

University of Strathclyde
Department of Pure and Applied Chemistry

***A Medicinal Chemistry Approach Towards
Bromodomain Epigenetic Modulators***

Robert Peter Law

PhD Pure and Applied Chemistry

2016

This thesis is the result of the author's original research. It has been composed by the author and has not been previously submitted for examination which has led to the award of a degree.

The copyright of this thesis belongs to GSK in accordance with the author's contract of engagement with GSK under the terms of the United Kingdom Copyright Acts. Due acknowledgement must always be made of the use of any material contained in, or derived from, this thesis.

Signed:

Date:

Abstract

Bromodomains are a family of epigenetic reader domains which recognize acetylated histone lysine residues, recruiting transcription factors to specific DNA locales. Aberrant bromodomain function is strongly implicated in a wide variety of diseases. Bromodomains are amenable to small-molecule inhibition, but in many cases either no inhibitor is known or a published inhibitor is only weakly selective.

The bromodomain and extra-terminal domain (BET) family of proteins are strongly linked to diverse cancers, autoimmune inflammation and other diseases, with several BET inhibitors in clinical trials. The BET family contains four proteins, Brd2, 3, 4, and T, which each contain two bromodomains, BD1 and BD2. BD2-selective BET inhibitors have received little attention, hindering the elucidation of the biological roles of the BD2 domains.

This work set out to develop potent BD2-selective BET inhibitors with drug-like properties. Using a strategy of late-stage synthetic diversity, parallel vector exploration, and structure- and knowledge-based optimisation, diverse analogues were synthesised and screened. The structure-activity relationships (SARs) of the template were elucidated, and the binding mode and selectivity rationale were determined through X-ray crystallography. This optimisation resulted in low-nanomolar, cell potent BD2 inhibitors with excellent wider bromodomain selectivity and good drug-like properties, suitable for use as *in vitro* or *in vivo* tools for target validation.

The function of the BRPF1 bromodomain is unknown, and while selective inhibitors have been developed their chemical diversity is poor. Starting from moderately potent but promiscuous hits, a structurally diverse series of BRPF1 inhibitors was investigated, aiming to improve potency and selectivity. Diverse, novel substitution patterns of the hit template and similar scaffolds were synthesised, investigated and SAR generated. Though increasing potency proved challenging, selectivity over other bromodomains was improved and the binding mode was elucidated through X-ray crystallography. This work has generated useful leads for further optimisation, thoroughly investigated the template and gained insights into BRPF1-ligand binding.

Acknowledgements

I would like to thank my GSK supervisions, David Hirst and Stephen Atkinson, for their generous help, advice and encouragement during my PhD, and my academic supervisor, Allan Watson, for his dedicated guidance and insightful support of my projects and development. Their assistance has given me vital skills and knowledge, guided my projects to success and helped shape my career aspirations. Thank you for your time, teaching me so much and making my PhD a success!

For their suggestions, discussions and camaraderie I am hugely grateful to everyone in Epinova chemistry; particularly Dominique Amans, Lee Harrison, Tom Hayhow, Alex Preston, Gail Seal, Jon Seal, Robert Sheppard, Bob Watson and Chris Wellaway. I would like to thank the project teams for allowing me to gain invaluable experience of medicinal chemistry, and managers Matt Lindon, Emmanuel Demont and Rab Prinjha for their support and allowing me to work on Epinova projects.

Thanks are due to Harry Kelly and Billy Kerr for their enthusiasm in setting up and running the industrial PhD programme and providing countless development opportunities. I am also grateful to Andrea Malley for her assistance with administration of the scheme.

I would also like to thank the IP students I have had the pleasure to work alongside, train and influence. I am particularly grateful to Liam Wilson, whose skill, eagerness and good humour made my first foray into student supervision highly enjoyable and mutually beneficial.

I am thankful to all the GSK staff who have kindly assisted me throughout my work; Eric Hortense for chiral HPLC analysis, Roy Copley for X-ray diffraction experiments, Bill Leavens for HRMS analysis, Sean Lynn for NMR spectroscopy; James Gray for DMPK experiments, Chun-wa Chung for X-ray protein crystallography and James Woolven and Armelle Le Gall for computational modelling. Special thanks are due to Laurie Gordon and Melanie Leveridge for running biochemical assays, data integrity checking and teaching me to run assays myself.

Thank you to the other industrial PhD students, particularly Ben, Natalie, Craig, Aymeric, JT and Sam, for the moral support and many hours of laughter, ridicule and complaining. I would also like to thank everyone in the Watson/Jamieson labs for making me so welcome during my Strathclyde secondment. Lastly, I am hugely grateful to Sarah McManus, for putting up with the long hours and weekends spent working, keeping me sane and helping me see the buffalo.

Contents

Abstract	3
Acknowledgements	4
Contents	5
List of Figures, Schemes and Tables	8
Figures	8
Schemes	10
Tables	11
Summary of Publications	13
List	13
of	13
Abbreviations	15
1. Introduction	18
1.1 Principles of Modern Medicinal Chemistry and Drug Design	18
1.1.1 The Medicinal Chemistry Process	18
1.1.2 The Goals of Medicinal Chemistry – Drug Candidates and Probes	19
1.1.3 Control of Physicochemical Properties	20
1.1.4 Ligand Efficiency	23
1.2 The Molecular Basis of Epigenetics	24
1.2.1 Histone Proteins, Nucleosomes and Chromatin	24
1.2.2 Histone Post-Translational Modifications	25
1.3 Bromodomains	27

1.4	BET Bromodomains	29
1.4.1	BET Proteins in Disease	30
1.4.2	Small Molecule BET Inhibitors	35
1.4.3	Domain-Selective BET Inhibitors	40
1.4.4	Dual Kinase-Bromodomain Inhibitors	43
1.4.5	Small Molecule-Induced Degradation	45
1.5	Non-BET Bromodomains.....	46
1.5.1	ATAD2	46
1.5.2	BAZ	49
1.5.3	BPTF	50
1.5.4	BRPF	51
1.5.5	Brd7 and Brd9	54
1.5.6	Brd8	55
1.5.7	BRWD	56
1.5.8	CECR2	56
1.5.9	CREBBP and EP300	56
1.5.10	PB1 and SMARCA2/4	58
1.5.11	PCAF	59
1.5.12	SP100/110/140	60
1.5.13	TAF1	61

1.5.14 TIF1 α	61
1.6 The Future of Bromodomains as Small-Molecule Targets	61
2. Design and Synthesis of Tetrahydroquinoxalines as BD2-Selective BET Inhibitors	63
2.1 Introduction	63
2.2 Aims	66
2.3 Results and Discussion	67
2.3.1 Previous GSK Work	67
2.3.2 Optimisation Strategy	68
2.3.3 The 2-Position	69
2.3.4 The KAc mimetic	76
2.3.5 The WPF-Shelf Group	77
2.3.6 Linker Substitution	81
2.3.7 6-Substitution	83
2.3.8 Aza Cores	88
2.3.9 The 3-Position – Lead-Hopping From a Screening Hit	90
2.3.10 Combination of Substituents	96
2.3.11 Single Enantiomer Synthesis	99
2.3.12 Profiling of Lead Molecules	103
2.4 Conclusions	107
2.5 Further Work	108
3. Design and Synthesis of BRPF1 Bromodomain Inhibitors	109

3.1	Introduction	109
3.2	Aims	112
3.3	Results and Discussion	113
3.3.1	Fragment Cores and Warhead Optimisation	113
3.3.2	The Pyrazolopyrimidine 5-Position	116
3.3.3	Azaindole (AI) Core	128
3.3.4	5,6-Disubstituted Pyrazolopyrimidines	132
3.3.5	Pyrazolopyrimidine 6-Substitution	139
3.3.6	X-Ray Crystallography	142
3.3.7	The 7-Position	144
3.3.8	Targeting the Phe-Ile Region	147
3.3.9	6-Aza Cores	154
3.3.10	Insights Into Wider Bromodomain Selectivity	156
3.3.11	Selectivity Within the BRPF Family	159
3.4	Conclusions	163
3.5	Future Work	165
4.	Experimental	166
4.1	General Chemistry Experimental	166
4.2	Compound Synthesis and Characterisation - Design and Synthesis of Tetrahydroquinoxalines as BD2-Selective BET Inhibitors	168
4.3	Compound Synthesis and Characterisation - Design and Synthesis of BRPF1 Bromodomain Inhibitors	224

4.4 Supplementary Protocols	316
5. References	318

List of Figures, Schemes and Tables

Figures

Figure No.	Title	Page
Figure 1.1	The process of iterative medicinal chemistry.	18
Figure 1.2	Basic structure of the chromatosome.	24
Figure 1.3	The roles of histone-modifying enzymes.	25
Figure 1.4	Drugs targeting histone-modifying proteins	26
Figure 1.5	Ribbon diagram of human bromodomain Brd4 BD1 and X-ray crystal structure of human Brd4 BD1 with acetylated lysine bound.	28
Figure 1.6	Phylogenetic tree showing structural similarities between bromodomains.	29
Figure 1.7	Schematic structure of human BET proteins.	30
Figure 1.8	Tumour volumes and survival rates in mouse NMC xenograft models treated with JQ1.	31
Figure 1.9	Effect of BET inhibitors on T-cell cytokine production.	32
Figure 1.10	Schematic of the relationship between Brd4, P-TEFb and HIV reactivation.	33
Figure 1.11	Selected BET inhibitors.	35
Figure 1.12	X-ray crystal structure of I-BET762 bound to Brd4 BD1.	37
Figure 1.13	X-ray crystal structures of dimethylisoxazole BET inhibitors bound to BET bromodomains.	38
Figure 1.14	X-ray crystal structure of I-BET726 bound to Brd2 BD2.	39
Figure 1.15	Nomenclature and predicted druggability of selective BET inhibitors.	40
Figure 1.16	Comparison of the BRD4 BD1 and BD2 X-ray apo structures.	41
Figure 1.17	Reported domain-selective BET inhibitors.	42
Figure 1.18	RVX-208 bound to Brd4 BD1 and Brd2 BD2.	42
Figure 1.19	Structures and BET biochemical potencies of reported dual kinase-bromodomain inhibitors.	44
Figure 1.20	Phthalimide-linked BET inhibitors for small molecule protein degradation.	45
Figure 1.21	Druggability analysis of human bromodomains.	46
Figure 1.22	Structures and biochemical potencies of reported ATAD2 bromodomain inhibitors.	47

Figure 1.23	X-ray crystal structure of an ATAD inhibitor bound to the bromodomain of ATAD2.	48
Figure 1.24	Structures and biochemical potencies of reported BAZ2B bromodomain inhibitors.	49
Figure 1.25	X-ray crystal structure of an BAZ inhibitors bound to the BAZ2B bromodomain.	50
Figure 1.26	Reported BPTF bromodomain inhibitor AU1.	51
Figure 1.27	Schematic of the quaternary MOZ HAT complex and sequence of BRPF1.	51
Figure 1.28	Reported BRPF family bromodomain inhibitors.	52
Figure 1.29	X-ray crystal structure of a benzimidazolone BRPF1 inhibitor bound to the bromodomain of BRPF1.	53
Figure 1.30	Structures and biochemical potencies of reported Brd7 and Brd9 bromodomain inhibitors.	54
Figure 1.31	X-ray structure of I-Brd9 bound to the Brd9 bromodomain.	55
Figure 1.32	Structures and biochemical potencies of reported CREBBP family bromodomain inhibitors.	57
Figure 1.33	X-ray crystal structures CREBBP inhibitors bound to the CREBBP bromodomain, showing interaction with Arg1173.	58
Figure 1.34	Structure and biochemical potencies of PFI-3.	59
Figure 1.35	Structure and potencies of PCAF inhibitors.	60
<hr/>		
Figure 2.1	Published THQ BET inhibitors and initial THQx hits.	63
Figure 2.2	X-ray crystal structures of THQx hits and a peptide bound to Brd4 BD2.	64
Figure 2.3	X-ray crystal structures of THQx hits and I-BET726 bound to BD2 domains.	65
Figure 2.4	Scatter plot of Brd4 BD1 vs BD2 FRET pIC ₅₀ for previously synthesised tetrahydroquinoxalines.	67
Figure 2.5	Current SAR knowledge for the THQx series, with key compounds from previous work.	68
Figure 2.6	Strategy for optimisation of the THQx series.	68
Figure 2.7	Initial THQx leads bound to the BD2 bromodomain.	73
Figure 2.8	Comparison of leads bound to the BD1 and BD2 domains.	74
Figure 2.9	Ring-fused THQx compound, and docking into Brd4 BD2.	75
Figure 2.10	Overlaid ¹ H NMR spectra of epoxide-opening products, showing enantiomeric pairs.	83
Figure 2.11	Biochemical potencies of aza core molecules.	90
Figure 2.12	Structures and potencies of BO hits.	90
Figure 2.13	X-ray crystal structures of BO and THQx compounds bound to Brd2 BD2.	91
Figure 2.14	DiscoverRx BROMOScan™ bromodomain selectivity tree for a THQx probe candidate.	105
Figure 2.15	X-ray structure of THQx probe candidates bound to Brd2 BD2.	106
Figure 2.16	Profile of THQx probe candidate.	107

Figure 3.1	Docking of a PP into the BRPF1 bromodomain	111
Figure 3.2	Docking of a PP into the BRPF1 bromodomain	124
Figure 3.3	Intermediates and potential product conformations of the Van Leusen cyanation	127
Figure 3.4	Modelled vector similarities and design strategy for disubstituted compounds.	132
Figure 3.5	X-ray crystal structure of a PP lead bound to the BRPF1 bromodomain.	143
Figure 3.6	X-ray crystal structure of a PP lead bound to the BRPF1 bromodomain.	143
Figure 3.7	Overlaid docking of an initial PP hit and X-ray crystallography of a lead compound bound to the BRPF1 bromodomain.	144
Figure 3.8	Biological activity of 7-substituted pyrazolopyrimidines.	145
Figure 3.9	X-ray structure of a phenylpiperidine PP analogue bound to the BRPF1 bromodomain.	153
Figure 3.10	Structures, dihedral angles and MMFF94x potential energies (calculated using Molecular Operating Environment, MOE) for phenylpiperidine PPs.	154
Figure 3.11	Alternative N6 cores.	154
Figure 3.12	FRET bromodomain selectivity profile of a PP lead, plotted onto the human bromodomain phylogenetic tree.	157
Figure 3.13	Apo X-ray crystal structures of the bromodomains of BRPF1 overlaid with Brd9, CECR2 and Brd4 BD1.	158
Figure 3.14	Overlay of the X-ray structure of a phenylpiperidien bound to the BRPF1 bromodomain and the apo structure of Brd9.	159
Figure 3.15	Plot of BRPF1 vs BRPF2 pIC ₅₀ .	160
Figure 3.16	Plot BRPF1 vs BRPF2 pIC ₅₀	160
Figure 3.17	Overlaid Apo structures of BRPF1 and BRPF2 and sequence homology of key KAc binding site residues for the BRPF family.	161
Figure 3.18	Future work.	165

Schemes

Scheme No.	Title	Page
Scheme 2.1	Representative synthesis of THQx building blocks.	69
Scheme 2.2	Representative synthesis of 6-H compounds.	70
Scheme 2.3	Synthesis of <i>gem</i> -dimethyl THQx compounds.	72
Scheme 2.4	Synthesis and biological activity of ring-fused THQx compounds.	75
Scheme 2.5	Synthesis and activity of alternative KAc mimetic THQx compounds.	76
Scheme 2.6	Synthesis of a WPF shelf array.	77
Scheme 2.7	Topliss scheme and potencies of the relevant compounds.	81

Scheme 2.8	Compound synthesis by epoxide ring-opening.	83
Scheme 2.9	Synthesis of 6-aryl compounds.	84
Scheme 2.10	Synthesis of 7-aza THQx.	89
Scheme 2.11	Synthesis of acid intermediate.	92
Scheme 2.12	Oxidation with a benzoyl (Bz) protecting group.	94
Scheme 2.13	Synthesis and potency of lead-hopping final compounds.	95
Scheme 2.14	Synthesis of combination compounds.	97
Scheme 2.15	Chiral separation of THQx leads and single enantiomer potencies.	99
Scheme 2.16	Single enantiomer synthesis of THQx leads.	100
Scheme 2.17	Completion of the single enantiomer synthesis.	102
<hr/>		
Scheme 3.1	Synthesis and activity of alternative KAc mimetics.	113
Scheme 3.2	Core modifications.	114
Scheme 3.3	Core modifications.	115
Scheme 3.4	Synthesis of a 5-substituted pyrazolopyrimidines intermediate.	116
Scheme 3.5	Synthesis of α -Me 5-substituted pyrazolopyrimidines and their BRPF1 activity.	119
Scheme 3.6	Methylation of a PP hit, potency and physicochemical properties.	124
Scheme 3.7	Synthesis of 5-(aminopiperidine) PPs.	127
Scheme 3.8	Synthesis of 5-substituted AI compounds.	129
Scheme 3.9	Synthesis of <i>N</i> -substituted AI compounds.	131
Scheme 3.10	Attempted synthesis of disubstituted pyrazolopyrimidines.	132
Scheme 3.11	Attempted synthesis of 5-C, 6- <i>N</i> disubstituted pyrazolopyrimidines and elaboration of the 7-cPr analogues.	133
Scheme 3.12	Attempted intermolecular cyclisation using a dimethylenone ester.	134
Scheme 3.13	Acylation of unprotected and protected aminopyrazoles.	135
Scheme 3.14	Stepwise formation of the PP bicyclic ring system.	135
Scheme 3.15	Synthesis of 5,6-disubstituted pyrazolopyrimidines.	136
Scheme 3.16	Further 6-benzyl and 6-alkyl substituents in the disubstituted PP series.	138
Scheme 3.17	Synthesis and biological activity of 6-substituted pyrazolopyrimidines.	140
Scheme 3.18	Proposed mechanism for the formation of 7-amino PPs.	140
Scheme 3.19	Synthesis and biological activity of 6-substituted pyrazolopyrimidines.	141
Scheme 3.20	Synthesis and biological activity of 6-OBn pyrazolopyrimidine.	142
Scheme 3.21	Synthesis of a pyrazolopyrimidone analogue.	145
Scheme 3.22	Synthesis of 7-amino PPs.	146
Scheme 3.23	Synthesis of 7-amino AIs.	147
Scheme 3.24	Benzylic and phenyl groups.	148
Scheme 3.25	Bridged and bicyclic 5-substituents.	148
Scheme 3.26	Phenyl groups at the 2-position of heterocycles.	149

Scheme 3.27	Synthesis of imidazole and amine 5-substituents.	151
Scheme 3.28	Synthesis of a 5,6-disubstituted pyrazolopyrimidine.	152
Scheme 3.29	Synthesis of 5-substituted pyrrolo[3,2-d]pyrimidine compounds.	155
Scheme 3.30	Proposed synthesis of pyrazolo[1,5-a]-1,3,5-triazine compounds.	165

Tables

Table No.	Title	Page
Table 1.1	Protein classes involved in histone post-translational modification.	25
Table 2.1	WPF shelf/2-position square array of THQx compounds.	71
Table 2.2	Optimisation of the WPF shelf binding group.	79
Table 2.3	Investigation of epoxide opening conditions.	82
Table 2.4	THQx 6-Aryl array.	85
Table 2.5	Attempted oxidation conditions.	93
Table 2.6	Target potencies and additional profiling of combination compounds.	98
Table 2.7	Optimisation of Suzuki-Miyaura cross-coupling.	101
Table 2.8	Extended profiles of THQx probe candidates.	103
Table 2.9	DiscoverRx BROMOScan™ Kd values.	105
Table 3.1	Bromodomain FRET potencies, LE and physicochemical properties of 109 initial pyrazolopyrimidine hits.	
Table 3.2	Synthesis, structures and potencies of initial 5-substituted PPs.	117
Table 3.3	Bromodomain FRET potencies, LE and physicochemical properties of 5-substituted PPs.	120
Table 3.4	Structures and potencies of amine array products.	120
Table 3.5	Bromodomain FRET potencies and physicochemical properties of 5-123 heterocyclic PPs.	
Table 3.6	Structures and potencies of aminopiperidine substituted PPs.	125
Table 3.7	Bromodomain FRET potencies, LE and physicochemical properties of 128 5-(aminopiperidine)-substituted PPs.	
Table 3.8	Bromodomain FRET potencies, LE and physicochemical properties of 5-substituted AIs.	130
Table 3.9	Azaindole <i>N</i> -substitution.	131
Table 3.10	Synthetic yields, BRPF1 pIC ₅₀ and LE for disubstituted PP compounds and monosubstituted comparators.	137
Table 3.11	Bromodomain FRET potencies, LE and physicochemical properties of 139 5,6-disubstituted PPs.	
Table 3.12	Structures and potencies of phenylpiperidine PPs.	150
Table 3.13	FRET potencies, LE and physicochemical properties of 152 methylpiperidine and phenylpiperidine PPs.	

Table 3.14	Bromodomain FRET potencies, LE and physicochemical properties of 156 pyrrolo[3,2-d]pyrimidines.	
Table 3.15	Bromodomain FRET potencies, LE and physicochemical properties of lead compounds.	163

Summary of Publications

A modular synthesis of functionalised phenols enabled by controlled boron speciation

John J. Molloy, Robert P. Law, James W. B. Fyfe, Ciaran P. Seath, David J. Hirst and Allan J. B. Watson, *Org. Biomol. Chem.*, **2015**, **13**, 3093-3102.

Abstract: A modular synthesis of functionalised biaryl phenols from two boronic acid derivatives has been developed via one-pot Suzuki-Miyaura cross-coupling, chemoselective control of boron solution speciation to generate a reactive boronic ester in situ, and oxidation. The utility of this method has been further demonstrated by application in the synthesis of drug molecules and components of organic electronics, as well as within iterative cross-coupling.

2,3-Disubstituted 1-acyl-4-amino-1,2,3,4-tetrahydroquinoline derivatives and their use as bromodomain inhibitors

WO 2014140076 A1; Dominique Amans, Stephen J. Atkinson, Lee A. Harrison, David J. Hirst, Robert P. Law, Matthew Lindon, Alexander Preston, Jonathan T. Seal and Christopher R. Wellaway, 12th March 2014.

Rationally designing safer anilines: the challenging case of 4-aminobiphenyls

Alan M. Birch, Sam Groombridge, Robert Law, Andrew G. Leach, Christine D. Mee, and Carolin Schramm; *J. Med. Chem.*, **2012**, **55** (8), 3923–3933.

Abstract: We describe how we have been able to design 4-aminobiphenyls that are nonmutagenic (inactive in the Ames test). No such 4-aminobiphenyls were known to us, but insights provided by quantum mechanical calculations have permitted us to design and synthesize some examples. Importantly, the quantum mechanical calculations could be combined with predictions of other properties of the compounds that contained the 4aminobiphenyls so that these remained druglike. Having found compounds that are not active, the calculations can provide insight into which factors (electronic and conformational in this case) are important. The calculations provided SAR-like information that was able guide the design of further examples of 4-aminobiphenyls that are not active in the Ames test.

Design and Synthesis of Tetrahydroquinoxalines as Domain Selective BET Inhibitors

Robert P. Law, Stephen J. Atkinson, Paul Bamborough, Chun-wa Chung, Emmanuel H. Demont, Matthew J. Lindon, Laurie J. Gordon, Rab K. Prinjha, Allan J.B. Watson, David J. Hirst. *Manuscript in preparation.*

Abstract: The bromodomain and extra-terminal domain (BET) family of proteins bind acetylated lysine residues on histone proteins. BET bromodomain inhibition is a potential therapy for various cancers and immunoinflammatory diseases, but few reported inhibitors show selectivity within the BET family. Inhibitors with selectivity for the first or second bromodomain are desired to aid investigation of the biological function of these domains. This paper describes the discovery and optimization of a series of tetrahydroquinoxalines with selectivity for the second bromodomains of the BET family (BD2), culminating in potent BET inhibitors with BD2 selectivity.

List of Abbreviations

μ W	Microwave Irradiation
ADMET	Absorption, Distribution, Metabolism, Excretion, and Toxicity
AGP	A-Glycoprotein
AI	Azaindole
AML	Acute Myeloid Leukaemia
AMP	Artificial Membrane Permeability
ANCCA	AAA Nuclear Coregulator Cancer-Associated Protein
ApoA1	Apolipoprotein A1
ATAD	Atpase Family AAA Domain-Containing Protein
BAH	Bromo-Adjacent Homology
BAZ	Bromodomain Adjacent To Zinc Finger Domain
BD	Bromodomain
BET	Bromodomain and Extra-terminal
Bn	Benzyl
BO	Benzoxazine
Boc	<i>tert</i> -Butoxycarbonyl
BPTF	Bromodomain/PHD Finger Transcription Factor
Brd	Bromodomain-Containing Protein
BRPF	Bromodomain and PHD-Finger Containing Protein
brsm	By Recovered Starting Material
BRWD	Bromodomain And WD Repeat-Containing Protein
Bt	Benzotriazole
Bz	Benzoyl
CAN	Ceric Ammonium Nitrate
Cbz	Carboxybenzyl
CDK	Cyclin-Dependant Kinase
CECR2	Cat Eye Syndrome Chromosome Region, Candidate 2
CETP	Cholesteryl Ester Transfer Protein
CLND	Chemiluminescent Nitrogen Detection
CREBBP	Camp Response Element Binding Protein Binding Protein
cPr	Cyclopropyl
CTCL	Cutaneous T-Cell Lymphoma
CTD	C-Terminal Domain
CXCL	Chemokine (C-X-C Motif) Ligand
DABAL-Me ₃	Triethylenediamine bis(trimethylaluminum)
DABCO	1,4-Diazabicyclo[2.2.2]octane
DBU	1,8-Diazabicyclo[5.4.0]undec-7-ene
DCE	1,2-Dichloroethane
DCM	Dichloromethane
DDB1	Damage-Specific DNA Binding Protein 1
DDQ	2,3-Dichloro-5,6-dicyano-1,4-benzoquinone
DIPEA	<i>N,N</i> -Diisopropylethylamine
DMAP	4- <i>N,N</i> -Dimethylaminopyridine
DME	1,2-Dimethoxyethane
DMEDA	<i>N,N</i> -Dimethylethylenediamine
DMF	<i>N,N</i> -Dimethylformamide
DMPK	Distribution, Metabolism, and Pharmacokinetics
DMSO	Dimethylsulphoxide

eq/equiv.	Equivalents
ET	Extra-terminal
FRET	Fluorescence Resonance Energy Transfer
GM-CSF	Granulocyte-Macrophage Colony Stimulating Factor
GSK	GlaxoSmithKline
h	Hours
HAT	Histone Acetyltransferase
HATU	(Dimethylamino)- <i>N,N</i> -dimethyl(3 <i>H</i> -[1,2,3]triazolo[4,5- <i>b</i>]pyridin-3yloxy)methaniminium hexafluorophosphate
HDAC	Histone De-acetylase
HEAF6	Human Esa1-Associated Growth Factor
hERG	Human Ether-A-Go-Go Related Gene
HFIP	1,1,1,3,3,3-Hexafluoroisopropanol
HIV	Human Immunodeficiency Virus
HMG	High-Mobility Group
HOX	Homeobox
HPLC	High Performance Liquid Chromatography
HSA	Human Serum Albumin
HWB	Human Whole Blood
ING5	Inhibitor Of Growth 5
JAK	Janus Kinase
KAc	Acetyl-Lysine
KAT	Lysine Acetyltransferases
KDM	Lysine Demethylase
KMT	Lysine Methyltransferase
LCMS	Liquid Chromatography-Mass Spectrometry
LDA	Lithium Diisopropylamide
LE	Ligand Efficiency
LH	Leucine-Rich Helical
LLE	Lipophilic Ligand Efficiency
LLE _{AT}	Astex Lipophilic Ligand Efficiency
LPS	Lipopolysaccharide
MCP-1	Monocyte Chemotactic Protein-1
MDAP	Mass Directed Automatic Purification
MM	Multiple Myeloma
MMP1	Matrix Metalloproteinase-1
MOZ	Monocytic Leukemic Zinc-Finger
MS	Molecular Sieves
MW	Molecular Weight
NFATC1	Nuclear Factor of Activated T-Cells, Cytoplasmic, Calcineurin-Dependent 1
NMC	NUT Midline Carcinoma
NMO	<i>N</i> -Methylmorpholine <i>N</i> -Oxide
NMP	<i>N</i> -Methyl pyrrolidinone
NORC	Nucleolar Remodelling Complex
NUT	Nuclear Protein <i>In Testis</i>
PAD	Protein Arginine Deiminase
PB	Polybromodomain-Containing Protein
PBAF	Polybromo/BRG1-Associated Factors
PBMC	Peripheral Blood Mononuclear Cells

PCAF	P300/CREBBP-Associated Factor
PCC	Pyridinium Chlorochromate
PDB	Protein Data Bank
PEL	Primary Effusion Lymphoma
PEPPSI	Pyridine-Enhanced Precatalyst Preparation Stabilization and Initiation
PFI	Property Forecast Index (PFI = ChromLogD _{pH7.4} + #Ar)
PHD	Plant Homeodomain
PHIP	Pleckstrin Homology Domain Interacting Protein
PIN	Pinacol
PK	Pharmacokinetics
PLK	Polo-Like Kinase
PMB	<i>para</i> -Methoxy Benzyl
PML	Pro-Myelocytic Leukaemia
Pol II	RNA Polymerase II
PP	Pyrazolo[1,5- <i>a</i>]Pyrimidine
PRMT	Protein Arginine Methyltransferase
PT	Pyrazolo[1,5- <i>a</i>]-1,3,5-Triazine
P-TEFb	Positive Transcription Elongation Factor B
PTM	Post-Translational Modification
PWWP	Proline-Tryptophan-Tryptophan-Proline
PZP	Double PHD and Zinc Finger Assembly
RANKL	Receptor Activator of Nuclear Factor Kappa-B Ligand
RING	Really Interesting New Gene
RNA	Ribonucleic acid
rt	Room Temperature
RVF	Arginine-Valine-Phenylalanine
SAM	S-Adenosyl Methionine
SAR	Structure-activity Relationship
SEM	[2-(Trimethylsilyl)Ethoxy]Methyl Acetal
SGC	Structural Genomics Consortium
SIRNA	Small Interfering RNA
SMARC	SWI/SNF-Related, Matrix-Associated, Actin-Regulator Dependent Chromatin
SUMO	Small Ubiquitin-like Modifier
SWI/SNF	Switch/Sucrose Non-Fermentable

TAF1	Transcription Initiation Factor TFIID Subunit 1
TEMPO	(2,2,6,6-Tetramethylpiperidin-1-Yl)Oxyl
TFA	Trifluoroacetic acid
THF	Tetrahydrofuran
THP	Tetrahydropyran
THQ	1,2,3,4-Tetrahydroquinoline
THQx	1,2,3,4-Tetrahydroquinoxaline
TIF1 α	Transcription Initiator Factor 1 α
TLC	Thin Layer Chromatography
TNF	Tumour Necrosis Factor
TPAP	Tetrapropylammonium Perruthenate
TPSA	Topological Polar Surface Area
TRIM24	Tripartite Motif 24
WPF	Tryptophan-Proline-Phenylalanine
ZNF	Zinc Finger

1. Introduction

1.1 Principles of Modern Medicinal Chemistry and Drug Design

1.1.1 The Medicinal Chemistry Process

Medicinal chemistry involves the design, synthesis and analysis of pharmaceuticals and bioactive compounds. No two medicinal chemistry projects are the same, as they employ a wide variety of biological targets, chemistries, technologies, and end goals, but all broadly follow a logical, iterative process (Figure 1.1).¹

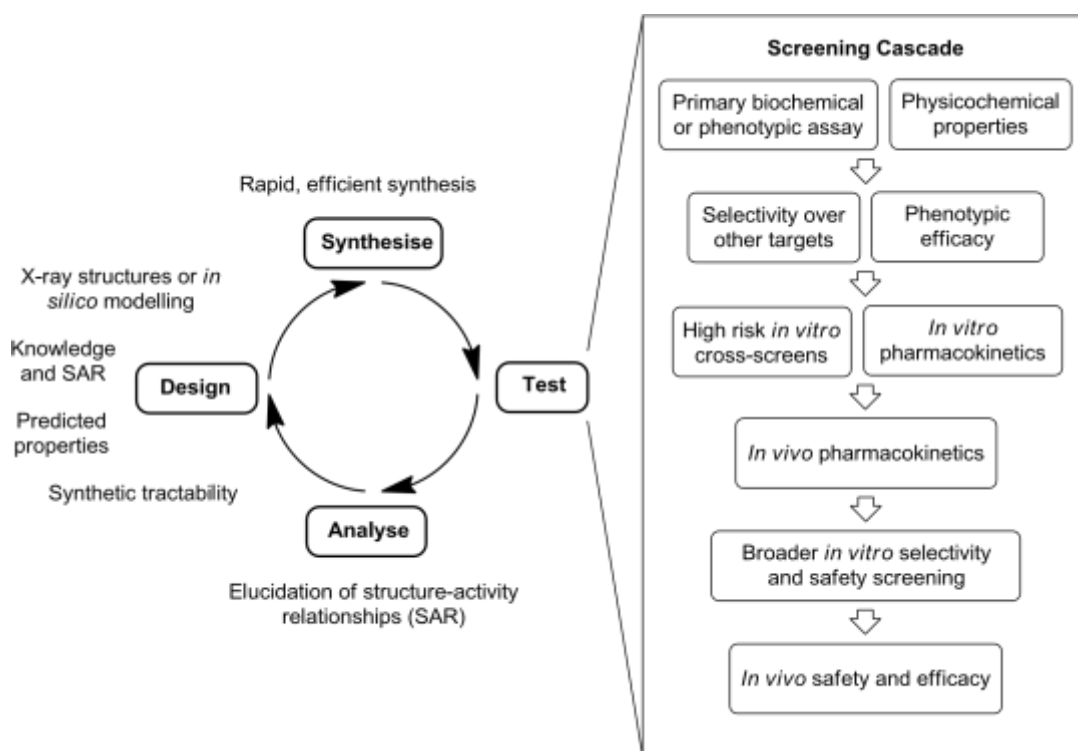


Figure 1.1. The processes of iterative medicinal chemistry.

The medicinal chemist designs potentially bioactive molecules based on previously known compounds which bind to the relevant biological target or produce a physiological effect. These are then synthesised, ideally as rapidly and efficiently as possible to expedite the process, and tested in a biological assay. Molecules typically progress through a screening cascade, with only compounds which meet a set of criteria at each level progressing to the next set of screens. Comparing the assay results for compounds of similar structure allows the formation of structure-activity relationships (SARs), which are then used to guide the design of further iterations. As a project progresses through multiple cycles, SAR becomes more complex and detailed as different areas of the molecule are explored, knowledge of the target grows and additional levels of the screening cascade are reached. The cycle continues until a compound is identified which meets all of the screening criteria (or is considered 'good enough'), or the goal is believed to be unobtainable and the series or project terminated.

Medicinal chemistry may use either phenotypic or target-based approaches. Phenotypic screening directly measures the biological effect of compounds in a relevant cellular system (e.g. the ability of an antibiotic to kill bacterial colonies) without precise knowledge of the molecular target. While this provides direct confirmation of the desired efficacy, the lack of knowledge around the compounds' binding mode makes analogue design more challenging and cellular assays are often less robust. Thus, even if a phenotypic approach is taken, there is often a subsequent move to understand molecular target and mechanism.

Target-based optimisation identifies a specific enzyme or protein which is known to be linked to a disease (e.g. a kinase which is upregulated in a particular cancer) and develops a compound which binds to that precise target. This often (but not always) allows the use of *in silico* modelling, X-ray protein crystallography and high-throughput biochemical assays, allowing the rapid development of highly potent inhibitors. However, should the target of interest not be the primary driver of disease or if alternative biological pathways exist, the compound may not be suitably efficacious in the clinic. To reduce this risk, target-based approaches usually utilise a phenotypic readout (e.g. cultivated cancer cell lines or xenograft models) alongside biochemical assays.

1.1.2 The Goals of Medicinal Chemistry – Drug Candidates and Probes

Traditionally, the end goal of medicinal chemistry has been the identification of a drug candidate; a molecule with suitable efficacy, pharmacokinetics and safety profile for progression into human clinical studies for a disease indication. The molecular target of the compound and its mechanism of action do not need to be known, and activity at multiple targets (polypharmacology) is acceptable provided the safety profile is uncompromised.² At the point of declaring a candidate, the structure of the compound (but not its salt form, particle morphology or formulation) becomes fixed. The discovery of a drug candidate is a lengthy, challenging, and expensive process,¹ and so ideally should only be undertaken for targets with a strong disease rationale.

Successful target-based drug discovery relies on thorough target validation – proving that the protein of interest has a key role in disease.¹ This may be accomplished by studying the up- or down-regulation of particular genes, proteins or biomarkers in disease, to elucidate biological signalling pathways and find weak points that can be targeted. Deactivating genes using RNA interference is commonly used, but this completely removes entire multidomain proteins and scaffolds - not representative of reversibly blocking a single protein domain.³ Increasingly, medicinal chemistry groups are turning their attention towards chemical probes, small molecules which bind to a specific protein domain and can be used to determine its biological role.⁴ Chemical probes are often more simple to develop compared to drug candidates as facets such as *in vivo* pharmacokinetics, chronic toxicity and dosing are of lesser importance. Target validation with chemical probes improves confidence in the therapeutic potential of a target, and more importantly invalidates targets to prevent unfruitful further investigation.⁵

Many pharmaceutical companies promote or enforce a set of property guidelines to ensure drug candidates are of high quality. Chemical probes are frequently developed by academic groups unfamiliar with such approaches, and concern over poor quality probes has led to

publication of several sets of probe guidelines.⁴⁻⁷ While suggested values vary between publications, the spirit of these guidelines can be summarised as follows:

- High, robust *in vitro* potency against a known biological target
- High selectivity against other proteins of the same target family, and selectivity profiling against common off-targets (10-100-fold is commonly suggested)^{6,8}
- Aqueous solubility and membrane permeability sufficiently high as to prevent assay interference and allow cellular studies
- Evidence of cellular penetration, target engagement and dose-dependent disruption of target protein activity in cells
- The availability of an inactive control analogue and additional probes from chemically distinct series

While suitability for *in vivo* experiments is not generally required, acceptable absorption, distribution, metabolism, excretion and toxicity (ADMET) parameters and target engagement in animal models greatly increases the utility of a probe.⁷ Such examples must normally be of a higher quality overall. Conversely, lower probe quality is somewhat more acceptable if the target is particularly challenging to drug or no chemical tools currently exist.⁶ Many confidential and proprietary probes are developed by industrial groups for internal use, and never released to the wider community. However, academic groups and academic/industrial consortia are increasingly promoting a pre-competitive model whereby probes and associated data are published and made publicly available without restriction.⁶

1.1.3 Control of Physicochemical Properties

When designing drug candidates (and to a lesser extent, probes) their potential ADMET properties must be considered. Despite huge investment in drug discovery, only 11% of projects which enter human clinical trials are successful and approved as medicines, with pharmacokinetics being a major cause of failure (referred to as attrition).⁹ It has been noted that to increase *in vitro* potency and permeability, excess lipophilicity (non-polar, fat-soluble functionality) and molecular weight is often designed into molecules, defined as 'molecular obesity' by Hann. High potency is often sought in order to lower the therapeutic dose, however as dose is dependent on ADMET properties, correlation between *in vitro* potency and the eventual therapeutic dose is poor.¹¹ Excess lipophilicity also correlates with compound promiscuity,^{10,11} and a marked decrease in molecular weight is shown as compounds progress through clinical phases.¹² Gleeson *et al.* assigned empirical ADMET property scores to a set of development compounds and found them to be far higher on average than those of marketed oral drugs.¹¹ To reduce this risk, a variety of metrics and guidelines for physicochemical properties have been developed.

The well-known 'Rule of Five', developed by Lipinski in 1997, was the first widely recognised attempt to determine if a drug will be orally bioavailable¹³ (though it is often misused as a definition of 'drug-like' space¹⁴). The 'Rule of Five' states that to achieve oral bioavailability compounds should have: <5 hydrogen bond donors, <10 hydrogen bond acceptors, MW<500, and logP<5.¹³ As the 'Rule of Five' does not include toxicological risk,¹⁵ more refined physicochemical metrics have since been developed.

The intrinsic hydrophobicity of a compound, LogP, is the most widely used measure of lipophilicity. However, LogP is only valid for a compound bearing no charge, so is a poor indicator for compounds such as amines which are ionised at physiological pH. To correct for this the effective hydrophobicity at pH = x, LogD_x, is often used. LogD_x can be measured in an octanol/water shake flask system as with LogP; however this has been shown to be unreliable for highly lipophilic compounds due to poor solubility. An alternative chromatographic measurement of hydrophobicity, ChromLogD, has been developed and shows good agreement with computationally calculated values.¹⁶

Investigation of 245 Pfizer compounds with animal *in vivo* toxicity data found that compounds with cLogP <3 and topological polar surface area (TPSA, a measure of polarity¹⁷) >75 Å² were 2.5-times more likely to be non-toxic at 10 µM doses. Compounds with cLogP >3 and TPSA<75 Å² were 2.5-times more likely to be toxic at the same dose, which correlated with increased promiscuity. This relationship was codified as the "3/75 rule".¹⁸

Aromatic rings provide rigid scaffolds that reduce the entropic penalty of binding to a receptor, are easily manipulated, and can bind strongly through hydrophobic interactions and π-stacking. However, MacDonald and Ritchie noted that the average number of aromatic rings decreases moving through development phases, with oral marketed drugs having an average 1.6 aromatic rings, compared to 3.3 for a selection of GSK preclinical candidates.¹⁹ Increasing aromatic ring count correlates with decreased aqueous solubility, increased plasma protein binding, higher cytochrome P450 activity and increased human ether-á-go-go (hERG) cardiac ion channel inhibition. Compared to carboaromatics, heteroaromatics have improved properties but are still detrimental overall compared to non-aromatic groups.

Heteroaliphatic rings, however, showed improved developability parameters. The authors therefore recommended a limit of three aromatic rings per molecule.^{19,20}

Following this, Young *et al.* developed the Property Forecast Index (PFI = LogD_{7.4} + #Ar), as a simple measure of developability that takes into account the effect of aromatic rings beyond their contribution to lipophilicity. Based on the trends in plasma protein binding, hERG binding, metabolic clearance, and promiscuity, a PFI limit of < 7 was recommended.¹⁶ In a similar vein, Lovering *et al.* demonstrated that the fraction of sp³ carbons (Fsp³ = #sp³ carbons/total

#carbons) increases on moving through development and correlates well with increased solubility.²¹ Increasing the 3D character of a molecule impairs crystal packing, evidenced by a reduction in melting point, and so improves solubility.²¹

The appropriateness of the use of simple physicochemical property guidelines is disputed, particularly the use of marketed drug properties as a benchmark. Failed drug candidates (which may provide a better indication of risks) are usually not included in such analyses, and candidates fail for reasons other than developability.²² It has been suggested that neglecting molecular weight and the use of binned data inflates the correlation between PFI and ADMET properties, needlessly restricting the chemical space available for drug design.²³ An analysis of 150 AstraZeneca candidates found no correlation between preclinical success and the 3/75 rule, Fsp³ or promiscuity, and noted that many recently approved drugs violate these guidelines.²² When attrition rates from four companies were collated, it was found that most fell within accepted drug-like space yet attrition remained at high levels. However, compounds failing due to safety in Ph1 were significantly more lipophilic than those which progressed. The authors recommend that tighter control of properties beyond the existing guidelines is unlikely to increase compound success.²⁴

Compliance with metrics aside, all compounds intended for biological use must be sufficiently soluble in aqueous physiological environments and able to cross biological membranes to reach intracellular targets. A poorly soluble compound limits the maximum available concentration in a biological assay, and may form precipitates which affect the results. 100-200 μM is generally considered a minimum for aqueous solubility.^{7,16} Highthroughput automated solubility measurements use very low amounts of compound, and often measure precipitation on aqueous dilution of DMSO stock solutions (thermodynamic solubility). After filtration, chemiluminescent nitrogen detection (CLND) pyrolyses the sample and measures the nitrogen content with very low detection limits, which can be extrapolated to determine the compounds concentration.²⁵ In later stage discovery kinetic solubility will often also be measured in simulated intestinal fluid, often using crystalline material.

Compounds may cross biological membranes through either passive permeation between the lipid molecules or active transport, whereby a transporter protein captures the compound and carries it through the membrane. The relative extent to which these processes govern permeability is disputed.^{26,27} Permeability is commonly measured in high-throughput assays using cultured monolayers of Caco-2 cells²⁸ or wholly synthetic artificial membranes.²⁹

It could be argued that, for a chemical probe not intended for the clinic, the control of physicochemical properties is unimportant compared to potency and selectivity. Probe design should not be needlessly restricted by such metrics, but as solubility, permeability and (lack

of) promiscuity are all important for high quality probes, this work will strive to maintain physicochemical properties within drug-like space where possible.

1.1.4 Ligand Efficiency

The concept of measuring how efficiently a ligand binds given its size was first proposed by Kuntz in 1999, who noted that as ligands get larger the binding contribution per atom decreases.³⁰ Comparing potency and molecular size allows consideration of how efficiently a compound binds, and is a useful way to limit excess molecular weight and lipophilicity. Hopkins *et al.* defined the binding energy per heavy atom as ligand efficiency (LE), which can be calculated either using K_d or pIC_{50} measurements (Equation 1).³¹

$$LE = \frac{\Delta G}{N_{Heavy\ Atoms}} = \frac{-RT \ln K_d}{N_{Heavy\ Atoms}} = 1.37 \times \frac{pIC_{50}}{N_{Heavy\ Atoms}} \quad (1)$$

Analysis of the Pfizer compound collection gave an estimated value of 38 heavy atoms for a 500 Da compound. If this compound has a K_d of 10 nM, a typical desired value for a medicinal chemistry project, then LE would equal 0.29. Based on this, a suggestion of $LE \approx 0.3$ or higher is proposed as reasonable efficiency.³¹ Allegations that LE may be mathematically invalid have emerged,³² and been refuted.³³ Although hard guidelines for LE values may be unhelpful, the model is a simple method for comparing hits and tracking increasing size during optimisation.

As LE only accounts for molecular size and not lipophilicity, Leeson and Springthorpe have developed the complementary measurement of ligand-lipophilicity efficiency (LLE), a measure of how effectively the lipophilicity of a molecule translates into potency (Equation 2). Based on average oral drug values, a target of $LLE = 5-7$ is suggested.¹⁵

$$LLE = pIC_{50}(\text{or } pK_i) - cLogP (\text{or } LogD) \quad (2)$$

LLE often cannot be used for fragments or initial hits, as their potency is sometimes too low to give sensible values. To counter this, LLE adjusted for heavy atom count (LLE_{AT} , Equation 3) has been designed for use in fragment-based drug design and is scaled to be comparable with LE.³⁴

$$LLE_{AT} = 0.111 + \frac{1.37 \times LLE}{N_{Heavy\ Atoms}} \quad (3)$$

A wide variety of other ligand efficiency and physicochemical property metrics and tools have also been developed^{35,36} – almost 40 according to a recent analysis.³² This has led to concern that the abundance of guidelines is confusing and could impede decision making.³²

1.2 The Molecular Basis of Epigenetics

1.2.1 Histone Proteins, Nucleosomes and Chromatin

The science of epigenetics ('above genetics') examines heritable changes in gene expression and phenotype that do not alter the underlying DNA sequence of an organism.³⁷ The human genome only contains around 20,000 – 25,000 protein-encoding genes, too few to account for the wide range of phenotypes observed in human cells,³⁸ and this extra complexity is believed to arise from selective activation and deactivation of the genome. Epigenetics has become an important field in biological and medical research in recent years, in particular due to the potential to deactivate disease-associated genes without the risk of permanent DNA alteration.

The mechanisms of selective gene transcription are complex, but many revolve around DNA access and storage. Within the nucleus of a cell, the DNA double helix wraps around octamers of histone proteins to form nucleosomes, which consist of two sets of four histones (H2A, H2B, H3, and H4) in a highly ordered octamer around which 145-147 base pairs of DNA are accommodated.³⁹ A fifth histone, H1, binds the DNA at the start and end of the turn to stabilise it. When H1 is bound, the structure is referred to as a chromatosome (Figure 1.2).⁴⁰ Each nucleosome is separated by a short length of unwrapped DNA, and the chain of chromatosomes pack further to form a chromatin fibre, which coils repeatedly to form the chromosomes. H1 is required for the formation of these higher order structures, with the H1 proteins linking together in the centre of the structure.⁴⁰

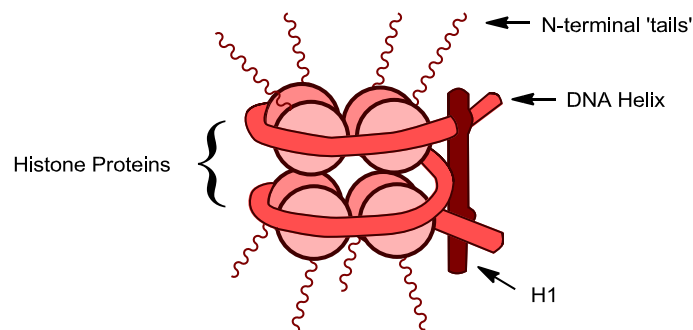


Figure 1.2. Basic structure of the chromatosome.

1.2.2 Histone Post-Translational Modifications

Each histone contains an N-terminal 'tail' that protrudes from the octamer and past the bound DNA. Amino acids on these tails are subject to a wide variety of post-translational modifications (PTMs, also referred to as 'histone marks').^{37,41} Over 60 amino acids within the histone tails are capable of being chemically modified in several different ways, giving a vast number of permutations.⁴² These combinations of PTMs are recognised by external proteins that mediate gene expression, leading to the hypothesis of a 'histone code' that directs precise control of transcription.^{43,44}

- Lysine residues can be acetylated and mono-, di-, or tri-methylated. Small proteins such as ubiquitin (which tags the protein for proteosomal degradation) or SUMO (small ubiquitin-like modifier, various functions) can be appended.
- Arginine can be mono- or di-methylated. The guanidine imine can be hydrolysed by protein arginine deiminase (PAD) enzymes to form citrulline.
- Serine, threonine and tyrosine can be phosphorylated.

PTMs may only persist due to positive maintenance and their heritability is unclear.^{45,46} A variety of enzymes dynamically add and remove histone marks, while certain PTMs are bound by reader domains to recruit protein complexes to chromatin (Figure 1.3, Table 1.1).

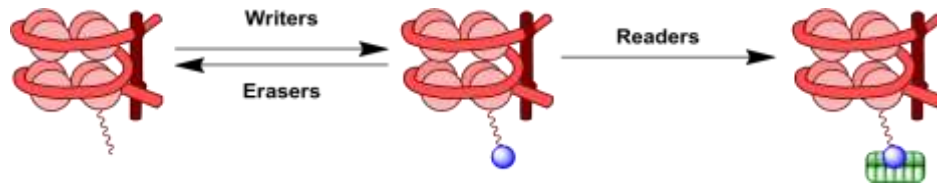


Figure 1.3. The roles of histone-modifying enzymes.

Table 1.1. Protein classes involved in histone post-translational modification.

	Writer	Eraser	Reader
Methylated Lysine	Lysine methyltransferase (KMT)	Lysine demethylase (KDM)	Tudor, MBT and PWWP domains, chromodomains, PHD-containing proteins
Acetylated Lysine	Histone acetyltransferases (HAT)	Histone deacetylase (HDAC)	Bromodomains
Methylated Arginine	Protein arginine methyltransferase (PRMT)	JMJD6, other erasers may exist but are unknown	Tudor domains

Histone Methylation and Demethylation

Methylation of histones is effected by *S*-adenosylmethionine (SAM)-dependant histone methyltransferases, with removal mediated by Jumonji 2-oxoglutarate-dependant demethylases⁴⁷ and lysine-specific histone demethylase 1 and 2. These erasers oxidise the methyl group to the methylene imine, which is then hydrolysed.⁴⁸ Lysine methylation is not a general marker for either the transcription or silencing of genes, and the precise biological effect is dependent on the particular lysine being methylated and whether it is mono-, di-, or tri-methylated. Lysine methyltransferases (KMTs), in particular KMT4 and KMT6, are strongly linked to cancer with KMT inhibitors **1.01** and **1.02** currently in clinical trials (Figure 1.4).^{41,49}

Methylated histones are read by chromodomains and tudor domains, which regulate gene expression and genome organisation.^{50,51}

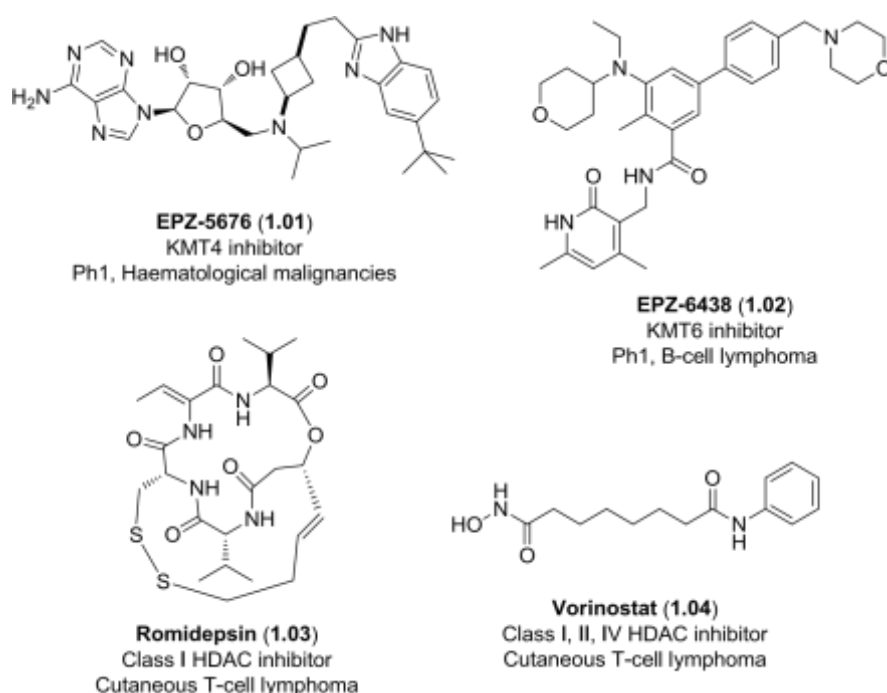


Figure 1.4. Drugs targeting histone-modifying proteins.

Lysine Acetylation and Deacetylation

Lysine acetylation is generally associated with active transcription,⁵² with dynamic acetylation of histones involved in the assembly of nucleosomes during cell division.⁵² Acetylation of lysine residues neutralises their positive charge and reduces the ionic interactions between the histones and the negatively charged phosphate groups of the DNA backbone. This causes the tightly packed heterochromatin, associated with repressed genes, to open up and form transcriptionally active euchromatin.⁵² However, it is thought that this model may be too simplistic and other factors are involved,⁴² such as altering the conformation of the intrinsically disordered and flexible histone tails.⁵³

Molecular dynamics simulations indicate that lysine acetylation has a dramatic effect on H4 conformation, with cumulative acetylation increasing hydrogen-bond contacts and helical propensity.⁵³ Monoacetylation of H4K16 in particular has a unique and dramatic effect, causing a significant structural rearrangement.⁵³ This may bring other acetylation sites into close proximity, creating 'recognition patches' to which transcriptional mediator proteins bind,^{53–55} or alter the accessibility of the nucleosome to transcription factors. Of the four lysines susceptible to acetylation on H4, only mutation of H4K16 resulted in degraded function,⁵⁶ while H4K16Ac plays a prominent role in chromatin compaction and euchromatin expression.⁵²

Lysine acetyltransferases (KATs, or histone acetyltransferases HATs) utilise acetyl CoA as their cofactor. Hyperacetylation of histones affects transcription in a small number of genes, causing repression of nuclear receptor coactivators and expression of tumour suppressors.⁵⁷ Acetyl marks are removed by Class I, II and IV histone deacetylases (HDACs), which contain a Zn²⁺ ion in their active site, and by sirtuins (SIRT, or Class III HDACs) which do not contain Zn and use NAD⁺ as a cofactor. HDAC inhibition causes diverse effects on multiple transcription pathways including anti-apoptotic signalling, disruption of the cell cycle, inhibition of mitosis, and immune modulation.⁵⁸ HDAC inhibitors are of interest as anticancer agents,⁵⁹ with the bacterial natural product romidepsin (**1.03**) and hydroxamic acid vorinostat (**1.04**) approved for the treatment of cutaneous T-cell lymphoma (Figure 1.4). **1.03** acts through *in vivo* cleavage of the disulphide bond to give a thiol which binds to the catalytically active zinc ion.^{60–62} The hydroxamic acid moiety of **1.04** also chelates the zinc ion, leading to a build-up of acetylated histones and other acetylated proteins.^{57,63} Several additional HDAC inhibitors are in clinical trials.^{37,41,63} Acetylated lysine residues are read by bromodomains (Section 1.3).

1.3 Bromodomains

Bromodomains, first identified from the *brahma* gene of *Drosophila* fruit flies in 1992, are a family of reader domains which recognise acetylated lysine (KAc) residues on histone tails.⁶⁴ Bromodomains act as scaffolds for the assembly of macromolecular protein complexes and their recruitment to acetylated nucleosomes, affecting transcription and chromatin remodelling. Bromodomains activate transcription factors, facilitating precise targeting of RNA polymerase II and chromatin-modifying enzymes such as HATs (which often contain reader domains in addition to their catalytic domains) to specific DNA loci.⁶⁵

Bromodomains are 110-amino acid proteins containing four left-handed α -helices (α Z, α A, α B, and α C) (Figure 1.5a) with a well conserved structure between bromodomains and across species, despite significant changes in the amino acid sequence. Two loop regions, BC and ZA, link the helices and contribute to the structure of the binding site and its selectivity (Figure 1.5a). The loops create a hydrophobic pocket in which the KAc residue binds, with a water network at the base of the pocket and binding of the acetyl carbonyl by highly conserved asparagine and tyrosine residues of the BC loop (Figure 1.5b).⁴² The BC loop also contains a 'gatekeeper' residue that varies between bromodomains, providing a hydrophobic interaction that restricts entry to the cavity. Bromodomains are also capable of binding to propionyl-lysine marks, with some able to accommodate larger PTMs such as butyryl- and crotonyl-lysine,⁶⁶ though these are much less abundant than KAc marks.⁶⁷

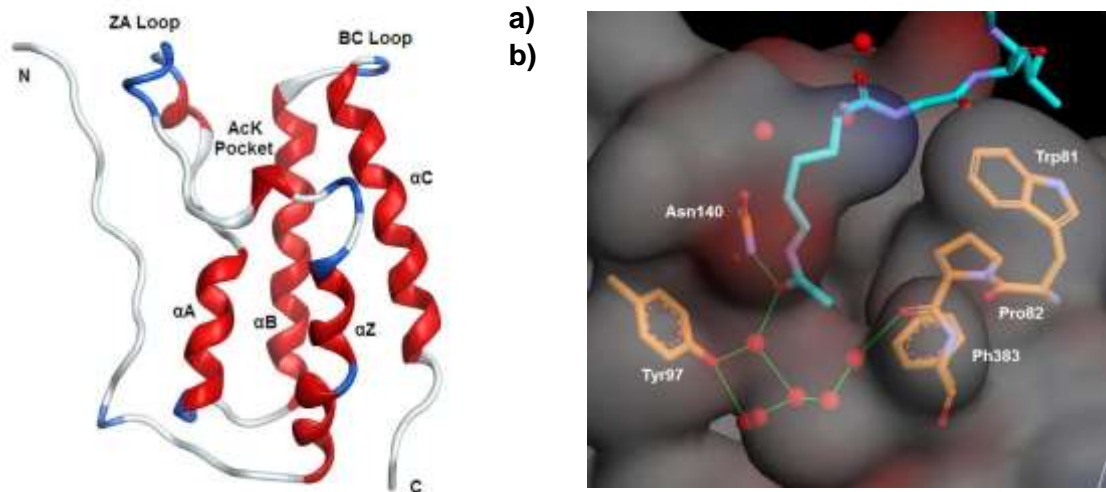


Figure 1.5. **a)** Ribbon diagram of human bromodomain Brd4 BD1 (PDB code: 3MUK). **b)** X-ray crystal structure of human Brd4 BD1 with acetylated lysine (cyan) bound, showing key residues and interactions (PDB code: 2DVQ).⁴² Red balls indicate water molecules and green lines hydrogen bonds.

Variations in bromodomain sequence homology allow the construction of a phylogenetic tree (Figure 1.6), with closely homologous domains occupying closer branches and distinct subfamilies. To date, 46 human proteins have been found to contain one or more bromodomains, with 61 distinct bromodomains identified (Figure 1.6).^{55,65} The biology of bromodomains is a rapidly expanding field, with many bromodomains being only lightly investigated thus far. Due to the early discovery of their ease of inhibition by small molecules (Section 1.4.2), strong phenotype, and clinical relevance (Section 1.4.1) the majority of work has focussed on the bromodomain and extra-terminal domain-containing (BET) family of proteins (Figure 1.6, red branches). However, focus is beginning to shift towards non-BET bromodomains, with several chemical probes developed and phenotypic investigations underway (*vide infra*).

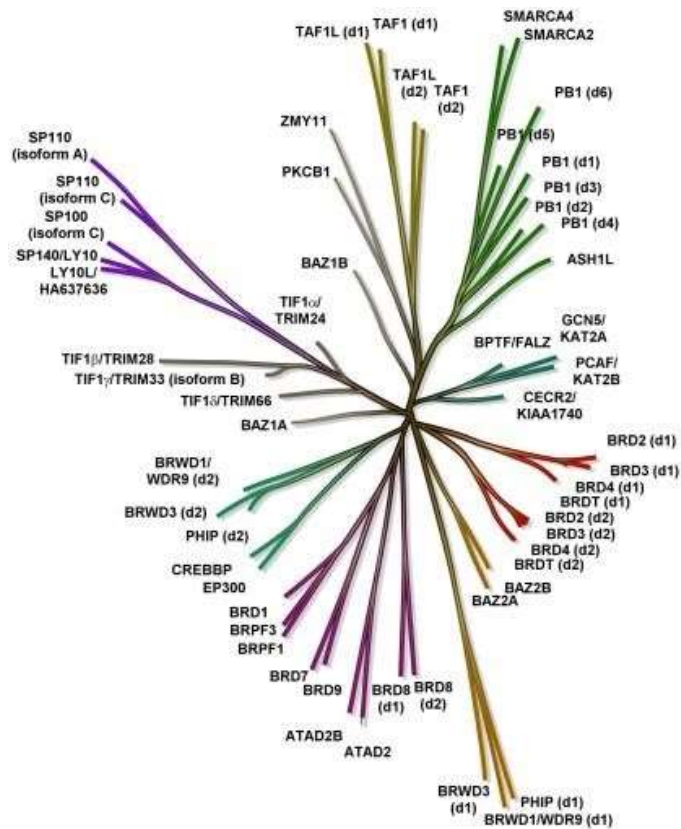


Figure 1.6. Phylogenetic tree showing structural similarities between bromodomains.⁶⁸

1.4 BET Bromodomains

The widely studied BET family consists of four proteins; Brd2, Brd3, Brd4, and BrdT (Figure 1.7). These proteins each contain two bromodomains, BD1 and BD2, together with an extraterminal (ET) domain nearer the C-terminus. Across the BET family, the four BD1 domains show a high degree of structural similarity, as do the four BD2 domains (Figure 1.7).⁶⁵ Motif A and Motif B contain nuclear localisation signals, which enable the protein to be recognised by nuclear transporters for active transport into the cell nucleus.⁶⁹ The well-conserved SEED domain, consisting of serine, aspartic acid, and glutamic acid residues, is found beyond the C-terminal end of the ET domain. Brd4 and BrdT are substantially longer than Brd2 and Brd3 and end with a C-terminal domain (CTD) which assists in maintaining the higher order structure of chromatin. The CTD binds positive transcription elongation factor B (P-TEFb), a kinase which activates RNA polymerase II (Pol II) to induce RNA transcription of the DNA strand bound to the histone.⁷⁰ The ET domain is also responsible for transcriptional regulation but is independent of P-TEFb, interacting with multiple transcription proteins and causing transcriptional activation.⁷¹

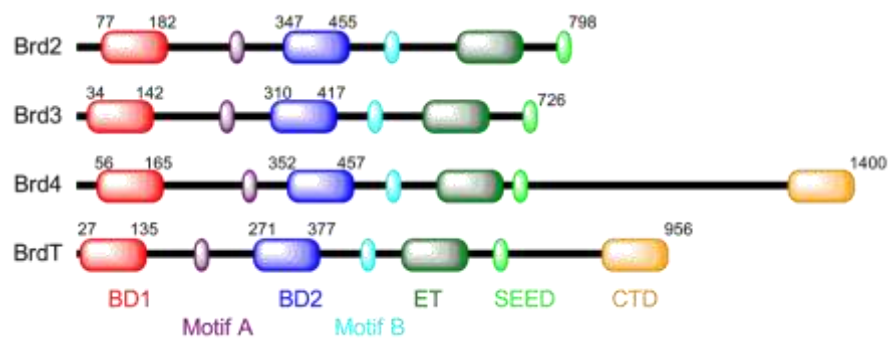


Figure 1.7. Schematic structure of human BET proteins, domain positions are not to scale.^{69,70}

BET proteins are vital for cell cycle function, with Brd4 directly required for the onset of mitosis⁷² and BET knockout or mutation causing death or severe defects across several species.⁶⁵ In addition to key biological roles in autoimmune responses, reproduction and metabolic processes (Section 1.4.1), Brd4 has been shown to be widely expressed in the brain and regulates the transcriptional processes involved in learning and memory. BET knockout or inhibition with the small-molecule BET inhibitor JQ1 (**1.05**, see Section 1.6.1) impaired memory consolidation, but also reduced susceptibility to seizures.⁷³ The role of BET proteins in several disease areas have been probed through gene knockout studies or small molecule inhibition (See Section 1.4.2 for details of specific small molecule BET inhibitors), producing strong disease rationales.

1.4.1 BET Proteins in Disease

Oncology

Studies of the rare but lethal cancer NUT (nuclear protein *in testis*) midline carcinoma (NMC) discovered a translocation of the NUT protein and Brd4, which fuse to form a Brd4-NUT oncogene. Knockdown studies confirmed that Brd4 attaches NUT to transcriptionally active chromatin and this association is instrumental in maintaining the tumour cells.⁷⁴ When dosed to patient-derived NMC tumour cells, **1.05** caused rapid differentiation, growth arrest and apoptosis. **1.05** also proved able to inhibit tumour growth and dramatically increased survival rates in NMC xenograft models in mice (Figure 1.8), with the compound being well tolerated throughout the trial.⁷⁵ The discovery of a direct link between Brd4 and NMC sparked significant interest into the BET family throughout the oncology field. BET bromodomain inhibition has been indicated as a potential therapy in a wide range of cancers, including Burkitt's lymphoma,⁷⁶ acute myeloid leukaemia,^{77,78} mixed lineage leukemia,⁷⁹ ovarian cancer,⁸⁰ prostate cancer,⁸¹ medulloblastoma,⁸² glioblastoma⁸³ and neuroblastoma.⁸⁴ Several

small-molecule BET inhibitors (Section 1.4.2) have entered human clinical trials in oncology.^{85–}

90

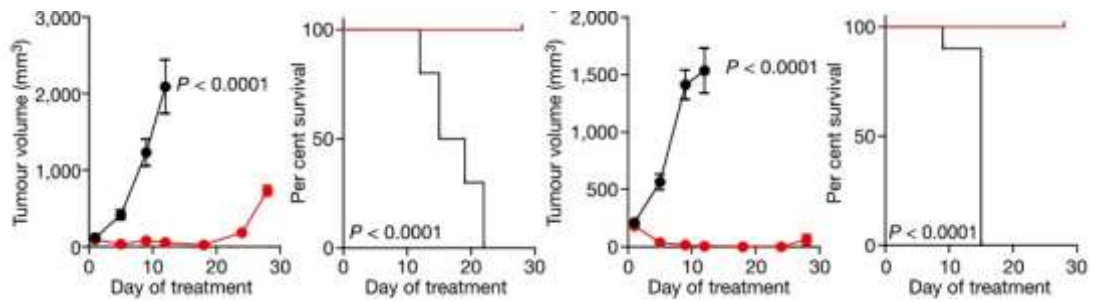


Figure 1.8. Tumour volumes and survival rates in mouse NMC xenograft models, using patient-derived 11060 (left) and Per403 (right) cell lines, treated with vehicle (black) or JQ1 (red).⁷⁵ Reproduced with permission from *Nature* **2010**, 468, 1067-1073.

The antitumor activity of BET inhibition is theorised to be partly, if not completely, due to suppression of the oncogene cMyc.^{76,77,91} Brd4, in combination with other transcriptional mediators, is recruited to enhancer regions of DNA to activate nearby genes. While the presence of Brd4-recruiting enhancers is ubiquitous, certain oncogenes, including cMyc, are activated by super-enhancer regions which are larger than normal enhancers and recruit significantly more Brd4.^{92,93} Treatment with **1.05** caused a disproportionate decrease in transcription for super-enhancer genes compared to typical enhancers.⁹² This may explain the relatively small number of genes affected by BET inhibitors and their generally good tolerability, despite the ubiquitous expression of Brd4. However, BET inhibition was also effective against primary effusion lymphoma (PEL), a non-Hodgkin's B-cell lymphoma where cMyc is not influenced by super-enhancers and is only modestly overexpressed.⁹⁴

Among the proteins recruited by Brd4 is the condensin II chromatin remodelling complex, which compacts the chromatin structure, reduces the effectiveness of the DNA damage response and was found to reduce cell survival following irradiation.⁹⁵ The inhibition of damage response signalling provides another possible mechanism for the antiproliferative effects of BET inhibitors. However, treatment of some cancer cell lines with small-molecule BET inhibitors has been reported to cause upregulation of BET proteins and their accumulation in cells.^{96,97} This may be due to feedback loops in which BET proteins inhibit their own production, allowing oncogenes to rebound quickly when treatment is withdrawn and reducing the therapeutic effect of the inhibitor.⁷⁶ Leukemia cells are able to develop resistance to BET inhibition, through increased recruitment of Wnt/ β -catenin signalling pathway proteins to cMyc.^{98,99}

Autoimmune Inflammation

When bone marrow-derived macrophages were stimulated with the bacterial endotoxin lipopolysaccharide (LPS), BET inhibition with another small-molecule inhibitor, I-BET762 (**1.06**), reduced the expression of multiple pro-inflammatory cytokines and chemokines (small signalling proteins, often involved in immune responses). Transcription factors involved in the initial expression of genes during an inflammatory immune response were also suppressed.¹⁰⁰ Prophylactic and therapeutic small-molecule BET inhibition also proved highly effective in increasing survival rates in murine models of endotoxic shock,¹⁰¹ severe sepsis,¹⁰⁰ and peritonitis.¹⁰⁰ Unaltered levels of tumour necrosis factor (TNF) cytokines, which mediate the inflammatory response to sepsis, suggests that this effect is not due to TNF downregulation but rather disruption of TNF-induced production of cytokines and chemokines.¹⁰⁰ However, parallel studies using an alternative inhibitor found that TNF- α levels were reduced both *in vitro* and in similarly performed *in vivo* models.¹⁰¹

Exposure of naïve T-cells to antigens causes them to differentiate into T-helper (T_H) cells, which produce cytokines – often generating a positive feedback loop (Figure 1.9). BET inhibition with **1.06** was shown to have an inhibitory effect on the production of proinflammatory cytokines IL-17 and GM-CSF (granulocyte-macrophage colony stimulating factor) when administered to naïve T-cells before differentiation.¹⁰² Anti-inflammatory gene products were also upregulated and transfer of the differentiated T-cells into mice led to decreased recruitment of inflammatory T-cells to the central nervous system. No effect was seen on T-cells that had already differentiated. These effects were mimicked by inhibition of cMyc, indicating this oncogene also plays a role in inflammation and may be responsible for a portion of this anti-inflammatory phenotype.¹⁰²

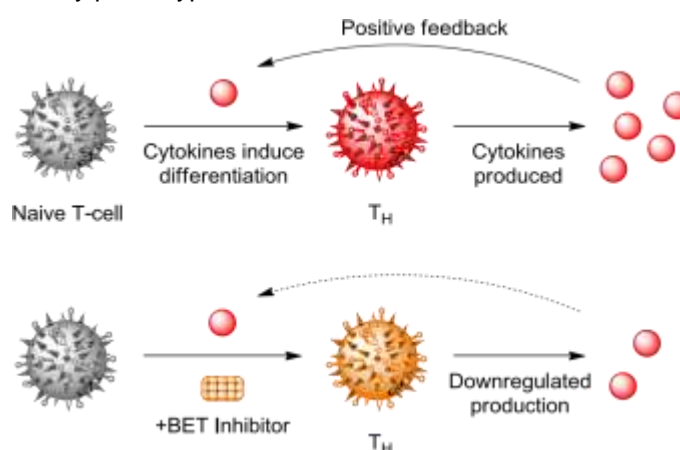


Figure 1.9. Effect of BET inhibitors on T-cell cytokine production.

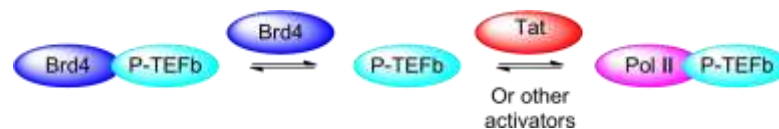
Osteoclast cells, which reabsorb bone, are overexpressed in rheumatoid arthritis where their differentiation is promoted by Myc, GM-CSF and the TNF-family cytokine RANKL. BET

inhibition with I-BET151 (**1.11**) suppressed osteoclast differentiation *in vitro* and *in vivo* while also reducing arthritic inflammation and strengthening bones. The action of **1.11** is believed to be through Myc suppression, which downregulates production of the master osteoclast regulator NFATC1.¹⁰³ BRD2, BRD3 and BRD4 have been detected in fibroblasts and macrophages in rheumatoid arthritis (RA) synovial tissue. Bromodomain inhibition with **1.11** again suppressed inflammatory gene products such as MMP1, CXCL10 and CXCL11, downregulating the majority of genes induced by TNF- α and IL-1 β .¹⁰⁴

In LPS-stimulated human monocytes, the BET inhibitor **1.11** was able to suppress the transcription and expression of cytokines CXCL10 and CXCL11. When stimulated with IFN γ , **1.11** inhibited proinflammatory transcription in a gene specific-manner which was independent of Myc inhibition,¹⁰⁵ indicating alternative autoimmune pathways may be operating. Overall, BET inhibitors show significant promise as anti-inflammatory agents.

HIV Reactivation

The binding of P-TEFb by Brd4 and the role of the resulting complex in transcriptional regulation makes BET inhibition an attractive target for the reactivation of human immunodeficiency virus (HIV) from latency. While active HIV is effectively treated with antiviral medication, reservoirs of inactive virions in CD4+T cells remain unaffected and reinfect the patient once the course of treatment ends. A therapy is sought that is capable of reactivating this latent virus in order to fully eliminate it from the body. The viral activator Tat recruits P-TEFb to Pol II to promote HIV transcription, however Brd4 and Tat compete to bind P-TEFb, preventing activation of the HIV transcription complex.¹⁰⁶ It is theorised that Brd4 inhibition will increase Tat-P-TEFb binding and hence recruitment of P-TEFb to HIV, increasing transcription (Figure 1.10).



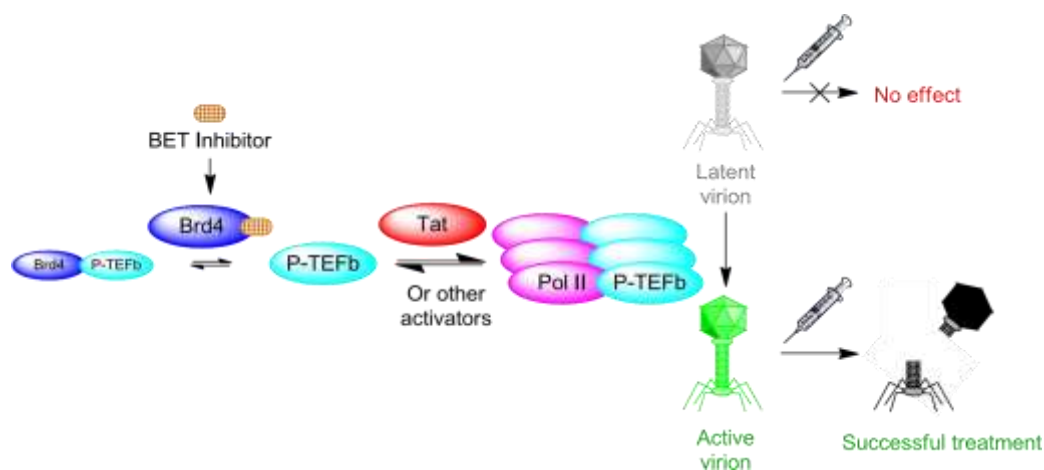


Figure 1.10. Schematic of the relationship between Brd4, P-TEFb and HIV reactivation.

Knockdown of BET or treatment of HIV-infected T-cells and monocytes with **1.05** significantly activated HIV from latency across multiple cell types.^{107–109} **1.05** showed low cytotoxicity in these models, but does suppress T-cell proliferation.¹⁰⁷ While HIV reactivation is dependent on P-TEFb, use of cell lines that lack the Tat gene had no effect on the results, showing that reactivation can proceed by Tat-independent mechanisms. However, specific knockdown of Brd2, which is also inhibited by JQ1, was effective in reactivating HIV.¹⁰⁹ Brd2 lacks a CTD and so cannot bind P-TEFb, as such the mechanism of Brd2-mediated HIV reactivation is currently unknown. It is theorised that Brd2 mediates recruitment of repressor complexes to the latent HIV activator complex, though how this involves P-TEFb is unclear.¹⁰⁹

Male Fertility

All BET proteins are required for spermatogenesis, with the expression levels of each of the four BET proteins highly dependent on the level of spermatozoa development.⁷⁰ BrdT, which is only found in the testes and ovaries,¹¹⁰ is particularly essential. Human BrdT BD1 mutation is linked to male infertility,¹¹¹ while knockout causes failures in sperm elongation and the development of structural deformities.⁷⁰ Studies in *Drosophila* have identified two novel testes-specific BET proteins, tBrd-2 and tBrd-3, which only contain a single bromodomain and may form acetylation-dependant complexes.¹¹²

The vital role of BrdT in fertility has led to suggestions that a pan-BET or BrdT inhibitor could perform a contraceptive role. In mice, small molecule BET inhibition reduced testis size, sperm count and quality, with almost complete reversibility observed 4 months after dosing was halted. Hormone levels or behaviour were not affected, and offspring born after withdrawal and recovery showed no adverse effects.¹¹³ However, the strong systemic phenotypes of pan-BET inhibitors would likely lead to side effects that prevent human contraceptive use.

Cardiovascular Disease

Several BET inhibitors have been shown to upregulate apolipoprotein A1 (ApoA1),^{100,114–117} a major component of high density lipoprotein (HDL) cholesterol. ApoA1 raises HDL levels, with increased HDL strongly linked to decreased risk of atherosclerosis.¹¹⁸ The mechanism by which BET inhibitors affect ApoA1 is unknown. In particular, RVX-208/apabetalone (**1.20**) has undergone several clinical trials in cardiovascular disease,^{119–122} being shown to increase ApoA1 and HDL levels in humans.^{123–125} The incidence of major adverse cardiac events was reduced, with improved responses in patients with higher systemic inflammation.¹²⁵ This suggests that the anti-inflammatory effect of BET inhibition may play a significant role. However, when progressed to Phase II trials, **1.20** failed to show statistically significant ApoA1 or HDL induction compared to placebo, with no significant regression of atherosclerosis.¹²⁶ The implications of this result for the role of BET proteins in cardiovascular disease are unclear, particularly as **1.20** was discovered through phenotypic screening and has only moderate BET potency, biased towards the four BD2 domains.^{117,127}

1.4.2 Small Molecule BET Inhibitors

The discovery of the significant role of the BET proteins in several diseases has led several academic groups and pharmaceutical companies to investigate inhibition of BET function. While many epigenetic targets have been considered undruggable, the deep and welldefined KAc binding pockets of the BET family have enabled effective small-molecule BET inhibition with a wide variety of chemotypes (Figure 1.11). All feature a KAc mimetic which forms the same key interactions as the native peptide, and often includes a lipophilic group to mimic an acetyl CH₃.

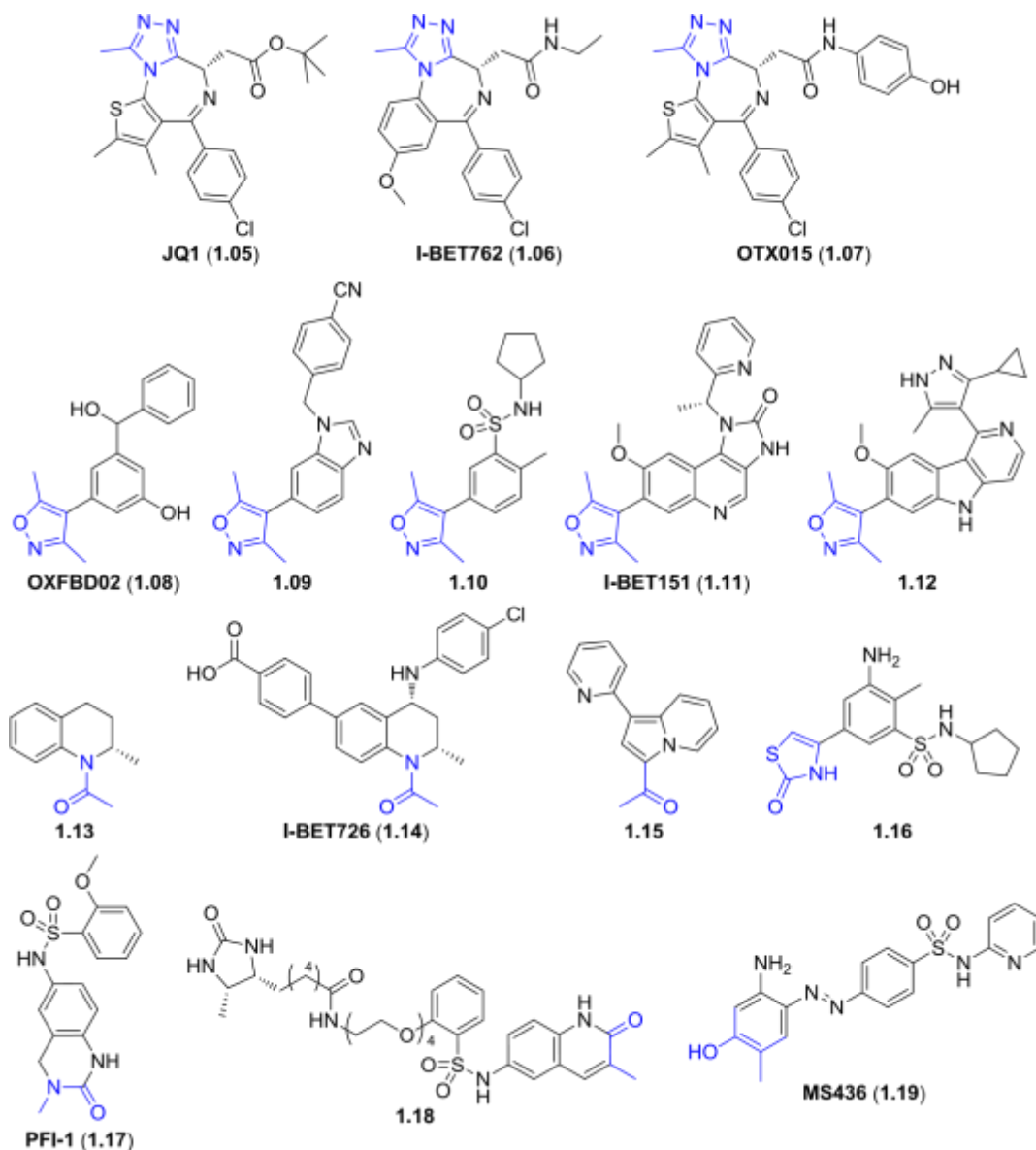


Figure 1.11. Selected BET inhibitors. The KAc mimetics are highlighted blue.

Triazolodiazepines

Several groups have reported triazolo-1,4-diazepines as BET inhibitors (Figure 1.11). Starting from a Mitsubishi-Tanabe patent which disclosed triazolo-1,4-diazepines as BET inhibitors, the University of Oxford and Harvard Medical School developed the freely available chemical probe JQ1 (**1.05**), which is highly potent and selective for the BET family.⁷⁵ GSK carried out phenotypic screening for upregulators of apolipoprotein A1 (ApoA1) as a potential therapy for atherosclerosis,¹¹⁸ identifying I-BET762 (**1.06**). Subsequent chemoproteomics showed that **1.06** was a potent and selective BET bromodomain inhibitor.^{100,128,129} Clinical trials of **1.06** in NMC, solid tumour cancers and haematological malignancies are currently underway.^{85,90}

Mitsubishi-Tanabe and OncoEthix have themselves developed OTX015 (**1.07**), also undergoing clinical trials in oncology,⁸⁶⁻⁸⁸ with **1.07** reported to show antiproliferative and apoptotic activity in B-cell lymphoma cell lines.¹³⁰ In addition, the BET inhibitor CPI-0610 (structure not yet disclosed) has entered trials for the treatment of lymphoma.⁸⁹

The binding mode of the triazolodiazepine scaffold is exemplified by **1.06**, shown bound to Brd4 BD1 in Figure 1.12. The triazole ring acts as the KAc mimetic, forming a hydrogen bond with the Asn140 residue and binding through the conserved water network to Tyr97. BET bromodomains contain a lipophilic region known as the WPF shelf, named after the tryptophan-proline-phenylalanine stack which neighbours it.¹³¹ The WPF shelf has been shown to increase the binding affinity of a diacetylated H4 histone, with the second KAc residue and the histone tail lying across this region.⁵⁴ The chlorobenzene group also binds to the WPF shelf and the Ile146 gatekeeper through π -stacking and hydrophobic interactions, while the methoxyphenyl groups extends through the narrow lipophilic ZA channel on the other side of the WPF stack.^{75,100,128,129} The bulky ester (**1.05**) and amide (**1.06**) functionalities prevent binding to benzodiazepine receptors and the resulting psychoactive effects; only the (S)-enantiomers have significant BET activity.⁷⁵ In the case of **1.06**, the amide is also capable of hydrogen bonding to Asn140.¹⁰⁰

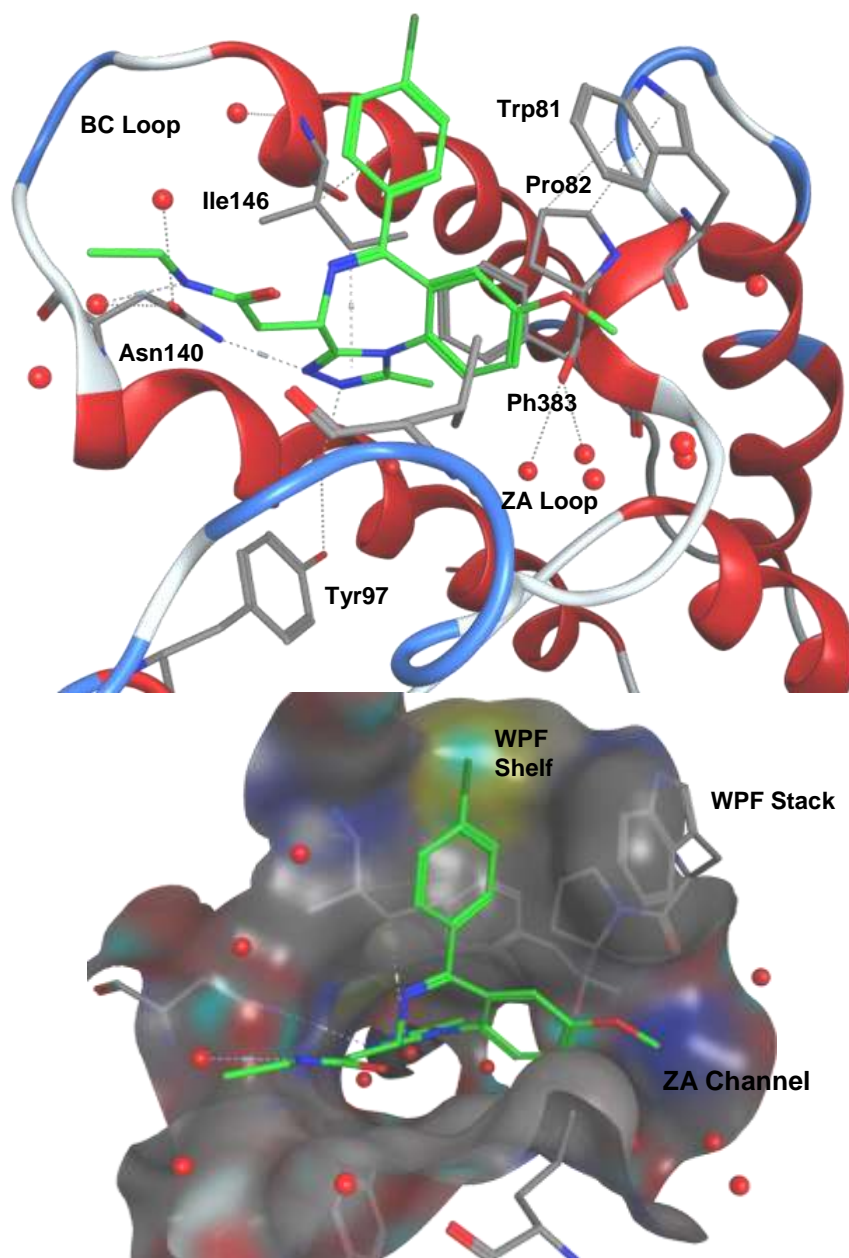


Figure 1.12. X-ray crystal structure of I-BET762 (**1.06**) bound to Brd4 BD1. PDB: 3P5O.¹⁰⁰

Dimethylisoxazoles

Several groups have independently discovered the 3,5-dimethylisoxazole moiety to be a suitable KAc mimetic. Observations that the solvent *N*-methyl-2-pyrrolidinone (NMP) bound weakly to KAc binding pockets led to a study of methylated heterocycles as BET inhibitors, culminating in the discovery of potent dimethylisoxazole-based ligand **1.08** (Figure 1.11), which was active in an isolated AML cell line.^{132–134} Both the nitrogen and oxygen of the isoxazole contribute to KAc mimetic binding, with the methyl groups occupying small lipophilic pockets. The secondary alcohol of **1.08** interacts with a water network on the outside edge of

the pocket, and the WPF shelf is occupied by the phenyl group (Figure 1.13a). Though almost inactive at most other bromodomains, **1.08** showed only 2-7 fold selectivity over the closely homologous cAMP response element binding protein (CREB) binding protein (CREBBP) bromodomain.¹³⁴ Combining an alternative benzimidazole core with the dimethylisoxazole KAc mimetic to give **1.09** increased Brd4 potency and achieved 100-fold selectivity over CREBBP.¹³⁵

The dimethylisoxazole moiety has also been utilised by GSK, with a fragment-based approach affording **1.10**, which utilises a sulphonamide linker to place a cyclopentyl group on the WPF shelf.¹³⁶ This KAc mimetic was also used in the development of I-BET151 (**1.11**), which showed good potency against Brd2-4 and excellent selectivity over other bromodomains.^{115,137} A water molecule bound to Gln101 solvates the quinoline nitrogen and contributes further binding, while the pyridine sits on the WPF shelf and the quinoline ring is bound by the ZA channel (Figure 1.13b). I-BET151 showed similar therapeutic effects to I-BET762 (**1.06**) in mouse models of LPS-induced endotoxicity and caused cell cycle arrest and apoptosis in models of mouse and human leukaemia.⁷⁹ Modification of the tricyclic core of **1.11** gave the carboline **1.12**, which bound in a similar manner but showed improved activity relative to **1.11** in acute leukaemia cell lines.¹³⁸

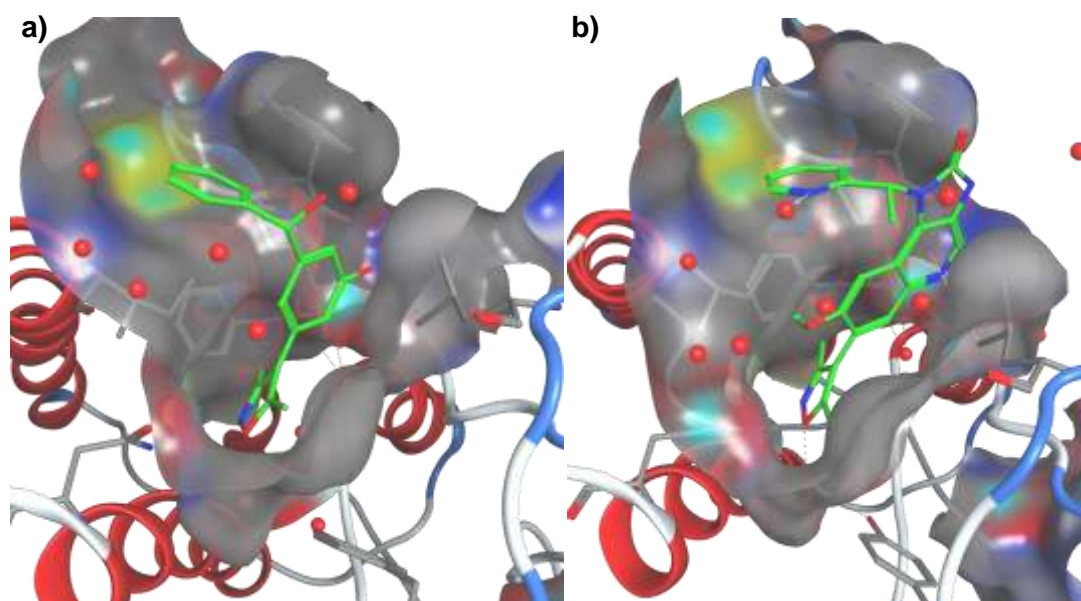


Figure 1.13. a) X-ray crystal structure of **1.08** bound to Brd4 BD1 (PDB 3SVG).¹³³ b) X-ray crystal structure of I-BET151 (**1.11**) bound to Brd2 BD1 (PDB: 4ALG).¹³⁷

Tetrahydroquinolines

A fragment screen carried out within GSK by Chung *et al.* identified several promising fragments which bound to the BET bromodomain, including the highly efficient

tetrahydroquinoline **1.13**.¹³⁹ The acetyl group acts as the KAc mimetic, with the ring system occupying the lipophilic areas of the binding pocket. The C2 methyl group enters a small lipophilic pocket, with only the (*S*)-enantiomer binding.¹³⁹ Subsequent screening of a series of tetrahydroquinoline ApoA1 up-regulators, which like **1.06** had been optimised using phenotypic screening without knowing their molecular target, identified them as BET inhibitors.¹¹⁴ The lead compound, I-BET726 (**1.14**), bound similarly to **1.13** with only the (*2S,4R*)-enantiomer displaying significant activity (Figure 1.14). The WPF shelf was tolerant of most substitutions, with *para*-chloro displaying a good balance of potency and physicochemical properties. The 6-position of the core projects through the ZA channel, and it was found that phenyl 6-substituents had increased potency due to lipophilic contact with the ZA loop and edge-to-face π -interactions with Trp81 of the WPF stack. The placement of polar groups at the *para* position of this ring was beneficial for both potency and solubility. In addition to potent ApoA1 activity, **1.14** successfully reduced the secretion of the proinflammatory cytokine IL-6 in human macrophages and whole blood, and like **1.06** showed therapeutic efficacy in a LPS-induced murine sepsis model.¹¹⁴

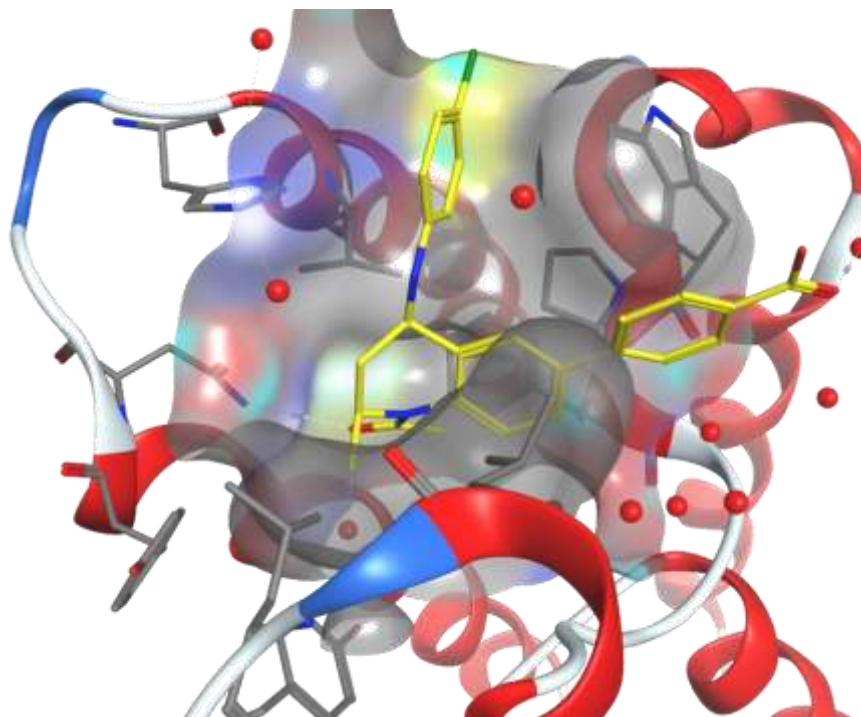


Figure 1.14. X-ray crystal structure of I-BET726 (**1.14**) bound to Brd2 BD2 (PDB 4UYG).¹¹⁴

Other Chemotypes

The fragment screen which discovered THQ **1.13** also identified indolizine **1.15**, again binding through the acetyl group with the pyridyl group packing against the WPF stack.¹³⁹ Other members of this series have been optimised into inhibitors of non-BET bromodomains (See

Sections 1.5.2 and 1.5.5). Thiazolidinones have also been utilised as KAc mimetics, despite not occupying the lipophilic warhead pocket as seen for most other inhibitors.

Discovered through an *in silico* fragment docking study, the thiazolidinone fragment was optimised to afford structurally diverse BET inhibitors, including **1.16**, which showed antiproliferative activity in HT-29, MV4-11 and MM-1S cancer cell lines.^{140,141}

A fragment-based approach was also utilised by Pfizer in the development of the methyl quinazolinone PFI-1 (**1.17**).^{142,143} The reverse sulphonamide creates a turn that allows the aryl group to access the WPF shelf, with electron-rich aryls favoured and methoxyphenyl **1.17** selected for further development on the basis of physicochemical properties and potency. PFI-1 showed anti-proliferative and apoptotic effects on leukaemia cell lines, with cMyc expression being downregulated.¹⁴³ However, **1.17** is susceptible to oxidative insertion of nucleophilic solvents^{142,144} and in the design of the *des*-thiobiotinylated analogue **1.18** an alternative quinolinone core was used. **1.18** is capable of being captured by streptavidin beads, and underwent chemoproteomic profiling which showed **1.18** to bind endogenous BET proteins in THP-1 cells.¹⁴⁴

Zhou *et al.* have developed a series of diazobenzene-based BET inhibitors with a novel *ortho*-methyl phenol as the KAc mimetic, exemplified by MS436 (**1.19**).¹⁴⁵ The rigid diazobenzene spacer interacts with the water network at the base of the pocket, while the second aromatic ring occupies the ZA channel and forms edge-to-face interactions with the WPF Trp. In contrast to the frequent occupation of the WPF shelf by BET inhibitors, the sulphonamide instead allows the pyridine ring to sit on top of the WPF stack and form π stacking interactions with the WPF Trp.¹⁴⁵

1.4.3 Domain-Selective BET Inhibitors

The majority of the BET inhibitors disclosed thus far show little or no selectivity between the four BET proteins or the BD1 and BD2 domains, and are referred to as pan-BET inhibitors (Figure 1.15). The development of more selective BET inhibitors is a logical next step in this field, to help fully elucidate the biological roles of BET proteins and potentially offer clinical advantages over pan-BET inhibitors in terms of safety, efficacy or disease scope.

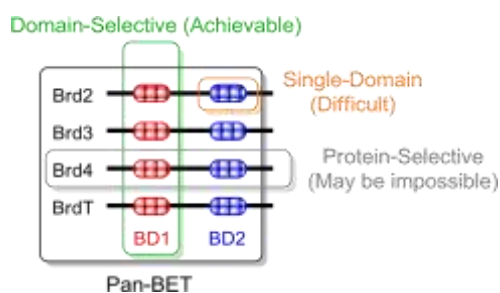


Figure 1.15. Nomenclature and predicted druggability of selective BET inhibitors.

The bromodomain sequence homology of the four dual-Brd BET proteins is very high, with the four BD1 and four BD2 domains showing closer homology than between BD1 and BD2 domains on each protein.⁶⁵ This will likely prevent the design of protein selective BET inhibitors, and make single-domain inhibitors extremely challenging to develop (Figure 1.15). However, significant differences exist between the BD1 and BD2 domains which allow selectivity to be obtained. Comparison of X-ray apo structures for the Brd4 BD1 and BD2 KAc binding pockets (Figure 1.16), shows that for the majority of the binding site the proteins are essentially identical. The ‘gatekeeper’ residue which restricts access to the WPF shelf is Ile in BD1 and Val in BD2, with a Lys/Gln switch at the base of the ZA channel. The greatest differences lie in the BC loop, with an Asp in BD1 exchanged for a His in BD2 and an Asp/Glu switch of the adjacent residue. This concentration of differences in one location close to the binding pocket is advantageous for the design of domain-selective inhibitors.

Brd4 BD1/Brd4 BD2

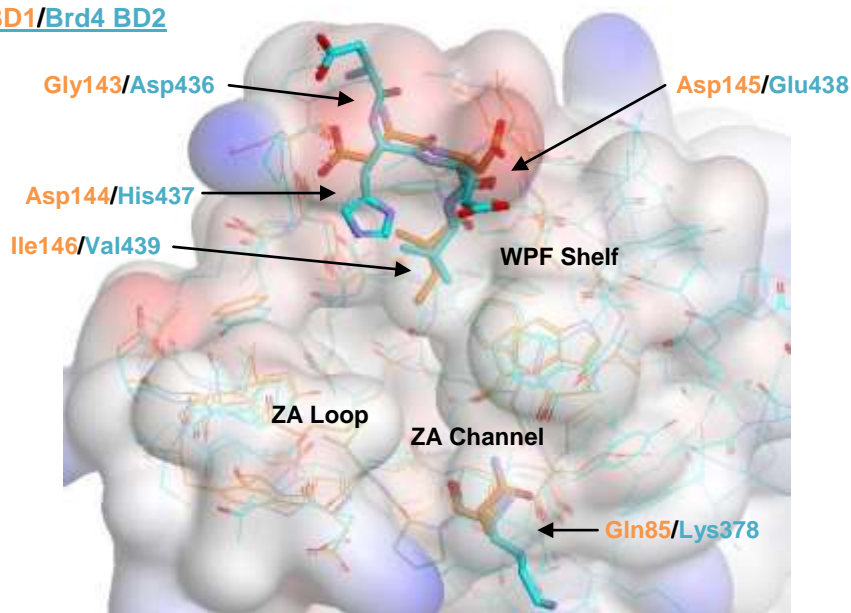


Figure 1.16. Comparison of the BRD4 BD1 (orange, PDB: 2OSS) and BD2 (cyan, PDB: 2DWW) X-ray apo structures, showing the BD1 surface. Water molecules are omitted for clarity. Differing residues are shown in bold.

From Figure 1.16, several potential strategies for domain selectivity can be formulated. The base of the binding pocket is smaller in BD1 due to the differing gatekeepers, and as such inhibitors with smaller cores are expected to exhibit BD1-bias due to increased lipophilic contacts. Larger molecules may clash with the extra methyl group in BD1, and so be BD2-biased. The BD2-specific histidine is the most significant difference, and may be critical for gaining BD2 selectivity either through ionic interactions, hydrogen bonding or π -

interactions. BD1 selectivity may be gained by placing a large enough group onto the WPF shelf that it clashes with the His and Glu in BD2.

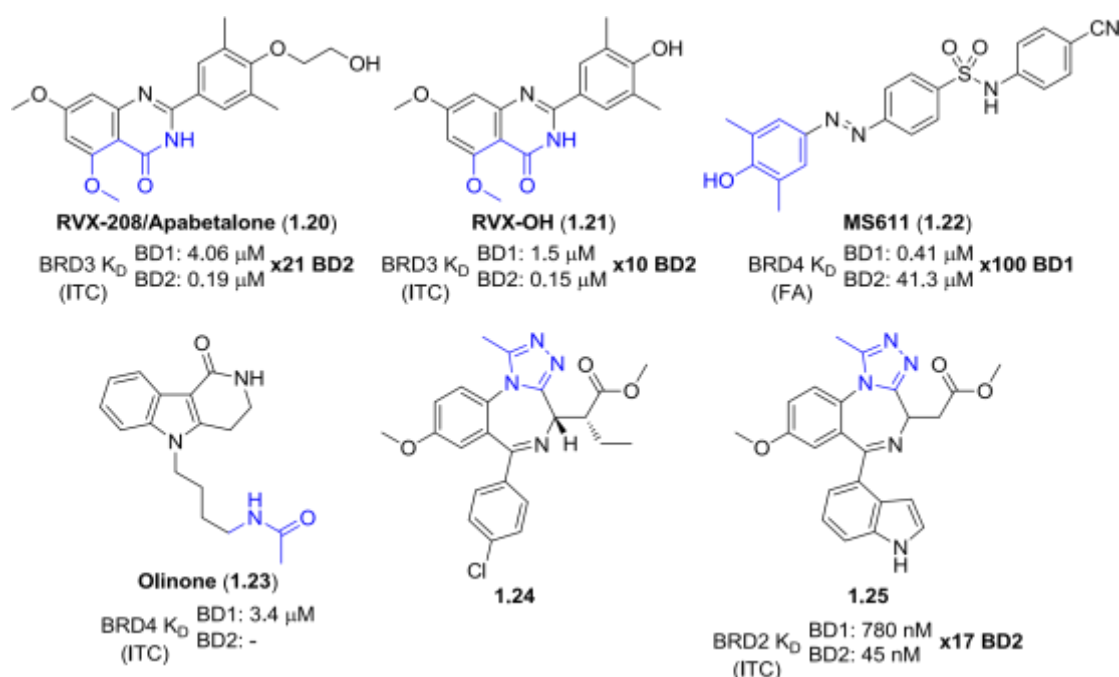


Figure 1.17. Reported domain-selective BET inhibitors.

Several reported inhibitors utilise these differences to gain selectivity (Figure 1.17). RVX-208/apabetalone (**1.20**, Figure 1.17) is currently in clinical trials for cardiovascular disease (Section 1.4.1). **1.20** was discovered through a phenotypic screen measuring ApoA1 upregulation and later shown to be an inhibitor of BET bromodomains with selectivity for BD2.^{117,127} Brd3 BD2 selectivity for this compound was measured at 170-fold (AlphaScreen) and 20-fold (ITC), with lesser selectivity and weaker binding to other members of the BET family. The differences in selectivity between assays were attributed to differences in peptide affinity for the two domains.¹²⁷ The molecular basis of selectivity is hypothesised to be packing of the BD2-specific His against the dimethylphenol ring (Figure 1.18).

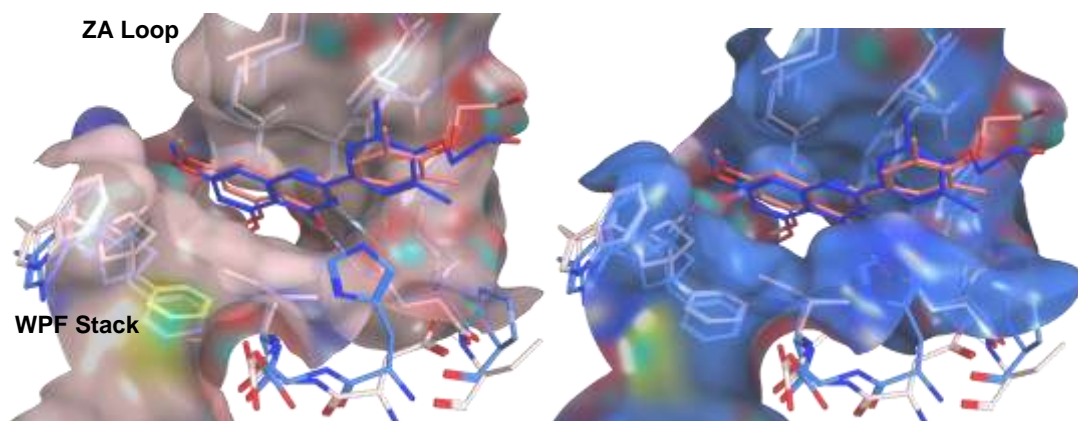


Figure 1.18. RVX-208 (**1.20**) bound to Brd4 BD1 (pink, PBD: 4MR4) overlaid with **1.20** bound to Brd2 BD2 (blue, PBD: 4MR6) showing the BD1 surface (left) and BD2 surface (right). Solvent is omitted for clarity.

Interestingly, the related compound RVX-OH (**1.21**), which lacks the hydroxyethyl moiety, showed much reduced selectivity. In BD1 **1.21** adopts an alternative binding mode, with the free phenol group acting as the KAc mimetic. RVX-208 **1.20** was only able to weakly displace chromatin from Brd3, and in a HepG2 cell line only affected the expression of 46 genes compared to 754 when the pan-BET inhibitor **1.05** was used. BD2 inhibition was not sufficient to produce a strong transcriptional response compared to pan-BET in a subset of these genes.¹²⁷ **1.20** also had no effect on oligodendrocyte progenitor differentiation, in contrast to the pan-BET phenotype where differentiation was inhibited.¹⁴⁶

The altered binding mode of RVX-OH **1.21** was exploited to develop MS611 (**1.22**),¹⁴⁶ like **1.19** a member of the diazobenzene family of BET inhibitors,¹⁴⁵ which exhibits ~100-fold selectivity for Brd4 BD1. Interestingly, this compound is significantly less selective at Brd2 and unselective at Brd3. The histidine clashing strategy was utilised to develop Olinone (**1.23**), the tricyclic system of which occupies the whole of the larger BD1 WPF shelf with a pendant KAc mimetic to bind to the Asn. Occupying the location of the BD2-specific His produced a compound with no detectable affinity for BD2. BD1 inhibition with **1.22** promoted oligodendrocyte progenitor differentiation, while pan-BET inhibitors inhibited it.¹⁴⁶

Ciulli *et al.* used an alternative 'bump-and-hole' strategy to investigate the roles of individual domains.¹⁴⁷ Mutating a leucine residue in the KAc binding site to alanine created an artificial lipophilic binding cavity, which could be occupied with high affinity by **1.24**, an alkylated variant of I-BET762 (**1.06**). **1.06** did not bind to the mutant Brd and the altered compound **1.24** was significantly less potent towards wild-type BET. The mutant Brd gene could be spliced into cells as either the BD1 or BD2 domain without loss of function, therefore allowing selective inhibition of either domain using **1.24** and showing that blockade of BD1 alone is able to prevent the binding of chromatin to Brd4.¹⁴⁷ During the development of **1.24**, it was observed that the indole **1.25** displayed moderate wild-type BD2 selectivity at Brd2, though this was reduced to ~10-fold at Brd4. The increased domain selectivity was attributed to improved edge-to-face π -stacking with the BD2-specific His.¹⁴⁸

1.4.4 Dual Kinase-Bromodomain Inhibitors

Several historical kinase inhibitors have subsequently shown activity against the bromodomain family. This is perhaps unsurprising, given the ability of bromodomains to bind

a variety of chemotypes and the absence of bromodomain-containing proteins from crossscreening panels at the time of their development. In addition, the N-terminal region of Brd4 contains several kinase-like motifs and the protein has been shown to act as an atypical kinase, selectively phosphorylating RNA Pol II.¹⁴⁹ Kinase-bromodomain inhibitors may derive some of their efficacy from disrupting this function in addition to their primary kinase inhibitory activity, and dual inhibitors may offer benefits over single target inhibitors.¹⁵⁰ The serendipitous kinase inhibitor hits contain interesting SAR and novel KAc mimetics, which can benefit the design of bromodomain inhibitors (Figure 1.19).

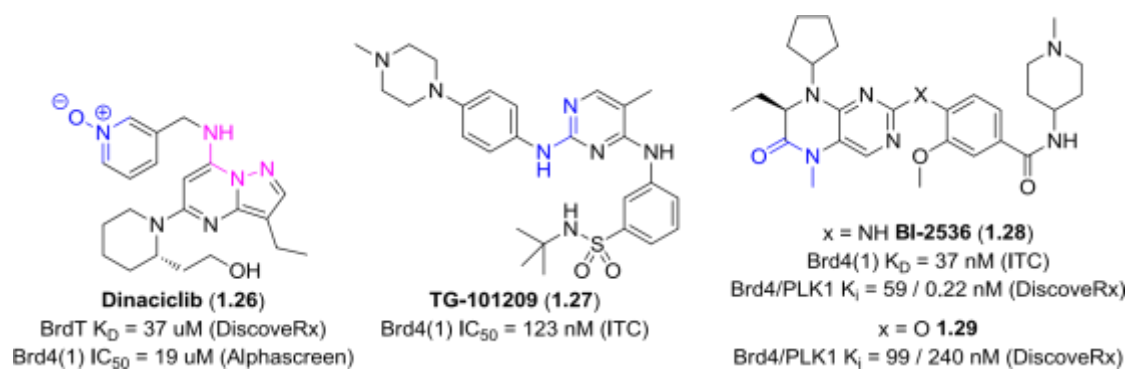


Figure 1.19. Structures and BET biochemical potencies of reported dual kinase-bromodomain inhibitors. For Dinaciclib, the alternative KAc mimetic observed for Brd4 is highlighted pink.

The cyclin-dependant kinase (CDK) inhibitor Dinaciclib **1.26**, currently in Phase III clinical trials for lymphocytic leukaemia, was shown to bind to BrdT by X-ray crystallography, though with relatively low potency. The pyridine *N*-oxide (blue) acts as the KAc mimetic, with the piperidine occupying the WPF shelf and the hinge binder forming hydrogen bonds to residues of the ZA loop.¹⁵¹ Interestingly, when crystallised in Brd4 a change in binding mode was observed, with the kinase hinge binding motif (pink) instead binding to the conserved Asn.¹⁵² This binding mode was also seen for TG-101209 (**1.27**), one of a series of structurally similar Janus kinase (JAK) inhibitors with BET activity.^{150,152} The piperazine packs against the ZA loop, while the *tert*-Bu group occupies the WPF shelf. **1.27** was also selective for the BET family over other bromodomains, and intriguingly showed bias for BrdT BD1 within the BET bromodomains.¹⁵²

Polo-like kinase 1 (PLK1) inhibitor BI-2536 (**1.28**) has been shown to be a highly potent BETselective bromodomain inhibitor,^{150,152,153} capable of suppressing c-Myc expression *in vitro*,¹⁵⁰ with the methyl quinoxalinone lactam forming the KAc mimetic. Surprisingly, given the high potency observed, the WPF shelf is not occupied – the phenyl ring passes through the ZA channel and packs against the WPF stack, while the cyclopentyl and piperidine point into solvent. The ethyl group occupies a lipophilic pocket on the side of the binding site and the pyrimidine amine forms a bidentate water-mediated hydrogen bond to a backbone Glu

residue.^{150,153} The high unoptimised potency of **1.28** offers opportunities to develop extremely potent BET inhibitors if regions such as the WPF shelf can be effectively accessed. Fletcher *et al.* carried out SAR studies and optimisation on **1.28**, and while little effort was made to access the WPF shelf, selectivity for PLK1 over Brd4 could be encouragingly reversed by simply changing the amine linker to an oxygen, giving **1.29**.¹⁵³

1.4.5 Small Molecule-Induced Degradation

The accessible KAc binding pocket of the BET bromodomains makes inhibitors amenable to linking to chemical biology tools. Parallel approaches by Crews⁹⁷ and Bradner¹⁵⁴ described linking of triazolodiazepine scaffolds to a thalidomide-based group, which itself binds to the E3 ubiquitin ligase cereblon. The resulting bifunctional molecules, dBET (**1.30**) and ARV-825 (**1.31**), simultaneously bind to BET proteins and cereblon and bring them into proximity, allowing cereblon to ubiquitinate the BET protein and mark it for proteosomal degradation.

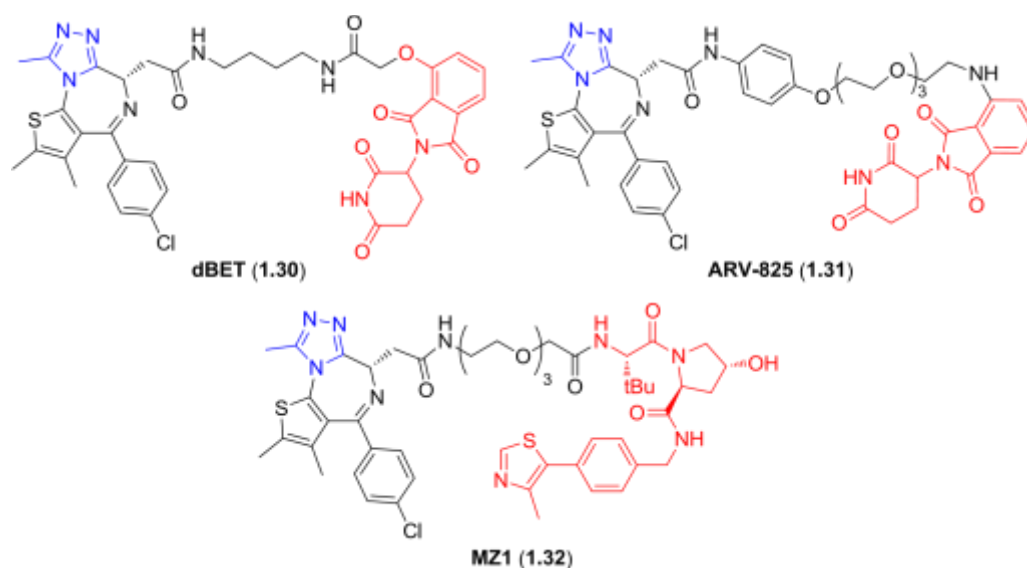


Figure 1.20. Chimeric BET inhibitors for small molecule protein degradation. The ligase-binding motif is shown in red.

1.30 was capable of significantly degrading Brd4 in MV411 cells, with up to 95% downregulation observed after 2 h. This degradation resulted in downstream reduction of MYC levels, and increased apoptosis significantly compared to treatment with JQ1. In a mouse MV411 xenograft model, **1.30** was effective at preventing tumour growth and downregulated MYC expression.¹⁵⁴ **1.31** acts through the same mechanism, with an EC_{50} below 1 nM. In Namalwa or Ramos cells, **1.31** treatment caused rapid and complete degradation of Brd4, whereas treatment with conventional inhibitors **1.05** and **1.07** caused protein accumulation. MYC levels remained reduced for 24 h, compared to 4 h with **1.05**, while antiproliferative and apoptotic activity in Burkitt's lymphoma cells was also superior to **1.05** and **1.07**.⁹⁷

MZ1 (**1.32**), developed by Ciulli *et al.*, instead targets the E3 ligase VHL.¹⁵⁵ Intriguingly, **1.32** showed preferential degradation of Brd4 over Brd2 and Brd3, possibly due to more efficient ubiquitinylation of Brd4 or preferential interaction of the VHL-binding motif with Brd4. As a result, **1.32** showed a gene expression profile more consistent with siBrd4 knockdown than pan-Brd inhibition (**1.05**),¹⁵⁵ and offers a mechanism for protein selective BET inactivation.

1.5 Non-BET Bromodomains

Despite extensive efforts in the development of BET bromodomain inhibitors and the elucidation of BET function, the remaining 56 human bromodomains have received comparatively little attention.¹⁵⁶ Most bromodomain-containing proteins are known as components of transcriptional mediator complexes, but their therapeutic potential and the specific roles of their bromodomain modules are unclear. The rapid discovery of BET phenotypes resulting from the disclosure of the initial BET chemical probes (in particular JQ1) has encouraged research into chemical probes for non-BET bromodomains. This is aided by the close homology of the bromodomain family, which allows knowledge of existing effective KAc mimetics to be transferred to novel targets. Based on published X-ray structures, an *in silico* druggability analysis of the bromodomain family examined pocket volume, shape and hydrophobicity using SiteMap software. Around 50% of bromodomains were predicted to be highly druggable, with 25% intermediate and 25% difficult to drug (Figure 1.21).¹⁵⁷ Nevertheless, potent chemical tools for several of the bromodomains classified 'difficult' in this analysis have subsequently been disclosed (*vide infra*).

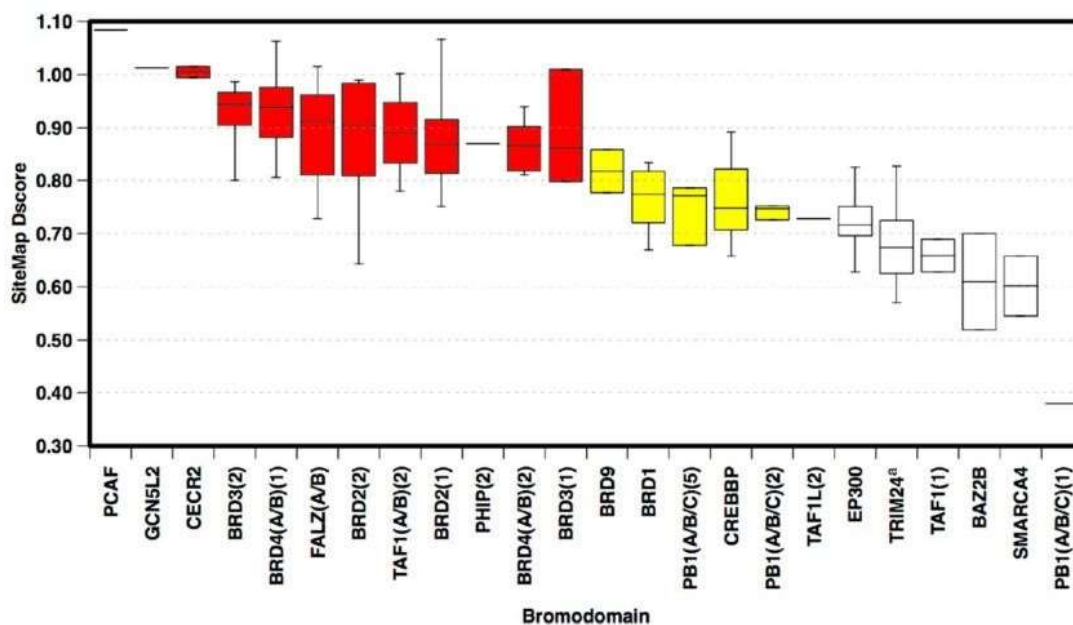


Figure 1.21. Druggability analysis of human bromodomains. Red = druggable, yellow = intermediate, white = difficult. Reproduced from *J. Med. Chem.* **2012**, *55*, 7346–7359 (open access).¹⁵⁷

1.5.1 ATAD2

ATAD2 (ATPase family AAA domain-containing protein 2, also known as (AAA nuclear coregulator cancer-associated protein (ANCCA)) is a transcriptional regulator which catalyses the decomposition of ATP to ADP through its AAA domain, and also contains a single bromodomain which may be linked to ATPase function.¹⁵⁸ ATAD2 is recruited by the oestrogen receptor and acts as a co-activator of oestrogen receptor genes¹⁵⁸ and the oncogene Myc.¹⁵⁹ Through activation of oestrogen and androgen receptors ATAD2 amplifies its own expression, leading to ATAD2 activation in diverse cancers where these receptors are dysregulated.¹⁵⁸ ATAD2 overexpression is indicative of higher mortality in lung,¹⁶⁰ breast,¹⁶⁰ hepatocellular,¹⁶¹ and prostate¹⁶² cancers, with siRNA silencing of ATAD2 moderating disease progression and promoting apoptosis.^{159–161} The closely homologous paralogue ATAD2B is less closely studied but has no strong link to human cancers.¹⁵⁸

ATAD2 is considered less druggable than other bromodomains,¹⁵⁷ and finding hits and leads has proved troublesome due to its shallow, flexible KAc binding site with several negatively charged residues on the ZA and BC loops.¹⁶³ Fragment screens have had some success; Fesik and co-workers used an NMR screen to identify diverse ATAD2-binding fragments with reasonable ligand efficiency, such as **1.33-1.35** (Figure 1.22).¹⁶⁴ The tricycle **1.34** shows an intriguing binding mode, with the triazole acting as the KAc mimetic, while the aniline occupies a pocket deeper within the ATAD2 binding site and displaces three water molecules, postulated to be the cause of the high potency. Thiazole **1.35** binds to the conserved Asn1046 through the lactam, with the aminothiazole pointing into the same pocket as **1.34**. The amine displaces a water molecule and makes multiple hydrogen bonds to solvent and backbone carbonyls.¹⁶⁴ However, 2-aminothiazoles can show highly promiscuous 'frequent hitter' behaviour, particularly in fragment screens, and hits which contain this moiety should be treated with caution.¹⁶⁵

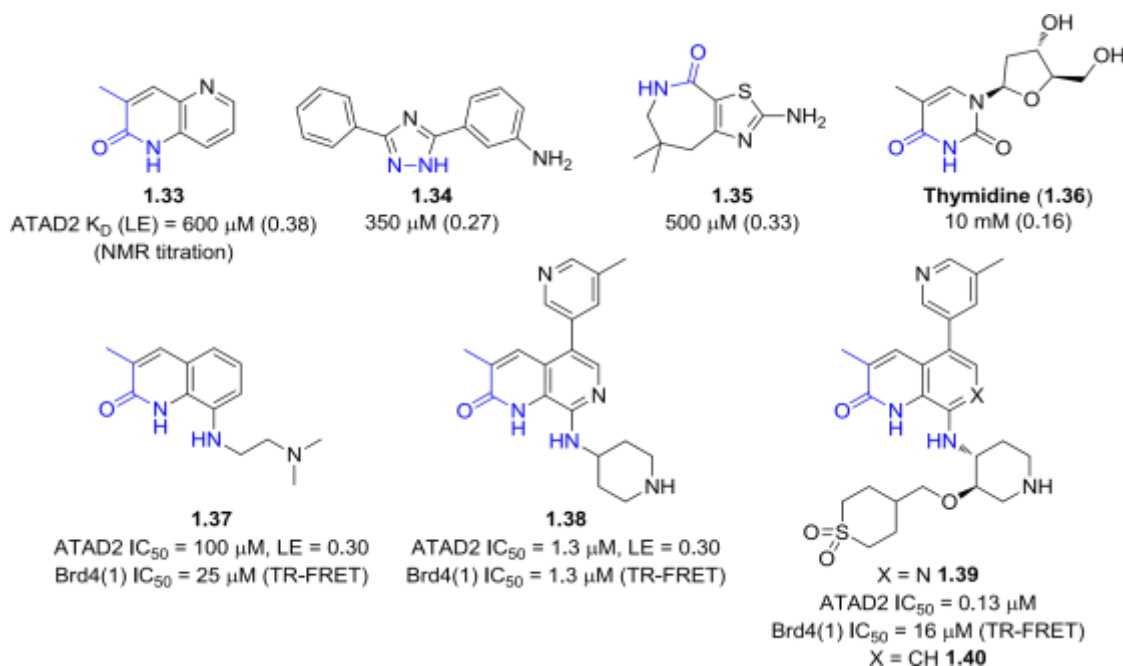


Figure 1.22. Structures and biochemical potencies of reported ATAD2 bromodomain inhibitors. Knapp *et al.* investigated the use of nucleoside bases in order to bind the negatively charged loop regions. Thymidine **1.36** bound with low affinity but showed interesting binding features, with the imide forming the KAc mimetic interaction and the furanose oxygen atoms displacing water molecules and forming water-mediated interactions with the protein backbone. Investigation of SAR around the sugar moiety failed to improve potency.¹⁶³

Concurrently with discovery of fragment **1.33** by Fesik, a fragment screen within GSK also identified quinolinones as ATAD2 bromodomain inhibitors, with initial investigation affording **1.37**.¹⁶⁶ The 8-amino substituent forms a bidentate hydrogen bond with the conserved Asn1064, improving potency compared to **1.33**. Optimisation resulted in **1.38**, which maintained the ligand efficiency of **1.37** and exhibited micromolar potency at ATAD2 but was equipotent at BET bromodomains, preventing the use of **1.38** as a chemical probe.¹⁶⁶ Further structure-based optimisation resulted in **1.39**, which showed improved ATAD2 potency and selectivity over the BET family.¹⁶⁷ The pyridine nitrogen displaces a water molecule and forms a hydrogen bond to Asp1014 of the ZA loop, while the piperidine nitrogen targets an acidic cluster formed of three Asp residues (Figure 1.23). The sulphone binds in a region termed the RVF shelf, analogous to the WPF shelf in BET bromodomains but significantly more polar, displacing a water molecule and hydrogen bonding to at least one arginine residue. This also reduces Brd4 potency due to the unfavourable placement of the polar sulphone on the lipophilic WPF shelf. However, **1.39** showed significant off-target activity at the bromodomains of TAF1(2) (2.5-fold selectivity) and BRPF2 (13-fold selectivity).¹⁶⁷ While this limits the utility of **1.39**, as the only highly potent ATAD2 inhibitor known **1.39** is suitable for use as a probe until more selective examples can be discovered.

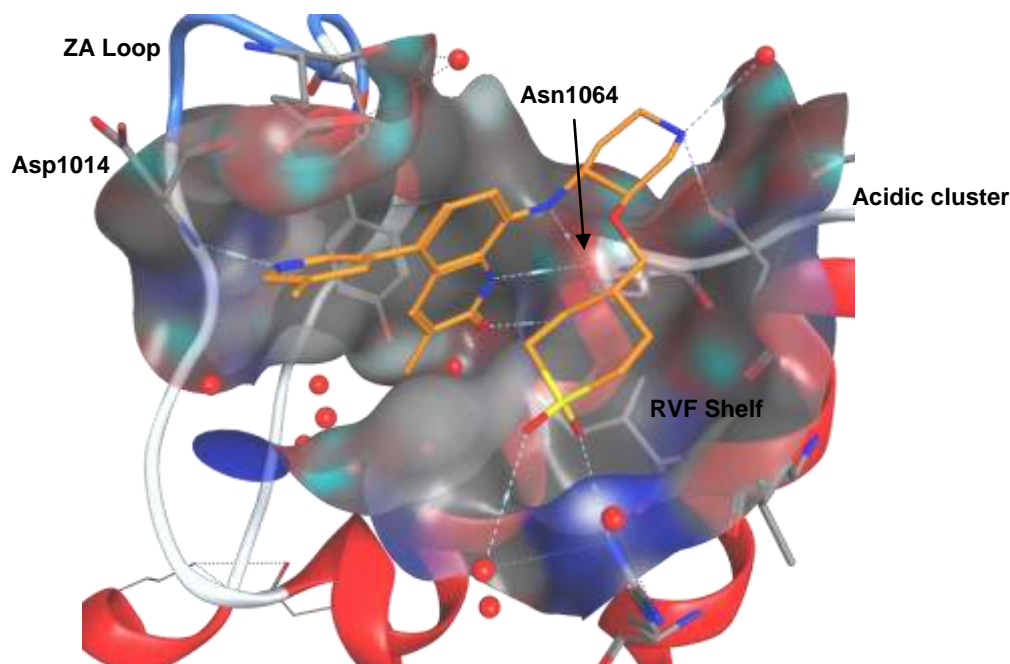


Figure 1.23. X-ray crystal structure of **1.40** bound to the bromodomain of ATAD2 (PDB: 5A83).¹⁶⁷

1.5.2 BAZ

The BAZ (bromodomain adjacent to zinc finger domain) family of bromodomain-containing proteins consist of a C-terminal bromodomain adjacent to a PHD finger (also known as a zinc finger), a region termed the WAKZ motif and a leucine-rich helical (LH) domain along with several other conserved motifs.¹⁶⁸ Four proteins make up the family; BAZ1A, BAZ1B, BAZ2A and BAZ2B. BAZ2B is considered among the least druggable bromodomains due to its shallow KAc binding pocket and lack of a WPF shelf or ZA channel.¹⁵⁷ In part due to the lack of a suitable chemical probe, the exact biological role of BAZ proteins is unclear, but they are thought to have a role in regulating the ISWI chromatin remodelling complex.¹⁶⁸ BAZ2A is a key component of the nucleolar remodelling complex (NoRC), which is responsible for heterochromatin formation and rRNA silencing.¹⁶⁹

Despite the low predicted druggability, several BAZ2 inhibitors have been developed (Figure 1.24). A fragment screen against BAZ2B revealed several weak hits, which were optimised to afford the potent tricyclic compound **1.41**, which utilises an *N*-methyl urea as the KAc mimetic and shows good selectivity over BET and CREBBP. The chlorophenyl packs against the WPF stack (Figure 1.25), which is conserved in the BET and BAZ bromodomains.¹⁷⁰

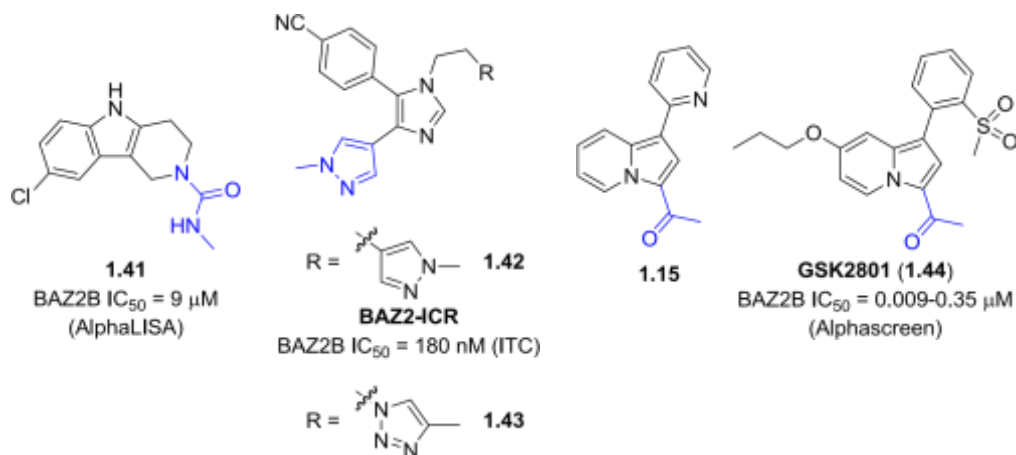


Figure 1.24. Structures and biochemical potencies of reported BAZ2B bromodomain inhibitors.

Optimisation of a virtual screening hit gave the potent and selective inhibitor BAZ2-ICR (**1.42**).¹⁷¹ Close analogue **1.43** was crystallised into BAZ2A and was seen to adopt an intriguing intramolecular stacking conformation between the phenyl and triazole rings, that allows it to efficiently occupy the wide, shallow KAc binding site. In comparison to the binding mode of **1.41**, the methyl and nitrile groups of **1.43** displace three water molecules from the binding site, which may account for the high potency observed (Figure 1.25).

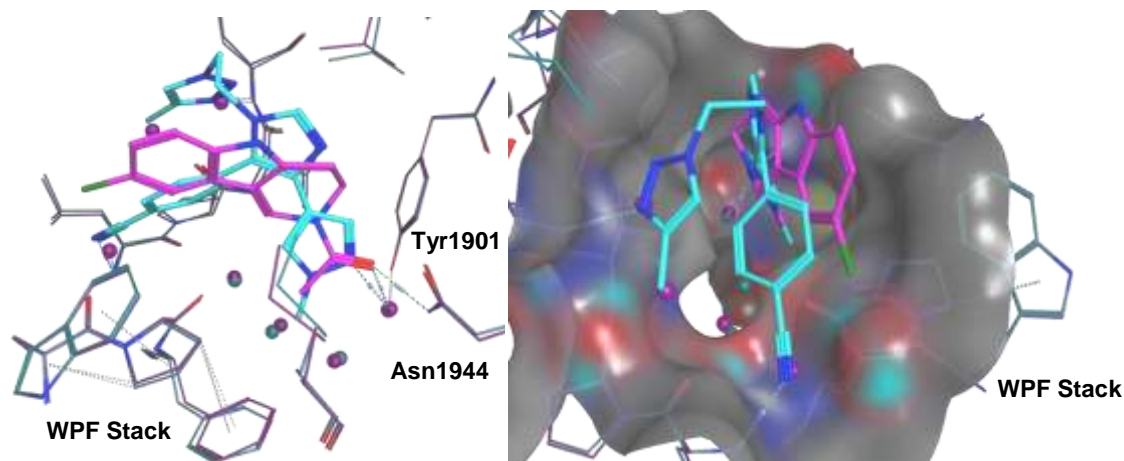


Figure 1.25. Overlaid X-ray crystal structures of **1.41** (magenta, PDB: 4XUB)¹⁷⁰ and **1.43** (cyan, PDB: 4NRA)¹⁷¹ bound to the BAZ2B bromodomain.

In addition to significant BET activity (Figure 1.11), indolizine **1.15** was also equipotent at BAZ2A. The indolizine series was optimised to give the potent and selective probe GSK2801 (**1.44**), with no detectable BET activity. The pendant aryls of **1.15** and **1.44** protrude through the ZA channel, which is narrower in the BET bromodomains - introducing *ortho* substituents twists the pendant phenyl ring out of plane of the core, causing a clash with the BET protein.¹⁷² Activity at BAZ1 was not discussed for any of the published inhibitors **1.41-1.44**.

1.5.3 BPTF

The Bromodomain/PHD finger Transcription Factor (BPTF) bromodomain-containing protein contains two PHD fingers (one of which co-locates with the bromodomain) and an extensive glutamine-rich acidic region.¹⁷³ BPTF forms part of the mammalian orthologue of the *Drosophila* NURF chromatin remodelling complex¹⁷⁴ and is essential for murine embryonic development.¹⁷⁵ The PHD fingers are involved in chromatin binding along with the bromodomain, with the co-located PHD binding to H3K4Me₃ and directing the bromodomain to bind selectively to H4K16Ac.¹⁷⁶ BPTF is recruited at higher levels to bladder cancer oncogenes,¹⁷⁷ while overexpression is correlated with tumour progression in colorectal cancer.¹⁷⁸ Melanoma patients with higher BPTF expression also show poorer survival and heightened resistance to BRAF inhibitor therapy.¹⁷⁹ Inhibitors of the BPTF bromodomain have received little attention, with the only inhibitor thus far disclosed being AU1 (**1.45**, Figure 1.26), discovered using a ¹⁹F NMR screen.¹⁸⁰ W2824 of the BPTF KAc pocket (analogous to that of the WPF stack in BET bromodomains) was benignly replaced with 5fluorotryptophan, allowing simple measurements of compound binding by ¹⁹F NMR. A screen of publicly available GSK kinase inhibitors identified **1.45** as selective for BPTF over Brd4(1), with good potency by ITC and cellular activity in a luciferase assay. The binding mode of **1.45** to the BPTF bromodomain is not known, but the ester group was shown to be required for activity.¹⁸⁰

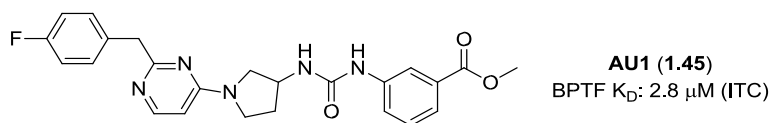


Figure 1.26. Reported BPTF bromodomain inhibitor AU1.

1.5.4 BRPF

The BRPF (Bromodomain and PHD Finger-containing) family of proteins consists of BRPF1, BRPF2 (also referred to as Brd1) and BRPF3. The BRPFs act as scaffolds to assemble complexes of MYST (MOZ, YBF2, SAS2 and TIP60) family histone acetyltransferases. BRPF1 is involved in the assembly of the MOZ (monocytic leukemic zinc-finger) HAT complex, a quaternary tetrameric complex between itself, the MOZ catalytic subunit, ING5 (inhibitor of growth 5) and hEAF6 (human Esa1-associated growth factor) (Figure 1.27a).¹⁸¹ The MOZ HAT can control the expression of homeobox (HOX) genes,^{182,183} which control the body plan of a developing embryo, and plays a direct role in blood cell formation (haematopoiesis) and the development of haematopoietic stem cells.¹⁸⁴ Mutation of BRPF1 affects skeletal development

and HOX transcription in zebrafish.¹⁸⁵ Fusion of MOZ and CBP genes results in a rare form of acute myeloid leukaemia (AML) with poor prognosis,¹⁸² and disruption of MOZ HAT activity is linked to leukaemia development.¹⁸¹ BRPF1 also has a critical role during brain development, with loss causing abnormal morphology in the hippocampus.¹⁸⁶ BRPF2 forms a tetramer with HBO1, another MYST family HAT, and the resulting complex acetylates H3K14 and may play a major role in the transcriptional activation of genes which regulate erythroid development.¹⁸⁷ In addition, BRPF2 is widely expressed in brain tissue, with mutation linked to abnormal brain development,¹⁸⁸ autism spectrum disorder,¹⁸⁹ schizophrenia and bipolar disorder.^{188,190,191} Interestingly, the link to schizophrenia was observed only in European populations.^{190,192} The role of BRPF3 is currently unclear.

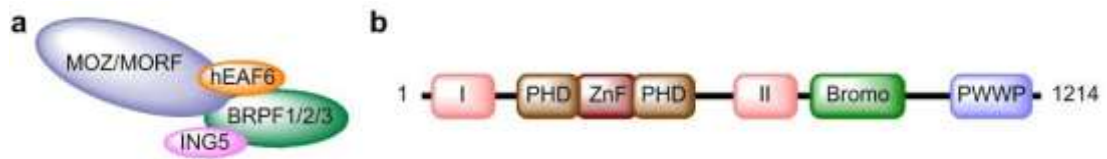


Figure 1.27. a Schematic of the quaternary MOZ HAT complex. **b** Sequence of BRPF1. The sequence of BRPF1 is shown in Figure 1.27b.¹⁹³ Two protein interaction domains, I and II, bind to MOZ and ING5/hEAF6 respectively to form the MOZ HAT tetramer. The bromodomain binds to acetylated histones and the PWWP domain binds histones independent of their acetylation marks, recruiting the MOZ complex to active chromatin.¹⁸³ A double PHD and Zinc finger (ZnF) assembly (PZP) binds unmodified histones and DNA. BRPF1 has two isoforms, 1A and 1B, of which only 1B is capable of binding histones due to a residue insertion in the ZA loop of 1A. BRPF1 shows specificity in its binding to KAc residues,^{55,193} with strong binding to H2AK5Ac, H4K12Ac and H2K14Ac due to hydrogen bonds between the peptide and bromodomain in addition to the KAc binding interaction. Apart from H2AK5Ac, all peptides binding to BRPF1 contain either sterically small glycine or alanine residues on either side of the acetylated lysine.¹⁹³

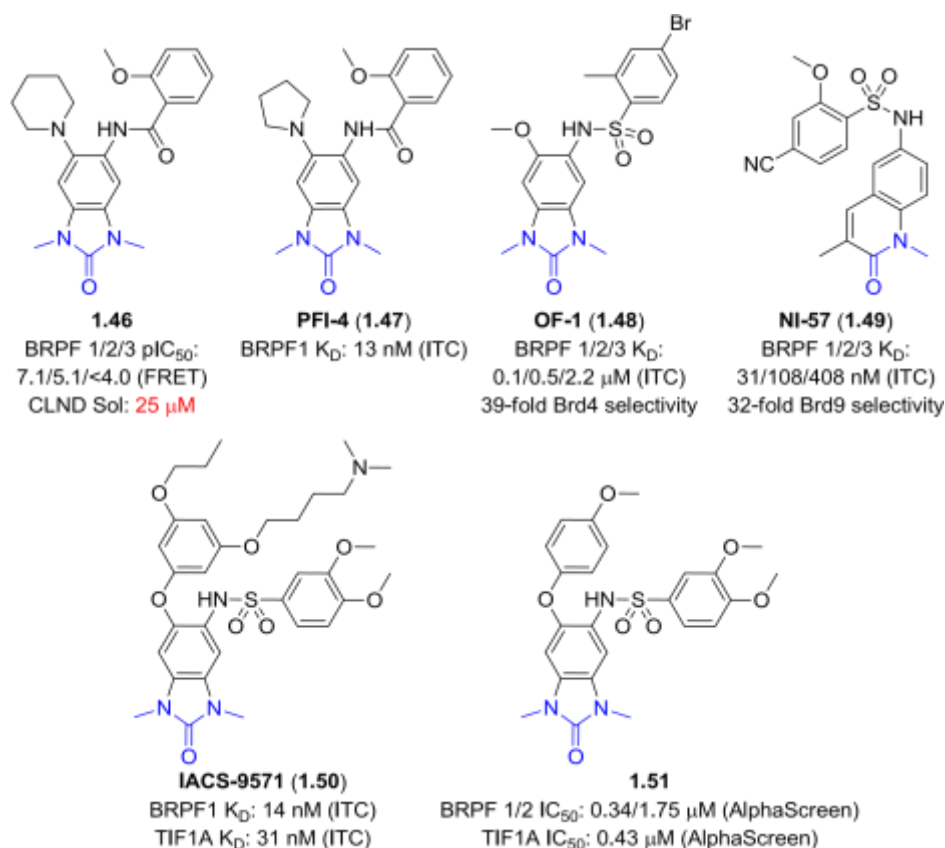


Figure 1.28. Reported BRPF family bromodomain inhibitors

BRPF1 is considered to be druggable (see Section 1.5),¹⁵⁷ and several groups have independently discovered potent BRPF inhibitors based on a 1,3-dimethylbenzimidazolone motif (Figure 1.28). Work within GSK to develop a knowledge-based library of potential KAc mimetics identified **1.46** as a potent, selective inhibitor of the BRPF1 bromodomain (Figure 1.28).¹⁹⁴ The imidazolone group acts as the KAc mimetic, with the aromatic amide resting on the ZA loop and binding to Glu661 (Figure 1.29). An intramolecular NH-OMe H-bond locks the amide in the bound conformation, also forcing the piperidine to twist out of plane and sit on a small lipophilic shelf region. BRPF bromodomains lack a WPF stack or shelf, with the gatekeeper being an aromatic Phe714 which forms π -stacking interactions with the benzimidazolone core. While potent and selective for BRPF1 over BRPF2/3 and other bromodomains, **1.46** is poorly soluble, which may limit its utility.¹⁹⁴ Coincidentally, work by Pfizer and the SGC produced the highly similar inhibitor PFI-4 (**1.47**).¹⁹⁵

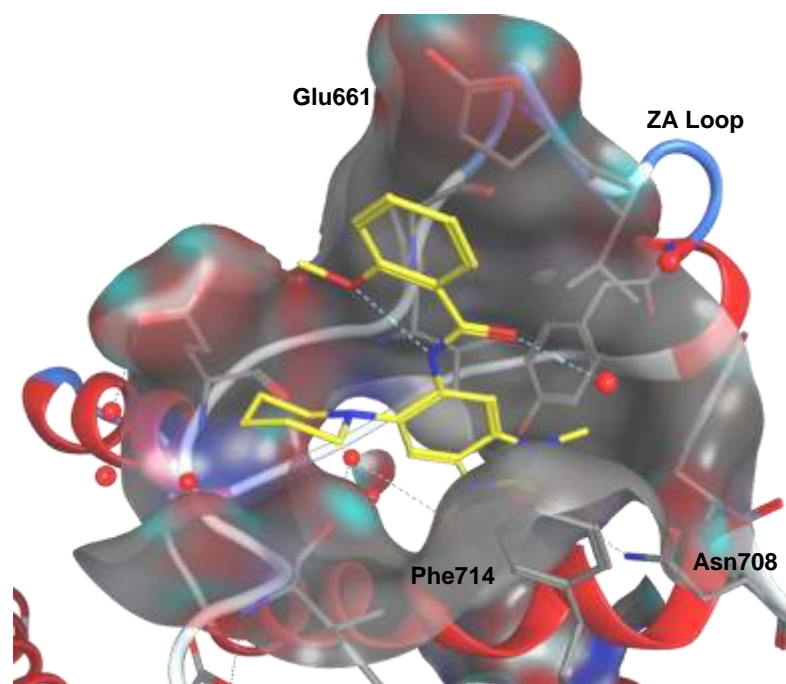


Figure 1.29. X-ray crystal structure of **1.46** bound to the bromodomain of BRPF1 (PDB 4UYE).¹⁹⁴

The benzimidazolone core was also optimised by the SGC into OF-1 (**1.48**), which was less potent at BRPF1 and showed lesser selectivity over BRPF2/3 compared to **1.46**. This panBRPF profile is potentially useful in determining the relative biological roles of the BRPF family members. However, **1.48** displays only 40-fold selectivity over the BET family.¹⁹⁶ Additionally, the SGC and University College London have developed NI-57 (**1.49**), the only non-benzimidazolone BRPF inhibitor currently disclosed.¹⁹⁷ The binding mode remains similar, with the *N*-Me quinoxalinone presumably acting as the KAc mimetic. Similar to **1.48**, **1.49** displays a relatively pan-BRPF selectivity profile and moderate selectivity over other bromodomains.¹⁹⁷

While **1.46-1.49** show good to moderate selectivity for BRPFs over other bromodomains, addition of a phenyl ring to the vector occupied by a methoxy group in **1.48** produced IACS-9571 (**1.50**),¹⁹⁸ and **1.51**¹⁹⁹ and which show high potency at both BRPF1 and the TIF1 α (transcription initiator factor 1A, also known as tripartite motif 24, TRIM24) bromodomains. Both compounds adopt similar binding modes, with the pendant aromatic rings stacking against each other and occupying the regions on the edge of the KAc pocket.

In the case of **1.50**, the butyl chain protrudes through the ZA channel and interacts with an ¹⁹⁸ acidic Asp in TIF1 α (and possibly a Glu in BRPF1). **1.51** had no significant cytotoxicity against a panel of cancer cell lines.¹⁹⁹ Interestingly, ATAD2 inhibitor **1.39** is the only compound disclosed with bias for BRPF2 over BRPF1,¹⁶⁷ and no BRPF3-biased examples or BRPF3 X-ray structures are known.

1.5.5 Brd7 and Brd9

The closely homologous bromodomain-containing proteins 7 (Brd7) and 9 (Brd9) are believed to play a role in chromatin remodelling, and are known to form part of the SWI/SNF (SWItch/Sucrose Non-Fermentable) nuclear remodelling complex.²⁰⁰ The SWI/SNF complex as a whole is known to play a significant role in various malignancies, and has been posited as a potential oncology target,^{201,202} though the exact roles of Brd7 and Brd9 within the complex is unclear. Brd7 binds to KAc residues on histones H3 and H4 but lacks binding specificity.²⁰³ A link has been shown between polymorphism of Brd7 and increased risk of pancreatic cancer,²⁰⁴ and Brd7 is widely thought to act as a tumour suppressor.^{205,206} Brd9, however, is frequently overexpressed in cervical cancer,²⁰⁷ though its biological role is less well known compared to Brd7. Brd9 is also one of the few BRDs able to bind butyryl-lysine.⁶⁶

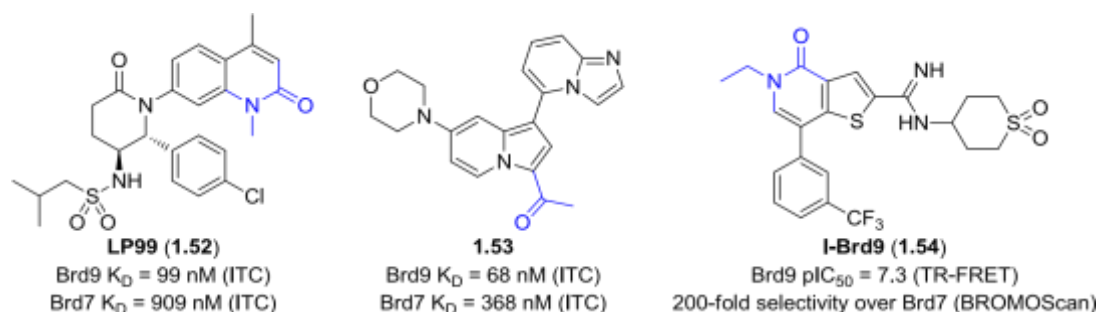


Figure 1.30. Structures and biochemical potencies of reported Brd7 and Brd9 bromodomain inhibitors.

Diverse small-molecule inhibitors of these bromodomains have been developed (Figure 1.30). LP99 (**1.52**) is a potent Brd9 inhibitor, but shows only 10-fold selectivity over Brd7. **1.52** binds to the conserved Asn and Tyr residues through its *N*-methyl quinolinone moiety, which also packs against the Tyr106 gatekeeper residue in Brd9. The piperidinone ring facilitates close shape complementarity with a more open portion of the binding site, while the sulphonamide NH and lactam carbonyl groups form hydrogen bonds to the protein backbone. When administered to LPS-stimulated THP cells, **1.52** downregulated the proinflammatory cytokine IL-6, indicating a possible immunological role for Brd7/9.²⁰⁸

During the development of the BAZ2 probe **1.44** (see Section 1.5.2) molecules with Brd9 activity were identified, and this series was optimised to give potent Brd7/9 inhibitor **1.53**. Selectivity is attributed to the imidazopyrimidine motif, which clashes with the BAZ and Brd4 KAc pockets and forms a π -stacking interaction with Tyr222 in Brd9.²⁰⁹ BI-9564, the structure of which has not been disclosed, is also available as a chemical probe with Brd9 $K_D=14$ nM (ITC) and reasonable selectivity (Brd7 $K_D=239$ nM, CECR2 $K_D=258$ nM (ITC)).²¹⁰

The thienopyridone I-Brd9 (**1.54**) also shows potent inhibition of Brd9, though with improved Brd7 selectivity compared to **1.52** and **1.53**. The ethyl pyridone forms the KAc mimetic, with the amidine forming hydrogen bonds through both NH motifs to the key Asn100 and backbone Ile53 (Figure 1.31). In addition, the amidine improves selectivity over the BET bromodomains due to the more lipophilic nature of the relevant region in the BET KAc pocket. Though capable of displacing endogenous Brd9 from HuT-78 cell lysates, no phenotypic data for **1.54** were reported.²¹¹

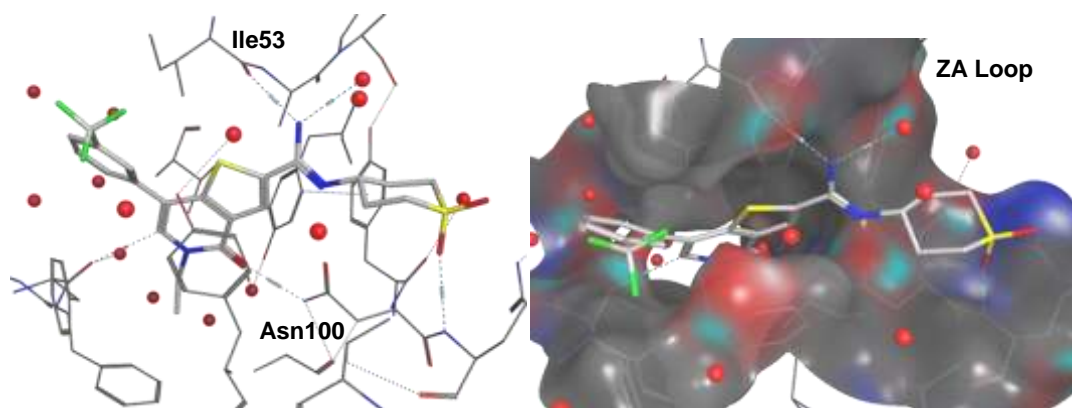


Figure 1.31. X-ray structure of I-Brd9 (**1.54**) bound to the Brd9 bromodomain (gray, PDB: 4UIW).²¹¹

1.5.6 Brd8

Brd8 (also known as p120), of which at least three isoforms exist, is a nuclear receptor coactivator which interacts with the thyroid hormone receptor through its bromodomain.²¹² Isoforms 1 and 2 are components of the NuA4 HAT complex, which coactivates diverse transcription processes and is critical for DNA repair.²¹³ Brd8 is overexpressed in several metastatic colorectal cancer cell lines, with knockdown of Brd8 using siRNA slowing cell growth and sensitising cells towards spindle poisons.²¹⁴ Brd8 also forms a chromatin remodelling complex with p400 which is required for fat cell differentiation.²¹⁵ Given the ability of BET bromodomains to affect lipoprotein expression^{114–116} this increases evidence that bromodomain inhibition may be of relevance in metabolic diseases. No inhibitors of the Brd8 bromodomain have been reported.

1.5.7 BRWD

The bromodomain and WD repeat-containing protein family consists of BRWD1 (also known as WRD9), PHIP (pleckstrin homology domain interacting protein, or BRWD2) and BRWD3.

WD repeats are 40-amino acid structural motifs which repeat up to 16 times, forming a circular β -propeller structure involved in protein complex assembly.²¹⁶ Each family member contains several WD repeats followed by two bromodomain modules, but are otherwise diverse.²¹⁷

As with BrdT,¹¹³ BRWD1 is required for spermatogenesis,²¹⁷ but in general its function is unknown. PHIP is involved in insulin signalling pathways and enhances the production of insulin-secreting beta cells,^{218,219} and may be involved in protein degradation through association with E3 ubiquitin ligases.²²⁰ A role in DNA damage repair through interaction with damage-specific DNA binding protein 1 (Ddb1) has also been suggested.²²⁰ BRDW3 is strongly implicated in neurological disorders, with mutations of BRDW3 observed in cases of intellectual disability with macrocephaly^{221,222} and West syndrome, a form of epileptic encephalopathy.²²³ Despite PHIP being classed as druggable,¹⁵⁷ no BRWD family inhibitors have been reported.

1.5.8 CECR2

CECR2 (cat eye syndrome chromosome region, candidate 2) forms part of the ATPdependant CECR2-containing remodelling factor (CERF) chromatin remodelling complex.²²⁴ The protein contains a single bromodomain, in addition to an AT hook motif which binds to A/T rich regions of DNA. CECR2 is highly expressed in the neural tube (the precursor to the CNS) in developing embryos,²²⁴ in addition to roles in spermatogenesis,²²⁵ and DNA damage repair following double strand breaks.²²⁶ Along with Brd9, CECR2 is also capable of binding butyryl-lysine.⁶⁶

NVS-1, a selective chemical probe for the CECR2 bromodomain with $K_D = 80$ nM (ITC), has been developed by the SGC and Novartis.²²⁷ ATAD2 inhibitor **1.39**¹⁶⁷ and unpublished Brd7/9 inhibitor BI-9564²¹⁰ also show moderate CECR2 activity.

1.5.9 CREBBP and EP300

Cyclic-AMP response element binding protein (CREBBP or CBP) and E1A binding protein (EP300 or p300) are closely related lysine acetyltransferases (KATs) that each contain a single, highly homologous bromodomain in addition to their KAT domain. K382 of the tumour suppressor p53 (which is mutated in 50% of human cancers²²⁸) is acetylated in response to cellular stress, and binds to CREBBP to initiate cell cycle arrest or apoptosis.²²⁹ CREBBP inhibitors are of interest to probe this interaction, investigate additional biological roles of the CREBBP bromodomain, and as potential treatments for diseases involving aberrant p53.

Despite low bromodomain sequence homology, CREBBP activity is often observed as an off-target for BET inhibitors.^{135,143,145} This has allowed a transfer of knowledge and chemotypes from BET inhibitor design, and has enabled the design of several CREBBP/p300-selective inhibitors (Figure 1.32). However, no strong CREBBP/EP300 phenotype or disease link has been disclosed thus far.

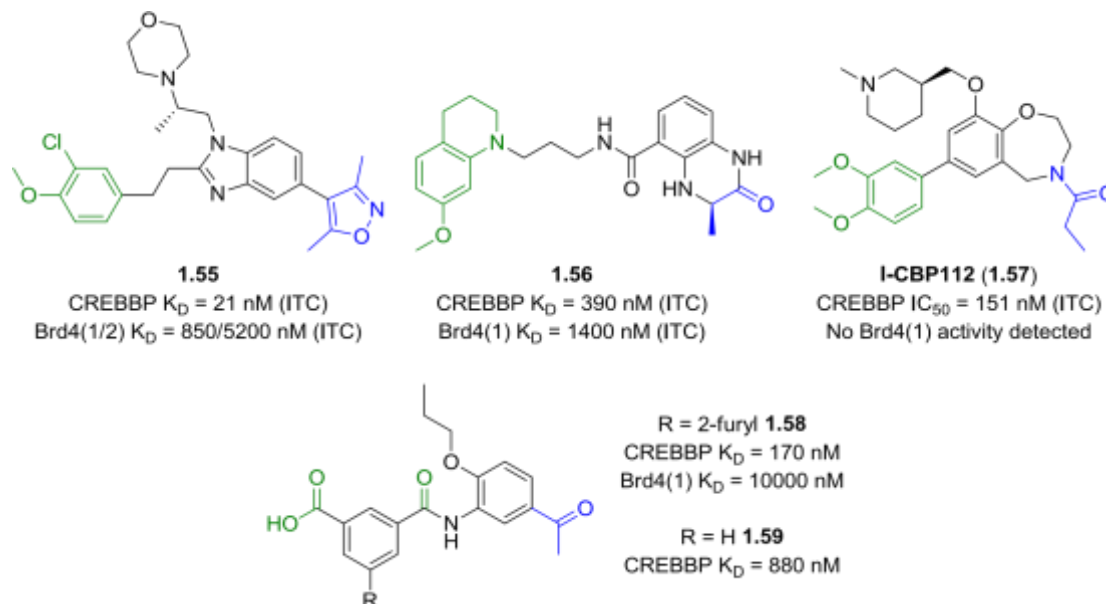


Figure 1.32. Structures and biochemical potencies of reported CREBBP family bromodomain inhibitors. the KAC mimetic is highlighted in blue, the arginine-binding group in green.

CREBBP activity was observed during early development of the dimethylisoxazole-based BET inhibitor **1.09** (which itself lacks measurable CREBBP activity),¹³⁵ and Hay *et al.* optimised the same template to obtain potent and selective inhibitor **1.55**.²³⁰ Key to their strategy was interaction with a CREBBP-specific Arg1173 in the region analogous to the BET WPF shelf, with the pendant phenyl forming cation- π interactions with this residue. The morpholine occupies the ZA channel, being conformationally restricted by the chiral methyl. Intriguingly, selectivity over Brd4 BD1 (40-fold) was significantly lower than over Brd4 BD2 (250-fold).²³⁰

Rooney *et al.* designed dihydroquinoxalinone inhibitor **1.56**, which was less potent and CREBBP/p300 selective but still capable of displacing the CREBBP bromodomain from chromatin. The amide and dihydroquinoxalinone form an intramolecular hydrogen bond which restricts the conformation of the side chain, allowing the tetrahydroquinoline to occupy an induced-fit pocket under Arg1173 and form a cation- π interaction (Figure 1.33).²³¹ I-CBP112 (**1.57**), developed by the SGC and GSK, inhibited renewal of AML cells *in vivo* and enhanced the cytotoxic effects of both BET inhibitors and doxorubicin.^{232,233}

Cafilisch and Nevado carried out a high throughput fragment-based docking screen to identify CREBBP inhibitors,²³⁴ identifying acetylbenzenes such as **1.58**,²³⁵ which showed good CREBBP/p300 potency and excellent selectivity over the BET family and other bromodomains. The acetyl group acts as KAc mimetic, while the benzoic acid forms an ion pair with Arg1173. The amide carbonyl also forms a through-water hydrogen bond to this residue (Figure 1.33) Although this series was generally inactive when dosed to a panel of cancer cell lines, it is speculated this is a result of poor permeability due to the acid group.²³⁵

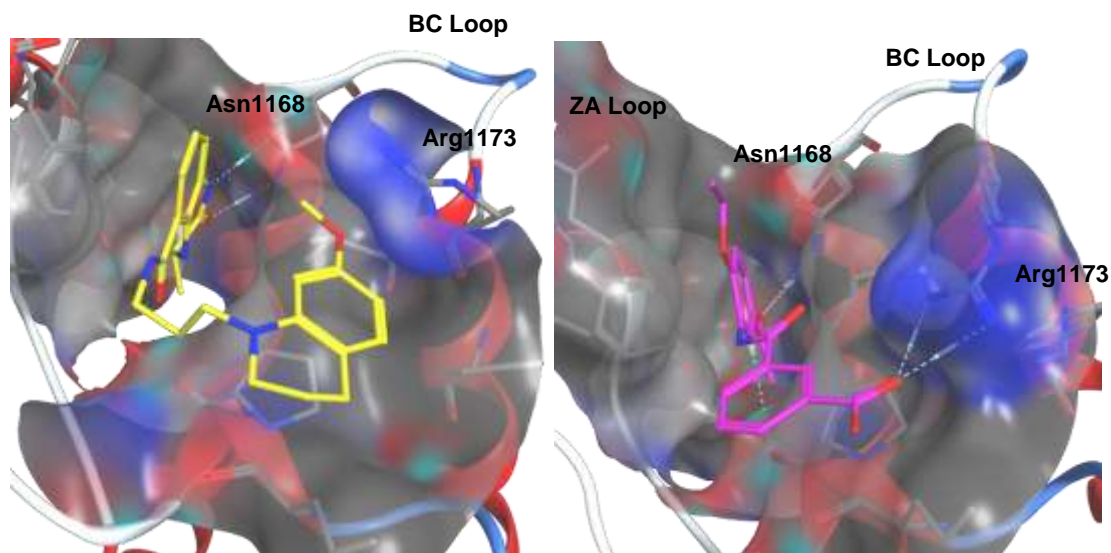


Figure 1.33. X-ray crystal structures of **1.56** (yellow, PDB: 4NYX)²³¹ and **1.59** (magenta, PDB: 4TQN)²³⁵ bound to the CREBBP bromodomain, showing interaction with Arg1173. Water molecules omitted for clarity.

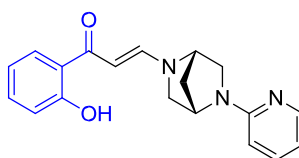
1.5.10 PB1 and SMARCA2/4

Polybromodomain-containing protein 1 (PB1, also known as BAF180) contains six bromodomain modules (BD1-6), two bromo-adjacent homology (BAH) domains, and a highmobility group (HMG) DNA-binding domain.²³⁶ The bromodomains bind to histone H3 preferentially,²³⁷ and may cooperate with the HMG domain to recruit PB1 to specific loci based on precise acetylation patterns. PB1 forms part of the polybromo/BRG1-associated factors (PBAF) complex, which is involved in cell cycle progression and mitosis.^{237,238} The PBAF complex and PB1 are essential for cardiac development,²³⁹ and PB1 is able to regulate the tumour suppressor p21, being mutated in breast^{236,240} and renal²⁴¹ cancers.

The PBAF complex is one of the human analogues of the SWI/SNF nuclear remodelling complex, as is the BRG1- or HRBM-associated factors (BAF) complex.²⁴² BRG1 and HRBM are more commonly known as SWI/SNF-related, Matrix-associated, Actin-dependent

Regulator Chromatin (SMARC)-A2 and SMARCA4. These closely related proteins contain bromodomains (closely homologous to those of PB1)¹⁵⁷ and ATPase domains, forming the mutually exclusive catalytic subdomains of the BAF/PBAF complexes.²⁴² The SWI/SNF complex is mutated in various cancers,^{201,202,242} and inactivation of SMARCA2 is lethal to SMARCA4-deficient cancers.^{243–245}

PFI-3 (**1.60**) is a potent inhibitor of the SMARCA2/4 and PB1(5) bromodomains with excellent selectivity over the other 5 PB1 bromodomains by T_m shift (Figure 1.34).^{246,247} Though the binding mode of **1.60** is unclear, crystallography of similar molecules in the PB1(5) bromodomain suggests that the salicylic acid motif acts as the KAc mimetic, binding deep within the KAc binding site and completely displacing the water network.^{248,249} However, in contrast to SMARCA2/4 knockdown, PFI-3 showed no effect when dosed to rhabdoid cancer or leukemia cells and was unable to displace the SWI/SNF complex from chromatin.²⁴⁶ This indicates that the bromodomain of SMARCA2/4 is not involved in SWI/SNF-dependant cancers, and other domains also influence chromatin binding.²⁴⁶



PFI-3 (1.60)
PB1 (5) K_D = 48 nM (ITC)
SMARCA4 K_D = 89 nM (ITC)

Figure 1.34. Structure and biochemical potencies of PFI-3. The KAc mimetic is highlighted in blue.

1.5.11 PCAF

P300/CREBBP-associated factor (PCAF/KAT2B) is a transcriptional coactivator which contains HAT and E3 ubiquitin ligase domains, and a single bromodomain. Zhou's seminal work on the PCAF bromodomain was the first to solve the 3D structure of a bromodomain and identify KAc as the endogenous binding partner.²⁵⁰ PCAF and TAF selectively recognise H3K14Ac over other bromodomains,²⁵¹ and PCAF is strongly implicated in HIV progression. The viral activator Tat is activated by p300-mediated K50 acetylation²⁵² allowing recruitment to the PCAF bromodomain to enable HIV transcription.²⁵³

This disease link lead to early investigation of PCAF inhibitors (Figure 1.35). PCAF bromodomain inhibitor **1.61** was the first KAc mimetic described, with highly efficient binding in an ELISA peptide displacement assay. Interestingly, an NMR structure indicates the compound does not bind to the conserved Asn, with the nitro binding to Tyr802 and the terminal amine making electrostatic interactions with Glu750.²⁵⁴ Using *in silico*-guided design

to identify potentially displaceable water molecules, the series was optimised further to give **1.62**, which was active in reducing Tat-mediated HIV-1 transcription.²⁵⁵ Further work identified the amino analogue **1.63**, which showed improved potency to **1.61** when dosed to C8166 cells infected with HIV-1.²⁵⁶

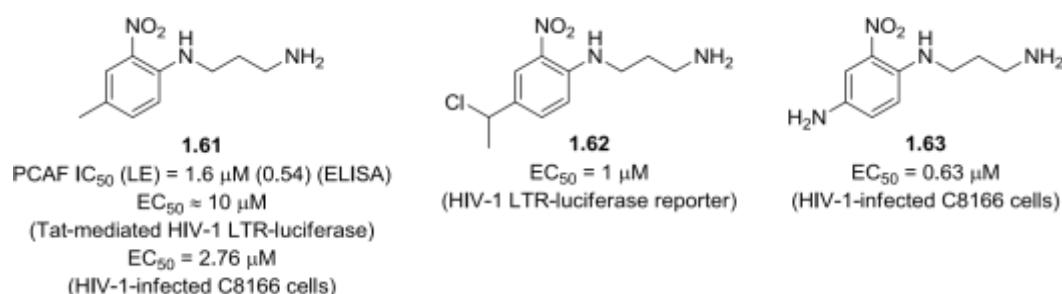


Figure 1.35. Structure and potencies of PCAF inhibitors.

1.5.12 SP100/110/140

The SP100/110/140 proteins contain chromatin-interacting regions such as bromodomains, PHD and SAND domains,^{257,258} and are found within pro-myelocytic leukaemia (PML) nuclear body complexes which act as tumour suppressors and regulate cellular function.²⁵⁹

The family appears to have a strong immunological role. SP100 represses viral replication during early stages of infection with human papillomavirus²⁶⁰ and cytomegalovirus.²⁶¹ SP100/140 are common autoantibodies in primary biliary cirrhosis patients.^{262,263} SP110 functions as a transcriptional coactivator of nuclear hormones²⁶⁴ and as an immunoprotectant against infectious organisms, being expressed in lymphocytes, spleen and liver. Mutations cause immunodeficiency and decreased T-cell production and are linked to hepatic veno-occlusive disease.²⁶⁵ SP140 is induced by the cytokine IFN γ ,²⁵⁷ and may also play a role in response to, and inactivation of, HIV-1 lacking the viral infectivity factor (Vif).²⁶⁶ The SP140 gene locus has been identified as a susceptible region for Crohn's disease²⁶⁷ and for single nucleotide polymorphisms in chronic lymphocytic leukemia.²⁶⁸

The SP100 bromodomain (and presumably those of the closely related SP110/140) is atypical, with a significantly smaller binding pocket due to increased numbers of Phe and Tyr residues in the loop regions.^{269,270} It is unknown whether KAc binding is possible, and no small-molecule bromodomain inhibitors have been reported.

1.5.13 TAF1

TAF1 (Transcription initiation factor TFIID subunit 1, also known as TAF_{II}-250 or p250) is a component of the TFIID basal transcription factor, which binds to DNA start sites to initiate transcription. TAF1 contains two bromodomains, which specifically recognise the diacetylated H4 tail,²⁷¹ and a TATA-box binding domain which recognises the TATA-binding protein, another component of TFIID which binds to DNA.²⁷² TAF1(2) is the only bromodomain capable of binding the uncommon crotonyl-lysine mark.⁶⁶ TAF1 has several testes-specific homologues with high sequence homology and similar function.^{112,273} TAF1 enhances the transcriptional activity of the androgen receptor (AR) and overexpression is linked to AR-mediated progression of prostate cancer,²⁷⁴ with mutation observed in some severe intellectual disabilities^{275,276} and progressive movement disorders.²⁷⁷ Silencing of TAF1 induces production of the tumour suppressor p53,²⁷⁸ and TAF1 is frequently mutated in uterine serous carcinoma.²⁷⁹ Although no selective TAF inhibitors have been disclosed, ATAD2 inhibitor **1.39** shows high TAF1(2) activity (BROMOscan pK_i = 7.3).¹⁶⁷

1.5.14 TIF1 α

The TIF1 α (transcription initiator factor 1 α , also known as tripartite motif 24, TRIM24) protein contains a dual PHD-bromodomain motif which is capable of combinatorial binding of both unmodified and acetylated histone lysines.²⁸⁰ TIF1 α acts as a coactivator of the estrogen receptor²⁸⁰ and as a mediator of nuclear receptor-ligand binding to represses the activity of the retinoic acid receptor.²⁸¹ TIF1 α also contains a RING-type E3 ubiquitin ligase which ubiquitinylates and degrades the tumour suppressor p53, with TIF1 α depletion in human breast cancer cells causing apoptosis.²⁸² TIF1 α is overexpressed in head and neck squamous cell carcinoma,²⁸³ glioblastoma,²⁸⁴ gastric cancer,²⁸⁵ and non-small cell lung cancer²⁸⁶ with raised TIF1 α expression levels correlated with poorer overall survival. Despite this strong disease link, the only TIF1 α inhibitors reported to date are the dual BRPF-TIF1 α inhibitors **1.50**¹⁹⁸ and **1.51**¹⁹⁹ (See Section 1.5.4).

1.6 The Future of Bromodomains as Small-Molecule Targets

Progress in the development of small-molecule bromodomain inhibitors continues to accelerate. Only a decade has elapsed since the first report of small-molecule bromodomain inhibitors,²⁵⁴ yet potent and selective inhibitors for the majority of human bromodomains have been discovered and several BET inhibitors have entered clinical trials.

The coming years are expected to see the maturation of the field. The plethora of BET inhibitors in oncology clinical trials will confirm or deny their potential as anti-cancer targets, and positive safety findings may see the launch of trials for more chronic conditions such as HIV and inflammation. Focus is beginning to shift towards non-BET bromodomains - the development of inhibitors for the remaining targets and discovery of probes with improved potency or selectivity is expected to continue. Reports are beginning to emerge of target validation/invalidation using these probes,^{233,246} and positive results may see non-BET bromodomain inhibitors enter clinical trials. Approaches such as designed polypharmacology,¹⁵⁰ targeted protein degradation,^{97,154} antibody or gene therapy may also be further investigated. Currently, opportunity exists in four underexplored areas:

- The development of BET inhibitors with selectivity within the BET family, which may offer differentiated pharmacology compared to pan-BET inhibitors. The BD2 domains in particular are poorly served, with only weakly selective inhibitors reported. Single domain inhibitors are also unknown.
- The development of chemical probes for bromodomains where no inhibitor currently exists, to enable target validation studies and explore the druggability of the target.
- The development of additional probes for bromodomains where existing inhibitors are weakly potent, poorly selective or only a single chemotype is known. High quality chemical probes are required to prevent ambiguity in phenotypic assay results, and testing multiple chemotypes reduces the likelihood of off-target driven effects.
- Development of bromodomain inhibitors with novel, patentable structures. The intellectual property landscape around the BET family is highly competitive, and progress in the field is fast-paced. Probes with drug-like properties or fast-following leads will expedite the development of bromodomain inhibitor candidates.

This work will seek to develop, through small-molecule medicinal chemistry, chemical probes to meet these requirements.

2. Design and Synthesis of Tetrahydroquinoxalines as BD2Selective BET Inhibitors

2.1 Introduction

The tetrahydroquinoline (THQ) fragment **1.13** is a known efficient BET inhibitor (Figure 2.1)¹³⁹ with high synthetic tractability.²⁸⁷ The THQ core has been successfully optimised against ApoA1 upregulation (without knowledge of molecular target) to give IBET-726 (**1.14**), subsequently shown to be a potent BET inhibitor.¹¹⁴ However, *in vivo* cleavage of the C4-N bond of **1.14** (a potential metabolic route could involve hydrolysis of the acetamide and

oxidative elimination of the aniline to afford a quinoline) would produce a potentially mutagenic free aniline.²⁸⁸ The mutagenicity risk of 4-chloroaniline is ambiguous, with both negative and positive responses observed,²⁸⁹ and bacterial or rodent *ex vivo* assays may not give the full picture of mutagenicity. To fully discharge the risk the masked aniline moiety could be removed from the structure - a potential alternative is the use of a tetrahydroquinoxaline (THQx) core, which shares the KAc mimetic and general core structure of **1.14** but removes the pendant aniline. It should be noted that the THQx core still contains two embedded anilines, but these are less likely to be fully unmasked *in vivo* due to their higher degree of substitution and position within the centre of the molecule, protecting them from metabolising enzymes. Within GSK, *N*-acetyl tetrahydroquinoxalines have shown activity as upregulators of ApoA1, and subsequently found to be active as BET inhibitors. When a selection of THQx compounds were tested against the Brd4 bromodomains, several showed BD2-biased profiles.²⁹⁰ The fragment **2.001** showed comparable Brd4 potency to **1.13** and a slight preference for BD2 over BD1, while the benzyl derivative **2.002** exhibited a significant increase in potency and an intriguing 30-fold BD2 selectivity.

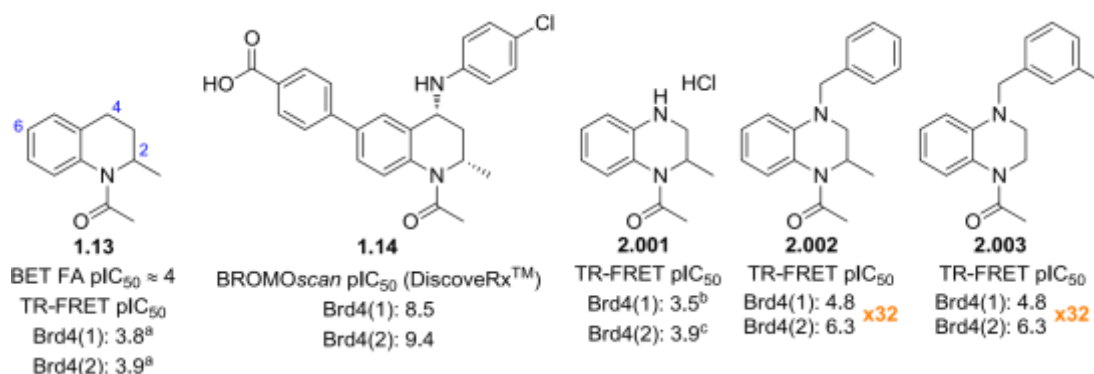


Figure 2.1. Published THQ BET inhibitors and initial THQx hits. FRET data are n=2 or greater unless otherwise specified. (a) n=2, <4.3 on two additional test occasions; (b) n=1, <3.3 on two additional test occasions, <4.3 on two further test occasions; (c) n=3, <4.3 on two additional test occasions.

An X-ray structure of the close analogue **2.003** bound to Brd4 BD2 was obtained (Figure 2.2). The acetyl group of **2.003** overlaid well with the acetyl group of a native ReIA K₃₁₀Ac peptide ligand,²⁹¹ with the tolyl group placed on the WPF shelf between the WPF stack and the BD2-specific histidine.

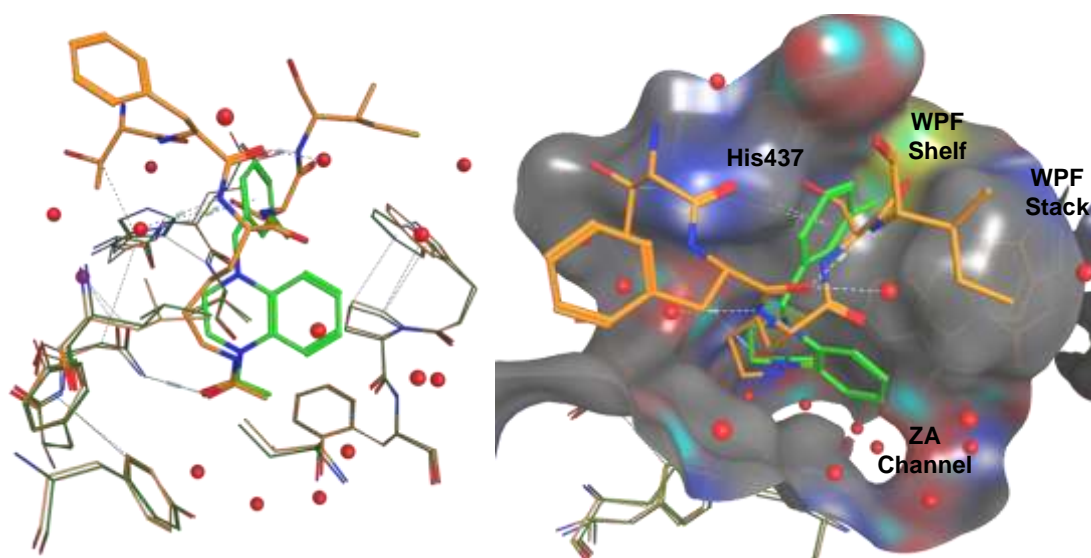


Figure 2.2 X-ray crystal structures of **2.003** bound to Brd4 BD2 (green, 1.83 Å),²⁹² showing the **2.003** BD2 surface and solvent (red), overlaid with RelA K₃₁₀Ac peptide (orange, 2.0 Å, PDB 4KV4)²⁹¹. Water molecules from the peptide are omitted for clarity.

THQx **2.003** adopted a very similar binding mode to THQ **1.14**¹³⁹ (Figure 2.3), with the KAc mimetic, fused phenyl ring and WPF shelf-occupying tolyl group overlaying closely. However, the saturated ring of the tetrahydroquinoxaline core adopts a flatter conformation that alters the angle onto the WPF shelf. The close overlay of the core and KAc mimetic with the peptide and an established ligand indicates that they may be near optimal and poorly tolerate substitution. The 2-methyl group of **1.14** occupies a small lipophilic pocket,¹³⁹ and the unsubstituted ring of **2.003** can be seen to pucker in order to fill this pocket. Placement of small alkyl substituents at this position may improve potency by occupying the pocket more effectively. The core 6-positions of **2.003** and **1.14** are also in very similar positions, indicating that substitution from the vector could allow access to the ZA channel.

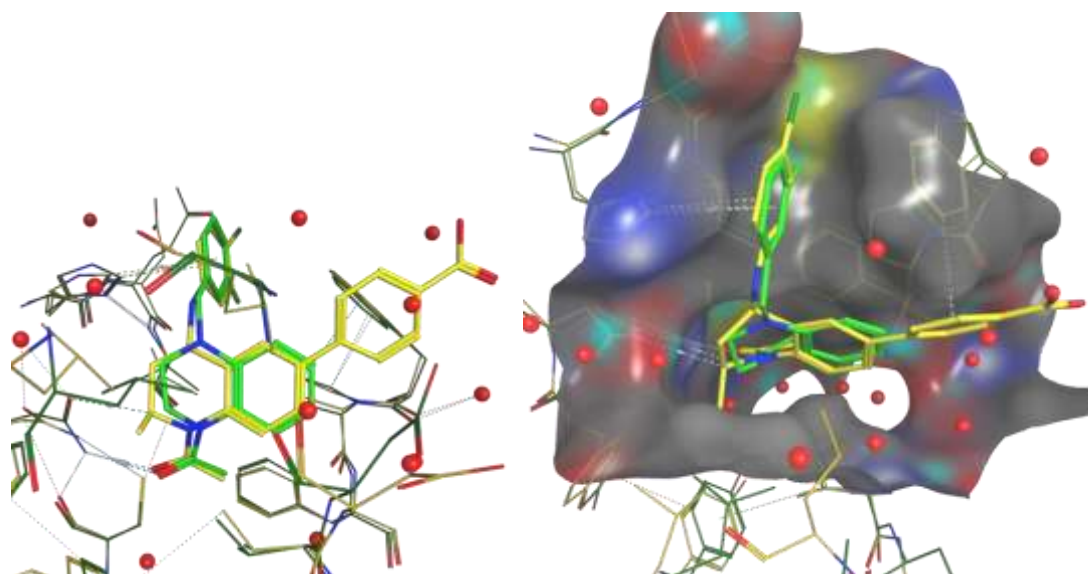


Figure 2.3. X-ray crystal structures of **2.003** bound to Brd4 BD2 (green, 1.83 Å),²⁹² showing the **2.003** BD2 surface and solvent (red spheres), overlaid with **1.14** bound to Brd4 BD2 (yellow, 2.0 Å, PDB 4UYG).¹³⁹

2.2. Aims

The promising potency and selectivity of the initial tetrahydroquinoxaline hits gave confidence that the series could be optimised to provide molecules with improved potency, selectivity and physicochemical properties. This work aimed to optimise the THQx series in order to identify a molecule which would be suitable for use as a BD2-domain selective *in vitro* tool to profile the biological role of BD2 in immune and cancer cells. Therefore, a molecule was desired which met the following criteria:

- 1) Brd4 BD2 $pIC_{50} > 7$ and 50-fold selectivity over BD1 (ideally 100-fold).
- 2) > 50 -fold selectivity over other bromodomain families.
- 3) Acceptable physicochemical properties (CLND solubility $> 100 \mu\text{M}$, artificial membrane permeability (AMP) $> 100 \text{ nms}^{-1}$, ChromLogD_{7.4} 2-4).¹⁶
- 4) Evidence of cellular target engagement.

In order to achieve these goals, the strategy to be followed was:

- Identify and explore the principal vectors for substitution from the THQx core and determine the optimal substituents for conferring potency and selectivity.
- Improve the physicochemical properties of the series by introducing polarity.
- Develop synthetic routes to facilitate the rapid and efficient synthesis of analogues, as single enantiomers if applicable.
- While an *in vitro* tool was initially desired, a compound suitable for *in vivo* experiments would also be highly beneficial. As such, compounds would be designed to minimise *in vivo* liabilities such as reactive groups, and adhere to the modern concepts of drug discovery and compound design.¹³

2.3. Results and Discussion

2.3.1 Previous GSK Work

The promising nature of the THQx hits motivated a GSK team to briefly investigate the series prior to this work.²⁹⁰ Plotting these previously developed compounds (Figure 2.4) showed that the template had moderate BD2 bias. Many of the previously synthesised examples contained a 6-Br substituent, and a weak correlation was observed between BD1 potency and this substitution pattern, suggesting the 6-Br causes a reduction in selectivity. The small number of compounds with an elaborated 6-substituent showed encouraging selectivity and potency, and the data confirmed that an amide linker between the core and WPF-shelf group was detrimental to potency. At the outset it was realised that the loss of a hydrogen bond donor and decreased availability of the N lone pair compared to the analogous THQ gives the THQx

series an inherently higher lipophilicity, and it was encouraging to note that reasonably selective molecules with low lipophilicity could also be obtained.

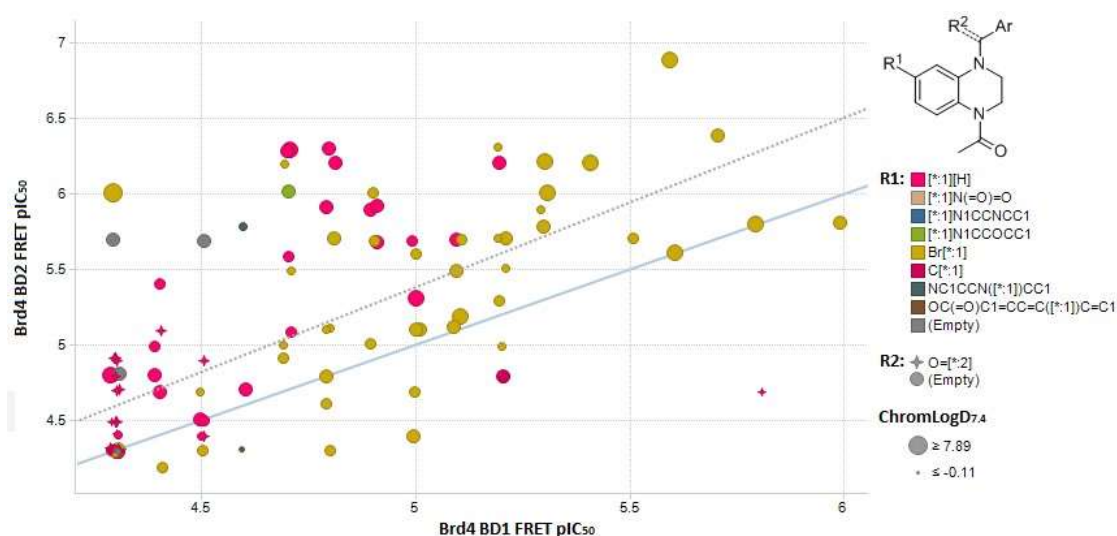


Figure 2.4. Scatter plot of Brd4 BD1 vs BD2 FRET pIC₅₀ for previously synthesised tetrahydroquinoxalines, showing lines of unity (blue) and best fit (dashed). Points are coloured by the 6-substituent (of note are gold for Br and magenta for H) and sized by ChromLogD_{7.4}. Stars indicate amide-linked shelf groups, circles CH₂-linked.

Optimisation efforts were largely limited to the WPF shelf-binding group and failed to deliver significant BD2 selectivity or potency, with no THQx molecules identified with either 50-fold BD2 selectivity or BD2 pIC₅₀ > 7. Simple lipophilic phenyls (**2.002-4**) were found to give the highest selectivity (Figure 2.5). Only H and Me were tested at the 2-position and a small number of 6-position groups were briefly investigated, with unsaturated heterocycles (**2.005**) appearing to reduce potency.²⁹⁰ Lipophilicity could be reduced by introducing an acid substituent (**2.006**), maintaining reasonable potency and selectivity. Heterocyclic WPF shelf groups were more polar but were poorly tolerated, as exemplified by pyridine **2.007**.

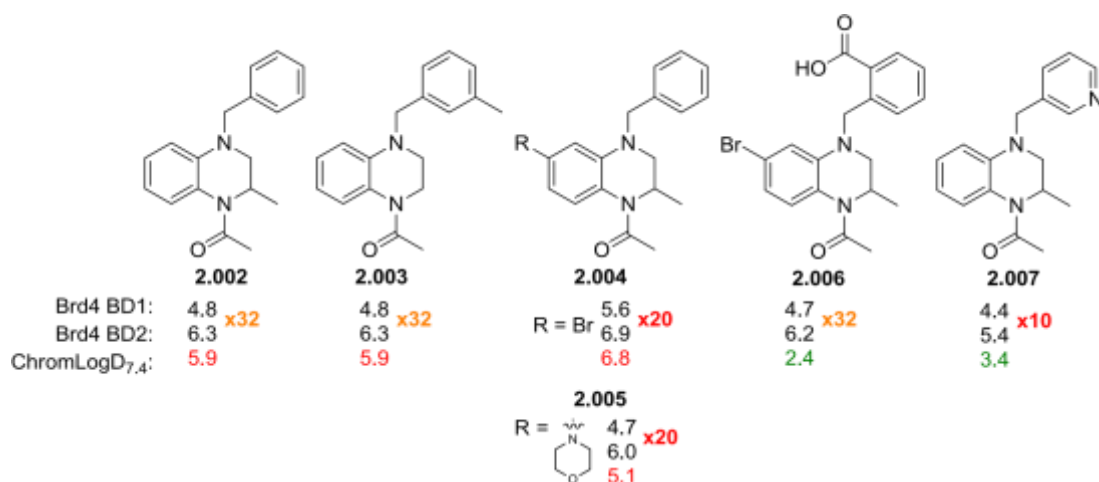


Figure 2.5. Current SAR knowledge for the THQx series, with key compounds from previous work. All potency data are n=3 or greater.

2.3.2 Optimisation Strategy

From the crystal structures (Figure 2.6), several main vectors were identified for optimization; a screen of small alkyl groups at the 2-position of the THQx ring to occupy the small lipophilic pocket, alternative substitution patterns on the phenyl ring interacting with the WPF shelf, and occupation of the ZA channel (Figure 2.2).²⁹³ The placement of sp^2 substituents at the 6-position may allow access to this region and confer potency due to lipophilic binding and π -interactions with the WPF Trp. These vectors were planned to be optimised individually, before combining the optimal substituents to give final compounds. To make the synthetic program as efficient as possible, optimisation was carried out on racemic compounds, with the role of individual enantiomers investigated once potent and selective compounds were obtained (*vide infra*). All compounds were tested in separate biochemical FRET assays against Brd4 BD1 and Brd4 BD2, in addition to physicochemical property assays and, later, *in vivo* phenotypic assays.

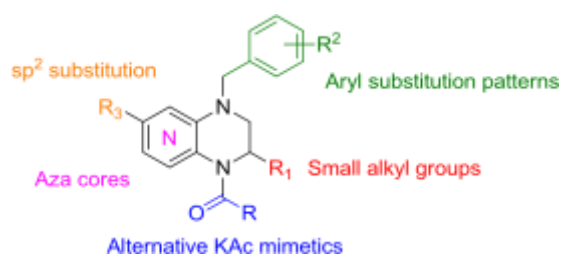
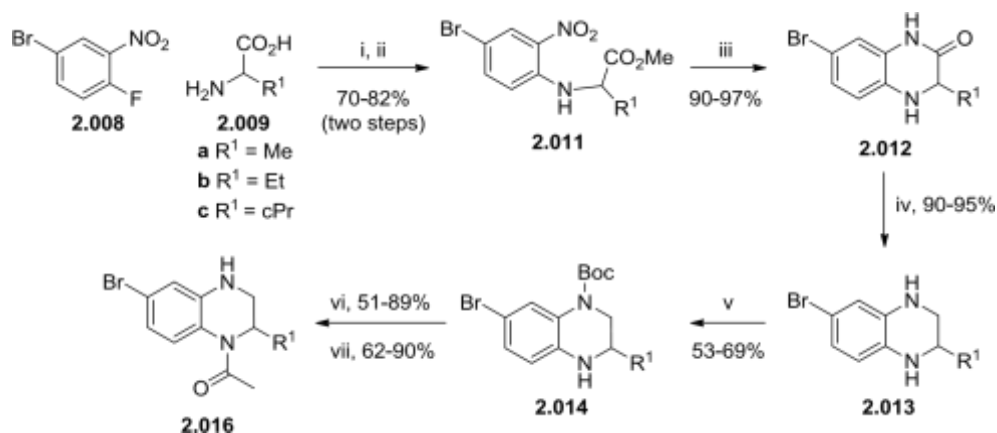


Figure 2.6. Strategy for optimisation of the THQx series.

2.3.3 The 2-Position

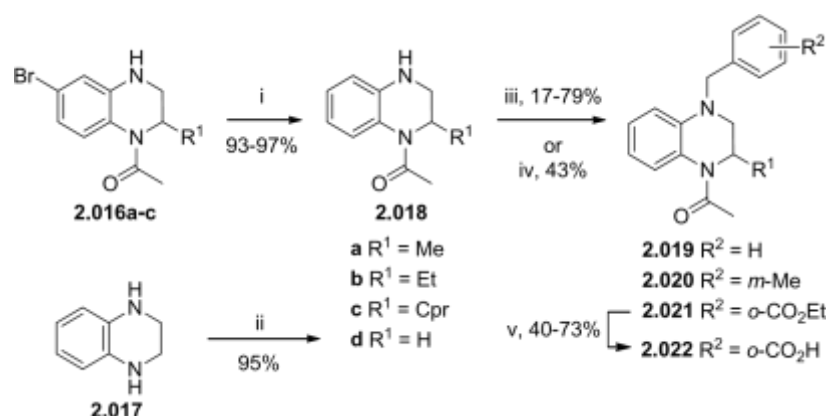
A strategy of late-stage diversity was chosen to enable rapid library synthesis. Pleasingly, the previous optimisation efforts generated a significant number of building blocks with varying C2 substitutions on multi-gram scale.²⁹⁰ The synthetic route used (Scheme 2.1) utilised a stepwise core construction to minimise regiochemical problems, synthesising intermediates as racemates for simplicity. It was envisioned that enantiopure compounds would be obtained by preparative chiral HPLC separation or single enantiomer synthesis when appropriate. An S_NAr reaction between fluorobenzene **2.008** and amino acids **2.009a-c** gave (after esterification) the amino ester **2.011**. Reduction of the nitro group and cyclisation with $SnCl_2$ gave quinoxalinone **2.012**, which could be reduced to the THQx **2.013** with borane-THF. The steric bulk of the 2-substituent and electron-withdrawing nature of the bromide allowed differentiation between the two amines, with Boc-protection affording **2.014** as the major product. Acetylation followed by Boc-deprotection gave **2.016a-c**, with synthetic handles at the 4- and 6-positions, on multi-gram scale.²⁹⁰ Although this route was effective, several limitations were evident. The frequent use of harsh reagents and conditions (e.g. thionyl chloride, gaseous HCl) was suboptimal from a safety and sustainability perspective, and the requirement for stoichiometric $SnCl_2$ was concerning. In addition, the yields for the acetylation and Boc deprotection were variable and lower than expected for such rudimentary steps. These concerns would be addressed when synthesising future batches of intermediates (*vide infra*).



Scheme 2.1. Representative synthesis of building blocks **2.15a-c**. Reagents and conditions: (i) K_2CO_3 , DMF, 80 °C; (ii) $SOCl_2$, MeOH, reflux; (iii) $SnCl_2$, EtOH, reflux; (iv) $BH_3 \cdot THF$, THF, 60 °C; (v) Boc_2O , DMAP, Et_3N , DCM, rt; (vi) Ac_2O , Et_3N , DCM, reflux; (vii) HCl, DCM, -20 °C.

To access compounds with no substituent at the 6-position and a variety of alkyl groups at the 2-position, the 6-Br moiety could be easily removed by hydrogenation under flow conditions to give **2.018b-c** in high yield (Scheme 2.2). The flow conditions were operationally simple and highly scalable, removing the need to handle flammable hydrogen gas and catalyst

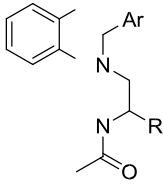
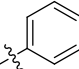
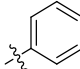
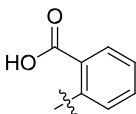
suspensions. Gram-scale batches of the 2-Me and 2-H analogues **2.018a** and **2.018d** were available from the previous GSK work,²⁹⁰ **2.018d** being synthesised from 1,2,3,4-tetrahydroquinoxaline **2.017** according to literature procedures.^{290,294} Subsequent reductive amination with substituted benzaldehydes (a precedent method of THQx benzylation²⁹⁵) or S_N2 displacement of a benzylic bromide gave the target compounds **2.019****2.021a-d**. For examples bearing a benzoic acid, the coupling reaction was undertaken using the corresponding ethyl esters and the product hydrolysed using aqueous LiOH to afford the final compounds **2.022a-d**. Yields for the coupling reactions were highly variable and at times low, due to incomplete reaction for some substrates and losses of material during HPLC purification.



Scheme 2.2 Representative synthesis of 6-H compounds. Reagents and conditions: (i) Flow hydrogenation, 10% Pd/C, H₂, MeOH, rt; (ii) Ac₂O, EtOH, 0 °C – rt; (iii) Benzylic bromide, K₂CO₃, DMF, 90-110 °C; (iv) Benzylic aldehyde, NaBH(OAc)₃, DCM, rt; (v) LiOH, H₂O, MeOH, THF, rt.

A small square array was performed, matching the three most promising WPF shelf aryls from the previous optimisation campaign (Ph, *m*-tolyl, and *o*-CO₂H) with varying C2 alkyl substitutions (H, Me, Et, cPr) intended to probe the lipophilic pocket identified from the crystal structure (Table 2.1). Unfortunately, the high potency and selectivity shown by *m*-toluyl **2.003** was lost when the C2 substituent was altered, and other substitutions of R=H tetrahydroquinoxalines **d** showed low potency and selectivity. This indicates that **2.003** is most likely an unreliable singleton, and the R=H series was not further investigated.

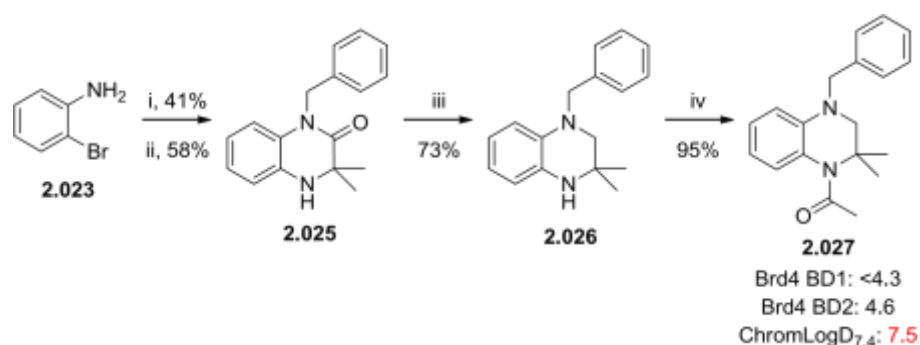
Table 2.1. WPF shelf/2-position square array of THQx compounds.

 Brd4 BD1, BD2 FRET pIC₅₀ (Selectivity) ChromLogD_{7.4}		Ar		
		 2.019	 2.020	 2.022
R	Me a	(2.002) 4.8, 6.3 (x32) 5.9	4.7, 6.0 (x20) 6.5	4.4 ^a , 5.8 (x25) 1.5
	Et b	5.0, 6.2 (x16) 6.5	4.9, 6.1 (x16) 7.1	4.5 ^b , 6.1 (x40) 1.9
	cPr c	4.7 ^c , 6.2 (x32) 6.7	4.6 ^c , 6.1 (x32) 7.2	<4.3, 6.1 (>x63) 2.2
	H d	5.0, 5.6 (x4) 5.6	(2.003) 4.8, 6.3 (x32) 5.9	<4.3, 5.3 (>x10) 1.2

Data are n=3 or greater unless otherwise specified. (a) n=1, <4.3 on two additional test occasions; (b) n=2, <4.3 on one additional test occasion; (c) n=3, <4.3 on one additional test occasion.

The simple phenyls **2.019** showed reasonable potency and selectivity, especially phenyl cyclopropyl **2.019c**, though no clear trend was evident. In contrast to the inconsistent SAR of the other groups tested, the acids **2.022** showed a consistent increase in BD2 potency and selectivity moving from H→Me→Et→cPr. Cyclopropyl acid **2.022c** had BD1 potency below the lower limit of the FRET assay, good BD2 potency and encouragingly consistent SAR. As such, **2.022c** was selected as a lead compound for further optimisation.

In addition to monosubstitution, *gem*-dimethyl substitution at C2 was investigated (Scheme 2.3). 2-Bromoaniline **2.023** was benzylated using reductive amination conditions, before undergoing a copper-catalysed Ullmann-type coupling with 2,2-dimethylglycine, followed by thermal cyclisation to give quinoxalinone **2.025**.²⁹⁶ Installing the benzyl group prior to cyclisation provided definitive differentiation between the tetrahydroquinoxaline nitrogen atoms and prevented the need for protecting groups. While the Ullman coupling/cyclisation proceeded in only moderate yield, this method was significantly shorter and more efficient than the previous method (Scheme 2.1) due to the one-pot methodology and lack of protecting groups. Lactam reduction with borane-THF gave **2.026**, before high-yielding acetylation to give the *gem*-dimethyl THQx **2.207**, which was poorly active against both BD1 and BD2. The methyl that occupies the lipophilic pocket most likely pushes the core too close to the opposite edge of the binding pocket to accommodate the second methyl group.



Scheme 2.3. Synthesis of *gem*-dimethyl THQx **2.027**. Potency data are n=3. Reagents and conditions: (i) PhCHO, AcOH, NaBH(OAc)₃, DCM, rt; (ii) 2,2-Dimethylglycine, CuCl, *N,N*-dimethylethylenediamine, K₃PO₄, DMSO, 110 °C; (iii) BH₃•THF, THF, 50 °C; (iv) AcCl, pyridine, DCM, rt.

X-ray crystal structures of phenyl **2.019c** and acid **2.022c** bound to the Brd2 BD2 bromodomain were obtained and compared to that of **2.003** bound to Brd4 BD2 (Figure 2.7). For the C-2-H compound **2.003** the saturated ring of the core twists to extend C2 towards the lipophilic pocket region formed from Val380, Leu387, Tyr390, and Tyr432 (Brd4 BD2 numbering). The 2-cyclopropyl substituent fully occupies this region, and as a consequence the saturated ring adopts a flatter conformation with N4 being pushed back and the position of the benzyl group on the WPF shelf changing. This causes the phenyl rings of **2.019c** and **2.022c** to occupy a similar position to the toluyl methyl of **2.003**, making the same lipophilic interactions. This offers an explanation as to the outlying activity of **2.003** and the nonadditive SAR.

The phenyl ring of **2.019c** makes the same interactions with the BD2-specific His433 (Brd2) as **2.003**. Although **2.019c** and **2.022c** overlay very closely, the acid group of **2.022c** does not interact with His433, forming a through-water interaction with Asp434. In this structure His433 instead adopts an alternative position to that seen for phenyl **2.019c**, being replaced by solvent. In Brd4 BD2 Asp343 is replaced by Glu438, so the observed interaction may not occur. In the structure of **2.019c**, a water molecule is seen close to the position of the acid group of **2.022c**, indicating this area is a favourable location for a polar group. The highly conserved nature of the water network at the base of the KAc binding pocket can also be observed. From racemic samples, only the (*S*)-enantiomer crystallised in the bromodomain, consistent with the higher activity observed for (*S*)-**1.14**.¹¹⁴

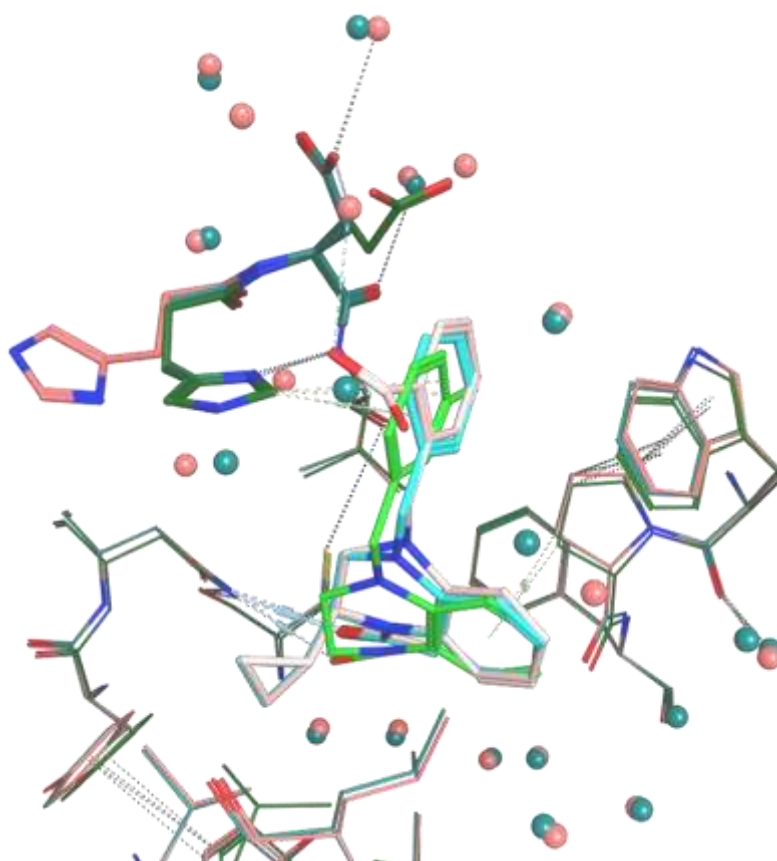


Figure 2.7. **2.003** bound to Brd4 BD2 (green, 1.83 Å, solvent omitted for clarity)²⁹² overlaid with **2.019c** (cyan, 1.78 Å)²⁹² and **2.022c** (pink, 1.78 Å)²⁹² bound to Brd2 BD2.

While these crystal structures explain the BD2 binding mode, it should be noted that the BD2 potency of most of the square array compounds is broadly similar, and the increased selectivity is due to reduced BD1 potency. To examine this, **2.019c** was also crystallised into Brd4 BD1 (Figure 2.8). The binding mode is highly similar in both bromodomains, though in BD2 His433 packs against the phenyl ring, making edge-to-face π -interactions and improving the contact between the ring and the WPF stack. In BD1, the phenyl ring adopts a slightly flatter orientation on the WPF shelf, so contact with the WPF stack is poorer. In addition, the gatekeeper differs between BD1 (Ile, Ile146 for Brd4 BD1) and BD2 (Val, Val 435 for Brd2 BD2), making the BD2 KAc pocket larger and so more accommodating of the THQx core. This is accentuated by the 2-cPr motif, which pushes the core closer to the gatekeeper.

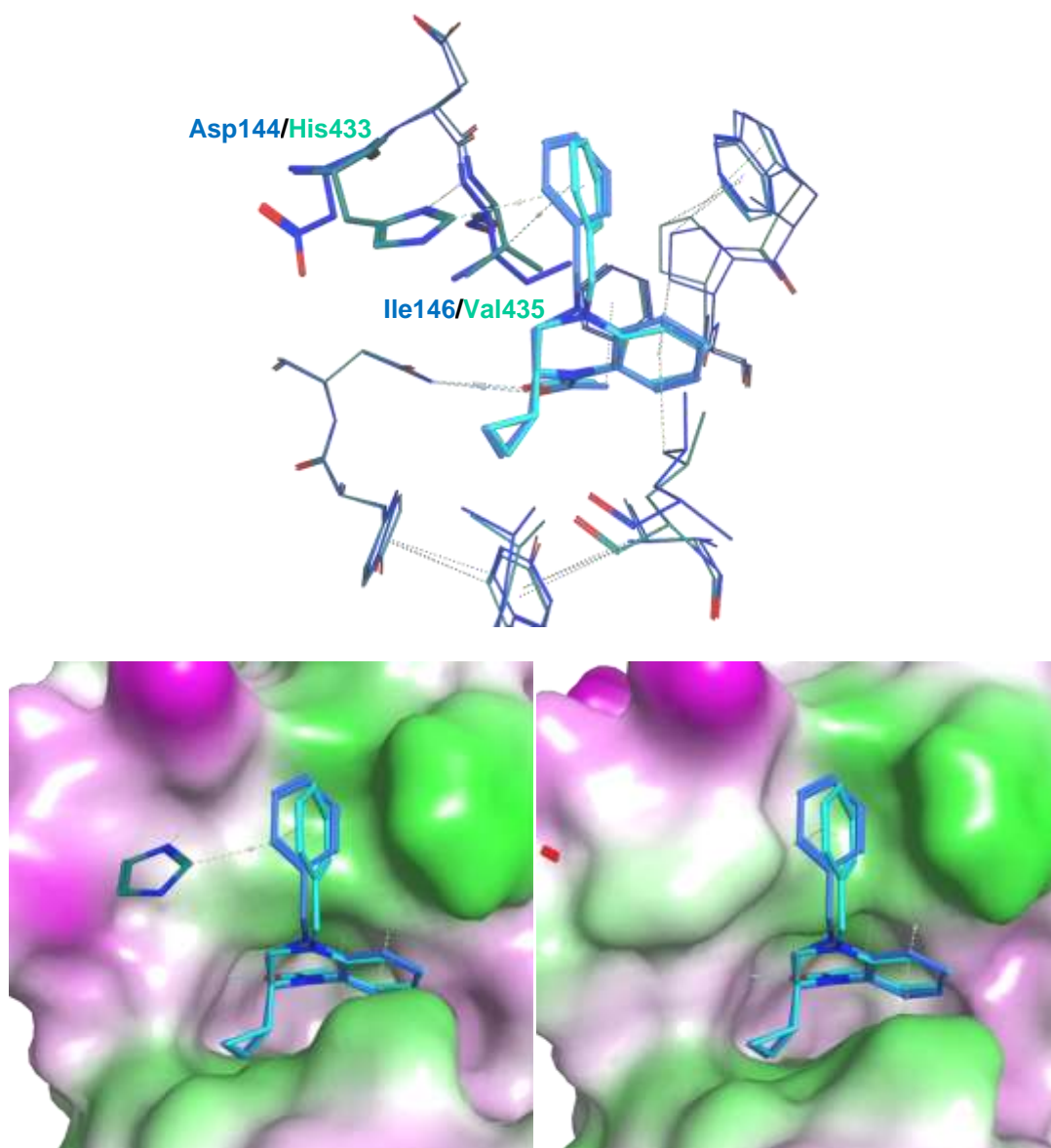


Figure 2.8. **2.019c** bound to Brd2 BD2 (cyan, 1.78 Å),²⁹² overlaid with **2.019c** bound to Brd4 BD1 (blue 1.50 Å).²⁹² *Top:* No surface, key residues are bolded. *Bottom left:* Showing the BD1 surface. *Bottom right:* Showing the BD2 surface. Surfaces are coloured by lipophilicity; green=hydrophobic, pink=hydrophilic.

From the crystal structure, it was theorised that introduction of a *cis*-fused ring at the 2- and 3-positions could better occupy the pocket where the 2-cPr sits and potentially pack against the underside of the His. This would also rigidify the saturated THQx ring and so reduce any entropy loss from conformational change and loss of degrees of freedom on binding.²⁹⁷ To this end, the ring-fused structure **2.028** (Figure 2.9) was designed, which is conformationally locked and has good shape complementarity with the BD2 binding site. The cyclopentylfused structure was chosen as larger rings clash with the edge of the binding pocket and are themselves flexible, while smaller rings were considered too strained to synthesise.

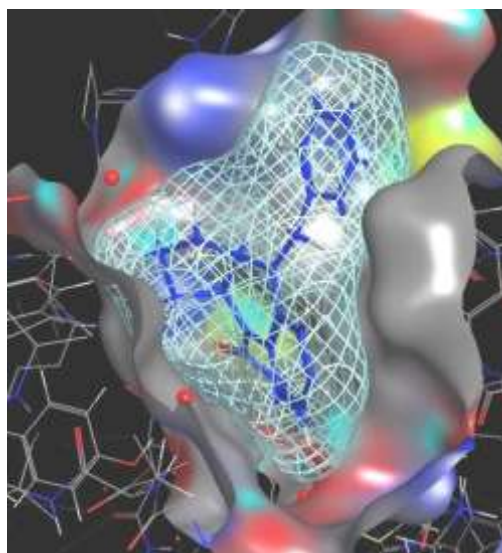
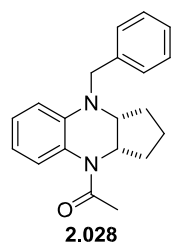
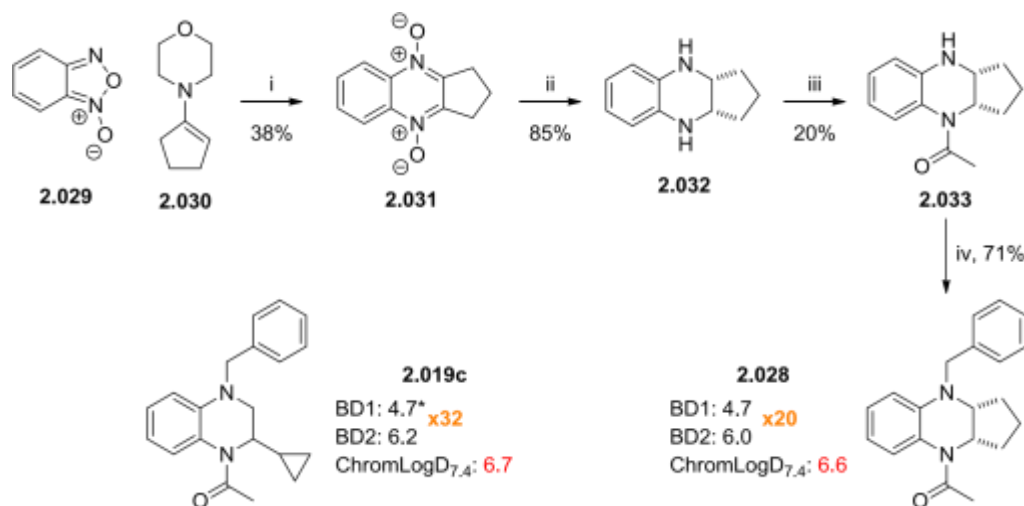


Figure 2.9. Ring-fused THQx **2.028**, and docking into Brd4 BD2.

The synthesis of **2.028** (Scheme 2.4) was achieved by Beirut cyclisation²⁹⁸ of benzofuroxan **2.029** and commercially available enamine **2.030**, to give the di-*N*-oxide **2.031** in reasonable yield.^{299–301} Reduction with sodium borohydride³⁰² gave exclusively the *cis*-regioisomer **2.032** in excellent yield, however acetylation proved difficult due to di-acetylation, with mono-acetyl product **2.033** isolated in poor but usable yield. Reductive amination gave the ring-fused product **2.028**, which disappointingly proved slightly less potent and selective than the 2cyclopropenyl THQx **2.019c**, though lipophilicity remained at a similar (albeit high) level. The reduced potency may be due to a minor clash with the binding site (Figure 2.9) or suboptimal occupation of the lipophilic pocket normally occupied by the cyclopropyl group.

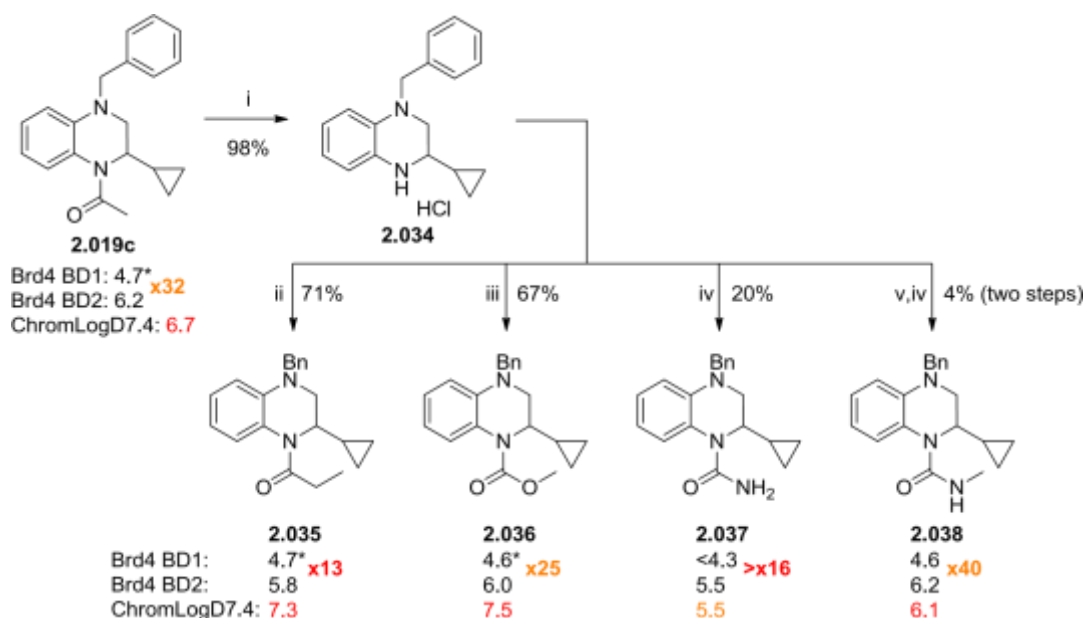


Scheme 2.4. Synthesis and biological activity of ring-fused THQx **2.028**. Reagents and conditions: (i) MeOH, rt; (ii) NaBH₄, MeOH, rt; (iii) AcCl, pyridine, DCM, rt; (iv) PhCHO, NaBH(OAc)₃, DCM, rt. Potency data are n=3 or greater unless specified. *n=3, <4.3 on one additional test occasion.

2.3.4 The KAc mimetic

While the X-ray crystal structures of **2.003** and **2.019c** showed good overlay of the THQx acetyl group and those of the native peptide and published inhibitor **1.14**, a brief investigation of the KAc mimetic was undertaken (Scheme 2.5). The amide of 2-cyclopropyl compound **2.019c** was removed by hydrolysis in quantitative yield using methanol and HCl, and the resulting amine **2.034** acylated to give **2.035-2.038**. Acylations with propionyl chloride and methyl chloroformate effectively gave **2.035** and **2.036**, and the urea **2.037** could be accessed using potassium cyanate under microwave irradiation, though in poor yield due to incomplete conversion and side reactions. However, the methyl urea **2.038** proved troublesome, with the common methyl isocyanate alternative *N*-succinimidyl

N-methylcarbamate³⁰³ giving no product. A two-step method with formation of an activated *p*-nitrophenol carbamate before displacement with methylamine²⁹⁵ gave the desired product, but in low yield. This may be due to the volatility of methylamine at the reaction temperature.



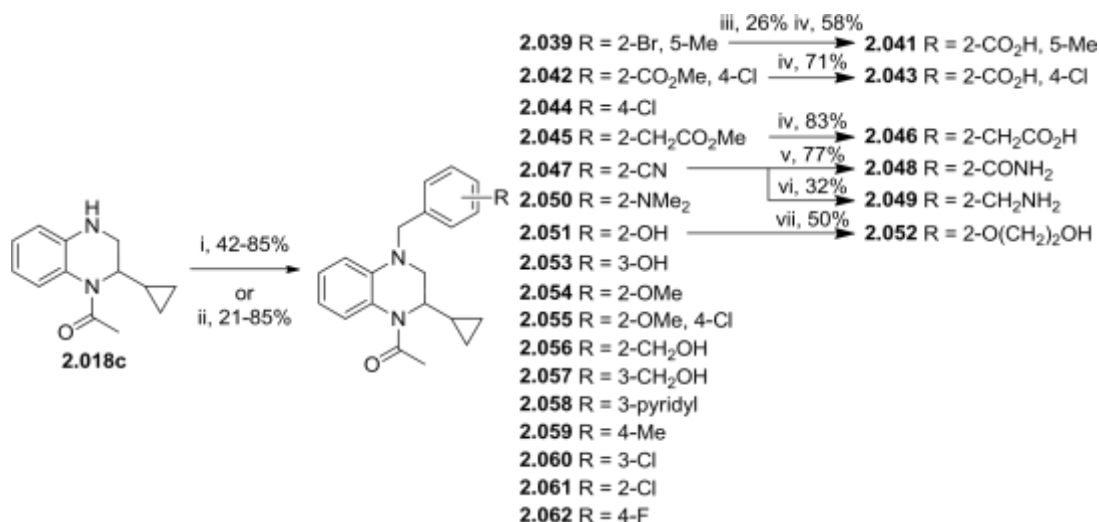
Scheme 2.5. Synthesis and activity of alternative KAc mimetic THQx compounds. Reagents and conditions: (i) 35% HCl, MeOH, 65 °C; (ii) Propionyl chloride, pyridine, DCM, rt; (iii) methyl chloroformate, pyridine, DCM, rt; (iv) KOCN, 1 M HCl, H₂O, 80 °C, μ W; (v) *p*-nitrophenol chloroformate, pyridine, DMAP, DCM, rt; (iv) 2 M MeNH₂ in THF, 50 °C. Potency data are n=3 or greater unless specified. *n=3, <4.3 on one additional test occasion.

The propyl analogue **2.035** and ester **2.036** were tolerated, but BD2 potency and selectivity were reduced slightly – most likely due to the KAc mimetic becoming too large. Urea **2.037** was not tolerated, unsurprising given the lipophilic nature of this region of the binding pocket, but was able to significantly reduce the lipophilicity of the template. Methyl urea **2.038** showed comparable potency and selectivity to the acetyl analogue **2.019c**, with a reasonable reduction

in ChromLogD_{7.4}, but given its onerous synthesis and lack of a significant benefit the acetyl KAc mimetic was maintained as the preferred group moving forwards.

2.3.5 The WPF-Shelf Group

While **2.022c** had good potency and selectivity, due to the acid moiety it was almost completely impermeable in an artificial membrane permeability assay (Table 2.2). A screen of WPF shelf groups was initiated, focussing on polar groups *ortho* to the benzyl linker. The compounds were synthesized from **2.018c** in a similar manner to Scheme 2.2, using benzylic bromide displacement or reductive amination as appropriate based on reagent availability (Scheme 2.6). As before (Scheme 2.2), benzylation yields were variable and substrate dependant, with incomplete reactions or HPLC losses accounting for the majority of the low yields. The trisubstituted benzoic acid **2.041** was synthesised by Pd-catalysed carbonylation/esterification of the corresponding bromide **2.039** with Mo(CO)₆ under microwave conditions,³⁰⁴ followed by saponification of the resulting ester **2.040** to give **2.041**. The carbonylation proceeded poorly and the use of stoichiometric Mo(CO)₆ is disfavoured due to its high toxicity, expense and the generation of high pressures in a sealed system. However, the method was known to be tolerant of *N*-acetyl groups,³⁰⁴ and on small scale these risks were sufficiently manageable to obtain the final compound. The nitrile **2.047** was converted to the primary amide **2.048** using the very mild H₂O₂ and K₂CO₃ conditions developed by Katritzky,³⁰⁵ and to the benzylamine **2.049** by flow hydrogenation over Raney Ni. Phenol **2.052** was alkylated with 2-bromoethanol to afford the hydroxyethanol analogue **2.052**.



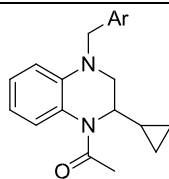
Scheme 2.6. Synthesis of WPF shelf array. Reagents and conditions: (i) Benzylic bromide, K₂CO₃, DMF, 90-110 °C, (**2.042**, **2.047**, **2.056-2.058**); (ii) Benzylic aldehyde, NaBH(OAc)₃, DCM, rt, (**2.039**, **2.044**, **2.045**, **2.050-2.055**, **2.059-2.062**); (iii) Mo(CO)₆, Herrmann's catalyst, DIPEA, 1-butanol, 1,4-dioxane, μW,

150 °C; (iv) LiOH, H₂O, MeOH, THF, rt; (v), H₂O₂, K₂CO₃, DMSO, rt; (vi) Flow hydrogenation, Raney Ni, 50 bar H₂, EtOH, 50 °C; (vii) 2-Bromoethanol, K₂CO₃, DMF, 110 °C.

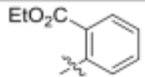
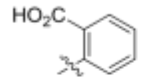
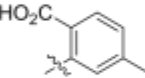
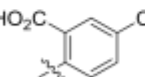
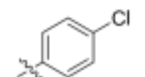
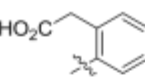
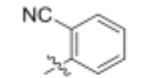
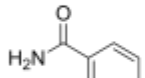
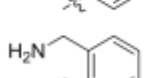
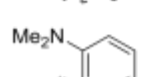
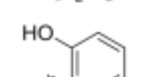
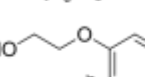
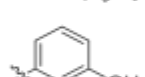
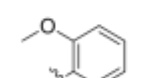
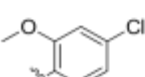
These compounds were tested in the Brd4 FRET assay and their physicochemical properties (lipophilicity represented by ChromLogD_{7.4},¹⁶ CLND solubility^{19,25} and artificial membrane permeability (AMP)²⁹) were profiled using GSK's high-throughput automated profiling systems. The results are shown in Table 2. The corresponding ethyl ester of **2.022c** (**2.021c**) displayed similar BD2 potency but increased BD1 potency, indicating that the polarity or charged nature of the acid is required for low BD1 potency. Combination of the tolyl and benzoic acid functionalities (**2.041**) was detrimental to BD2 potency, while addition of a *p*-Cl (**2.043**) or a methylene spacer (**2.046**) had no significant effect on binding. As with **2.022c**, the acids showed poor permeability, though aqueous solubility (as measured by CLND) was good. *Para*-chlorophenyl is a common WPF shelf-binding group, utilised in BET inhibitors such as **1.06**¹²⁹ and **1.14**.¹¹⁴ However, the 4-Cl analogue **2.044** was potent but less selective compared to **2.022c**, again showing the role of the *ortho* acid in increasing selectivity, and while the increased lipophilicity improved permeability it decreased solubility. Though the nitrile **2.047** was poorly selective, the corresponding amide **2.048** maintained BD2 potency and was pleasingly selective with excellent physicochemical properties, indicating that the beneficial effect of the 2-substituent is not necessarily ionic in nature. Indeed, the basic compounds **2.049** and **2.050** showed high BD2 potencies and reasonable selectivities, as did the neutral phenols **2.051**, **2.053** and methoxy **2.054**. However, these examples generally showed higher ChromLogD, and as such were less soluble. Intriguingly, addition of a 4-Cl substituent to the methoxy compound **2.054** gave **2.055**, which showed a significant increase in selectivity at the cost of BD2 potency, increased lipophilicity and poor solubility. The *ortho*- and *meta*- phenols **2.051** and **2.053** were also well tolerated, though potency fell when the substituent was moved from the *ortho* to the *meta* position.

The *ortho*-benzylic alcohol **2.056** gave excellent selectivity and BD2 potency in excess of the original acid **2.022c**, again with a drop in potency seen on moving substitution to the *meta* position (**2.057**). Separation and testing of the two enantiomers of **2.056** showed the biological activity is derived solely from one enantiomer, **2.056a**, which was also highly permeable. The binding preference observed for the (*S*)-enantiomer in the crystal structures of **2.019c** and **2.022c**, and difference in enantiomer activity for **1.14**, allows speculation that (*S*)-**2.056** would be the more potent isomer. The ethylene glycol derivative **2.052** was tested, and found to maintain the high potency and selectivity of **2.056** with similar properties. The 3pyridyl **2.058** (the best shelf heterocycle from the legacy work²⁹⁰) exhibited excellent physicochemical properties, but was poorly potent and selective.

Table 2.2. Optimisation of the WPF shelf binding group.



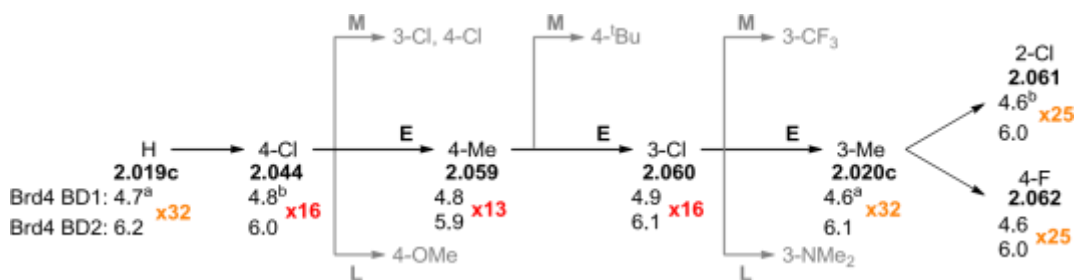
Cpd	Ar	Brd4 FRET	pIC ₅₀	BD2	Chrom-	AMP	CLND
		BD1	BD2	Sel.	LogD _{7.4}	(nm/s)	Sol. (uM)

2.021c		4.9	6.0	x13	7.2	230	32
2.022c		<4.3 ^b	6.1	>x63	2.2	36	399
2.041		<4.3 ^b	5.6	>x20	2.4	80	402
2.043		4.4 ^b	5.9	x32	2.9	33	321
2.044		4.8 ^b	6.0	x16	7.2	270	8
2.046		<4.3 ^b	6.0	x50	2.4	19	249
2.047		4.6	5.6	x10	6.0	510	179
2.048		<4.3 ^b	5.9	>x40	3.9	620	363
2.049		4.7	6.2	x32	2.7	540	279
2.050		4.7	6.3	x40	7.5	120	39
2.051		4.7	6.3	x40	5.2	560	131
2.052		4.6	6.5	x79	4.7	450	184
2.053		4.8	6.2	x25	4.9	600	237
2.054		4.8	6.4	x40	6.9	430	30
2.055		<4.3 ^b	6.0	x50	7.5	410	2
		Brd4 FRET pIC₅₀	BD2	Chrom-	AMP	CLND	

Cpd	Ar	BD1	BD2	Sel.	LogD _{7.4}	(nm/s)	Sol. (uM)
(±)- 2.056		4.5	6.3	x63	4.9	610	183
2.056a		4.8	6.7	x79	4.7	620	290
2.056b		<4.3 ^b	<4.3 ^b	-	4.7	530	302
2.057		4.6	6.1	x32	4.7	800	499
2.058		<4.3 ^b	5.2	x8	4.0	830	321
2.059		4.8	5.9	x13	7.2	260	44
2.060		4.9	6.1	x16	7.2	200	4
2.061		4.6 ^b	6.0	x25	7.8	270	33
2.062		4.6	6.0	x25	8.7	380	191

All potency data are n = 3 or greater unless specified. (a) Lower binding limit of the assay; (b) n=2, <4.3 on one additional test occasion.

In order to gain quantitative insights into the role of the steric, electronic, and lipophilic properties of the shelf group, a Topliss analysis was undertaken. This QSAR method involves the stepwise application of a decision tree to rapidly access the most potent compounds from a series, based on whether the previous iteration increased, decreased or did not affect potency.³⁰⁶ Following this approach for the THQx WPF-shelf group (Scheme 2.7), moving from phenyl **2.019c** to 4-Cl **2.044** did not affect potency so the 4-Me analogue **2.059** was synthesised. This was also equipotent, as was the 3-Cl **2.060**, and the remaining three compounds from this branch (3-Me **2.020c**, 2-Cl **2.061**, and 4-F **2.062**) were tested. No increase in BD2 potency was observed throughout but this approach did lead to a moderate increase in selectivity over the course of the scheme. While encouraging, this selectivity was below that seen for **2.022c** and **2.056a**, indicating it is the result of specific interactions with the protein and not stereoelectronic factors.

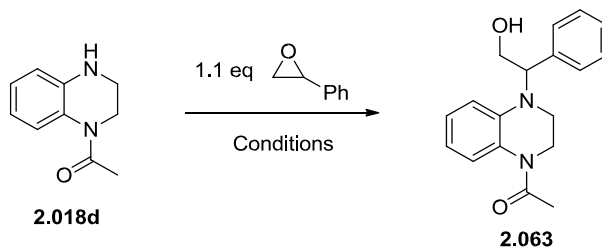


Scheme 2.7. Topliss scheme (non-progressed branches omitted for clarity) and potencies of the relevant compounds. M = more potent, E = equipotent, L = less potent. All data are n=3 or greater unless specified. (a) n=3, <4.3 on one additional test occasion; (b) n=2, <4.3 on one additional test occasion.

The origin of selectivity of these compounds is as yet unknown, with only subtle changes in potency and selectivity achieved through this optimisation. The relatively flat SAR may be due to the vertical alignment adopted by the aryl group in order to stack between the His and WPF stack in BD2, with substituents pointing into solvent and making no significant interactions to the protein, aside from certain polar *ortho* substituents such as those included in **2.056** and **2.052**, which are encouragingly potent and selective.

2.3.6 Linker Substitution

The two benzylic centres present in **2.056** are potentially sites of oxidative metabolism by cytochrome P450 enzymes.³⁰⁷ It was theorised that moving the CH₂OH group to the benzylic linker position could prevent this, or open up a new vector for substitution and access to the crucial histidine residue. It was envisioned that these compounds could be accessed by regioselective ring-opening of epoxides, and as such a variety of conditions^{308–314} were examined for the synthesis of model substrate **2.063** (Table 2.3).

Table 2.3. Investigation of epoxide opening conditions

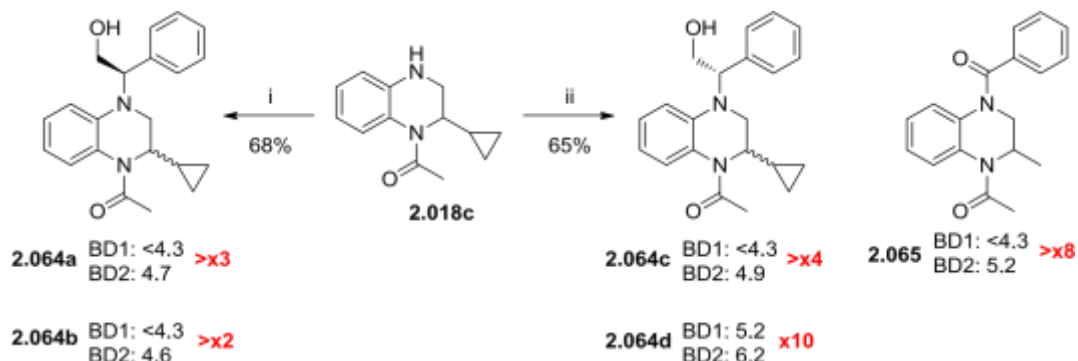
Entry	Conditions	Conversion (%)	2.063 (%)
1 ₃₀₈	10 mol% Sm(OTf) ₃ , DCM, rt, 24 h	43	23 ^a
2 ₃₀₉	10 mol% InBr ₃ , DCM, rt, 24 h	52	33 ^a
3 ₃₀₉	10 mol% BiCl ₃ , DCM, rt, 24 h	15	0 ^a
4 ₃₁₀	10 mol% ZrCl ₄ , DCM, rt, 24 h	26	13 ^a
5 ₃₁₁	1.4 eq Ti(O ⁱ Pr) ₄ , 2-MeTHF, 75°C, 24 h	66	20 ^b
6 _{312,313}	Trifluoroethanol, 75 °C, 24 h	90	60 ^b
7 ₃₁₄	Water, 75 °C, 24 h	23	18 ^b
8 ₃₁₄	1:1 Water/1,4-Dioxane, 80°C, 24 h	0 ^a	0

^a ^b
By LCMS. Isolated yield

Metal halides^{308,309} (Entries 1, 2, 4) all gave limited conversion to the desired product except for bismuth trichloride (Entry 3).³⁰⁹ The use of stoichiometric titanium(IV) isopropoxide³¹¹ with heating gave better conversion but a low isolated yield (Entry 5). However, simply refluxing the THQx **2.018d** and styrene oxide in the weakly acidic solvent trifluoroethanol (TFE)^{312,313} gave excellent conversion and a good isolated yield (Entry 6). Ring opening of epoxides in hot water has been reported as a more sustainable procedure,³¹⁴ and these conditions gave slow but clean conversion (Entry 7), with limited solubility of **2.018d** hindering the reaction. Introduction of an organic co-solvent (Entry 8) gave no reaction.

With the TFE ring-opening conditions in hand, the 2-cyclopropyl derivatives were synthesised (Scheme 2.8). Given that **2.018c** is a racemic mixture and the epoxide opening creates a new chiral centre, enantiopure epoxides were used to produce diastereomeric pairs. Ring opening gave the two diastereomers, which could easily be separated by HPLC, in 1:1 mixtures, and was assumed to proceed with inversion of stereochemistry. The absolute configuration of the products could not be assigned by 2D NMR and the compounds were tested with the C2 stereochemistry unknown, though ¹H NMR spectra (Figure 2.10) clearly showed that **2.064a/c** and **2.064b/d** were the enantiomeric pairs. All the isomers **2.064a-d** tested had very low potency and selectivity and compounds of this type were not further investigated. The higher

potency of **2.064d** allows speculation this may be the *S,S*-diastereomer, where the cyclopropyl group occupies the lipophilic pocket as seen in Figure 2.7 and the CH₂OH group avoids a clash with the WPF stack. In addition, the amidelinked analogue **2.065** was obtained from the GSK compound collection and found to also exhibit BD2 potency and bias, though potency was significantly lower than for **2.002**.



Scheme 2.8. Compound synthesis by epoxide ring-opening. Potency data are n=3 or greater. Reagents and conditions: (i): (*R*)-styrene oxide, TFE, 75 °C; (ii): (*S*)-styrene oxide, TFE, 80 °C.

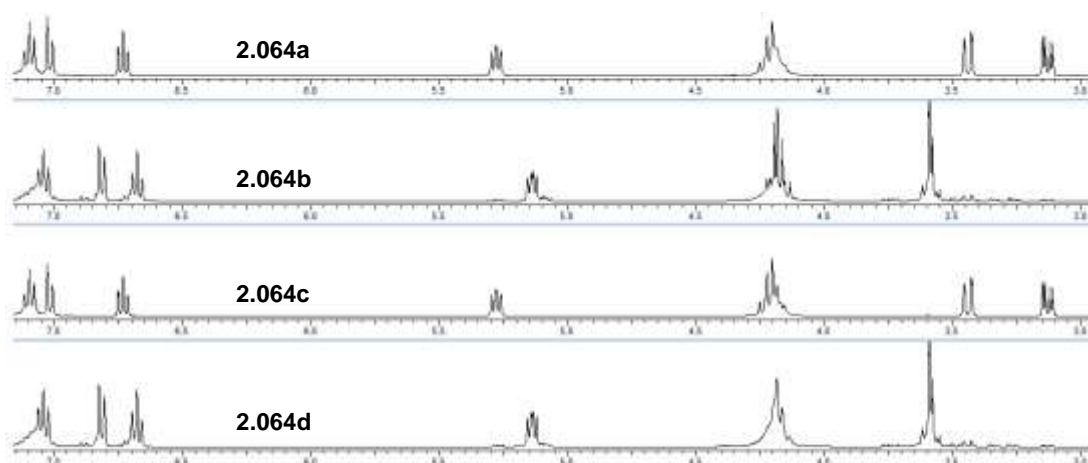


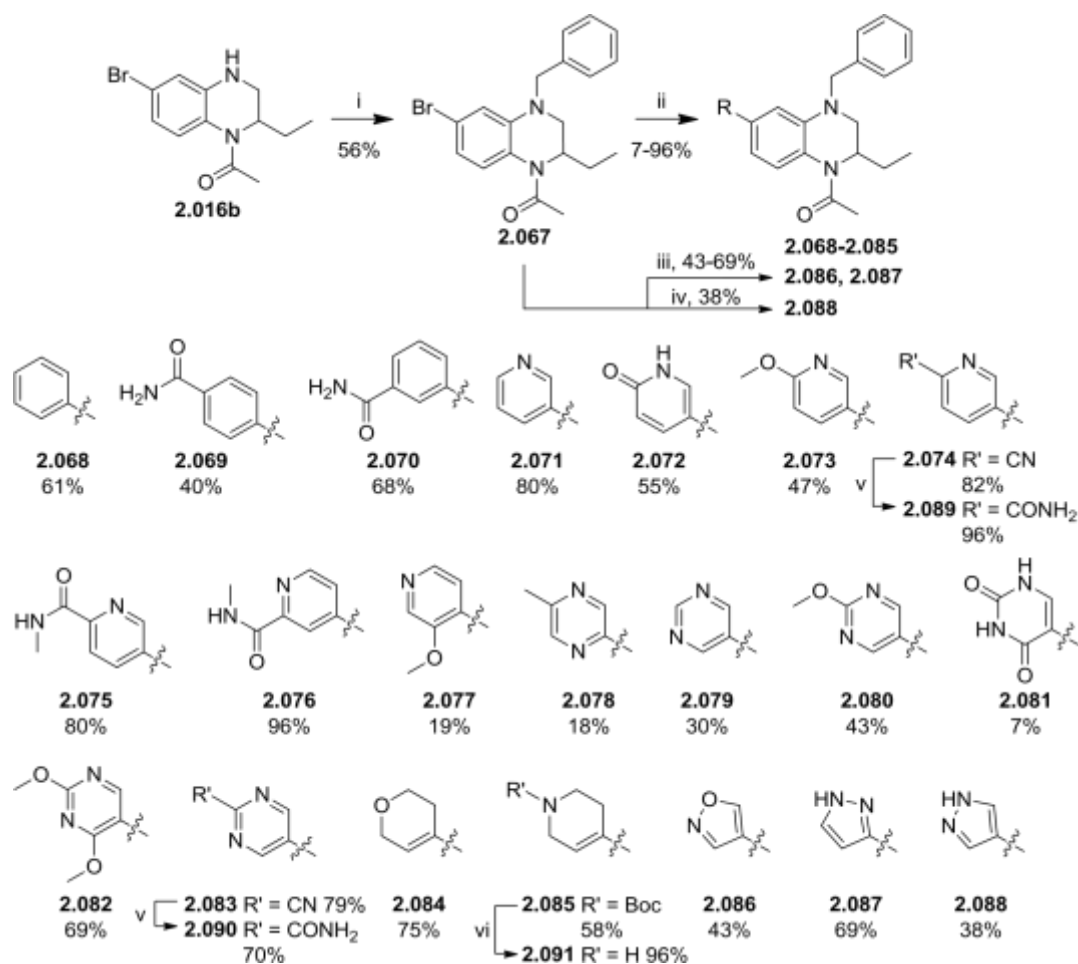
Figure 2.10. Overlaid ¹H NMR spectra of **2.064a-d**, showing enantiomeric pairs.

2.3.7 6-Substitution

At the onset of this investigation, the 6-position of the THQx series was relatively unexplored, with examples limited to bromides and *N*-linked saturated heterocycles (see **2.005**) which were generally less potent and selective compared to the unsubstituted compounds.²⁹⁰ The X-ray crystal structures of 6-unsubstituted compounds (Figure 2.3) show that the 6-position of the THQx core overlays closely with that of **1.14**, from which an aryl group is attached to occupy the ZA channel. For **1.14**, the placement of π -character at this vector increased potency by

forming edge-to-face π -interactions with the WPF tryptophan,¹¹⁴ and so this vector was examined in the THQx series in the hope of eliciting a similar effect. High numbers of aromatic rings are associated with decreased aqueous solubility, p450 inhibition, and promiscuity,^{16,19,20} and the array was designed to minimise these potential liabilities. Heteroaromatics and some non-aromatic 6-substituents were primarily targeted, as they have been shown to present a reduced developability risk compared to carboaromatics.²⁰

Therefore, 6-aryl compounds were synthesised *via* benzylation of **2.016b** to give **2.067**, followed by Suzuki-Miyaura coupling to afford **2.068-2.088** (Scheme 2.9). Carried out under microwave conditions, the reactions were rapid and well-suited to parallel synthesis methods. Although most reactions proceeded well under Pd(dppf)Cl₂/Cs₂CO₃ conditions, some electron-deficient examples (such as **2.078** and **2.081**) coupled in poor yield due to competing protodeboronation and poor reagent stability.³¹⁵ *Ortho*-substitution of the boronic acid or ester (**2.077**) was also detrimental to yield as a result of increased steric hindrance.



Scheme 2.9. Synthesis of 6-aryl compounds. Reagents and conditions: (i) BnBr, K₂CO₃, DMF, 90 °C; (ii) ArB(OH)₂ or ArBPin, Pd(dppf)Cl₂, Cs₂CO₃, 1,4-dioxane, H₂O, μ W, 110 °C; (iii) ArBPin, Pd(dppf)Cl₂,

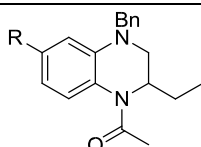
DIPEA, 1,4-dioxane, H₂O, μ W, 110 °C; (iv) (1-(Boc)-1*H*-pyrazol-4-yl)boronic acid pinacol ester, Pd₂(dba)₃, XPhos, K₃PO₄, 1-butanol, μ W, 115 °C; (v) H₂O₂, K₂CO₃, DMSO, rt; (vi) TFA, DCM, rt.

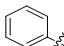
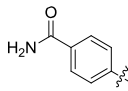
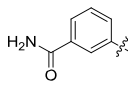
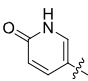
Due to competing protodeboronation, 5-membered heterocycles required modified conditions, specifically DIPEA as base for isoxazole **2.086** and Pd₂(dba)₃ with XPhos for pyrazole **2.088**.³¹⁶ For the preparation of **2.088**, the use of the Boc-protected pyrazole improved the stability of the boronic ester, with the Boc group being removed from the product under the reaction conditions. Amidopyridine **2.089** and amidopyrimidine **2.090** were synthesised by H₂O₂/K₂CO₃ oxidation of the corresponding nitriles **2.074** and **2.083**, while the Boc group was removed from tetrahydropyridine **2.085** with TFA to give **2.091**.

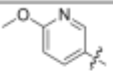
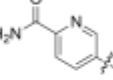
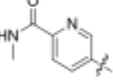
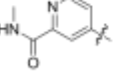
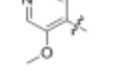
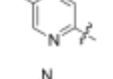
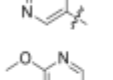
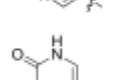
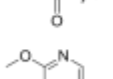
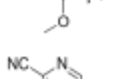
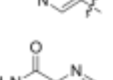
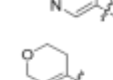
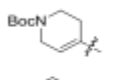
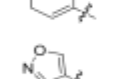
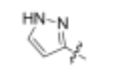
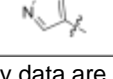
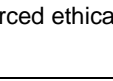

The biochemical potencies and physicochemical properties of the 6-substituted THQxs are shown in Table 2.4. In addition to Brd4 potency and selectivity, a 6-substituent was desired that was not detrimental (and ideally beneficial) to the overall physicochemical properties of the molecule. In addition to ChromLogD_{7.4},¹⁶ CLND solubility^{19,25} and AMP,²⁹ human serum albumin (HSA) binding³¹⁷ was measured. Compounds with pIC₅₀ > 6.8 were progressed to the next level of the screening cascade, being profiled in cellular assays using human isolated peripheral blood mononuclear cells (PBMCs) and whole blood (hWB). Treatment of the cells with the bacterial endotoxin lipopolysaccharide (LPS) causes the PBMCs (and other immune cells in the hWB) to elicit an immune response and release the proinflammatory cytokine MCP1. MCP1 production is reduced by treatment of the cells with pan-BET inhibitors,¹⁰¹ allowing this assay to be used as a test for cellular penetration and the compounds' ability to mediate an immune response.

Table 2.4 Optimisation of the 6-aryl group.

Cpd	R	Brd4 BD1/BD2 pIC ₅₀	BD2 Sel.	Chrom LogD _{7.4}	CLND Sol. (μ M)	AMP (nm/s)	HSA bind. (%)	PBMC/hWB MCP1 pIC ₅₀
2.019 b	H	5.0 / 6.2	x16	6.5	171	620	97	-



-		2.068 5.8 / 6.6 x6	7.9	47	550	99
6.8 / 5.7		2.069 6.4 / 7.3 x8	4.4	143	440	98
7.0 / 5.2		2.070 6.3 / 7.2 x8	4.7	146	430	97
6.4 / <5		2.071 5.8 / 7.0 x16	5.6	198	550	97
2.072 6.1 / 7.1	x10	3.5	239	550	95	7.1 / 6.0 Brd4 CLND HSA

Cpd	R	BD1/BD2 pIC ₅₀	BD2 Sel.	Chrom LogD _{7.4}	Sol. (μ M)	AMP (nm/s)	bind. (%)	PBMC/hWB MCP1 pIC ₅₀
2.073		5.9 / 7.0	x13	7.0	94	300	98	6.2 / 5.3
2.089		6.2 / 7.2	x10	4.5	36	510	96	6.9 / 5.7
2.075		6.1 / 7.2	x13	5.3	209	560	97	6.5 / 5.6
2.076		5.9 / 7.0	x13	5.4	145	630	97	6.7 / 5.3
2.077		5.3 / 6.3	x10	5.4	205	530	98	-
2.078		5.7 / 6.9	x16	5.9	158	530	-	6.4 / 5.1
2.079		5.5 / 6.8	x20	4.9	307	720	96	6.5 / <5
2.080		5.6 / 7.0	x25	5.8	91	520	97	6.5 / 5.4
2.081		5.2 / 6.3	x13	3.0	65	92	94	-
2.082		5.4 / 6.4	x10	6.3	95	420	96	-
2.083		6.6 / 7.0	x3	6.3	27	340	97	7.4 / 6.1
2.090		5.7 / 7.0	x20	3.6	308	410	94	7.1 / 6.0
2.084		5.8 / 6.8	x10	6.5	142	470	97	6.6 / -
2.085		5.8 / 6.8	x6	8.1	27	370	98	6.5 / -
2.091		5.5 / 6.8	x20	2.8	368	270	90	6.8 / -
2.086		5.8 / 6.9	x13	5.9	138	370	97	6.4 / 5.1
2.087		6.2 / 7.1	x8	4.6	125	340	97	6.8 / 5.4
2.088		6.4 / 7.3	x8	4.2	113	570	97	7.3 / 5.4

All potency data are n=2 or greater. Dashes indicate no data available. The human biological samples were sourced ethically and their research use was in accord with the terms of the informed consents.

Phenyl **2.068**, synthesised as a baseline compound, was around 3-fold more potent at BD2 but over 15-fold more potent at BD1 compared to the 6-H analogue **2.019b** – while it was expected that the ZA channel would not confer BD2 selectivity this apparent BD1 bias was surprising. The addition of the 6-phenyl group produced a dramatic increase in lipophilicity and decrease in solubility. It was found that introducing a primary amide at the *para* (**2.069**) or *meta* (**2.070**) positions gave an increase in potency to nanomolar levels and a very slight increase in selectivity, also improving solubility through a drastic drop in lipophilicity compared to **2.068**. Amides **2.069** and **2.070** were pleasingly active in the cellular assays, with both showing similar reductions in potency of ~3-fold in PBMCs and between 30-100fold in whole blood. Pyridine **2.071** also exhibited good biochemical BD2 potency and another slight rise in selectivity, though with no detectable whole blood activity. Unlike the isolated PBMC assay the whole blood assay contains plasma proteins such as serum albumin,³¹⁷ and so highly protein bound compounds such as these will display a reduction in hWB activity due to a reduced free fraction.

To introduce more polarity pyridone **2.072** was synthesised, which maintained BD2 potency but reduced ChromLogD_{7.4} by almost 100-fold compared to **2.071**. This increase in polarity caused a concomitant improvement in solubility, reduced protein binding and much improved cellular potency. Methoxypyridine **2.073** reversed these improvements, indicating that hydrogen bond donors or other highly polar groups may be beneficial. Combining the similarly selective 3-pyridyl group (**2.071**) with the primary amide functionality of **2.069** gave **2.089**, which showed improved BD2 potency, though the decrease in lipophilicity was not additive and solubility was poor. Mono-methylation of **2.089** to give **2.075** caused no significant change in potency or selectivity, with increased lipophilicity again adversely affecting whole blood activity. The isomer **2.076** showed no significant difference to **2.075**. *Ortho*-substitution of the pyridine ring (**2.077**) was detrimental, potentially due to either a clash with the water network at the base of the ZA channel or from increasing the dihedral angle between the 6-aryl and the core, leading to a poorer fit. Methylpyrazine **2.078** again showed good BD2 potency and selectivity, though with high lipophilicity due to the methyl group, and poor cellular activity.

To further increase polarity, pyrimidines were investigated. Unsubstituted pyrimidine **2.079** showed good potency and 20-fold BD2 selectivity which translated well into PBMC potency. No whole blood activity was detected, an unusual response given the slightly lower lipophilicity and plasma protein binding of **2.079**. The more lipophilic methoxypyrimidine **2.080** maintained potency and selectivity, with a slight increase in whole blood activity and a PBMC to hWB reduction around the expected 10-fold. However, the solubility of **2.080** was poor and whole blood activity again was low. The uracil derivative **2.081** was highly polar and displayed low

protein binding. However, as seen with **2.077**, *ortho*-substitution again lowered BD2 potency and selectivity. A similar effect was observed for the dimethoxy variant

2.082. Cyanopyrimidine **2.083** was poorly selective but displayed excellent PBMC potency, despite having similar BD2 potency and physicochemical properties to **2.080**. The cellular potency may be driven by the very high BD1 potency of **2.083**, as the exact roles of the BD1 and BD2 domains and the extent to which they each affect MCP-1 production are unknown. Indeed, one of the purposes of this work is to provide a domain-selective BET inhibitor to determine the relative roles of BD1 and BD2 in cytokine production and immunology. Oxidation of **2.083** to amide **2.090** gave a large boost in selectivity, maintaining good cellular potencies, while also significantly improving physicochemical properties. While the x-ray structure of **1.14** (Figure 2.3) indicates this amide is probably not making direct interactions with the protein, the formation of hydrogen bonds to the water network at the exit of the ZA channel is a potential rationale for this boost in selectivity.

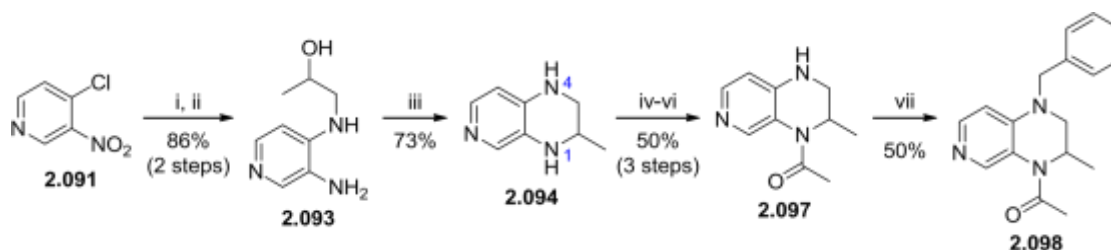
Tetrahydropyran **2.084** showed greater selectivity than the 6-phenyl analogue **2.068**, while the *N*-Boc tetrahydropyridine **2.085** had similar activity. Removing the Boc group gave **2.091**, which had lower BD2 potency compared to the aryl analogues but very high selectivity. HSA binding may not give an accurate picture of total protein binding, as HSA is a generally neutral protein and the basic amine may also bind to acidic phospholipids. All partially saturated examples were highly permeable, but tetrahydropyran **2.084** was relatively lipophilic and so only moderately soluble. However, the inclusion of a hydrogen bond donor and basic centre in **2.091** gave a sharp reduction in lipophilicity, and hence an improvement in solubility, while maintaining good permeability. 5-Membered heterocycles were also briefly investigated – oxazole **2.086** was potent and reasonably selective but was considered too lipophilic and insufficiently potent in cells. Pyrazoles **2.087** and **2.088** increased biochemical potency but selectivity, lipophilicity and solubility worsened. A pleasing increase in PBMC activity was seen but this did not translate into whole blood potency.

In summary, the pyrimidine amide **2.090** and the tetrahydropyran **2.091** appeared most promising and were carried forward for combination with the optimal substituents from the other vectors.

2.3.8 Aza Cores

Introduction of nitrogen atoms into the aromatic ring of the core has the potential to reduce the intrinsically high lipophilicity of the series. The 5-, 6-, and 8-aza cores had been investigated in the previous optimisation campaign,²⁹⁰ and the 7-aza was synthesised to complete the set. Intermediate **2.094** was synthesised using a method based on that developed by Hepworth

and Tittensor (Scheme 2.10).³¹⁸ Substitution of chloropyridine **2.091** with 2-hydroxypropylamine, followed hydrogenation under flow conditions to reduce the nitro group, gave aminopyridine **2.093**. This catalytic reduction is significantly milder, more atom-efficient and sustainable compared to the SnCl₂-mediated reduction previously utilised for THQx core construction (Scheme 2.1). Heating to reflux in aqueous acid gave the cyclised core **2.094** in three high-yielding steps.



Scheme 2.10. Synthesis of 7-aza THQx **2.098**. Reagents and conditions: (i) 2-Hydroxypropylamine, DIPEA, EtOH, μ W, 150 °C; (ii) H₂, 10% Pd/C, H-Cube, MeOH; (iii) HBr, reflux; (iv) Boc₂O, pyridine, rt; (v) AcCl, DMAP, pyridine, DCM, rt; (vi) 4 M HCl in 1,4-dioxane, rt; (vii) NaH, BnBr, DMF, 0 °C.

Unfortunately, acetylation of **2.094** proved difficult – the highly polar core was poorly soluble, necessitating the use of neat pyridine as solvent. Despite the electron density on N4 being more readily delocalised into the pyridine ring, acetylation gave a mixture of 4-Ac and diacetylated products, with none of the desired 1-Ac product **2.097** isolated. Taking advantage of this regiochemical preference, Boc protection occurred solely on N4 and the N1 acetyl group was installed on the protected material, though more forcing conditions were required and yields were moderate. Deprotection of the Boc group gave **2.097** in a reasonable 50% yield from **2.094**. Benzylation again proved problematic, with reductive amination or substitution under the previously developed conditions giving complex mixtures with none of the observed product observed, even when the BnBr/K₂CO₃ substitution was carried out at rt. However, deprotonation with sodium hydride followed by addition of benzyl bromide gave the desired product **2.098** in acceptable yield.

Regrettably, **2.098** was poorly potent at Brd4 BD2, though BD1 potency was below the lower binding limit of the assay at the concentration tested. Of the alternative aza cores **2.098**, **2.101**, the 8-aza THQx **2.101** showed the best potency and selectivity profile (Figure 2.11).²⁹⁰ This may be due to a reduced steric clash between the acetyl CH₃ and the 8-position of the ring when the 8-H is removed, making adoption of the binding conformation (Figure 2.2) more favourable. Although the BD2 potency of **2.101** was still reduced significantly compared to **2.002**, BD1 potency was also reduced to below the lower assay limit. The 5-aza **2.099** was slightly less selective and the 6-aza **2.100** had no measurable activity at either bromodomain. All four aza-isomers were less potent and appear to be less selective compared to the phenyl

core analogue **2.002**, though a pleasing reduction in lipophilicity was achieved for all compounds and in particular **2.098** and **2.100**. Nonetheless, the poorer potencies led to no further work being carried out on aza-core analogues.

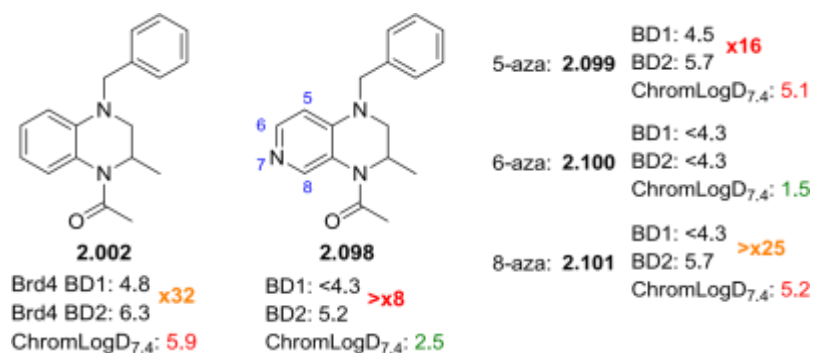


Figure 2.11. Biochemical potencies of aza core molecules. Potency data are n=2 or greater.

3.3.9 The 3-Position – Lead-Hopping From a Screening Hit

During a screen against Brd4 of compounds containing potential KAc mimetics, a series of benzoxazines (BOs), structurally similar to the THQx series, were identified which showed promising BD2 selectivity (Figure 2.12).³¹⁶ These compounds exhibited interesting SAR, with the pendant heterocycles of **2.102**³¹⁹ and **2.103**³¹⁹ seemingly required for activity – truncation to sulphone **2.104**³¹⁹ removed almost all BD2 activity. Selectivity could not be accurately measured for **2.102** and **2.104** due to the assay concentration limit but **2.103** was screened at higher concentration to give an accurate BD1 potency. The ligand efficiency (LE) and lipophilic ligand efficiency (LLE) of these compounds were poor, though the addition of the morpholine maintained and improved efficiency due to the increase in potency and polarity it conferred.

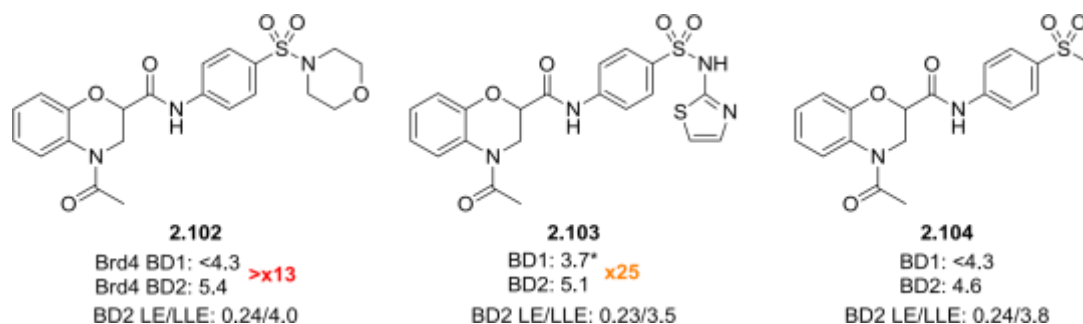


Figure 2.12. Structures and potencies of BO hits **2.102-2.104**. All potency data are n=3 or greater unless specified. *n=2, <4.3 on three other test occasions.

It was theorised that these compounds may bind in a similar manner to the THQx series, with the acetyl group acting as the warhead and the amide pointing out of the binding pocket along

a cleft formed by the ZA loop and the BD2-specific His. Notably, this region is also occupied by the BD2-biased BET inhibitor RVX-208 (**1.20**, see Figure 1.18).^{117,127}

These theories were confirmed by crystallography of **2.103** bound to Brd2 BD2 (Figure 2.13),²⁹² which showed that the amide NH forms a bidentate hydrogen bond to the key Asp140 residue. The phenyl ring projects through the expected channel, packing against His433 and making lipophilic contact with Leu383. The sulphonamide provides a crucial 90° turn, which orientates the thiazole to form edge-to-face π -interactions with His433. Given that the morpholine **2.102** is more potent than **2.103** despite being lacking π -character, the key interaction may in fact be hydrogen bonds to Asp434 and the backbone beyond His433, or simply lipophilic contact with His433. The THQx scaffold overlays reasonably well with the BO core, with the 3- and 4-positions of the respective cores in reasonably similar locations. It can also be seen that the region occupied by the thiazole of **2.102** contains two water molecules in the **2.019c** structure, one in close proximity to the thiazole sulphur, which may be displaced by the binding of **2.102**.

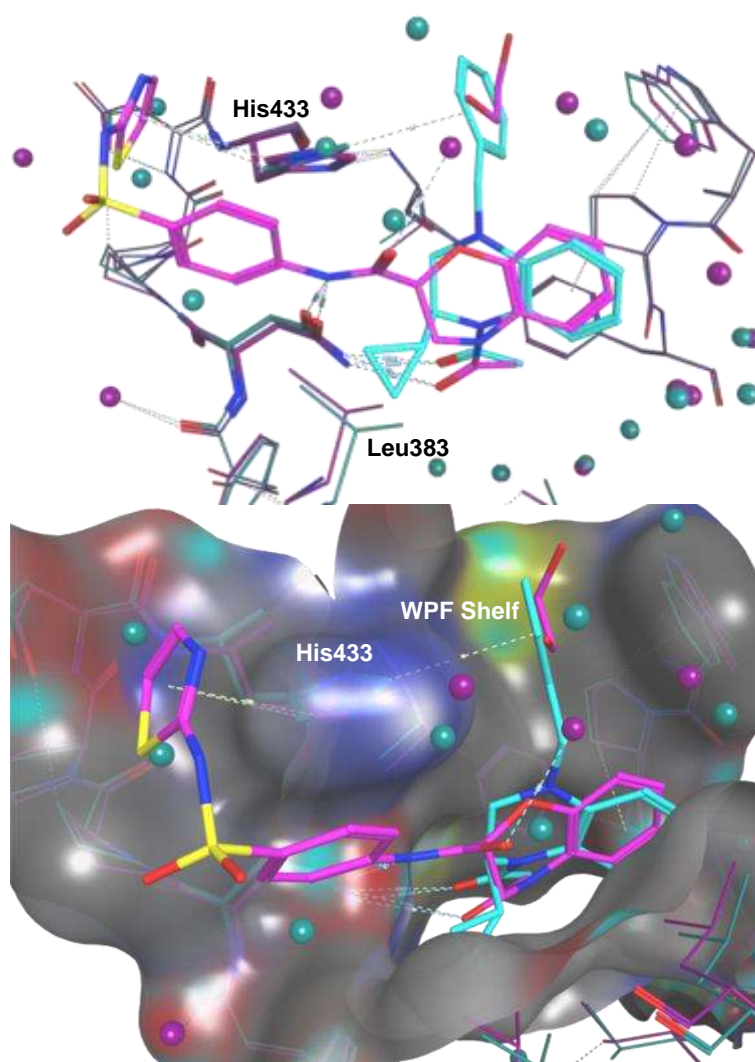
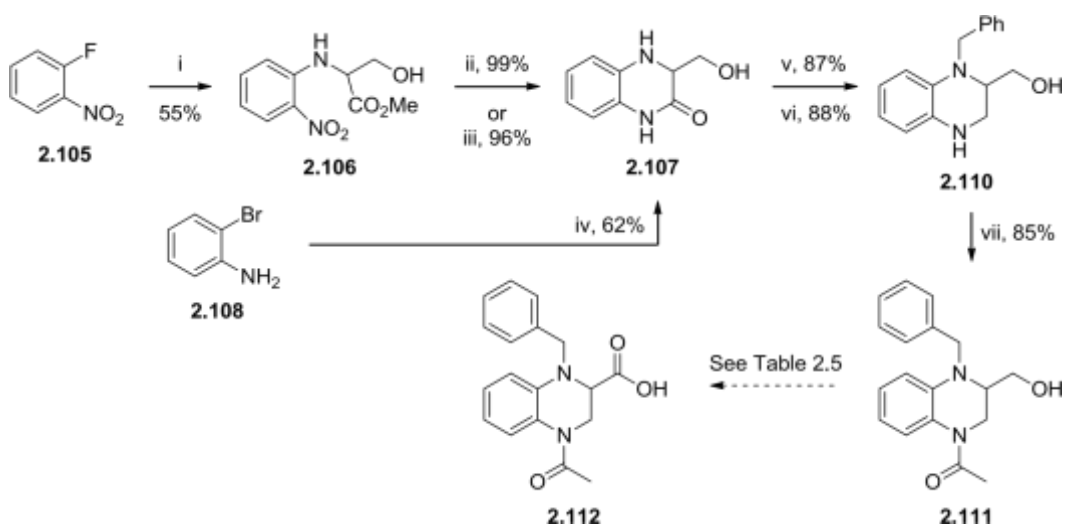


Figure 2.13. X-ray crystal structures of **2.103** (magenta, 1.63 Å)²⁹² and **2.019c** bound to Brd2 BD2 (cyan, 1.78 Å).²⁹² Key residues are bolded. *Top:* No surface, some residues omitted for clarity. *Bottom:* Showing the **2.103** structure surface. The good overlay of the cores indicated that replacing the BO oxygen with an *N*-benzyl group could enable access to the WPF shelf. Given the >100-fold increase in potency observed on accessing the WPF shelf (*c.f.* **2.001** and **2.002**, Figure 2.1) and high selectivity of the BO hits, this lead-hopping approach had the potential to generate highly potent and selective compounds.

It was envisaged that compounds of this type could originate from a THQx with a carboxylic acid at the 3-position, and to allow pairwise comparison with the BO series and simplify synthesis, compounds were synthesised with no 2-substituent. A high yielding, gram-scale synthesis of the 3-substituted core (Scheme 2.11) was developed utilising known methodology²⁹⁰ and modified literature precedent.³²⁰



Scheme 2.11. Synthesis of acid intermediate **2.112**. Reagents and conditions: (i) Serine methyl ester, DIPEA, MeCN, μ W, 130 °C; (ii) SnCl₂, EtOH, reflux; (iii) H₂, 10% Pd/C, MeOH, rt; (iv) (\pm)-serine, CuCl, *N,N*-dimethylethylenediamine, K₃PO₄, DMSO, 110 °C; (v) PhCHO, PhSiH₃, Bu₂SnCl₂, 2:1 THF:DMF, rt; (vi) BH₃·THF, THF, 50 °C; (vii) AcCl, pyridine, DCM, rt.

An S_NAr reaction between fluorobenzene **2.105** and serine methyl ester gave **2.106** in reasonable yield. Nitro reduction could be achieved in excellent yield with either SnCl₂ reduction or a more sustainable catalytic hydrogenation. As before, cyclisation to **2.107** occurred spontaneously in the SnCl₂ reduction or when the hydrogen reaction mixture was left to stand after catalyst removal. Alternatively, **2.107** could be constructed in one step from 2-bromoaniline **2.108** using the copper catalysed method developed by Tanimori,²⁹⁶ though this route was poorly scalable due the requirement for a sealed tube and difficulties in removing

DMSO from the polar product. At this stage the lower reactivity of the lactam nitrogen was exploited to selectively add a benzyl group to N4, however functionalisation of **2.107** by reductive amination proved difficult, with standard reductive amination conditions ($\text{NaBH}(\text{OAc})_3$) failing to produce any product. The electron-withdrawing lactam may deactivate the amine, or intermolecular hydrogen bonds may form with the OH which hinder reactivity. Alternatively, the boron hydride may be chelated by the carbonyl and alcohol, preventing reaction. The tin catalysed conditions utilised by Apodaca³²¹ and Smil³²² gave the desired product but conversion was slow, increasing the catalyst loading and adding DMF as a co-solvent³²³ gave the benzylated product in good yield. Lactam reduction with boraneTHF gave amine **2.110**, which was acetylated with acetyl chloride to give **2.111** in good yield.

However, obtaining acid **2.112** proved extremely challenging (Table 2.5). Although oxidation for **2.111** to aldehyde **2.113** was facile under Swern conditions (Entry 1), a variety of stepwise and one-step oxidations to acid **2.112** or methyl ester **2.114** failed, giving either complex mixtures or lactam **2.115**. The mechanism of this process is unknown, but the radical homolysis of amino alcohol C-C bonds is known to occur.³²⁴ It is possible that **2.115** arises from this homolytic cleavage followed by oxidative quenching of the resulting radical cation at C3. Alternatively, polar decarboxylation could occur, followed by hemiaminal formation and oxidation.

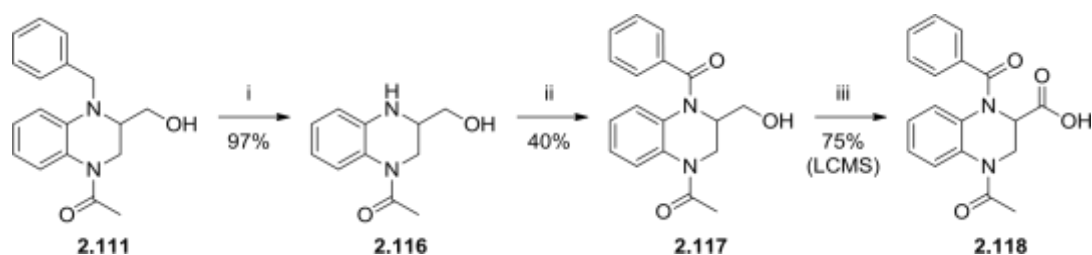
Table 2.5. Attempted oxidation conditions.

$\text{2.111} \xrightarrow{\text{Oxidation}} \text{2.113} \text{ (R = COOH)}$
 $\text{2.113} \xrightarrow{\text{Oxidation}} \text{2.112} \text{ (R = CHO)}$
 $\text{2.112} \xrightarrow{\text{Oxidation}} \text{2.114} \text{ (R = CO}_2\text{Me)}$
 $\text{2.111} \xrightarrow{\text{Oxidation}} \text{2.115}$

Entry	Oxidation	Conditions	Outcome
1	2.111 → 2.113	DMSO, $(\text{COCl})_2$, Et_3N , DCM -78 °C – rt.	85% yield
2	2.113 → 2.112	7 eq NaClO 7 eq NaH_2PO_4 , 2-methylbut-2-ene, 3:1 BuOH/H ₂ O, rt	2.115 55% yield
3	"	Oxone, DMF, rt	Complex mixture, major product 2.115
4 ³²⁵	"	5 mol% CuCl, ^t BuOOH, MeCN, rt	"
5 ³²⁶	"	4 mol% VO(acac) ₂ , 3 eq H ₂ O ₂ , MeCN, rt	"
6	2.113 → 2.114	Oxone, MeOH, rt "	"
7	"	5 mol% CuCl, ^t BuOOH, MeOH, rt "	"

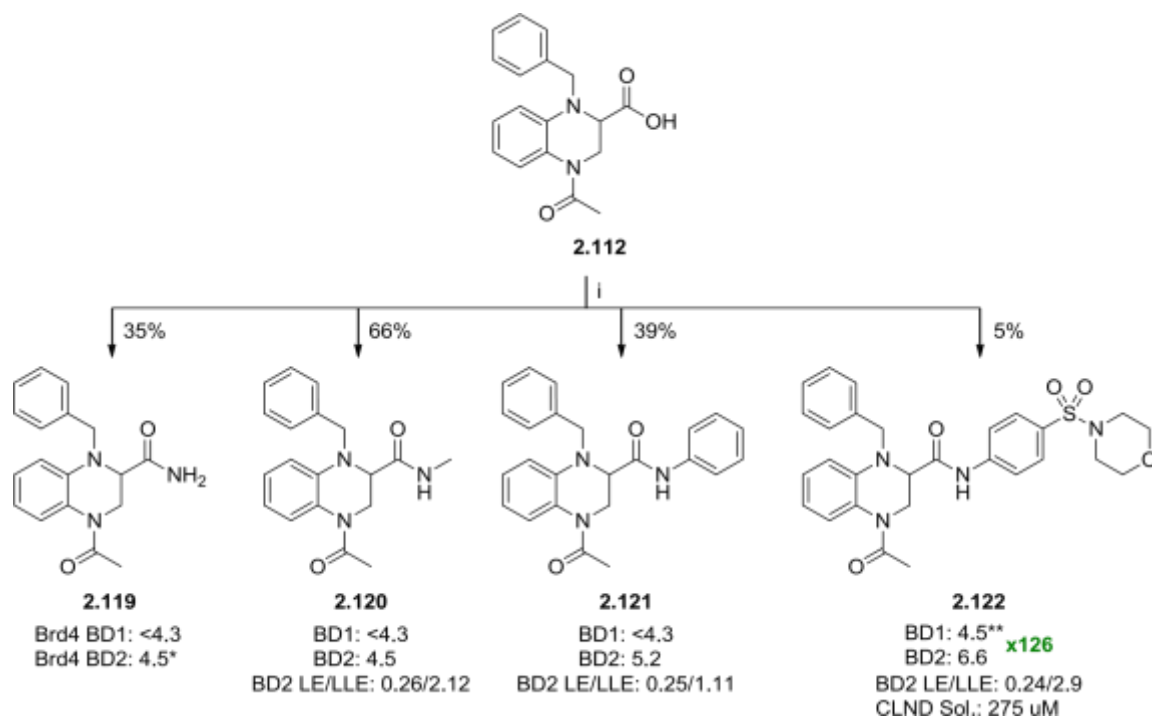
8	"	4 mol% VO(acac) ₂ , 3 eq H ₂ O ₂ , MeOH, rt	"
9	2.111 → 2.112	4eq PCC, DMF, rt	Complex mixture
10 ³²⁷	"	5 mol% PCC, 2 eq H ₃ IO ₄ , MeCN, rt	"
11 ³²⁸	"	20 mol% RuO ₂ .H ₂ O, 7 eq NaIO ₄ , 2:1 Acetone/H ₂ O, 0°C - rt	"
12 ³²⁹	"	7 mol% TEMPO, 2 mol% NaOCl, 2 eq NaClO ₂ , MeCN, H ₂ O, pH=7, rt	No reaction
13	"	1 eq CrO ₃ , H ₂ SO ₄ , 2:1 Acetone/H ₂ O, rt	Complex mixture
14	"	4 eq CrO ₃ , H ₂ SO ₄ , 2:1 Acetone/H ₂ O, No 2.112 observed -10 °C - rt	"
15 ³³⁰	"	5 mol% RuCl ₃ , 3 eq NaIO ₄ , 1:1:1.5 MeCN/CCl ₄ /H ₂ O, rt	"
16 ³³¹	"	3mol% TPAP, 3 eq NMO, MeCN, rt	4% 2.112 , major product 2.115
17	"	10mol% TPAP, 6 eq NMO, MeCN, -15°C	22% 2.112 (isolated yield)
18 ³³²	"	2 mol% [Cp*IrCl ₂] ₂ , 6 mol% 2.111 → 2.114 MeNHCH ₂ CH ₂ OH, 10 mol% Cs ₂ CO ₃ , 4 eq Trace 2.114 , SM unreacted MeOH, Acetone, rt.	"
19 ^{333,334}	"	5 mol% [RuH ₂ (CO)(PPh ₃) ₃], 5 mol% Xantphos, 3 eq crotononitrile, 2 eq H ₂ O, 1:1 MeOH/Toluene, 110 °C.	5% 2.114 , complex mixture

Small amounts of the desired product were obtained when TPAP oxidation was attempted (Entry 16), and an increase in the catalyst and reagent loading at -10 °C giving a usable 22% yield of **2.112** (Entry 17). Attempts to isolate **2.112** by chromatography failed, with the acid being unstable to silica but isolable in usable purity by acid-base aqueous extraction. The methyl ester **2.114** could also be obtained in low yield directly from the alcohol **2.111** using 'borrowing hydrogen' catalysis (Entries 18, 19).³³²⁻³³⁴ Interestingly, when the benzyl group was converted to a benzoyl (Bz) group (**2.117**), oxidation under the above conditions gave the acid product **2.118** cleanly with only a trace of the lactam byproduct, even after several hours at rt (Scheme 2.12). This indicates that the nitrogen lone pair may be involved in the formation of **2.115**, potentially through charge stabilisation or formation of an intermediate imine.



Scheme 2.12. Oxidation with a benzoyl (Bz) protecting group. Reagents and conditions: (i) 10% Pd/C, H₂, MeOH, rt, H-Cube flow hydrogenation reactor; (ii) BzCl, pyridine, DCM, 0 °C; (iii) 6 eq NMO, 10 mol% TPAP, MeCN, -15 °C - rt, (75% by LCMS).

Despite the low yields, sufficient amounts of **2.112** were obtained to synthesise final compounds using HATU-mediated amide couplings (Scheme 2.13). The primary amide **2.119** had no measurable pIC₅₀ at the concentration tested against either bromodomain of Brd4, whereas methyl amide **2.120** showed a weak but still measurable BD2 potency. Phenyl amide **2.121** gave no measurable BD1 pIC₅₀ and was weakly potent against BD2, as expected from comparison to the non-sulphonamide BO **2.104**. Addition of the morpholine sulphonamide moiety found in **2.102** gave **2.122**, albeit in very low yield, which was over 120-fold selective for Brd4 BD2 over BD1, showed reasonable BD2 potency, and was pleasingly soluble.



Scheme 2.13. Synthesis and potency of lead-hopping final compounds. All potency data are n=3 or greater unless specified. *n=1, <4.3 on two additional test occasions. **n=2, <4.3 on one additional test occasion. Reagents and conditions: (i) Amine or amine HCl salt, HATU, DIPEA, DMF, rt.

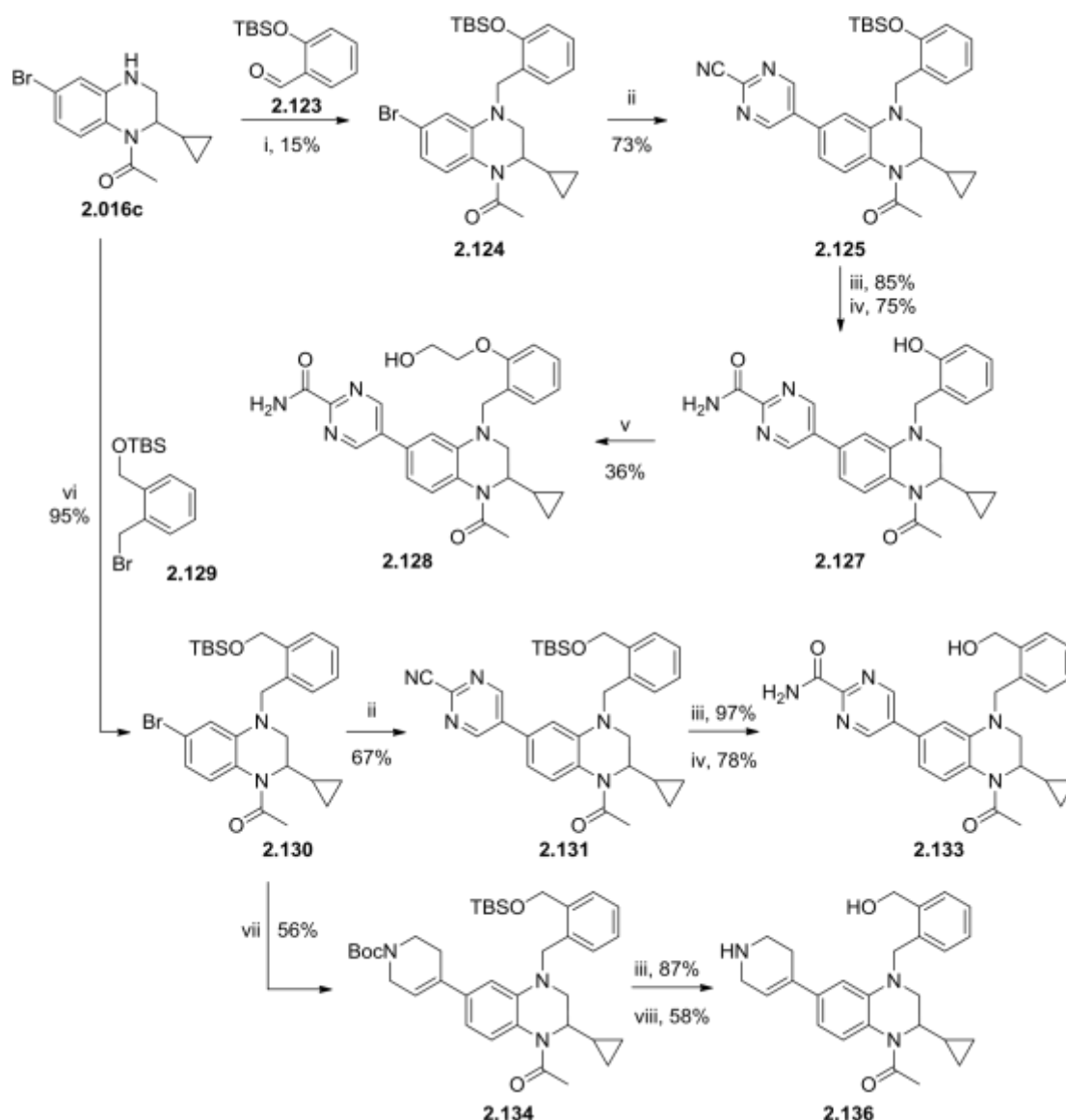
While this result was pleasing and validated the lead-hopping hypothesis, it should be noted that the addition of the shelf group gives a much smaller boost in BD2 potency from **2.102** to **2.122** (x16) when compared to **2.001** and **2.002** (x316). Ligand efficiency³¹ is much the same for **2.102** and **2.122**, though it is below the desired minimal value of 0.3. However, the related lipophilic ligand efficiency (LLE)³³⁵ value drops sharply, showing that the additional lipophilicity of the benzyl group is not well used. Comparison of these compounds to the 2-H, 4-Bn THQx **2.019d** (BD1/BD2 pIC₅₀: 5.0/5.6, BD2 LE: 0.38) shows that a 3-amide substituent is a poorly efficient means of increasing potency and selectivity due to the large 3-substituents required to pack against the His and make this interaction significant. Due to this inefficiency, 3-substitution was not further optimised.

2.3.10 Combination of Substituents

With the 2-, 3-, 4-, and 6- position investigations complete, the previously investigated substitution patterns were combined in the hope that SAR would be additive and afford potent and selective probe molecules. For the 2-position, the cyclopropyl group was preferred, and the *o*-CH₂OH and *o*-O(CH₂)₂OH phenyls were the most selective examples for the WPF-shelf group. The optimal 6-substituent was less clear as many of the compounds tested had similar profiles, so it was decided that both the pyrimidine 1-amide of **2.090**, which had the best physicochemical properties among the most selective aryls, and the promisingly selective but less potent tetrahydropyridine group of **2.091** would be utilised. From the crystal structures of **2.022c** and **2.019c** (Figure 2.7) and from comparison to I-BET726,¹¹⁴ it appears that the (*S*)-enantiomer is the stronger binder and single enantiomer compounds would be required for definitive profiling, for synthetic ease the compounds were initially prepared as racemates pending a single enantiomer synthesis (*vide infra*).

Unfortunately, the 6-bromo substitution of **2.016c** slowed the rate of reductive amination or benzyl bromide displacement compared to the 6-H compounds described earlier, possibly due to inductive electron withdrawal. This resulted in diminished yields due to competitive side reactions of the aryl aldehyde or benzylic bromide with the alcohol group, and the alcohol group was introduced protected with TBS (**2.123**) to prevent this (Scheme 2.14). However, the TBS group proved to still be relatively labile under reductive amination conditions resulting in a poor yield. Following reductive amination, **2.124** underwent SuzukiMiyaura cross-coupling to **2.125** in good yield, followed by efficient deprotection with TBAF and mild nitrile oxidation using H₂O₂. The resulting phenol **2.127** could be alkylated with 2bromoethanol to afford the final product **2.128**, though reaction was slow and yield poor. In the case of **2.130** the use of NaH appended the benzyl group in excellent yield, a significant improvement on the previous reductive amination or benzylic displacement conditions. Following cross-coupling, affording **2.131**, the TBS-groups were easily removed with TBAF, with nitrile oxidation giving **2.133**.

Efforts to streamline the synthesis by installing the benzyl group as the final step were unsuccessful due to the poor solubility and reactivity of compounds containing the pyrimidine group. The Boc-protected tetrahydropyridine was introduced using identical Suzuki conditions, giving **2.134** which was doubly deprotected to afford **2.136**.



Scheme 2.14. Synthesis of combination compounds. Reagents and conditions: (i) NaBH(OAc)₃, DCM, rt; (ii) Pyrimidine-2-carbonitrile-5-boronic acid pinacol ester, Pd(dppf)Cl₂, Cs₂CO₃, 1,4-dioxane, H₂O, μW, 110 °C; (iii) TBAF, THF, rt; (iv) H₂O₂, K₂CO₃, DMSO, rt; (v) 2-Bromoethanol, K₂CO₃, DMF, 110 °C; (vi) NaH, DMF, 0 °C; (vii) *tert*-butyl 5,6-dihydropyridine-1(2*H*)-carboxylate-4-boronic acid pinacol ester, Pd(dppf)Cl₂, Cs₂CO₃, 1,4-dioxane, H₂O, μW, 110 °C; (viii) TFA, DCM, rt.

All four combination compounds (**2.127**, **2.128**, **2.133**, **2.136**) were profiled, and showed good BD2 potency and selectivity (Table 2.6). SAR was additive, with the BD2 potencies of **2.090** and **2.091** being maintained while the WPF-shelf groups reduced BD1 potency. The combination of substituents successfully brought physicochemical properties into more druglike space through the introduction of polar functionality (and a basic centre in **2.136**). As expected from the earlier results (Section 2.3.3), phenol **2.127** was less selective, though active in the phenotypic PBMC MCP1 assay. Alkylation to give **2.128** improved selectivity and solubility at the cost of increased lipophilicity, though ChromLogD_{7.4} was still within the desired range. Benzylic alcohol **2.133** was also a promising lead, and though permeability and solubility were slightly lower than desired **2.133** had good cellular potency. Tetrahydropyridine **2.136** was also highly selective and had the highest LE of the combination set, with the basic centre producing a large decrease in ChromLogD. Solubility and permeability were both improved compared to **2.133** and no reduction in potency was observed between the FRET and cellular assays. From these data, the benzylic alcohol shelf group was selected for investigation as a single enantiomer with both 6-substituents.

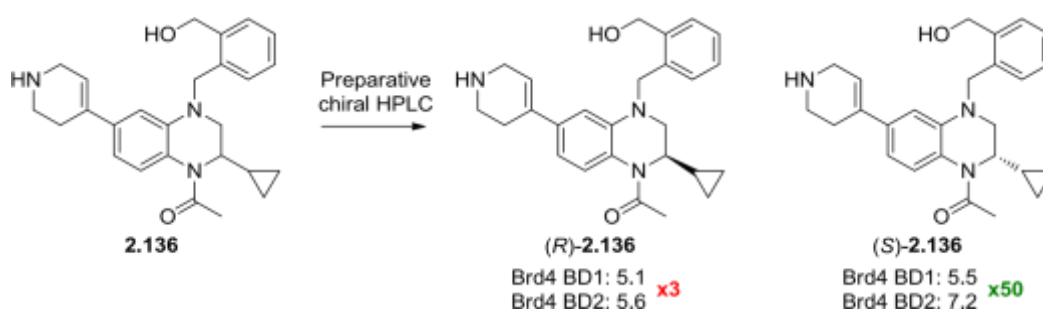
Table 2.6. Target potencies and additional profiling of combination compounds.

Compound	2.127	2.128	2.133	2.136
BRD4 BD1/BD2				
pIC₅₀ (Selectivity)	5.5 / 7.0 (x32)	5.2 / 6.9 (x50)	5.2 / 7.0 (x63)	5.0 / 6.8 (x63)
BRD4 BD2 LE/LLE	0.29 / 4.34	0.26 / 4.48	0.28 / 4.72	0.30 / 3.64
ChromLogD_{7.4}	3.2	3.0	2.8	2.2
CLND Sol (μM)	41	344	130	312
AMP_{7.4} (nm/s)	500	200	86	120
HSA binding (%)	96	92	91	90
PBMC MCP1 pIC₅₀	6.7	-	6.8	6.8

All potency data are n = 3 or greater.

The effect of separating the racemate into its constituent isomers was investigated for **2.136**. Chiral HPLC separation³³⁶ afforded the two isomers (Scheme 2.15), the absolute configuration of which was confirmed by X-ray crystallography (Figure 2.15) and comparison with homochiral synthetic material (*vide infra*). As hypothesised, the *S*-enantiomer exhibited a slight

boost in potency and was pleasingly selective. However, unlike the 6-H analogue **2.056b**, the *R*-enantiomer maintained a low level of unselective Brd4 potency. Preparative chiral HPLC conditions could not be developed for pyrimidine amide **2.133** due to poor solubility, and a synthetic solution was sought.



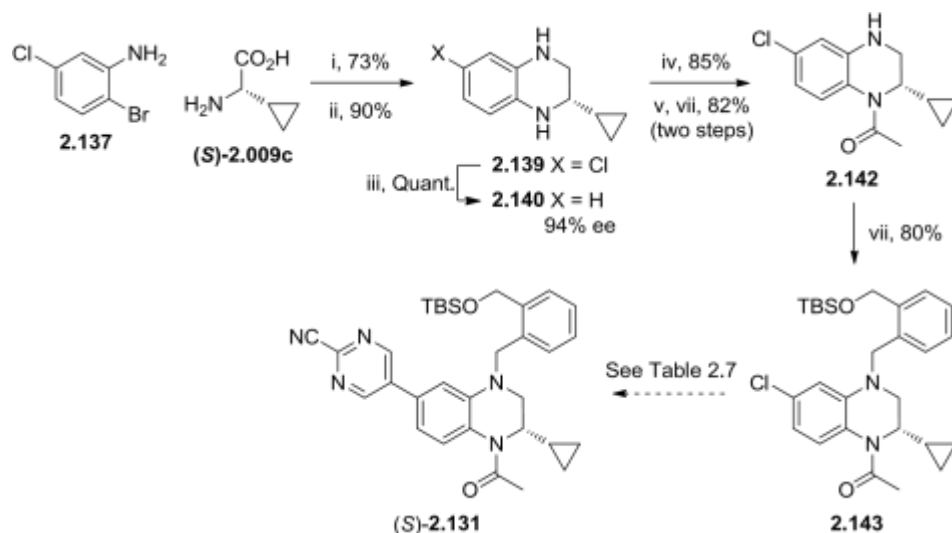
Scheme 2.15. Chiral separation of **2.136** and potencies of the single enantiomers. Potency data are n=3 or greater.

2.3.11 Single Enantiomer Synthesis

With historical and crystallographic data strongly suggesting that the (*S*)-enantiomer of the THQx series was the more active enantiomer, a synthesis of enantiopure products was desired. Though **2.136** could be separated into its constituent isomers by preparative chiral HPLC, poor solubility prevented this for the 6-pyrimidine compounds and separation earlier in the synthetic route would be required. To prevent this wasteful and poorly scalable method, and confirm the absolute configuration of the active isomer, a method of preparing enantiomerically pure final compounds was desired. Asymmetric hydrogenation of 2-alkyl quinoxalines^{337–341} was considered but the high H₂ pressures often utilised were considered poorly practical and incompatible with an aryl halide substituent. The Ullmann-type cyclisations used in the synthesis of *gem*-dimethyl (Scheme 2.3) and 3-amido (Scheme 2.11) compounds were reported to proceed without racemisation of the amino acid and were tolerant of some aryl halides.²⁹⁶ Given these advantages, and to make use of the previously developed synthetic route, this method was utilised (Scheme 2.16).

(*S*)-Cyclopropylglycine (commercially available or accessible enzymatically from cyclopropylglyoxylic acid³⁴²) underwent Cu-catalysed coupling-cyclisation with bromoaniline **2.137** to give the quinoxalinone core **2.138** in high yield, which was efficiently reduced to THQx **2.139** using borane-THF. To determine enantiopurity, **2.139** was hydrogenated to give **2.140**, which was compared with an available racemic sample by chiral HPLC and shown to be an acceptable 94%*ee*. **2.139** was acetylated and the WPF shelf aryl group added using the previously developed chemistry (Scheme 2.14), giving **2.143**. Although this route is inherently

inefficient due to the protection and deprotection steps, installation of the substituted benzyl group earlier in the synthesis (as done for **2.027**, Scheme 2.3) was not considered practical due to the harsh conditions of the Ullmann and borane reduction steps. However, yields for the protection/acetylation/deprotection were significantly improved over the initial route (Scheme 2.1). This route necessitated the use of a less reactive 6-Cl substituent to avoid chemoselectivity issues in the Ullman coupling step and therefore a reassessment of the Suzuki-Miyaura coupling conditions was required. This proved to be non-trivial, and none of the pyrimidine product (*S*)-**2.131** was observed under the previously competent Pd(dppf)Cl₂-catalysed conditions.

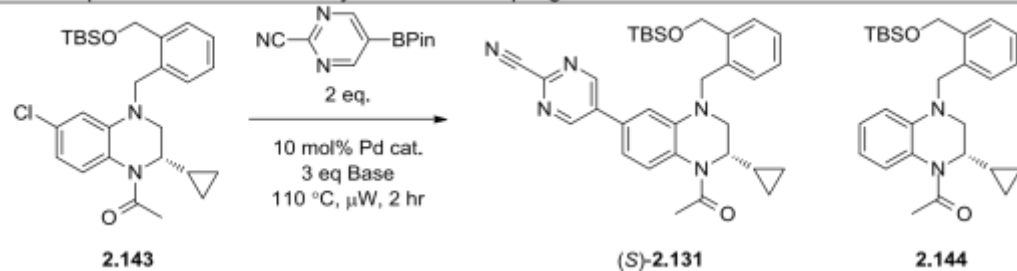


Scheme 2.16. Single enantiomer synthesis of **2.143**. Reagents and conditions: (i) CuCl, DMEDA, DBU, DMSO, 110 °C; (ii) BH₃·THF, THF, 60 °C; (iii) 10% Pd/C, H₂, EtOH, rt; (iv) Boc₂O, DMAP, Et₃N, DCM rt; (v) Ac₂O, Et₃N, 2-MeTHF, 90 °C; (vi) TFA, DCM, rt; (vii) **2.129**, NaH, THF, 0 °C.

A campaign of catalyst, ligand and condition screening was undertaken to identify a suitable method for this transformation (Table 2.7). Initial investigations of palladium catalysts and pre-catalysts with additional ligands gave only traces of the desired product (*S*)-**2.131** (Entries 1-4). The NHC-stabilised pre-catalyst PEPPSI was marginally better (Entry 6), though yields remained low. Palladacycle pre-catalysts gave improved yields (Entries 7-11), though increased levels of the proto-dehalogenation product **2.144** were also observed. XPhos palladacycle catalysts gave good conversion which improved upon moving to the third generation catalyst, giving >50% conversion to the desired product (Entry 11). A screen of solvents (Entries 12-15) and bases (Entries 16-20) did not improve on this yield, though pleasingly low levels of proto-dehalogenation were observed in DME (Entry 20). Alcoholic solvents completely inhibited the reaction (Entry 13), and the addition of water inhibited, but did not prevent reaction (Entries 11, 12, 18). Given the increase in efficiency seen on moving

from the first to the third generation palladacycle catalysts, BrettPhosPd G3 was tested and gave comparable conversion to XPhosPd G3 (Entry 21). The use of DME solvent with this catalyst again reduced dehalogenation (Entry 22), and these conditions allowed (S)-**2.131** to be obtained in a useable 43% isolated yield (Entry 23).

Table 2.7. Optimisation of Suzuki-Miyaura cross-coupling

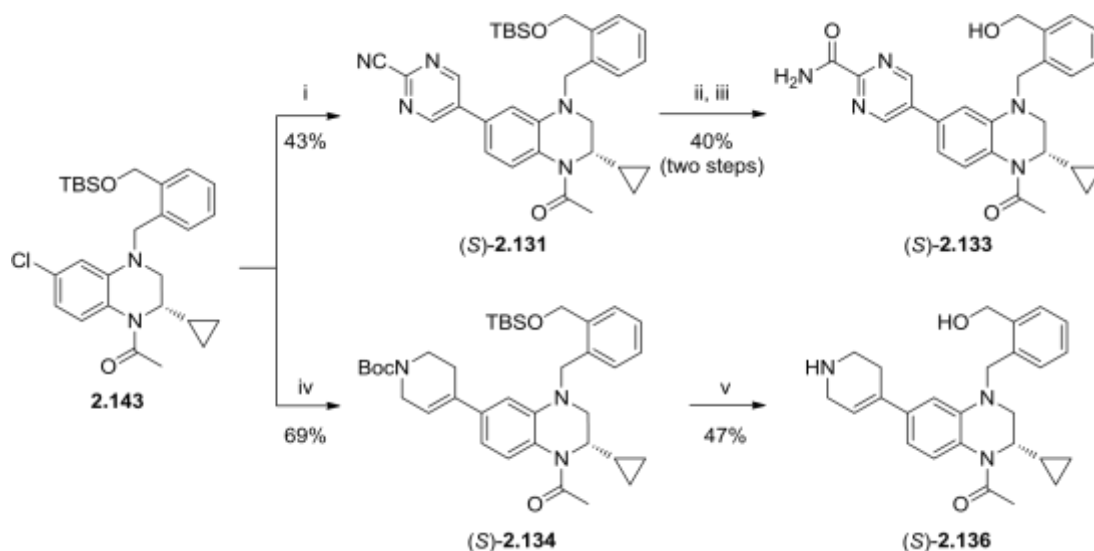


Entry	Catalyst/Ligand	Base/ Additive	Solvent	% by LCMS		
				2.143	(S)-2.131	2.144
1	Pd(dppf)Cl ₂	Cs ₂ CO ₃	10:1 1,4-dioxane:H ₂ O	No reaction		
2	Pd(PPh ₃) ₄	Na ₂ CO ₃	4:1 1,4-dioxane:EtOH	No reaction		
3	Pd ₂ (dba) ₃ , SPhos (10 mol%)	KOAc	1,4-dioxane	No reaction		
4	Pd(OAc) ₂ , RuPhos (10 mol%)	Na ₂ CO ₃	10:1 1,4-dioxane:H ₂ O	No reaction		
5	Pd(OAc) ₂ , XPhos (10 mol%)	K ₃ PO ₄ , 5 eq H ₂ O	THF, 100 °C	74	8	-
6	Pd-PEPPSI-IPent	Cs ₂ CO ₃	1,4-dioxane	75	10	-
7	Xphos Pd G2	K ₃ PO ₄ , 5 eq H ₂ O	1,4-dioxane	50	18	9
8	Xphos Pd G2	Cs ₂ CO ₃	1,4-dioxane	49	23	6
9	SPhos Pd G2	Cs ₂ CO ₃	1,4-dioxane	71	2	-
10	BrettPhos Pd G1	Cs ₂ CO ₃	1,4-dioxane	42	31	17
11	XPhos Pd G3	Cs ₂ CO ₃	1,4-dioxane	18	43	19
12	XPhos Pd G3	Cs ₂ CO ₃	10:1 1,4-dioxane:H ₂ O	67	14	-
13	XPhos Pd G3	Cs ₂ CO ₃	tBuOH	No reaction		
14	XPhos Pd G3	Cs ₂ CO ₃	Toluene	41	29	12
15	XPhos Pd G3	Cs ₂ CO ₃	DME	40	30	2
16	XPhos Pd G3	Et ₃ N	1,4-dioxane	66	2	12
17	XPhos Pd G3	K ₃ PO ₄	1,4-dioxane	65	13	11

18	XPhos Pd G3	K ₃ PO ₄ , 5 eq H ₂ O	1,4-dioxane	70	19	10
19	XPhos Pd G3	KO ^t Bu	1,4-dioxane		No reaction	
20	XPhos Pd G3	K ₂ CO ₃	1,4-dioxane	58	20	5
21	BrettPhos Pd G3	Cs ₂ CO ₃	1,4-dioxane	33	41	8
22	BrettPhos Pd G3	Cs₂CO₃	DME	5	52	13
23	BrettPhos Pd G3	Cs₂CO₃	DME		43^a	

‘Pd’ = Palladacycle pre-catalyst. ‘G1’ = First generation, etc. ^aIsolated yield

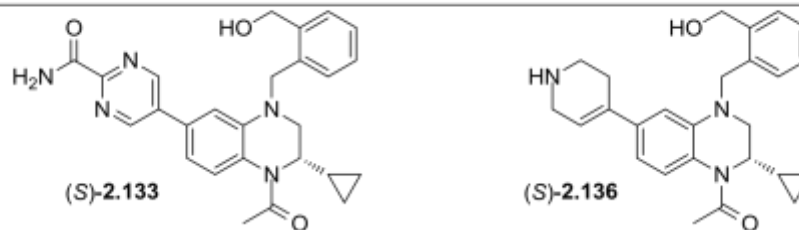
With these optimised conditions in hand, (*S*)-**2.131** was desilylated and the nitrile was oxidised to give (*S*)-**2.133**. The optimised Suzuki conditions were also applicable to the tetrahydropyridine substituent, which was coupled in improved yield to give (*S*)-**2.134**, followed by double deprotection affording (*S*)-**2.136** (Scheme 2.17).



Scheme 2.17. Completion of the single enantiomer synthesis. ^aReagents and conditions: (i) Pyrimidine-2-carbonitrile-5-boronic acid pinacol ester, BrettPhos Pd G3, Cs₂CO₃, DME, 110 °C, μW, 2 hr; (ii) TBAF, THF, rt; (iii) H₂O₂, K₂CO₃, DMSO, rt; (iv) *tert*-butyl 5,6-dihydropyridine-1(2*H*)-carboxylate-4-boronic acid pinacol ester, BrettPhos Pd G3, Cs₂CO₃, DME, 110 °C, μW, 2 hr; (v) HCl, MeOH, rt.

2.3.12 Profiling of Lead Molecules

With the single enantiomer products in hand, full profiling was undertaken (Table 2.8).

Table 2.8. Extended profiles of THQx probe candidates,

	(S)-2.133	(S)-2.136
Brd4 BD1/BD2 FRET pIC₅₀ (xSel)	5.7 / 7.3 (x40)	5.5 / 7.2 (x50)
Brd2 BD1/BD2 FRET pIC₅₀ (xSel)	5.8 / 7.0 (x16)	5.5 / 6.4 (x8)
Brd3 BD1/BD2 FRET pIC₅₀ (xSel)	6.1 / 7.5 (x25)	5.9 / 7.3 (x25)
BrdT BD1/BD2 FRET pIC₅₀ (xSel)	6.3 / 7.0 (x5)	5.8 / 6.7 (x8)
MCP1 PBMC pIC₅₀	7.1	7.4
MCP1 hWB pIC₅₀	6.0	5.7
BRPF1 FRET pIC₅₀	<4	4.7
hERG pIC₅₀	<4.3	<4.3
Rat Hepatocyte Stability (mL/min/g liver)	23.0	8.66
Human Hepatocyte Stability (mL/min/g liver)	1.57	1.81
ChromLogD_{7.4}	3.0	2.3
AMP (nm/s)	135	110
CLND Solubility (μM)	87	418
HSA Binding (%)	91	85
AGP Binding (%)	-	84

All FRET and cellular potency data are n=3 or greater. Other data are n=2 or greater. The human biological samples were sourced ethically and their research use was in accord with the terms of the informed consents.

Mirroring the results seen for (S)-2.136, the single enantiomer (S)-2.133 was around half a log unit more potent than the racemate (\pm)-2.133 but was less selective – in contrast to 2.056 where the single enantiomer proved to be more selective. Both compounds were also potent at the other members of the BET family, Brd2, 3 and T, with poor selectivity observed at Brd2 and BrdT in particular. The KAc binding pockets of Brd4 and BrdT BD1 are highly homologous, with the only significant residue difference being exchange of a glutamine beyond the ZA channel in Brd4 for an arginine in BrdT, which may be capable of folding into the ZA channel and interacting with the pyrimidine amide. Potency in PBMCs was good, with (S)-2.136 showing particular efficacy but ~100-fold reduction in the whole blood assay, despite lower HSA binding. Binding to acidic A-glycoprotein (AGP) through the basic nitrogen was thought to be responsible, but was measured as moderate at 84%. (S)-2.133 showed slightly improved whole blood potency, but it should be noted that cellular assays have a higher variability than

biochemical assays that use purified protein and both compounds are capable of inhibiting an immune response in hWB to a similar degree.

Both compounds showed minimal inhibition of the hERG cardiac ion channel, especially gratifying for (S)-**2.136** as amines adjacent to lipophilic regions are a common hERG pharmacophore. The compounds had good ChromLogD_{7.4} and reasonable permeability, though (S)-**2.136** was significantly more soluble and had marginally lower protein binding. Both compounds were weighable solids and bench stable at room temperature in air.

These data suggested advantages and disadvantages to both compounds as probes. (S)-**2.133** has marginally improved whole blood activity and permeability, with a more consistent profile across the BET family. However, (S)-**2.136** was more selective at the primary target of Brd4 BD2, showed excellent potency in isolated cells, and had much improved solubility. On balance, it was decided to take forward (S)-**2.136** as the lead compound from the THQx series.

To determine the wider bromodomain selectivity profile of (S)-**2.136**, the compound was screened against a panel of 35 bromodomains using DiscoverX's BROMOscan™ assay platform (Figure 2.14, Table 2.9).³⁴³ The screen showed low-nanomolar potency at each of the BET BD2 domains and good selectivity over BD1, especially for Brd4 where over 200fold selectivity was recorded. Domain selectivity was lesser against the other BET Brds, particularly Brd2 and Brd3, but was still at acceptable levels. In contrast to the FRET data, selectivity at BrdT was higher than Brd2 and 3. BROMOscan potency was generally higher than in the FRET assays, a phenomenon also seen for other BET¹¹⁴ and non-BET bromodomain^{167,194,211} inhibitors. The closest non-BET activity was BRPF1, the only significant off-target identified, with an ~360-fold window of selectivity compared to Brd4 BD2. A pIC₅₀ of 4.7 (316-fold selectivity) was obtained when (S)-**2.136** was screened in GSK's BRPF1 FRET assay (Table 2.8). No BROMOscan data for RVX-208 or other BD2biased BET inhibitors have been reported, but these data will allow direct comparison to any inhibitors disclosed in the future.

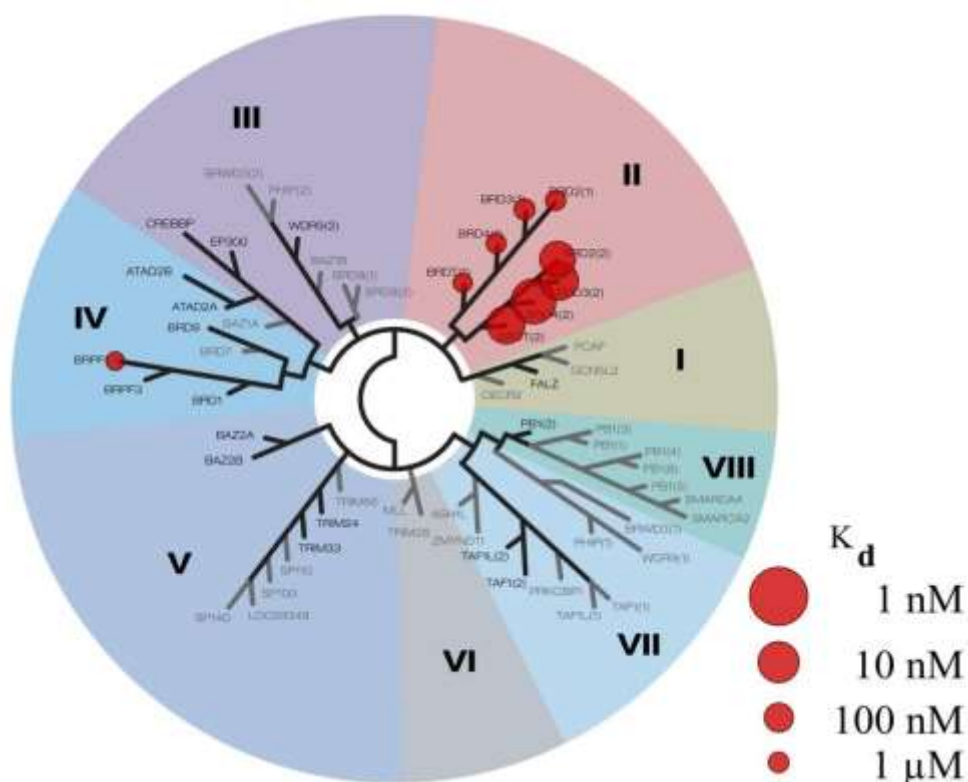


Figure 2.14. DiscoverX BROMOscan™ bromodomain selectivity tree for (S)-2.136, showing K_d as circles. Targets with activity <3000 nM are shown. Targets with greyed out names were not screened.

Table 2.9. DiscoverX BROMOscan™ K_d values for (S)-2.136.

Target	K_d (nM)	Domain Selectivity
Brd4 BD1	1500	x227
Brd4 BD2	6.6	
Brd2 BD1	1300	x40
Brd2 BD2	32	
Brd3 BD1	910	x48
Brd3 BD2	19	
BrdT BD1	1900	x90
BrdT BD2	21	
BRPF1	2400	x363 (vs Brd4 BD2)
TAF1(2)	15000	
WRD9(2)	15000	
ATAD2A/B, BAZ2A/B, BRD1, BRD7, BRD8, BRD9, BRPF3, CECR2, CRE1.14P, EP300, FALZ, GCN5L2, PBRM1(2/5), PCAF, SMARCA2/4, TAF1L(2), TRIM24(Bromo/PHD), TRIM33(Bromo/PHD),	>30000	

X-ray crystal structures of (S)-**2.133** and (S)-**2.136** bound to Brd2 BD2 were obtained²⁹² and showed very similar binding to the KAc pocket (Figure 2.15). Core binding is as seen for the less elaborated THQx **2.019c** (Table 2.1, Figure 2.7) with the cyclopropyl groups filling the lipophilic pocket and the core phenyls packing against the WPF stack. The benzyl alcohol points into solvent above the binding pocket and appears to be flexible, interacting with a water network above His433 in the (S)-**2.136** structure but facing the opposite way in the (S)-**2.133** structure. Both aryl groups adopt an approximately 36° dihedral angle to the core (close to the energy minimised dihedral angle of 44°) that improves contact and π -stacking with Trp370 of the WPF stack. The pyrimidine nitrogen atoms and primary amide of (S)-**2.133** make several interactions with the water network around the exit of the ZA channel, as does the amine of (S)-**2.136**.

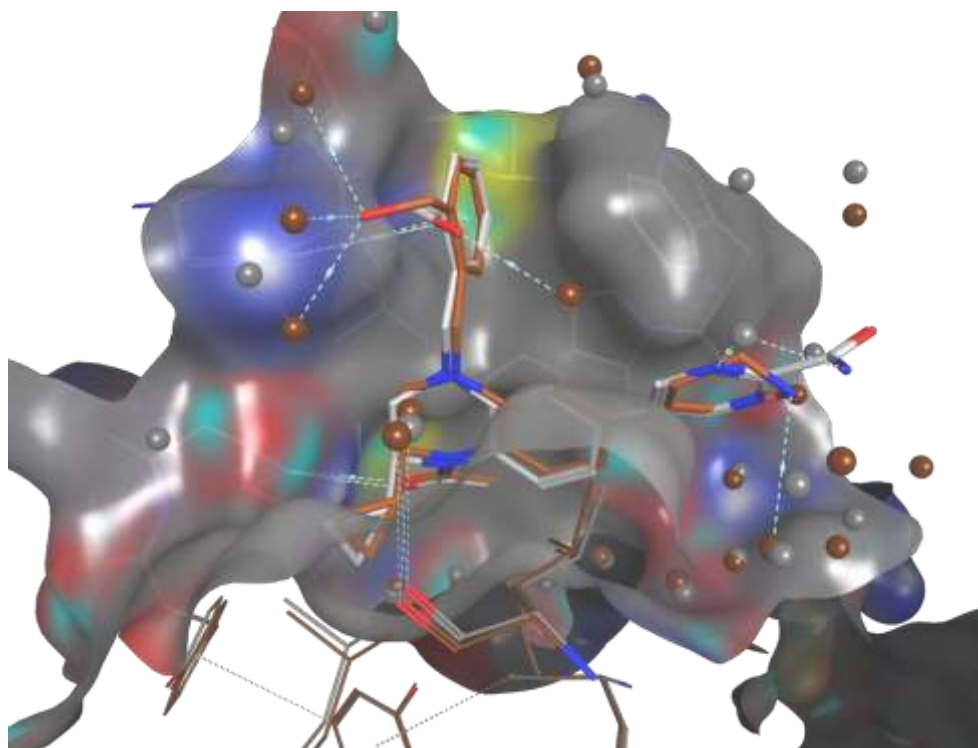


Figure 2.15. X-ray structure of (S)-**2.133** (grey, 1.60 Å)²⁹² and (S)-**2.136** (brown, 1.59 Å)²⁹² bound to Brd2 BD2 showing the (S)-**2.136** surface.

2.4 Conclusions

This work set out to develop BD2-selective BET bromodomain inhibitors with high BET family selectivity and good physicochemical properties. The SAR around the THQx template has been explored and robust, scalable methods suitable for analogue synthesis have been developed. Iterative, structure-guided design has successfully optimised the THQx series from

weakly potent, moderately selective and highly lipophilic initial hits to produce (S)-**2.136**. (S)-**2.136** meets the majority of the aforementioned probe criteria, being potent, selective and showing excellent physicochemical properties. The compound also proved to be cell permeable and able to mediate an autoimmune inflammatory response *in vitro* (Figure 2.16).

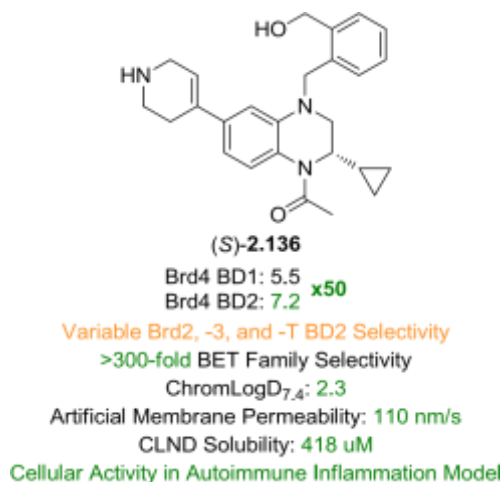


Figure 2.16. Profile of (S)-**2.136**.

One caveat is the lower BD2 selectivity at Brd2, 3 and T, which also varied between the inhouse FRET and DiscoverX BROMOscan™ assays. Some assay variability can be explained by the differing conditions under which the assays are run, but this should not affect the fold-selectivities within the same assay set. Both FRET and BROMOscan assays use recombinant protein truncates, and differences in their preparation and structure may be responsible. It should be noted that the instances of low BD2 selectivity are due to reduced BD2 potency, not increased BD1 activity, allowing a selectivity window for Brd4 BD2 to be exploited. Nonetheless, (S)-**2.136** is significantly more potent and selective than reported BD2-selective inhibitors and is suitable for use as an *in vitro* tool to examine BD2 inhibition.

Between the completion of this work and its publication, a patent was released describing a structurally similar series of tetrahydroquinoxalines as BD2-selective BET inhibitors.³⁴⁴ As potency data were binned, exact selectivities of these compounds are unknown, though no examples of >200-fold BD2 selectivity were reported.³⁴⁴ The majority of the substituents exemplified differed from those focussed on in this work.

2.5 Further Work

Although (S)-**2.136** broadly meets the specified probe criteria, future work in this series could consist of:

- Further improvement in BD2 potency and selectivity. The 50-fold selectivity window of (S)-**2.136** may be too narrow to unambiguously assign biological activity to particular

domains, particularly for the strong and varied phenotypes of the BET proteins. Ideally, BD1 potency would be further reduced to inactive levels, or BD2 potency improved compared to BD1. Work in this or other chemical series could build upon the learnings from this work to develop more selective inhibitors.

- Further investigation of the BD2 selectivity of (S)-**2.136** across the BET family. The use of alternative biochemical assays, ITC or biophysical measurements may allow definitive determination of the wider BD2-selectivity profile. Screening of (S)-**2.136** against full-length endogenous protein would also be desirable.
- Investigation of the biological effect of (S)-**2.136** in other cell lines, phenotypic assays and disease models, in an effort to elucidate the biological roles of the BD2 domains.
- Further exploration of the 3-substituted examples (Section 2.3.9), particularly through improvement of ligand efficiency, optimisation of the WPF shelf group, more thorough exploration of the pendant His-binding group and improvement of physicochemical properties. Although synthesis would be challenging, 2,3-disubstituted examples would also be of significant interest. Such efforts have the potential to further improve on the high selectivity of **2.122** and generate second-generation BD2-selective probes.

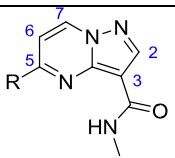
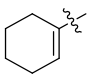
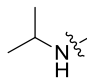
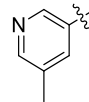
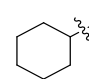
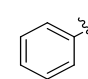
3. Design and Synthesis of BRPF1 Bromodomain Inhibitors

3.1. Introduction

Several BRPF1 bromodomain inhibitors (**1.46-1.51**) have been reported (See Section 1.5.4),^{194–199} but all except **1.49**¹⁹⁷ share the benzimidazolone chemotype and **1.48-1.51** show poor selectivity among other bromodomains.^{198,199} The benzimidazolones **1.46** and **1.47**, discovered by GSK and Pfizer, show the best potency and selectivity profile but are poorly soluble. To properly validate phenotypic data obtained with members of the benzimidazolone class and mitigate any potential series-specific liabilities, a selective inhibitor from an alternative chemotype is required.

During efforts to identify novel cores for the GSK bromodomain focussed set, several series' of 5,6-fused heterocycles with a methyl amide KAc mimetic were identified.³⁴⁵ Of these, pyrazolo[1,5-*a*]pyrimidines showed promise when docked into the BRPF1 bromodomain, and several examples were synthesised and screened in FRET assays against BRPF1, other bromodomains and in physicochemical property assays (Table 3.1).³⁴⁵

Table 3.1. Bromodomain FRET potencies, LE and physicochemical properties of initial pyrazolopyrimidine hits.

	 3.001	 3.002	 3.003	 3.004	 3.005
BRPF1 pIC₅₀ / LE	6.6 / 0.48	6.1 / 0.49	5.7 / 0.39	5.4 / 0.39	6.0 / 0.43
BRPF2 pIC₅₀	4.8	4.8	4.2 _a	-	<4
BRPF3 pIC₅₀	4.4	4.4	<4	-	4.1 ^a
Brd4 BD1 / BD2 pIC₅₀	4.4 ^b / <4.3	<4.3 / <4.3	4.6 / <4.3	<4.3 / <4.3	4.5 / 4.4 ^c
BPTF pIC₅₀	5.1	4.7	5.4	-	-
Brd7 pIC₅₀	5.1	4.8	-	-	5.0
Brd9 pIC₅₀	5.6	5.5	-	-	5.8
CECR2 pIC₅₀	5.5	4.4	-	-	5.5
PCAF pIC₅₀	5.2	5.2	-	-	5.1
ChromLogD_{7.4}	4.0	2.1	1.6	4.3	3.1
CLND Solubility (μM)	545	467	500	588	504
AMP (nm/s)	640	130	170	650	670

All potency data are n=2 or greater unless otherwise specified. Dashes indicate no data available. a) n=1, <4 on one other test occasion; b) n=3, <4.3 on two other test occasions; c) n=2, <4.3 on one other test occasion.

The pyrazolo[1,5-a]pyrimidine (PP) series showed micromolar potency against BRPF1, with high ligand efficiency for even the weaker inhibitors. Partially saturated rings (**3.001**) and secondary amines (**3.002**) at the 5-position of the core showed high potency and efficiency, while aromatics (**3.003**, **3.005**) were tolerated but less potent. Reducing the double bond of **3.001** gave **3.004**, which was over 10-fold less potent. Within the BRPF family, the series appeared to be BRPF1-selective, with the choice of 5-substituent affecting the degree of selectivity over BRPF2, from 20-fold (**3.002**) to >100-fold (**3.005**), with very low BRPF3 potency for all examples tested.

All examples tested had no significant activity against Brd4 (as a general measure of BET activity) – given the strong phenotype observed for BET inhibition this is a prerequisite for any non-BET bromodomain probe. Though TIF1α has been observed as an off-target for certain BRPF1 inhibitors of the benzimidazolone class,^{198,199} **3.001** showed low TIF1α potency (pIC₅₀ = 4.7). Aside from this, the pan-bromodomain selectivity of the series was poor. Relatively high potency was observed against Brd9 and CECR2, with lower but still significant activity seen for BPTF, Brd7 and PCAF. The high Brd9 potency is unsurprising, as Brd9 is closely homologous to the BRPF family (Figure 1.6) and BRPF1 was noted as a common off-target during the synthesis of Brd9 inhibitors.^{209,211} CECR2, BPTF and PCAF are much less closely

related to BRPF1, but share some key similarities in the KAc binding site (most notably an aromatic gatekeeper residue) which are the cause of the non-selective binding (See Section 3.3.10).

Interestingly, compared to cyclohexene **3.001**, amine **3.002** was over 10-fold less potent at CECR2 but had lower selectivity over Brd9. These data indicated that optimisation of the 5-substituent could potentially enable improved selectivity. Aromatic substituents at the 5-position proved even more promiscuous, with methylpyridine **3.003** almost equipotent at BPTF. To confirm that this was not due to the pyridyl nitrogen or methyl group, phenyl **3.005** was synthesised (See Table 3.2), and also showed poor selectivity over CECR2 and Brd9.

As well as high LE, the physicochemical properties of the series were generally good, with high aqueous solubility and both ChromLogD_{7.4} and artificial membrane permeability (AMP) within druglike space. However, it was noted that the addition of heteroatoms to the 5-substituent (**3.002** and **3.003**) caused a large drop in lipophilicity and hence reduced AMP, though it remained in acceptable space. In addition, **3.001** showed poor chemical stability, with solid samples gradually degrading under bench conditions. It is thought the conjugated alkene may act as a Michael acceptor or oxidation site, and therefore removing this motif was a priority.

Docking of **3.001** into the BRPF1 bromodomain (Figure 3.1)³⁴⁵ suggested that the methyl amide functions as the KAc mimetic and is constrained by an intramolecular H-bond to the pyrimidine nitrogen. The planar core packs against the Phe714 'gatekeeper' residue, while an overlay with the X-ray structure of the benzimidazolone **1.46** showed that the 5-cyclohexene may occupy much the same space as the piperidine of **1.46**, although the docking orientated the alkene in the plane of the PP ring system. Such an orientation would allow conjugation of the alkene π -system into that of the core and allow lipophilic contact with the ZA loop. Tuning the orientation and interactions in this region may offer the opportunity to improve BRPF1 potency and selectivity over other bromodomains. In addition, the 6- and 7- positions of the PP core may offer the opportunity to interact with the ZA loop, in a similar manner to the methoxyphenyl ring of **1.46** which forms cation- π interactions with Glu661 and increases potency.

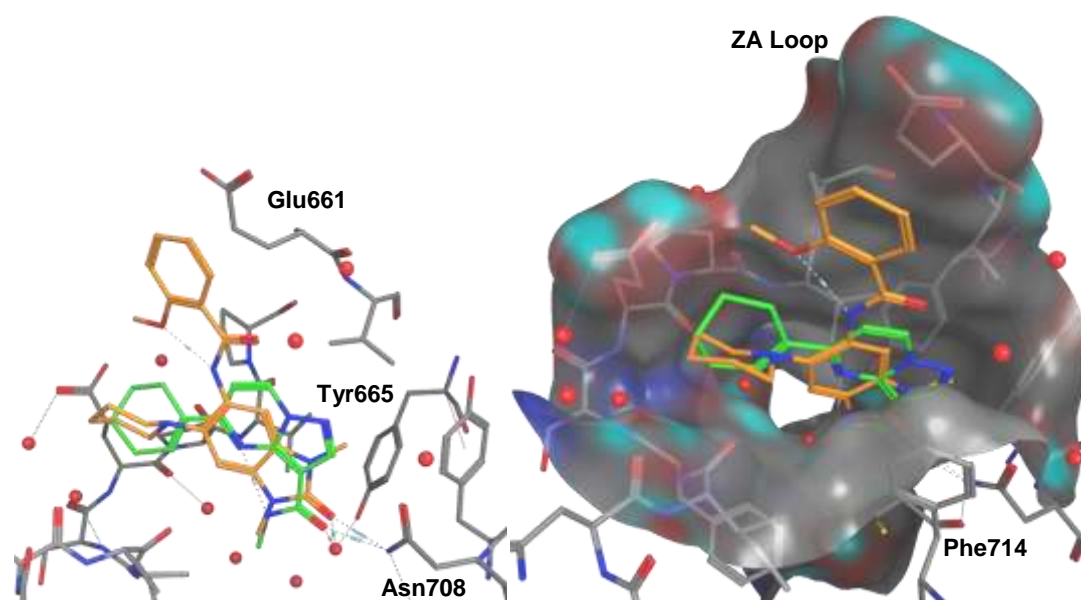


Figure 3.1. Docking of **3.001** (green, Armelle le Gall³⁴⁵) into the X-ray structure of **1.46** bound to the BRPF1 bromodomain (orange, PDB:4UYE) showing the warhead binding (left, Phe714 omitted for clarity) and surface (right).

3.2. Aims

This work aimed to optimise the PP series, or related novel scaffolds, to develop a second generation BRPF probe. The criteria for this probe would be:

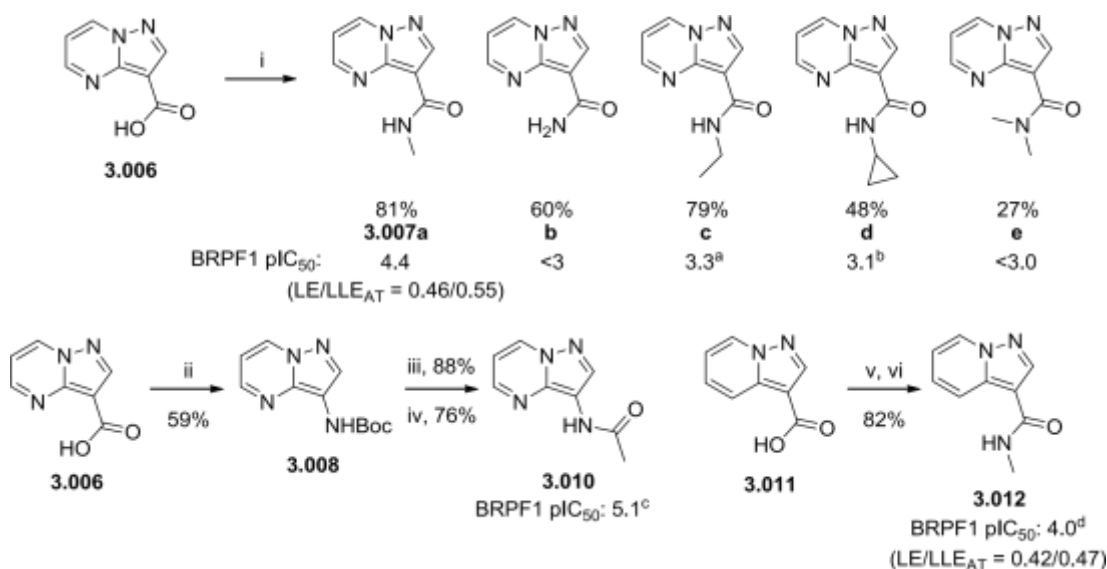
- BRPF1 $pIC_{50} > 7.0$.
- Defined BRPF1/2/3 selectivity profile (both pan-BRPF and single-bromodomain probes would be desirable)
- 100-fold selectivity over BET bromodomains, >50-fold selectivity against other nonBET bromodomains
- CLND solubility >100 μM , AMP >100 nm/sec, ChromLogD_{7.4} 2-4.
- Structurally differentiated from existing probe chemotypes

To achieve this, the following strategy was devised. The basic binding of the core would be investigated by synthesising various 5,6-fused fragment-like heterocycles. Although docking predicted the methyl amide with an internal hydrogen bond would likely be critical for activity, this would also be confirmed experimentally. Concurrently, the 5-substituent would be investigated. Due to the apparently broad tolerability observed at this vector, synthetic tractability and the varied effects on selectivity, a wide range of substituents would be screened initially before focussing on the most promising. Substitution at the 6- and 7- positions, and disubstitution, would also be investigated.

3.3. Results and Discussion

3.3.1 Fragment Cores and Warhead Optimisation

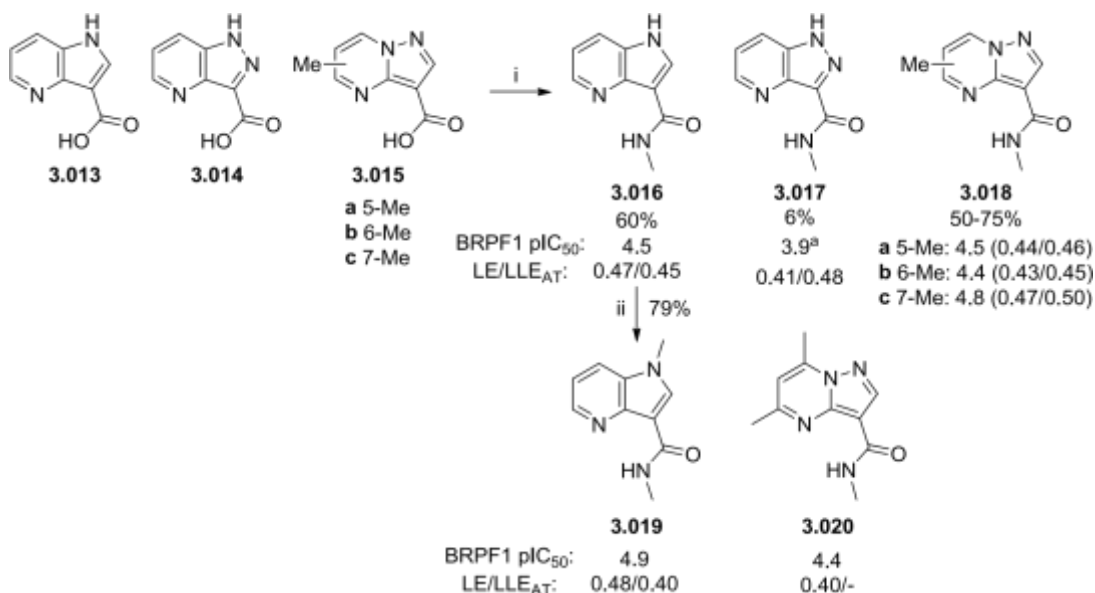
Although methyl groups are most commonly used as the lipophilic portion of the KAc mimetic,¹⁵⁶ larger alkyl groups are known to fulfil this role.²¹¹ To explore this, the postulated KAc mimetic was investigated by coupling the commercially available PP acid **3.006** with a small array of amines using HATU (Scheme 3.1). Only the methyl amide **3.007a** showed any significant activity, maintaining the high ligand efficiency of the initial hits. All other amides **3.007b-e** were inactive, even when tested at higher concentration. Reversal of the amide was achieved by subjecting **3.006** to a Curtius rearrangement, quenching with *tert*-butanol to form the Boc protected amine **3.008**. Deprotection and acetylation gave **3.010**, which showed no improvement over **3.007a**. To test the contribution of the intramolecular hydrogen bond, pyrazolo[1,5-*a*]pyridine **3.011** was amidated in a two-step procedure using oxalyl chloride and methylamine, giving **3.012**. Although **3.012** was less potent than **3.007a**, the drop in potency was reasonably small. It is hypothesised that the desired *trans* amide, with the carbonyl in plane with the core and methyl group in the least sterically hindered position, is intrinsically the most stable conformation and the contribution of the intramolecular hydrogen bond is small. Additionally, while the LE of **3.007a** and **3.012** was relatively similar, the higher lipophilicity of **3.012** resulted in a much lower LLE_{AT} – hence **3.007a** is more efficient in terms of lipophilicity. As lipophilicity often increases during optimisation,¹⁰ leads with low LLE_{AT} are important in striving for optimal physicochemical property space.



Scheme 3.1. Synthesis and activity of alternative KAc mimetics. a) n=1, <3 on two other test occasions; b) n=2, <3 on one other test occasion; c) n=1, <4 on three other test occasions; d) n=2, <4 on four other test occasions. LLE_{AT} calculated using ChromLogD_{7.4}. Reagents and conditions: (i) Amine, HATU,

DIPEA, DMF, rt; (ii) diphenyl phosphorazidate, Et₃N, toluene, 100 °C, then ^tBuOH, 100 °C; (iii) TFA, DCM, rt; (iv) AcCl, pyridine, DCM, rt; (v) (COCl)₂, DMF, DCM, rt; (vi) MeNH₂, THF, rt.

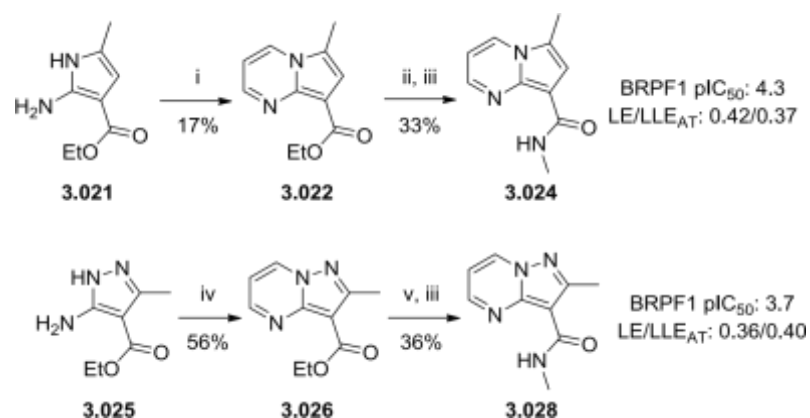
With the methyl amide and intramolecular hydrogen bond confirmed as optimal, alternative cores with these motifs were investigated. To probe tolerability towards substitution, a methyl group was also placed at each position in turn (Scheme 3.2). Commercially available acids **3.013-3.015a-c** were amidated with HATU to give **3.016-3.018a-c**. Indole **3.016** was subsequently methylated in good yield using phase-transfer alkylation, affording **3.019**.³⁴⁶ Dimethyl PP **3.020** was obtained from the GSK compound collection.



Scheme 3.2. Core modifications. All potency data are n=2 or greater unless specified. a) n=1, <4 on one additional test occasion. LLE_{AT} calculated using ChromLogD_{7.4}. Reagents and conditions: (i) MeNH₂, HATU, DIPEA, DMF, rt; (ii) MeI, KOH, Bu₄NSO₄H, H₂O, DCM, rt.

Azaindole **3.016** was slightly more potent than **3.007a** with reduced LLE_{AT} due to increased lipophilicity. Pyrazolopyridine **3.017** showed reduced potency and efficiency, potentially due to unfavourable placement of the N2 nitrogen lone pair in the lipophilic edge of the binding pocket. *N*-Methyl azaindole **3.019** showed a further improvement in potency compared to **3.016**, with LE higher than the initial core **3.007a** but LLE_{AT} substantially reduced, indicating the lipophilic methyl group is not an efficient addition. Methyl substitution in the 5- (**3.018a**) and 6- (**3.018b**) positions was tolerated but gave no significant benefit, whilst the 7-Me analogue **3.018c** gave a half log unit increase in activity compared to **3.007a**. Of these three examples, 7-Me **3.018c** showed the highest efficiency, with only a small drop in LLE_{AT}. However, this SAR did not prove additive in the case of the dimethyl **3.020**. It is hypothesised

that introduction of the 5-methyl causes the core to adopt a subtly different orientation in the binding site which disrupts the beneficial contacts being made by the 7methyl substituent. Other cores required *de novo* synthesis. The bicyclic esters **3.022** and **3.026** were generated by condensation of aminopyrrole **3.021** and aminopyrazole **3.025** with 1,1,3,3-tetramethoxypropane under acidic conditions. Although pyrazolopyrimidine **3.022** was obtained in good yield using HCl, these conditions gave a poor yield for pyrrolopyrimidine **3.026**, however switching to acetic acid improved the yield to a usable 17%. This may be due to the greater nucleophilicity of pyrazoles due to the alpha-effect of the adjacent nitrogen, and the lower stability of pyrroles causing degradation during the reaction. Ester hydrolysis and amide formation gave the desired products **3.024** and **3.028** in 33-36% yield over the two steps.



Scheme 3.3. Core modifications. All potency data are n=3. LLE_{AT} calculated using ChromLogD_{7.4}.

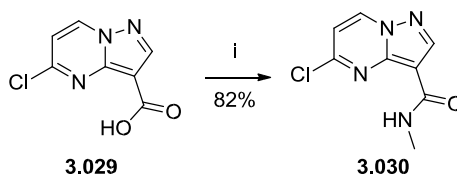
Reagents and conditions: (i) 1,1,3,3-tetramethoxypropane, AcOH, 100 °C; (ii) 1 M KOH, MeOH, rt; (iii) MeNH₂, HATU, DIPEA, DMF, rt; (iv) 1,1,3,3-tetramethoxypropane, 5 M HCl, 95 °C; (v) 1 M NaOH, MeOH, THF, rt

Pyrrolopyrimidine **3.024** was tolerated but with no improvement in potency over **3.007a**, and lesser activity compared to *N*-Me AI **3.019**. Substitution from the 2-position (**3.028**) was detrimental, in accordance with computational modelling (Figure 3.1) where the methyl group of **3.028** would be predicted to clash with the protein. Overall, the SAR of these fragments supported the hypothesised binding mode, but only small and weakly efficient improvements in potency were obtained. The PP and *N*-Me azaindole (AI) cores were taken forward to further optimisation, while also noting the promise of the 7-position as a vector for increasing potency.

3.3.2 The Pyrazolopyrimidine 5-Position

Initial Exploration

To further explore the SAR around the potent cyclohexene hit **3.001**, a number of 5-substituted compounds were synthesised. Whilst HATU is a highly effective amide coupling reagent, it is expensive and wasteful on scale, producing multiple byproducts which often must be removed using chromatography. Commercially available acid **3.029** was amidated in a two-step procedure using inexpensive oxalyl chloride, which produces only gaseous or inorganic byproducts, to give the 5-chloro intermediate **3.030** on gram scale (Scheme 3.4).



Scheme 3.4. Synthesis of 5-substituted pyrazolopyrimidines intermediate **3.030**. Reagents and conditions: (i) (COCl)₂, DMF, DCM, rt; then MeNH₂, rt.

The desired 5-substituent was then appended using Suzuki-Miyaura cross-coupling (**3.005**, **3.031-3.040**), Sonogashira coupling (**3.041**) or S_NAr (**3.042-3.044**) (Table 3.2). While many of the Suzuki-Miyaura couplings proceeded in good yield, poor stability of the boronic acid reduced the yield for some of the alkene examples. Where the building blocks contained Boc-protected amine groups, these were deprotected with TFA in high yield after the coupling. **3.037** and **3.039** proved unstable as the free base and so were isolated as hydrochloride salts – this instability may explain the low yields observed but raised concerns around the suitability of these examples for use as chemical tools. Cyclopropyl **3.040** was synthesised in excellent yield using the corresponding trifluoroborate, using the conditions developed by Molander for the coupling of this reagent to heteroaryl chlorides.³⁴⁷ The chloroPP **3.030** proved highly amenable to S_NAr reactions, and it was noted (initially from side products observed during the synthesis of **3.030**) that methylamine underwent this reaction at room temperature to give **3.043** in good yield. The room temperature reaction was not investigated for **3.042** and **3.044**. Aniline **3.045** was obtained from the GSK compound collection.

Table 3.2. Synthesis, structures and potencies of initial 5-substituted PPs.

3.030 Conditions 3.005, 3.031-3.044

Cpd	Reagents	Method	R	Yield(s)	BRPF1 pIC ₅₀	LE
3.005		i		67%	6.0	0.43
3.031		i		21%	6.3	0.48
3.032		i		25%	6.2	0.42
3.033		i		62%	5.9	0.43
3.034		i		72%	5.6	0.40
3.035		i		11%	5.9	0.40
3.037		i, ii		64%, 49%	6.4	0.46
3.039		i, ii		40%, 11%	5.6	0.37
3.040		iii		94%	5.5	0.47
3.041		iv		49%	5.0	0.38
3.042		v		89%	6.0	0.43
3.043		v*		72%	5.4	0.49
3.044		v		79%	6.1	0.44
3.045	-**	-**		-**	5.4	0.37

All potency data are n=3 or greater. Reagents and conditions: (i) RB(OH)₂ or RBPIn, Pd(PPh₃)₄, Na₂CO₃, 2:1:1 Toluene:EtOH:H₂O, 120 °C, μW; (ii) TFA, DCM, rt; (iii) cPrBF₃K, Pd(OAc)₂, CataCXium A, Cs₂CO₃, 10:1 Toluene:H₂O, 100 °C, μW; (iv) cPrCCH, Pd(PPh₃)₂Cl₂, CuI, Et₃N, DMF, 120 °C, μW; (v) Amine, DIPEA, DMSO, 120 °C, μW. *Reaction carried out at rt. **Obtained from the GSK compound collection.

Unfortunately, all of these examples proved less potent than cyclohexene **3.001** (BRPF1 pIC₅₀ = 6.6). Even close analogues to **3.001**, such as cyclopentene **3.031**, showed a drop in potency, though ligand efficiency was maintained. Norbornene **3.032** was synthesised to introduce 3D character to the otherwise flat molecule, but potency and LE were again lowered. The introduction of an oxygen atom (**3.033** and **3.034**) gave varying reductions in potency compared to **3.001** depending on its position. Methyl tetrahydropyridine **3.035** showed similar

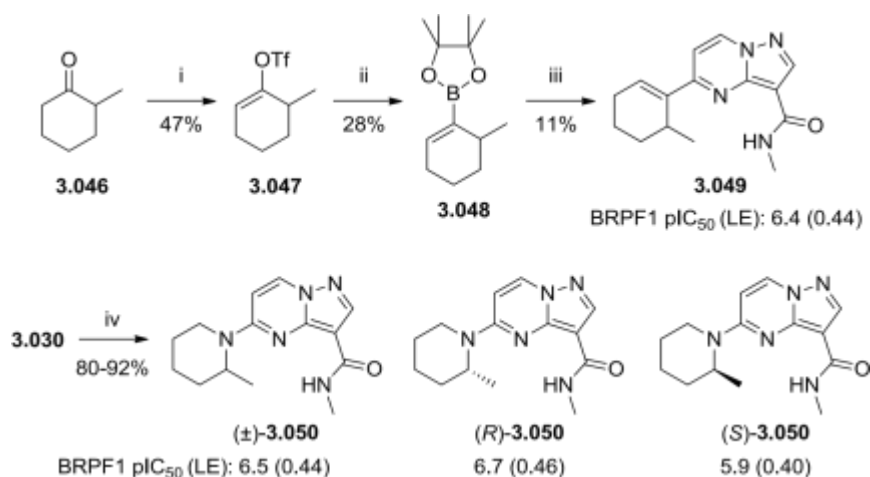
potency, though the NH analogue **3.037** showed a 0.5 log unit increase in potency and LE compared to **3.035**, indicating that the NH may be forming a hydrogen bonding interaction. Protonation of **3.035** could also allow it to act as a hydrogen bond donor. Bridged variant **3.039** was less potent, potentially due to an altered hydrogen bond vector or steric clash with the binding site. Cyclopropyl **3.040** was a relatively weak but highly efficient binder, while alkyne **3.041** was poorly potent, potentially due to the highly directional nature of the alkyne substituent. Given the efficient binding of isopropylamine **3.002**, *N*-linked secondary amines were tested; while bulky alkyl substituents such as **3.042** were tolerated, moving to smaller alkyls (**3.043**) or anilines (**3.045**) was detrimental. However, methylamine **3.043** maintained high ligand efficiency, suggesting that the amine nitrogen plays a significant role in binding. Piperidine **3.044** was also reasonably potent, though LE was reduced compared to **3.043**, again indicating that the alkyl section of the substituent contributes to binding with lower efficiency than does the nitrogen.

While offering no insight into the reduction in potency seen compared to **3.001**, comparing the docking of **3.001** and the crystal structure of benzimidazolone **1.46** in BRPF1 (Figure 3.1) may rationalise the relatively flat SAR of the PP series compared to benzimidazolones such as **1.46**. For **1.46**, the piperidine is twisted out of the plane of the core and occupies a lipophilic shelf region, whereas for **3.001** the cyclohexene group is postulated to be in the plane of the core and contact with this region is poorer. While the introduction of a 6-substituent may force the 5-substituent to twist out of plane due to steric clashes, it was thought that increasing steric hindrance around the linker could have the same effect.

α -Methyl Substituents

To test this hypothesis, an α -methyl substituent was appended to both the cyclohexene and piperidine analogues (Scheme 3.5). For the cyclohexene example, the enantiotopic position was chosen to introduce the maximum degree of 3D character. Reaction of methyl cyclohexanone **3.046** with LDA gave the kinetic enolate, which was trapped with phenyl triflimide to form the enol triflate **3.047**.³⁴⁸ Purification of **3.047** proved problematic due to coeluting impurities, and the material was used impure in a Suzuki-Miyaura cross-coupling with **3.030** to produce racemate **3.049** in low but usable yield. While **3.049** showed an improvement in potency compared to other analogues (Table 3.2), it was still less potent and had lower LE than **3.001**. Racemic and enantiopure 2-methyl piperidines **3.050** were synthesised by S_NAr in high yield. Although initially carried out with microwave heating, it was subsequently found that the reaction also proceeded at room temperature with longer reaction times. Racemate (\pm)-**3.050** gave a boost in potency compared to **3.044**, with most activity residing in the *R*-enantiomer. Pleasingly, (*R*)-**3.050** showed potency equal to the initial hit

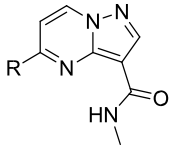
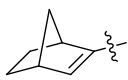
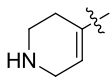
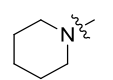
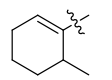
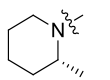
3.001 and only a small reduction in LE. The methyl group may occupy a small pocket at the edge of the ZA loop (Figure 3.2).



Scheme 3.5. Synthesis of α -Me 5-substituted pyrazolopyrimidines and their BRPF1 activity. All potency data are $n=3$ or greater. Reagents and conditions: (i) PhNTf₂, LDA, DME, -78 - 0 °C; (ii) B₂Pin₂, PdCl₂(dppf), KOAc, DMF, 85 °C; (iii) **3.030**, Pd(PPh₃)₄, Na₂CO₃, 2:1:1 Toluene:EtOH:H₂O, 120 °C, μ W; (iv) 2-methylpiperidine, DIPEA, DMSO, rt or 120 °C, μ W.

While potency had not been improved relative to the initial hit **3.001**, it was also important to examine the broader profiles of representative 5-substituents to select areas for further optimisation (Table 3.3). Norborene **3.032** showed improved selectivity over CECR2 compared to **3.001**, but Brd9 selectivity worsened. Tetrahydropyridine **3.037** had a much improved selectivity profile, with >25-fold selectivity over all other Brds tested, but was highly polar and completely impermeable in the AMP assay due to the basic centre. Piperidine **3.044** had good selectivity over Brd7 and CECR2 but Brd9 and Brd4 selectivity were relatively poor. Methyl cyclohexene **3.049** was poorly selective, being only 2-fold less potent at Brd9 and less selective than the parent **3.001**. Although relatively lipophilic, **3.049** maintained high aqueous solubility. Interestingly, the methyl group had the opposite effect in the piperidine series ((*R*)-**3.050**), slightly improving Brd9 selectivity compared to **3.049** and removing Brd4 activity. Piperidines **3.044** and **3.050** both showed excellent physicochemical property profiles, with removal of the alkene moiety and introduction of a heteroatom having a striking effect on lipophilicity compared to methylcyclohexene **3.049**. The *N*-linked piperidines also removed the potentially unstable alkene moiety. BRPF2/3 potency was similar to the initial hits and was relatively unaffected by the choice of substituent, though alkenes **3.032** and **3.049** showed slightly lower selectivity over BRPF2.

Table 3.3. Bromodomain FRET potencies, LE and physicochemical properties of 5-substituted PPs.

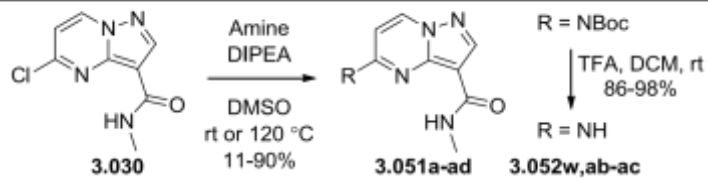
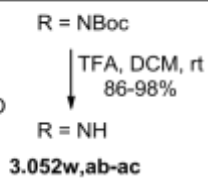
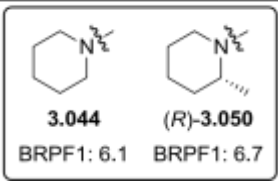
	R				
	 3.032	 3.037	 3.044	 (±)-3.049	 (R)-3.050
BRPF1 pIC₅₀ / LE	6.2 (0.42)	6.4 (0.46)	6.1 (0.44)	6.4 (0.44)	6.7 (0.46)
BRPF2 pIC₅₀	4.8	4.7	4.6	4.9	4.7
BRPF3 pIC₅₀	4.2	4.5	4.0 ^a	4.3	4.2
Brd4 BD1 / BD2 pIC₅₀	<4.3 / <4.3	<4.3 / <4.3	5.4 ^b / 4.6 ^b	4.4 / 4.7	4.6 ^c / 4.5 ^d
Brd7 pIC₅₀	4.9	4.4	4.9	5.3	5.1
Brd9 pIC₅₀	5.5	5.0	5.3	6.1	5.8
CECR2 pIC₅₀	4.9	5.0	4.7	5.3	4.8
ChromLogD_{7.4}	4.2	-0.4	2.8	4.8	3.3
CLND Solubility (μM)	456	405	441	513	610
AMP (nm/s)	500	<3	260	620	307

All potency data are n=2 or greater unless otherwise specified. a) n=1, <4 on one other test occasion; b) n=1, <4.3 on two other test occasions; c) n=3, <4.3 on two other test occasions; d) n=4, <4.3 on one other test occasion.

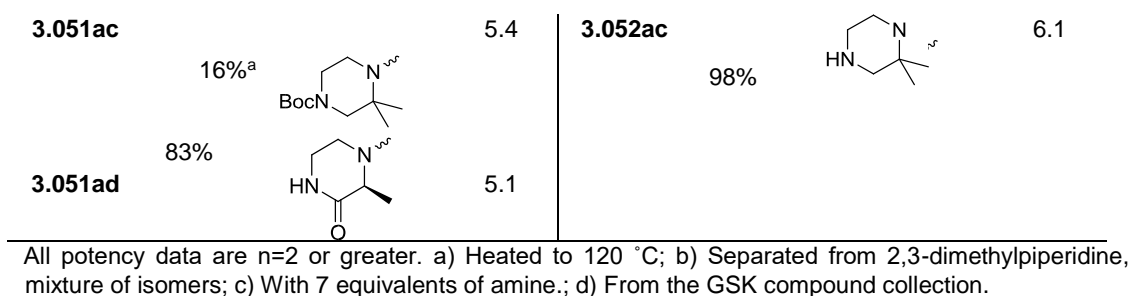
2-Methyl *N*-Linked Heterocycles

From these data, it was decided that *N*-linked heterocycles with α -Me substituents were a promising area for further investigation, as were substituents with free NH motifs analogous to **3.037** (provided the permeability could be improved). To thoroughly investigate this area, an array of cyclic *N*-linked heterocycles with α -Me groups was undertaken (Table 3.4). Pleasingly, the S_NAr reactions utilised to access these compounds were found to proceed in high yield at room temperature for all but the most hindered substrates, allowing efficient parallel synthesis. Where the amine was more sterically hindered or zwitterionic, the mass balance generally consisted of unreacted starting material. Where the products **3.051** contained a Boc protected amine, this was removed with TFA to give **3.052**.

Table 3.4. Structures and potencies of amine array products **3.051a-ad** and **3.052**

							
Cpd	Yield	5-Amine	BRPF1 pIC₅₀	Cpd	Yield	5-Amine	BRPF1 pIC₅₀

(S)- 3.051a	70%		5.7	(R)- 3.051a	72%		6.4
3.051b	66%		5.8	3.051c	68% ^a		5.9
3.051d	55% ^a		6.3	3.051e	52% ^a		6.7
3.051f	87%		6.1	3.051g	82%		6.3
3.051h	30%		4.9	3.051i	46%		4.7
3.051j	67%		6.4	3.051k	32% ^a		6.3
3.051l	71%		5.9	3.051m	15% ^a		6.4
3.051n	90%	Isomeric mixture	Not tested	3.051o	-	Isomer 1	6.8
3.051p	-	Isomer 1	5.9	3.051q	-	Isomer 2	6.7
3.051r	6% ^b		6.2	3.051s	79% ^b		6.2
3.051t	83%		6.5	3.051u	66%		6.5
3.051v	61% ^c		5.6	3.051w	69%	BocN	5.9
3.052w	94%		6.0	3.053	- ^d		5.7
3.051x	63%		6.0	3.051y	11% ^a		5.8
3.051z	45% ^a 73%		6.1	3.051aa	85% ^c		6.4
(R)- 3.051ab		BocN	5.5	(R)- 3.052ab	86%		6.7
(S)- 3.051ab	64%	BocN	5.2	(S)- 3.052ab	98%		6.1



Pyrrolidines were poorer than their piperidine analogues, with (*R*)-**3.051a** around half a log unit less potent than (*R*)-**3.050**. The *R*-enantiomer was the more potent throughout this exploration. Though *gem*-disubstitution was tolerated (**3.051d**), substitution of the methyl group with a hydroxyl (**3.051b**) or exchange for a trifluoromethyl (**3.051c**) was detrimental. *Trans*-disubstituted pyrrolidine **3.051e** was highly potent, possibly as a result of increased steric clashes twisting the pyrrolidine out of plane of the core.

Moving the methyl group to the 3- (**3.051f**) or 4-position (**3.051g**) of the piperidine caused a reduction in potency, though **3.051g** had a similar potency to bare piperidine **3.044**, suggesting improved contact with the lipophilic surface of the pocket. Introduction of acids (**3.051h**, **3.051i**) was highly detrimental, unsurprising given the lipophilic nature of this region of the binding pocket.

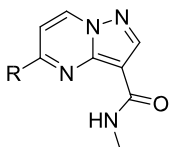
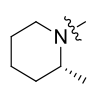
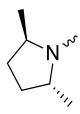
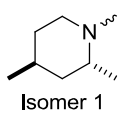
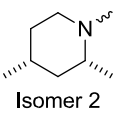
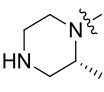
In terms of the 2-position, an ethyl group (**3.051j**) was tolerated with little loss of potency, with isopropyl **3.051k** also well tolerated. Hydroxyethyl **3.051l**, however, was detrimental - as expected from comparison to pyrrolidine **3.051b**. As seen with pyrrolidine **3.051e**, piperidine 2,6-disubstitution (**3.051m**) was tolerated, though **3.051m** did not improve on the monosubstituted analogues and the *trans* enantiomers were not tested due to monomer unavailability. The use of 2,4-dimethylpiperidine gave a mixture of isomers **3.051n**, which was separated by chiral HPLC to give **3.051o-q**. Both **3.051o** and **3.051q** displayed equivalent potency to (*R*)-**3.050**, and the observed potencies allow speculation that these are the 2*R*-enantiomers, with **3.051p** being the corresponding *cis*-2*S*-isomer. Following the pattern observed for **3.051g** and **3.044**, the 4-Me group appears to add little additional potency in either configuration. Unfortunately, the alternative *trans* isomer could not be isolated, but as the 2*S* isomer would be predicted to be less potent. The 2,3-dimethyl analogues were synthesised from a mixture of isomers to give separable diastereomers **3.051r** and **3.051s**, which also showed a reduction in potency compared to (\pm)-**3.050**.

Increasing the ring size to azepane **3.051t** afforded a small potency improvement over piperidine **3.044**, but no increase in potency was seen on addition of a methyl group (**3.051u**). Homopiperazines **3.051v** and **3.052w** were also less well tolerated. For 6-membered rings bearing an additional heteroatom, a general increase in potency of ~0.4 log units was observed

on addition of the 2-methyl group, exemplified by comparison of morpholines **3.053** (obtained from the GSK compound collection) and **3.051x**. Once again, the addition of a second methyl group at the 6-position did not improve potency relative to **3.051x**, although of the two 2,6-dimethylmorpholine isomers tested, (*R*),(*R*)-*trans* **3.051z** was the more potent compared to the *cis* isomer **3.051y**. The (*S*),(*S*)-*trans* starting material was unavailable. Unsubstituted piperazine **3.051aa** was more potent than **3.044** and similar to tetrahydropyridine **3.037**, but unfortunately addition of the 2-methyl group (**3.052ab**) gave a smaller gain in potency than for the piperidine examples. *Gem*-disubstitution was somewhat detrimental for 6-membered rings (**3.052ac**) due to the difference in ring size and conformation compared to the pyrrolidine **3.051d**. Addition of a carbonyl group to the 3-position of the piperazine ring was highly detrimental (**3.051ad**) and in all cases the *N*-Boc analogues **3.051w,ab,ac** were poorly tolerated, again unsurprising given the small size of the binding pocket these substituents occupy.

Unfortunately, none of these amines surpassed the potency of (*R*)-**3.050** within statistical significance, with **3.051e,o,q** and (*R*)-**3.052ab** being the most potent. The wider selectivity and physicochemical properties of these examples were investigated and compared to (*R*)-**3.050** (Table 3.5).

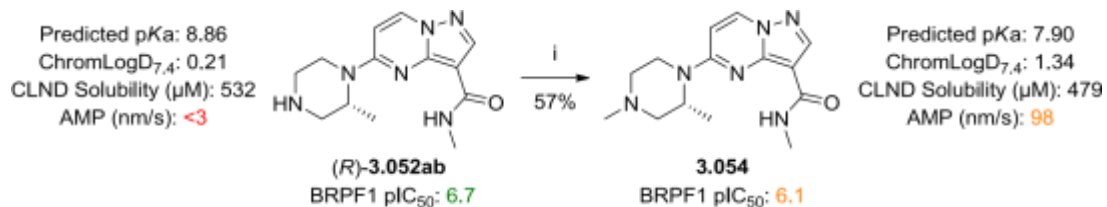
Table 3.5. Bromodomain FRET potencies and physicochemical properties of 5-heterocyclic PPs.

	R				
	 (<i>R</i>)- 3.050	 3.051e	 Isomer 1 3.051o	 Isomer 2 3.051q	 (<i>R</i>)- 3.052ab
BRPF1 pIC₅₀ / LE	6.7 (0.46)	6.7 (0.46)	6.8 (0.44)	6.7 (0.44)	6.7 (0.46)
BRPF2 pIC₅₀	4.7	5.5	-	5.4	4.9
BRPF3 pIC₅₀	4.2	5.1	-	4.9	4.8
Brd4 BD1 / BD2 pIC₅₀	4.6 ^a / 4.5 ^b	4.6 / 4.4	<4.3 ^c / 4.6 ^c	4.5 ^d / <4.3	<4.3 / <4.3
BPTF pIC₅₀	5.1	5.6	5.0	5.2	5.3
Brd7 pIC₅₀	5.1	5.7	-	5.5	-
Brd9 pIC₅₀	5.8	6.6	5.9	6.5	5.4
CECR2 pIC₅₀	4.8	5.0	-	4.9	4.8
ChromLogD_{7.4}	3.3	3.6	4.2	4.2	0.2
CLND Solubility (μM)	610	491	467	452	532
AMP (nm/s)	307	360	-	600	<3

All potency data are n=2 or greater unless otherwise specified. Dashes indicate no data available. a) n=3, <4.3 on two other test occasions; b) n=4, <4.3 on one other test occasion; c) n=1; d) n=2, <4.3 on one other test occasion.

For all examples, selectivity for BRPF1 was reduced compared to (*R*)-**3.050**, with **3.051e** and **3.051q** in particular showing increased BRPF2 potency. The region in which the 5-substituent binds is wider in BRPF2 (See Section 3.3.11), so larger substituents may occupy it more closely. The rationale for the increased BRPF3 potency of these examples is unclear. As expected, the nature of the 5-substituent had a dramatic effect on wider bromodomain selectivity. Dimethylpyrrolidine **3.051e** and dimethylpiperidine **3.051q** were almost equipotent at Brd9, with increases in Brd7 and BPTF potency also observed. Although **3.051o** showed a similar selectivity profile to (*R*)-**3.050**, the additional methyl group has no significant benefit. (*R*)-**3.052ab** displayed marginally improved Brd9 selectivity and similar BPTF potency. Despite the likely reduction in p*K*_a for **3.052ab** vs tetrahydropyridine **3.037**, the basic amine is still protonated at pH 7.4, resulting in a very low ChromLogD_{7.4} and no measurable artificial membrane permeability.

Methylation of (*R*)-**3.052ab** under Eschweiler–Clarke conditions gave **3.054**, which significantly improved physicochemical properties but reduced BRPF1 potency (Scheme 3.6). Calculation of p*K*_a values for **3.052ab** and **3.054** showed that the methyl group of **3.054** reduced p*K*_a by around 10-fold, due to steric disruption of ion solvation by the methyl group. The reduced ionisation level of **3.054** allows improved permeation through the neutral and lipophilic artificial membrane. However, the α-methyl piperidine (*R*)-**3.050** remained the optimal substituent moving forwards.



Scheme 3.6. Synthesis, potency and physicochemical properties of **3.054**. Potency data are n=3. p*K*_a calculated using ChemAxon. Reagents and conditions: (i) CH₂O, CHO₂H, H₂O, 70 °C.

Aminopiperidines

Modelling showed the presence of Glu655 and several backbone carbonyls at the edge of the pocket in which the 5-substituent is theorised to bind (Figure 3.2). It was thought that the placement of amines in this region could form hydrogen bonds or ionic interactions with these residues, and this may explain the tolerability of piperazines such as **3.052ab**. Several aminopiperidines were examined to attempt to optimise this putative interaction.

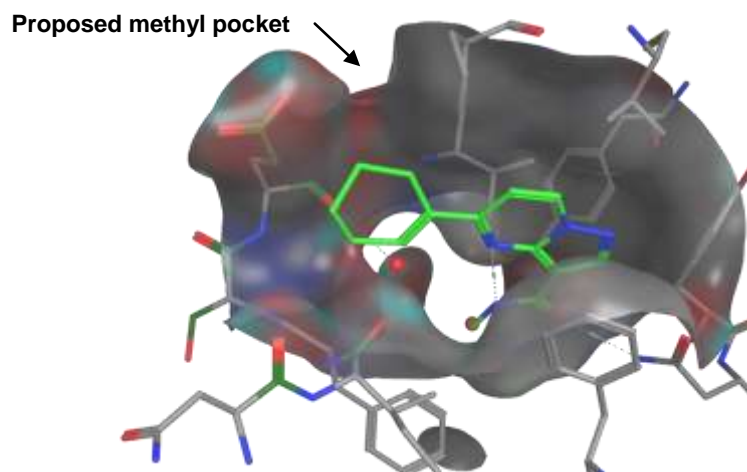


Figure 3.2. Docking of **3.001** in the BRPF1 bromodomain (green, Armelle le Gall³⁴⁵), with hydrogenbond acceptors near to the 5-position vector highlighted dark green. The pocket where the methyl group was hypothesised to bind is highlighted.

Though the poor permeability of analogues such as (*R*)-**3.052ab** was a concern, pendant primary or tertiary amines were expected to be less basic, and so have improved permeability. These amino-substituted piperidines **3.051ae-ao** were synthesised through S_NAr under the previously developed conditions, with reactions proceeding smoothly at rt.

Where the pendant amine was protected with a Boc group, this was again removed with TFA (Table 3.6). Yields were generally good to excellent, with fused tricycles **3.051al-am** showing reduced yield due to chiral HPLC separation and poor separation of impurities.

Table 3.6. Structures and potencies of aminopiperidine substituted PPs.

Cpd	Yields	5-Amine	BRPF1 pIC ₅₀	Cpd	Yields	5-Amine	BRPF1 pIC ₅₀
3.051ae	87%		5.5	3.052ae	82%		6.1
3.052af	83%, 98%		6.4	3.052ag	98%, 73%		6.4
3.051ah	94%		6.1	3.052ai	81%, 69%		6.5
3.051aj	77%		6.1	3.052ak	17% ^a		6.2
3.052al	16% ^a		6.0	3.052am	- ^b		6.0
(±)-3.052an	- ^b		6.6	3.051ao	55%		6.2
3.055	- ^b		5.7				

All potency data are n=2 or greater. a) Separated from the same reaction using racemic starting material by chiral HPLC. Yield is over 2 steps; b) See Scheme 3.7 for synthesis.

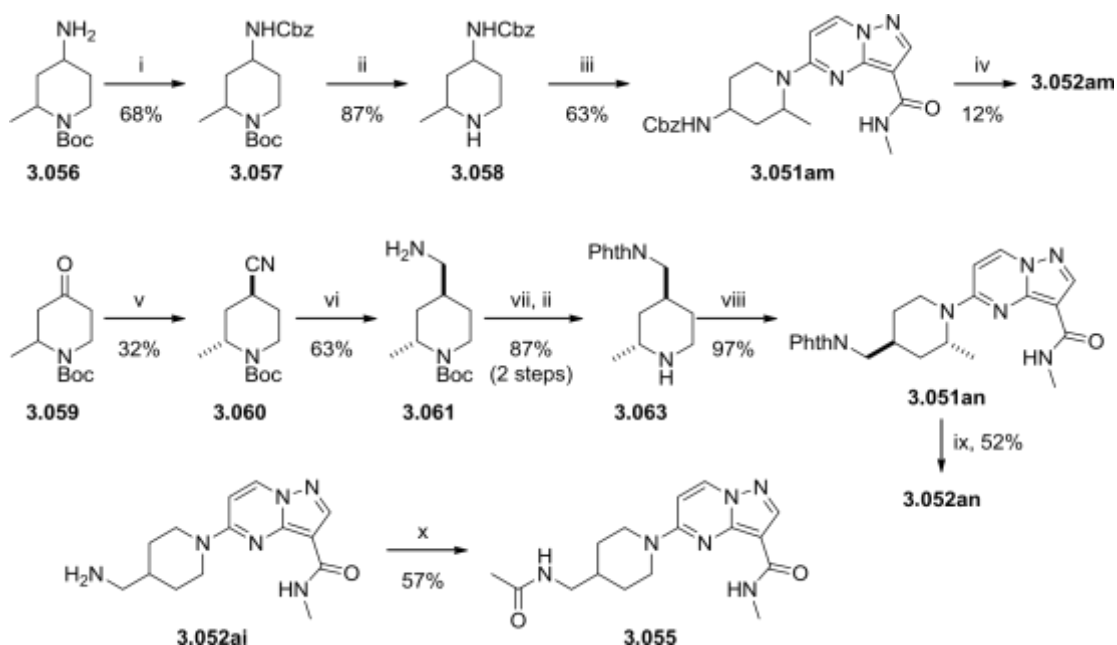
A 3-amino group (**3.052ae**) was tolerated but similar in potency to **3.044**, whilst combination with the 2-methyl group gave **3.052af**, which exhibited a very slight increase in potency. The binding mode of the amine is not established, and if it were to prefer binding on the same face as the methyl group then the alternative 2,3-regioisomer may be favoured. However, this compound was not prepared as building blocks were unavailable.

In general, amines were tolerated at the 4-position of the piperidine. Primary amine **3.052ag** had slightly improved potency relative to the parent piperidine **3.044**, while the tertiary amine variant **3.051ah** was equipotent. When the amines were homologated one carbon out from the ring (**3.052ai** and **3.051aj**), potency was essentially unchanged relative to **3.052ag** and **3.051ah**. Given that the formation of an electrostatic interaction typically produces large increases in potency (>1000-fold in some examples²³⁵), an ion pair is most likely not being formed. The loss of potency on dimethylation (**3.051aj**) and removal of hydrogen bond-donor

capability suggests that weak and subtle hydrogen bonding interactions may be responsible for the observed potency.

Cyclisation of the amines into 5,6-bicycles **3.052ak** and **3.052al** somewhat reduced potency – the respective *trans* bicycles were not available. Combining the 4-amino substituent with the 2-methylpiperidine motif resulted in **3.052am** and **3.052an**. Interestingly, **3.052am** showed reduced potency compared to both (\pm)-**3.050** and **3.052ag**. The *trans* diastereomer of **3.051am** was observed as a minor product in the S_NAr reaction, but unfortunately in insufficient quantity for isolation. The *trans*-4-aminomethyl variant maintained the higher potency of **3.050** and **3.052ai**. To further investigate the role of the amine substituent, amide **3.051o**, which lacks basic character, was synthesised and showed slightly reduced potency compared to **3.052ai**. Though the relatively flat SAR makes definitive explanations difficult, based on this result and the lower potency of **3.052aj** it is suggested that any interactions being formed are not ionic in nature. It is important to note that the amide of **3.051o** will also change the hydrogen-bonding vectors of the nitrogen, a possible explanation for reduced potency. Acetylation of **3.052ai** with acetyl chloride (See Scheme 3.7) gave the amide **3.055**, which showed reduced potency due to a suspected steric or electronic clash with the protein.

While the majority of amines used in this investigation were available from commercial sources, some building blocks required *de novo* synthesis (Scheme 3.7). To produce **3.052am**, the corresponding piperidine **3.056** was purchased (majority *cis*, small amount of *trans*) as an unequal mixture of diastereomers. Protecting group manipulation gave **3.058** before coupling to the core and separation of the diastereomers. Although the deprotection proceeded in good yield (74%), the poor separation of the resulting diastereomers by HPLC resulted in a low yield of the pure products **3.051am**.



Scheme 3.7. Synthesis of 5-(aminopiperidine) PPs. Reagents and conditions: (i) CbzCl, K₂CO₃, THF, rt; (ii) TFA, DCM, rt; (iii) **3.030**, DIPEA, DMSO, 90 °C, μ W; (iv) HBr, AcOH, rt then HPLC; (v) TosMIC, KO^tBu, DME, rt; (vi) BH₃•THF, THF, 75 °C; (vii) Phthalic anhydride, toluene, 120 °C; (viii) **3.030**, DIPEA, DMSO, rt; (ix) MeNH₂, EtOH, 120 °C, μ W; (x) AcCl, pyridine, DCM, rt.

The synthesis of homologated example **3.052an** proved more challenging. Ketone **3.059** underwent Van Leusen cyanation to give nitrile **3.060**,³⁴⁹ producing a single diastereomer which was inferred to be the *trans* product based on the confirmed stereochemistry of **3.063**. The high stereocontrol was intriguing, as Van Leusen cyanation of the analogous 3methylcyclohexanone has been reported to give a mixture of diastereomers.³⁵⁰ Though KO^tBu is an insufficiently strong base (pK_a ~17) to deprotonate the nitrile α -position (pK_a ~33)³⁵¹ and thus epimerise the stereocenter, the Van Leusen mechanism does proceed through anion **A** (Figure 3.3).³⁵² As a completely diastereoselective protonation of **A** is unlikely, it can be hypothesised that **3.060** is in fact the thermodynamic product. The small nature of a nitrile group means an axial conformation is disfavoured relative to an equatorial conformation to a lesser extent.³⁵³ Additionally, placing the methyl group equatorial (**B**) may cause a clash with the Boc group - if the methyl adopts an axial orientation to avoid this then an equatorial nitrile (**C**) would be preferred over a *bis*-axial conformation (**D**).

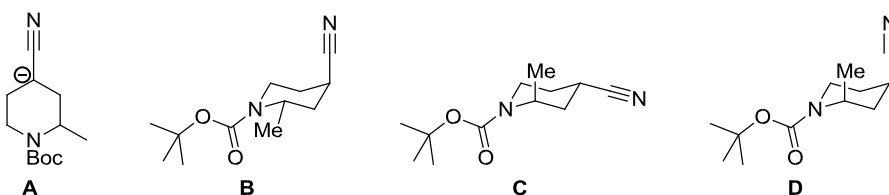
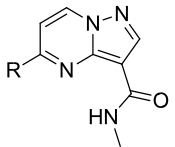
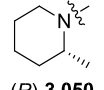
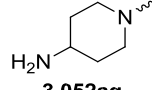
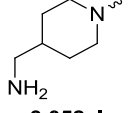
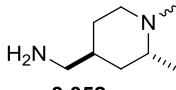


Figure 3.3. Intermediates and potential product conformations of the Van Leusen cyanation. Nitrile **3.060** was reduced to the primary amine **3.061** using borane-THF in good yield. Phthalimide protection of the amine and Boc deprotection with TFA gave **3.063** in high yield, which was determined to be wholly the *trans* diastereomer by NMR. Coupling to the core efficiently gave **3.051an**, with the phthalimide group removed using methylamine (avoiding the use of toxic hydrazine) to produce the final compound **3.052an**. Acetamide **3.055** was synthesised from **3.052ai** by reaction with acetyl chloride and pyridine in good yield.

The extended profiles of selected aminopiperidines were investigated (Table 3.7). 4-Amino substitution reduced selectivity over BRPF2/3. The hydrogen bond-donor residues these compounds targeted are a significant area of difference within the BRPF family (See Section 3.3.11), and subtle interactions and effects on solvation may be responsible. All amines showed no Brd4 activity and were significantly more selective over Brd9 than **3.050**. Wider selectivity profiling of **3.052an** is ongoing. All amines were highly soluble but had very low ChromLogD_{7.4}, and similar to the piperazine **3.051ab** were highly impermeable in the AMP

assay. For this reason, and the loss of efficiency compared to **3.050** (indicating no significant interaction with the protein has been formed) aminopiperidines were not further investigated.

Table 3.7. Bromodomain FRET potencies, LE and physicochemical properties of 5(aminopiperidine)-substituted PPs.

	R			
	 (R)- 3.050	 3.052ag	 3.052ai	 3.052an
BRPF1 pIC₅₀ / LE	6.7 (0.46)	6.4 (0.44)	6.5 (0.42)	6.6 (0.41)
BRPF2 pIC₅₀	4.7	5.1	5.2	5.0
BRPF3 pIC₅₀	4.2	4.6	4.7	4.9
Brd4 BD1 / BD2 pIC₅₀	4.6 ^a / 4.5 ^b	<4.3 / <4.3	<4.3 / <4.3	<4.3 / <4.3
Brd7 pIC₅₀	5.1	-	5.0	-
Brd9 pIC₅₀	5.8	5.0	5.1	5.4
CECR2 pIC₅₀	4.8	-	5.0	-
ChromLogD_{7.4}	3.3	-0.3	-0.2	-0.1
CLND Solubility (μM)	610	574	470	431
AMP (nm/s)	307	<10	<10	<10

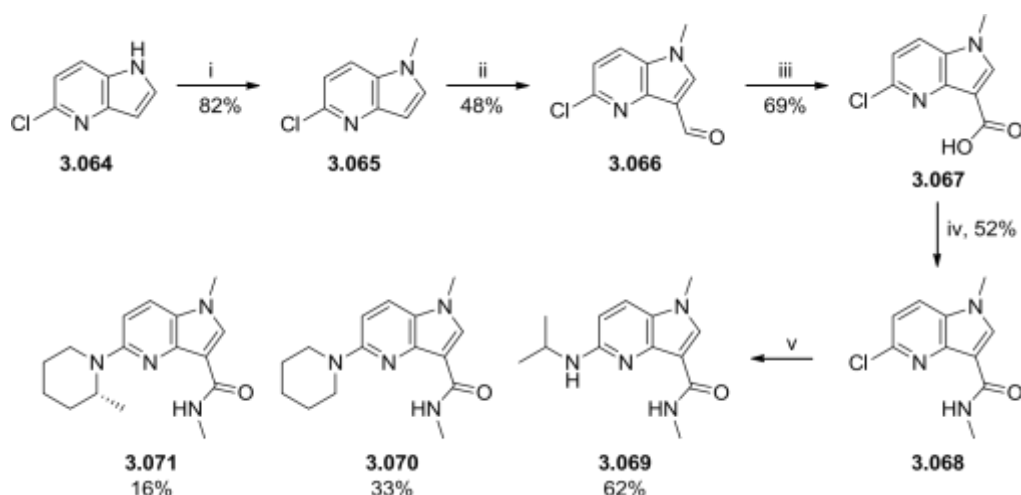
All potency data are n=2 or greater unless otherwise specified. Dashes indicate no data available. a) n=3, <4.3 on two other test occasions; b) n=4, <4.3 on one other test occasion.

3.3.3 Azaindole (AI) Core

As part of the investigation of the core fragment, the *N*-methyl 4-azaindole (AI) fragment **3.019** was shown to have superior BRPF1 potency to the PP core fragment **3.007a** (Scheme 3.2). This increase in potency warranted further investigation, and 5-substituted AI compounds were synthesised to compare against the PP series (Scheme 3.8).

5-Chloro-4-azaindole **3.064** was methylated with MeI in good yield to give **3.065**, which underwent Vilsmeier-Haack formylation to aldehyde **3.066**. Pinnick oxidation gave acid **3.067**, which was amidated with oxalyl chloride and methylamine to afford key intermediate **3.068**. Attempts to directly amidocarbonylate **3.065** using Li's I₂-mediated methodology³⁵⁴ were unsuccessful, possibly due to the volatility of methylamine. Due to the altered electronics of the core and inability to delocalise charge into the carbonyl group, S_NAr was unsuccessful in introducing the 5-substituent. Pleasingly, Buchwald-Hartwig cross-coupling allowed access to elaborated compounds **3.069-3.071**, with isopropylamine (**3.069**) giving the best yield.

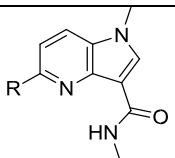
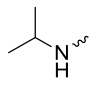
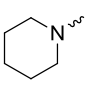
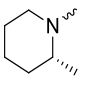
Piperidines were less effective coupling partners, in particular hindered 2methylpiperidine (**3.071**) for which the yield was poor but usable.



Scheme 3.8. Synthesis of 5-substituted AI compounds. Reagents and conditions: (i) NaH, MeI, DMF, rt; (ii) POCl₃, DMF, 0 °C – rt; (iii) NaClO₂, NaH₂PO₄, H₃NSO₃, THF, H₂O, rt; (iv) (COCl)₂, DCM, rt; then MeNH₂, THF, 0 °C – rt; (v) Amine, NaO^tBu, Pd(OAc)₂, BINAP, 1,4-dioxane, 110 °C.

The potency, selectivity and physicochemical property profiles of the AI compounds **3.069-3.071** were investigated (Table 3.8). While BRPF1 potencies were good and LE was broadly maintained, the AI compounds failed to improve on their respective PP analogues **3.002**,

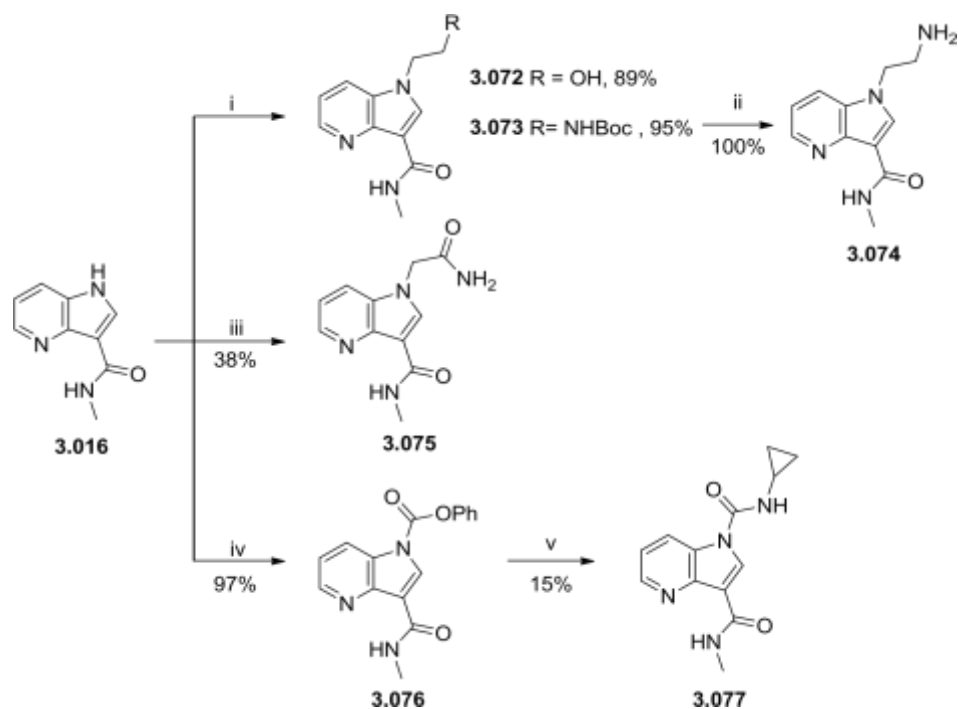
3.044, and (*R*)-**3.050**. Notably, BRPF family selectivity was significantly worsened, with **3.070** only 10-fold selective over BRPF2 (*c.f.* **3.044**, 100-fold selective). A significant increase in off-target activity at the BPTF bromodomain was also noted, though Brd9 selectivity was slightly improved. The removal of a heteroatom and addition of a methyl group resulted in a 100-fold increase in lipophilicity, producing a decrease in aqueous solubility (though this remained within desired space) and increased permeability.

Table 3.8. Bromodomain FRET potencies, LE and physicochemical properties of 5-substituted AIs.				
	(<i>R</i>)- 3.050	R		
		 3.069	 3.070	 3.071
BRPF1 pIC₅₀ / LE	6.7 (0.46)	5.5 (0.42)	6.2 (0.42)	6.7 (0.44)
BRPF2 pIC₅₀	4.7	<4	5.2	5.7
BRPF3 pIC₅₀	4.2	4.5	4.4	4.8

Brd4 BD1 / BD2 pIC₅₀	4.6 ^a / 4.5 ^b	<4.3 / <4.3	<4.3 / <4.3	<4.3 / <4.3
BPTF pIC₅₀	5.1	-	5.4	5.9
Brd7 pIC₅₀	5.1	-	4.8	4.8
Brd9 pIC₅₀	5.8	-	5.2	5.4
CECR2 pIC₅₀	4.8	-	5.0	5.2
ChromLogD_{7.4}	3.3	3.6	4.8	5.4
CLND Solubility (μM)	610	416	378	356
AMP (nm/s)	307	370	560	500

All potency data are n=2 or greater unless otherwise specified. Dashes indicate no data available. a) n=3, <4.3 on two other test occasions; b) n=4, <4.3 on one other test occasion.

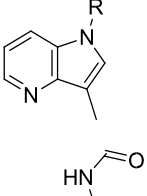
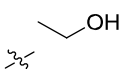
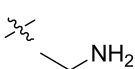
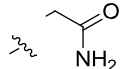
While the AI series did not improve potency or selectivity compared to the PP series, the methyl group is predicted to protrude into solvent and offers an alternative vector for substitution. It is possible that hydrogen bond donor groups projecting from this vector could form H-bonds to the key Asn708 residue, forming a strong bidentate interaction along with the methyl amide. To test this, a variety of H-bond donor substituents were synthesised (Scheme 3.9). The NH azaindole **3.016** could be readily alkylated in excellent yield with ethylene carbonate (**3.072**) or alkyl bromides (**3.073**), with the Boc protecting group removed from **3.073** with TFA in quantitative yield to give **3.074**. Reaction with iodoacetamide gave primary amide **3.075**, while for the synthesis of carbonyl linked amides the indole was first acylated with phenyl chloroformate to give **3.076** in excellent yield. Addition of amine nucleophiles to the activated carbamate proved difficult, with ammonium chloride and methylamine giving only the NH indole **3.016**. However, cyclopropylurea **3.077** was isolated in usable yield. The indole urea moiety proved too unstable for successful screening, with **3.077** rapidly degrading in the DMSO stock solution, as a result carbonyl linkers were not further explored.



Scheme 3.9. Synthesis of *N*-substituted AI compounds. Reagents and conditions: (i) Ethylene carbonate or *tert*-butyl (2-chloroethyl)carbamate, K_2CO_3 , DMF, 110 °C; (ii) TFA, DCM, rt; (iii) 2-Iodoacetamide, K_2CO_3 , DMF, 80 °C; (iv) Phenyl chloroformate, Et_3N , THF, 0 °C - rt; (v) Cyclopropylamine, Et_3N , DMSO, rt.

Regrettably, the *N*-substituted AI compounds lost all activity at BRPF1 (Table 3.9). It is possible that the angle of the core in the binding pocket would require the substituent to twist unfavourably out of plane in order to form a bidentate interaction, or that the substituents simply clash with the binding pocket when groups larger than methyl are introduced. Given that the 5-substituted examples **3.069-3.071** were also suboptimal compared to the PP series, and the indole nitrogen appeared to be an unproductive vector for substitution, the azaindole core was not further investigated.

Table 3.9. Azaindole *N*-substitution

	R				
	H	Me			
3.016	3.019	3.072	3.074	3.075	
BRPF1 pIC₅₀	4.5	4.9	<4	<4	<4

All potency data are n=3.

3.3.4 5,6-Disubstituted Pyrazolopyrimidines

The 6-position of the PP core has the potential to interact with the ZA loop, in addition to twisting the 5-substituent out of plane through steric repulsion. Substitution from this position has the potential to increase potency and selectivity, as the 6-position vector is similar to that of the amide vector of benzimidazolone **1.46**¹⁹⁴ (Figure 3.1). Key learnings from the ZA loop binders of published BRPF1 inhibitors, such as linking through an amide (**1.46**, **1.47**)^{194,195} or sulphonamide (**1.48-1.51**)¹⁹⁶⁻¹⁹⁹ and restraining the amide conformation,^{194,195} were to be applied during compound design while maintaining a distinct chemotype.

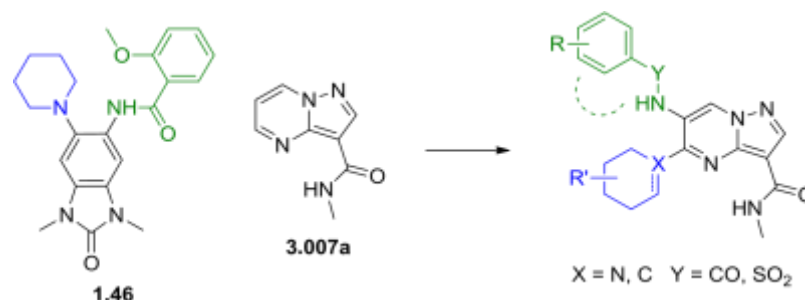
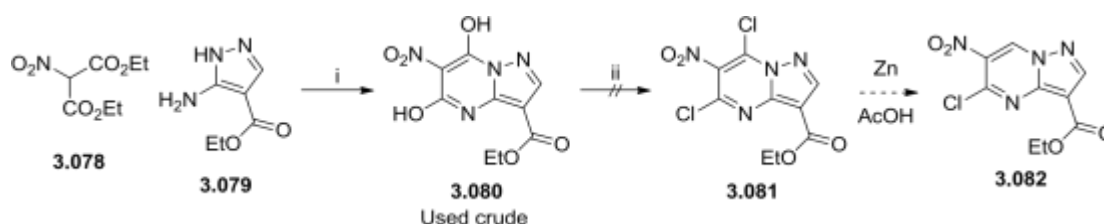


Figure 3.4. Modelled vector similarities and design strategy for disubstituted compounds.

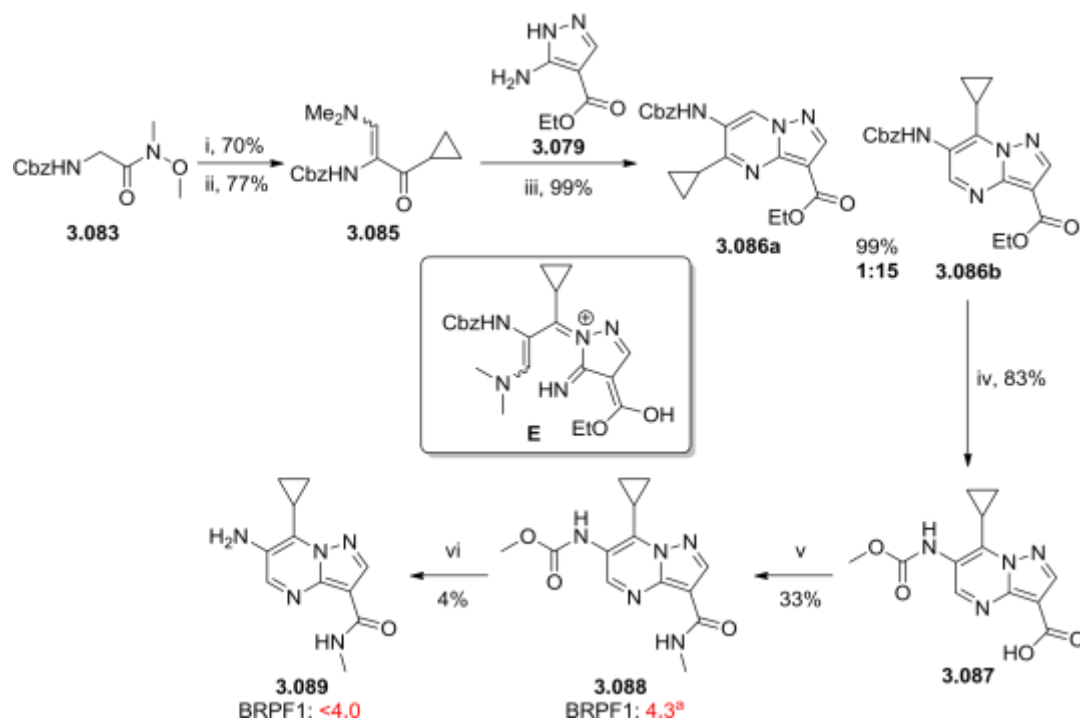
The synthesis of these analogues was not predicted to be straightforward. No pyrazolopyrimidines with heteroatoms at both the 5- and 6-positions have been reported, but condensation of aminopyrazoles with malonates and chlorination of the resulting diol is common.^{355,356} Subsequent selective removal of the 7-Cl with Zn in AcOH has been reported.³⁵⁷ To pursue this, nitromalonate **3.078** and aminopyrazole **3.079** were reacted to give **3.080**, through long reaction times were required and the highly polar product was difficult to isolate (Scheme 3.10). Chlorination of the crude material with POCl₃ failed to give the dichloride **3.081**, with the isolated product degrading to an unknown product on isolation.



Scheme 3.10. Attempted synthesis of disubstituted pyrazolopyrimidines. Reagents and conditions: (i) Na, EtOH, 90 °C, 7 days; (ii) POCl₃, 60 °C.

Where a carbon substituent is required at the 5-position, γ -(dimethylamino)enones have been used as the 1,3-dielectrophile.³⁵⁸ Given the ligand efficiency of the 5-cyclopropyl substituent and the difficulties encountered in the above steps, this method was investigated (Scheme 3.11). Cbz-glycine Weinreb amide **3.083** (commercially available, or obtainable from Cbz-glycine³⁵⁹) was reacted with cyclopropylmagnesium bromide to give the cyclopropyl ketone

3.084, which underwent Knoevenagel-type condensation with DMFDMA³⁵⁸ to give **3.085** in good yield, as an inconsequential 3:1 mixture of geometric isomers. Acid-promoted cyclisation with **3.079** under microwave conditions was facile, but the use of alcoholic solvents (EtOH, iPrOH) led to transesterification of the carbamate, whilst the reaction did not occur in aprotic media (DMSO). The use of glacial acetic acid as the solvent gave the cyclised products in quantitative yield, but with the undesired regioisomer **3.086b** as the major product (~15:1). Cyclisations of aminopyrazoles with γ -(dimethylamino)enones have been reported to produce both the 5-³⁶⁰ and 7-substituted^{361,362} products, though only 7-substituted examples are known for 3-acylpyrazoles.³⁶² The amine lone pair of **3.079** is delocalised into the ester, and so the pyrazole nitrogen generally reacts first and condenses with the ketone, generating intermediate **E** which undergoes Michael attack to cyclise.

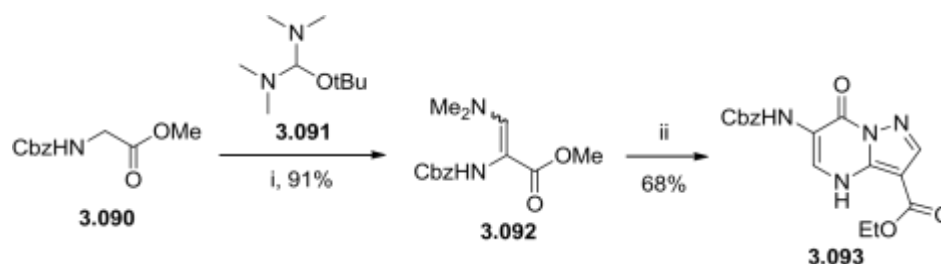


Scheme 3.11. Attempted synthesis of 5-C, 6-N disubstituted pyrazolopyrimidines and elaboration of the 7-cPr analogues. Potency data are n=3 unless specified. a) n=2, <4 on one additional test occasion. Reagents and conditions: (i) cPrMgBr, THF, -5 °C-rt; (ii) DMF-DMA, 85 °C; (iii) **3.07**, AcOH, 120 °C, μ W; (iv) KOH, H₂O, MeOH, 80 °C; (v) (COCl)₂, DCM, rt; then MeNH₂, THF, rt; (vi) NaOH, H₂O, MeOH, 80 °C.

Although the undesired regioisomer was the predominant product, it offered an opportunity to explore the 7-position. Ester hydrolysis of **3.086b** gave acid **3.087**, with the carbamate undergoing transesterification with MeOH. Throughout the synthesis, the 6-carbamate was found to be highly labile. Amide formation gave **3.088**, with carbamate hydrolysis giving amide **3.089** in low yield due to losses on purification. Unfortunately, despite the activity of 7Me PP **3.018c**, **3.088** and **3.089** had very poor BRPF1 potency. The cyclopropyl substituent may be

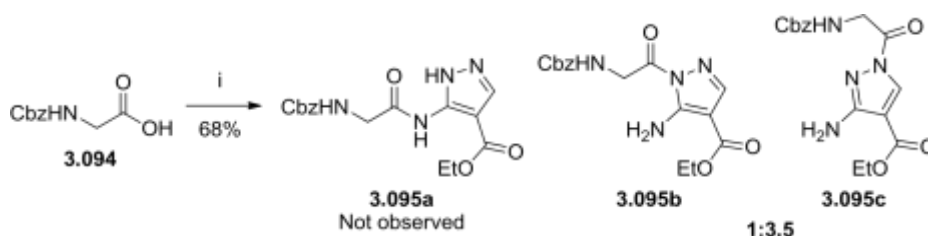
too large and clash with the ZA loop, though the amine may also form an unfavourable interaction. Later results showed that a 6-NH₂ was well tolerated (See Section 3.3.7), indicating the cyclopropyl substituent is likely the cause of the poor potency.

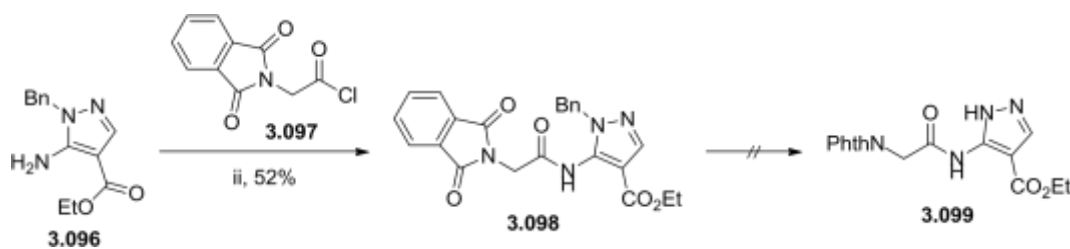
Returning to 5,6-disubstitution, it was envisioned that a cyclisation to place an oxygen at the 5-position followed by chlorination would generate a functional handle (Scheme 3.12). Formation of the dimethylenone ester **3.092** from Z-glycine methyl ester **3.090** with DMFDMA was sluggish, whereas the alternative reagent **3.091** gave **3.092** in excellent yield.³⁶³ Cyclisation with **3.079** under the previously developed conditions was again facile, but gave **3.093** as a single regioisomer with the carbonyl in the undesired 7-position. In the literature, only cyclisations to give 7-hydroxy products are reported for similar ring systems.^{363–365} The resulting product **3.093** was not converted to final products as other data suggested that a 7-position carbonyl was detrimental to potency (See Section 3.3.7).



Scheme 3.12. Attempted intermolecular cyclisation using a dimethylenone ester. Reagents and conditions: (i) **3.091**, toluene, 110 °C; (ii) **3.079**, AcOH, 140 °C, μ W.

To circumvent the regioselectivity issues, a two step cyclisation process was envisaged. Formation of the N5-C6 bond as an amide bond in the first step, followed by cyclisation, was expected to give the product as the desired regioisomer. However, amide coupling of Zglycine **3.094** with the aminopyrazole monomer **3.079** gave only the ring-acylated products **3.095b** and **3.095c** (Scheme 3.13). To circumvent this a protecting group strategy was devised, also protecting the 6-amine with a robust phthalimido group due to the lability of the carbamates observed in previous attempts (Scheme 3.11). Commercially available benzylpyrazole **3.096** could be acylated with phthalimido glycyl chloride **3.097** to give **3.098**, but attempts to remove the benzyl group with hydrogenolysis or BBr₃ failed.

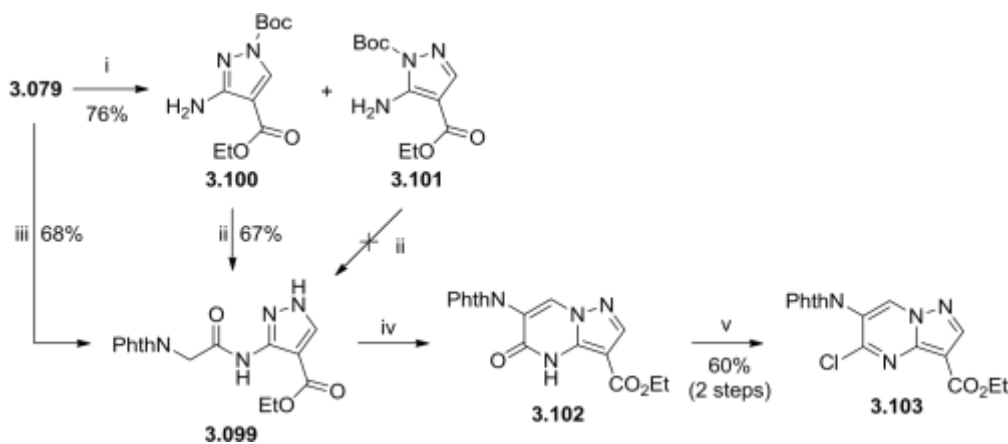




Scheme 3.13. Acylation of unprotected and protected aminopyrazoles. Reagents and conditions: (i) **3.079**, HATU, DIPEA, DMF, rt; (ii) Pyridine, CHCl_3 , rt.

The protecting group was exchanged for a more readily removable Boc group (Scheme 3. 14). Pleasingly, Boc protection of **3.079** proceeded exclusively on the ring nitrogens, giving

3.100 as the major product, along with small amounts of **3.101**. Amidation of **3.100** with **3.097** and *in situ* deprotection gave the desired amide **3.099**, but minor Boc isomer **3.101** did not react under these conditions. **3.099** could also be obtained *via* a one-pot sequence of protection, amidation and deprotection with TFA, with an improved overall yield. Whereas the two-step route involved two chromatographic purifications to reach **3.101**, the one-pot route enabled purification by precipitation and trituration in a more scalable and efficient procedure. The enone was formed using **3.091**, and after removal of solvent cyclised with AcOH to give **3.102**. The highly polar and insoluble pyrimidone **3.102** proved difficult to purify, so was telescoped into the chlorination with POCl_3 to provide key intermediate **3.103**.

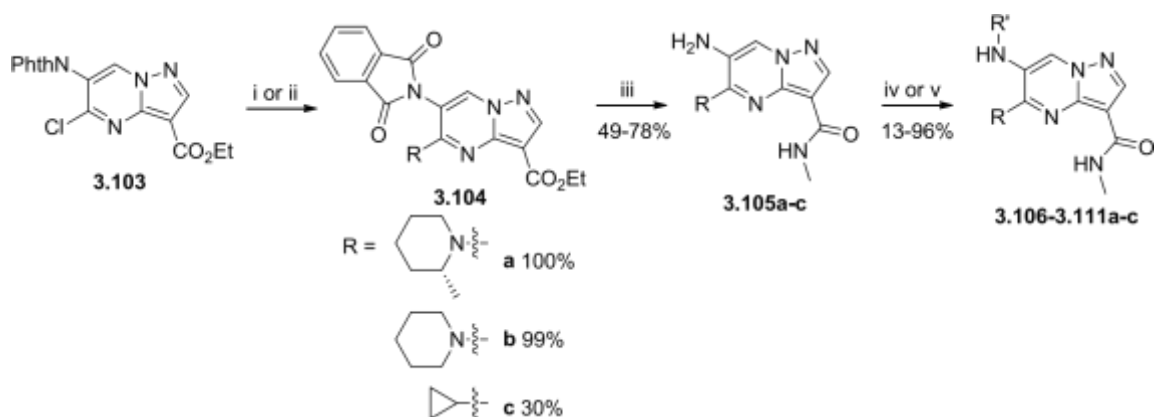


Scheme 3.14. Stepwise formation of the PP bicyclic ring system. Reagents and conditions: (i) Boc_2O , pyridine, DCM, rt. Yield is for **3.100**; (ii) **3.097**, pyridine rt, then TFA, rt; (iii) Boc_2O , pyridine, DCM, rt, then **3.097**, rt, then TFA, rt; (iv) **3.091**, toluene, 110°C , then AcOH, 110°C ; (v) POCl_3 , DMF, 100°C .

Chloride **3.103** proved extremely reactive, degrading under attempts to hydrolyse the ester and install the amide warhead with partial opening of the phthalimide also observed. It was decided to introduce the 5-substituent first, then form the amide directly from the ester using DABAL- Me_3 (AlMe_3 -DABCO adduct).³⁶⁶ *N*-Linked 5-substituents **a** and **b** were introduced through $\text{S}_\text{N}\text{Ar}$ in high yield, whereas *C*-linked cyclopropyl **c** required Suzuki-Miyaura coupling.

This proceeded in lower yield relative to cores lacking the 6-substituent, due to the less reactive and more sterically hindered chloride (Scheme 3.15). The chosen 5substituents were selected to accommodate and identify any significant differences in 5position SAR once a 6-substituent was added, with piperidine **b** included to allow direct comparison to benzimidazolone **1.46**.

DABAL-Me₃-mediated direct ester amination³⁶⁶ proceeded with complete deprotection of the phthalimide to give intermediates **3.105a-c** in good yield. The 6-substituent was readily functionalised with acyl chlorides and sulphonamides or by reductive amination to give a library of disubstituted compounds and form a small square array (Table 3.10).

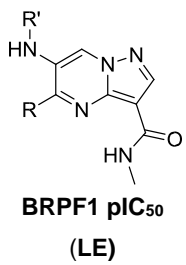
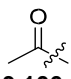
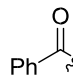
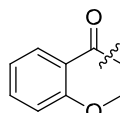
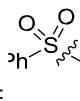
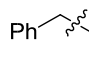
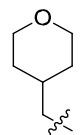
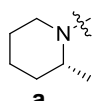
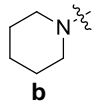
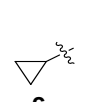
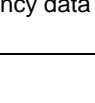


Scheme 3.15. Synthesis of 5,6-disubstituted pyrazolopyrimidines. Reagents and conditions: (i) Piperidine, DIPEA, DMSO, rt; (ii) Cyclopropylboronic acid, Pd(PPh₃)₄, K₂CO₃, 100 °C; (iii) DABAL-Me₃, MeNH₂, 40 – 70 °C; (iv) Acyl chloride or sulphonyl chloride, pyridine, DCM, rt; (v) Aldehyde, MgSO₄, DCM, rt; then NaBH₄, MeOH, rt.

Disappointingly, the theorised improvement in potency on disubstitution did not occur (Table 3.10). For the piperidines **a** and **b** the addition of a 6-NH₂ (**3.015a,b**) gave a slight drop in potency, with a large decrease occurring when an acetyl (**3.106a**), benzoyl (**3.107a**) or benzenesulfonyl (**3.109a**) group was introduced. Constraining the aryl substituent with an internal hydrogen bond, as seen in the benzimidazolone BRPF1 inhibitors **1.46** and **1.47**, improved potency relative to **3.107a**. However, the potencies of **3.108a** and **3.108b** were still below that of the initial monosubstituted leads ((*R*)-**3.050**, **3.04**) and **3.108b** was over a log unit less potent than the direct comparator **1.46**. This discrepancy indicates that the PP and benzimidazolone series bind in different ways and SAR is not transferable between them. A benzyl group (**3.110a**) was tolerated but did not improve potency, with similar results seen on replacing the aryl group with a tetrahydropyran (**3.111a**). For the cyclopropyls **c**, an improvement in potency was observed when adding the 6-NH₂, (**3.105c**) benzyl (**3.110c**) or THP (**3.111c**) groups, when compared to the unsubstituted analogue **3.040**. Overall, cyclopropyl examples remained less potent compared to the methylpiperidines **a**. For piperidines **a** and **b** the large 6-substituent may force an unfavourable change in the

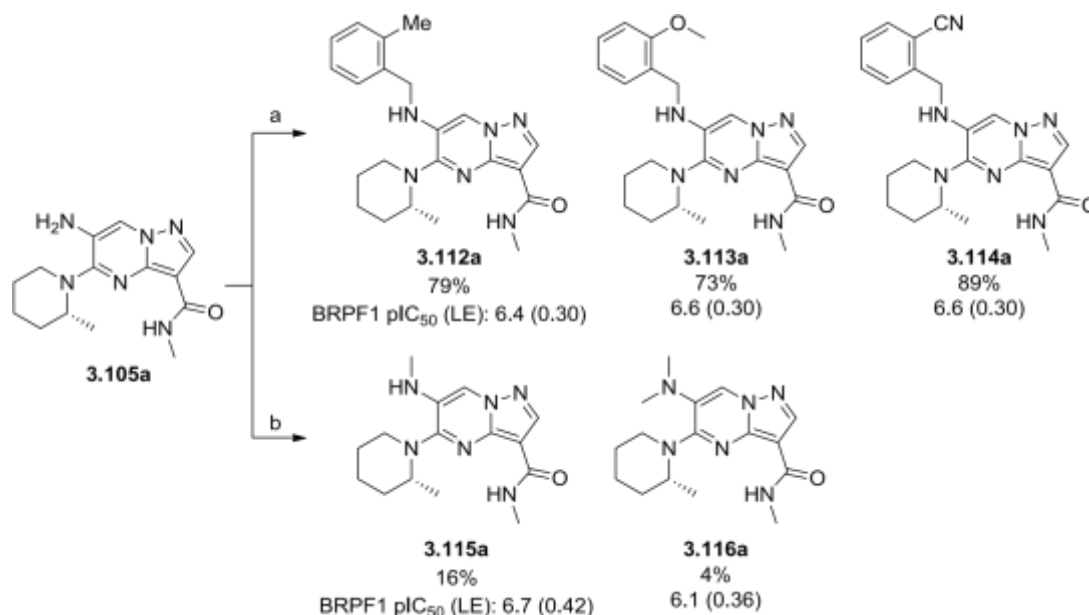
conformation of the piperidine ring, negating the increase in potency gained from binding to the ZA loop.

Table 3.10. Yields, BRPF1 pIC₅₀ and LE for disubstituted PPs and monosubstituted comparators.

 BRPF1 pIC ₅₀ (LE)		R'							
		6-H	H						
R		(R)- 3.050			84%				
		3.044	6.7 (0.46)	83%	5.3 (0.25)	96%	40%	31%	45%
		3.040	6.1 (0.44)	5.4 (0.31)	-	6.2 (0.27)	5.6 (0.26)	6.7 (0.33)	6.5 (0.32)
		3.040	6.0 (0.41)	6.4 (0.42)	-	76%	-	-	-
			5.5 (0.47)	5.7	55%	-	5.8 (0.27)	-	-
			5.7 (0.46)	5.2 (0.36)	-	-	5.3 (0.28)	13%	18%

All potency data are n=3 or greater. Dashes indicate compound was not synthesised.

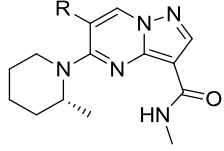
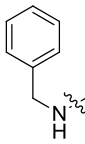
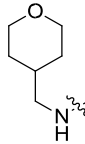
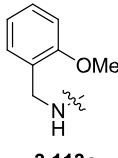
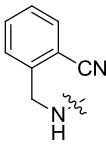
Benzyl and alkyl substitution of the 6-position was briefly investigated further (Scheme 3.16). Amine **3.105a** was alkylated with electron neutral (**3.112a**), rich (**3.113a**) and deficient (**3.114a**) benzyl groups – methoxy benzyl **3.113a** is capable of conformational restriction through an intramolecular hydrogen bond and also serves as a single-point comparator to **3.108a**. While *ortho*-substitution was tolerated with no loss of activity, modification of the electronics of the ring had no significant effect on potency compared to **3.110a**. Methylation of the amine with MeI proceeded in poor yield but gave both the monomethyl (**3.115a**) and dimethyl (**3.116a**) products. Monomethyl **3.115a** gave a small boost in potency compared to **3.105a** which was lost on dimethylation (**3.116a**), though the potency of **3.115a** was not significantly different to that of monosubstituted PP (*R*)-**3.050**.



Scheme 3.16. Further 6-benzyl and 6-alkyl substituents in the disubstituted PP series. All potency data are $n=3$. Reagents and conditions: a) i) Aldehyde, MgSO₄, AcOH, DCM, rt; ii) NaBH₄, MeOH, rt; b) MeI, K₂CO₃, DMF, 90 °C.

The selectivity and physicochemical property profiles of the most potent disubstituted examples were compared to (*R*)-**3.050** (Table 3.11). In general, the 6-substituents improved selectivity over other bromodomains, though as expected BRPF1 ligand efficiencies were reduced. Selectivity over BRPF2/3 was generally maintained compared to (*R*)-**3.050**, though appeared dependant on the substitution pattern of the benzene ring. Benzyl **3.110a** showed only marginal improvements in Brd9 selectivity with a thousand-fold increase in ChromLogD_{7.4}, resulting in poor aqueous solubility. Tetrahydropyran **3.11a** was slightly less selective due to reduced BRPF1 potency but displayed improved solubility (though still reduced compared to (*R*)-**3.050**). Methoxybenzyl **3.113a** and cyanobenzyl **3.114a** had poorer ligand efficiency due to the additional atoms, but displayed particularly improved selectivity over Brd9, with **3.113a** being ~50-fold selective. Activity at CECR2 and Brd7 was also significantly reduced. However, as with benzyl **3.110a**, solubility was worsened due to increased lipophilicity, and **3.113a** was very poorly permeable due to the additional hydrogen bond acceptor. The mono-methyl amine **3.115a** was equipotent to (*R*)-**3.050** with only a slight drop in LE and good physicochemical properties. BPTF and Brd9 potency were reduced by half a log unit compared to (*R*)-**3.050**, giving 25-fold selectivity over Brd9, but remained lower than the high selectivity of the benzyls **3.113a** and **3.114a**.

Table 3.11. Bromodomain FRET potencies, LE and physicochemical properties of 5,6-disubstituted PPs.

	R					
	H (R)-3.050					NHMe 3.115a
BRPF1 pIC₅₀ / LE	6.7 (0.46)	6.7 (0.33)	6.5 (0.32)	6.6 (0.30)	6.6 (0.30)	6.7 (0.42)
BRPF2 pIC₅₀	4.7	5.1	4.5 ^a	4.7	5.1	4.7
BRPF3 pIC₅₀	4.2	4.9	<4	4.2	<4	4.3
Brd4 BD1/BD2 pIC₅₀	4.6 ^b /4.5 ^c	4.4 ^d /4.7	<4.3/<4.3	4.4 ^e /4.6	<4.3/4.5 ^e	<4.3/<4.3
BPTF pIC₅₀	5.1	5.0	4.5	-	-	4.6
Brd7 pIC₅₀	5.1	-	4.5	4.7	5.1	4.7
Brd9 pIC₅₀	5.8	5.4	5.4	4.9	5.3	5.3
CECR2 pIC₅₀	4.8	-	4.5	4.4	4.5	4.5
ChromLogD_{7.4}	3.3	6.3	5.1	6.3	5.3	4.3
CLND Solubility (μM)	610	68	324	97	88	361
AMP (nm/s)	307	320	490	<30	440	560

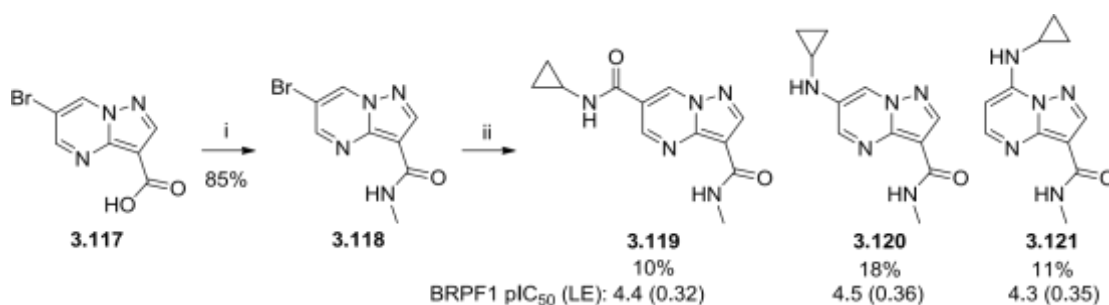
All potency data are n=2 or greater unless otherwise specified. Dashes indicate no data available. a) n=1, <4 on one additional test occasion; b) n=3, <4.3 on two other test occasions; c) n=4, <4.3 on one other test occasion; d) n=3, <4.3 on one other test occasion; e) n=1, <4.3 on two other test occasions.

The rationale behind these disappointing results was initially unclear. The lack of a positive binding interaction from the 6-substituent indicated that the predicted binding mode of the PP series may not completely accurate. Alternatively, small differences in vector position between the PP and benzimidazolone series' (as shown in Figure 3.1) may lead to pronounced differences in SAR.

3.3.5 Pyrazolopyrimidine 6-Substitution

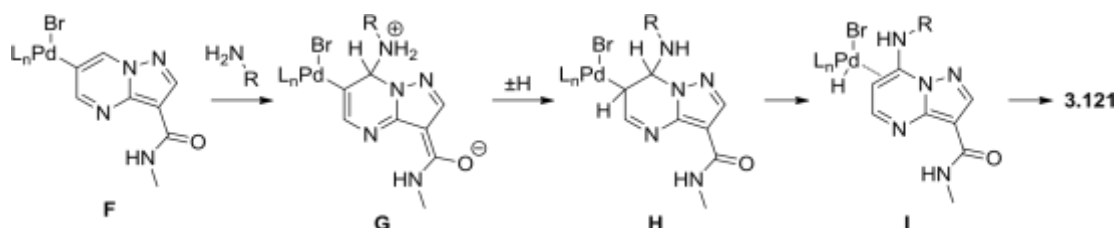
To provide insights into the impact and role of the 6-substituent, a series of 6monosubstituted PPs were synthesised. 6-Br pyrazolopyrimidine acid **3.117** was obtained from the GSK compound collection, and the warhead installed using the previously developed methodology. The resulting bromide **3.118** was utilised in metal-catalysed crosscouplings (Scheme 3.17). An attempted amidocarbonylation using CO gas gave three major products – the desired amide **3.119**, the Buchwald-Hartwig amination product **3.120** and unexpected 7-amino product

3.121. None showed a statistically significant improvement in BRPF1 potency over 6-H analogue **3.007a** (BRPF1 pIC₅₀ = 4.4).



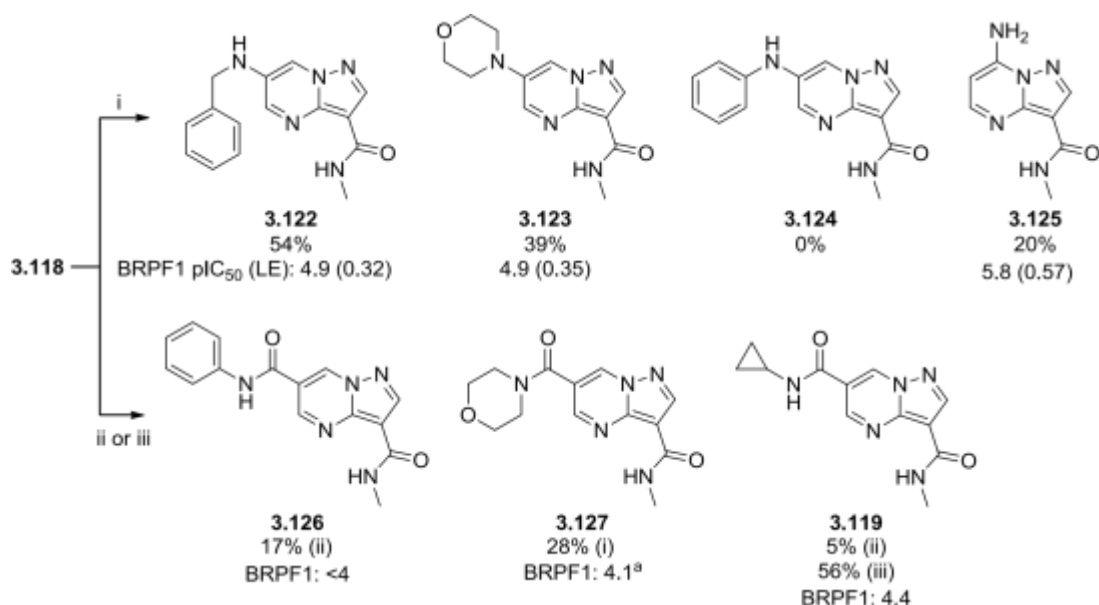
Scheme 3.17. Synthesis and biological activity of 6-substituted pyrazolopyrimidines. All potency data are n=2 or greater unless otherwise specified. Reagents and conditions: (i) (COCl)₂, DMF, DCM, rt then MeNH₂, THF, 0 °C; (ii) Cyclohexylamine, Pd(OAc)₂, Xantphos, Et₃N, DMF, CO, 60 °C.

The mechanism for the formation of 7-amine **3.121** is unclear. It is proposed that after oxidative addition (**F**) the amine attacks the 7-position, which is the most acidic and reactive to nucleophilic attack,^{367–369} giving **G**. Following reprotonation at the 6-position (**H**) aromaticity is restored by β-hydride elimination (**I**) (Scheme 3.18).



Scheme 3.18. Proposed mechanism for the formation of **3.121**.

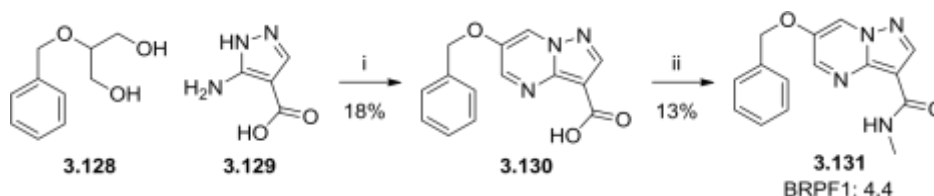
Since 6-amino Buchwald-Hartwig products were also observed, this chemistry was utilised to further investigate the SAR. Simply running the reaction under N₂ instead of CO gave amines **3.122** and **3.123**, though aniline gave none of the desired product **3.124** and the 7-amination product **3.125** was the sole product observed when ammonium chloride was used. Carbonylation could be successfully achieved using Co₂(CO)₈ as the CO source in the presence of DMAP,³⁷⁰ affording amides **3.126** and **3.127** in low but usable yield. No 7-amino product was observed under these conditions, however, only a trace of cyclopropyl amide **3.119** was obtained. Switching the catalyst to the highly efficient Xantphos 3rd Generation palladacycle,³⁷¹ and generation of CO *ex situ* using two-chamber glassware,³⁷² allowed the reaction to be run under milder conditions with a much improved yield of **3.119**. This method also simplifies the procedure, removing the need for gas cylinders or toxic metal carbonyls.



Scheme 3.19. Synthesis and biological activity of 6-substituted pyrazolopyrimidines. All potency data are $n=2$ or greater unless otherwise specified. a) $n=1, < 4$ on two additional test occasions. Reagents and conditions: (i) Amine, $\text{Pd}(\text{OAc})_2$, Xantphos, Et_3N , DMF, 60–80 °C; (ii) Amine, $\text{Co}_2(\text{CO})_8$, $\text{Pd}(\text{OAc})_2$, Xantphos, DMAP, DMF, 75 °C; (iii) cPrNH_2 , Xantphos Pd G3, Et_3N , $\text{CO}_{(g)}$ (generated *ex situ* using COware 2-chamber system³⁷²), 1,4-dioxane, 50 °C.

The BRPF1 data for these compounds is intriguing and supports the poor activity of the 5,6-disubstituted examples previously described. The cyclopropyl amide **3.119** and amine **3.121** were weakly potent. Increasing the size of the 6-substituent to benzyl **3.122** or morpholine **3.123** did give a small boost in potency, though with much reduced LE. Surprisingly, the larger amides **3.126** and **3.127** had no detectable potency at BRPF1, suggesting a steric or electronic clash with the binding site. The beneficial effect of the benzyl in **3.122** is consistent with the higher potency of disubstituted analogues bearing 6-*N*-benzyl groups (**3.110a,c**, Section 3.3.4). Most notably, the unexpected 7-amine product **3.125** was significantly more potent than **3.007a**, and this was further explored (see Section 3.3.7).

Given the slightly higher potency of benzylamine **3.122**, and to rule out the linker atom being the reason for low activity, the effect of an oxygen linker was investigated. To synthesise the oxygen-linked analogue, diol **3.128** was oxidised to the corresponding dialdehyde under Swern conditions, followed by a one-pot cyclisation with pyrazole **3.129** to give the 6-OBn PP **3.130**.³⁷³ Amidation of the crude acid gave **3.131** in low but usable yield, the ether linkage proved detrimental to BRPF1 potency compared to benzylamine **3.122** and oxygen linkers were not further explored.



Scheme 3.20. Synthesis and biological activity of 6-OBn pyrazolopyrimidine **3.131**. Potency data are $n=3$. Reagents and conditions: (i) **3.128**, $(\text{COCl})_2$, DMSO, Et_3N , $-78\text{ }^\circ\text{C}$ then 6 M HCl, **3.129**, $70\text{ }^\circ\text{C}$; (ii) MeNH_2 , HATU, DIPEA, DMF, rt.

3.3.6 X-Ray Crystallography

The poor potency of 6-substituted compounds indicated that the binding mode of the PP series differed from the initial *in silico* modelling, and these speculations were confirmed when an X-ray crystal structure of (*R*)-**3.050** bound to BRPF1 was obtained (Figure 3.5). The warhead and core bound as predicted, while Glu661 was seen to pack over the top of the pyrimidine ring, which may explain the poor tolerability of 6-substituents. The methyl piperidine was observed to bind in an unexpected configuration, with the ring parallel to the core and the methyl group failing to occupy the pocket at the edge of the ZA channel as expected. Instead, the methyl group adopts an axial orientation, being mostly solventexposed but making slight lipophilic contact with the Phe714 ‘gatekeeper’ residue and Ile652 of the neighbouring lipophilic shelf. This area, which we term the ‘Phe-Ile region’, is an intriguing vector for further investigation. Given the boost in potency observed on addition of the chiral methyl, these interactions (or the effect it has on the conformation of the piperidine ring) must be significant. It might be expected that the methyl group prefers an equatorial conformation, and so pay an energy penalty on binding in a lower energy state, which reduces affinity for the protein. This energy penalty is ~ 1.9 kcal/mol for *N*-acetyl-2-methyl piperidine³⁷⁴ though will be dependent on the nature of the N-substituent. However, as for the Van Leusen cyanation result (Section 3.3.2, Figure 3.3) it is possible that for bulkier N-substituents (such as the PP core) the axial conformation is in fact lower in energy as it avoids clashes with the methyl group.

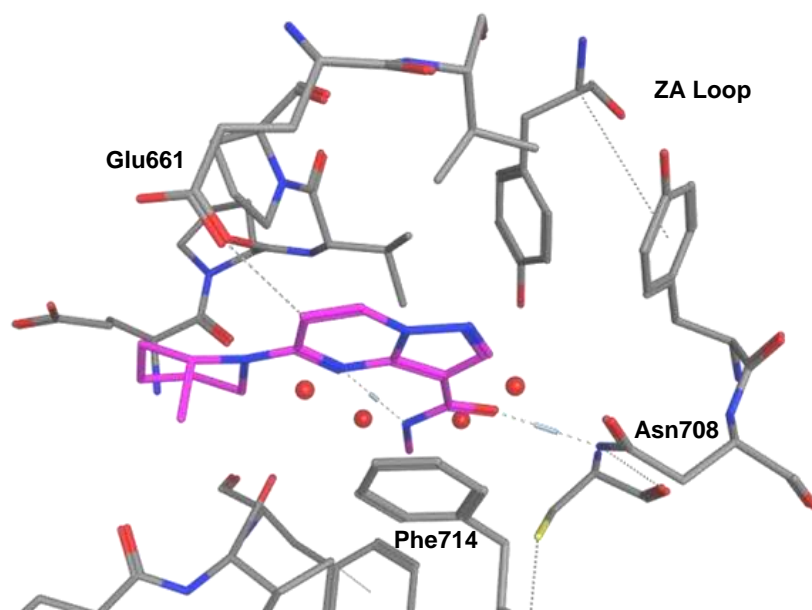


Figure 3.5. X-ray crystal structure of (*R*)-**3.050** (magenta, 1.95 Å)²⁹² bound to the BRPF1 bromodomain, showing the water network at the base of the pocket.

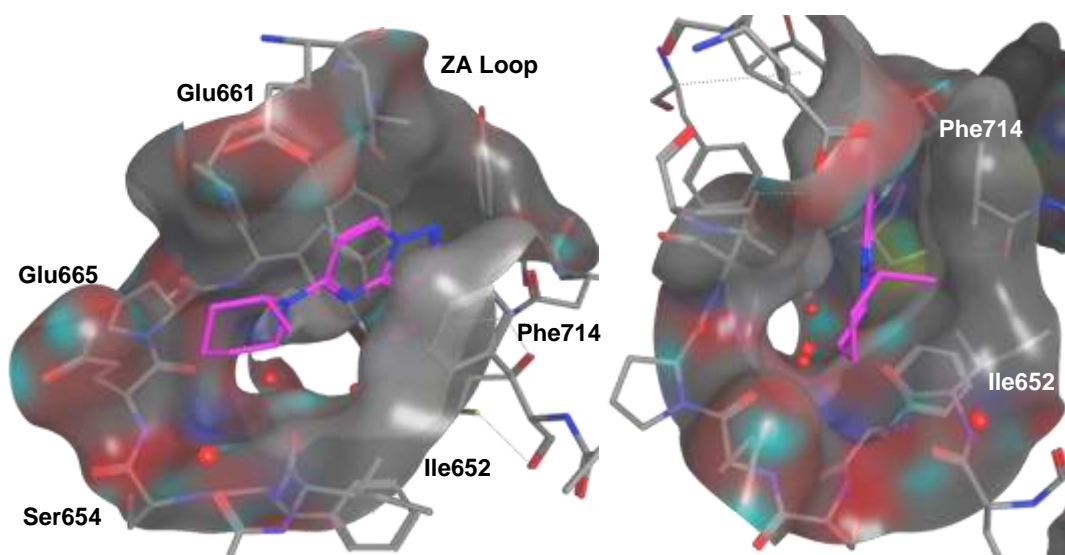


Figure 3.6. X-ray crystal structure of (*R*)-**3.050** (magenta, 1.95Å)²⁹² bound to the BRPF1 bromodomain, showing the protein surface.

Comparison of the original *in silico* modelling of **3.001** and the X-ray structure of (*R*)-**3.050** (Figure 3.7) showed excellent agreement in the binding mode and position of the core. Although most residues are in identical places in the docking and X-ray structures, the flexibility of the ZA loop and movement of Glu661 to pack onto the core is clearly visible.

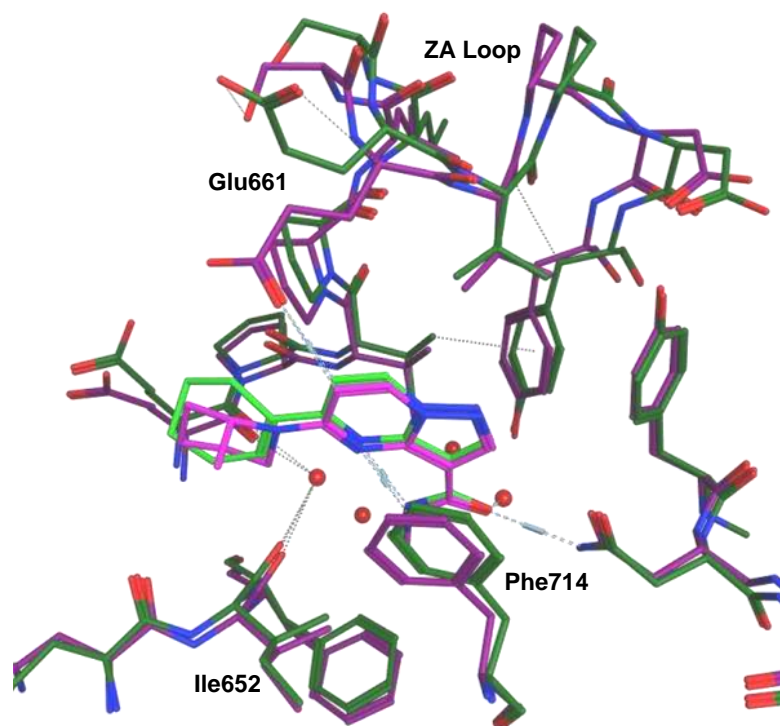


Figure 3.7. Overlaid docking of **3.001** (greens, Armelle le Gall³⁴⁵) and X-ray crystal structure of (*R*)-**3.050** (magenta, 1.95Å)²⁹² bound to the BRPF1 bromodomain.

The crystal structure presented intriguing new vectors for exploration. The proximity of Glu661 to the 7-position may allow interactions to be formed with appropriate 7-substituents. Extension of the methyl group may enable improved occupation the lipophilic pocket, the formation of π -interactions with the Phe714 residue, and altered bromodomain selectivity.

3.3.7 The 7-Position

Several 7-substituted PPs have shown an improvement in potency compared to the unsubstituted core **3.007a** (Figure 3.8). In summary, although the addition of 7-methyl **3.018c** efficiently increased BRPF1 activity by half a log unit, the larger 7-cyclopropyl group **3.089** had no measurable potency. This is not thought to be due to the 6-NH₂ motif as this was well-tolerated for other PPs (*c.f.* **3.105**, Table 3.10). Cyclopropylamine **3.120**, however, maintained potency, while primary amine **3.125** showed high potency and a significant increase in LE and warrants further investigation. Pyrrolidine **3.132** was obtained from the GSK compound collection and showed poor potency, again indicating that larger substituents at the 7-position were not tolerated. The amine NH motifs may be forming interactions with Glu661 or influencing the electronics of the core; cyclopropyl groups have some π -character which may disrupt subtly beneficial electronic effects. Larger 7substituents may clash with

Glu661 or other residues of the ZA loop, with flexible substituents such as **3.121** able to rotate away from the clashing residue.

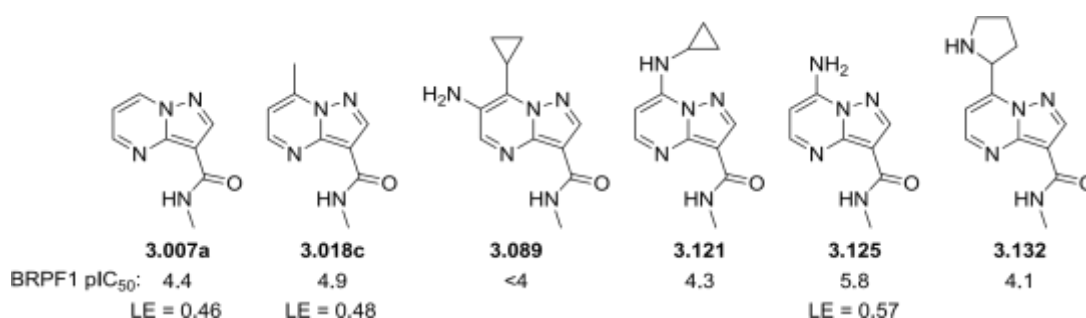
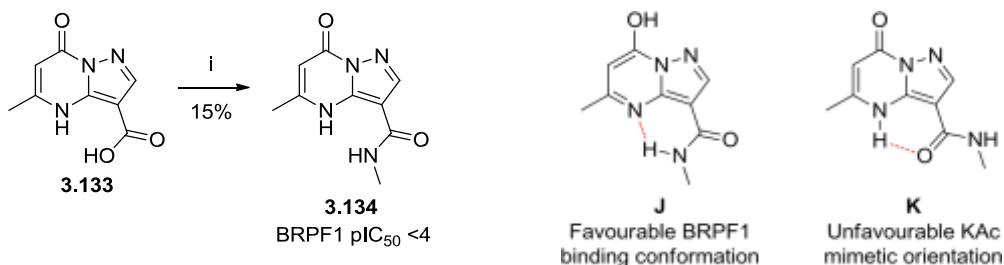


Figure 3.8. Biological activity of 7-substituted pyrazolopyrimidines. Potency data are n=3 or greater.

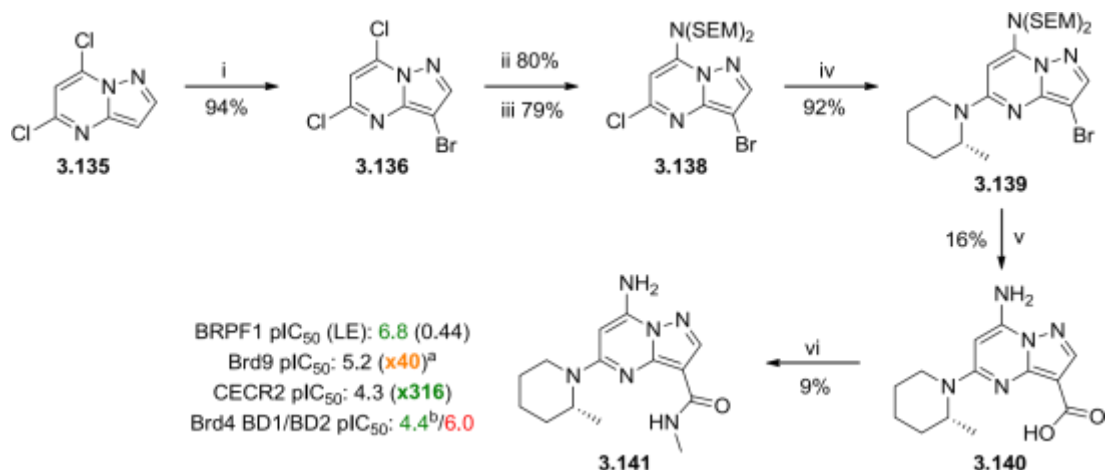
Given that the amine of **3.125** may be acting as a hydrogen bond donor or acceptor (or neither), an oxygen at the 7-position was investigated. Pyrimidone acid **3.133** was obtained from the GSK compound collection and the warhead amide installed using HATU to give **3.134**. However, the BRPF1 potency of **3.134** was below the lower binding limit of the assay. **3.134** exists in equilibrium between the hydroxypyrimidine (**J**) and pyrimidone (**K**) tautomers; while **J** adopts the required amide conformation for BRPF1 binding (c.f. Figure 3.7) in **K** the 4-NH may hydrogen-bond to the carbonyl and cause the amide to rotate. Investigation of the IR spectrum of **3.134** in an attempt to elucidate the preferred tautomer was inconclusive, with multiple absorbencies in the amide/lactam regions (See Experimental).



Scheme 3.21. Synthesis of pyrazolopyrimidone **3.134** and its potential conformations. Potency data are n=3. Reagents and conditions: (i) MeNH₂, HATU, DIPEA, DMF, rt.

To investigate the effect of the 7-NH₂ in more elaborated compounds, 5,7-disubstituted examples were desired. Commercially available dichloropyrazolopyrimidine **3.135** was brominated in the 3-position with NBS, before undergoing a 7-selective S_NAr with ammonia. Subsequent *bis*-SEM protection gave **3.138** (Scheme 3.22).³⁷⁵ For 5,7-disubstituted PPs, the 7-position is the most electron deficient due to the electronegative diazo-motif adjacent to it and S_NAr occurs there preferentially.^{355,356,376} The favoured 2-methylpiperidine was introduced

in a second S_NAr , affording **3.139** in high yield with complete regiocontrol. Lithium-halogen exchange and quench with CO_2 afforded the 3-acid. The SEM protecting group was partially removed during the reaction, so the mixture was stirred with HCl to effect complete deprotection, giving **3.140** in low but usable yield. Amide coupling with HATU provided final compound **3.141**, though the yield was diminished by incomplete reaction of acid **3.140** and losses on purification.



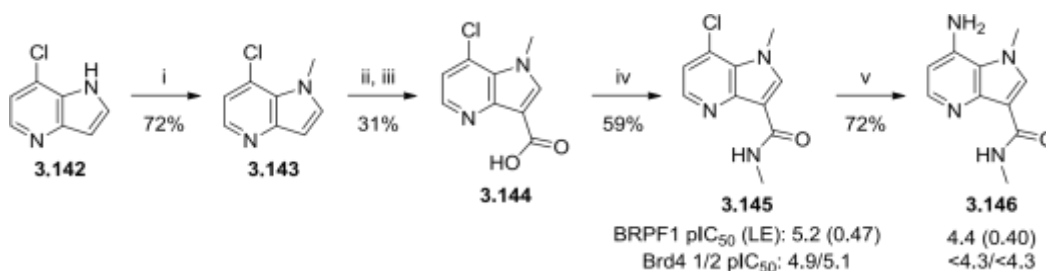
Scheme 3.22. Synthesis of 7-amino PPs. Potency data are n=2 or greater unless otherwise stated. a) n=1; b) n=1, <4.3 on three other test occasions. Reagents and conditions: (i) NBS, $CHCl_3$, rt; (ii) NH_4OH , H_2O , 85 °C; (iii) SEM-Cl, DIPEA, DCM, 45 °C; (iv) (*R*)-2-methylpiperidine, Na_2CO_3 , NMP, 110 °C; (v) $nBuLi$, CO_2 , THF, -78 °C - rt then HCl, H_2O , rt; (vi) $MeNH_2$, HATU, DIPEA, DMF, rt.

Unfortunately, the potency contribution of the 5-(2-methylpiperidine) group to the potent 7-amine **3.125** did not prove to be additive, with **3.141** only equipotent with 6-H analogue (*R*)-**3.050** at BRPF1. However, while selectivity over Brd9 did improve to 40-fold (with the caveat that this is n=1 data) and CECR2 potency was further reduced compared to (*R*)-**3.050**, interestingly high and domain selective Brd4 BD2 activity was also observed, in sharp contrast to (*R*)-**3.050**. The kinase inhibitor Dinaciclib (**1.25**, Section 1.4.4) contains a similar 7-amino pyrazolo[1,5-*a*]pyrimidine scaffold, and has been reported to bind to BET bromodomains (but not to BRPF1).¹⁵¹ The amine and pyrazole nitrogens are capable of acting as a KAc mimetic,¹⁵² and it is possible that **3.141** binds to Brd4 in a similar manner with the amide or piperidine conferring domain selectivity.

The effect of the 7-amine was also investigated in the AI series (Scheme 3.23). 7-Chloro-4-azaindole **3.142** was methylated to **3.143**, followed by Vilsmier-Haack formylation and telescoped Pinnick oxidation to give acid **3.144** in reasonable yield. Amide coupling produced the key 7-chloro intermediate **3.145**. Attempted Buchwald-Hartwig coupling with ammonium chloride gave no product, so the reaction was instead carried out with

paramethoxybenzylamine and the PMB group removed from the crude coupling product with TFA to give primary amine **3.146** in good yield. Chloride **3.145** was pleasingly potent but showed poor selectivity over Brd4, while in contrast to PP **3.125**, amine **3.146** showed poor BRPF1 potency. The 7-amino appeared to be detrimental compared to the parent AI **3.019** and chloride **3.145**. Additionally, no Brd4 activity was observed for **3.146**; given that 7-amino PP **3.125** also showed no measurable potency at Brd4 it was theorised that the 5-substituent of

3.141 also contributes to its Brd4 activity.



Scheme 3.23. Synthesis of 7-amino AIs. Potency data are n=3 or greater. (i) MeI, NaH, DMF, 0 °C; (ii) POCl₃, DMF, 0 - 60 °C; (iii) NaClO₂, NaH₂PO₄, H₃NSO₃, THF, H₂O, 0 °C - rt; (iv) MeNH₂, HATU, DIPEA, DMF, rt; (v) PMBNH₂, NaO^tBu, Pd(OAc)₂, BINAP, 1,4-dioxane, 110 °C, then TFA, rt.

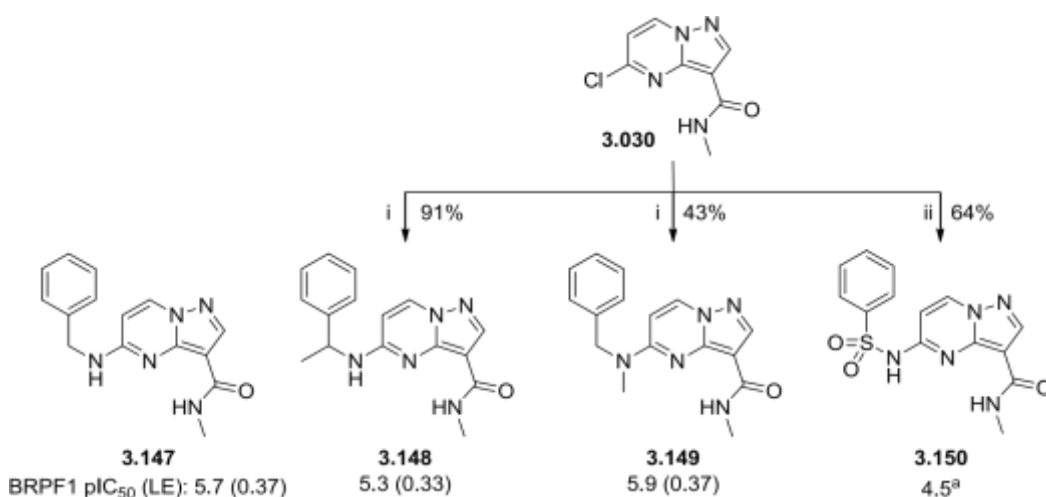
As no improvement in potency had been obtained, and off-target selectivity worsened, the 7-amino was not further investigated.

3.3.8 Targeting the Phe-Ile Region

With the X-ray structure of **3.050** (Figure 3.5) in hand, we aimed to generate an edge-to-face π -interaction with the Phe714 gatekeeper. Various aromatics were investigated at the 5position of the pyrazolopyrimidine, and given that directly 5-linked aromatics (**3.003**, **3.005**) or anilines (**3.045**) were detrimental to potency, extending the linker was also explored.

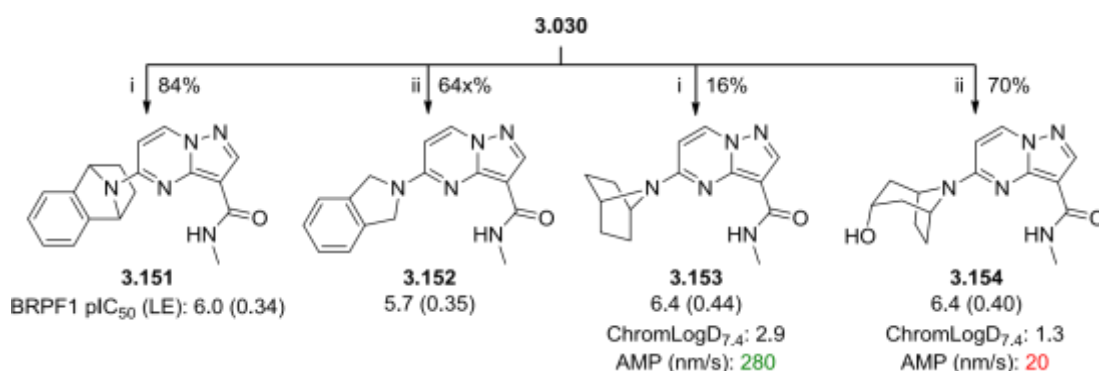
Benzylamine **3.147** was obtained from the GSK compound collection and shown to have moderate BRPF1 potency and reduced LE. In an attempt to constrain the conformation of the benzyl group the racemic α -Me benzylamine **3.148** was synthesised, but exhibited reduced potency and LE, potentially due to a clash with the binding site. Tertiary benzylamine **3.149** was synthesised and showed a marginal improvement in potency compared to **3.147**, but the lack of a large increase in potency indicated an interaction was not occurring. Sulphonamides have a 90° N-S-C bond angle which would place the phenyl ring in the ideal position for contact with the Phe714 gatekeeper. The acidity of the sulphonamide NH allows them to participate in S_NAr reactions,³⁷⁶ and so phenyl sulphonamide **3.149** was readily synthesised. However, the BRPF1 potency of **3.149** was below the lower limit of the assay, most likely due to the

sulphonamide oxygen lone pairs clashing with the Glu661 which packs onto the top of the core.



Scheme 3.24. Benzylic and phenyl groups. Potency data are n=3 or greater unless otherwise stated. a) n=1, <4 on two other test occasions. Reagents and conditions: (i) α -Methylbenzylamine or N-methylbenzylamine, DIPEA, DMSO, rt; (ii) PhSO₂NH₂, Cs₂CO₃, DME, 90 °C.

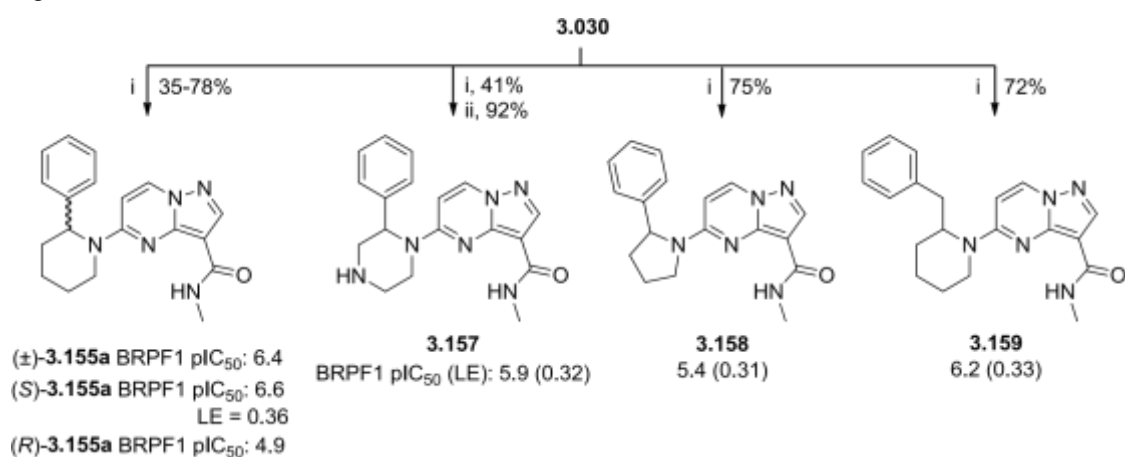
With flexible benzyl substituents proving unfruitful, conformationally restricted examples and bridged substituents were investigated, again through facile S_NAr of the corresponding amine onto 5-chloro intermediate **3.030** (Scheme 3.25). The aza-bridged tetrahydronaphthalene **3.151** was synthesised in an attempt to place a conformationally restricted phenyl group in the Phe¹¹⁶ region, but showed only moderate potency and low LE. Isoindoline **3.152** showed similar potency and slightly higher LE, indicating the bridge and resulting conformational restriction contributed little to the binding of **3.151**. Bicycloheptane **3.153** and nortropine derivative **3.154** proved relatively potent and efficient, potentially due to improved contact with the 5-position pocket. The similar potency of **3.153** and **3.154**, and higher LE of **3.153**, indicates that the alcohol of **3.154** does not form positive interactions with the protein. This group also had a detrimental effect on permeability.



Scheme 3.25. Bridged and bicyclic 5-substituents. Potency data are n=3. Reagents and conditions: (i) Amine, DIPEA, DMSO, 90 °C, μ W; (i) Amine, DIPEA, DMSO, rt.

Attention turned to placing the aromatic ring at the α -position of the piperidine ring, in the hope that the ring would again adopt the desired axial conformation. The A value for an N -substituted 2-methylpiperidine is estimated at 1.9 kcal/mol,³⁷⁴ not dissimilar to that of cyclohexane (1.74 kcal/mol),³⁵³ enabling comparison to the A value for phenylcyclohexane (2.7 kcal/mol).³⁵³ As such it was noted that a significantly greater energy penalty would be paid for phenylpiperidine PPs on adopting the required axial conformation.

Phenylpiperidines underwent S_NAr reaction with **3.030** in good yield, although heating was required due to greater steric hindrance around the nitrogen (Scheme 3.26). Encouragingly, the racemate (\pm)-**3.155a** showed good BRPF1 potency. The enantiomers (R)-**3.155a** and (S)-**3.155a** were readily synthesised using commercially available enantiopure phenylpiperidines. As predicted from the crystallography, (S)-**3.155a** was the more potent, with (R)-**3.155a** significantly less active as it cannot adopt the most favourable vertical/axial binding conformation and engage the same pocket of the protein. The beneficial effect of constraining the phenyl ring can be seen through comparison to benzylamine **3.147**, with addition of the piperidine ring maintaining LE. However, the LE of (S)-**3.155a** is still below that of the methyl analogue (R)-**3.050**, possibly indicating that beneficial hydrophobic or π -interactions are being counteracted by the energy penalty of adopting the axial phenyl conformation. It was thought that different linker rings might improve binding through reduced $A^{1,3}$ -strain; phenyl piperazine **3.157** (*via* Boc derivative **3.156**) and pyrrolidine **3.158** were synthesised in a similar manner but both were less potent and efficient than (\pm)-**3.155a**. Extending the phenyl ring out by one atom, in the form of 2-benzylpiperidine **3.159**, was relatively well tolerated but gave a slight reduction in potency compared to (\pm)-**3.155a**. The 2phenylpiperidine appears to be optimal in terms of the phenyl ring vector angle and the contact between substituents and the Phe-Ile region.



Scheme 3.26. Phenyl groups at the 2-position of heterocycles. Potency data are n=3. Reagents and conditions: (i) Amine, DIPEA, DMSO, 90 °C, μ W; (ii) TFA, DCM, rt.

The nature of the aromatic ring was investigated with an array of 2-phenylpiperidines (Table 3.12). Monomers were chosen to probe the effect of changing the electronics of the ring and tolerability towards substitution at different positions. The S_NAr reactions to form these products proceeded smoothly and in good yield under microwave heating. A methoxy substituent was tolerated at all positions of the ring (**3.155c-d**), with *para*-methoxy **3.155d** being the most potent out of this set of analogues. However, **3.155d** was only marginally more potent (within assay error limits of 0.3 log units) than unsubstituted phenyl **3.155a**. Fluorine was tolerated at the *meta* (**3.155e**) and *para* (**3.155f**) positions, but showed reduced potency compared to *para*-methoxy **3.155d**. *Para*-chloro (**3.155g**) and *para*-methyl (**3.155h**) were also active but did not improve on the potency of **3.155a** or **3.155d**. The relatively flat SAR suggests that the electronics of the phenyl ring are unimportant and no specific interactions with the protein are being made by the substituents.

Pyridyl substitution was unfavourable, with racemic 2-pyridyl **3.155i** significantly less potent than **3.155a**. The 3-pyridyl (*S*)-**3.155**, obtained from the natural product (-)-anabasine, was slightly more potent than **3.155i** (accounting for the expected 0.2-0.3 log increase in potency for the (*S*)-enantiomer compared to the corresponding racemate, c.f. (\pm)-**3.155a** and (*S*)-**3.155a**). 5-Membered heterocycles proved more potent than the pyridine analogues, with oxadiazole **3.155k** and thiazole **3.155l** showing reasonable potency. In an attempt to form hydrogen bonding interactions with the backbone carbonyls on the side of the pocket opposite the Phe, imidazole **3.155m** was synthesised (Scheme 3.27). However, **3.155m** was poorly potent, indicating a hydrogen bond donor is not tolerated in this region.

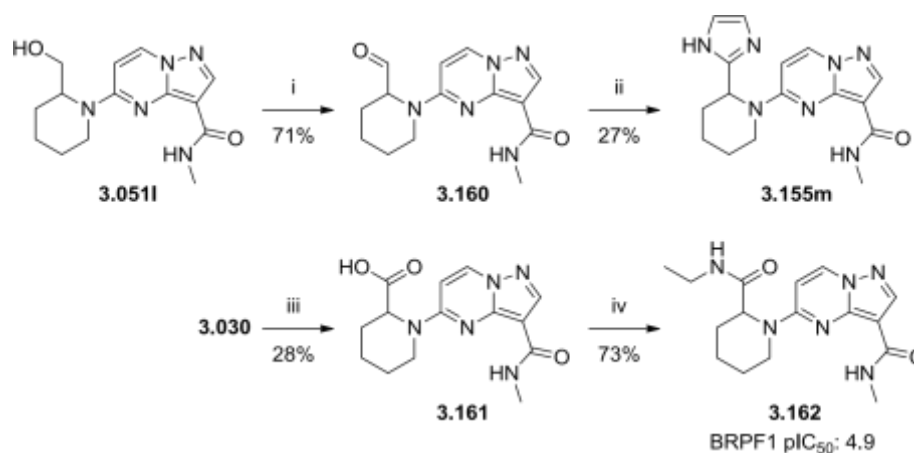
Table 3.12. Structures and potencies of phenylpiperidine products **3.155a-m**

Cpd	Yield	Ar	BRPF1 pIC ₅₀	Cpd	Yield	Ar	BRPF1 pIC ₅₀
3.155b	75%		6.4	3.155c	61%		6.2
3.155d	81%		6.5	3.155e	75%		6.1
3.155f	60%		6.2	3.155g	66%		6.1
3.155h	72%		6.4	3.155i	75%		5.6

(S)- 3.155j	53%		6.1	3.155k	68%		6.2
3.155l	65%		6.1	3.155m	-a		5.5

Potency data are n=3. a) For synthesis see Scheme 3.27.

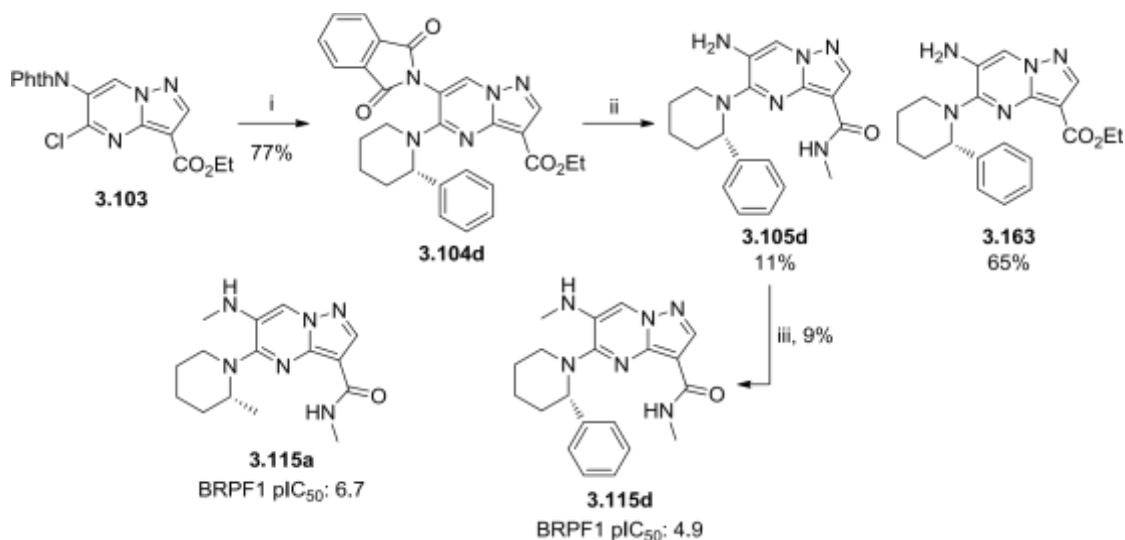
To synthesise imidazole **3.155m**, hydroxymethyl piperidine **3.051l** was oxidised to the corresponding aldehyde **3.160** with DMP, followed by thermal cyclisation with aqueous ammonia and glyoxal to give **3.155m** in reasonable yield. Amides could potentially also form π -interactions with Phe714, without the detrimental effects of an aromatic ring on developability and physicochemical properties (Section 1.1.3). Acid **3.161** was synthesised by S_NAr (in low yield due to poor solubility and the electron-deficient piperidine) and the ethyl amide **3.162** formed using HATU. The potency of **3.162** was very poor, potentially as a result of the hydrogen bond donor not adopting the required conformation, or the amide being too far from the Phe to interact. Amides were not further investigated.



Scheme 3.27. Synthesis of imidazole **3.155m** and amine **3.162**. Potency data are n=3. Reagents and conditions: (i) Dess-Martin periodinane, DCM, rt; (ii) NH_4OH , glyoxal, MeOH, H_2O , rt; (iii) piperidine-2-carboxylic acid, DIPEA, DMSO, 90 °C, μW ; (iv) $EtNH_2$, HATU, DIPEA, DMF, rt.

Given the promising potency and selectivity profile of 5,6-disubstituted PP **3.115a**, the *N*-methyl 6-substituent was combined with the (S)-2-phenylpiperidine 5-substituent to test whether these benefits would be additive (Scheme 3.28). The phthalimide intermediate **3.103** was reacted with (S)-2-phenylpiperidine under the previously developed S_NAr conditions to give **3.104d** in good yield. Amidation/deprotection under the previously facile DABAL- Me_3 conditions proceeded poorly, giving only 11% of the desired amide product **3.105d** (unoptimised yield). The amine/ester product **1.63**, resulting from phthalimide deprotection

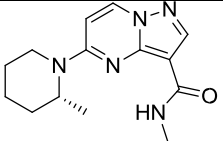
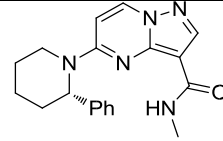
without reaction of the ester, was also isolated in 65% yield. Sufficient quantities of **3.105d** were obtained to alkylate with methyl iodide, giving **3.115d** in poor yield – the reaction was sluggish with the formation of multiple byproducts from alkylation at other sites of the molecule. **3.115d** showed very poor potency – the 6-substituent may prevent rotation of the phenylpiperidine into the preferred axial binding conformation. Given that the poor BRPF1 potency of **3.115d** would also be expected for other 6-substituents, no attempt was made to improve the low synthetic yields or investigate alternative substitution.



Scheme 3.28. Synthesis of 5,6-disubstituted pyrazolopyrimidine **3.115d**. Potency data are n=3. Reagents and conditions: (i) (*S*)-2-Phenylpiperidine, DIPEA, DMSO, 90 °C, μ W; (ii) DABAL-Me₃, MeNH₂, THF, 40 – 70 °C; (iii) MeI, K₂CO₃, DMF, 90 °C, μ W.

The potency and selectivity profile of the phenylpiperidine (*S*)-**3.155a** was compared to (*R*)-**3.050** (Table 3.13). (*S*)-**3.155a** showed much reduced ligand efficiency as a result of the additional phenyl ring, with an essentially unchanged selectivity profile. The additional phenyl was not overly detrimental to physicochemical properties, raising the ChromLogD_{7.4} by 1.4. Solubility was reduced but remained in good space, while permeability increased. However, overall (*S*)-**3.155a** offered no benefit compared to (*R*)-**3.050**.

Table 3.13. FRET potencies, LE and physicochemical properties of (*R*)-**3.050** and (*S*)-**3.155a**.

	 (R)-3.050	 (S)-3.155a
BRPF1 pIC₅₀ / LE	6.7 (0.46)	6.6 (0.36)
BRPF2 pIC₅₀	4.7	4.6
BRPF3 pIC₅₀	4.2	4.4

Brd4 BD1 / BD2 pIC₅₀	4.6 ^a / 4.5 ^b	4.6 / 4.4
Brd7 pIC₅₀	5.1	5.3
Brd9 pIC₅₀	5.8	5.6
CECR2 pIC₅₀	4.8	4.7
ChromLogD_{7.4}	3.3	4.7
CLND Solubility (μM)	610	464
AMP (nm/s)	307	490

Potency data are n=2 or greater unless otherwise stated. Dashes indicate data not available. a) n=3, <4.3 on two other test occasions; b) n=4, <4.3 on one other test occasion.

An X-ray crystal structure of (*S*)-**3.155a** bound to the BRPF1 bromodomain was obtained (Figure 3.9). The core binds as before with Glu661 packing onto the top of the pyrimidine ring, though slightly further away compared to (*R*)-**3.050**. This underlines the flexibility of this residue and the subtle effects it may have on binding affinity. The piperidine again adopts an axial conformation to place the phenyl in the Ph-Ile region at a 90° angle to the core and Phe714. No edge-to-face interaction with Phe714 is made, only edge-to-edge contact, and the ring sits too high above Ile652 for meaningful lipophilic contacts. This could explain the lack of an increase in potency between methyl piperidine (*R*)-**3.050** and the phenylpiperidine analogues, in addition to the energy penalty required to adopt the axial bound conformation. Disappointingly, occupying this region failed to improve selectivity despite it being more crowded in Brd9 – again, the ring may bind too far away for a significant steric clash.

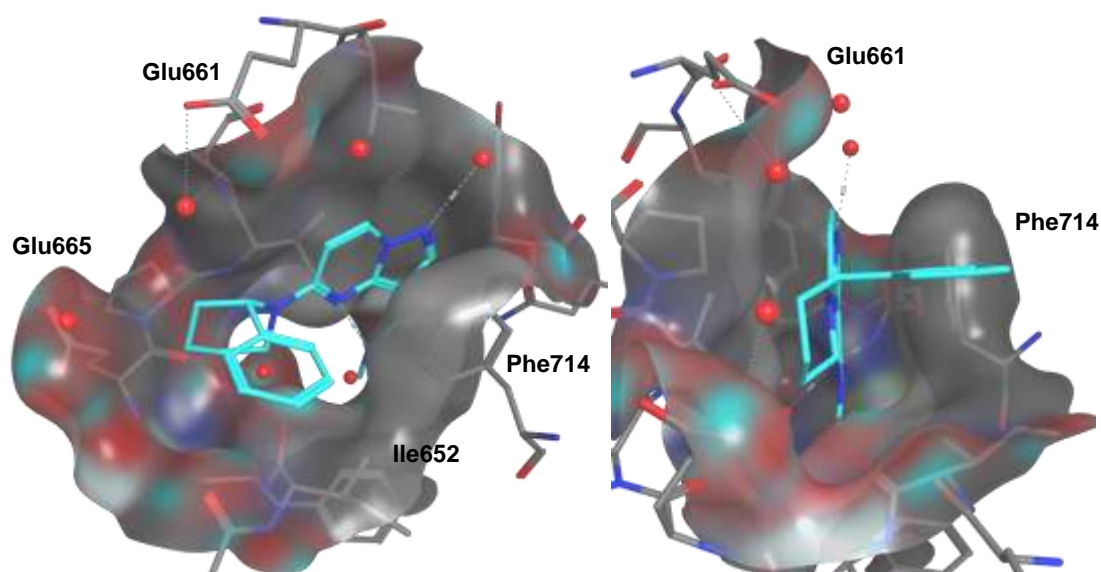


Figure 3.9. X-ray structure of phenylpiperidine (*S*)-**3.155a** (cyan, 1.9 Å)²⁹² bound to the BRPF1 bromodomain.

To further explain this binding mode, the relative potential energies of the rotational conformations of (*S*)-**3.155a** were calculated (Figure 3.10). The protein atoms and solvent

were removed and the potential energy of the bound conformation (**L**) was measured using a MMFF94x forcefield to be 59.8 kcal/mol. The corresponding vertical phenyl conformation, **M**, has a higher potential energy due to increased steric clash with the axial protons at the 2- and 4-positions of the piperidine, but could compensate for this to some degree through the formation of an edge-to-face interaction with Phe714. However, in order to rotate from **L** to **M** (with no change in conformation of the piperidine chair) the molecule must pass through the high energy structure **N**, with eclipsed protons. This forms a high energy barrier to rotation which reinforces the preference for the low-energy bound conformation.

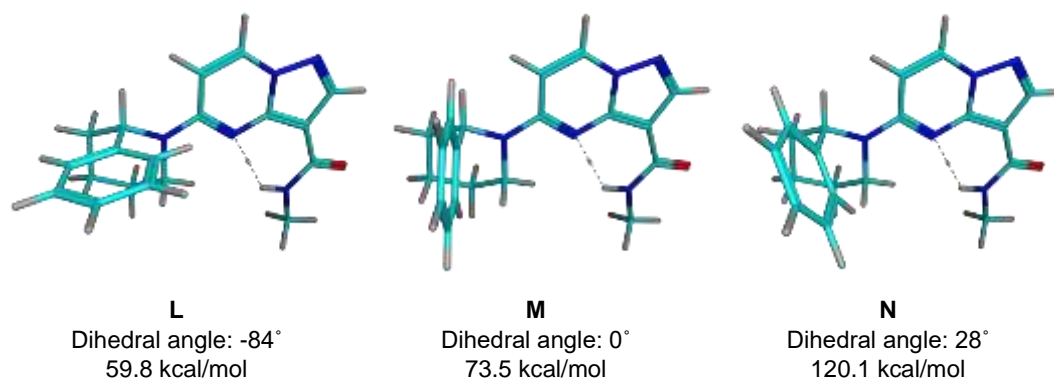


Figure 3.10. Structures, dihedral angles and MMFF94x potential energies (calculated using Molecular Operating Environment, MOE) for phenylpiperidine (*S*)-**3.155a**.

3.3.9 6-Aza Cores

Although the protons of the core 6-position and the piperidine α -position do not clash in the crystal structures, they remain in close proximity and the 6-H proton may affect the rotational freedom of the 5-substituent. This is of particular concern for larger 5-substituents such as phenylpiperidines, and indeed it was observed that a larger 6-substituent dramatically reduced BRPF1 activity (**3.115a**). Replacing the 6-position with a heteroatom could reduce this and improve potency, and the effect of introducing a lone pair close to Glu661 was considered worthy of investigation. Two alternative cores, the pyrazolo[1,5-*a*]-1,3,5-triazines (**3.164**) and pyrrolo[3,2-*d*]pyrimidines (**3.165**) were proposed to explore this (Figure 3.11).

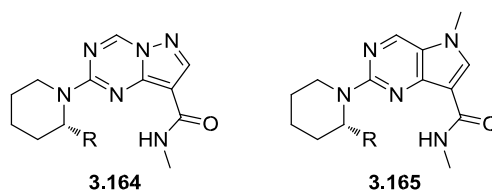
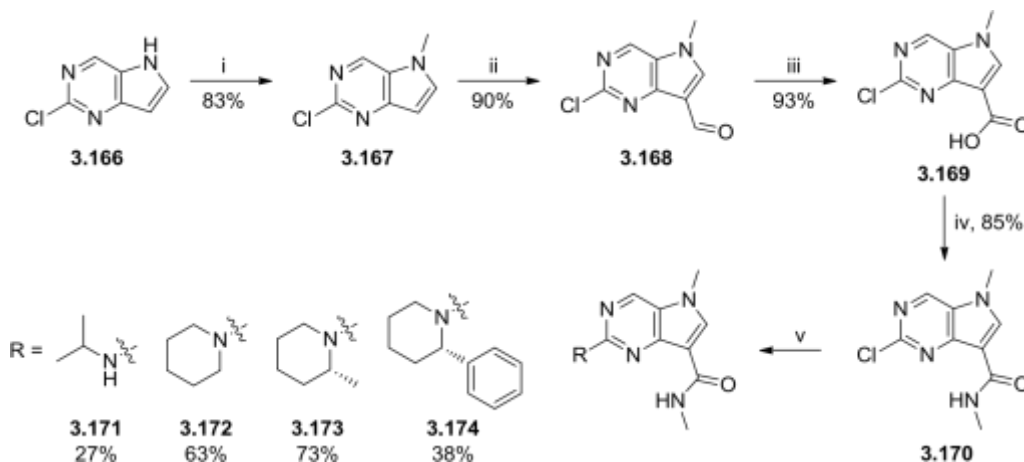


Figure 3.11. Alternative N6 cores.

The pyrazolo[1,5-a]-1,3,5-triazine (PT) core is predated in medicinal chemistry,^{356,377,378} with one compound containing this structure progressing to late-stage development.³⁷⁹ However, almost all syntheses involve a 7-substituent,^{356,377-379} with known methods for synthesising 7-H PT analogues incompatible with heteroatom 5-substituents.³⁸⁰ As such, the synthesis of **3.164** was considered to be challenging but achievable. In contrast, pyrrolo[3,2d]pyrimidines with 5-N, 7-H substitution are known,³⁸¹ while 5-chloro building blocks are commercially available and compatible with the previously developed azaindole chemistry (Section 3.3.3). Given that 6-N cores have the potential to be detrimental should a lonepair/lone-pair clash with Glu661 occur, the pyrrolopyrimidine core was chosen in order to rapidly investigate this series and hypothesis.

The pyrrolopyrimidine series was synthesised using the previously developed AI synthetic route (Scheme 3.29). Methylation of commercially available **3.166** gave **3.167**, which was formylated to give **3.168** and the aldehyde then oxidised under Pinnick conditions to give acid **3.169** in high yield. Considering the lower yield obtained for amidation of AI **3.067** with oxalyl chloride, **3.169** was instead reacted with HATU and methylamine to produce the amide **3.170**, with a significant improvement in yield. The additional electronegative nitrogen in the core compared to the AI series made S_NAr a viable route for the synthesis of 5-N derivatives, though high temperatures and long reaction times (160 °C, 3 days) were required. The derivatives **3.171-3.174** were obtained in moderate to good yields.

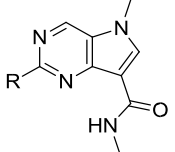
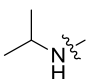
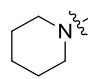
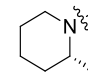
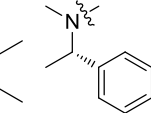


Scheme 3.29. Synthesis of 5-substituted pyrrolo-pyrimidine compounds. Reagents and conditions: (i) NaH, MeI, DMF, rt, 1 hr; (ii) POCl₃, DMF, 0 °C – rt, 3 hr; (iii) NaClO₂, NaH₂PO₄, H₃NSO₃, THF, H₂O, rt, 18 hr; (iv) MeNH₂, HATU, DIPEA, DMF, rt; (v) Amine, DIPEA, DMSO, 90-160 °C, μW (**3.171**, **3.172**) or thermal (**3.173**, **3.174**).

When screened against the BRPF1 bromodomain, the pyrrolopyrimidine core proved to be potent (Table 3.14). Isopropylamine **3.171** was less potent than the initial PP hit **3.002**, but

showed a marginal improvement in potency over AI analogue **3.069** and improved solubility and permeability compared to **3.002** despite a small increase in ChromLogD_{7.4}. Piperidine **3.172** was very similar in potency and properties to AI **3.070**, though selectivity over Brd7 and CECR2 was reduced compared to **3.070** and PP analogue **3.044**. Methylpiperidine (*R*)-**3.173** was slightly more potent than the PP analogue (*R*)-**3.055** (though still within assay error limits) but showed a more marked increase in lipophilicity. However, solubility remained high and permeability improved. Similar to the PP series, phenylpiperidine (*S*)-**3.174** showed good activity but was slightly less potent than (*R*)-**3.173**, with significantly worsened solubility. Although **3.172** and (*R*)-**3.173** showed very low BET activity, (*S*)-**3.174** showed higher activity, in particular against BD1. As seen for the AI series (Table 1.8), BRPF family selectivity was worse than for the PP series, though to a lesser extent. Brd9 potency was significantly increased, producing a lower selectivity window compared to the PPs. Given the high potency observed from the pyrrolopyrimidine series, the pyrazolotriazine series will also be investigated (see Section 3.5).

Table 3.14. Bromodomain FRET potencies, LE and physicochemical properties of pyrrolo[3,2-d]pyrimidines.

	R			
	 3.171	 3.172	 (<i>R</i>)-3.173	 (<i>S</i>)-3.174
BRPF1 pIC₅₀ / LE	5.8 (0.44)	6.3 (0.43)	6.9 (0.45)	6.8 (0.36)
BRPF2 pIC₅₀	5.0	4.6	5.4	5.0 _a
BRPF3 pIC₅₀	4.4	4.4	4.6	4.3
Brd4 BD1 / BD2 pIC₅₀	4.4 ^b / 4.4 ^c	<4.3 / 4.3 ^b	4.4 / 4.5	5.2 / 4.7
Brd7 pIC₅₀	5.5	5.1	5.8	5.4 _a
Brd9 pIC₅₀	6.0	5.7	6.2	5.9

¹ 3.10 Insights Into Wider Bromodomain Selectivity

The wider bromodomain selectivity profile of methylpiperidine (*R*)-**3.050** is shown on the bromodomain phylogenetic tree (Figure 3.12). Good selectivity over the BETs and more distant branches of the phylogenetic tree are observed, with higher activity at Brd9 and Brd7 which can be rationalised by their close sequence homology. However, the higher potencies observed at BPTF, PCAF and CECR2 are less intuitive due to their lower homology.

CECR2 pIC₅₀	5.3	5.5	5.6	5.2
ChromLogD_{7.4}	2.7	4.3	5.0	6.1
CLND Solubility (μM)	552	357	535	128
AMP (nm/s)	480	570	630	680

Potency data are n=2 or greater unless otherwise stated. Dashes indicate data not available. a) n=1; b) n=1, <4.3 on two other test occasions; c) n=2, <4.3 on one other test occasion.

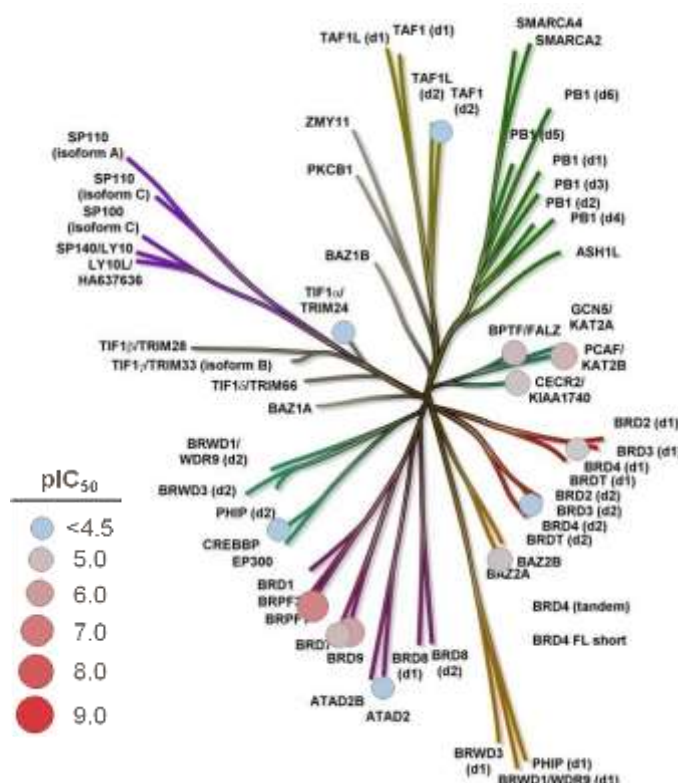


Figure 3.12. FRET bromodomain selectivity profile of (*R*)-3.050, plotted as circles onto the human bromodomain phylogenetic tree.

These differences can be rationalised from examination of the crystal structures (Figure 3.13). Brd9 and CECR2, though quite separate on the phylogenetic tree, both have a similar KAc binding pocket to BRPF1 with an aromatic 'gatekeeper' (Phe714 in BRPF1, Tyr in Brd9 and CECR2) which forms π -stacking interactions with the PP core. However, in Brd4 the gatekeeper is an Ile which cannot form this interaction and causes the binding pocket to adopt a significantly different shape. In addition, the WPF stack of Brd4 blocks the region in which the methylpiperidine binds.

The gatekeeper is also non-aromatic in ATAD (Ile), BAZ2A (Val), TIF1 α (Val) and CREBBP (Val), at which the PP series shows low activity, indicating that the gatekeeper-core interaction is a significant driver of potency for this series. In TAF1 the gatekeeper is a Tyr, but is held

away from the binding pocket by a movement of the BC loop. The only other bromodomains with aromatic gatekeepers which have not been screened against are KAT2A/GCN5 (Tyr), and the SP100/110/140 family (Phe). Binding to KAT2A/GCN5 is expected to be similar to the homologous PCAF, BPTF and CECR2, while the SP family are atypical bromodomains with significantly altered KAc pockets which may prevent binding. In BAZ1A, PB1(1) and TIF1 β the gatekeeper is an Asp or Glu and may be able to form cation- π interactions with the core, however no assays for these targets are currently available.

The majority of changes between the bromodomains are in the ZA loop, with only BRPF1 containing the crucial Glu661 which packs onto the top of the core. The ZA loop of BRPF1 is more similar to that of Brd9 than CECR2, which contains a Tyr which projects down into the pocket. The presence of this residue rationalises why the PP 5-substituent has a significant effect on CECR2 potency, with planar substituents containing π -character (e.g. cyclohexene **3.001** and phenyl **3.005**) forming π -stacking interactions with the Tyr, while bulky nonaromatic groups such as isopropylamine **3.002** clash with it.

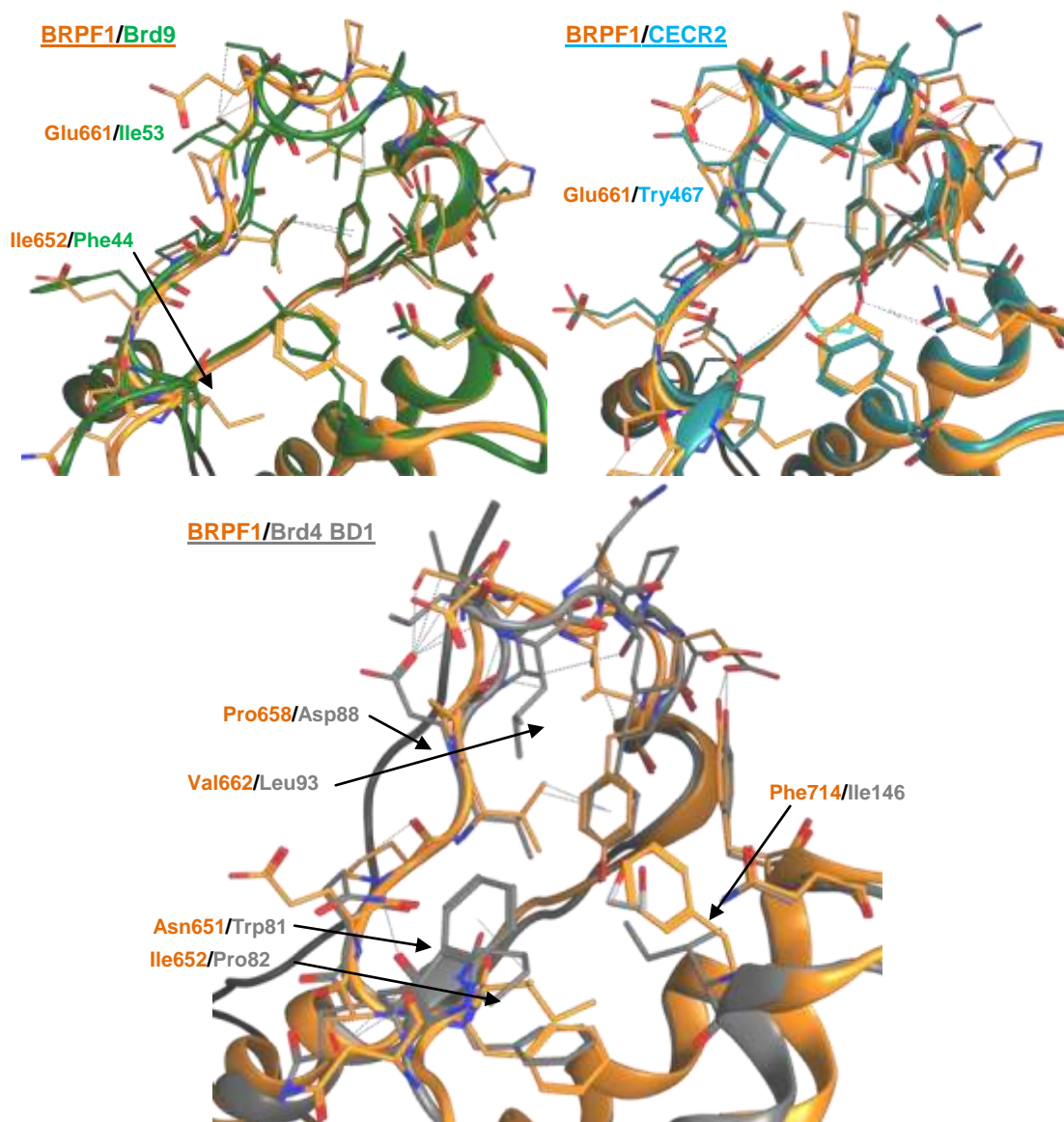


Figure 3.13. Apo X-ray crystal structures of the bromodomains of BRPF1 (orange, PDB: 4LC2) overlaid with Brd9 (dark green, PDB: 3HME), CECR2 (dark cyan, PDB: 3NXB) and Brd4 BD1 (gray, PDB: 2OSS), showing the KAc binding pocket. Crystallised solvent is shown in a lighter hue.

For gaining selectivity over Brd9, the main areas of difference are the ZA loop in the region of Glu661 (which is a bulkier Ile in Brd9) and the Phe-Ile region (where Ile652 is a Phe in Brd9). The large 6-substituents of the most selective examples such as **3.113a** most likely clash with the Ile of the ZA loop on Brd9. Overlay of the X-ray structure of (S)-**3.155a** with the apo structure of Brd9 showed that Phe44 is oriented away from the binding site and only minor clashes are predicted (Figure 3.14). This may explain why phenylpiperidine substitution (Section 2.2.8) failed to produce a significant reduction in Brd9 potency.

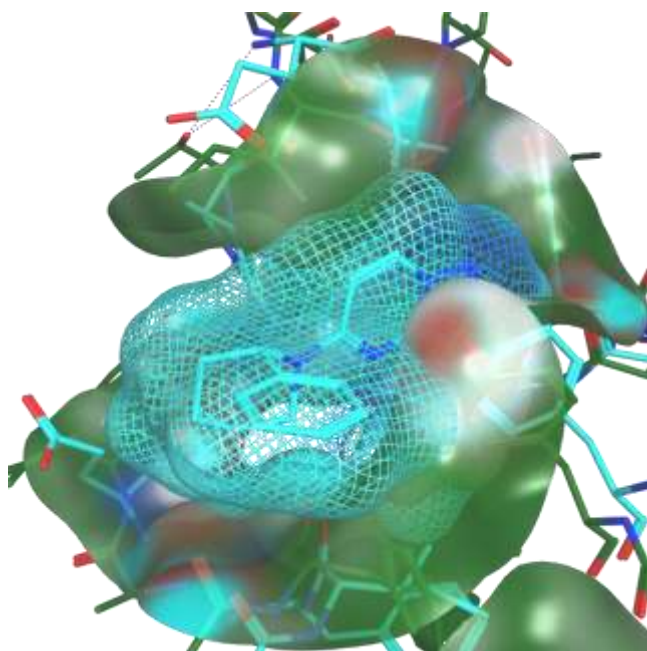


Figure 3.14. Overlay of the X-ray structure of (*S*)-**3.155a** bound to the BRPF1 bromodomain (cyan, 1.9 Å)²⁹² and the apo structure of Brd9 (dark green, PDB: 3HME), showing the Brd9 surface (solid) and ligand surface (mesh).

3.3.11 Selectivity Within the BRPF Family

To examine BRPF family selectivity, the respective potencies of the entire series were plotted (Figures 3.15, 3.16), showing all exemplars were selective for BRPF1 over BRPF2 (x2-x158) and BRPF3 (x10-x398). Some of the highest selectivities over BRPF2 were observed for *o*-nitrile benzyl **3.114a** (x158), methylpiperazine (*R*)-**3.052ab** (x126) and 6NHMe **3.115a** (x100). Intriguingly low selectivity was seen for 5-*c*Pr,6-NHSO₂Ph **3.109c** (x3) and 5-(2-methylpiperidine), 6-NHBz **3.107a** (x2). The bulky groups of **3.109c** and **3.107a** probably make close contact with the more open BRPF2 binding site. **3.109c** also displayed low selectivity over BRPF3 (x20), while the 5-NH^{*i*}Pr AI **3.069** was the least selective (x10) of the compounds discussed in this work. Most compounds with the highest BRPF1 potency showed >100-fold selectivity over BRPF3, with **3.114a** being the most selective (x398).

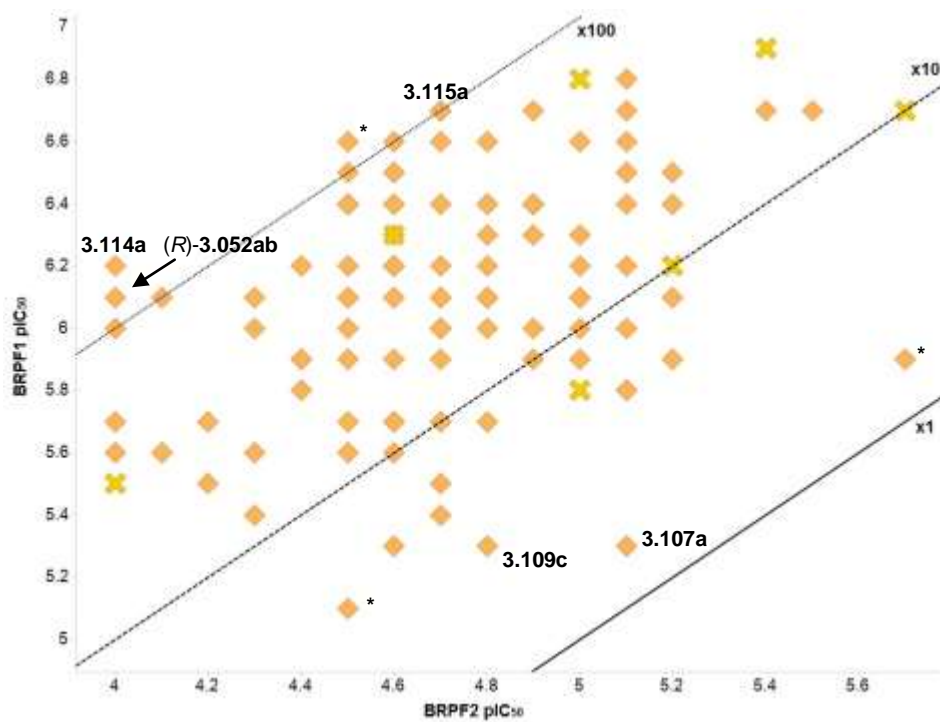


Figure 3.15. BRPF1 vs BRPF2 pIC₅₀. Orange diamonds are the PP series, gold crosses are the AI and pyrrolo-pyrimidine series'. Lines of fold selectivity are shown. *Compound not disclosed in this work.

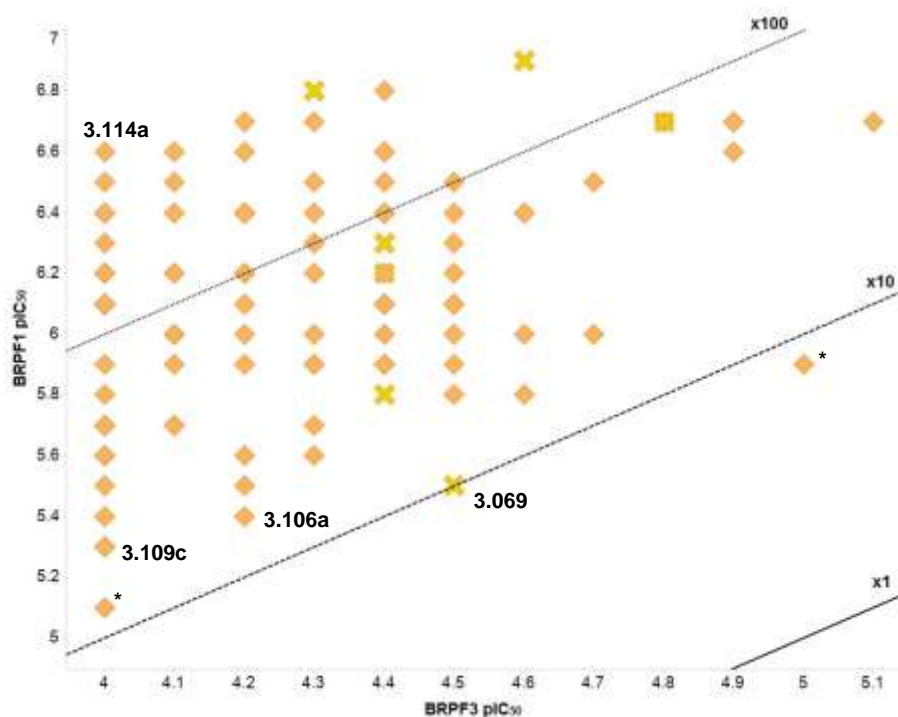


Figure 3.16. BRPF1 vs BRPF3 pIC₅₀. Orange diamonds are the PP series, gold crosses are the AI and pyrrolo-pyrimidine series'. Lines of fold selectivity are shown. *Compound not disclosed in this work.

The selectivities can be somewhat rationalised by comparing the X-ray crystal structures of BRPF1 and BRPF2. No X-ray structure of the BRPF3 bromodomain is known, but the

sequence homology can also be compared (Figure 3.17). The KAc binding-region is highly conserved, as is the edge of the ZA loop adjacent to the crucial Asn708, however, several residue differences exist on the far side of the binding pocket.

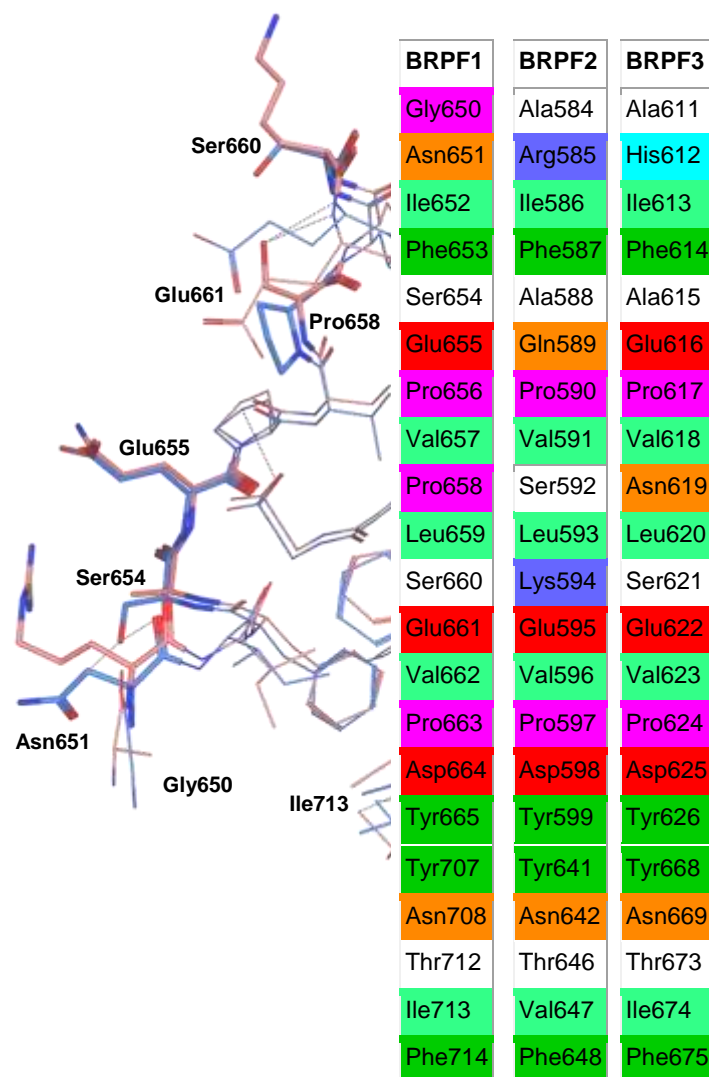


Figure 3.17. *Left:* Overlaid Apo structures of BRPF1 (blue, PDB: 4LC2) and BRPF2 (pink, PDB: 3RCW) bromodomains, key differing residues are bolded and labelled with BRPF1 numbering. *Right:* Sequence homology of key KAc binding site residues for the BRPF family, coloured by amino acid type.

The major difference between the bromodomains is the change of Pro658, against which the 5-substituent makes lipophilic contact, for a Ser in BRPF2 and an Asn in BRPF3. This makes this region of the BRPF2 binding pocket wider and more polar, reducing binding affinity. While the preferred orientation of the Asn in BRPF3 is unclear, it will make this region of the pocket smaller and so prevent compound binding, rationalising the low BRPF3 potencies observed.

Glu655 is maintained in BRPF3 but is a glutamine in BRPF2; compounds forming ionic interactions here would show increased selectivity over BRPF2. Indeed, it was observed that amines **3.052ag** and **3.052al** (Table 3.7) showed increased BRPF3 potency (but still too low

for an electrostatic interaction). The other residue changes in this region (Ser654, Asn651, Gly650) are somewhat further away from the compound binding region and likely do not significantly affect selectivity.

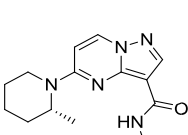
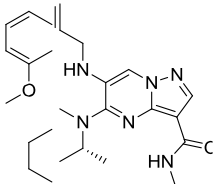
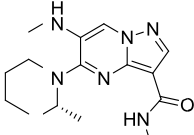
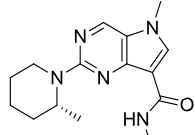
The lack of residue changes around the KAc-binding region complicates explanation of why the AI and pyrrolopyrimidine series' are less BRPF1 selective compared to the PP series. However, the methyl group and altered electronics of the core likely cause a subtle change in binding conformation, which changes the position of the 5-substituent into a more favourable location for BRPF2 binding.

3.4. Conclusions

The potency and selectivity profiles of the most promising phenylpiperidines to date were compared (Table 3.15). This work identified (*R*)-2-methylpiperidine as the best substituent at the 5-position of the bicyclic core, as exemplified by (*R*)-**3.050**, which displayed good BRPF1 potency and high ligand efficiency with an excellent physicochemical property profile. Although Brd4 potency was low and CECR2 potency was reduced compared to the initial hit **3.001**, Brd9 selectivity remained poor. Selectivity over other bromodomains was largely unchanged compared to the hits.

A screen of amine and amide substituents at the 6-position revealed methoxybenzyl **3.113a** and methyl amine **3.115a**, which maintained the potency of (*R*)-**3.050** (though with a large loss of ligand efficiency for **3.113a**) while improving selectivity. **3.113a** is the most selective example of this series over all other bromodomains tested, with the next closest activity being at BAZ2A (40-fold selectivity). However, the ChromLogD_{7.4} of **3.113a** is outside the desired parameters, solubility is relatively low, and permeability is very poor, potentially restricting the use of **3.113a** in cellular experiments.

Table 3.15. Bromodomain FRET potencies, LE and physicochemical properties of lead compounds.

	 (<i>R</i>)-3.050	 3.113a	 3.115a	 3.173
BRPF1 pIC₅₀ / LE	6.7 (0.46)	6.6 (0.30)	6.7 (0.42)	6.9 (0.45)
BRPF2	4.7	4.7	4.7	5.4
BRPF3	4.2	4.2	4.3	4.6
Brd4 BD1 / BD2 pIC₅₀	4.6 ^a / 4.5 ^b	4.4 ^c / 4.6	<4.3 / <4.3	4.4 / 4.5
BPTF pIC₅₀	5.1	-	4.6	-
Brd7 pIC₅₀	5.1	4.7	4.7	5.8
Brd9 pIC₅₀	5.8	4.9	5.3	6.2
CECR2 pIC₅₀	4.8	4.4	4.5	5.6
PCAF pIC₅₀	5.2	-	5.0	-
BAZ2A pIC₅₀	4.9	5.0	4.9	-
ChromLogD_{7.4}	3.3	6.3	4.3	5.0
CLND Sol. (μM)	610	97	361	535
AMP (nm/s)	307	<30	560	630

Potency data are n=2 or greater unless otherwise stated. Dashes indicate data not available. a) n=3, <4.3 on two other test occasions; b) n=4, <4.3 on one other test occasion; c) n=1, <4.3 on two other test occasions; d) n=1.

Methyl amine **3.115a** shows good potency, ligand efficiency and physicochemical properties in addition to reasonable (25-fold) selectivity over Brd9. Selectivity over other bromodomains was also reasonable. Pyrrolopyrimidine **3.173** is the most potent compound developed in this work and exhibits good physicochemical properties. Selectivity profiling is ongoing, but initial results show a smaller BRPF1 selectivity window over Brd7 and CECR2 compared to (*R*)**3.050** and high Brd9 potency. BRPF family selectivity was also altered, with increased BRPF2 potency.

These examples (with the exception of **3.173**, for which some data is not currently available) showed low but consistent potency against PCAF and BAZ2A, and ~100-fold or greater selectivity for BRPF1 within the BRPF family.

These data indicate that although the PP series and similar chemotypes are promising BRPF1 inhibitors, no compounds have been identified which fully meet the specified probe criteria (Section 3.2). Given that the AMP assay is an artificial model and not fully representative of a biological system (*e.g.* does not account for active transport), methoxybenzylamine **3.113a** may be sufficiently cell-permeable for use as a probe molecule. Alternatively, methyl amine **3.115a** may be sufficiently selective to provide meaningful data in biological experiments, depending on dose levels and the strengths of various target and offtarget phenotypes. Overall, the potency of the series is at a usable level but does not improve on existing inhibitors, with the most BRPF1-selective inhibitors also being less potent. While final SAR investigations may yield examples with improved selectivity and physicochemical properties (Section 3.5), if more potent inhibitors are required then an alternative chemotype should be sought.

3.5. Future Work

Further work in this area will seek to complete the selectivity profiles of many of the examples described thus far. In addition, further compounds are of interest (Figure 3.18).

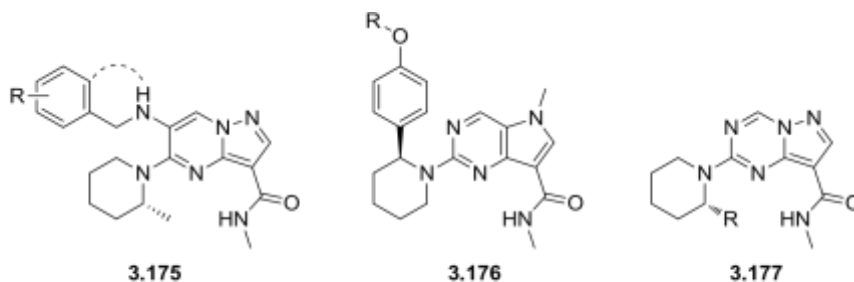
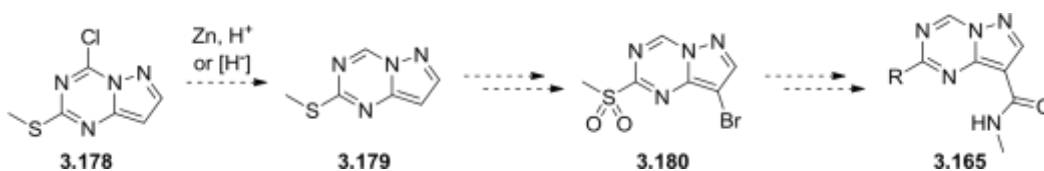


Figure 3.18. Future work.

- A thorough investigation of disubstituted PPs with a 6-*N*-benzyl group (**3.175**) including investigation of other substitution sites on the phenyl ring. The effect of substitution patterns on BRPF1 potency is expected to be relatively neutral based on previous data (Scheme 3.16), but have subtle and unpredictable effects on the bromodomain selectivity profile.
- Closer examination of the methoxyphenylpiperidine **3.155d**, including synthesis or separation of the single enantiomers, alternative ethers (**3.176**) and inclusion into the pyrrolopyrimidine core to test if potency gains are additive. Again, the wider selectivity profile of these compounds also warrants investigation.
- Synthesis of the pyrazolo[1,5-*a*]-1,3,5-triazine (PT) core and substituted examples (Scheme 3.30). Such a synthesis could stem from commercially available bicycle **3.178**, the 7-Cl of which could potentially be selectively removed as seen for the PP series.³⁵⁷ Bromination of PT scaffolds is known to occur at the 3-position,³⁷⁸ allowing amide synthesis through carbonylation or lithiation and trapping. Oxidation of the methyl thiol, and use of the resulting sulphone **3.180** in S_NAr reactions, is well precedented.^{356,378}



Scheme 3.30. Proposed synthesis of pyrazolo[1,5-*a*]-1,3,5-triazine compounds.

4. Experimental

4.1 General Chemistry Experimental

Unless otherwise stated, all reactions were carried out under an atmosphere of nitrogen in heat or oven dried glassware and anhydrous solvent. Solvents and reagents were purchased from commercial suppliers and used as received.

Reactions were monitored by thin layer chromatography (TLC) or LCMS. TLC was carried out on glass or aluminium-backed 60 silica plates coated with UV₂₅₄ fluorescent indicator. Spots were visualised using UV light (254 or 365 nm) or common staining methods as appropriate. Flash column chromatography was carried out using Biotage SP4 or Isolera One apparatus with SNAP KP or SNAP ULTRA pre-packed silica cartridges. Ion exchange chromatography was carried out using Biotage Isolute cartridges and extracted organic mixtures were dried using Biotage PTFE hydrophobic phase separator frits.

NMR spectra were recorded at rt (unless otherwise stated) using standard pulse methods on any of the following spectrometers and signal frequencies: Bruker AV-400 (¹H = 400 MHz, ¹³

¹³C = 101 MHz), Bruker AV-600 (¹H = 600 MHz, ¹³C = 150 MHz), Bruker DPX-250 spectrometer at 250 MHz or Varian INOVA spectrometer at 300 MHz. Chemical shifts are referenced to trimethylsilane (TMS) or the residual solvent peak, and are reported in ppm. Coupling constants are quoted to the nearest 0.1 Hz and multiplicities are given by the following abbreviations and combinations thereof: s (singlet), d (doublet), ABq (AB quartet), t (triplet), q (quartet), quin (quintet), sxt (sextet), m (multiplet), br. (broad). Where products were isolated as single unknown enantiomers, this is indicated by an asterisks following the stereochemical assignment.

IR spectra were obtained on a Perkin Elmer Spectrum 1 FTIR apparatus, with major peaks reported. Optical rotation of chiral products was measured using a Jasco P1030 polarimeter. Melting point analysis was carried out using a Stuart SMP40 melting point apparatus, melting points are uncorrected.

IR spectra were obtained on a Perkin Elmer Spectrum 1 FTIR apparatus, with major peaks reported. Optical rotation of chiral products was measured using a Jasco P1030 polarimeter. Melting point analysis was carried out using a Stuart SMP40 melting point apparatus, melting points are uncorrected.

Liquid chromatography high resolution mass spectra were recorded on a Micromass Q-Tof Ultima hybrid quadrupole time-of-flight mass spectrometer, with analytes separated on an Agilent 1100 Liquid Chromatograph equipped with a Phenomenex Luna C18(2) reversed phase column (100 mm x 2.1 mm, 3 μm packing diameter). LC conditions were 0.5 mL/min flow rate, 35 °C, injection volume 2-5 μL. Gradient elution with (A) water containing 0.1% (v/v)

formic acid and (B) acetonitrile containing 0.1% (v/v) formic acid. Gradient conditions were initially 5% B, increasing linearly to 100% B over 6 min, remaining at 100% B for 2.5 min then decreasing linearly to 5% B over 1 min followed by an equilibration period of 2.5 min prior to the next injection.

LCMS analysis was carried out on a Waters Acquity UPLC instrument equipped with a BEH or CSH column (50 mm x 2.1 mm, 1.7 μ m packing diameter) and Waters micromass ZQ MS using alternate-scan positive and negative electrospray. Analytes were detected as a summed UV wavelength of 210 – 350 nm. Two liquid phase methods were used:

Formic – 40 °C, 1 mL/min flow rate. Gradient elution with the mobile phases as (A) water containing 0.1% volume/volume (v/v) formic acid and (B) acetonitrile containing 0.1% (v/v) formic acid. Gradient conditions were initially 1% B, increasing linearly to 97% B over 1.5 min, remaining at 97% B for 0.4 min then increasing to 100% B over 0.1 min.

High pH – 40 °C, 1 mL/min flow rate. Gradient elution with the mobile phases as (A) 10 mM aqueous ammonium bicarbonate solution, adjusted to pH 10 with 0.88 M aqueous ammonia and (B) acetonitrile. Gradient conditions were initially 1% B, increasing linearly to 97% B over 1.5 min, remaining at 97% B for 0.4 min then increasing to 100% B over 0.1 min.

Mass directed automatic purification (MDAP) preparative HPLC was carried out using a Waters ZQ MS using alternate-scan positive and negative electrospray and a summed UV wavelength of 210 – 350 nm. Three liquid phase methods were used:

Formic MDAP – Sunfire C18 column (100 mm x 19 mm, 5 μ m packing diameter, 20 mL/min flow rate) or Sunfire C18 column (150 mm x 30 mm, 5 μ m packing diameter, 40 mL/min flow rate). Gradient elution at rt with the mobile phases as (A) water containing 0.1% volume/volume (v/v) formic acid and (B) acetonitrile containing 0.1% (v/v) formic acid.

High pH MDAP – Xbridge C18 column (100 mm x 19 mm, 5 μ m packing diameter, 20 mL/min flow rate) or Xbridge C18 column (150 mm x 30 mm, 5 μ m packing diameter, 40 mL/min flow rate). Gradient elution at rt with the mobile phases as (A) 10 mM aqueous ammonium bicarbonate solution, adjusted to pH 10 with 0.88 M aqueous ammonia and (B) acetonitrile.

TFA MDAP – XSELECT CSH column (150 mm x 30 mm, 5 μ m packing diameter, 40 mL/min flow rate). Gradient elution at rt with the mobile phases as (A) 0.1% v/v solution of TFA in H₂O and (B) 0.1% v/v solution of TFA in acetonitrile.

Appropriate MDAP fractions were concentrated under a stream of nitrogen in a blowdown apparatus or evaporated *in vacuo* to afford the products.

4.2 Compound Synthesis and Characterisation - Design and Synthesis of Tetrahydroquinoxalines as BD2-Selective BET Inhibitors

General Procedure 1 – Reductive amination

To a solution of amine (1 equiv.) and benzylic aldehyde (2 equiv.) in DCM (0.05 M) at rt under N₂ was added NaBH(OAc)₃ (4 equiv.). The mixture was stirred at rt until complete by LCMS (24-96 h). Sat. aq. NaHCO₃ was added and the phases vigorously mixed. The aqueous layer was extracted with DCM, the combined organics were dried through a hydrophobic frit, and the solvent was concentrated *in vacuo*. The crude product was purified by silica chromatography or MDAP to afford the pure product.

General Procedure 2 – Amine benzylation

A solution of amine (1 equiv.) and K₂CO₃ (3 equiv.) in DMF (0.3 M) was treated with a benzylic bromide (2 equiv.) and stirred under N₂ at 90 °C until complete by LCMS (12-40 h). The reaction mixture was cooled, diluted with MeOH (0.3 volumes), and filtered. The filtrate was concentrated *in vacuo* and the residue was purified by MDAP to afford the pure product.

General Procedure 3 – Suzuki-Miyaura cross-coupling with aryl bromides

The aryl bromide, aryl boronic acid or boronic acid pinacol ester (1.5-2 equiv.), Cs₂CO₃ (4 equiv.), and Pd(dppf)Cl₂ (10 mol%) were placed in a microwave vial and suspended in 1,4-dioxane and H₂O (10:1, 0.1 M). The vial was sealed, evacuated and refilled with N₂. The reaction was heated in a Biotage Initiator microwave reactor at 110 °C for 2 h. The reaction mixture was cooled, filtered through Celite, and evaporated to dryness. The crude product was purified by silica chromatography or MDAP to afford the pure product.

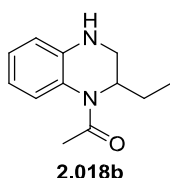
General Procedure 4 – Nitrile oxidation with H₂O₂.

To a stirred solution of aryl nitrile in DMSO (0.08 M) was added K₂CO₃ (2 equiv.), followed by 35% aq. H₂O₂ (10 equiv.). The reaction mixture was stirred at rt for 1 h, then filtered, concentrated and the residue purified by MDAP to afford the pure products.

General Procedure 5 – HATU-mediated amidation

To a solution of the carboxylic acid (1 equiv.) and HATU (1.5 equiv.) in DMF (0.15 M) was added the respective amine (2 equiv.) and DIPEA (3 equiv., 5 equiv. if using the amine HCl

salt). The reaction mixture was stirred at rt for 30 min, then filtered and purified by MDAP to afford the products.



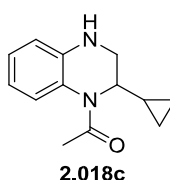
1-(2-Cyclopropyl-3,4-dihydroquinoxalin-1(2H)-yl)ethanone

A solution of 1-(6-bromo-2-ethyl-3,4-dihydroquinoxalin-1(2H)-yl)ethanone hydrochloride **2.016b** (260 mg, 0.918 mmol) in MeOH (23 mL) was passed through a Thales H-cube Flow Hydrogenator with a 10% Pd/C CatCart in full H₂ mode at a rate of 1 mL/min. Two passes of the reaction mixture through the CatCart were required for full conversion. The solvent was evaporated *in vacuo* and the residue purified by ion exchange chromatography (sulphonic acid (SCX), 5 g, sequential solvents: MeOH, 2 M NH₃/MeOH). The appropriate fractions were combined and evaporated *in vacuo* to give 1-(2-ethyl-3,4-dihydroquinoxalin-1(2H)-yl)ethanone (181 mg, 0.886 mmol, 97%) as a yellow oil.

LCMS (Formic, ES⁺): t_R = 0.79 min, [M+H⁺] 205.1, (98% pure).

¹H NMR (400 MHz, DMSO-d₆): δ 0.85 (t, *J* = 7.4 Hz, 3H), 1.16-1.44 (m, 2H), 2.15 (s, 3H), 3.11-3.37 (m, 2H), 4.48-4.65 (m, 1H), 5.64 (s, 1H), 6.53 (td, *J* = 8.1, 1.3 Hz, 1H), 6.62 (dd, *J* = 8.1, 1.3 Hz, 1H), 6.89 (td, *J* = 8.1, 1.5 Hz, 1H), 7.17 (d, *J* = 8.1 Hz, 1H).

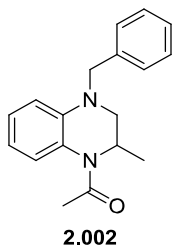
1-(2-Cyclopropyl-3,4-dihydroquinoxalin-1(2H)-yl)ethanone



A solution of 1-(6-bromo-2-cyclopropyl-3,4-dihydroquinoxalin-1(2H)yl)ethanone **2.016c** (352 mg, 1.193 mmol) in MeOH (40 mL) was passed through a Thales H-cube Flow Hydrogenator with a 10% Pd/C CatCart in full H₂ mode at a rate of 1 mL/min. Two passes of the reaction mixture through the CatCart were required for full conversion. The solvent was evaporated *in vacuo* and the residue purified by ion exchange chromatography (sulphonic acid (SCX), 5 g, sequential solvents MeOH, 2 M NH₃/MeOH). The appropriate fractions were combined and evaporated *in vacuo* to give 1-(2-cyclopropyl-3,4-dihydroquinoxalin-1(2H)yl)ethanone (256 mg, 1.184 mmol, 99%) as an off-white solid. LCMS (High pH, ES⁺): t_R = 0.84 min, [M+H⁺] 217.1, (100% pure). ¹H NMR (400 MHz, CDCl₃): δ 0.33-0.57 (m, 4H), 0.83 (br. s., 1H), 2.27 (s, 3H), 3.44 (dd, *J* = 11.5, 4.2 Hz, 1H), 3.47-3.54 (m, 1H), 4.06-4.30 (m, 2H), 6.62 (dd, *J* = 8.1, 1.3 Hz, 1H), 6.68 (ddd, *J* = 8.1, 7.6, 1.3 Hz, 1H), 7.01 (ddd, *J* = 8.1, 7.6, 1.3 Hz, 1H), 7.04-7.12 (m, 1H).

C NMR (101 MHz, CDCl₃): δ 3.8, 4.2, 11.9, 22.9, 46.0, 50.7, 113.9, 116.3, 122.8, 125.7, 126.1, 137.6, 169.0. M.pt.:114-120 C. ν_{\max} (neat): 3361, 2843, 1622, 1517, 1467, 1439, 1383, 1364, 1313, 1283, 1234, 1123, 1070, 1019, 952, 905, 831, 762, 740 cm⁻¹.

HRMS: (C₁₃H₁₆N₂O) [M+H⁺] requires 217.1335, found [M+H⁺] 217.1342. **1-(4-Benzyl-2-methyl-3,4-dihydroquinoxalin-1(2H)-yl)ethanone**

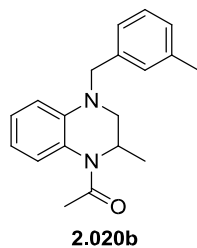


Prepared from **2.018a** (25 mg, 0.131 mmol) and benzaldehyde (0.027 mL, 0.263 mmol) according to General Procedure 1. Purification of the crude product by High pH MDAP afforded 1-(4-benzyl-2-methyl-3,4-dihydroquinoxalin-1(2H)-yl)ethanone (16 mg, 0.057 mmol, 43%).

LCMS (High pH, ES⁺): t_R = 1.16 min, [M+H⁺] 281.3, (100% pure). ¹H NMR (400 MHz, CDCl₃): δ 1.14 (d, J = 7.1 Hz, 3H), 2.27 (s, 3H), 3.17 (dd, J = 11.4, 1.8 Hz, 1H), 3.59 (dd, J = 11.4, 4.8 Hz, 1H), 4.55 (d, J = 4.5 Hz, 2H), 5.17-5.35 (m, 1H), 6.65-6.73 (m, 2H), 6.99-7.10 (m, 2H), 7.23-7.38 (m, 5H).

HRMS: (C₁₈H₂₀N₂O) [M+H⁺] requires 281.1648, found 281.1651.

1-(2-Methyl-4-(3-methylbenzyl)-3,4-dihydroquinoxalin-1(2H)-yl)ethanone

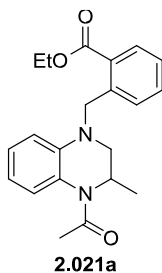


Prepared from **2.018a** (35 mg, 0.18 mmol) and 3-methylbenzyl bromide (50 μ L, 0.552 mol) according to General Procedure 2. Purification of the crude product by High pH MDAP afforded 1-(2-methyl-4-(3-methylbenzyl)-3,4-dihydroquinoxalin-1(2H)-yl)ethanone (26 mg, 0.088 mmol, 48%) as a yellow oil.

LCMS (High pH, ES⁺): t_R = 1.23 min, [M+H⁺] 295.1, (86% pure).

¹H NMR (400 MHz, CDCl₃): δ 1.13 (d, J = 6.8 Hz, 3H), 2.27 (s, 3H), 2.35 (s, 3H), 3.16 (dd, J = 11.4, 1.3 Hz, 1H), 3.58 (dd, J = 11.2, 4.6 Hz, 1H), 4.51 (d, J = 5.1 Hz, 2H), 5.26 (br s, 1H), 6.65-6.73 (m, 2H), 6.98-7.12 (m, 5H), 7.23 (t, J = 7.3 Hz, 1H).

Ethyl 2-((4-acetyl-3-methyl-3,4-dihydroquinoxalin-1(2H)-yl)methyl)benzoate



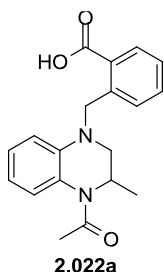
Prepared from **2.018a** (35 mg, 0.18 mmol) and ethyl 2-(bromomethyl)benzoate (0.096 mL, 0.552 mmol) according to General Procedure 2. Purification of the crude product by High pH MDAP afforded ethyl 2-((4-acetyl-3-methyl-3,4-dihydroquinoxalin-1(2H)-yl)methyl)benzoate (11 mg, 0.031 mmol, 17%) as a yellow oil.

LCMS (High pH, ES⁺): t_R = 1.23 min, [M+H⁺] 353.1, (100% pure).

¹H NMR (400 MHz, CDCl₃): δ 1.19 (d, J = 6.8 Hz, 3H), 1.43 (t, J = 7.1 Hz, 3H), 2.29 (s, 3H), 3.16 (dd, J = 11.4, 1.2 Hz, 1H), 3.64 (dd, J = 11.4, 4.5 Hz, 1H), 4.40 (q, J = 7.1 Hz, 2H), 4.89 (d, J = 18.6 Hz, 1H), 5.00 (d, J = 18.6 Hz, 1H), 5.30 (br s, 1H), 6.50 (dd, J = 8.3, 1.2 Hz, 1H), 6.68 (td, J = 7.3, 1.0 Hz, 1H), 7.00 (td, J = 7.7, 1.0 Hz, 1H), 7.05 (br s, 1H), 7.31

(d, $J = 7.8$ Hz, 1H), 7.36 (td, $J = 7.7, 1.0$ Hz, 1H), 7.46 (td, $J = 7.7, 1.2$ Hz, 1H), 8.07 (dd, $J = 7.8, 1.5$ Hz, 1H).

2-((4-Acetyl-3-methyl-3,4-dihydroquinoxalin-1(2H)-yl)methyl)benzoic acid



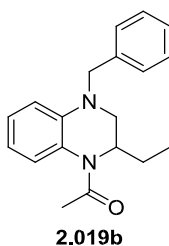
2.022a

A solution of **2.021a** (8.0 mg, 0.02 mmol) and LiOH.H₂O (5.4 mg, 0.23 mmol) in THF (0.45 mL), MeOH (0.23 mL) and H₂O (0.45 mL) was stirred at rt for 24 h. The reaction mixture was concentrated *in vacuo* and the residue was purified by Formic MDAP to afford 2-((4-acetyl-3-methyl-3,4-dihydroquinoxalin-1(2H)-yl)methyl)benzoic acid (5.0 mg, 0.015 mmol, 68%) as a white solid.

LCMS (Formic, ES⁺): $t_R = 0.93$ min, [M+H⁺] 325.2, (100% pure).

¹H NMR (400 MHz, MeOD-*d*4): δ 1.16 (br s, 3H), 2.26 (s, 3H), 3.23 (d, $J = 11.0$ Hz, 1H), 3.56-3.67 (m, 1H), 4.87 (d, $J = 17.9$ Hz, 1H), 5.01 (d, $J = 17.9$ Hz, 1H), 5.20 (br s, 1H), 6.56 (d, $J = 8.1$ Hz, 1H), 6.67 (t, $J = 7.6$ Hz, 1H), 7.01 (t, $J = 7.3$ Hz, 1H), 7.12 (br s, 1H), 7.31 (d, $J = 7.6$ Hz, 1H), 7.34 (t, $J = 7.6$ Hz, 1H), 7.45 (td, $J = 7.6, 1.2$ Hz, 1H), 7.97 (dd, $J = 7.6, 1.2$ Hz, 1H). The exchangeable acid proton was not observed.

1-(4-Benzyl-2-ethyl-3,4-dihydroquinoxalin-1(2H)-yl)ethanone



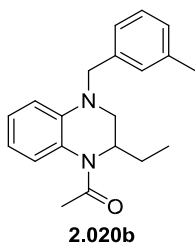
2.019b

Prepared from **2.018b** (45 mg, 0.22 mmol) and benzyl bromide (52 μ L, 0.44 mmol) according to General Procedure 2. Purification of the crude product by High pH MDAP afforded 1-(4-benzyl-2-ethyl-3,4-dihydroquinoxalin-1(2H)-yl)ethanone (43 mg, 0.15 mmol, 66%) as a brown oil.

LCMS (High pH, ES⁺): $t_R = 1.23$ min, [M+H⁺] 295.2, (100% pure). ¹

¹H NMR (400 MHz, CDCl₃): δ 0.89 (t, $J = 7.3$ Hz, 3H), 1.31-1.55 (m, 2H), 2.28 (s, 3H), 3.26 (d, $J = 11.5$ Hz, 1H), 3.57 (dd, $J = 11.5, 4.9$ Hz, 1H), 4.50 (d, $J = 16.9$ Hz, 1H), 4.60 (d, $J = 16.9$ Hz, 1H), 5.00 (br s, 1H), 6.61-6.74 (m, 2H), 7.02 (s, 1H), 7.03 (t, $J = 7.3$ Hz, 1H), 7.12-7.40 (m, 5H).

1-(2-Ethyl-4-(3-methylbenzyl)-3,4-dihydroquinoxalin-1(2H)-yl)ethanone



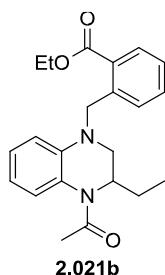
2.020b

Prepared from **2.018b** (45 mg, 0.22 mmol) and 3-methyl benzylbromide (60 μ L, 0.44 mmol) according to General Procedure 2. Purification of the crude product by High pH MDAP afforded 1-(2-ethyl-4-(3-methylbenzyl)-3,4-dihydroquinoxalin-1(2H)-yl)ethanone (43 mg, 0.15 mmol, 63%) as a brown oil.

LCMS (High pH, ES⁺): $t_R = 1.30$ min, [M+H⁺] 309.3, (100% pure). ¹H NMR (400 MHz, CDCl₃): δ 0.89 (t, $J = 7.3$ Hz, 3H), 1.33-1.51 (m, 2H), 2.28 (s, 3H), 2.34 (s,

3H), 3.26 (d, $J = 11.5$ Hz, 1H), 3.56 (dd, $J = 11.4, 4.8$ Hz, 1H), 4.46 (d, $J = 16.9$ Hz, 1H), 4.56 (d, $J = 16.9$ Hz, 1H), 4.99 (br s, 1H), 6.59-6.74 (m, 2H), 6.98-7.07 (m, 4H), 7.09 (d, $J = 7.6$ Hz, 1H), 7.23 (t, $J = 7.6$ Hz, 1H).

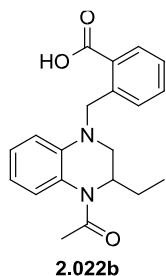
Ethyl 2-((4-acetyl-3-ethyl-3,4-dihydroquinoxalin-1(2H)-yl)methyl)benzoate



Prepared from **2.018b** (45 mg, 0.22 mmol) and ethyl 2-(bromomethyl)benzoate (0.096 mL, 0.552 mmol) according to General Procedure 2. Purification of the crude product by High pH MDAP afforded ethyl 2-((4-acetyl-3-ethyl-3,4-dihydroquinoxalin-1(2H)-yl)methyl)benzoate (30 mg, 0.082 mmol, 37%) as a yellow oil.

LCMS (High pH, ES⁺): $t_R = 1.29$ min, $[M+H]^+$ 367.3, (100% pure). ¹H NMR (400 MHz, CDCl₃): δ 0.93 (t, $J = 7.2$ Hz, 3H), 1.43 (t, $J = 7.2$ Hz, 3H), 1.47-1.57 (m, 2H), 2.30 (s, 3H), 3.25 (d, $J = 11.5$ Hz, 1H), 3.62 (dd, $J = 11.4, 4.3$ Hz, 1H), 4.40 (q, $J = 7.2$ Hz, 2H), 4.94 (dd, $J = 35.0, 18.6$ Hz, 2H), 5.02 (s, 1H), 6.48 (d, $J = 8.3$ Hz, 1H), 6.68 (t, $J = 7.2$ Hz, 1H), 6.99 (t, $J = 7.8$ Hz, 1H), 7.03 (br s, 1H), 7.26 (br s, 1H), 7.35 (t, $J = 7.2$ Hz, 1H), 7.46 (td, $J = 7.5, 1.3$ Hz, 1H), 8.07 (dd, $J = 7.8, 1.2$ Hz, 1H).

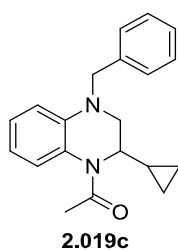
2-((4-Acetyl-3-ethyl-3,4-dihydroquinoxalin-1(2H)-yl)methyl)benzoic acid



A solution of **2.021b** (30 mg, 0.82 mmol) and LiOH·H₂O (20 mg, 0.82 mmol) in THF (0.82 mL), MeOH (0.41 mL) and H₂O (0.82 mL) was stirred at rt for 24 h. The reaction mixture was concentrated *in vacuo* and purified by Formic MDAP, followed by silica chromatography (0-10% 2 M NH₃ in MeOH/DCM). Appropriate fractions were evaporated *in vacuo* to afford 2-((4-acetyl-3-ethyl-3,4-dihydroquinoxalin-1(2H)-yl)methyl)benzoic acid (6 mg, 0.018 mmol, 22%) as a brown solid.

LCMS (Formic, ES⁺): $t_R = 0.98$ min, $[M+H]^+$ 339.3, (100% pure). ¹H NMR (400 MHz, CDCl₃): δ 0.92 (t, $J = 7.0$ Hz, 3H), 1.40-1.56 (m, 2H), 2.29 (s, 3H), 3.22 (d, $J = 11.2$ Hz, 1H), 3.61 (dd, $J = 10.0, 3.9$ Hz, 1H), 4.96 (dd, $J = 34.0, 19.1$ Hz, 2H), 5.035.08 (m, 1H), 6.47 (d, $J = 8.3$ Hz, 1H), 6.67 (t, $J = 7.3$ Hz, 1H), 6.92-7.06 (m, 2H), 7.24-7.32 (m, 1H), 7.35 (t, $J = 7.3$ Hz, 1H), 7.48 (t, $J = 7.3$ Hz, 1H), 8.14 (d, $J = 7.3$ Hz, 1H). Acid proton was not observed.

1-(4-Benzyl-2-cyclopropyl-3,4-dihydroquinoxalin-1(2H)-yl)ethanone



Prepared from **2.018c** (50 mg, 0.23 mmol) and benzyl bromide (55 μ L, 0.462 mmol) according to General Procedure 2. Purification of the crude product by High pH MDAP afforded 1-(4-benzyl-2-cyclopropyl-3,4-dihydroquinoxalin-1(2H)-yl)ethanone (56 mg, 0.18 mmol, 79%) as a yellow oil.

LCMS (High pH, ES⁺): t_R = 1.24 min, [M+H⁺] 307.1, (100% purity). ¹H NMR (400 MHz, CDCl₃): δ 0.30-0.42 (m, 1H), 0.42-0.57 (m, 3H), 0.87-0.97

(m, 1H), 2.28

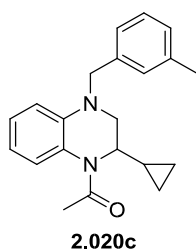
(s, 3H), 3.47 (dd, J = 11.1, 1.5 Hz, 1H), 3.60 (dd, J = 11.1, 4.6 Hz, 1H), 4.27 (br s, 1H), 4.59 (d, J = 3.9 Hz, 2H), 6.64-6.75 (m, 2H), 7.03 (td, J = 7.8, 1.5 Hz, 1H), 7.07-7.13 (m, 1H), 7.25-7.37 (m, 5H).

¹³

C NMR (101 MHz, CDCl₃): δ 4.0, 4.1, 12.5, 22.8, 52.0, 53.3, 54.4, 111.2, 115.7, 123.3, 125.6, 126.5, 126.5, 127.2, 128.7, 138.0, 139.1, 169.0. ν_{max} (neat): 2895, 2835, 1638, 1599, 1510, 1372, 1359, 1321, 1256, 1238, 1089, 1022, 964, 939, 910, 831, 750, 728, 693 cm⁻¹.

HRMS: (C₂₀H₂₂N₂O) [M+H⁺] requires 307.1805, found 307.1803.

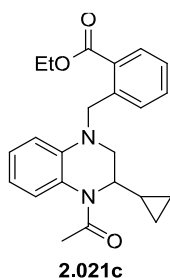
1-(2-Cyclopropyl-4-(3-methylbenzyl)-3,4-dihydroquinoxalin-1(2H)-yl)ethanone



Prepared from **2.018c** (50 mg, 0.23 mmol) and 3-methyl benzylbromide (62 μ L, 0.462 mmol) according to General Procedure 2. Purification of the crude product by High pH MDAP afforded 1-(2-cyclopropyl-4-(3-methylbenzyl)-3,4-dihydroquinoxalin-1(2H)-yl)ethanone (55 mg, 0.17 mmol, 74%) as a yellow oil.

LCMS (High pH, ES⁺): t_R = 1.31 min, [M+H⁺] 321.1, (89% pure). ¹H NMR (400 MHz, CDCl₃): δ 0.32-0.43 (m, 1H), 0.43-0.59 (m, 3H), 0.93 (br s, 1H), 2.28 (s, 3H), 2.34 (s, 3H), 3.47 (dd, J = 11.1, 1.5 Hz, 1H), 3.59 (dd, J = 11.1, 4.6 Hz, 1H), 4.27 (br s, 1H), 4.56 (d, J = 5.6 Hz, 2H), 6.63-6.73 (m, 2H), 7.01-7.13 (m, 5H), 7.17-7.30 (m, 1H).

Ethyl 2-((4-acetyl-3-cyclopropyl-3,4-dihydroquinoxalin-1(2H)-yl)methyl)benzoate



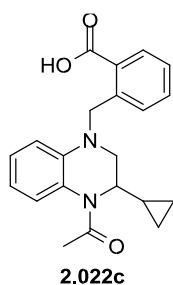
Prepared from **2.018c** (50 mg, 0.23 mmol) and ethyl 2(bromomethyl)benzoate (80 μ L, 0.462 mmol) according to General Procedure 2. The reaction was not complete after 40 h so further ethyl 2(bromomethyl)benzoate (98 μ L, 0.57 mmol) and potassium carbonate (118 mg, 0.85 mmol) were added and the reaction stirred at 100 °C for 20 h.

Purification of the crude product by High pH MDAP afforded ethyl 2-((4-acetyl-3-cyclopropyl-3,4-dihydroquinoxalin-1(2H)-yl)methyl)benzoate (36 mg, 0.095 mmol, 41%) as a yellow oil.

LCMS (High pH, ES⁺): t_R = 1.30 min, [M+H⁺] 379.2, (94% pure). ¹H NMR (400 MHz, CDCl₃): δ 0.32-0.43 (m, 1H), 0.43-0.63 (m, 3H), 0.97 (br s, 1H), 1.44 (t, J = 7.1 Hz, 3H), 2.30 (s, 3H), 3.45 (dd, J = 11.2, 1.0 Hz, 1H), 3.64 (dd, J = 11.2, 4.6 Hz, 1H), 4.30 (br s, 1H), 4.41 (q, J = 7.1 Hz, 2H), 4.99 (d, J = 10.3 Hz, 2H), 6.51 (d, J = 8.1 Hz, 1H),

6.69 (ddd, $J = 7.8, 7.8, 1.2$ Hz, 1H), 6.99 (ddd, $J = 8.1, 8.1, 1.2$ Hz, 1H), 7.11 (br s, 1H), 7.32-7.41 (m, 2H), 7.45 (ddd, $J = 8.1, 8.1, 1.2$ Hz, 1H), 8.08 (d, $J = 8.1$ Hz, 1H).

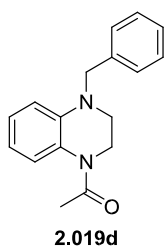
2-((4-Acetyl-3-cyclopropyl-3,4-dihydroquinoxalin-1(2H)-yl)methyl)benzoic acid



2.022c

A solution of **2.021c** (30 mg, 0.08 mmol) and LiOH.H₂O (57 mg, 2.38 mmol) in THF (1.3 mL), MeOH (1.3 mL) and H₂O (1.3 mL) was stirred at rt for 4 days. The reaction mixture was concentrated *in vacuo* and purified by Formic MDAP to afford 2-((4-acetyl-3-cyclopropyl-3,4-dihydroquinoxalin-1(2H)-yl)methyl)benzoic acid (11 mg, 0.031 mmol, 40%) as a brown solid. LCMS (Formic, ES⁺): $t_R = 1.01$ min, $[M+H]^+$ 351.3, (100% pure). ¹H NMR (400 MHz, CDCl₃): δ 0.32-0.46 (m, 1H), 0.46-0.64 (m, 3H), 0.98 (br s, 1H), 2.31 (s, 3H), 3.45 (dd, $J = 11.2, 1.2$ Hz, 1H), 3.66 (dd, $J = 11.2, 4.6$ Hz, 1H), 4.32 (br s, 1H), 5.01 (d, $J = 8.1$ Hz, 2H), 6.52 (dd, $J = 8.2, 1.1$ Hz, 1H), 6.71 (ddd, $J = 7.6, 7.6, 1.2$ Hz, 1H), 6.95-7.06 (m, 1H), 7.13 (br s, 1H), 7.35-7.47 (m, 2H), 7.51 (ddd, $J = 7.6, 7.6, 1.5$ Hz, 1H), 8.19 (dd, $J = 8.2, 1.3$ Hz, 1H). Acid proton was not observed.

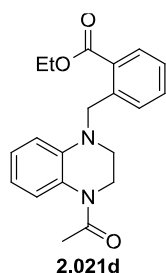
1-(4-Benzyl-3,4-dihydroquinoxalin-1(2H)-yl)ethanone



2.019d

Prepared from **2.018d** (50 mg, 0.28 mmol) and benzyl bromide (68 μ L, 0.567 mmol) according to General Procedure 2. Purification of the crude product by High pH MDAP afforded 1-(4-benzyl-3,4-dihydroquinoxalin-1(2H)-yl)ethanone (46 mg, 0.17 mmol, 61%) as a brown oil. LCMS (High pH, ES⁺): $t_R = 1.11$ min, $[M+H]^+$ 267.2, (100% pure). ¹H NMR (400 MHz, CDCl₃): δ 2.30 (s, 3H), 3.48 (t, $J = 5.4$ Hz, 2H), 3.98 (t, $J = 4.6$ Hz, 2H), 4.58 (s, 2H), 6.60-6.75 (m, 2H), 7.03 (t, $J = 7.7$ Hz, 1H), 7.07 (br. s, 1H), 7.24 (d, $J = 7.1$ Hz, 2H), 7.26-7.44 (m, 3H).

Ethyl 1-((4-acetyl-3,4-dihydroquinoxalin-1(2H)-yl)methyl)ethanone

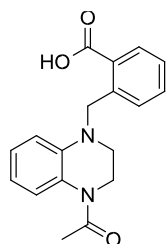


2.021d

Prepared from **2.018d** (50 mg, 0.28 mmol) and ethyl 2-(bromomethyl)benzoate (98 μ L, 0.57 mmol) according to General Procedure 2. Reaction was not complete after 40 h so further ethyl 2-(bromomethyl)benzoate (98 μ L, 0.57 mmol) and potassium carbonate (118 mg, 0.85 mmol) were added and the reaction stirred at 100 °C for 20 h. Purification by High pH MDAP afforded ethyl 1-((4-acetyl-3,4-dihydroquinoxalin-1(2H)-yl)methyl)ethanone (32 mg, 0.095 mmol, 33%) as a yellow oil. LCMS (High pH, ES⁺): $t_R = 1.18$ min, $[M+H]^+$ 339.0, (85% pure). ¹H NMR (400 MHz, CDCl₃): δ 1.44 (t, $J = 7.2$ Hz, 3H), 2.32 (s, 3H), 3.50 (t, $J = 5.4$ Hz, 2H), 4.02 (br s, 2H), 4.40 (q, $J = 7.2$ Hz, 2H), 4.96 (s, 2H), 6.50 (dd, $J = 8.3, 1.0$ Hz, 1H), 6.67 (td, $J = 7.6, 0.7$ Hz, 1H), 6.99 (td, $J = 7.8, 1.2$ Hz, 1H), 7.06 (br s, 1H), 7.24 (d, $J = 7.6$ Hz, 1H),

7.36 (td, $J = 7.5, 0.7$ Hz, 1H), 7.46 (td, $J = 7.6, 1.5$ Hz, 1H), 8.08 (dd, $J = 7.8, 1.2$ Hz, 1H).

2-((4-Acetyl-3,4-dihydroquinoxalin-1(2H)-yl)methyl)benzoic acid



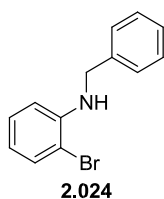
2.022d

A solution of **2.021d** (27 mg, 0.08 mmol) and LiOH.H₂O (38 mg, 1.60 mmol) in THF (0.5 mL), MeOH (0.3 mL) and H₂O (1 mL) was stirred at rt for 24 h. The reaction mixture was concentrated and purified by Formic MDAP to afford 2-((4-acetyl-3,4-dihydroquinoxalin-1(2H)-yl)methyl)benzoic acid (18 mg, 0.058 mmol, 73%).

LCMS (Formic, ES⁺): $t_R = 0.88$ min, [M+H⁺] 311.2, (100% pure).

¹H NMR (400 MHz, MeOD-*d*₄): δ 2.28 (s, 3H), 3.49 (br s, 2H), 3.98 (t, $J = 5.3$ Hz, 2H), 4.95 (s, 2H), 6.52 (d, $J = 8.3$ Hz, 1H), 6.65 (t, $J = 7.6$ Hz, 1H), 6.98 (br s, 1H), 7.15 (br s, 1H), 7.26 (d, $J = 7.6$ Hz, 1H), 7.36 (t, $J = 7.3$ Hz, 1H), 7.47 (td, $J = 7.6, 1.2$ Hz, 1H), 8.01 (dd, $J = 7.7, 1.3$ Hz, 1H). Acid proton was not observed.

N-Benzyl-2-bromoaniline



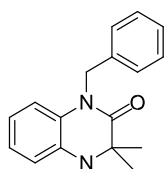
2.024

2-Bromoaniline **2.023** (1.00 g, 5.81 mmol) was dissolved in DCM (8 mL) at rt, then benzaldehyde (0.59 mL, 5.81 mmol) was added. The reaction mixture was stirred at rt for 2 h, then acetic acid (0.33 mL, 5.81 mmol) was added, followed by sodium triacetoxyborohydride (1.97 g, 9.30 mmol). The reaction mixture was stirred at rt for 16 h. The reaction mixture was diluted

with DCM (20 mL) and water (20 mL) and the aqueous layer was extracted with DCM (2 x 20 mL). The combined organics were dried, evaporated to dryness and purified by silica chromatography (0-30% EtOAc/cyclohexane). Collected fractions were combined and concentrated to give *N*-benzyl-2-bromoaniline (650 mg, 2.36 mmol, 41%) as a clear oil.

LCMS (High pH, ES⁺): $t_R = 1.33$ min, [M+MeCN]⁺ 303.2, (100% pure). ¹H NMR (400 MHz, CDCl₃): δ 4.43 (d, $J = 5.6$ Hz, 2H), 4.78 (br. s., 1H), 6.56-6.66 (m, 2H), 7.15 (ddd, $J = 7.7, 1.5$ Hz, 1H), 7.29-7.34 (m, 1H), 7.35-7.42 (m, 4H), 7.46 (dd, $J = 7.7, 1.5$ Hz, 1H). Analysis consistent with literature.³⁸²

1-Benzyl-3,3-dimethyl-1,2,3,4-tetrahydroquinoxalin-2(1H)-one



2.025

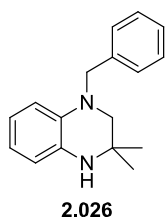
2-Amino-2-methylpropanoic acid (412 mg, 4.00 mmol), *N*-benzyl-2-bromoaniline **2.024** (524 mg, 2 mmol), copper(I) chloride (9.90 mg, 0.100 mmol), *N*1,*N*2-dimethylethane-1,2-diamine (43.1 μ L, 0.400 mmol) and potassium phosphate tribasic (849 mg, 4.00 mmol) were placed in an oven-dried microwave tube which was sealed and placed under N₂. Anhydrous, degassed DMSO (7 mL) was added by syringe and the reaction evacuated and placed under N₂ three times. The reaction mixture was heated to 110 °C in an oil bath for 40 h, then 130 °C

for 40 h. The reaction mixture was cooled, diluted with EtOAc (10 mL) and filtered through Celite. The filtrate was washed with water (2 x 5 mL) and the combined aqueous phases were extracted with CHCl₃ (2 x 10 mL). The combined organics were dried, evaporated, and the residue was purified by silica chromatography (0-40% EtOAc/cyclohexane) to afford 1-benzyl-3,3-dimethyl-3,4-dihydroquinoxalin-2(1*H*)-one (343 mg, 1.159 mmol, 58%) as an off-white oil which solidified on standing.

LCMS (High pH, ES⁺): $t_R = 1.09$ min, [M+H⁺] 267.1, (100% purity).

¹H NMR (400 MHz, CDCl₃): δ 1.46 (s, 6H), 3.77 (s, 1H), 5.15 (s, 2H), 6.66-6.74 (m, 2H), 6.80 (dd, $J = 8.1, 1.5$ Hz, 1H), 6.88 (ddd, $J = 7.5, 1.2$ Hz, 1H), 7.19-7.25 (m, 3H), 7.27-7.34 (m, 2H).

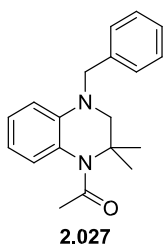
1-Benzyl-3,3-dimethyl-1,2,3,4-tetrahydroquinoxaline



To a solution of 1-benzyl-3,3-dimethyl-3,4-dihydroquinoxalin-2(1*H*)-one **2.025** (160 mg, 0.601 mmol) in THF (4 mL) stirred under N₂ at rt was added BH₃·THF (1.8 mL, 1.802 mmol, 1 M in THF) dropwise. The reaction mixture was heated to 50 °C for 4 h. The reaction mixture was cooled to rt, quenched with MeOH (1 mL) and 1 M HCl (1 mL) and stood overnight. The mixture was basified with 1 M NaOH and extracted with ethyl acetate (3 x 20 mL). The combined organics were dried, evaporated to dryness and the residue was purified by silica chromatography (0-40% EtOAc/cyclohexane) to afford 1-benzyl-3,3dimethyl-1,2,3,4-tetrahydroquinoxaline (123 mg, 0.439 mmol, 73%) as an off-white gum.

LCMS (High pH, ES⁺): $t_R = 1.03$ min, [M+H⁺] 253.1, (81% pure). ¹H NMR (400 MHz, CDCl₃): δ 1.30 (s, 6H), 3.11 (s, 2H), 4.52 (s, 2H), 6.56 (dd, $J = 7.3, 2.0$ Hz, 1H), 6.59-6.70 (m, 3H), 7.26-7.34 (m, 1H), 7.34-7.42 (m, 4H). NH not observed.

1-(4-Benzyl-2,2-dimethyl-3,4-dihydroquinoxalin-1(2*H*)-yl)ethanone

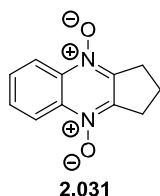


To a solution of 1-benzyl-3,3-dimethyl-1,2,3,4-tetrahydroquinoxaline **2.026** (120 mg, 0.476 mmol) and pyridine (77 μ L, 0.951 mmol) in DCM (4 mL) stirred under N₂ at rt was added acetyl chloride (51 μ L, 0.713 mmol). The reaction mixture was stirred at rt for 30 min. The reaction mixture was cooled to rt, quenched with sat. aq. NaHCO₃ (5 mL), extracted with DCM (3 x 15 mL) and the combined organics dried and evaporated to dryness. The residue was purified by silica chromatography (0-40% EtOAc/cyclohexane). Appropriate fractions were evaporated *in vacuo* to afford 1-(4-benzyl-2,2-dimethyl-3,4-dihydroquinoxalin-1(2*H*)-yl)ethanone (133 mg, 0.452 mmol, 95%) as a white solid

LCMS (High pH, ES⁺): $t_R = 1.27$ min, [M+H⁺] 295.1, (100% pure). ¹H NMR (400 MHz, CDCl₃): δ 1.56 (s, 6H), 2.16 (s, 3H), 2.87 (s, 2H), 4.31 (s, 2H), 6.74-6.80 (m, 1H), 6.78 (d, $J = 7.8$ Hz, 1H), 6.94 (dd, $J = 8.1, 1.3$ Hz, 1H), 7.05 (ddd, $J = 7.8, 1.5$ Hz, 1H), 7.29-7.35 (m, 1H), 7.36-7.41 (m, 4H). ¹³

C NMR (101 MHz, CDCl₃): δ 25.1, 26.2, 54.6, 61.1, 64.0, 111.9, 118.1, 125.1, 125.3, 127.4, 127.9, 128.6, 129.4, 137.6, 143.9, 171.5. M.pt.: 94-95 °C. ν_{\max} (neat): 3012, 2960, 2841, 2813, 1645, 1595, 1500, 1454, 1365, 1319, 1268, 1237, 1176, 1138, 1028, 914, 831, 794, 747, 702, 768 cm⁻¹.

HRMS: (C₁₉H₂₂N₂O) [M+H⁺] requires 295.1805, found [M+H⁺] 295.1786. **2,3-Dihydro-1H-cyclopenta[b]quinoxaline 4,9-dioxide**

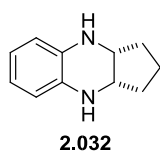


To a solution of benzofuroxan **2.029** (300 mg, 2.20 mmol) in MeOH (6 mL) stirred under N₂ at rt was added 4-(cyclopent-1-en-1-yl)morpholine **2.030** (0.35 mL, 2.20 mmol). A deep red colour developed. The reaction mixture was stirred at 50 °C for 5 min, then cooled to rt and evaporated *in vacuo*.

The residue was recrystallised from methanol to afford 2,3-dihydro-1H-cyclopenta[b]quinoxaline 4,9-dioxide **2.031** (170 mg, 0.84 mmol, 38%) as black crystals.

LCMS (Formic, ES⁺): t_R = 0.42 min, [M+H⁺] 203.2, (100% purity). ¹H NMR (400 MHz, CDCl₃): δ 2.38 (quin, *J* = 7.8 Hz, 2H), 3.42 (t, *J* = 7.7 Hz, 4H), 7.79-7.88 (m, 2H), 8.60-8.68 (m, 2H). ν_{\max} (neat): 3076, 2965, 1547, 1603, 1423, 1339, 1292, 1098, 1038, 870, 788, 697 cm⁻¹. M.pt. (EtOH): 159 °C (dec). Analysis consistent with literature.^{299,300}

Cis-2,3,3a,4,9,9a-Hexahydro-1H-cyclopenta[b]quinoxaline



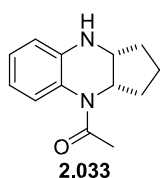
To a solution of 2,3-dihydro-1H-cyclopenta[b]quinoxaline 4,9-dioxide **2.031** (150 mg, 0.74 mmol) in MeOH (8 mL) stirred under N₂ at rt was added sodium borohydride (168 mg, 4.45 mmol) portionwise over 1 h. The reaction mixture became a deep red colour, with an exotherm and gas evolution

observed. The reaction mixture was stirred at rt for 3 h and the red colour faded to dark yellow. The reaction was quenched with water, concentrated *in vacuo* and partitioned between ethyl acetate (25 mL) and water (10 mL). The aqueous layer was extracted with ethyl acetate (2 x 20 mL) and the combined organics dried and evaporated to dryness. The residue was purified by silica chromatography (0-40% EtOAc/cyclohexane). Appropriate fractions were evaporated *in vacuo* to afford *cis*-2,3,3a,4,9,9a-hexahydro-1H-cyclopenta[b]quinoxaline **2.032** (110 mg, 0.63 mmol, 85%) as a white solid.

LCMS (High pH, ES⁺): t_R = 0.85 min, [M+H⁺] 175.2, (92% purity). ¹H NMR (400 MHz, CDCl₃): δ 1.59-1.72 (m, 3H), 1.83-2.02 (m, 3H), 3.56-3.62 (m, 2H), 3.66 (br. s., 2H), 6.50-6.56 (m, 2H), 6.57-6.63 (m, 2H).

ν_{\max} (neat): 3341, 2961, 2866, 1595, 1508, 1473, 1307, 1284, 1251, 732 cm⁻¹. M.pt.: 102-104 °C. Analysis consistent with literature.³⁰²

(±)-1-(*cis*-3,3a,9,9a-Tetrahydro-1H-cyclopenta[b]quinoxalin-4(2H)-yl)ethanone

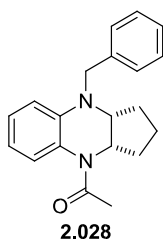


To a solution of *cis*-2,3,3a,4,9,9a-hexahydro-1*H*-cyclopenta[*b*]quinoxaline **2.032** (90 mg, 0.52 mmol) in DCM (4 mL) stirred under N₂ at 0 °C was added acetyl chloride (40 μL, 0.57 mmol) dropwise. The reaction mixture was stirred at 0 °C for 30 min. The reaction was warmed to rt and further acetyl chloride (40 μL, 0.57 mmol) was added. The reaction was stirred for 30 min,

then diluted with DCM (5 mL) and sat. aq. NaHCO₃ (5 mL). The aqueous layer was extracted with DCM (2 x 10 mL) and the combined organics were dried and evaporated to dryness.

The residue was purified by silica chromatography (0-100% EtOAc/cyclohexane), appropriate fractions were evaporated *in vacuo* to afford (±)-1-(*cis*-3,3a,9,9a-tetrahydro-1*H*-cyclopenta[*b*]quinoxalin-4(2*H*)-yl)ethanone **2.033** (22 mg, 0.10 mmol, 20%) as a yellow oil. LCMS (High pH, ES⁺): t_R = 0.82 min, [M+H⁺] 217.3, (100% pure). ¹H NMR (400 MHz, DMSO-*d*₆, 393K): δ 1.14-1.28 (m, 1H), 1.66 (d, *J* = 1.5 Hz, 3H), 1.83 (d, *J* = 7.1 Hz, 2H), 2.14 (s, 3H), 3.69-3.74 (m, 1H), 5.00 (td, *J* = 8.8, 6.7 Hz, 1H), 5.27 (br. s, 1H), 6.54 (ddd, *J* = 7.5, 1.5 Hz, 1H), 6.65 (dd, *J* = 8.0, 1.5 Hz, 1H), 6.89 (ddd, *J* = 8.1, 7.5, 1.4 Hz, 1H), 7.21 (dd, *J* = 7.5, 1.5 Hz, 1H).

(±)-1-(*cis*-9-Benzyl-3,3a,9,9a-tetrahydro-1*H*-cyclopenta[*b*]quinoxalin-4(2*H*)-yl)ethanone



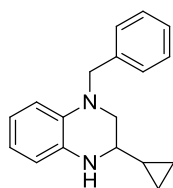
To a stirred solution of (±)-1-(*cis*-3,3a,9,9a-tetrahydro-1*H*-cyclopenta[*b*]quinoxalin-4(2*H*)-yl)ethanone **2.033** (20 mg, 0.092 mmol) and benzaldehyde (0.019 mL, 0.19 mmol) in DCM (2 mL) at rt under N₂ was added sodium triacetoxyborohydride (59 mg, 0.28 mmol). The mixture was stirred at rt for 80 h. Further benzaldehyde (0.019 mL, 0.19 mmol) and sodium triacetoxyborohydride (59 mg, 0.28 mmol) were added after 24 h. The

reaction was diluted with sat. aq. NaHCO₃ (2 mL) and DCM (2 mL), and the aqueous phase was extracted with DCM (2 x 10 mL). The combined organic phases were dried through a hydrophobic frit and evaporated *in vacuo*. The crude product was purified by High pH MDAP to afford (±)-1-(*cis*-9-benzyl-3,3a,9,9a-tetrahydro-1*H*-cyclopenta[*b*]quinoxalin-4(2*H*)-yl)ethanone **2.028** (20 mg, 0.07 mmol, 71%) as a brown gum. LCMS (High pH, ES⁺): t_R = 1.23 min, [M+H⁺] 307.3, (91% pure). ¹H NMR (400 MHz, CDCl₃): δ 1.25-1.47 (m, 3H), 1.51-1.64 (m, 1H), 1.68-1.83 (m, 1H), 1.94-2.08 (m, 1H), 2.19 (s, 3H), 3.85 (dt, *J* = 9.8, 6.4 Hz, 1H), 4.08 (d, *J* = 14.8 Hz, 1H), 4.51 (d, *J* = 14.8 Hz, 1H), 5.41-5.57 (m, 1H), 6.71 (d, *J* = 8.1 Hz, 1H), 6.81 (ddd, *J* = 7.6, 1.0 Hz, 1H), 7.01-7.05 (m, 1H), 7.09 (ddd, *J* = 7.6, 1.0 Hz, 1H), 7.25-7.38 (m, 5H). ¹³C NMR (101 MHz, CDCl₃): δ 22.5, 22.7, 28.7, 30.1, 52.4, 57.7, 63.5, 114.8, 118.3, 125.7, 126.8, 127.2, 127.7, 128.6, 129.1, 137.6, 142.8, 169.5.

*v*_{max} (neat): 3031, 2954, 2866, 1651, 1599, 1502, 1452, 1389, 1332, 1287, 1255, 1155, 1113, 1030, 984, 921, 842, 741, 700 cm⁻¹.

HRMS: (C₂₀H₂₂N₂O) [M+H⁺] requires 307.1805, found [M+H⁺] 307.1800.

1-Benzyl-3-cyclopropyl-1,2,3,4-tetrahydroquinoxaline



2.034

To a solution of 1-(4-benzyl-2-cyclopropyl-3,4-dihydroquinoxalin-1(2*H*))yl)ethanone **2.019c** (106 mg, 0.346 mmol) in MeOH (5 mL) was added conc. HCl (2 mL, 65.8 mmol). The reaction was heated to 65 °C for 5 h, then evaporated to afford 1-benzyl-3-cyclopropyl-1,2,3,4-

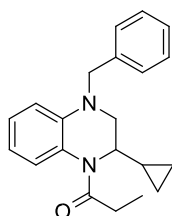
tetrahydroquinoxaline hydrochloride (106 mg, 0.338 mmol, 98%) as a white

solid.

LCMS (High pH, ES⁺): $t_R = 1.32$ min, $[M+H]^+$ 265.3, (93% purity). ¹

¹H NMR (400 MHz, MeOD-*d*₄): δ 0.47-0.58 (m, 1H), 0.67-0.88 (m, 3H), 0.99-1.12 (m, 1H), 3.06 (td, $J = 9.1, 3.3$ Hz, 1H), 3.60 (dd, $J = 13.0, 9.1$ Hz, 1H), 3.73 (dd, $J = 13.0, 3.3$ Hz, 1H), 4.66 (dd, $J = 44.5, 16.1$ Hz, 2H), 6.81 (t, $J = 7.6$ Hz, 1H), 6.94 (d, $J = 8.6$ Hz, 1H), 7.20-7.40 (m, 7H). Exchangeable protons were not observed.

1-(4-Benzyl-2-cyclopropyl-3,4-dihydroquinoxalin-1(2*H*))yl)propan-1-one



2.035

To a solution of 1-benzyl-3-cyclopropyl-1,2,3,4-tetrahydroquinoxaline hydrochloride **2.034** (25 mg, 0.083 mmol) and pyridine (0.020 mL, 0.249 mmol) in DCM (2 mL) was added propionyl chloride (11 μ L, 0.125 mmol). The reaction was stirred at rt under N₂ for 2 h, then diluted with water (2 mL) and DCM (5 mL) and extracted. The aqueous layer was extracted with

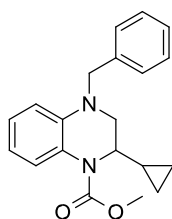
DCM (2 x 5 mL) and the combined organics were dried through a

hydrophobic frit, evaporated and purified by High pH MDAP. The solvent was evaporated *in vacuo* to afford 1-(4-benzyl-2-cyclopropyl-3,4-dihydroquinoxalin-1(2*H*))yl)propan-1-one (19 mg, 0.059 mmol, 71%).

LCMS (High pH, ES⁺): $t_R = 1.33$ min, $[M+H]^+$ 321.2, (100% purity). ¹H NMR (400 MHz, CDCl₃): δ 0.31-0.40 (m, 1H), 0.41-0.56 (m, 3H), 0.84-0.98 (m, 1H), 1.17 (t, $J = 7.5$ Hz, 3H), 2.44-2.57 (m, 1H), 2.59-2.74 (m, 1H), 3.46 (dd, $J = 11.2, 1.7$ Hz, 1H), 3.59 (dd, $J = 11.2, 4.6$ Hz, 1H), 4.17-4.35 (m, 1H), 4.59 (d, $J = 3.7$ Hz, 2H), 6.64-6.74 (m, 2H), 7.04 (ddd, $J = 8.5, 7.2, 1.7$ Hz, 1H), 7.12 (br. s., 1H), 7.23-7.39 (m, 5H).

HRMS: (C₂₁H₂₄N₂O) $[M+H]^+$ requires 321.1961, found $[M+H]^+$ 321.1970.

Methyl 4-benzyl-2-cyclopropyl-3,4-dihydroquinoxaline-1(2*H*)-carboxylate



2.036

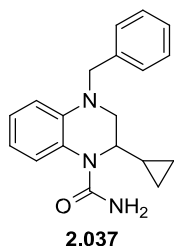
To a solution of 1-benzyl-3-cyclopropyl-1,2,3,4-tetrahydroquinoxaline hydrochloride **2.034** (25 mg, 0.083 mmol) and pyridine (0.020 mL, 0.249 mmol) in DCM (2 mL) was added methyl chloroformate (10 μ L, 0.125 mmol).

The reaction was stirred at rt under N₂ for 2 h, then diluted with water (2 mL) and DCM (5 mL) and extracted. The aqueous layer was extracted with DCM (2 x 5 mL) and the combined organics were dried

through a hydrophobic frit, evaporated and purified by High pH MDAP. The solvent was evaporated *in vacuo* to afford methyl 4-benzyl-2-cyclopropyl-3,4-dihydroquinoxaline-1(2*H*)carboxylate (18 mg, 0.056 mmol, 67%).

LCMS (High pH, ES⁺): $t_R = 1.35$ min, $[M+H]^+$ 323.2, (100% purity). ¹H NMR (400 MHz, CDCl₃): δ 0.33 (dd, $J = 4.8, 2.3$ Hz, 1H), 0.46-0.60 (m, 3H), 1.01-1.14 (m, 1H), 3.46 (dd, $J = 11.0, 1.8$ Hz, 1H), 3.63 (dd, $J = 11.0, 4.2$ Hz, 1H), 3.81 (s, 3H), 3.83-3.90 (m, 1H), 4.59 (d, $J = 1.2$ Hz, 2H), 6.65-6.75 (m, 2H), 6.97 (ddd, $J = 8.3, 7.2, 1.6$ Hz, 1H), 7.24-7.39 (m, 5H), 7.56 (d, $J = 8.3$ Hz, 1H).

HRMS: (C₂₀H₂₂N₂O₂) $[M+H]^+$ requires 323.1754, found $[M+H]^+$ 323.1764. **4-Benzyl-2-**

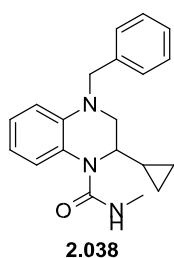


cyclopropyl-3,4-dihydroquinoxaline-1(2*H*)-carboxamide To a solution of 1-benzyl-3-cyclopropyl-1,2,3,4-tetrahydroquinoxaline hydrochloride **2.034** (25 mg, 0.083 mmol) and 1 M HCl (0.083 mL, 0.083 mmol) in water (0.5 mL) was added potassium cyanate (34 mg, 0.416 mmol). The reaction vessel was sealed and heated in a Biotage Initiator microwave reactor to 80 °C for 1 h. The reaction mixture was diluted with

EtOAc (5 mL) and water (2 mL) and extracted. The aqueous layer was extracted with EtOAc (2 x 10 mL) and the combined organics were dried through a hydrophobic frit and evaporated to dryness. The residue was purified by High pH MDAP. The solvent was evaporated to afford 4-benzyl-2-cyclopropyl-3,4-dihydroquinoxaline-1(2*H*)carboxamide (5 mg, 0.016 mmol, 20%).

LCMS (High pH, ES⁺): $t_R = 1.13$ min, $[M+H]^+$ 308.4, (100% purity). ¹H NMR (400 MHz, CDCl₃): δ 0.27-0.42 (m, 1H), 0.42-0.62 (m, 3H), 0.83-0.99 (m, 1H), 3.46 (dd, $J = 11.1, 1.3$ Hz, 1H), 3.62 (dd, $J = 11.2, 4.4$ Hz, 1H), 4.02 (dd, $J = 10.1, 3.3$ Hz, 1H), 4.60 (s, 2H), 5.03 (br. s., 2H), 6.61-6.78 (m, 2H), 7.01 (ddd, $J = 8.4, 7.2, 1.6$ Hz, 1H), 7.227.42 (m, 6H).

4-Benzyl-2-cyclopropyl-*N*-methyl-3,4-dihydroquinoxaline-1(2*H*)-carboxamide To a

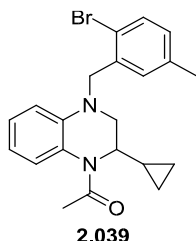


solution of 1-benzyl-3-cyclopropyl-1,2,3,4-tetrahydroquinoxaline hydrochloride **2.034** (29 mg, 0.096 mmol) and pyridine (0.023 mL, 0.289 mmol) in DCM (2 mL) was added 4-nitrophenyl carbonochloridate (29 mg, 0.145 mmol). The reaction was stirred at rt under N₂ for 2 h. DMAP (6 mg, 0.048 mmol), pyridine (0.023 mL, 0.289 mmol) and 4-nitrophenyl carbonochloridate (29 mg, 0.145 mmol) were added and the reaction

stirred for a further 3 days. The reaction mixture was diluted with water (2 mL) and DCM (5 mL) and extracted. The aqueous layer was extracted with DCM (2 x 5 mL) and the combined organics were dried through a hydrophobic frit, evaporated and purified by silica chromatography (0-100% EtOAc/cyclohexane). Appropriate fractions were evaporated *in vacuo* and the residue was dissolved in methanamine (2 mL, 4.00 mmol, 2 M in THF) and stirred at 50°C for 48 h. Every 8 h, further methanamine (2 mL, 4.00 mmol, 2 M in THF) was

added. The reaction mixture was evaporated to dryness and purified by High pH MDAP. The solvent was evaporated *in vacuo* to give 4-benzyl-2-cyclopropyl-*N*-methyl-3,4-dihydroquinoxaline-1(2*H*)-carboxamide (1.5 mg, 4.67 μ mol, 20%) as a yellow gum.

LCMS (High pH, ES⁺): t_R = 1.19 min, [(M-CONHMe)+H]⁺ 265.3, (100% pure). ¹H NMR (400 MHz, CDCl₃): δ 0.31-0.37 (m, 1H), 0.44-0.58 (m, 3H), 0.84-0.96 (m, 1H), 2.85 (d, J = 4.5 Hz, 3H), 3.44 (dd, J = 11.1, 1.3 Hz, 1H), 3.57 (dd, J = 11.1, 4.4 Hz, 1H), 4.01 (ddd, J = 10.0, 4.4, 1.3 Hz, 1H), 4.59 (s, 2H), 5.27 (q, J = 4.5 Hz, 1H), 6.65-6.73 (m, 2H), 6.99 (ddd, J = 7.7, 1.5 Hz, 1H), 7.21 (dd, J = 7.7, 1.3 Hz, 1H), 7.25-7.37 (m, 5H). **1-(4-(2-**



Bromo-5-methylbenzyl)-2-cyclopropyl-3,4-dihydroquinoxalin-1(2*H*)-yl)ethanone Prepared from **2.018c** (40 mg, 0.19 mmol) and 2-bromo-

5methylbenzaldehyde (74 mg, 0.370 mmol) according to General

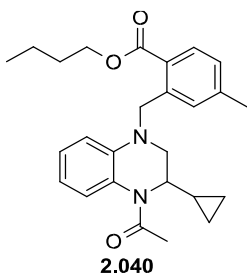
Procedure 1. The reaction was not complete after 18 h so further 2-bromo-5-methylbenzaldehyde (74 mg, 0.37 mmol) and sodium

triacetoxyborohydride (118 mg, 0.56 mmol) were added and the reaction was stirred at rt for 24 h. Purification of the crude product by silica

chromatography (0-40% EtOAc/cyclohexane) and High pH MDAP afforded 1-(4-(2-bromo-5-methylbenzyl)-2-cyclopropyl-3,4-dihydroquinoxalin-1(2*H*)-yl)ethanone (40 mg, 0.10 mmol, 54%) as an off-white gum.

LCMS (High pH, ES⁺): t_R = 1.43, [M+H⁺] 399.3, 401.3, (96% pure). ¹H NMR (400 MHz, CDCl₃): δ 0.37-0.45 (m, 1H), 0.46-0.60 (m, 3H), 0.90-1.05 (m, 1H), 2.22 (s, 3H), 2.30 (d, J = 1.0 Hz, 3H), 3.47 (td, J = 11.2, 1.3 Hz, 1H), 3.62 (dd, J = 11.2, 4.6 Hz, 1H), 4.23-4.37 (m, 1H), 4.56 (d, J = 4.4 Hz, 2H), 6.53 (d, J = 8.3 Hz, 1H), 6.67-6.75 (m, 1H), 6.95-7.00 (m, 1H), 7.01-7.07 (m, 2H), 7.08-7.16 (m, 1H), 7.49 (d, J = 8.1 Hz, 1H).

Butyl 2-((4-acetyl-3-cyclopropyl-3,4-dihydroquinoxalin-1(2*H*)-yl)methyl)-4-methylbenzoate

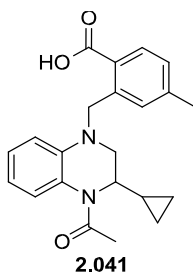


A mixture of **2.039** (36 mg, 0.09 mmol), DMAP (22 mg, 0.18 mmol), Herrmann's catalyst (4.2 mg, 0.0045 mmol), butan-1-ol (0.12 mL, 1.35 mmol), Mo(CO)₆ (12 mg, 0.05 mmol) and DIPEA (0.03 mL, 0.18 mmol) were sealed into a microwave vial and placed under N₂. 1,4Dioxane (1 mL) was added and the reaction was heated to 150 °C for

6 h in a Biotage Initiator microwave reactor. Further Herrmann's catalyst (4.2 mg, 0.0045 mmol) and Mo(CO)₆ (12 mg, 0.05 mmol) were added and the reaction was heated to 150 °C for 3 h. The reaction mixture was filtered through Celite and evaporated to dryness. The residue was purified by High pH MDAP to afford butyl 2-((4-acetyl-3-cyclopropyl-3,4-dihydroquinoxalin-1(2*H*)-yl)methyl)-4-methylbenzoate (10 mg, 0.023 mmol, 26%).

LCMS (High pH, ES⁺): t_R = 1.51 min, [M+H⁺] 421.5, (91% purity). ¹

¹H NMR (400 MHz, CDCl₃): δ 0.33-0.42 (m, 1H), 0.44-0.58 (m, 3H), 0.94 – 1.03 (m, 1H), 0.99 (t, *J* = 7.5 Hz, 3H), 1.42-1.56 (m, 2H), 1.71-1.81 (m, 2H), 2.27 (s, 3H), 2.29 (s, 3H), 3.43 (d, *J* = 11.2 Hz, 1H), 3.60 (dd, *J* = 11.2, 4.6 Hz, 1H), 4.23-4.31 (m, 1H), 4.31 (t, *J* = 6.6 Hz, 2H), 4.95 (s, 2H), 6.49 (dd, *J* = 7.8, 0.7 Hz, 1H), 6.67 (ddd, *J* = 7.0, 0.7 Hz, 1H), 6.98 (ddd, *J* = 7.8, 1.2 Hz, 1H), 7.08 (br s, 1H), 7.11-7.18 (m, 2H), 7.97 (d, *J* = 7.8 Hz, 1H). **2-((4-Acetyl-3-cyclopropyl-3,4-dihydroquinoxalin-1(2*H*)-yl)methyl)-4-methylbenzoic acid**



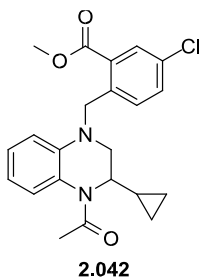
A solution of **2.040** (10 mg, 0.02 mmol) and LiOH·H₂O (29 mg, 1.19 mmol) in THF (1 mL), MeOH (1 mL) and H₂O (1 mL) was stirred at rt for 72 h. Further LiOH·H₂O (15 mg, 0.63 mmol) was added and the reaction stirred at rt for 72 h. The reaction mixture was evaporated and the residue partitioned between ethyl acetate (5 mL) and 2 M HCl (5 mL).

The aqueous layer was extracted with EtOAc (3 x 10 mL) and the combined organics dried and concentrated *in vacuo*. Purification by Formic MDAP afforded 2-((4-acetyl-3-cyclopropyl-3,4-dihydroquinoxalin-1(2*H*)-yl)methyl)-4-methylbenzoic acid (5 mg, 0.014 mmol, 58%) as a yellow solid.

LCMS (Formic, ES⁺): *t_R* = 1.07 min, [M+H⁺] 365.3, (87% purity). ¹H NMR (400 MHz, CDCl₃): δ 0.35-0.44 (m, 1H), 0.45-0.59 (m, 3H), 0.92-1.06 (m, 1H), 2.29 (s, 3H), 2.30 (s, 3H), 3.44 (dd, *J* = 11.2, 1.5 Hz, 1H), 3.61 (dd, *J* = 11.2, 4.6 Hz, 1H), 4.23-4.38 (m, 1H), 4.98 (d, *J* = 4.9 Hz, 2H), 6.50 (dd, *J* = 8.3, 1.5 Hz, 1H), 6.68 (ddd, *J* = 7.7, 7.7, 1.5 Hz, 1H), 7.00 (ddd, *J* = 7.7, 7.7, 1.5 Hz, 1H), 7.05-7.14 (m, 1H), 7.15-7.22 (m, 2H), 8.09 (d, *J* = 7.7 Hz, 1H). Acid proton was not observed.

HRMS: (C₂₂H₂₄N₂O₃) [M+H⁺] requires 365.1860, found 365.1855.

Methyl 2-((4-acetyl-3-cyclopropyl-3,4-dihydroquinoxalin-1(2*H*)-yl)methyl)-5-chlorobenzoate



Prepared from **2.018c** (40 mg, 0.19 mmol) and methyl 2-(bromomethyl)5-chlorobenzoate (97 mg, 0.370 mmol) according to General Procedure

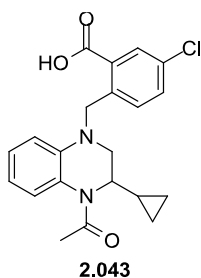
2. Reaction was not complete after 18 h so further methyl 2-(bromomethyl)-5-chlorobenzoate (97 mg, 0.37 mmol) and potassium carbonate (77 mg, 0.56 mmol) were added and the reaction stirred at 100 °C for 24 h. Purification of the crude product by silica chromatography (0-

50% EtOAc/cyclohexane) afforded methyl 2-((4-acetyl-3-cyclopropyl-3,4-dihydroquinoxalin-1(2*H*)-yl)methyl)-5-chlorobenzoate (36 mg, 0.09 mmol, 49%) as a yellow oil.

LCMS (High pH, ES⁺): *t_R* = 1.35, [M+H⁺] 399.3 (100% pure). ¹H NMR (400 MHz, CDCl₃): δ 0.32-0.43 (m, 1H), 0.44-0.61 (m, 3H), 0.89-1.01 (m, 1H), 2.30 (s, 3H), 3.42 (dd, *J* = 11.2, 1.5 Hz, 1H), 3.62 (dd, *J* = 11.2, 4.6 Hz, 1H), 3.95 (s, 3H), 4.30 (br s, 1H), 4.93 (d, *J* = 6.6 Hz, 2H),

6.45 (dd, $J = 8.4, 1.4$ Hz, 1H), 6.70 (td, $J = 7.6, 1.2$ Hz, 1H), 7.00 (td, $J = 7.6, 1.4$ Hz, 1H), 7.07-7.17 (m, 1H), 7.31 (d, $J = 8.4$ Hz, 1H), 7.42 (dd, $J = 8.4,$

2.4 Hz, 1H), 8.06 (d, $J = 2.4$ Hz, 1H). **2-((4-Acetyl-3-cyclopropyl-3,4-dihydroquinoxalin-**

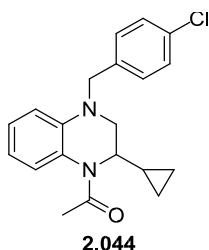


1(2H)-yl)methyl)-5-chlorobenzoate A solution of **2.042** (25 mg, 0.06 mmol) and LiOH.H₂O (15 mg, 0.63 mmol) in THF (1.5 mL), and H₂O (1.5 mL) was stirred at rt for 72 h. Further LiOH.H₂O (15 mg, 0.63 mmol) was added and the reaction stirred at rt for 72 h. The reaction mixture was concentrated and purified by Formic MDAP to afford 2-((4-acetyl-3-cyclopropyl-3,4-dihydroquinoxalin-1(2H)-yl)methyl)-5-

chlorobenzoate (17 mg, 0.044 mmol, 71%) as an off-white solid.

LCMS (Formic, ES⁺): $t_R = 1.12$ min, $[M+H]^+$ 385.3, (94% purity). ¹H NMR (400 MHz, CDCl₃): δ 0.33-0.45 (m, 1H), 0.46-0.61 (m, 3H), 0.96 (br s, 1H), 2.32 (s, 3H), 3.43 (dd, $J = 11.3, 1.2$ Hz, 1H), 3.65 (dd, $J = 11.3, 4.6$ Hz, 1H), 4.32 (br s, 1H), 4.96 (d, $J = 2.0$ Hz, 2H), 6.47 (dd, $J = 8.3, 1.2$ Hz, 1H), 6.72 (ddd, $J = 7.8, 7.8, 1.2$ Hz, 1H), 7.01 (ddd, $J = 7.8, 7.8, 1.5$ Hz, 1H), 7.12 (br s, 1H), 7.35 (d, $J = 8.3$ Hz, 1H), 7.47 (dd, $J = 8.4, 2.3$ Hz, 1H), 8.16 (d, $J = 2.4$ Hz, 1H). Acid proton was not observed.

1-(4-(4-Chlorobenzyl)-2-cyclopropyl-3,4-dihydroquinoxalin-1(2H)-yl)ethanone

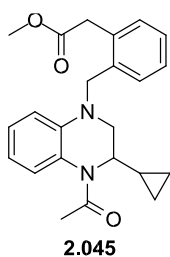


Prepared from **2.018c** (25 mg, 0.116 mmol) and 4-chlorobenzaldehyde (33 mg, 0.231 mmol) according to General Procedure 1. Purification of the crude product by High pH MDAP afforded 1-(4-(4-chlorobenzyl)-2-cyclopropyl-3,4-dihydroquinoxalin-1(2H)-yl)ethanone (14 mg, 0.041 mmol, 36%).

LCMS (High pH, ES⁺): $t_R = 1.32$ min, $[M+H]^+$ 341.2, (100% pure). ¹H NMR (400 MHz, CDCl₃): δ 0.31-0.55 (m, 4H), 0.81-0.96 (m, 1H), 2.27 (s, 3H), 3.44 (dd, $J = 11.1, 1.7$ Hz, 1H), 3.58 (dd, $J = 11.1, 4.6$ Hz, 1H), 4.18-4.34 (m, 1H), 4.55 (d, $J = 6.4$ Hz, 2H), 6.64 (dd, $J = 8.3, 1.3$ Hz, 1H), 6.70 (ddd, $J = 7.4, 1.3$ Hz, 1H), 7.03 (ddd, $J = 8.3, 7.4, 1.7$ Hz, 1H), 7.07-7.14 (m, 1H), 7.19-7.24 (m, 2H), 7.29-7.33 (m, 2H).

HRMS: (C₂₀H₂₁ClN₂O) $[M+H]^+$ requires 341.1415, found $[M+H]^+$ 341.1415.

Methyl 2-(2-((4-acetyl-3-cyclopropyl-3,4-dihydroquinoxalin-1(2H)-yl)methyl)phenyl)acetate



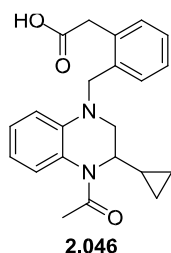
Prepared from **2.018c** (40 mg, 0.19 mmol) and methyl 2-(2-formylphenyl)acetate (85 μ L, 0.555 mmol) according to General Procedure 1. The reaction was not complete after 24 h so further methyl 2-(2-formylphenyl)acetate (85 μ L, 0.555 mmol) was added and the reaction stirred at rt for 24 h. Purification of the crude product by silica chromatography (0-50% EtOAc/cyclohexane) and High pH MDAP afforded

methyl 2-(2-((4-acetyl-3-cyclopropyl-3,4-dihydroquinoxalin-1(2*H*)-yl)methyl)phenyl)acetate (51 mg, 0.14 mmol, 73%) as a yellow oil.

LCMS (High pH, ES⁺): t_R = 1.19, [M+H⁺] 379.3 (100% pure).

¹H NMR (400 MHz, CDCl₃): δ 0.31-0.42 (m, 1H), 0.43-0.58 (m, 3H), 0.88-1.03 (m, 1H), 2.28 (s, 3H), 3.41 (dd, *J* = 11.1, 1.7 Hz, 1H), 3.56 (dd, *J* = 11.1, 4.8 Hz, 1H), 3.73 (d, *J* = 1.5 Hz, 2H), 3.74 (s, 3H), 4.28 (br s, 1H), 4.61 (s, 2H), 6.59 (dd, *J* = 8.2, 1.3 Hz, 1H), 6.70 (ddd, *J* = 7.6, 7.6, 1.3 Hz, 1H), 7.03 (ddd, *J* = 7.8, 7.8, 1.6 Hz, 1H), 7.06-7.15 (m, 1H), 7.21-7.31 (m, 4H).

2-(2-((4-Acetyl-3-cyclopropyl-3,4-dihydroquinoxalin-1(2*H*)-yl)methyl)phenyl)acetic acid



A solution of **2.045** (40 mg, 0.11 mmol) and LiOH·H₂O (25 mg, 1.06 mmol) in THF (2.5 mL) and H₂O (2.5 mL) was stirred at rt for 24 h. The reaction mixture was concentrated *in vacuo* and the residue partitioned between ethyl acetate (25 mL) and 2 M HCl (10 mL). The aqueous layer was extracted with EtOAc (3 x 20 mL) and the combined organics were dried and concentrated *in vacuo*.

Purification by Formic MDAP afforded 2-(2-((4-

acetyl-3-cyclopropyl-3,4-dihydroquinoxalin-1(2*H*)-yl)methyl)phenyl)acetic acid (32 mg, 0.09 mmol, 83%) as a yellow oil.

LCMS (Formic, ES⁺): t_R = 1.00 min, [M+H⁺] 365.3 (100% purity). ¹H NMR (400 MHz, CDCl₃): δ 0.28-0.37 (m, 1H), 0.40-0.56 (m, 3H), 0.86-0.97 (m, 1H), 2.28 (s, 3H), 3.32 (dd, *J* = 11.0, 2.0 Hz, 1H), 3.52 (dd, *J* = 11.0, 5.3 Hz, 1H), 3.72 (d, *J* = 1.5 Hz, 2H), 4.28 (br s, 1H), 4.52 (d, *J* = 16.5 Hz, 1H), 4.64 (d, *J* = 16.5 Hz, 1H), 6.64 (d, *J* = 8.2 Hz, 1H), 6.71 (ddd, *J* = 7.4, 7.4, 1.0 Hz, 1H), 7.04 (ddd, *J* = 8.2, 7.4, 1.6 Hz, 1H), 7.07-7.15 (m, 1H), 7.20-7.32 (m, 4H). Acid proton was not observed.

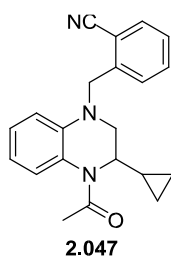
¹³

C NMR (101 MHz, CDCl₃): δ 3.9, 4.1, 12.8, 22.7, 38.2, 52.6, 52.8, 53.3, 111.6, 116.4, 123.8, 125.6, 126.8, 126.9, 127.6, 127.9, 131.3, 132.0, 135.8, 139.7, 169.8, 175.2. M. pt.: 157-160 °C.

ν_{max} (neat): 3005, 1724, 1600, 1514, 1392, 1343, 1323, 1247, 1168, 1085, 910, 732 cm⁻¹.

HRMS: (C₂₂H₂₄N₂O₃) [M+H⁺] requires 365.1860, found [M+H⁺] 365.1860.

2-((4-Acetyl-3-cyclopropyl-3,4-dihydroquinoxalin-1(2*H*)-yl)methyl)benzonitrile



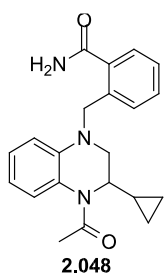
Prepared from **2.018c** (44 mg, 0.20 mmol) and 2-(bromomethyl)benzonitrile (80 mg, 0.407 mmol) according to General Procedure 2. Purification of the crude product by High pH MDAP afforded 2-((4-acetyl-3-cyclopropyl-3,4-dihydroquinoxalin-1(2*H*)-yl)methyl)benzonitrile (56 mg, 0.17 mmol, 83%) as a light yellow solid.

LCMS (High pH, ES⁺): t_R = 1.15 min, [M+H⁺] 332.3 (100% pure).

1

¹H NMR (400 MHz, CDCl₃): δ 0.30-0.58 (m, 4H), 0.83-0.99 (m, 1H), 2.28 (s, 3H), 3.45 (dd, *J* = 11.1, 1.6 Hz, 1H), 3.65 (dd, *J* = 11.1, 4.8 Hz, 1H), 4.18-4.38 (m, 1H), 4.80 (d, *J* = 12.7 Hz, 2H), 6.56 (dd, *J* = 8.1, 1.2 Hz, 1H), 6.73 (ddd, *J* = 8.1, 8.1, 1.2 Hz, 1H), 7.03 (ddd, *J* = 7.9, 7.9, 1.2 Hz, 1H), 7.07-7.19 (m, 1H), 7.36-7.42 (m, 1H), 7.36-7.40 (m, 1H), 7.53 (td, *J* = 7.9, 1.5 Hz, 1H), 7.68-7.76 (m, 1H).
HRMS: (C₂₁H₂₁N₃O) [M+H⁺] requires 332.1757, found [M+H⁺] 332.1746.

2-((4-Acetyl-3-cyclopropyl-3,4-dihydroquinoxalin-1(2*H*)-yl)methyl)benzamide



Prepared from **2.047** (27 mg, 0.08 mmol) according to General Procedure 4. Purification of the crude product by High pH MDAP afforded 2-((4-acetyl-3-cyclopropyl-3,4-dihydroquinoxalin-1(2*H*)-yl)methyl)benzamide (22 mg, 0.06 mmol, 77%) as a yellow solid.

LCMS (High pH, ES⁺): *t*_R = 0.91 min, [M+H⁺] 350.3 (100% pure). ¹

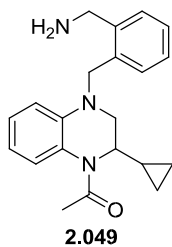
¹H NMR (400 MHz, CDCl₃): δ 0.30-0.39 (m, 1H), 0.41-0.57 (m, 3H), 0.84-0.97 (m, 1H), 2.27 (s, 3H), 3.39 (dd, *J* = 11.1, 1.8 Hz, 1H), 3.57 (dd, *J* = 11.1, 4.9 Hz, 1H), 4.18-4.33 (m, 1H), 4.85 (d, *J* = 4.0 Hz, 2H), 5.92-6.07 (m, 1H), 6.08-6.26 (m, 1H), 6.64 (dd, *J* = 8.0, 1.3 Hz, 1H), 6.70 (ddd, *J* = 7.6, 7.6, 1.3 Hz, 1H), 7.01 (td, *J* = 8.0, 1.6 Hz, 1H), 7.07-7.17 (m, 1H), 7.30-7.44 (m, 3H), 7.59 (dd, *J* = 7.6, 1.5 Hz, 1H).

¹³C NMR (101 MHz, CDCl₃): δ 4.0, 4.1, 12.6, 22.8, 52.1, 53.0, 53.5, 111.5, 116.2, 123.6, 125.6, 126.6, 127.2, 127.3, 127.7, 131.0, 133.8, 137.2, 139.1, 169.0, 171.1. M.pt.: 194-196 °C.

*v*_{max} (neat): 3338, 3188, 1626, 1513, 1383, 1322, 1256, 1086, 909, 733 cm⁻¹.

HRMS: (C₂₁H₂₃N₃O₂) [M+H⁺] requires 350.1863, found 350.1853.

1-(4-(2-(Aminomethyl)benzyl)-2-cyclopropyl-3,4-dihydroquinoxalin-1(2*H*)-yl)ethanone

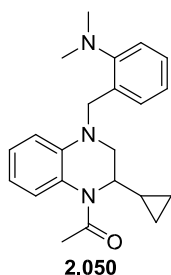


A solution of **2.047** (40 mg, 0.12 mmol) in EtOH (10 mL) was hydrogenated over Raney Ni using a H-CubeTM hydrogenation flow reactor (Raney Ni CatCart 30, 50 °C, 50 bar, 1 mL/min flow rate, 2H). The reaction was concentrated and purified by ion exchange chromatography (1 g SCX cartridge, MeOH/2 M NH₃ in MeOH) followed by High pH MDAP to afford 1-(4-(2-(aminomethyl)benzyl)-2-cyclopropyl-3,4-dihydroquinoxalin-1(2*H*)-yl)ethanone (13 mg, 0.04 mmol, 32%) as a yellow solid. LCMS

(High pH, ES⁺): *t*_R = 0.95 min, [M+H⁺] 336.3 (100% pure). ¹

¹H NMR (400 MHz, DMSO-*d*₆): δ 0.24-0.53 (m, 4H), 0.78-0.91 (m, 1H), 2.16 (s, 3H), 3.34-3.41 (m, 1H), 3.42-3.52 (m, 1H), 3.79 (s, 2H), 4.01-4.21 (m, 1H), 4.68 (dd, *J* = 34.0, 17.4 Hz, 2H), 6.53-6.63 (m, 2H), 6.86-6.97 (m, 1H), 7.09 (dd, *J* = 7.5, 1.5 Hz, 1H), 7.14 (td, *J* = 7.5, 1.5 Hz, 1H), 7.17-7.29 (m, 2H), 7.42 (dd, *J* = 7.5, 1.5 Hz, 1H). Amine protons were not observed.

HRMS: (C₂₁H₂₅N₃O) [M+H⁺] requires 336.2070, found 336.2072. **1-(2-Cyclopropyl-4-(2-(dimethylamino)benzyl)-3,4-dihydroquinoxalin-1(2H)-yl)ethanone**

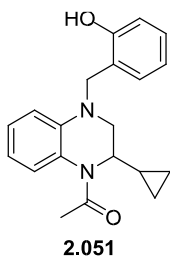


Prepared from **2.018c** (25 mg, 0.11 mmol) and 2-(dimethylamino)benzaldehyde (35 mg, 0.23 mmol) according to General Procedure 1. Purification of the crude product by High pH MDAP afforded 1-(2-cyclopropyl-4-(2-(dimethylamino)benzyl)-3,4-dihydroquinoxalin-1(2H)-yl)ethanone (30 mg, 0.09 mmol, 74%).

LCMS (High pH, ES⁺): t_R = 1.33 min, [M+H⁺] 350.4 (100% pure). ¹H NMR (400 MHz, CDCl₃): δ 0.32-0.57 (m, 4H), 0.88-1.00 (m, 1H), 2.28 (s, 3H), 2.76 (s, 6H), 3.47 (dd, J = 11.2, 1.2 Hz, 1H), 3.63 (dd, J = 11.2, 4.6 Hz, 1H), 4.20-4.34 (m, 1H), 4.64 (d, J = 10.0 Hz, 2H), 6.62 (dd, J = 8.3, 0.7 Hz, 1H), 6.67 (s, 1H), 6.96-7.04 (m, 2H), 7.04-7.12 (m, 1H), 7.18 (dd, J = 8.3, 1.5 Hz, 1H), 7.22-7.29 (m, 2H).

HRMS: (C₂₂H₂₇N₃O) [M+H⁺] requires 350.2227, found 350.2233.

1-(2-Cyclopropyl-4-(2-hydroxybenzyl)-3,4-dihydroquinoxalin-1(2H)-yl)ethanone

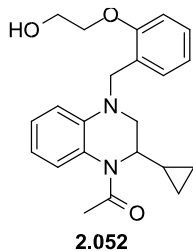


Prepared from **2.018c** (30 mg, 0.14 mmol) and 2-hydroxybenzaldehyde (0.03 mL, 0.28 mmol) according to General Procedure 1. Further 2-hydroxybenzaldehyde (0.03 mL, 0.28 mmol) and sodium triacetoxyborohydride (88 mg, 0.42 mmol) were added after 24 and 48 h and the reaction stirred at rt for a further 24 h. Purification of the crude product by High pH MDAP afforded 1-(2-cyclopropyl-4-(2-hydroxybenzyl)-3,4-

dihydroquinoxalin-1(2H)-yl)ethanone (23 mg, 0.07 mmol, 51%) as a white solid.

LCMS (High pH, ES⁺): t_R = 1.08 min, [M+H⁺] 323.3 (100% pure). ¹H NMR (400 MHz, CDCl₃): δ 0.28-0.37 (m, 1H), 0.39-0.58 (m, 3H), 0.79-0.93 (m, 1H), 2.27 (s, 3H), 3.28 (dd, J = 11.1, 2.9 Hz, 1H), 3.48 (dd, J = 11.1, 5.6 Hz, 1H), 4.23-4.41 (m, 1H), 4.56 (s, 2H), 6.81-6.96 (m, 4H), 7.05-7.25 (m, 4H), 7.32-7.51 (m, 1H).

1-(2-Cyclopropyl-4-(2-(2-hydroxyethoxy)benzyl)-3,4-dihydroquinoxalin-1(2H)-yl)ethanone



A solution of **2.051** (23 mg, 0.07 mmol) and K₂CO₃ (30 mg, 0.21 mmol) in DMF (1 mL) was treated with 2-bromoethanol (15 μL, 0.21 mmol) and stirred under N₂ at 110 °C for 20 h. The reaction mixture was cooled, diluted with MeOH and filtered. The filtrate was purified by High pH MDAP to afford 1-(2-cyclopropyl-4-(2-(2-hydroxyethoxy)benzyl)-3,4-dihydroquinoxalin-1(2H)-yl)ethanone (13 mg, 0.04 mmol, 50%) as a

beige solid.

LCMS (High pH, ES⁺): t_R = 1.07 min, [M+H⁺] 367.3 (90% purity). ¹H NMR (400 MHz, CDCl₃): δ 0.28-0.39 (m, 1H), 0.40-0.55 (m, 3H), 0.84-0.97 (m, 1H), 2.27 (s, 3H), 3.42 (dd, J = 11.2, 1.5 Hz, 1H), 3.53 (dd, J = 11.2, 4.6 Hz, 1H), 3.91-4.00 (m, 2H),

4.13 (dd, $J = 5.1, 3.9$ Hz, 2H), 4.19-4.32 (m, 1H), 4.61 (dd, $J = 43.8, 17.1$ Hz, 2H), 6.65-6.73 (m, 2H), 6.89-6.95 (m, 2H), 7.00-7.13 (m, 2H), 7.18 (dd, $J = 7.7, 1.8$ Hz, 1H), 7.23-7.30 (m, 1H). Alcohol proton not observed.

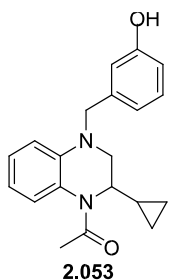
¹³

C NMR (101 MHz, CDCl₃): δ 4.0, 4.1, 12.5, 22.8, 50.0, 51.9, 52.8, 61.5, 69.4, 111.1, 111.3, 115.5, 120.9, 123.2, 125.5, 125.7, 126.5, 127.6, 128.3, 139.1, 156.5, 169.1.

ν_{\max} (neat): 3397, 2928, 1625, 1600, 1513, 1452, 1384, 1341, 1322, 1240, 1089, 1048, 918, 749 cm⁻¹.

HRMS: (C₂₂H₂₆N₂O₃) [M+H⁺] requires 367.2016, found 367.2011.

1-(2-Cyclopropyl-4-(3-hydroxybenzyl)-3,4-dihydroquinoxalin-1(2H)-yl)ethanone

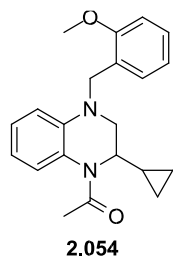


Prepared from **2.018c** (25 mg, 0.11 mmol) and 2-hydroxybenzaldehyde (25 μ L, 0.23 mmol) according to General Procedure 1. Purification of the crude product by High pH MDAP afforded 1-(2-cyclopropyl-4-(3-hydroxybenzyl)-3,4-dihydroquinoxalin-1(2H)-yl)ethanone (8 mg, 0.02 mmol, 21%).

LCMS (High pH, ES⁺): $t_R = 1.05$ min, [M+H⁺] 323.3 (100% pure). ¹

¹H NMR (400 MHz, CDCl₃): δ 0.27-0.39 (m, 1H), 0.41-0.58 (m, 3H), 0.78-1.03 (m, 1H), 2.27 (s, 3H), 3.45 (dd, $J = 11.2, 1.7$ Hz, 1H), 3.58 (dd, $J = 11.2, 4.6$ Hz, 1H), 4.14-4.36 (m, 1H), 4.53 (s, 2H), 5.57-5.98 (m, 1H), 6.65-6.71 (m, 2H), 6.73-6.79 (m, 1H), 6.76-6.79 (m, 1H), 6.83 (dd, $J = 7.7, 1.1$ Hz, 1H), 7.04 (td, $J = 7.8, 1.5$ Hz, 1H), 7.06-7.12 (m, 1H), 7.20 (t, $J = 7.7$ Hz, 1H).

1-(2-Cyclopropyl-4-(2-methoxybenzyl)-3,4-dihydroquinoxalin-1(2H)-yl)ethanone



Prepared from **2.018c** (25 mg, 0.11 mmol) and 2-methoxybenzaldehyde (28 μ L, 0.23 mmol) according to General Procedure 1. Purification of the crude product by High pH MDAP afforded 1-(2-cyclopropyl-4-(2-methoxybenzyl)-3,4-dihydroquinoxalin-1(2H)-yl)ethanone (33 mg, 0.10 mmol, 85%).

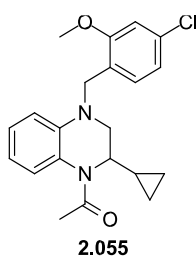
LCMS (High pH, ES⁺): $t_R = 1.27$ min, [M+H⁺] 337.3 (100% pure). ¹

¹H NMR (400 MHz, CDCl₃): δ 0.32-0.59 (m, 4H), 0.88-1.04 (m, 1H), 2.29 (s, 3H), 3.48 (dd, $J = 11.3, 1.5$ Hz, 1H), 3.62 (dd, $J = 11.3, 4.6$ Hz, 1H), 3.90 (s, 3H), 4.22-4.36 (m, 1H), 4.58 (d, $J = 7.6$ Hz, 2H), 6.62 (dd, $J = 8.3, 1.5$ Hz, 1H), 6.67 (ddd, $J = 7.6, 7.6, 1.2$ Hz, 1H), 6.89 (ddd, $J = 7.4, 7.4, 0.9$ Hz, 1H), 6.93 (dd, $J = 8.1, 1.0$ Hz, 1H), 7.01 (ddd, $J = 8.4, 7.2, 1.5$ Hz, 1H), 7.05-7.12 (m, 1H), 7.14-7.19 (m, 1H), 7.24-7.30 (m, 1H).

¹³

C NMR (101 MHz CDCl₃): δ 4.0, 4.1, 12.5, 22.9, 49.9, 51.9, 53.3, 55.2, 110.1, 111.2, 115.4, 120.5, 123.0, 125.4, 125.5, 126.5, 126.6, 128.0, 139.2, 157.2, 169.0. M. pt.: 125-126 °C ν_{\max} (neat): 2837, 1650, 1601, 1512, 1490, 1461, 1376, 1320, 1238, 1088, 1027, 745 cm⁻¹.

HRMS: (C₂₁H₂₄N₂O₂) [M+H⁺] requires 337.1911, found 337.1915 **1-(4-(4-Chloro-2-methoxybenzyl)-2-cyclopropyl-3,4-dihydroquinoxalin-1(2H)yl)ethanone**

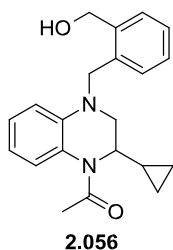


Prepared from **2.018c** (25 mg, 0.11 mmol) and 4-chloro-2-methoxybenzaldehyde (24 mg, 0.23 mmol) according to General Procedure 1. Purification of the crude product by High pH MDAP afforded 1-(4-(4-chloro-2-methoxybenzyl)-2-cyclopropyl-3,4-dihydroquinoxalin-1(2H)yl)ethanone (18 mg, 0.049 mmol, 70%)

LCMS (High pH, ES⁺): t_R = 1.35 min, [M+H⁺] 371.2, (100% pure). ¹H NMR (400 MHz, CDCl₃): δ 0.33-0.58 (m, 4H), 0.85-0.99 (m, 1H), 2.28 (s, 3H), 3.43 (dd, *J* = 11.2, 1.5 Hz, 1H), 3.59 (dd, *J* = 11.2, 4.6 Hz, 1H), 3.88 (s, 3H), 4.21-4.35 (m, 1H), 4.51 (d, *J* = 4.9 Hz, 2H), 6.56 (dd, *J* = 8.3, 1.2 Hz, 1H), 6.63-6.71 (m, 1H), 6.84-6.89 (m, 1H), 6.91 (d, *J* = 2.0 Hz, 1H), 6.98-7.14 (m, 3H).

HRMS: (C₂₁H₂₃ClN₂O₂) [M+H⁺] requires 371.1521, found [M+H⁺] 371.1521.

1-(2-Cyclopropyl-4-(2-(hydroxymethyl)benzyl)-3,4-dihydroquinoxalin-1(2H)yl)ethanone



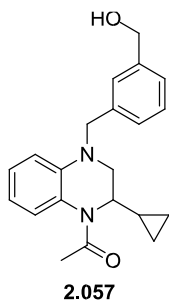
Prepared from **2.018c** (25 mg, 0.12 mmol) and (2-(bromomethyl)phenyl)methanol (47 mg, 0.231 mmol) according to General Procedure 2. Purification of the crude product by High pH MDAP afforded

1-(2-cyclopropyl-4-(2-(hydroxymethyl)benzyl)-3,4-dihydroquinoxalin-1(2H)yl)ethanone (33 mg, 0.10 mmol, 85%) as a light yellow solid. LCMS (High pH, ES⁺): t_R = 1.02 min, [M+H⁺] 337.2, (98% pure). ¹H NMR (400 MHz, CDCl₃): δ 0.30-0.38 (m, 1H), 0.41-0.64 (m, 3H), 0.83-1.05 (m, 1H), 2.26 (s, 3H), 3.37 (dd, *J* = 11.2, 1.2 Hz, 1H), 3.53 (dd, *J* = 11.2, 4.9 Hz, 1H), 4.07-4.40 (m, 1H), 4.68 (s, 2H), 4.76 (s, 2H), 6.64 (d, *J* = 8.2 Hz, 1H), 6.72 (t, *J* = 7.5 Hz, 1H), 7.03 (ddd, *J* = 8.2, 6.4, 1.2 Hz, 1H), 7.11 (br s, 1H), 7.21-7.37 (m, 3H), 7.43 (d, *J* = 7.1 Hz, 1H). Alcohol proton not observed.

HRMS: (C₂₁H₂₄N₂O₂) [M+H⁺] requires 337.1911, found 337.1907.

The racemic mixture (**±**)-**2.056** (25 mg, 0.07 mmol) was separated into individual enantiomers by chiral HPLC (15% EtOH/Heptane, f=25ml/min, 30mm x 25cm Chiralcel ODH), affording the individual isomers **2.056a** (1st eluting isomer, 11 mg, 0.03 mmol, 98%*ee*, 100% LC purity) and **2.056b** (2nd eluting isomer, 9 mg, 0.03 mmol, 99%*ee*, 100% LC purity).

1-(2-Cyclopropyl-4-(3-(hydroxymethyl)benzyl)-3,4-dihydroquinoxalin-1(2H)-yl)ethanone

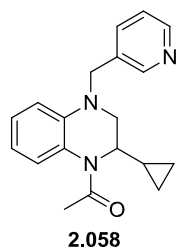


Prepared from **2.018c** (20 mg, 0.09 mmol) and (3-(bromomethyl)phenyl)methanol (56 mg, 0.277 mmol) according to General Procedure 2. Purification of the crude product by High pH MDAP afforded 1-(2-cyclopropyl-4-(3-(hydroxymethyl)benzyl)-3,4-dihydroquinoxalin-1(2H)-yl)ethanone (13 mg, 0.04 mmol, 42%) as a light yellow solid.

LCMS (High pH, ES⁺): t_R = 1.01 min, [M+H⁺] 337.3 (100% pure). ¹H NMR (400 MHz, CDCl₃): δ 0.30-0.40 (m, 1H), 0.41-0.59 (m, 3H), 0.84-1.00 (m, 1H), 2.27 (s, 3H), 3.47 (dd, J = 11.2, 1.5 Hz, 1H), 3.59 (dd, J = 11.2, 4.6 Hz, 1H), 4.20-4.32 (m, 1H), 4.59 (s, 2H), 4.68 (s, 2H), 6.65-6.72 (m, 1H), 6.68 (d, J = 7.7 Hz, 1H), 7.03 (td, J = 7.7, 1.6 Hz, 1H), 7.06-7.14 (m, 1H), 7.19-7.23 (m, 1H), 7.26-7.37 (m, 3H). Alcohol proton was not observed.

HRMS: (C₂₁H₂₄N₂O₂) [M+H⁺] requires 337.1911, found 337.1900.

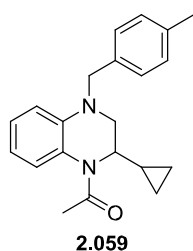
1-(2-Cyclopropyl-4-(pyridin-3-ylmethyl)-3,4-dihydroquinoxalin-1(2H)-yl)ethanone



Prepared from **2.018c** (50 mg, 0.23 mmol) and 3-(bromomethyl)pyridine hydrobromide (88 mg, 0.35 mmol) according to General Procedure 2. Purification of the crude product by High pH MDAP and silica chromatography (0-10% 2 M NH₃ in MeOH/DCM) afforded 1-(2-cyclopropyl-4-(pyridin-3-ylmethyl)-3,4-dihydroquinoxalin-1(2H)-yl)ethanone (23 mg, 0.075 mmol, 32%) as a white solid.

LCMS (High pH, ES⁺): t_R = 0.93 min, [M+H⁺] 306.1 (91% pure). ¹H NMR (400 MHz, CDCl₃): δ 0.28-0.40 (m, 1H), 0.40-0.59 (m, 3H), 0.87 (br. s., 1H), 2.26 (s, 3H), 3.45 (dd, J = 11.1, 1.3 Hz, 1H), 3.60 (dd, J = 11.1, 4.8 Hz, 1H), 4.27 (br. s., 1H), 4.60 (d, J = 2.2 Hz, 2H), 6.66 (dd, J = 8.3, 1.0 Hz, 1H), 6.71 (td, J = 7.6, 1.1 Hz, 1H), 7.04 (td, J = 8.1, 1.5 Hz, 1H), 7.10 (br. s., 1H), 7.26 (dd, J = 8.6, 4.9 Hz, 1H), 7.59 (d, J = 7.8 Hz, 1H), 8.58 (s, 1H), 8.55 (s, 1H).

1-(2-Cyclopropyl-4-(4-methylbenzyl)-3,4-dihydroquinoxalin-1(2H)-yl)ethanone

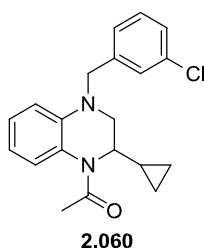


Prepared from **2.018c** (20 mg, 0.09 mmol) and 4-methylbenzaldehyde (22 μ L, 0.19 mmol) according to General Procedure 1. After 48 h further 4-methylbenzaldehyde (22 μ L, 0.19 mmol) and sodium triacetoxyborohydride (58.8 mg, 0.277 mmol) were added and the reaction mixture was stirred at rt for 24 h. Purification of the crude product by High pH MDAP afforded 1-(2-cyclopropyl-4-(4-methylbenzyl)-3,4-dihydroquinoxalin-1(2H)-yl)ethanone (25 mg, 0.078 mmol, 84%) as an off-white gum.

LCMS (High pH, ES⁺): t_R = 1.31 min, [M+H⁺] 321.3, (99% pure). ¹H NMR (400 MHz, CDCl₃): δ 0.31-0.40 (m, 1H), 0.42-0.56 (m, 3H), 0.82-0.99 (m, 1H), 2.27 (s, 3H), 2.36 (s, 3H), 3.46 (dd,

$J = 11.2, 1.7 \text{ Hz, 1H}$), 3.59 (dd, $J = 11.2, 4.6 \text{ Hz, 1H}$), 4.164.35 (m, 1H), 4.47-4.63 (m, 2H), 6.63-6.75 (m, 2H), 7.03 (ddd, $J = 8.4, 7.2, 1.7 \text{ Hz, 1H}$), 7.06-7.12 (m, 1H), 7.13-7.20 (m, 4H).

HRMS: ($\text{C}_{21}\text{H}_{24}\text{N}_2\text{O}$) [$\text{M}+\text{H}^+$] requires 321.1961, found [$\text{M}+\text{H}^+$] 321.1967. **1-(2-Cyclopropyl-4-(3-chlorobenzyl)-3,4-dihydroquinoxalin-1(2H)-yl)ethanone**



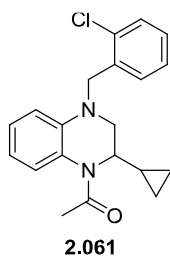
Prepared from **2.018c** (20 mg, 0.09 mmol) and 3-chlorobenzaldehyde (26 mg, 0.19 mmol) according to General Procedure 1. After 48 h further 3-chlorobenzaldehyde (26 mg, 0.19 mmol) and sodium triacetoxyborohydride (58.8 mg, 0.277 mmol) were added and the reaction mixture was stirred at rt for 24 h. Purification of the crude product by High pH MDAP afforded 1-(4-(3-chlorobenzyl)-2-cyclopropyl-3,4-

dihydroquinoxalin-1(2H)-yl)ethanone (21 mg, 67%) as an off-white gum.

LCMS (High pH, ES⁺): $t_R = 1.31 \text{ min}$, [$\text{M}+\text{H}^+$] 341.2, 343.2, (99% pure). ¹H NMR (400 MHz, CDCl_3): δ 0.31-0.63 (m, 4H), 0.82-1.00 (m, 1H), 2.28 (s, 3H), 3.46 (dd, $J = 11.1, 1.6 \text{ Hz, 1H}$), 3.60 (dd, $J = 11.1, 4.6 \text{ Hz, 1H}$), 4.19-4.36 (m, 1H), 4.56 (ABq, $J = 17.1 \text{ Hz, 2H}$), 6.63 (dd, $J = 8.3, 1.5 \text{ Hz, 1H}$), 6.71 (ddd, $J = 7.6, 1.2 \text{ Hz, 1H}$), 7.04 (ddd, $J = 8.3, 7.2, 1.5 \text{ Hz, 1H}$), 7.07-7.14 (m, 1H), 7.15-7.19 (m, 1H), 7.23-7.31 (m, 3H).

HRMS: ($\text{C}_{20}\text{H}_{21}\text{ClN}_2\text{O}$) [$\text{M}+\text{H}^+$] requires 341.1415, found [$\text{M}+\text{H}^+$] 341.1416.

1-(2-Cyclopropyl-4-(2-chlorobenzyl)-3,4-dihydroquinoxalin-1(2H)-yl)ethanone

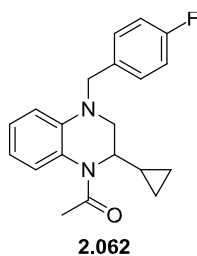


Prepared from **2.018c** (20 mg, 0.09 mmol) and 2-chlorobenzaldehyde (20 mg, 0.14 mmol) according to General Procedure 1. Purification of the crude product by High pH MDAP afforded 1-(4-(2-chlorobenzyl)-2-cyclopropyl-3,4-dihydroquinoxalin-1(2H)-yl)ethanone (11 mg, 0.032 mmol, 47%).

LCMS (High pH, ES⁺): $t_R = 1.33 \text{ min}$, [$\text{M}+\text{H}^+$] 341.1, (96% pure). ¹H NMR (400 MHz, CDCl_3): δ 0.33-0.60 (m, 4H), 0.89-1.03 (m, 1H), 2.29 (s, 3H), 3.47 (dd, $J = 11.1, 1.6 \text{ Hz, 1H}$), 3.64 (dd, $J = 11.1, 4.6 \text{ Hz, 1H}$), 4.20-4.38 (m, 1H), 4.65 (d, $J = 4.4 \text{ Hz, 2H}$), 6.53 (dd, $J = 8.3, 1.5 \text{ Hz, 1H}$), 6.71 (ddd, $J = 7.6, 1.3 \text{ Hz, 1H}$), 7.02 (ddd, $J = 8.4, 7.2, 1.5 \text{ Hz, 1H}$), 7.06-7.16 (m, 1H), 7.17-7.27 (m, 3H), 7.40-7.46 (m, 1H).

HRMS: ($\text{C}_{20}\text{H}_{21}\text{ClN}_2\text{O}$) [$\text{M}+\text{H}^+$] requires 341.1415, found [$\text{M}+\text{H}^+$] 341.1416.

1-(2-Cyclopropyl-4-(4-fluorobenzyl)-3,4-dihydroquinoxalin-1(2H)-yl)ethanone



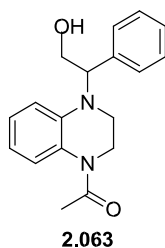
Prepared from **2.018c** (15 mg, 0.07 mmol) and 4-fluorobenzaldehyde (15 μL , 0.14 mmol) according to General Procedure 1. After 24 h further 4-fluorobenzaldehyde (15 μL , 0.139 mmol) and sodium triacetoxyborohydride (44.1 mg, 0.208 mmol) were added and the reaction mixture was stirred at rt for 24 h. Purification of the crude product by High

pH MDAP afforded 1-(2-cyclopropyl-4-(4-fluorobenzyl)3,4-dihydroquinoxalin-1(2*H*)-yl)ethanone (17 mg, 0.052 mmol, 76%) as a beige solid.

LCMS (High pH, ES⁺): t_R = 1.24 min, [M+H⁺] 325.3, (100% purity). ¹H NMR (400 MHz, CDCl₃): δ 0.31-0.40 (m, 1H), 0.41-0.55 (m, 3H), 0.88 (br. s., 1H), 2.27 (s, 3H), 3.44 (dd, *J* = 11.1, 1.3 Hz, 1H), 3.58 (dd, *J* = 11.1, 4.7 Hz, 1H), 4.17-4.35 (m, 1H), 4.56 (dd, *J* = 22.5, 16.7 Hz, 2H), 6.64-6.74 (m, 2H), 6.98-7.30 (m, 6H).

HRMS: (C₂₀H₂₁FN₂O) [M+H⁺] requires 325.1711, found [M+H⁺] 325.1713.

1-(4-(2-Hydroxy-1-phenylethyl)-3,4-dihydroquinoxalin-1(2*H*)-yl)ethanone



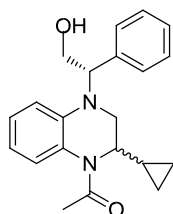
A mixture of 1-(3,4-dihydroquinoxalin-1(2*H*)-yl)ethanone **2.018d** (30 mg, 0.170 mmol) and 2-phenyloxirane (0.021 mL, 0.187 mmol) in trifluoroethanol (2 mL) was stirred at rt for 3 h, then heated to 75 °C for 18 h. The reaction mixture was evaporated and the residue was purified by silica chromatography (0-100% EtOAc/cyclohexane), appropriate fractions were evaporated *in vacuo* to afford 1-(4-(2-hydroxy-1-phenylethyl)-3,4-

dihydroquinoxalin-1(2*H*)-yl)ethanone (30 mg, 0.101 mmol, 60%). LCMS

(High pH, ES⁺): t_R = 0.90 min, [M+H⁺] 297.3, (100% purity).

¹H NMR (400 MHz, CDCl₃): δ 2.23 (s, 3H), 2.50-2.68 (m, 1H), 3.30-3.42 (m, 1H), 3.46-3.55 (m, 1H), 3.63 (ddd, *J* = 12.4, 8.1, 3.9 Hz, 1H), 4.10-4.23 (m, 3H), 5.13 (dd, *J* = 8.6, 5.6 Hz, 1H), 6.67 (td, *J* = 7.6, 1.5 Hz, 1H), 6.84 (d, *J* = 8.1 Hz, 1H), 6.97-7.02 (m, 1H), 7.03 (t, *J* = 7.3 Hz, 2H), 7.24 (d, *J* = 7.1 Hz, 1H), 7.27-7.39 (m, 3H).

1-(2-Cyclopropyl-4-((*S*)-2-hydroxy-1-phenylethyl)-3,4-dihydroquinoxalin-1(2*H*)-yl)ethanone



A mixture of 1-(2-cyclopropyl-3,4-dihydroquinoxalin-1(2*H*)-yl)ethanone **2.018c** (30 mg, 0.139 mmol) and (*R*)-2-phenyloxirane (22 mg, 0.180 mmol) in trifluoroethanol (2 mL) was stirred at 75 °C for 18 hr. The reaction mixture was evaporated and the residue purified by MDAP (High pH). The solvent was evaporated *in vacuo* to afford the products as separate

diastereomers-relative stereochemistry could not be assigned by NMR.

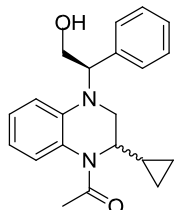
2.064c 1-(2-Cyclopropyl-4-((*S*)-2-hydroxy-1-phenylethyl)-3,4-dihydroquinoxalin-1(2*H*)-yl)ethanone (14 mg, 0.042 mmol, 30%).

LCMS (High pH, ES⁺): t_R = 1.00 min, [M+H⁺] 337.2, (95% purity). ¹H NMR (400 MHz, CDCl₃): δ 0.34-0.63 (m, 4H), 0.78-0.92 (m, 1H), 2.22 (s, 3H), 3.13 (dd, *J* = 11.4, 4.3 Hz, 1H), 3.44 (dd, *J* = 11.5, 2.0 Hz, 1H), 4.11-4.28 (m, 3H), 5.28 (dd, *J* = 8.6, 5.9 Hz, 1H), 6.73 (td, *J* = 7.5, 1.5 Hz, 1H), 6.98-7.05 (m, 1H), 7.05-7.17 (m, 2H), 7.23-7.39 (m, 5H). OH not observed.

2.064d 1-(2-Cyclopropyl-4-((*S*)-2-hydroxy-1-phenylethyl)-3,4-dihydroquinoxalin-1(2*H*)-yl)ethanone (18 mg, 0.054 mmol, 39%).

LCMS (High pH, ES⁺): t_R = 1.06 min, [M+H⁺] 337.3, (92% purity). ¹H NMR (400 MHz, CDCl₃): δ 0.20-0.29 (m, 1H), 0.31-0.48 (m, 3H), 0.69-0.81 (m, 1H), 2.24 (s, 3H), 3.54-3.63 (m, 2H), 4.11-4.27 (m, 3H), 5.14 (dd, J = 8.3, 5.4 Hz, 1H), 6.68 (td, J = 7.6, 1.5 Hz, 1H), 6.82 (d, J = 8.1 Hz, 1H), 7.04 (ddd, J = 8.5, 7.2, 1.7 Hz, 1H), 7.03-7.12 (m, 1H),

7.27-7.42 (m, 5H). OH not observed. **1-(2-cyclopropyl-4-((R)-2-hydroxy-1-phenylethyl)-3,4-dihydroquinoxalin-1(2H)yl)ethanone**



A mixture of 1-(2-cyclopropyl-3,4-dihydroquinoxalin-1(2H)-yl)ethanone **2.018c** (30 mg, 0.139 mmol) and (S)-2-phenyloxirane (22 mg, 0.180 mmol) in trifluoroethanol (2 mL) was stirred at 80 °C for 18 hr. The reaction mixture was evaporated and the residue purified by silica chromatography (25-100% EtOAc/cyclohexane). The solvent was evaporated *in vacuo* to

afford the products as separate diastereomers-relative stereochemistry could not be assigned by NMR. NMR spectra matched **2.064c** and **2.064d** respectively.

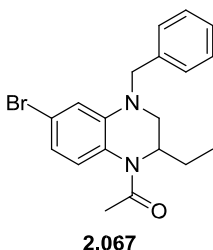
2.064a 1-(2-Cyclopropyl-4-((R)-2-hydroxy-1-phenylethyl)-3,4-dihydroquinoxalin-1(2H)yl)ethanone (11 mg, 0.033 mmol, 24%).

LCMS (High pH, ES⁺): t_R = 1.01 min, [M+H⁺] 337.4, (95% purity).

2.064b 1-(2-Cyclopropyl-4-((R)-2-hydroxy-1-phenylethyl)-3,4-dihydroquinoxalin-1(2H)yl)ethanone (19 mg, 0.056 mmol, 41%).

LCMS (High pH, ES⁺): t_R = 1.06 min, [M+H⁺] 337.4, (84% purity).

1-(4-Benzyl-2-ethyl-6-bromo-3,4-dihydroquinoxalin-1(2H)-yl)ethanone



2.067

Prepared from **2.016b** (140 mg, 0.49 mmol) and benzyl bromide (88 μL, 0.74 mmol) according to General Procedure 2. The reaction was not complete after 18 h so further benzyl bromide (88 μL, 0.74 mmol) and potassium carbonate (205 mg, 1.48 mmol) were added and the reaction stirred at 90 °C for 18 h. The reaction mixture was cooled, diluted with

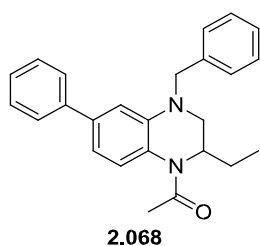
H₂O (40 mL) and extracted with Et₂O (3 x 25 mL). The combined organics were dried through a hydrophobic frit and evaporated to dryness. The crude product was purified by silica chromatography (0-40% EtOAc/cyclohexane), appropriate fractions were evaporated *in vacuo* to afford 1-(4-benzyl-2-ethyl-6-bromo-3,4-dihydroquinoxalin-1(2H)-yl)ethanone (103 mg, 0.28 mmol, 56%) as a yellow solid.

LCMS (High pH, ES⁺): t_R = 1.33 min, [M+H⁺] 373.3, 375.3 (100% pure). ¹H NMR (400 MHz, CDCl₃): δ 0.86 (t, J = 7.0 Hz, 3H), 1.32-1.44 (m, 2H), 2.25 (s, 3H), 3.24

(d, J = 11.5 Hz, 1H), 3.54 (dd, J = 11.5, 4.6 Hz, 1H), 4.52 (dd, J = 34.5, 16.9 Hz, 2H), 4.91-5.04 (m, 1H), 6.76-6.90 (m, 3H), 7.22 (d, J = 7.3 Hz, 2H), 7.29-7.40 (m, 3H). ¹³C NMR (101 MHz, CDCl₃): δ 10.4, 22.9, 23.5, 47.5, 51.8, 54.2, 113.7, 118.5, 120.0, 121.6, 126.5, 126.7, 127.5, 128.9, 137.1, 140.2, 169.5. M.pt. (Et₂O): 112-114 °C.

ν_{\max} (neat): 2928, 1639, 1595, 1510, 1451, 1395, 1361, 1335, 1318, 1253, 1112, 832, 803, 725, 694 cm^{-1} .

HRMS: ($\text{C}_{19}\text{H}_{21}\text{BrN}_2\text{O}$) $[\text{M}+\text{H}^+]$ requires 373.0910, found $[\text{M}+\text{H}^+]$ 373.0914. **1-(4-Benzyl-2-ethyl-6-phenyl-3,4-dihydroquinoxalin-1(2H)-yl)ethanone**



2.068

Prepared from **2.067** (25 mg, 0.07 mmol) and phenyl boronic acid (16 mg, 0.13 mmol) according to General Procedure 3. Purification of the crude product by High pH MDAP afforded 1-(4-benzyl-2-ethyl-6-phenyl-3,4-dihydroquinoxalin-1(2H)-yl)ethanone (15 mg, 0.04 mmol, 61%).

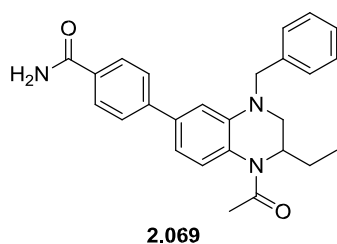
LCMS (High pH, ES^+): t_{R} = 1.39 min, $[\text{M}+\text{H}^+]$ 371.4 (100% purity).

1

$^1\text{H NMR}$ (400 MHz, CDCl_3): δ 0.92 (t, J = 7.3 Hz, 3H), 1.33-1.63 (m, 2H), 2.33 (s, 3H), 3.30 (d, J = 11.4 Hz, 1H), 3.61 (dd, J = 11.4, 4.9 Hz, 1H), 4.56 (d, J = 17.0 Hz, 1H), 4.69 (d, J = 17.0 Hz, 1H), 4.92-5.12 (m, 1H), 6.79-6.96 (m, 2H), 7.08 (d, J = 8.6 Hz, 1H), 7.25-7.43 (m, 8H), 7.46-7.52 (m, 2H).

HRMS: ($\text{C}_{25}\text{H}_{26}\text{N}_2\text{O}$) $[\text{M}+\text{H}^+]$ requires 371.2118, found 371.2124.

4-(1-Acetyl-4-benzyl-2-ethyl-1,2,3,4-tetrahydroquinoxalin-6-yl)benzamide



2.069

Prepared from **2.067** (25 mg, 0.07 mmol) and (4-carbamoylphenyl)boronic acid (22 mg, 0.13 mmol) according to General Procedure 3. Purification of the crude product by High pH MDAP afforded 4-(1-acetyl-4-benzyl-2-ethyl-1,2,3,4-tetrahydroquinoxalin-6-yl)benzamide (11 mg, 0.03 mmol, 40%) as an off-white solid.

LCMS (High pH, ES^+): t_{R} = 1.02 min, $[\text{M}+\text{H}^+]$ 414.5, (96% purity).

$^1\text{H NMR}$ (400 MHz, CDCl_3): δ 0.91 (t, J = 7.3 Hz, 3H), 1.35-1.60 (m, 2H), 2.32 (s, 3H), 3.32 (d, J = 11.7 Hz, 1H), 3.62 (dd, J = 11.7, 4.5 Hz, 1H), 4.57 (d, J = 16.9 Hz, 1H), 4.67 (d, J = 16.9 Hz, 1H), 4.95-5.10 (m, 1H), 5.73-6.00 (m, 1H), 6.04-6.31 (m, 1H), 6.89 (d, J = 2.0 Hz, 1H), 6.90-6.95 (m, 1H), 7.05-7.14 (m, 1H), 7.24-7.40 (m, 5H), 7.53 (d, J = 8.3 Hz, 2H), 7.83 (d, J = 8.3 Hz, 2H).

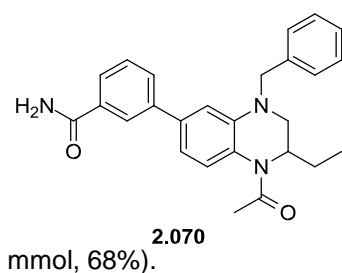
^{13}C

$^{13}\text{C NMR}$ (126 MHz, CDCl_3): δ 10.4, 23.1, 23.6, 47.9, 52.3, 54.5, 109.8, 114.8, 122.5, 126.0, 126.5, 127.1, 127.4, 127.8, 128.9, 131.7, 137.8, 138.2, 139.3, 144.8, 169.0, 169.7. M.pt.: 153-156 $^{\circ}\text{C}$.

ν_{\max} (neat): 3532, 3352, 3171, 2977, 2928, 2836, 1674, 1624, 1571, 1504, 1437, 1380, 1325, 1253, 1114, 1068, 1014, 865, 838, 809, 709, 692 cm^{-1} .

HRMS: ($\text{C}_{26}\text{H}_{27}\text{N}_3\text{O}_2$) $[\text{M}+\text{H}^+]$ requires 414.2176, found 414.2180.

3-(1-Acetyl-4-benzyl-2-ethyl-1,2,3,4-tetrahydroquinoxalin-6-yl)benzamide

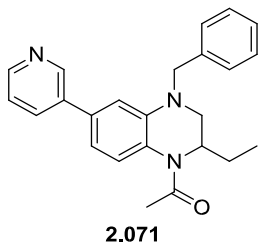


mmol, 68%).

Prepared from **2.067** (24 mg, 0.06 mmol) and (3-carbamoylphenyl)boronic acid (21 mg, 0.13 mmol) according to General Procedure 3. Purification of the crude product by High pH MDAP afforded 3-(1-acetyl-4-benzyl-2-ethyl-1,2,3,4-tetrahydroquinoxalin-6-yl)benzamide (18 mg, 0.04

LCMS (High pH, ES⁺): t_R = 1.05 min, [M+H⁺] 414.5 (100% purity). ¹H NMR (400 MHz, CDCl₃): δ 0.91 (t, J = 7.3 Hz, 3H), 1.37-1.59 (m, 2H), 2.31 (s, 3H), 3.31 (d, J = 11.6 Hz, 1H), 3.61 (dd, J = 11.6, 4.6 Hz, 1H), 4.62 (ABq, J = 16.9 Hz, 2H), 4.93-5.11 (m, 1H), 5.79-6.06 (m, 1H), 6.08-6.34 (m, 1H), 6.87 (d, J = 2.1 Hz, 1H), 6.91 (dd, J = 8.1, 2.1 Hz, 1H), 7.01-7.13 (m, 1H), 7.23-7.39 (m, 5H), 7.45 (t, J = 7.7 Hz, 1H), 7.62 (ddd, J = 7.7, 7.7, 1.5 Hz, 1H), 7.75 (ddd, J = 7.7, 7.7, 1.4 Hz, 1H), 7.89 (s, 1H).

1-(4-Benzyl-2-ethyl-6-(pyridin-3-yl)-3,4-dihydroquinoxalin-1(2H)-yl)ethanone



Prepared from **2.067** (30 mg, 0.08 mmol) and pyridin-3-ylboronic acid (20 mg, 0.16 mmol) according to General Procedure 3.

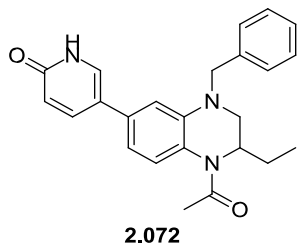
Purification of the crude product by High pH MDAP afforded 1-(4-benzyl-2-ethyl-6-(pyridin-3-yl)-3,4-dihydroquinoxalin-1(2H)yl)ethanone (24 mg, 0.06 mmol, 80%).

LCMS (High pH, ES⁺): t_R = 1.12 min, [M+H⁺] 372.4, (98% purity).

¹H NMR (400 MHz, CDCl₃): δ 0.92 (t, J = 7.5 Hz, 3H), 1.46 (br s, 2H), 2.32 (s, 3H), 3.33 (d, J = 11.4 Hz, 1H), 3.63 (dd, J = 11.4, 4.5 Hz, 1H), 4.57 (d, J = 17.0 Hz, 1H), 4.67 (d, J = 17.0 Hz, 1H), 4.94-5.14 (m, 1H), 6.84 (d, J = 2.0 Hz, 1H), 6.85-6.91 (m, 1H), 7.00-7.18 (m, 1H), 7.23-7.40 (m, 6H), 7.74 (td, J = 8.0, 2.0 Hz, 1H), 8.54 (dd, J = 4.8, 1.5 Hz, 1H), 8.72 (d, J = 1.5 Hz, 1H).

HRMS: (C₂₄H₂₅N₃O) [M+H⁺] requires 372.2070, found 372.2077.

1-(4-Benzyl-2-ethyl-6-(6-hydroxypyridin-3-yl)-3,4-dihydroquinoxalin-1(2H)-yl)ethanone



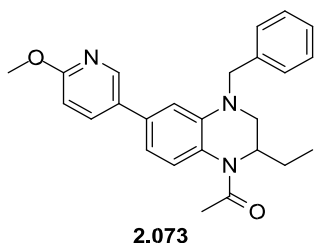
Prepared from **2.067** (30 mg, 0.08 mmol) and (6-hydroxypyridin-3-yl)boronic acid pinacol ester (36 mg, 0.16 mmol) according to General Procedure 3. Purification of the crude product by High pH MDAP afforded 1-(4-benzyl-2-ethyl-6-(6-hydroxypyridin-3-yl)-3,4-dihydroquinoxalin-1(2H)-yl)ethanone (17 mg, 0.04 mmol, 55%).

LCMS (High pH, ES⁺): t_R = 0.91 min, [M+H⁺] 388.4 (100% purity).

¹H NMR (400 MHz, CDCl₃): δ 0.90 (t, J = 7.5 Hz, 3H), 1.35-1.57 (m, 2H), 2.30 (s, 3H), 3.29 (d, J = 11.5 Hz, 1H), 3.59 (dd, J = 11.5, 4.4 Hz, 1H), 4.59 (ABq, J = 17.1 Hz, 2H), 4.94-5.07 (m,

1H), 6.62 (d, $J = 9.5$ Hz, 1H), 6.67 (d, $J = 2.0$ Hz, 1H), 6.68-6.74 (m, 1H), 6.98-7.10 (m, 1H), 7.21-7.39 (m, 5H), 7.52 (d, $J = 2.5$ Hz, 1H), 7.64 (dd, $J = 9.5, 2.5$ Hz, 1H), 13.43 (br. s, 1H).

HRMS: (C₂₄H₂₅N₃O₂) [M+H⁺] requires 388.2020, found 388.2014. **1-(4-Benzyl-2-ethyl-6-(6-methoxypyridin-3-yl)-3,4-dihydroquinoxalin-1(2H)-yl)ethanone**



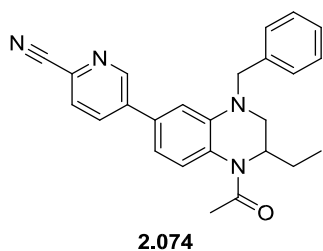
Prepared from **2.067** (30 mg, 0.08 mmol) and 2-methoxypyridine-5-boronic acid pinacol ester (38 mg, 0.16 mmol) according to General Procedure 3. Purification of the crude product by High pH MDAP afforded 1-(4-benzyl-2-ethyl-6-(6-methoxypyridin-3-yl)-3,4-dihydroquinoxalin-1(2H)-yl)ethanone (15 mg, 0.037 mmol, 47%).

LCMS (High pH, ES⁺): $t_R = 1.29$ min, [M+H⁺] 402.5, (100% purity). ¹H NMR (400 MHz, CDCl₃): δ 0.91 (t, $J = 7.6$ Hz, 3H), 1.36-1.60 (m, 2H), 2.32 (s, 3H), 3.31 (d, $J = 11.3$ Hz, 1H), 3.62 (dd, $J = 11.3, 4.5$ Hz, 1H), 3.96 (s, 3H), 4.61 (ABq, $J = 16.9$ Hz, 2H), 4.95-5.11 (m, 1H), 6.76 (d, $J = 8.6$ Hz, 1H), 6.79 (d, $J = 2.2$ Hz, 1H), 6.80-6.85 (m, 1H),

7.03-7.12 (m, 1H), 7.23-7.39 (m, 5H), 7.67 (dd, $J = 8.7, 2.6$ Hz, 1H), 8.28 (d, $J = 2.7$ Hz, 1H).

HRMS: (C₂₅H₂₇N₃O₂) [M+H⁺] requires 402.2176, found [M+H⁺] 402.2169.

5-(1-Acetyl-4-benzyl-2-ethyl-1,2,3,4-tetrahydroquinoxalin-6-yl)picolinonitrile

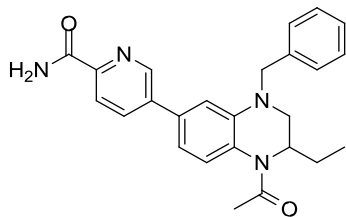


Prepared from **2.067** (30 mg, 0.08 mmol) and 5-picolinonitrileboronic acid pinacol ester (37 mg, 0.16 mmol) according to General Procedure 3. Purification of the crude product by High pH MDAP afforded 5-(1-acetyl-4-benzyl-2ethyl-1,2,3,4-tetrahydroquinoxalin-6-yl)picolinonitrile (26 mg, 0.066 mmol, 82%) as a yellow solid.

LCMS (High pH, ES⁺): $t_R = 1.21$ min, [M+H⁺] 397.7, (97% purity). ¹H NMR (400 MHz, CDCl₃): δ 0.93 (t, $J = 7.5$ Hz, 3H), 1.49 (br. s., 2H), 2.32 (s, 3H), 3.37 (d, $J = 11.7$ Hz, 1H), 3.67 (dd, $J = 11.5, 4.4$ Hz, 1H), 4.54-4.70 (m, 2H), 4.94-5.15 (m, 1H), 6.81 (d, $J = 2.1$ Hz, 1H), 6.89 (dd, $J = 8.1, 2.1$ Hz, 1H), 7.06-7.21 (m, 1H), 7.23-7.41 (m, 5H), 7.69 (d, $J = 8.1$ Hz, 1H), 7.84 (dd, $J = 8.1, 2.4$ Hz, 1H), 8.78 (d, $J = 2.4$ Hz, 1H).

HRMS: (C₂₅H₂₄N₄O) [M+H⁺] requires 397.2023, found [M+H⁺] 397.2028.

5-(1-Acetyl-4-benzyl-2-ethyl-1,2,3,4-tetrahydroquinoxalin-6-yl)picolinamide



2.089

Prepared from **2.074** (20 mg, 0.050 mmol) according to General Procedure 4. Purification of the crude product by High pH MDAP afforded 5-(1-acetyl-4-benzyl-2-ethyl-1,2,3,4-tetrahydroquinoxalin-6-yl)picolinamide (20 mg, 0.05 mmol, 79%) as a yellow solid.

LCMS (High pH, ES⁺): t_R = 1.02 min, [M+H⁺] 415.4 (100% 1

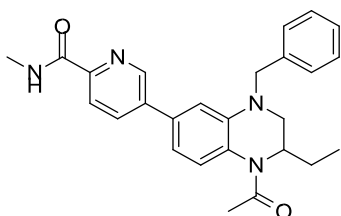
purity).

¹H NMR (400 MHz, CDCl₃): δ 0.93 (t, *J* = 7.3 Hz, 3H), 1.39-1.60 (m, 2H), 2.33 (s, 3H), 3.34

(d, *J* = 11.7 Hz, 1H), 3.65 (dd, *J* = 11.6, 4.5 Hz, 1H), 4.63 (ABq, *J* = 17.6 Hz, 2H), 4.94-5.12 (m, 1H), 5.73-5.87 (m, 1H), 6.86 (d, *J* = 2.0 Hz, 1H), 6.92 (dd, *J* = 8.1, 2.0 Hz, 1H), 7.06-7.19 (m, 1H), 7.23-7.41 (m, 5H), 7.76-7.85 (m, 1H), 7.89 (dd, *J* = 8.1, 2.4 Hz, 1H), 8.20 (d, *J* = 8.1 Hz, 1H), 8.66 (d, *J* = 2.4 Hz, 1H).

HRMS: (C₂₅H₂₆N₄O₂) [M+H⁺] requires 415.2129, found 415.2129.

5-(1-Acetyl-4-benzyl-2-ethyl-1,2,3,4-tetrahydroquinoxalin-6-yl)picolinonitrile



2.075

Prepared from **2.067** (24 mg, 0.064 mmol), (6-(methylcarbamoyl)pyridin-3-yl)boronic acid (34 mg, 0.129 mmol) according to General Procedure 3. Purification of the crude product by High pH MDAP afforded 5-(1-acetyl-4-benzyl-2-ethyl-1,2,3,4-tetrahydroquinoxalin-6-yl)-*N*-methylpicolinamide (22 mg, 0.051 mmol, 80%) as a yellow

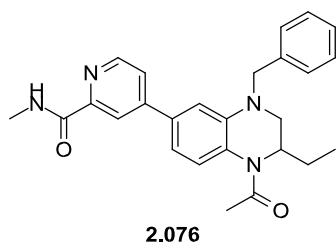
solid.

LCMS (High pH, ES⁺): t_R = 1.10 min, [M+H⁺] 429.5, (94% purity). ¹H NMR (400 MHz, CDCl₃): δ 0.92 (t, *J* = 7.3 Hz, 3H), 1.39-1.60 (m, 2H), 2.32 (s, 3H), 3.05 (d, *J* = 5.1 Hz, 3H), 3.34 (d, *J* = 11.5 Hz, 1H), 3.64 (dd, *J* = 11.5, 4.4 Hz, 1H), 4.62 (ABq, *J* = 17.1 Hz, 2H), 4.97-5.10 (m, 1H), 6.85 (d, *J* = 2.0 Hz, 1H), 6.87-6.94 (m, 1H), 7.06-7.17 (m, 1H), 7.23-7.40 (m, 5H), 7.87 (dd, *J* = 8.1, 2.2 Hz, 1H), 7.94-8.04 (m, 1H), 8.19 (d, *J* = 8.1 Hz, 1H), 8.62 (d, *J* = 2.2 Hz, 1H). ¹³C NMR (101 MHz, CDCl₃): δ 10.4, 23.1, 23.6, 26.1, 47.8, 52.4, 54.6, 109.7, 114.7, 122.0, 123.1, 126.2, 126.5, 127.5, 128.9, 135.2, 135.3, 137.5, 139.0, 139.4, 146.4, 148.5, 164.9, 169.5.

M.pt.: 78-81 °C v_{max} (neat): 3391, 2931, 1649, 1601, 1517, 1468, 1374, 1323, 1238, 1111, 1014, 840, 790, 729, 696 cm⁻¹.

HRMS: (C₂₆H₂₈N₄O₂) [M+H⁺] requires 429.2285, found [M+H⁺] 429.2279.

4-(1-Acetyl-4-benzyl-2-ethyl-1,2,3,4-tetrahydroquinoxalin-6-yl)-*N*-methylpicolinamide

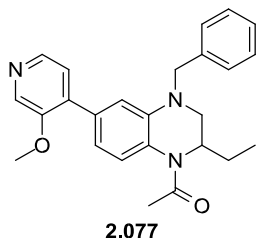


Prepared from **2.067** (30 mg, 0.08 mmol) and (2(methylcarbamoyl)pyridin-4-yl)boronic acid (42 mg, 0.16 mmol) according to General Procedure 3. Purification of the crude product by High pH MDAP afforded 4-(1-acetyl-4-benzyl-2-ethyl-1,2,3,4-tetrahydroquinoxalin-6-yl)-*N*-methylpicolinamide (33 mg, 0.077 mmol, 96%).

LCMS (High pH, ES⁺): t_R = 1.12 min, [M+H⁺] 429.5, (100% purity). ¹H NMR (400 MHz, CDCl₃): δ 0.91 (t, *J* = 7.5 Hz, 3H), 1.35-1.56 (m, 2H), 2.31 (s, 3H), 3.05 (d, *J* = 5.1 Hz, 3H), 3.32 (d, *J* = 11.6 Hz, 1H), 3.61 (dd, *J* = 11.6, 4.8 Hz, 1H), 4.63 (ABq, *J* = 16.6 Hz, 2H), 4.96-5.08 (m, 1H), 6.96-6.99 (m, 1H), 6.99-7.03 (m, 1H), 7.08-7.16 (m, 1H), 7.24-7.39 (m, 5H), 7.47 (dd, *J* = 5.1, 2.0 Hz, 1H), 8.01-8.12 (m, 1H), 8.31-8.37 (m, 1H), 8.50 (d, *J* = 5.1 Hz, 1H).

HRMS: (C₂₆H₂₈N₄O₂) [M+H⁺] requires 429.2285, found [M+H⁺] 429.2272.

1-(4-Benzyl-2-ethyl-6-(3-methoxypyridin-4-yl)-3,4-dihydroquinoxalin-1(2*H*)-yl)ethanone



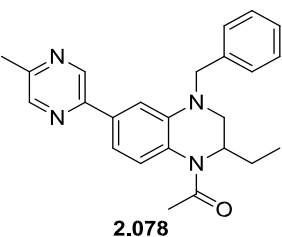
Prepared from **2.067** (30 mg, 0.08 mmol) and (3-methoxypyridin-4-yl)boronic acid (25 mg, 0.16 mmol) according to General Procedure 3. Purification of the crude product by High pH MDAP afforded 1-(4-benzyl-2-ethyl-6-(3-methoxypyridin-4-yl)-3,4-dihydroquinoxalin-1(2*H*)-yl)ethanone (6 mg, 0.01 mmol, 17%).

LCMS (High pH, ES⁺): t_R = 1.11 min, [M+H⁺] 402.4 (100% purity).

¹H NMR (400 MHz, CDCl₃): δ 0.91 (t, *J* = 7.3 Hz, 3H), 1.36-1.58 (m, 2H), 2.33 (s, 3H), 3.32 (d, *J* = 11.5 Hz, 1H), 3.62 (dd, *J* = 11.5, 4.6 Hz, 1H), 3.77 (s, 3H), 4.57 (ABq, *J* = 17.1 Hz, 2H), 4.94-5.11 (m, 1H), 6.88 (dd, *J* = 8.1, 2.0 Hz, 1H), 6.96 (d, *J* = 2.0 Hz, 1H), 7.03-7.12 (m, 1H), 7.19 (d, *J* = 4.8 Hz, 1H), 7.26-7.39 (m, 5H), 8.26 (d, *J* = 4.8 Hz, 1H), 8.30 (s, 1H).

HRMS: (C₂₅H₂₇N₃O₂) [M+H⁺] requires 402.2176, found 402.2166.

1-(4-Benzyl-2-ethyl-6-(5-methylpyrazin-2-yl)-3,4-dihydroquinoxalin-1(2*H*)-yl)ethanone



Prepared from **2.067** (60 mg, 0.16 mmol) and (5-methylpyrazin-2-yl)boronic acid pinacol ester (88 mg, 0.40 mmol) at 120 °C for 3 h according to General Procedure 3. Further (5-methylpyrazin-2-yl)boronic acid pinacol ester (88 mg, 0.40 mmol) and Pd(dppf)Cl₂ (12 mg, 0.016 mmol) were added and the reaction heated to 120

°C for 2 h. Purification of the crude product by High pH MDAP

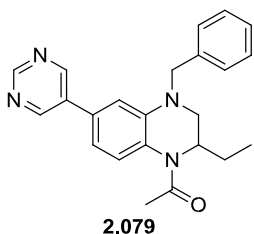
afforded 1-(4-benzyl-2-ethyl-6-(5-methylpyrazin-2-yl)-3,4-dihydroquinoxalin-1(2*H*)-yl)ethanone (11 mg, 0.03 mmol, 18%).

LCMS (High pH, ES⁺): t_R = 1.17 min, [M+H⁺] 387.3 (100% pure). ¹H NMR (400 MHz, CDCl₃): δ 0.90 (t, *J* = 7.3 Hz, 3H), 1.35-1.57 (m, 2H), 2.31 (s, 3H), 2.58 (s, 3H), 3.30 (dd, *J* = 11.5, 1.3

Hz, 1H), 3.60 (dd, $J = 11.5, 4.6$ Hz, 1H), 4.64 (ABq, $J = 16.9$ Hz, 2H), 4.91-5.12 (m, 1H), 7.06-7.19 (m, 1H), 7.24-7.38 (m, 7H), 8.40-8.47 (m, 1H), 8.74 (d, $J = 1.7$ Hz, 1H).

HRMS: (C₂₄H₂₆N₄O) [M+H⁺] requires 387.2179, found 387.2189.

1-(4-Benzyl-2-ethyl-6-(pyrimidin-5-yl)-3,4-dihydroquinoxalin-1(2H)-yl)ethanone



Prepared from **2.067** (30 mg, 0.08 mmol) and pyrimidin-5-ylboronic acid (20 mg, 0.16 mmol) according to General Procedure 3.

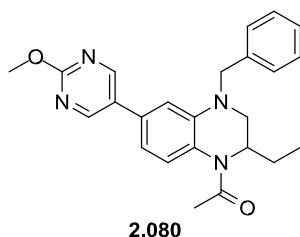
Purification of the crude product by High pH MDAP afforded 1-(4benzyl-2-ethyl-6-(pyrimidin-5-yl)-3,4-dihydroquinoxalin-1(2H)-yl)ethanone (9 mg, 0.02 mmol, 30%).

LCMS (High pH, ES⁺): t_R = 1.05 min, [M+H⁺] 373.3 (100% purity).

¹H NMR (400 MHz, CDCl₃): δ 0.86-0.99 (m, 3H), 1.45-1.56 (m, 2H), 2.32 (s, 3H), 3.36 (d, $J = 11.5$ Hz, 1H), 3.67 (dd, $J = 11.5, 4.3$ Hz, 1H), 4.59 (d, $J = 17.1$ Hz, 1H), 4.66 (d, $J = 17.1$ Hz, 1H), 4.97-5.11 (m, 1H), 6.78 (d, $J = 2.0$ Hz, 1H), 6.87 (td, $J = 8.2, 0.9$ Hz, 1H), 7.09-7.19 (m, 1H), 7.22-7.33 (m, 3H), 7.33-7.41 (m, 2H), 8.80 (s, 2H), 9.15 (s, 1H).

HRMS: (C₂₃H₂₄N₄O) [M+H⁺] requires 373.2023, found 373.2028.

1-(4-Benzyl-2-ethyl-6-(2-methoxypyrimidin-5-yl)-3,4-dihydroquinoxalin-1(2H)yl)ethanone

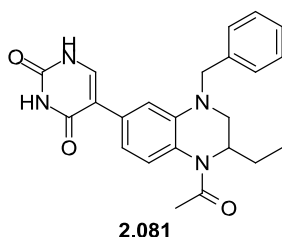


Prepared from **2.067** (30 mg, 0.08 mmol) and (2-methoxypyrimidin-5-yl)boronic acid (25 mg, 0.161 mmol), according to General Procedure 3. Purification of the crude product by High pH MDAP afforded 1-(4-benzyl-2-ethyl-6-(2-methoxypyrimidin-5-yl)-3,4-dihydroquinoxalin-1(2H)-yl)ethanone (14 mg, 0.035 mmol, 43%).

LCMS (High pH, ES⁺): t_R = 1.15 min, [M+H⁺] 403.4, (98% purity). ¹H NMR (400 MHz, CDCl₃): δ 0.87-0.99 (m, 3H), 1.40-1.58 (m, 2H), 2.31 (s, 3H), 3.34 (d, $J = 11.5$ Hz, 1H), 3.65 (dd, $J = 11.5, 4.6$ Hz, 1H), 4.05 (s, 3H), 4.60 (ABq, $J = 17.1$ Hz, 2H), 4.945.13 (m, 1H), 6.73 (d, $J = 1.5$ Hz, 1H), 6.80 (dd, $J = 8.1, 1.5$ Hz, 1H), 7.04-7.17 (m, 1H), 7.21-7.40 (m, 5H), 8.59 (s, 2H).

HRMS: (C₂₄H₂₆N₄O₂) [M+H⁺] requires 403.2129, found [M+H⁺] 403.2117.

5-(1-Acetyl-4-benzyl-2-ethyl-1,2,3,4-tetrahydroquinoxalin-6-yl)pyrimidine-2,4(1H,3H)dione



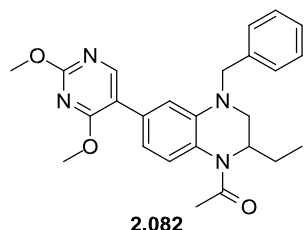
Prepared from **2.067** (63 mg, 0.169 mmol) and (2,4-dioxo-1,2,3,4-tetrahydropyrimidin-5-yl)boronic acid (79 mg, 0.506 mmol) according to General Procedure 3 with heating for 4 h. Further (2,4-dioxo-1,2,3,4-tetrahydropyrimidin-5-yl)boronic acid (2 eq) and Pd(dppf)Cl₂ (12 mg, 0.017 mmol) were added and the reaction was

heated to 110 °C for 2 h. Purification of the crude

product by High pH MDAP afforded 5-(1-acetyl-4-benzyl-2-ethyl-1,2,3,4-tetrahydroquinoxalin-6-yl)pyrimidine-2,4(1*H*,3*H*)-dione (5 mg, 0.012 mmol, 7%) as a white solid.

LCMS (High pH, ES⁺): *t*_R = 0.82 min, [M+H⁺] 405.4, (100% pure). ¹H NMR (500 MHz, DMSO-*d*₆): δ 0.70-0.85 (m, 3H), 1.27-1.42 (m, 2H), 2.16 (s, 3H), 3.23 – 3.48 (m, 2H), 4.51-4.66 (m, 2H), 4.73-4.88 (m, 1H), 6.71-6.86 (m, 1H), 6.96 (s, 1H), 7.03-

7.17 (m, 1H), 7.21-7.29 (m, 3H), 7.30-7.37 (m, 2H), 7.50 (s, 1H), 11.09 (br. s, 2H). **1-(4-benzyl-6-(2,4-dimethoxypyrimidin-5-yl)-2-ethyl-3,4-dihydroquinoxalin-1(2*H*)yl)ethanone**



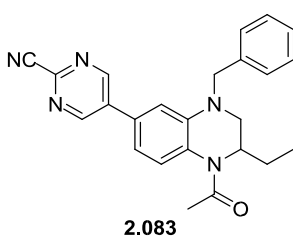
Prepared from **2.067** (30 mg, 0.08 mmol) and (2,4-dimethoxypyrimidin-5-yl)boronic acid (30 mg, 0.16 mmol), according to General Procedure 3. Purification of the crude product by High pH MDAP afforded 1-(4-benzyl-6-(2,4-dimethoxypyrimidin-5-yl)-2-ethyl-3,4-dihydroquinoxalin-

1(2*H*)yl)ethanone (24 mg, 0.055 mmol, 69.0%).

LCMS (High pH, ES⁺): *t*_R = 1.22 min, [M+H⁺] 433.4, (98% purity). ¹H NMR (400 MHz, CDCl₃): δ 0.91 (t, *J* = 7.3 Hz, 3H), 1.37-1.59 (m, 2H), 2.32 (s, 3H), 3.32 (d, *J* = 11.2 Hz, 1H), 3.62 (dd, *J* = 11.5, 4.4 Hz, 1H), 3.89 (s, 3H), 4.02 (s, 3H), 4.56 (dd, *J* = 39.4, 16.6 Hz, 2H), 4.93-5.10 (m, 1H), 6.79 (dd, *J* = 8.1, 2.0 Hz, 1H), 6.83 (d, *J* = 2.0 Hz, 1H), 6.99-7.12 (m, 1H), 7.21-7.39 (m, 5H), 8.20 (s, 1H).

HRMS: (C₂₅H₂₈N₄O₃) [M+H⁺] requires 433.2234, found [M+H⁺] 433.2231.

5-(1-Acetyl-4-benzyl-2-ethyl-1,2,3,4-tetrahydroquinoxalin-6-yl)pyrimidine-2-carbonitrile



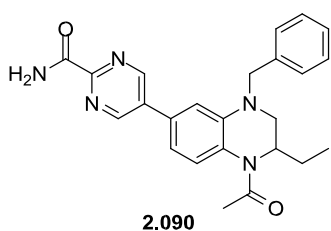
Prepared from **2.067** (50 mg, 0.13 mmol) and (2-cyanopyrimidin-5-yl)boronic acid (40 mg, 0.27 mmol) according to General Procedure 3. Purification of the crude product by silica chromatography (0-50% EtOAc/cyclohexane) afforded 5-(1-acetyl-

4-benzyl-2-ethyl-1,2,3,4-tetrahydroquinoxalin-6-yl)pyrimidine-2-carbonitrile (42 mg, 0.11 mmol, 79%) as a yellow solid.

LCMS (High pH, ES⁺): *t*_R = 1.22 min, [M+H⁺] 398.3 (94% purity). ¹H NMR (400 MHz, CDCl₃): δ 0.94 (t, *J* = 7.1 Hz, 3H), 1.90-2.04 (m, 2H), 2.32 (s, 3H), 3.40 (d, *J* = 11.6 Hz, 1H), 3.70 (dd, *J* = 11.6, 4.5 Hz, 1H), 4.62 (s, 2H), 4.96-5.14 (m, 1H), 6.77 (d, *J* = 1.9 Hz, 1H), 6.89 (dd, *J* = 8.2, 1.9 Hz, 1H), 7.09-7.22 (m, 1H), 7.23-7.27 (m, 2H), 7.29-7.40 (m, 3H), 8.86 (s, 2H).

HRMS: (C₂₄H₂₃N₅O) [M+H⁺] requires 398.1975, found 398.1979.

5-(1-Acetyl-4-benzyl-2-ethyl-1,2,3,4-tetrahydroquinoxalin-6-yl)pyrimidine-2-carboxamide



Prepared from **2.083** (15 mg, 0.04 mmol) according to General Procedure 4. Purification of the crude product by High pH MDAP afforded

5-(1-acetyl-4-benzyl-2-ethyl-1,2,3,4-tetrahydroquinoxalin-6-yl)pyrimidine-2-carboxamide (11 mg, 0.03 mmol, 70%) as a yellow solid.

LCMS (High pH, ES⁺): t_R = 0.92 min, [M+H⁺] 416.4 (100%

pure).

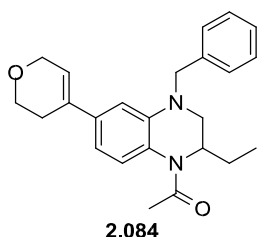
¹H NMR (500 MHz, CDCl₃): δ 0.94 (t, *J* = 7.5 Hz, 3H), 1.41-1.59 (m, 2H), 2.33 (s, 3H), 3.40 (d, *J* = 11.5 Hz, 1H), 3.71 (dd, *J* = 11.5, 3.6 Hz, 1H), 4.63 (ABq, *J* = 17.3 Hz, 2H), 4.99-5.14 (m, 1H), 6.14 (br s, 1H), 6.80 (d, *J* = 1.8 Hz, 1H), 6.92 (dd, *J* = 8.2, 1.8 Hz, 1H), 7.12-7.21 (m, 1H), 7.24-7.33 (m, 3H), 7.35-7.40 (m, 2H), 7.80 (br s, 1H), 8.90 (s, 2H).

¹³C

NMR (126 MHz, CDCl₃): δ 10.5, 23.1, 23.7, 47.7, 52.7, 54.8, 109.5, 114.5, 123.9, 126.5, 126.3, 127.6, 129.0, 131.4, 135.5, 137.3, 139.5, 155.1, 155.6, 164.4, 169.4. M.pt.: 106-109 °C
ν_{max} (neat): 3464, 3254, 2965, 2932, 2873, 2235, 1699, 1649, 1601, 1571, 1518, 1451, 1380, 1326, 1254, 1112, 910, 841, 730 cm⁻¹.

HRMS: (C₂₄H₂₅N₅O₂) [M+H⁺] requires 416.2081, found 416.2075.

1-(4-Benzyl-6-(3,6-dihydro-2H-pyran-4-yl)-2-ethyl-3,4-dihydroquinoxalin-1(2H)yl)ethanone

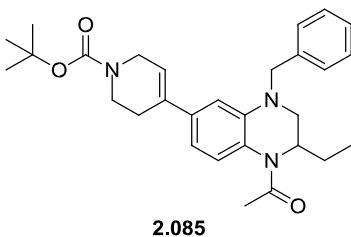


Prepared from **2.067** (45 mg, 0.121 mmol) and (3,6-dihydro-2H-pyran-4-yl)boronic acid pinacol ester (51 mg, 0.24 mmol) according to General Procedure 3. The crude product was purified by silica chromatography (0-50% EtOAc/cyclohexane) to afford 1-(4-benzyl-

6-(3,6-dihydro-2H-pyran-4-yl)-2-ethyl-3,4-dihydroquinoxalin-1(2H)yl)ethanone (34 mg, 0.090 mmol, 75%)..

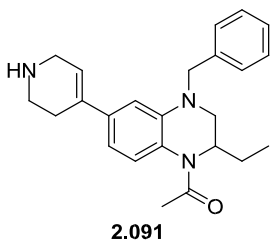
LCMS (High pH, ES⁺): t_R = 1.25 min, [M+H]⁺ 377.3, (100% purity). ¹H NMR (400 MHz, CDCl₃): δ 0.89 (t, *J* = 7.2 Hz, 3H), 1.35 – 1.52 (m, 2H), 2.28 (s, 3H), 2.38-2.44 (m, 2H), 3.27 (d, *J* = 11.5 Hz, 1H), 3.57 (dd, *J* = 11.5, 4.6 Hz, 1H), 3.89 (t, *J* = 5.4 Hz, 2H), 4.28 (q, *J* = 2.7 Hz, 2H), 4.57 (ABq, *J* = 16.6 Hz, 2H), 4.98 (br. s., 1H), 5.98 (br. s., 1H), 6.68-6.75 (m, 2H), 6.94-7.02 (m, 1H), 7.23-7.32 (m, 3H), 7.32-7.38 (m, 2H).

tert-Butyl 4-(1-acetyl-4-benzyl-2-ethyl-1,2,3,4-tetrahydroquinoxalin-6-yl)-5,6-dihydropyridine-1(2H)-carboxylate



Prepared from **2.067** (45 mg, 0.121 mmol) and (1-(tert-butoxycarbonyl)-1,2,3,6-tetrahydropyridin-4-yl)boronic acid pinacol ester (75 mg, 0.24 mmol) according to General Procedure 3. The crude product was purified by

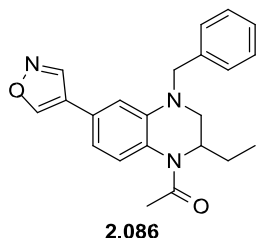
silica chromatography (0-50% EtOAc/cyclohexane) to afford *tert*-butyl 4-(1-acetyl-4-benzyl-2-ethyl-1,2,3,4-tetrahydroquinoxalin-6-yl)-5,6-dihydropyridine-1(2*H*)-carboxylate (33 mg, 0.069 mmol, 58%) LCMS (High pH, ES⁺): *t*_R = 1.46 min, [M+H]⁺ 476.4 (95% purity). ¹H NMR (400 MHz, CDCl₃): δ 0.86 (t, *J* = 7.2 Hz, 3H), 1.47 (s, 9H), 2.25 (s, 3H), 2.40 (br. s., 2H), 3.20-3.28 (m, 1H), 3.56 (t, *J* = 5.6 Hz, 3H), 4.00 (q, *J* = 2.4 Hz, 3H), 4.54 (ABq, *J* = 16.6 Hz, 3H), 4.91-5.02 (m, 1H), 5.84-5.91 (m, 1H), 6.63-6.71 (m, 2H), 6.89-6.98 (m, 1H), 7.19-7.29 (m, 3H), 7.30-7.36 (m, 2H). **1-(4-Benzyl-2-ethyl-6-(1,2,3,6-tetrahydropyridin-4-yl)-3,4-dihydroquinoxalin-1(2*H*))ethanone**



To a solution of **2.085** (29 mg, 0.061 mmol) in DCM (0.6 mL) was added TFA (94 μL, 1.219 mmol), and the reaction was stirred at rt for 6 h. The reaction mixture was purified by ion exchange chromatography (sulphonic acid (SCX) 1 g, sequential solvents MeOH, 2 M NH₃/MeOH). The appropriate fractions were evaporated *in vacuo* to afford 1-(4-benzyl-2-ethyl-6-(1,2,3,6-tetrahydropyridin-4-yl)-3,4-dihydroquinoxalin-1(2*H*))ethanone (22 mg, 0.059 mmol, 96%) as a brown gum.

LCMS (High pH, ES⁺): *t*_R = 1.09 min, [M+H]⁺ 376.2, (94% purity). ¹H NMR (400 MHz, CDCl₃): δ 0.86 (t, *J* = 7.2 Hz, 3H), 1.30-1.51 (m, 1H), 1.75 (br. s., 1H), 2.25 (s, 3H), 2.30-2.37 (m, 2H), 3.05 (t, *J* = 5.7 Hz, 2H), 3.23 (d, *J* = 11.5 Hz, 1H), 3.44-3.50 (m, 2H), 3.53 (dd, *J* = 11.5, 4.6 Hz, 1H), 4.53 (ABq, *J* = 17.1 Hz, 2H), 4.96 (br. s., 1H), 5.97 (br. s., 1H), 6.66-6.72 (m, 2H), 6.93 (br. s., 1H), 7.20-7.28 (m, 3H), 7.29-7.35 (m, 2H). NH was not observed.

1-(4-Benzyl-2-ethyl-6-(isoxazol-4-yl)-3,4-dihydroquinoxalin-1(2*H*))ethanone A

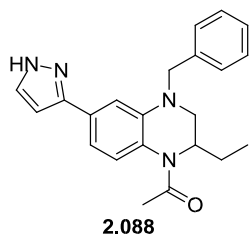


mixture of **2.067** (24 mg, 0.064 mmol), isoxazole-4-boronic acid pinacol ester (19 mg, 0.096 mmol), DIPEA (34 μL, 0.19 mmol) and Pd(dppf)Cl₂ (4.7 mg, 0.0064 mmol) were placed in a microwave vial and suspended in 1,4-dioxane (0.58 mL) and H₂O (0.12 mL). The vial was sealed, evacuated and refilled with N₂. The reaction was heated in a Biotage Initiator microwave at 110 °C for 1 h. The

reaction mixture was cooled, filtered through Celite and evaporated to dryness. Purification of the crude product by High pH MDAP afforded 1-(4-benzyl-2-ethyl-6-(isoxazol-4-yl)-3,4-dihydroquinoxalin-1(2*H*))ethanone (10 mg, 0.03 mmol, 43%) as a yellow gum.

LCMS (High pH, ES⁺): *t*_R = 1.16 min, [M+H]⁺ 362.4, (96% purity). ¹H NMR (400 MHz, CDCl₃): δ 0.91 (t, *J* = 7.5 Hz, 3H), 1.37-1.57 (m, 2H), 2.30 (s, 3H), 3.32 (d, *J* = 11.5 Hz, 1H), 3.62 (dd, *J* = 11.5, 4.4 Hz, 1H), 4.59 (ABq, *J* = 16.9 Hz, 2H), 4.91-5.10 (m, 1H), 6.71 (d, *J* = 2.0 Hz, 1H), 6.79 (d, *J* = 0.7 Hz, 1H), 6.98-7.11 (m, 1H), 7.21-7.41 (m, 5H), 8.39 (s, 1H), 8.51 (s, 1H).

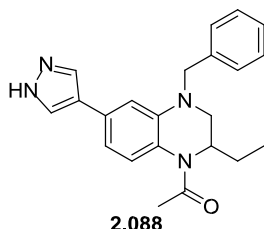
HRMS: (C₂₂H₂₃N₃O₂) [M+H]⁺ requires 362.1863, found 362.1861.

1-(4-Benzyl-2-ethyl-6-(1H-pyrazol-3-yl)-3,4-dihydroquinoxalin-1(2H)-yl)ethanone A

solution of **2.067** (24 mg, 0.064 mmol), (1*H*-pyrazol-3-yl)boronic acid (14 mg, 0.129 mmol), DIPEA (34 μ L, 0.193 mmol) and Pd(dppf)Cl₂ (5 mg, 6.43 μ mol) in water (0.15 mL) and 1,4-dioxane (0.75 mL) was sealed in a microwave vial, placed under N₂ and

heated in a Biotage Initiator microwave to 110 °C for 1 h. The reaction mixture was filtered through Celite and evaporated to dryness. Purification of the crude product by High pH MDAP afforded 1-(4-benzyl-2-ethyl-6-(1*H*-pyrazol-3-yl)-3,4-dihydroquinoxalin-1(2*H*)-yl)ethanone (16 mg, 0.044 mmol, 69%) as a yellow solid. LCMS (High pH, ES⁺): t_R = 1.03 min, [M+H⁺] 361.4, (99% purity). ¹H NMR (400 MHz, CDCl₃): δ 0.88 (t, *J* = 7.3 Hz, 3H), 1.33-1.59 (m, 2H), 2.30 (s, 3H), 3.26 (d, *J* = 11.5 Hz, 1H), 3.56 (dd, *J* = 11.5, 4.5 Hz, 1H), 4.54 (d, *J* = 16.9 Hz, 1H), 4.66 (d, *J* = 16.9 Hz, 1H), 4.95-5.06 (m, 1H), 6.47 (d, *J* = 2.2 Hz, 1H), 7.00-7.09 (m, 2H), 7.12 (s, 1H), 7.22-7.37 (m, 5H), 7.54 (d, *J* = 2.2 Hz, 1H). NH not observed. ¹³C NMR (101 MHz, CDCl₃): δ 10.4, 23.0, 23.5, 48.0, 52.0, 54.3, 102.6, 108.3, 113.5, 122.4, 126.0, 126.7, 126.8, 127.3, 128.8, 133.1, 137.8, 139.4, 148.5, 169.7. M.pt.: 88-93 °C v_{max} (neat): 3195, 2964, 2929, 1619, 1514, 1542, 1395, 1321, 1251, 1114, 1048, 965, 925, 848, 765, 731 698 cm⁻¹.

HRMS: (C₂₂H₂₄N₄O) [M+H⁺] requires 361.2023, found [M+H⁺] 361.2023.

1-(4-Benzyl-2-ethyl-6-(1H-pyrazol-4-yl)-3,4-dihydroquinoxalin-1(2H)-yl)ethanone A

mixture of **2.067** (30 mg, 0.60 mmol), (1-(*tert*-butoxycarbonyl)-1*H*-pyrazol-4-yl)boronic acid pinacol ester (36 mg, 0.12 mmol), Pd₂(dba)₃ (3.7 mg, 0.004 mmol), XPhos (3.8 mg, 0.008 mmol) and K₃PO₄ (34 mg, 0.16 mmol) were suspended in 1-butanol (1 mL) in a microwave vial. The vial was sealed, evacuated and placed under

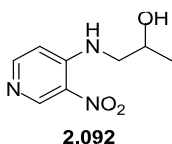
N₂. The reaction was heated in a Biotage Initiator microwave at 115 °C for 3 h. The reaction mixture was cooled, filtered through Celite and evaporated to dryness. Purification of the crude product by High pH MDAP afforded 1-(4-benzyl-2-ethyl-6-(1*H*-pyrazol-4-yl)-3,4-dihydroquinoxalin-1(2*H*)-yl)ethanone (11 mg, 0.030 mmol, 38%).

LCMS (High pH, ES⁺): t_R = 0.98 min, [M+H⁺] 361.4, (99% purity). ¹H NMR (400 MHz, CDCl₃): δ 0.82-0.96 (m, 3H), 1.39-1.49 (m, 2H), 2.30 (s, 3H), 3.28 (d, *J* = 11.5 Hz, 1H), 3.59 (dd, *J* = 11.5, 4.9 Hz, 1H), 4.54 (d, *J* = 16.8 Hz, 1H), 4.64 (d, *J* = 16.8 Hz, 1H), 4.94-5.07 (m, 1H), 6.79-6.86 (m, 2H), 7.00 (br s, 1H), 7.22-7.41 (m, 5H), 7.72 (s, 2H).

NH proton not observed.

HRMS: (C₂₂H₂₄N₄O) [M+H⁺] requires 361.2023, found 361.2014.

1-((3-Nitropyridin-4-yl)amino)propan-2-ol

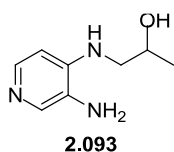


A solution of 4-chloro-3-nitropyridine **2.091** (780 mg, 4.92 mmol), 1-aminopropan-2-ol (399 μ L, 5.17 mmol) and DIPEA (902 μ L, 5.17 mmol) in EtOH (7 mL) heated to 150 °C in a Biotage Initiator microwave for 15 min. After cooling, the reaction was evaporated and purified by silica chromatography (75-100% EtOAc) to afford 1-((3-nitropyridin-4-yl)amino)propan-2-ol (846 mg, 4.29 mmol, 87%) as a bright yellow solid.

LCMS (High pH, ES⁺): t_R = 0.55 min, [M+H⁺] 198.2, (100% pure). ¹

¹H NMR (400 MHz, CDCl₃): δ 1.38 (d, J = 6.1 Hz, 3H), 1.94-2.16 (m, 1H), 3.31 (ddd, J = 13.3, 7.8, 5.1 Hz, 1H), 3.45 (ddd, J = 13.3, 6.1, 3.9 Hz, 1H), 4.05-4.32 (m, 1H), 6.76 (d, J = 6.1 Hz, 1H), 8.31 (dd, J = 6.1, 0.7 Hz, 1H), 8.37-8.56 (m, 1H), 9.23 (s, 1H).

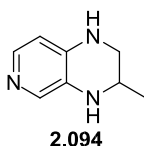
1-((3-Aminopyridin-4-yl)amino)propan-2-ol



A solution of 1-((3-nitropyridin-4-yl)amino)propan-2-ol **2.092** (825 mg, 4.18 mmol) in MeOH (8.5 mL) was passed through a Thales H-cube Flow Hydrogenator with a 10% Pd/C CatCart in full H₂ mode at a rate of 1 mL/min. The solvent was evaporated *in vacuo* to afford 1-((3-aminopyridin-4-yl)amino)propan-2-ol (695 mg, 4.16 mmol, 99%) as a beige solid.

LCMS (High pH, ES⁺): t_R = 0.40 min, [M+H⁺] 168.1, (100% purity). ¹H NMR (400 MHz, DMSO-d₆): δ 1.12 (d, J = 6.1 Hz, 3H), 2.87-3.14 (m, 2H), 3.83 (sxt, J = 6.1 Hz, 1H), 4.57 (br. s., 2H), 5.32 (t, J = 5.6 Hz, 1H), 6.38 (d, J = 5.5 Hz, 1H), 7.59 (d, J = 5.5 Hz, 1H), 7.64 (s, 1H). OH not observed.

3-Methyl-1,2,3,4-tetrahydropyrido[3,4-*b*]pyrazine



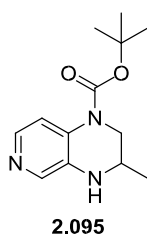
A solution of 1-((3-aminopyridin-4-yl)amino)propan-2-ol **2.093** (668 mg, 4.00 mmol) in HBr (48 wt. % in water) (25 mL, 221 mmol) was heated to 130 °C for 24 h. The solvent was evaporated *in vacuo* and the residue was purified by silica chromatography (0-20% 2 M NH₃ in MeOH/DCM). The product was purified by ion exchange chromatography (sulphonic acid (SCX), 20 g, sequential solvents MeOH, 2 M NH₃/MeOH), appropriate fractions were evaporated *in vacuo* to afford 3-methyl-1,2,3,4-tetrahydropyrido[3,4-*b*]pyrazine (437 mg, 2.93 mmol, 73%) as a brown gum.

LCMS (High pH, ES⁺): t_R = 0.42 min, [M+H]⁺ 150.1, (100% purity). ¹H NMR (400 MHz, DMSO-d₆): δ 1.09 (d, J = 6.3 Hz, 3H), 2.85 (dd, J = 10.9, 7.8 Hz, 1H), 3.15-3.23 (m, 1H), 3.26 (dt, J = 10.9, 3.3 Hz, 1H), 5.36 (br. s., 1H), 6.23 (br. s., 1H), 6.28 (d, J = 5.3 Hz, 1H), 7.45 (d, J = 5.3 Hz, 1H), 7.52 (s, 1H).

¹³

C NMR (101 MHz, DMSO-d₆): δ 19.7, 44.0, 47.3, 107.1, 130.5, 133.9, 139.6, 140.2.

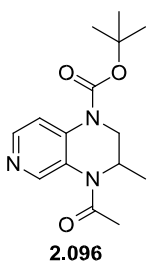
ν_{max} (neat): 3231, 2965, 2926, 2853, 1597, 1524, 1348, 1297, 1274, 1180, 1074, 1053, 891, 862, 810, 691 cm⁻¹.



tert-Butyl 3-methyl-3,4-dihydropyrido[3,4-*b*]pyrazine-1(2*H*)-carboxylate To a solution of 3-methyl-1,2,3,4-tetrahydropyrido[3,4-*b*]pyrazine **2.095** (300 mg, 2.011 mmol) in pyridine (12 mL) at 0 °C stirred under N₂ was added *di*tert-butyl dicarbonate (1.5 mL, 3.02 mmol, 2 M in DCM) dropwise. The reaction mixture was gradually allowed to warm to rt and stirred for 1 h. The reaction was concentrated, then azeotroped with toluene. The crude product was purified by silica chromatography (EtOAc), appropriate fractions were evaporated *in vacuo* to afford *tert*-butyl 3-methyl-3,4-dihydropyrido[3,4-*b*]pyrazine-1(2*H*)-carboxylate (381 mg, 1.528 mmol, 76%) as a white solid.

LCMS (High pH, ES⁺): t_R = 0.94 min, [M+H]⁺ 250.3, (100% purity). ¹H NMR (400 MHz, CDCl₃): δ 1.21 (d, *J* = 6.3 Hz, 3H), 1.53 (s, 9H), 3.07 (dd, *J* = 12.7, 8.3 Hz, 1H), 3.43-3.53 (m, 1H), 4.09 (dd, *J* = 12.7, 3.0 Hz, 1H), 7.58 (d, *J* = 5.4 Hz, 1H), 7.83 (d, *J* = 5.4 Hz, 1H), 7.92 (s, 1H). NH not observed. ¹³

C NMR (101 MHz, CDCl₃): δ 19.3, 28.3, 45.9, 48.0, 82.0, 116.5, 131.1, 133.0, 136.8, 138.6, 152.6.

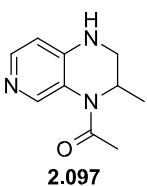


tert-Butyl 4-acetyl-3-methyl-3,4-dihydropyrido[3,4-*b*]pyrazine-1(2*H*)-carboxylate To a solution of *tert*-butyl 3-methyl-3,4-dihydropyrido[3,4-*b*]pyrazine-1(2*H*)carboxylate **2.095** (380 mg, 1.524 mmol), pyridine (740 μL, 9.15 mmol) and DMAP (186 mg, 1.524 mmol) in DCM (14 mL) stirred under N₂ was added acetyl chloride (434 μL, 6.10 mmol) dropwise. The reaction mixture was stirred at rt for 3 days. The reaction was quenched with water (20 mL) and extracted. The organic layer was washed with water (2 x 20 mL), dried

through a hydrophobic frit and evaporated to dryness. The crude product was purified by silica chromatography (0-100% EtOAc/cyclohexane), appropriate fractions were evaporated *in vacuo* to afford *tert*-butyl 4-acetyl-3-methyl-3,4-dihydropyrido[3,4-*b*]pyrazine-1(2*H*)carboxylate (285 mg, 0.978 mmol, 64%) as a brown oil. LCMS (High pH, ES⁺): t_R = 0.89 min, [M+H]⁺ 292.2, (100% purity).

¹H NMR (400 MHz, CDCl₃): δ 1.04 (d, *J* = 6.8 Hz, 3H), 1.56 (s, 9H), 2.25 (s, 3H), 3.69 (dd, *J* = 12.7, 5.4 Hz, 1H), 3.82 (d, *J* = 12.7 Hz, 1H), 5.13-5.28 (m, 1H), 8.11 (d, *J* = 5.7 Hz, 1H), 8.31 (d, *J* = 5.7 Hz, 1H), 8.34-8.45 (m, 1H).

1-(3-Methyl-2,3-dihydropyrido[3,4-*b*]pyrazin-4(1*H*)-yl)ethanone



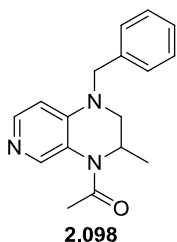
A suspension of *tert*-butyl 4-acetyl-3-methyl-3,4-dihydropyrido[3,4-*b*]pyrazine-1(2*H*)-carboxylate **2.096** (285 mg, 0.978 mmol) in HCl (4 M in 1,4-dioxane) (20 mL, 78 mmol) was stirred at rt for 18 h. The solvent and excess HCl were removed under reduced pressure and the crude product was purified by ion exchange chromatography (sulphonic acid (SCX), 5 g, sequential solvents MeOH, 2 M

NH₃/MeOH). The appropriate fractions were evaporated *in vacuo* to afford 1-(3-methyl-2,3-dihydropyrido[3,4-*b*]pyrazin-4(1*H*)-yl)ethanone (183 mg, 0.957 mmol, 98%) as a brown solid.

LCMS (High pH, ES⁺): t_R = 0.48 min, [M+H⁺] 192.2, (94% purity).

¹H NMR (400 MHz, CDCl₃): δ 0.97-1.14 (m, 3H), 2.27 (s, 3H), 3.27 (dd, *J* = 12.0, 3.8 Hz, 1H), 3.45 (dd, *J* = 12.0, 4.3 Hz, 1H), 5.09-5.19 (m, 1H), 5.20-5.32 (m, 1H), 6.50 (d, *J* = 5.2 Hz, 1H), 7.99 (d, *J* = 5.2 Hz, 1H), 8.05-8.17 (m, 1H).

1-(1-Benzyl-3-methyl-2,3-dihydropyrido[3,4-*b*]pyrazin-4(1*H*)-yl)ethanone



A mixture of 1-(3-methyl-2,3-dihydropyrido[3,4-*b*]pyrazin-4(1*H*)-yl)ethanone **2.097** (40 mg, 0.21 mmol) and sodium hydride (60% in mineral oil, 17 mg, 0.42 mmol) in DMF (2 mL) was stirred at 0 °C for 5 min then treated with benzyl bromide (30 μL, 0.25 mmol) and stirred under N₂ at 0 °C for 45 min. The reaction was quenched with sat. aq. NH₄Cl solution and evaporated to dryness. The crude product was combined with that from an identically

performed reaction with 11 mg **2.097**. The residues were purified by silica chromatography (0-20% 2 M NH₃ in MeOH/DCM), fractions were evaporated to dryness and further purified by High pH MDAP to afford 1-(1-benzyl-3-methyl-2,3-dihydropyrido[3,4-*b*]pyrazin-4(1*H*)-yl)ethanone (37 mg, 0.13 mmol, 49% based on combined reactions) as a yellow oil.

LCMS (High pH, ES⁺): t_R = 0.85 min, [M+H⁺] 282.2, (100% purity). ¹H NMR (600 MHz, CDCl₃): δ 1.08 (d, *J* = 7.3 Hz, 3H), 2.27 (s, 3H), 3.19 (d, *J* = 11.7 Hz, 1H), 3.60 (dd, *J* = 11.7, 4.4 Hz, 1H), 4.53 (d, *J* = 17.0 Hz, 1H), 4.60 (d, *J* = 17.0 Hz, 1H),

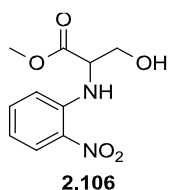
5.18-5.33 (m, 1H), 6.59 (d, *J* = 5.9 Hz, 1H), 7.20 (d, *J* = 7.3 Hz, 2H), 7.28-7.32 (m, 1H), 7.32-7.37 (m, 2H), 8.06 (d, *J* = 5.9 Hz, 1H), 8.08-8.15 (m, 1H).¹³

C NMR (151 MHz, CDCl₃): δ 16.8, 22.7, 40.7, 53.3, 53.7, 105.3, 119.3, 126.6, 127.8, 129.0, 136.2, 143.5, 145.3, 147.1, 168.7.

v_{max} (neat): 3381, 3030, 2973, 2931, 2871, 1651, 1593, 1522, 1453, 1379, 1324, 1241, 1203, 1113, 1064, 942, 805, 732, 701 cm⁻¹.

HRMS: (C₁₇H₁₉N₃O) [M+H⁺] requires 282.1601, found [M+H⁺] 282.1600.

Methyl 3-hydroxy-2-((2-nitrophenyl)amino)propanoate



A solution of 1-fluoro-2-nitrobenzene **2.105** (3.82 mL, 36.1 mmol), *DL*serine methyl ester hydrochloride (8.44 g, 54.2 mmol) and DIPEA (15.78 mL, 90 mmol) in acetonitrile (41 mL) was divided between three 20 mL microwave vials, placed under N₂, the vessels sealed and heated in a

Biotage Initiator microwave at 130 °C for 40 min. The reaction mixtures were combined, evaporated and purified by silica chromatography (0-100% EtOAc/cyclohexane), appropriate fractions were evaporated *in vacuo* to afford methyl 3-hydroxy-2-((2-nitrophenyl)amino)propanoate (4.36 g, 18.14 mmol, 50%) as a bright yellow solid.

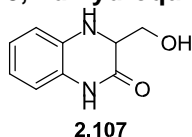
LCMS (High pH, ES⁺): $t_R = 0.79$ min, $[M+H]^+$ 240.1, (100% purity).

¹H NMR (500 MHz, CDCl₃): δ 2.23 (br. s, 1H), 3.85 (s, 3H), 4.04-4.17 (m, 2H), 4.38-4.46 (m, 1H), 6.77 (ddd, $J = 8.4, 7.1, 1.0$ Hz, 1H), 6.82 (d, $J = 8.5$ Hz, 1H), 7.48 (ddd, $J = 8.5, 7.1, 1.0$ Hz, 1H), 8.24 (dd, $J = 8.5, 1.0$ Hz, 1H), 8.60 (d, $J = 7.1$ Hz, 1H). ¹³C NMR (126 MHz, CDCl₃): δ 53.0, 57.4, 62.8, 113.8, 116.7, 127.1, 133.2, 136.2, 143.8, 171.0.

M.pt.: 138-141 °C. ν_{max} (neat): 3490, 3359, 1730, 1621, 1567, 1509, 1350, 1311, 1258, 1218, 1149, 1064, 1037, 964, 863, 784, 749, 695 cm⁻¹.

HRMS: (C₁₀H₁₂N₂O₅) $[M+H]^+$ requires 241.0819, found $[M+H]^+$ 241.0815. Analysis consistent with literature.³²⁰

(Hydroxymethyl)-3,4-dihydroquinoxalin-2(1H)-one



Hydrogenation method

A solution of methyl 3-hydroxy-2-((2-nitrophenyl)amino)propanoate **2.106** (3.648 g, 15.19 mmol) and 10% Pd/C (0.646 g, 3.04 mmol) in MeOH (250 ml) was stirred under an atmosphere of hydrogen at rt. The reaction was stirred for 3 h then filtered through Celite and stood overnight. The reaction mixture was evaporated to dryness to afford (hydroxymethyl)-3,4-dihydroquinoxalin-2(1H)-one (2.59 g, 14.54 mmol, 96%) as a brown gum.

SnCl₂ Reduction method

To a solution of methyl 3-hydroxy-2-((2-nitrophenyl)amino)propanoate **2.106** (60 mg, 0.250 mmol) in EtOH (5 mL) was added SnCl₂ (237 mg, 1.249 mmol). The reaction mixture was stirred at 90 °C for 24 h. The reaction mixture was evaporated to dryness and partitioned between EtOAc (10 mL) and sat. aq. NaHCO₃ (10 mL). The aqueous phase was extracted with EtOAc (3 x 25 mL) and DCM (3 x 25 mL) and the combined organics were dried through a hydrophobic frit and evaporated to dryness. The residue was purified by silica chromatography (50-100% EtOAc/cyclohexane) to afford 3-(hydroxymethyl)-3,4-dihydroquinoxalin-2(1H)-one (47 mg, 0.237 mmol, 95%) as a brown-red gum.

Copper-catalysed coupling/cyclisation method

DL-serine (210 mg, 2.00 mmol), 2-bromoaniline **2.108** (172 mg, 1.00 mmol), copper(I) chloride (4.95 mg, 0.05 mmol), *N*1,*N*2-dimethylethane-1,2-diamine (22 μ L, 0.20 mmol) and potassium phosphate tribasic (425 mg, 2.000 mmol) were placed in an oven-dried tube which was sealed and placed under N₂. Anhydrous, degassed DMSO (3.5 mL) was added and the reaction was evacuated and placed under N₂ three times. The reaction mixture was heated to 110 °C in an oil bath for 40 h. The reaction mixture was cooled, diluted with EtOAc (10 mL) and filtered

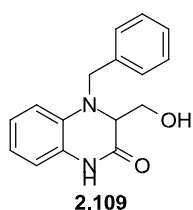
through Celite. The filtrate was washed with water (2 x 10 mL) and the combined aqueous phases extracted with ethyl acetate (3 x 20 mL) and chloroform (3 x 20 mL). The product could not be fully extracted from the aqueous phase – the aqueous and organics were evaporated to dryness and the residue was purified by silica chromatography (0-100% EtOAc/cyclohexane) to afford 3-(hydroxymethyl)-3,4-dihydroquinoxalin-2(1*H*)-one (110 mg, 0.617 mmol, 62%) as a yellow oil that solidified on standing.

LCMS (High pH, ES⁺): $t_R = 0.48$ min, $[M+H]^+$ 179.2, (72% purity).

¹H NMR (400 MHz, MeOD-*d*₄): δ 3.72-3.82 (m, 2H), 3.93 (dd, $J = 7.1, 3.9$ Hz, 1H), 6.67 (ddd, $J = 7.7, 1.2$ Hz, 1H), 6.73-6.78 (m, 2H), 6.85 (ddd, $J = 7.7, 1.5$ Hz, 1H).

Exchangeable protons were not observed. Analysis consistent with literature.²⁹⁶

(Hydroxymethyl)-3,4-dihydroquinoxalin-2(1*H*)-one



To a solution of 3-(hydroxymethyl)-3,4-dihydroquinoxalin-2(1*H*)-one **2.107** (350 mg, 1.964 mmol) and benzaldehyde (200 μ L, 1.964 mmol) in THF (5 mL) and DMF (2.5 mL) was added dibutylchlorostannane (30 mg, 0.098 mmol), and the reaction was stirred for 2 h before adding phenylsilane (266 μ L, 2.161 mmol). The reaction mixture was stirred at rt for 40 h, then

concentrated and purified by silica chromatography (0-100% EtOAc/cyclohexane). Appropriate fractions were evaporated to afford 4-benzyl-3-(hydroxymethyl)-3,4-dihydroquinoxalin-2(1*H*)-one (490 mg, 1.826 mmol, 93%) as a white solid.

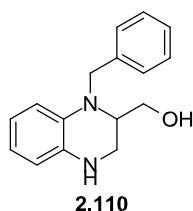
LCMS (High pH, ES⁺): $t_R = 0.85$ min, $[M+H]^+$ 269.1, (100% purity).

¹H NMR (500 MHz, DMSO-*d*₆): δ 3.58 (d, $J = 4.7$ Hz, 2H), 3.92 (t, $J = 4.7$ Hz, 1H), 4.46 (d, $J = 15.9$ Hz, 1H), 4.71 (d, $J = 15.9$ Hz, 1H), 4.82-5.04 (m, 1H), 6.55-6.61 (m, 2H), 6.71-6.76 (m, 2H), 7.24 (m, $J = 4.4$ Hz, 1H), 7.32 (d, $J = 4.4$ Hz, 4H), 10.43 (s, 1H).

¹³C NMR (126 MHz, DMSO-*d*₆): δ 52.4, 61.0, 64.9, 112.7, 115.0, 117.8, 123.2, 127.1, 127.4, 127.6, 128.9, 134.4, 138.7, 166.5. M.pt.: 199- 201 °C. ν_{max} (neat): 3327, 3215, 3156, 3099, 2927, 2869, 1680, 1509, 1415, 1348, 1311, 1251, 1165, 1127, 1061, 855, 788, 731, 692 cm^{-1} .

HRMS: (C₁₆H₁₆N₂O₂) $[M+H]^+$ requires 269.1285, found $[M+H]^+$ 269.1279.

(1-Benzyl-1,2,3,4-tetrahydroquinoxalin-2-yl)methanol



To a solution of 4-benzyl-3-(hydroxymethyl)-3,4-dihydroquinoxalin-2(1*H*)-one **2.109** (3.96 g, 14.8 mmol) in THF (200 mL) stirred under N₂ at rt was added BH₃·THF (44.3 mL, 44.3 mmol, 1 M in THF) over 10 min. The reaction mixture was stirred at rt for 3 hr then heated to 60 °C for 3 h. The reaction mixture was cooled to rt, quenched with MeOH (5 mL) and 1 M HCl (5 mL) and stirred for 30 min. The mixture was basified with 1 M NaOH and extracted with

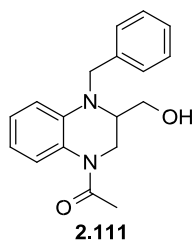
EtOAc (3 x 100 mL). The combined organics were dried through a hydrophobic frit and evaporated to dryness. The residue was purified by silica chromatography (40-100% EtOAc/cyclohexane) to afford (1-benzyl-1,2,3,4-tetrahydroquinoxalin-2-yl)methanol (3.31 g, 13.0 mmol, 88%) as a clear oil, which solidified on standing.

LCMS (High pH, ES⁺): t_R = 0.99 min, [M+H⁺] 255.2, (98% purity). ¹H NMR (400 MHz, CDCl₃): δ 3.28 (br. s, 2H), 3.34 (dd, J = 11.0, 3.4 Hz, 1H), 3.47 (dd, J = 11.0, 2.0 Hz, 1H), 3.49-3.54 (m, 1H), 3.75 (dd, J = 11.0, 4.4 Hz, 1H), 3.85 (dd, J = 11.0, 6.1 Hz, 1H), 4.60 (d, J = 2.7 Hz, 2H), 6.56-6.63 (m, 3H), 6.66-6.72 (m, 1H), 7.24-7.32 (m, 1H), 7.32-7.40 (m, 4H). ¹³

C NMR (101 MHz, CDCl₃): δ 41.5, 55.0, 58.4, 63.5, 112.8, 114.7, 117.3, 120.2, 126.8, 127.0, 128.7, 133.0, 134.6, 138.8. M.pt.: 96-98 °C. ν_{max} (neat): 3273, 3059, 2936, 2873, 1602, 1507, 1450, 1351, 1296, 1238, 1171, 1032, 912, 788, 743, 721, 695 cm⁻¹.

HRMS: (C₁₆H₁₈N₂O) [M+H⁺] requires 255.1492, found [M+H⁺] 255.1479.

1-(4-Benzyl-3-(hydroxymethyl)-3,4-dihydroquinoxalin-1(2H)-yl)ethanone



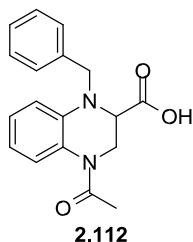
To a solution of (1-benzyl-1,2,3,4-tetrahydroquinoxalin-2-yl)methanol **2.110** (3.01 g, 11.84 mmol) and pyridine (1.91 mL, 23.67 mmol) in DCM (96 ml) stirred under N₂ at 0 °C was added acetyl chloride (0.97 mL, 13.61 mmol). The reaction mixture was stirred at 0 °C for 15 min, then quenched with water (15 mL) and extracted with DCM (3 x 30 mL). The combined organics were dried through a hydrophobic frit and evaporated to dryness.

The residue was purified by silica chromatography (0-100% EtOAc/cyclohexane), appropriate fractions were evaporated *in vacuo* to afford 1-(4-benzyl-3-(hydroxymethyl)-3,4-dihydroquinoxalin-1(2H)-yl)ethanone (2.99 g, 10.09 mmol, 85%) as a white solid.

LCMS (High pH, ES⁺): t_R = 0.97 min, [M+H⁺] 297.3, (92% pure). ¹H NMR (400 MHz, CDCl₃): δ 2.37 (s, 3H), 2.81-2.91 (m, 1H), 2.96 (d, J = 13.0 Hz, 1H), 3.25 (t, J = 11.6 Hz, 1H), 3.62-3.85 (m, 2H), 4.65 (s, 2H), 5.12 (d, J = 13.0 Hz, 1H), 6.59 (dd, J = 8.3, 1.0 Hz, 1H), 6.69 (ddd, J = 7.5, 1.0 Hz, 1H), 6.98-7.05 (m, 1H), 7.12 (d, J = 7.5 Hz, 1H), 7.18 (d, J = 7.3 Hz, 2H), 7.24-7.37 (m, 3H). ¹³

C NMR (101 MHz, CDCl₃): δ 22.0, 38.8, 53.4, 60.2, 60.4, 112.1, 115.7, 124.4, 124.9, 126.1, 127.1, 127.2, 128.8, 137.5, 138.3, 171.2. M.pt.: 159-161 °C
 ν_{max} (neat): 3389, 3042, 2912, 2867, 1624, 1596, 1504, 1412, 1396, 1357, 1061, 1031, 982, 925, 740, 696 cm⁻¹.

HRMS: (C₁₈H₂₀N₂O₂) [M+H⁺] requires 297.1598, found [M+H⁺] 297.1599. **4-Acetyl-1-benzyl-1,2,3,4-tetrahydroquinoxaline-2-carboxylic acid**



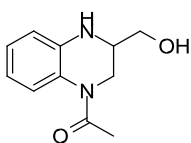
2.112

1-(4-Benzyl-3-(hydroxymethyl)-3,4-dihydroquinoxalin-1(2*H*)-yl)ethanone **2.111** (400 mg, 1.350 mmol), NMO (949 mg, 8.10 mmol) and TPAP (47.4 mg, 0.135 mmol) were dissolved in precooled wet MeCN (16 mL) at -15 °C. The mixture was stirred at -15 °C for 4 h and was then and evaporated *in vacuo* to give 4-acetyl-1-benzyl-1,2,3,4-tetrahydroquinoxaline-2-carboxylic acid (108 mg, 0.296 mmol, 22%) as a

black gum which was used crude without further purification. LCMS

(High pH, ES⁺): t_R = 0.68 min, [M+H⁺] 311.2, (71% purity).

1-(3-(Hydroxymethyl)-3,4-dihydroquinoxalin-1(2*H*)-yl)ethanone



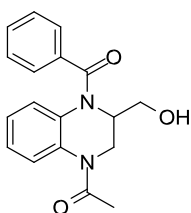
2.116

A solution of 1-(4-benzyl-3-(hydroxymethyl)-3,4-dihydroquinoxalin-1(2*H*)-yl)ethanone **2.111** (200 mg, 0.675 mmol) in MeOH (23 mL) was cycled through a Thales H-cube Flow Hydrogenator (10% Pd/C CatCart, full H₂, 1 mL/min) for 7 h. The solvent was then evaporated *in vacuo* to afford 1-(3-(hydroxymethyl)-3,4-dihydroquinoxalin-1(2*H*)-yl)ethanone (135 mg, 0.655 mmol, 97%) as a white solid.

LCMS (High pH, ES⁺): t_R = 0.60 min, [M+H⁺] 207.2, (85% pure). ¹H NMR (400 MHz, 303 K, DMSO-d₆): δ 2.18 (s, 3H), 3.31-3.56 (m, 4H), 3.81 (dd, *J* = 12.6,

3.5 Hz, 1H), 4.34 (t, *J* = 5.1 Hz, 1H), 5.66 (br. s., 1H), 6.52 (ddd, *J* = 7.6, 7.1, 1.5 Hz, 1H), 6.67 (dd, *J* = 8.0, 1.5 Hz, 1H), 6.88 (ddd, *J* = 8.0, 7.1, 1.5 Hz, 1H), 7.25 (dd, *J* = 7.6, 1.5 Hz, 1H).

1-(4-Benzoyl-3-(hydroxymethyl)-3,4-dihydroquinoxalin-1(2*H*)-yl)ethanone

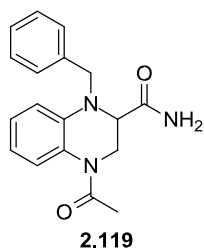


2.117

To a solution of 1-(3-(hydroxymethyl)-3,4-dihydroquinoxalin-1(2*H*)-yl)ethanone **2.116** (100 mg, 0.485 mmol) and pyridine (78 μL, 0.970 mmol) in DCM (4 mL) stirred under N₂ at 0 °C, was added benzoyl chloride (56 μL, 0.485 mmol). The reaction mixture was stirred at 0 °C for 15 min then quenched with water (1 mL) and extracted with DCM (3 x 5 mL). The combined organics were dried through a hydrophobic frit and evaporated

to dryness. The residue was purified by silica chromatography (0-100% EtOAc/cyclohexane), appropriate fractions were evaporated *in vacuo* and the product was further purified by High pH MDAP to afford 1-(4-benzoyl-3-(hydroxymethyl)-3,4-dihydroquinoxalin-1(2*H*)-yl)ethanone (60 mg, 0.193 mmol, 40%).

LCMS (High pH, ES⁺): t_R = 0.73 min, [M+H⁺] 311.2, (95% pure). ¹H NMR (400 MHz, CDCl₃): δ 2.36 (s, 3H), 3.02 (br. s., 1H), 3.62-3.80 (m, 3H), 5.12 (m, *J* = 5.1 Hz, 2H), 6.67 (d, *J* = 7.8 Hz, 1H), 6.92 (t, *J* = 7.3 Hz, 1H), 7.13-7.20 (m, 1H), 7.24-7.31 (m, 5H), 7.35-7.42 (m, 1H). **4-Acetyl-1-benzyl-1,2,3,4-tetrahydroquinoxaline-2-carboxamide**



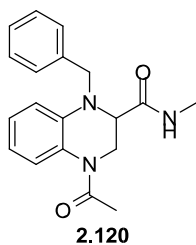
Prepared from 4-acetyl-1-benzyl-1,2,3,4-tetrahydroquinoxaline-2-carboxylic acid **2.112** (27 mg, 0.074 mmol) and ammonium chloride (8 mg, 0.148 mmol) according to General Procedure 5. Purification of the crude product by High pH MDAP afforded 4-acetyl-1-benzyl-1,2,3,4-tetrahydroquinoxaline-2-carboxamide (8 mg, 0.026 mmol, 35%) as a beige solid.

LCMS (High pH, ES⁺): t_R = 0.85 min, [M+H⁺] 310.2, (100% purity). ¹

¹H NMR (400 MHz, DMSO-*d*₆, 393K): δ 2.10 (s, 3H), 3.36 (dd, *J* = 13.1, 4.3 Hz, 1H), 4.07 (dd, *J* = 4.3, 3.1 Hz, 1H), 4.30 (d, *J* = 16.9 Hz, 1H), 4.56 (dd, *J* = 13.1, 3.1 Hz, 1H), 4.78 (d, *J* = 16.9 Hz, 1H), 6.60 (ddd, *J* = 7.3, 1.3 Hz, 1H), 6.73 (dd, *J* = 8.3, 1.3 Hz, 1H), 6.86 (br. s., 1H), 6.92 (ddd, *J* = 8.3, 7.3, 1.3 Hz, 1H), 7.18-7.35 (m, 5H). Amide protons not observed.

HRMS: (C₁₈H₁₉N₃O₂) [M+H⁺] requires 310.1550, found [M+H⁺] 310.1558.

4-Acetyl-1-benzyl-*N*-methyl-1,2,3,4-tetrahydroquinoxaline-2-carboxamide

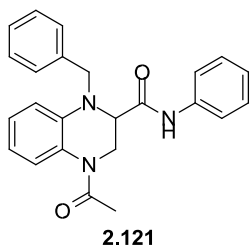


Prepared from 4-acetyl-1-benzyl-1,2,3,4-tetrahydroquinoxaline-2-carboxylic acid **2.112** (31 mg, 0.080 mmol) and methanamine hydrochloride (8.09 mg, 0.120 mmol) according to General Procedure 5. Purification of the crude product by High pH MDAP afforded 4-acetyl-1-benzyl-*N*-methyl-1,2,3,4-tetrahydroquinoxaline-2-carboxamide (17 mg, 0.053 mmol, 66%) as a white solid.

LCMS (High pH, ES⁺): t_R = 0.88 min, [M+H⁺] 324.2, (100% purity). ¹ ¹H NMR (400 MHz, DMSO-*d*₆, 393 K): δ 2.08 (s, 3H), 2.56 (d, *J* = 4.8 Hz, 3H), 3.33 (dd, *J* = 13.2, 4.0 Hz, 1H), 4.06 (dd, *J* = 4.0, 3.1 Hz, 1H), 4.28 (d, *J* = 16.9 Hz, 1H), 4.51 (dd, *J* = 13.2, 3.1 Hz, 1H), 4.77 (d, *J* = 16.9 Hz, 1H), 6.61 (ddd, *J* = 7.4, 1.4 Hz, 1H), 6.75 (dd, *J* = 8.4, 1.4 Hz, 1H), 6.93 (ddd, *J* = 8.4, 7.4, 1.4 Hz, 1H), 7.18-7.32 (m, 6H), 7.37-7.47 (m, 1H).

HRMS: (C₁₉H₂₁N₃O₂) [M+H⁺] requires 324.1707, found [M+H⁺] 324.1715.

4-Acetyl-1-benzyl-*N*-phenyl-1,2,3,4-tetrahydroquinoxaline-2-carboxamide



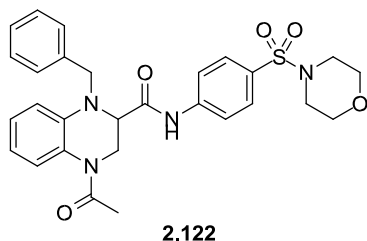
Prepared from 4-acetyl-1-benzyl-1,2,3,4-tetrahydroquinoxaline-2-carboxylic acid **2.112** (27 mg, 0.074 mmol) and aniline (14 μL, 0.148 mmol) according to General Procedure 5. Purification of the crude product by High pH MDAP afforded 4-acetyl-1-benzyl-*N*-phenyl-1,2,3,4-tetrahydroquinoxaline-2-carboxamide (11 mg, 0.029 mmol, 39%) as a brown gum.

LCMS (High pH, ES⁺): t_R = 1.12 min, [M+H⁺] 386.3, (98% purity). ¹

¹H NMR (400 MHz, DMSO-*d*₆, 393K): δ 2.12 (s, 3H), 3.48 (dd, *J* = 13.4, 4.1 Hz, 1H), 4.34 (dd, *J* = 4.1, 3.0 Hz, 1H), 4.41 (d, *J* = 16.9 Hz, 1H), 4.73 (dd, *J* = 13.4, 3.0 Hz, 1H), 4.84 (d, *J* = 16.9 Hz, 1H), 6.67 (ddd, *J* = 7.6, 1.5 Hz, 1H), 6.81 (dd, *J* = 8.3, 1.2 Hz, 1H), 7.00 (ddd, *J* = 8.3, 7.2, 1.5 Hz, 1H), 7.07 (ddd, *J* = 7.2, 1.2 Hz, 1H), 7.22-7.36 (m, 8H), 7.43-7.51 (m, 2H), 9.52 (br. s., 1H).

HRMS: (C₂₄H₂₃N₃O₂) [M+H⁺] requires 386.1863, found [M+H⁺] 386.1859.

4-Acetyl-1-benzyl-N-(4-(morpholinofonyl)phenyl)-1,2,3,4-tetrahydroquinoxaline-2carboxamide

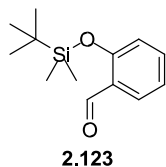


Prepared from 4-acetyl-1-benzyl-1,2,3,4-tetrahydroquinoxaline-2-carboxylic acid **2.112** (27 mg, 0.074 mmol) and 4-(morpholinofonyl)aniline (36 mg, 0.148 mmol) according to General Procedure 5. Purification of the crude product by High pH MDAP afforded 4acetyl-1-benzyl-N-(4-(morpholinofonyl)phenyl)-1,2,3,4-

tetrahydroquinoxaline-2-carboxamide (2 mg, 3.74 μmol, 5%) as a brown gum.

LCMS (High pH, ES⁺): t_R = 1.10 min, [M+H⁺] 535.5, (100% purity). ¹H NMR (400 MHz, CDCl₃): δ 2.22 (s, 3H), 2.96-3.03 (m, 4H), 3.24-3.42 (m, 1H), 3.72-3.78 (m, 4H), 4.28-4.33 (m, 1H), 4.59 (d, *J* = 16.5 Hz, 1H), 4.87 (d, *J* = 16.5 Hz, 1H), 5.05-5.35 (m, 1H), 6.91 (t, *J* = 7.5 Hz, 1H), 7.01-7.09 (m, 1H), 7.18 (t, *J* = 7.5 Hz, 1H), 7.22-7.41 (m, 6H), 7.57 (d, *J* = 8.8 Hz, 2H), 7.68 (d, *J* = 8.8 Hz, 2H), 8.08-8.51 (m, 1H).

2-((tert-Butyldimethylsilyl)oxy)benzaldehyde

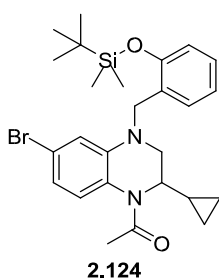


To a solution of 2-hydroxybenzaldehyde (0.87 mL, 8.19 mmol) and imidazole (1.67 g, 24.57 mmol) in DCM (12 ml) under N₂ at rt was added a solution of TBDMSCl (1.85 g, 12.28 mmol) in DCM (4 ml) dropwise. The reaction mixture was stirred at rt for 18 h, then quenched with saturated

ammonium chloride (10 mL) and the aqueous phase extracted with DCM (3 x 10 mL). The combined organic phases were dried using a hydrophobic frit, and concentrated *in vacuo*. Purification by silica chromatography (0-6% EtOAc/cyclohexane), appropriate fractions were evaporated *in vacuo* to afford 2-((tert-butyl dimethylsilyl)oxy)benzaldehyde (1.4 g, 5.93 mmol, 72%) as a colourless oil.

LCMS (Formic, ES⁺): t_R = 1.38 min, [M+H⁺] 237.4 (100% purity).

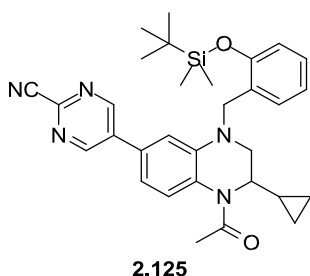
¹H NMR (400 MHz, CDCl₃): δ 0.28 (s, 6H), 1.03 (s, 9H), 6.89 (dd, *J* = 8.3, 0.7 Hz, 1H), 7.017.06 (m, 1H), 7.46 (ddd, *J* = 8.3, 7.3, 1.8 Hz, 1H), 7.81 (dd, *J* = 7.7, 1.8 Hz, 1H), 10.47 (d, *J* = 0.7 Hz, 1H). Analysis consistent with literature.³⁸³ **1-(6-Bromo-4-(2-((tert-butyl dimethylsilyl)oxy)benzyl)-2-cyclopropyl-3,4-dihydroquinoxalin-1(2H)-yl)ethanone**



Prepared from **2.016c** (64 mg, 0.22 mmol) and **2.123** (103 mg, 0.43 mmol) according to General Procedure 1, with further **2.123** (103 mg, 0.43 mmol), NaBH(OAc)₃ (86 mg, 0.41 mmol) and MgSO₄ added after 24 and 96 h. Purification of the crude product by High pH MDAP afforded 1-(6-bromo-4-(2-((*tert*-butyldimethylsilyl)oxy)benzyl)-2-cyclopropyl-3,4-dihydroquinoxalin-1(2*H*)-yl)ethanone (17 mg, 0.06 mmol, 15%).

LCMS (High pH, ES⁺): t_R = 1.70 min, [M+H⁺] 515.3, 517.3 (100% pure). ¹H NMR (400 MHz, CDCl₃): δ 0.33 (d, *J* = 4.4 Hz, 6H), 0.34-0.41 (m, 1H), 0.46 (br s, 2H), 0.51-0.59 (m, 1H), 0.85-0.99 (m, 1H), 1.06 (s, 9H), 2.25 (s, 3H), 3.46 (dd, *J* = 11.5, 0.7 Hz, 1H), 3.57 (dd, *J* = 11.5, 4.6 Hz, 1H), 4.18-4.33 (m, 1H), 4.52 (d, *J* = 5.9 Hz, 2H), 6.73 (d, *J* = 2.0 Hz, 1H), 6.78 (dd, *J* = 8.3, 2.0 Hz, 1H), 6.84-6.98 (m, 3H), 7.12 (d, *J* = 7.3 Hz, 1H), 7.18 (ddd, *J* = 7.7, 2.0 Hz, 1H).

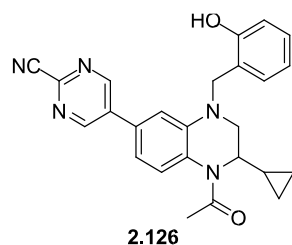
5-(1-Acetyl-4-(2-((*tert*-butyldimethylsilyl)oxy)benzyl)-2-cyclopropyl-1,2,3,4-tetrahydroquinoxalin-6-yl)pyrimidine-2-carbonitrile



Prepared from **2.124** (17 mg, 0.03 mmol) and (2-cyanopyrimidin-5-yl)boronic acid pinacol ester (15 mg, 0.07 mmol) according to General Procedure 3. Purification of the crude product by silica chromatography (0-80% EtOAc/cyclohexane) afforded 5-(1-acetyl-4-(2-((*tert*-butyldimethylsilyl)oxy)benzyl)-2-cyclopropyl-1,2,3,4-tetrahydroquinoxalin-6-yl)pyrimidine-2-carbonitrile (13 mg, 0.02 mmol, 73%) as a yellow solid.

LCMS (High pH, ES⁺): t_R = 1.57 min, [M+H⁺] 540.4 (100% purity). ¹H NMR (400 MHz, CDCl₃): δ 0.30 (d, *J* = 4.2 Hz, 6H), 0.39-0.46 (m, 1H), 0.46-0.57 (m, 2H), 0.55-0.64 (m, 1H), 0.93-0.99 (m, 1H), 1.01 (s, 9H), 2.30 (s, 3H), 3.58 (d, *J* = 11.5 Hz, 1H), 3.72 (dd, *J* = 11.5, 4.5 Hz, 1H), 4.19-4.38 (m, 1H), 4.59 (s, 2H), 6.70 (d, *J* = 2.0 Hz, 1H), 6.83-6.92 (m, 3H), 7.11-7.25 (m, 3H), 8.85 (s, 2H).

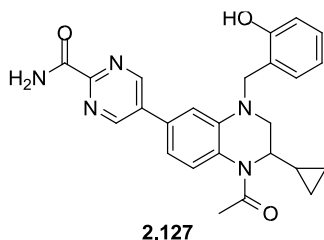
5-(1-Acetyl-2-cyclopropyl-4-(2-hydroxybenzyl)-1,2,3,4-tetrahydroquinoxalin-6-yl)pyrimidine-2-carbonitrile



A solution of 5-(1-acetyl-4-(2-((*tert*-butyldimethylsilyl)oxy)benzyl)-2-cyclopropyl-1,2,3,4-tetrahydroquinoxalin-6-yl)pyrimidine-2-carbonitrile **2.125** (13 mg, 0.02 mmol) and TBAF (25 μL, 0.03 mmol, 1 M in THF) in THF (0.36 mL) was stirred at rt for 30 min. The reaction mixture was filtered through a plug of silica and evaporated to *in vacuo* to afford 5-(1-acetyl-2-cyclopropyl-4-(2-hydroxybenzyl)-1,2,3,4-tetrahydroquinoxalin-6-yl)pyrimidine-2-carbonitrile (7 mg, 0.02 mmol, 85%) as a yellow solid.

LCMS (High pH, ES⁺): t_R = 1.12 min, [M-H⁻] 424.1 (100% purity). ¹H NMR (400 MHz, CDCl₃): δ 0.38-0.47 (m, 1H), 0.48-0.66 (m, 3H), 0.94 (br s, 1H), 2.32 (s, 3H), 3.58 (dd, *J* = 11.5, 1.7 Hz, 1H), 3.70 (dd, *J* = 11.5, 4.6 Hz, 1H), 4.20-4.35 (m, 1H), 4.67 (s, 2H), 6.29-6.38 (m, 1H), 6.85-6.99 (m, 3H), 7.00 (d, *J* = 1.2 Hz, 1H), 7.21 (ddd, *J* = 7.2, 4.3, 2.7 Hz, 2H), 7.30-7.40 (m, 1H), 8.91 (s, 2H).

5-(1-Acetyl-2-cyclopropyl-4-(2-hydroxybenzyl)-1,2,3,4-tetrahydroquinoxalin-6-yl)pyrimidine-2-carboxamide



2.127

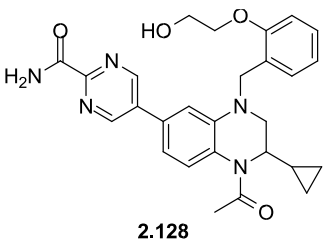
Prepared from 5-(1-acetyl-2-cyclopropyl-4-(2-hydroxybenzyl)-1,2,3,4-tetrahydroquinoxalin-6-yl)pyrimidine-2-carbonitrile **2.126** (10 mg, 0.02 mmol) according to General Procedure 4.

Purification of the crude product by High pH MDAP afforded 5-(1-acetyl-2-cyclopropyl-4-(2-hydroxybenzyl)-1,2,3,4-tetrahydroquinoxalin-6-yl)pyrimidine-2-carboxamide (7 mg,

0.02 mmol, 75%) as a yellow solid.

LCMS (High pH, ES⁺): t_R = 0.86 min, [M+H⁺] 444.5 (100% pure). ¹H NMR (400 MHz, DMSO-d₆): δ 0.26-0.52 (m, 4H), 0.81 (br. s., 1H), 2.20 (s, 2H), 3.48-3.63 (m, 2H), 3.99-4.15 (m, 1H), 4.54-4.75 (m, 2H), 6.73 (t, *J* = 7.5 Hz, 1H), 6.87 (d, *J* = 7.1 Hz, 1H), 7.01-7.18 (m, 5H), 7.43 (br. s., 1H), 7.77 (br. s., 1H), 8.16 (br. s., 1H), 9.10 (s, 2H), 9.72 (s, 1H).

5-(1-Acetyl-2-cyclopropyl-4-(2-(2-hydroxyethoxy)benzyl)-1,2,3,4-tetrahydroquinoxalin-6-yl)pyrimidine-2-carboxamide



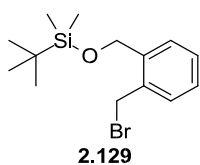
2.128

A mixture of 5-(1-acetyl-2-cyclopropyl-4-(2-hydroxybenzyl)-1,2,3,4-tetrahydroquinoxalin-6-yl)pyrimidine-2-carboxamide **2.127** (5 mg, 0.011 mmol) and potassium carbonate (5 mg, 0.034 mmol) in DMF (0.5 mL) was treated with 2-bromoethanol (2.4 μL, 0.034 mmol) and the reaction was stirred under N₂ at

110 °C for 40 h. The reaction mixture was cooled to rt, filtered and purified by High pH MDAP to afford 5-(1-acetyl-2-cyclopropyl-4-(2-(2-hydroxyethoxy)benzyl)-1,2,3,4-tetrahydroquinoxalin-6-yl)pyrimidine-2-carboxamide (2 mg, 4.10 μmol, 36%) as a yellow solid.

LCMS (High pH, ES⁺): t_R = 0.89 min, [M+H⁺] 488.5, (83% purity). ¹H NMR (400 MHz, CDCl₃): δ 0.37-0.62 (m, 4H), 0.83-1.04 (m, 1H), 2.32 (s, 3H), 3.56 (dd, *J* = 11.4, 1.1 Hz, 1H), 3.70 (dd, *J* = 11.4, 4.5 Hz, 1H), 3.94-4.03 (m, 2H), 4.14-4.20 (m, 2H), 4.21-4.38 (m, 1H), 4.69 (ABq, *J* = 17.6 Hz, 2H), 5.86 (br. s., 1H), 6.83 (d, *J* = 1.7 Hz, 1H), 6.89-6.98 (m, 3H), 7.17-7.24 (m, 1H), 7.24-7.32 (m, 2H), 7.79 (br. s., 1H), 8.94 (s, 2H). OH proton not observed.

((2-(Bromomethyl)benzyl)oxy)(*tert*-butyl)dimethylsilane

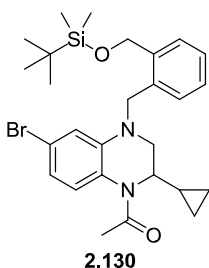


To a solution of (2-(bromomethyl)phenyl)methanol (330 mg, 1.64 mmol) in DCM (7 mL) under N₂ at rt was added 2,6-lutidine (0.38 mL, 3.28 mmol) and TBDMSOTf (0.57 mL, 2.46 mmol). The reaction mixture was stirred at rt for 1 h, then quenched with H₂O (5 mL) and the aqueous layer extracted with EtOAc (2 x 15 mL). The combined organics were dried, evaporated and the crude product purified by silica chromatography (0-20% EtOAc/cyclohexane) to afford ((2(bromomethyl)benzyl)oxy)(*tert*-butyl)dimethylsilane (490 mg, 1.56 mmol, 95%) as a clear oil.

LCMS (High pH, ES⁺): t_R = 1.61 min (100% purity). No mass ion observed.

¹H NMR (400 MHz, CDCl₃): δ 0.14 (s, 6H), 0.97 (s, 9H), 4.61 (s, 2H), 4.89 (s, 2H), 7.28 (s, 3H), 7.44-7.49 (m, 1H). Analysis consistent with literature.³⁸⁴

1-(6-Bromo-4-(2-(((*tert*-butyldimethylsilyl)oxy)methyl)benzyl)-2-cyclopropyl-3,4-dihydroquinoxalin-1(2*H*)-yl)ethanone



To a solution of **2.016c** (175 mg, 0.59 mmol) in DMF (7 mL) at 0 °C was added NaH (60% dispersion in mineral oil, 71 mg, 1.77 mmol), and the reaction was stirred under N₂ at 0 °C for 5 min. A solution of ((2(bromomethyl)benzyl)oxy)(*tert*-butyl)dimethylsilane **2.129** (240 mg, 0.76 mmol) in DMF (1 mL) was added dropwise and the reaction stirred at 0

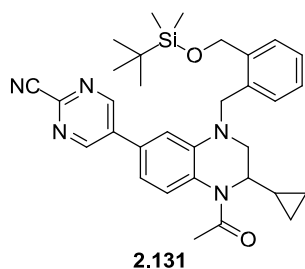
°C for 90 min. The reaction mixture was poured into H₂O (30 mL) and extracted with Et₂O (3 x 20 mL). The combined organics were dried, evaporated to dryness and the residue was purified by silica chromatography (0-20% EtOAc/cyclohexane). Appropriate fractions were evaporated *in vacuo* to afford 1-(6-bromo-4-(2-(((*tert*-butyldimethylsilyl)oxy)methyl)benzyl)-2-cyclopropyl-3,4-dihydroquinoxalin-1(2*H*)-yl)ethanone (299 mg, 0.57 mmol, 95%) as a colourless gum.

LCMS (Formic, ES⁺): t_R = 1.70 min, [M+H⁺] 529.3, 531.3 (100% purity).

¹H NMR (400 MHz, CDCl₃): δ 0.13 (s, 6H), 0.30-0.40 (m, 1H), 0.42-0.60 (m, 3H), 0.86-1.04 (m, 10H), 2.26 (s, 3H), 3.40 (d, *J* = 11.4 Hz, 1H), 3.52 (dd, *J* = 11.4, 4.6 Hz, 1H), 4.15-4.35 (m, 1H), 4.63 (d, *J* = 5.4 Hz, 2H), 4.76 (s, 2H), 6.72 (d, *J* = 2.1 Hz, 1H), 6.81 (dd, *J* = 8.3, 2.1 Hz, 1H), 6.87-7.01 (m, 1H), 7.12-7.33 (m, 3H), 7.44 (d, *J* = 7.3 Hz, 1H). ¹³C NMR (101 MHz, CDCl₃): δ -5.2, 4.1, 4.2, 12.5, 18.4, 22.8, 26.0, 51.6, 51.7, 52.9, 63.4, 113.7, 118.6, 120.0, 122.5, 125.4, 126.6, 127.2, 127.8, 128.0, 134.3, 138.4, 140.4, 168.7 v_{max} (neat): 2953, 2929, 2856, 1655, 1595, 1508, 1471, 1386, 1336, 1310, 1251, 1188, 1120, 1076, 836, 776, 744 cm⁻¹.

1.

HRMS: (C₂₇H₃₇BrN₂O₂Si) [M+H]⁺ requires 529.1880, found [M+H]⁺ 529.1876. **5-(1-Acetyl-4-(2-(((*tert*-butyldimethylsilyl)oxy)methyl)benzyl)-2-cyclopropyl-1,2,3,4-tetrahydroquinoxalin-6-yl)pyrimidine-2-carbonitrile**



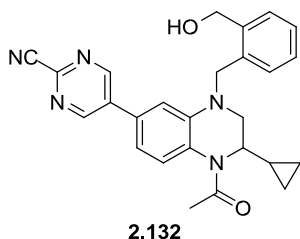
Prepared from 1-(6-bromo-4-(2-(((*tert*-butyldimethylsilyl)oxy)methyl)benzyl)-2-cyclopropyl-3,4-dihydroquinoxalin-1(2*H*)-yl)ethanone **2.130** (80 mg, 0.15 mmol) and (2-cyanopyrimidin-5-yl)boronic acid pinacol ester (70 mg, 0.30 mmol) according to General Procedure 3. Purification of the crude product by silica chromatography (0-30%

EtOAc/cyclohexane), appropriate fractions were evaporated *in vacuo* to afford 5-(1-acetyl-4-(2-(((*tert*-butyldimethylsilyl)oxy)methyl)benzyl)-2-cyclopropyl-1,2,3,4-tetrahydroquinoxalin-6-yl)pyrimidine-2-carbonitrile (70 mg, 0.13 mmol, 67%) as a yellow solid.

LCMS (High pH, ES⁺): t_R = 1.58 min, [M+H]⁺ 554.4, (95% purity).

¹H NMR (400 MHz, CDCl₃): δ 0.10 (s, 6H), 0.37-0.47 (m, 1H), 0.48-0.65 (m, 3H), 0.91 (s, 9H), 0.95-1.06 (m, 1H), 2.33 (s, 3H), 3.54 (dd, *J* = 11.4, 1.1 Hz, 1H), 3.68 (dd, *J* = 11.4, 4.5 Hz, 1H), 4.18-4.38 (m, 1H), 4.75 (s, 2H), 4.78 (s, 2H), 6.68 (d, *J* = 2.0 Hz, 1H), 6.90 (dd, *J* = 8.3, 2.0 Hz, 1H), 7.20-7.35 (m, 4H), 7.41-7.45 (m, 1H), 8.82 (s, 2H).

5-(1-Acetyl-2-cyclopropyl-4-(2-(hydroxymethyl)benzyl)-1,2,3,4-tetrahydroquinoxalin-6yl)pyrimidine-2-carbonitrile



A solution of 5-(1-acetyl-4-(2-(((*tert*-butyldimethylsilyl)oxy)methyl)benzyl)-2-cyclopropyl-1,2,3,4-tetrahydroquinoxalin-6-yl)pyrimidine-2-carbonitrile **2.131** (70 mg, 0.10 mmol) and TBAF (131 μL, 0.13 mmol, 1 M in THF) in THF (2 mL) was stirred at rt for 30 min. The reaction mixture was partitioned between EtOAc (10 mL) and H₂O (10 mL) and the

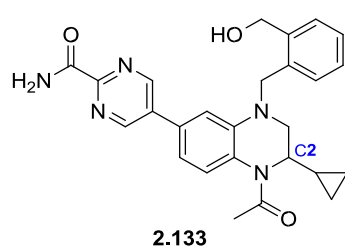
aqueous phase extracted with EtOAc (3 x 15 mL). The combined organics were evaporated to dryness and the residue was purified by silica chromatography (25-100%

EtOAc/cyclohexane), appropriate fractions were evaporated *in vacuo* to afford 5-(1-acetyl-2-cyclopropyl-4-(2-(hydroxymethyl)benzyl)-1,2,3,4-tetrahydroquinoxalin-6-yl)pyrimidine-2-carbonitrile (43 mg, 97%) as a yellow solid.

LCMS (High pH, ES⁺): t_R = 1.08 min, [M+H]⁺ 440.3, (97% purity). ¹H NMR (400 MHz, CDCl₃): δ 0.34-0.65 (m, 4H), 0.89-1.04 (m, 1H), 1.89 (t, *J* = 5.7 Hz, 1H),

2.32 (s, 3H), 3.54 (d, *J* = 11.5 Hz, 1H), 3.70 (dd, *J* = 11.5, 4.4 Hz, 1H), 4.13-4.38 (m, 1H), 4.80 (d, *J* = 4.9 Hz, 2H), 4.83 (s, 2H), 6.83 (s, 1H), 6.92 (s, 1H), 7.23-7.36 (m, 4H), 7.41 (d, *J* = 7.6 Hz, 1H), 8.88 (s, 2H).

HRMS: (C₂₆H₂₅N₅O₂) [M+H⁺] requires 440.2081, found 440.2075. **5-(1-Acetyl-2-cyclopropyl-4-(2-(hydroxymethyl)benzyl)-1,2,3,4-tetrahydroquinoxalin-6-yl)pyrimidine-2-carboxamide**



Prepared from 5-(1-acetyl-2-cyclopropyl-4-(2-(hydroxymethyl)benzyl)-1,2,3,4-tetrahydroquinoxalin-6-yl)pyrimidine-2-carbonitrile **2.132** (43 mg, 0.10 mmol) according to General Procedure 4. Purification of the crude product by High pH MDAP afforded 5-(1-acetyl-2-cyclopropyl-4-(2-(hydroxymethyl)benzyl)-1,2,3,4-

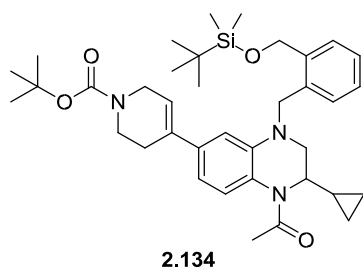
tetrahydroquinoxalin-6-yl)pyrimidine-2-carboxamide (35 mg, 78%) as a yellow-green solid.

LCMS (High pH, ES⁺): t_R = 0.82 min, [M+H⁺] 458.5 (100% pure). ¹H NMR (500 MHz, DMSO-*d*₆): δ 0.25-0.58 (m, 4H), 0.77-1.00 (m, 1H), 2.23 (s, 3H), 3.45 (d, *J* = 10.7 Hz, 1H), 3.50-3.64 (m, 1H), 3.96-4.02 (m, 1H), 4.64 (d, *J* = 5.2 Hz, 2H), 4.81 (dd, *J* = 43.6, 17.3 Hz, 2H), 5.24 (t, *J* = 5.2 Hz, 1H), 7.02 (d, *J* = 1.7 Hz, 1H), 7.09 (dd, *J* = 8.1, 1.7 Hz, 1H), 7.15-7.21 (m, 2H), 7.24 (ddd, *J* = 7.1, 1.9 Hz, 1H), 7.45 (d, *J* = 7.1 Hz, 1H), 7.47 (br s, 1H), 7.78 (br s, 1H), 8.17 (br s, 1H), 9.09 (s, 2H).

¹³C NMR (126 MHz, DMSO-*d*₆): δ 4.0, 4.6, 13.2, 23.3, 51.3, 53.2, 61.1, 109.5, 114.6, 124.3 (HMBC), 125.8, 126.6, 127.1, 127.5, 128.1, 130.6 (HMBC), 134.4, 135.4, 139.4, 140.2, 155.2, 157.2, 164.7, 168.5. C2 carbon not observed due to peak broadening. M.pt. 131-134 °C. ν_{max} (neat): 2838, 2572, 2498, 2342, 1689, 1627, 1601, 1568, 1516, 1448, 1382, 1320, 1261, 1090, 1007, 978, 855, 819, 748, 705 cm⁻¹.

HRMS: (C₂₆H₂₇N₅O₃) [M+H⁺] requires 458.2187, found 458.2189.

***tert*-Butyl 4-(1-acetyl-4-(2-(((*tert*-butyldimethylsilyl)oxy)methyl)benzyl)-2-cyclopropyl-1,2,3,4-tetrahydroquinoxalin-6-yl)-5,6-dihydropyridine-1(2*H*)-carboxylate**



Prepared from 1-(6-bromo-4-(2-(((*tert*-butyldimethylsilyl)oxy)methyl)benzyl)-2-cyclopropyl-3,4-dihydroquinoxalin-1(2*H*)-yl)ethanone **2.130** (100 mg, 0.19 mmol) and (1-(*tert*-butoxycarbonyl)-1,2,3,6-tetrahydropyridin-4-yl)boronic acid pinacol ester (88 mg, 0.28 mmol) according to General Procedure 3. After 2 h

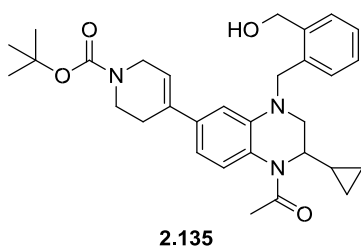
further (1-(*tert*-butoxycarbonyl)-1,2,3,6-tetrahydropyridin-4-yl)boronic acid pinacol ester (88 mg, 0.28 mmol) and PdCl₂(dppf) (7 mg, 9.44 μmol) were added and the reaction was heated to 100 °C for 2 h. Purification of the crude product by silica chromatography (0-30%

EtOAc/cyclohexane) afforded *tert*-butyl 4-(1-acetyl-4-(2-(((*tert*-butyldimethylsilyl)oxy)methyl)benzyl)-2-cyclopropyl-1,2,3,4-tetrahydroquinoxalin-6-yl)-5,6-dihydropyridine-1(2*H*)-carboxylate (67 mg, 0.106 mmol, 56%) as a yellow solid.

LCMS (High pH, ES⁺): t_R = 1.78 min, [M+H⁺] 632.6, (99% purity).

¹H NMR (400 MHz, CDCl₃): δ 0.12 (s, 6H), 0.31-0.39 (m, 1H), 0.42-0.57 (m, 3H), 0.95 (s, 9H), 0.95-1.02 (m, 1H), 1.48 (s, 9H), 2.29 (s, 3H), 2.34-2.42 (m, 2H), 3.41 (d, *J* = 11.2 Hz, 1H), 3.51-3.60 (m, 3H), 3.94-4.04 (m, 2H), 4.21-4.33 (m, 1H), 4.65 (s, 2H), 4.78 (s, 2H), 5.78-5.91 (m, 1H), 6.57 (d, *J* = 2.0 Hz, 1H), 6.71 (dd, *J* = 8.3, 1.7 Hz, 1H), 6.99-7.10 (m, 1H), 7.19-7.26 (m, 2H), 7.28 (s, 1H), 7.45 (d, *J* = 7.3 Hz, 1H).

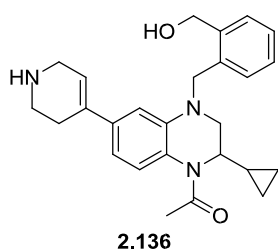
***tert*-Butyl 4-(1-acetyl-2-cyclopropyl-4-(2-(hydroxymethyl)benzyl)-1,2,3,4-tetrahydroquinoxalin-6-yl)-5,6-dihydropyridine-1(2*H*)-carboxylate**



A solution of *tert*-butyl 4-(1-acetyl-4-(2-(((*tert*-butyldimethylsilyl)oxy)methyl)benzyl)-2-cyclopropyl-1,2,3,4-tetrahydroquinoxalin-6-yl)-5,6-dihydropyridine-1(2*H*)-carboxylate **2.134** (67 mg, 0.106 mmol) and TBAF (138 μL, 0.138 mmol, 1 M in THF) in THF (2 mL) was stirred at rt for 2 h. The reaction mixture was purified by silica

chromatography (0-100% EtOAc/cyclohexane) to afford *tert*-butyl 4-(1-acetyl-2-cyclopropyl-4-(2-(hydroxymethyl)benzyl)-1,2,3,4-tetrahydroquinoxalin-6-yl)-5,6-dihydropyridine-1(2*H*)carboxylate (48 mg, 0.093 mmol, 87%) as a yellow solid. LCMS (High pH, ES⁺): t_R = 1.31 min, [M+H⁺] 518.5, (97% purity). ¹H NMR (400 MHz, CDCl₃): δ 0.29-0.37 (m, 1H), 0.42-0.56 (m, 3H), 0.87-0.98 (m, 1H), 1.48 (s, 9H), 2.27 (s, 3H), 2.36-2.44 (m, 2H), 3.36 (dd, *J* = 11.2, 1.2 Hz, 1H), 3.48-3.61 (m, 3H), 4.01 (d, *J* = 2.4 Hz, 2H), 4.19-4.32 (m, 1H), 4.71 (s, 2H), 4.78 (s, 2H), 5.85-5.93 (m, 1H), 6.67 (d, *J* = 1.2 Hz, 1H), 6.74 (dd, *J* = 8.1, 1.5 Hz, 1H), 7.01-7.13 (m, 1H), 7.23-7.35 (m, 3H), 7.43 (d, *J* = 7.1 Hz, 1H). OH not observed.

1-(2-Cyclopropyl-4-(2-(hydroxymethyl)benzyl)-6-(1,2,3,6-tetrahydropyridin-4-yl)-3,4-dihydroquinoxalin-1(2*H*)-yl)ethanone

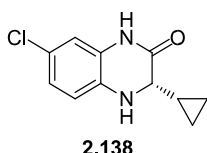


To a solution of *tert*-butyl 4-(1-acetyl-2-cyclopropyl-4-(2-(hydroxymethyl)benzyl)-1,2,3,4-tetrahydroquinoxalin-6-yl)-5,6-dihydropyridine-1(2*H*)-carboxylate **2.135** (60 mg, 0.116 mmol) in DCM (2 mL) was added TFA (1 mL, 12.98 mmol), and the reaction was stirred at rt for 2 h. The reaction was evaporated to dryness and purified by High pH MDAP to afford 1-(2-cyclopropyl-4-(2-(hydroxymethyl)benzyl)-6-(1,2,3,6-tetrahydropyridin-4-yl)-3,4-dihydroquinoxalin-1(2*H*)yl)ethanone (28 mg, 0.067 mmol, 58%) as a white solid. LCMS (High pH, ES⁺): t_R = 0.98 min, [M+H⁺] 418.6, (79% purity). ¹H NMR (400 MHz, CDCl₃): δ 0.27-0.36 (m, 1H), 0.39-0.55 (m, 3H), 0.86-0.98 (m, 1H), 2.26 (s, 3H), 2.30-2.36 (m, 2H), 3.03 (t, *J* = 5.6 Hz, 2H), 3.33 (dd, *J* = 11.1, 1.5 Hz, 1H), 3.44-3.47 (m, 2H), 3.50 (dd, *J* = 11.1, 5.0 Hz, 1H), 4.16-4.31 (m, 1H), 4.68 (s, 2H), 4.76 (s, 2H), 5.95-

6.00 (m, 1H), 6.68 (d, $J = 1.7$ Hz, 1H), 6.74 (dd, $J = 8.1, 1.7$ Hz, 1H), 6.98-7.11 (m, 1H), 7.22-7.33 (m, 3H), 7.41 (d, $J = 6.6$ Hz, 1H). NH and OH were not observed. ^{13}C NMR (151 MHz, CDCl_3): δ 3.9, 4.1, 12.7, 22.8, 27.7, 43.2, 45.4, 52.2, 52.3, 53.4, 63.4, 108.3, 113.2, 123.0, 123.2, 125.3, 127.0, 127.5, 128.3, 128.9, 135.3, 135.9, 138.3, 139.1, 139.8, 169.0. M.pt. 170-173 °C ν_{max} (neat): 3343, 2865, 1621, 1518, 1395, 1375, 1314, 1241, 1088, 961, 842, 795, 745 cm^{-1} .

HRMS: ($\text{C}_{26}\text{H}_{31}\text{N}_3\text{O}_2$) $[\text{M}+\text{H}]^+$ requires 418.2489, found $[\text{M}+\text{H}]^+$ 418.2491.

(S)-7-Chloro-3-cyclopropyl-3,4-dihydroquinoxalin-2(1H)-one



(S)-2-Amino-2-cyclopropylacetic acid (S)-**2.009c** (230 mg, 2.00 mmol), 2-bromo-5-chloroaniline **2.137** (206 mg, 1.00 mmol), CuCl (4.95 mg, 0.05 mmol), DMEDA (22 μL , 0.20 mmol) and DBU (301 μL , 2.00 mmol) were placed in an oven-dried microwave tube which was sealed and placed under N_2 . Anhydrous degassed DMSO (3.5 mL) was added and the reaction mixture was heated to 110 °C in an oil bath for 48 h. The reaction mixture was cooled, diluted with EtOAc (10 mL) and filtered through Celite. The filtrate was washed with H_2O (2 x 5 mL) and the combined aqueous phases extracted with CHCl_3 (2 x 5 mL). The combined organics were dried through a hydrophobic frit and evaporated *in vacuo*. Purified by silica chromatography (0-100% EtOAc/cyclohexane), appropriate fractions were evaporated *in vacuo* to afford (S)-7-chloro-3-cyclopropyl-3,4-dihydroquinoxalin-2(1H)-one (162 mg, 73%) as an off-white oil, which solidified on standing.

LCMS (High pH, ES^+): $t_{\text{R}} = 0.86$ min, No mass ion detected, (85% purity).

^1H NMR (400 MHz, CDCl_3): δ 0.21-0.33 (m, 1H), 0.50-0.65 (m, 2H), 0.67-0.78 (m, 1H), 1.161.30 (m, 1H), 3.16 (d, $J = 8.8$ Hz, 1H), 4.04 (br. s., 1H), 6.63 (d, $J = 8.5$ Hz, 1H), 6.72 (d, $J =$

2.1 Hz, 1H), 6.85 (dd, $J = 8.5, 2.1$ Hz, 1H), 8.03 (br. s., 1H).

^{13}C NMR (101 MHz, CDCl_3): δ 2.5, 3.2, 14.0, 61.2, 114.9, 115.1, 123.5, 124.0, 126.1, 131.8, 167.5.

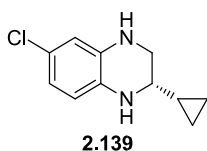
M.pt.: 165-168 °C

$[\alpha_{\text{D}}]^{25} = -4$ ($c = 1.0$, CDCl_3).

ν_{max} (neat): 3369, 3206, 2954, 1681, 1598, 1500, 1375, 1289, 1230, 1077, 868, 796 cm^{-1}

HRMS: ($\text{C}_{11}\text{H}_{11}\text{ClN}_2\text{O}$) $[\text{M}+\text{H}]^+$ requires 223.0633, found $[\text{M}+\text{H}]^+$ 223.0630.

(S)-6-Chloro-2-cyclopropyl-1,2,3,4-tetrahydroquinoxaline



To a solution of (S)-7-chloro-3-cyclopropyl-3,4-dihydroquinoxalin-2(1H)one **2.138** (1095 mg, 4.92 mmol) in THF (49 mL) stirred under N₂ at rt was added BH₃•THF (14.75 mL, 14.75 mmol, 1 M in THF) dropwise.

The reaction mixture was heated to 50 °C for 3 h. The reaction mixture was then cooled to rt, quenched with MeOH (5 mL) and 1 M HCl (5 mL) and stirred for 30 min. The mixture was basified with 1 M NaOH and extracted with ethyl acetate (3 x 50 mL). The combined organics were dried through a hydrophobic frit and evaporated to dryness. Purification of the crude product by silica chromatography (0-40% EtOAc/cyclohexane) and evaporation *in vacuo* of appropriate fractions afforded (S)-6-chloro-2-cyclopropyl-1,2,3,4-tetrahydroquinoxaline (920 mg, 4.41 mmol, 90%) as an off-white solid.

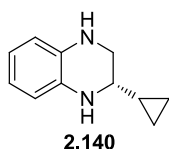
LCMS (High pH, ES⁺): t_R = 1.11 min, [M+H⁺] 209.3, (93% pure). ¹H NMR (400 MHz, CDCl₃): δ 0.25-0.37 (m, 2H), 0.51-0.64 (m, 2H), 0.81-0.93 (m, 1H), 2.482.56 (m, 1H), 3.26 (dd, J = 10.8, 8.1 Hz, 1H), 3.45 (dd, J = 10.8, 3.2 Hz, 1H), 3.75 (br. s., 1H), 3.84 (br. s., 1H), 6.42 (d, J = 8.3 Hz, 1H), 6.47 (d, J = 2.2 Hz, 1H), 6.53 (dd, J = 8.3, 2.2 Hz, 1H). ¹³C NMR (101 MHz, CDCl₃): δ 2.0, 2.8, 14.5, 46.4, 55.8, 113.6, 114.7, 118.0, 122.9, 132.0, 134.3.

M.pt.: 145-147 °C.

[α_D]^{25 °C} = -84 (c = 1.0, CDCl₃).

ν_{max} (neat): 3381, 3078, 3003, 2821, 1602, 1508, 1461, 1349, 1307, 1269, 1250, 1137, 1122, 1086, 1017, 957, 845, 795, 705 cm⁻¹. HRMS analysis failed.

(S)-2-Cyclopropyl-1,2,3,4-tetrahydroquinoxaline



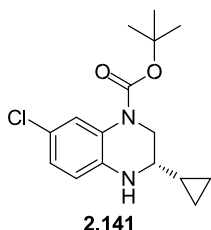
A mixture of (S)-6-chloro-2-cyclopropyl-1,2,3,4-tetrahydroquinoxaline **2.139** (37 mg, 0.18 mmol) and 10% Pd/C (8 mg, 0.04 mmol, 50% wt.) in EtOH (5 mL) was stirred under an atmosphere of H₂ at rt for 6 h. The reaction mixture was filtered through Celite and the filtrate was evaporated to dryness. The

residue was purified by ion exchange chromatography (1 g SCX cartridge, MeOH/2 M NH₃ in MeOH) to afford (S)-2-cyclopropyl-1,2,3,4-tetrahydroquinoxaline (31 mg, 100%) as a brown solid.

LCMS (High pH, ES⁺): t_R = 0.83 min, [M+H⁺] 175.2 (100% pure).

¹H NMR (400 MHz, CDCl₃): δ 0.20-0.42 (m, 2H), 0.48-0.68 (m, 2H), 0.78-1.01 (m, 1H), 2.57 (td, J = 8.3, 2.9 Hz, 1H), 3.29 (dd, J = 10.5, 8.3 Hz, 1H), 3.47 (dd, J = 10.5, 2.9 Hz, 1H), 3.58-3.90 (m, 2H), 6.48-6.67 (m, 4H).

(S)-tert-Butyl 7-chloro-3-cyclopropyl-3,4-dihydroquinoxaline-1(2H)-carboxylate To



2.141

a solution of (S)-6-chloro-2-cyclopropyl-1,2,3,4-tetrahydroquinoxaline **2.139** (840 mg, 4.03 mmol), triethylamine (1122 μL , 8.05 mmol) and DMAP (246 mg, 2.013 mmol) in DCM (16 mL) at 0 $^{\circ}\text{C}$ was added di-*tert*-butyl dicarbonate (966 mg, 4.43 mmol). The reaction mixture was gradually allowed to warm to rt and stirred for 24 h. Further di-*tert*-butyl dicarbonate (200 mg, 0.92 mmol) was added and the reaction was stirred for 24 h. The reaction mixture was diluted with DCM (10 mL) and sat. aq. NaHCO_3 (15 mL). The aqueous layer was extracted with DCM (2 x 20 mL) and the combined organics were dried through a hydrophobic frit and evaporated to dryness. The crude product was purified by silica chromatography (0-35% EtOAc/cyclohexane), appropriate fractions were evaporated *in vacuo* to afford (S)-*tert*-butyl 7-chloro-3-cyclopropyl-3,4-dihydroquinoxaline-1(2H)-carboxylate (1060 mg, 3.43 mmol, 85%) as an off-white solid.

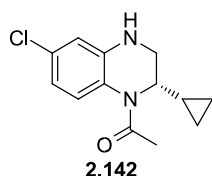
LCMS (High pH, ES⁺): $t_R = 1.43$ min, $[\text{M}+\text{H}^+]$ 307.3, (98% pure). ^1H NMR (400 MHz, CDCl_3): δ 0.26-0.39 (m, 2H), 0.51-0.63 (m, 2H), 0.74-0.91 (m, 1H), 1.54 (s, 9H), 2.61 (s, 1H), 3.18-3.33 (m, 1H), 4.00-4.24 (m, 2H), 6.49 (d, $J = 8.6$ Hz, 1H), 6.86 (dd, $J = 8.6, 2.2$ Hz, 1H), 7.55 (br. s., 1H). ^{13}C NMR (101 MHz, CDCl_3): δ 1.8, 2.6, 14.3, 28.3, 46.2, 56.4, 81.3, 114.8, 120.9, 124.2, 124.4, 125.1, 135.4, 153.0. M.pt.: 142-144 $^{\circ}\text{C}$.

$[\alpha_D]^{25\text{ }^{\circ}\text{C}} = -65$ ($c = 1.0$, CDCl_3).

ν_{max} (neat): 3368, 2988, 1675, 1560, 1501, 1454, 1401, 1374, 1294, 1237, 1153, 1098, 1077, 1046, 1035, 1018, 984, 869, 860, 804, 766 cm^{-1} .

HRMS: ($\text{C}_{16}\text{H}_{21}\text{ClN}_2\text{O}_2$) $[\text{M}+\text{H}]^+$ requires 309.1364, found $[\text{M}+\text{H}]^+$ 309.1363.

(S)-1-(6-Chloro-2-cyclopropyl-3,4-dihydroquinoxalin-1(2H)-yl)ethanone To



2.142

a solution of (S)-*tert*-butyl 7-chloro-3-cyclopropyl-3,4-dihydroquinoxaline-1(2H)-carboxylate **2.141** (1.06 g, 3.43 mmol) in 2-MeTHF (35 mL) was added triethylamine (5.74 mL, 41.2 mmol) and acetic anhydride (3.24 mL, 34.3 mmol). The reaction mixture was stirred at 90 $^{\circ}\text{C}$ for 18 h. The reaction mixture was cooled, diluted with EtOAc (20 mL) and washed with 1 M HCl (3 x 20 mL) and sat. aq. NaHCO_3 (3 x 20 mL). The organic layer was dried through a hydrophobic frit and evaporated to afford (S)-*tert*-butyl 4-acetyl-7-chloro-3-cyclopropyl-3,4-dihydroquinoxaline-1(2H)-carboxylate (1.234 g). The crude product was dissolved in DCM (3 mL) and TFA (3 mL) was added. The reaction was stirred at rt for 3 h, then evaporated and the residue partitioned between EtOAc (20 mL) and sat. aq. NaHCO_3 solution (20 mL). The aqueous layer was extracted with EtOAc (2 x 20 mL) and the combined organics were dried through a hydrophobic frit and evaporated to dryness. Purified by silica chromatography (0-100% EtOAc/cyclohexane), appropriate fractions were

evaporated to afford (S)-1-(6-chloro-2-cyclopropyl-3,4-dihydroquinoxalin-1(2H)-yl)ethanone (680 mg, 2.71 mmol, 80%) as a white solid.

LCMS (High pH, ES⁺): t_R = 1.04 min, [M+H]⁺ 251.16, (94% purity). ¹H NMR (400 MHz, CDCl₃): δ 0.29-0.59 (m, 4H), 0.70-0.88 (m, 1H), 2.23 (s, 3H), 3.40 (dd, J = 11.5, 4.2 Hz, 1H), 3.49 (ddd, J = 11.5, 4.9, 1.2 Hz, 1H), 4.08-4.30 (m, 1H), 4.37 (br. s., 1H),

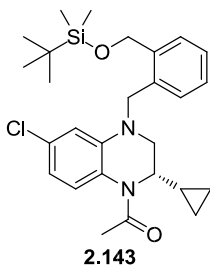
6.57-6.65 (m, 2H), 6.87-7.04 (m, 1H). ¹³C NMR (101 MHz, CDCl₃): δ 3.8, 4.3, 11.9, 22.8, 45.8, 50.5, 113.3, 116.0, 121.2, 126.5, 131.3, 138.5, 168.9. M.pt.: 122-126 °C.

[α]_D^{25 °C} = +208 (c = 1.0, CDCl₃).

ν_{max} (neat): 3299, 3004, 2866, 1630, 1603, 1502, 1444, 1380, 1313, 1238, 1227, 1095, 1067, 1023, 874, 849, 788 cm⁻¹.

HRMS: (C₁₃H₁₅ClN₂O) [M+H]⁺ requires 251.0946, found [M+H]⁺ 251.0948.

(S)-1-(4-(2-(((*tert*-Butyldimethylsilyl)oxy)methyl)benzyl)-6-chloro-2-cyclopropyl-3,4-dihydroquinoxalin-1(2H)-yl)ethanone



To a solution of (S)-1-(6-chloro-2-cyclopropyl-3,4-dihydroquinoxalin-1(2H)-yl)ethanone **2.142** (130 mg, 0.518 mmol) in DMF (6 mL) at 0 °C was added sodium hydride (62 mg, 60% in mineral oil, 1.555 mmol), and the reaction was stirred under N₂ at 0 °C for 5 min. A solution of ((2(bromomethyl)benzyl)oxy)(*tert*-butyl)dimethylsilane (204 mg, 0.648 mmol) in DMF (0.6 mL) was added dropwise and the

reaction was stirred

at 0 °C for 90 min. The reaction mixture was poured into water (30 mL) and extracted with Et₂O (3 x 10 mL). The combined organics were dried through a hydrophobic frit, evaporated to dryness and the residue was purified by silica chromatography (0-20%

EtOAc/cyclohexane), appropriate fractions were evaporated *in vacuo* to afford (S)-1-(4-(2-(((*tert*-butyldimethylsilyl)oxy)methyl)benzyl)-6-chloro-2-cyclopropyl-3,4-dihydroquinoxalin-1(2H)-yl)ethanone (200 mg, 0.412 mmol, 80%).

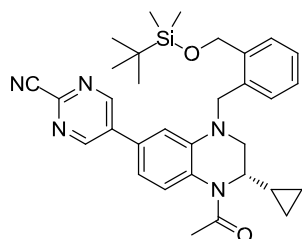
LCMS (High pH, ES⁺): t_R = 1.73 min, [M+H]⁺ 485.4, 487.4, (97% purity). ¹H NMR (400 MHz, CDCl₃): δ 0.10 (s, 6H), 0.29-0.38 (m, 1H), 0.40-0.57 (m, 3H), 0.85-0.93 (m, 1H), 0.94 (s, 9H), 2.24 (s, 3H), 3.38 (dd, J = 11.3, 1.0 Hz, 1H), 3.51 (dd, J = 11.5, 4.7 Hz, 1H), 4.13-4.34 (m, 1H), 4.61 (d, J = 4.9 Hz, 2H), 4.74 (s, 2H), 6.55 (d, J = 2.2 Hz, 1H), 6.64 (dd, J = 8.3, 2.2 Hz, 1H), 6.92-7.06 (m, 1H), 7.13-7.31 (m, 3H), 7.42 (dd, J = 7.3, 1.0 Hz, 1H). ¹³C NMR (101 MHz, CDCl₃): δ -5.2, 4.0, 4.2, 12.5, 18.3, 22.7, 25.9, 51.7, 51.8, 52.9, 63.4, 110.9, 115.6, 121.9, 125.5, 126.3, 127.2, 127.8, 128.1, 132.1, 134.3, 138.4, 140.1, 168.8. M.pt.: 136-139 °C.

[α]_D^{25 °C} = +50 (c = 1.0, CDCl₃).

ν_{max} (neat): 2956, 2928, 2893, 2855, 1644, 1597, 1511, 1392, 1359, 1337, 1306, 1256, 1094, 1057, 1041, 833, 777, 742 cm⁻¹.

HRMS: (C₂₇H₃₇ClN₂O₂Si) [M+H]⁺ requires 485.2386, found [M+H]⁺ 485.2400.

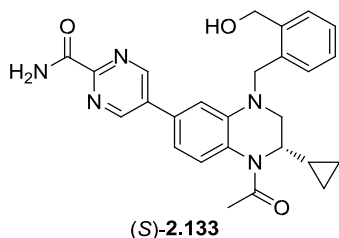
(S)-5-(1-Acetyl-4-(2-(((tert-butyl)dimethylsilyloxy)methyl)benzyl)-2-cyclopropyl-1,2,3,4-tetrahydroquinoxalin-6-yl)pyrimidine-2-carbonitrile



(S)-2.131

A solution of (S)-1-(4-(2-(((tert-butyl)dimethylsilyloxy)methyl)benzyl)-6-chloro-2-cyclopropyl-3,4-dihydroquinoxalin-1(2H)-yl)ethanone **2.129** (109 mg, 0.225 mmol), (2-cyanopyrimidin-5-yl)boronic acid pinacol ester (104 mg, 0.449 mmol), BrettPhos Pd G3 (20 mg, 0.022 mmol) and cesium carbonate (220 mg, 0.674 mmol) in DME (2.2 mL) was sealed in a microwave vial, placed under N₂ and heated in a Biotage Initiator microwave to 110 °C for 2 h. The reaction mixture was filtered through Celite and evaporated to dryness. The residue was purified by silica chromatography (0-40% EtOAc/cyclohexane) and High pH MDAP to afford (S)-5-(1-acetyl-4-(2-(((tert-butyl)dimethylsilyloxy)methyl)benzyl)-2-cyclopropyl-1,2,3,4-tetrahydroquinoxalin-6-yl)pyrimidine-2-carbonitrile (53 mg, 0.096 mmol, 42%) as a bright yellow solid. Analysis matched racemate (pp 215).

(S)-5-(1-Acetyl-2-cyclopropyl-4-(2-(hydroxymethyl)benzyl)-1,2,3,4-tetrahydroquinoxalin-6-yl)pyrimidine-2-carboxamide

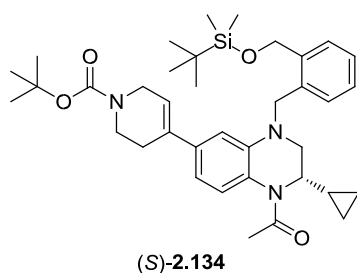


(S)-2.133

A solution of (S)-5-(1-acetyl-4-(2-(((tert-butyl)dimethylsilyloxy)methyl)benzyl)-2-cyclopropyl-1,2,3,4-tetrahydroquinoxalin-6-yl)pyrimidine-2-carbonitrile (S)-**2.131** (29 mg, 0.052 mmol) and TBAF (68 μL, 0.068 mmol, 1 M in THF) in THF (1 mL) was stirred at rt for 2 h. The reaction mixture was filtered through a plug of silica, eluting with 75% EtOAc/cyclohexane. The eluate was evaporated *in vacuo* and taken up in DMSO (0.7 mL). and H₂O₂ (37 μL, 37% wt. aq., 0.432 mmol) and potassium carbonate (12 mg, 0.086 mmol) were added. The reaction mixture was stirred at rt for 1 h and then purified directly by High pH MDAP to afford (S)-5-(1-acetyl-2-cyclopropyl-4-(2-(hydroxymethyl)benzyl)-1,2,3,4-tetrahydroquinoxalin-6-yl)pyrimidine-2-carboxamide (9 mg, 0.020 mmol, 38%).

[α_D]^{25 °C} = +114 (c = 0.5, CDCl₃). Analysis matched racemate (pp 216).

(S)-tert-Butyl 4-(1-acetyl-4-(2-(((tert-butyl)dimethylsilyloxy)methyl)benzyl)-2-cyclopropyl-1,2,3,4-tetrahydroquinoxalin-6-yl)-5,6-dihydropyridine-1(2H)-carboxylate



A solution of (S)-1-(4-(2-(((*tert*-butyldimethylsilyl)oxy)methyl)benzyl)-6-chloro-2-cyclopropyl-3,4-dihydroquinoxalin-1(2*H*)-yl)ethanone **2.143** (29 mg, 0.060 mmol), (1-(*tert*-butoxycarbonyl)-1,2,3,6-tetrahydropyridin-4-yl)boronic acid (37 mg, 0.120 mmol),

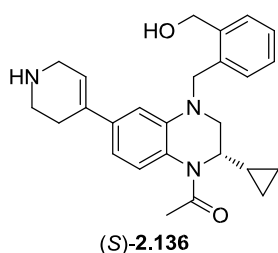
BrettPhos Pd G3 (5 mg, 5.98 μ mol) and cesium carbonate (58 mg, 0.179 mmol) in degassed DME (0.6 mL) was sealed in a microwave vial, placed under N_2 and heated in a Biotage Initiator microwave to 110 $^\circ C$ for 2 h. The reaction mixture was filtered through Celite and evaporated to dryness. The residue was purified by silica chromatography (0-35% EtOAc/cyclohexane), appropriate fractions were evaporated *in vacuo* and further purified by High pH MDAP to give (S)-*tert*-butyl 4-(1-acetyl-4-(2-(((*tert*-butyldimethylsilyl)oxy)methyl)benzyl)-2-cyclopropyl-1,2,3,4-tetrahydroquinoxalin-6-yl)-5,6-dihydropyridine-1(2*H*)-carboxylate (26 mg, 0.041 mmol, 69%) as an off-white gum.

LCMS (High pH, ES⁺): t_R = 1.76 min, $[M+H]^+$ 632.5, (93% pure). 1H NMR (400 MHz, $CDCl_3$): δ 0.10 (s, 6H), 0.29-0.37 (m, 1H), 0.41-0.55 (m, 3H), 0.89-0.98 (m, 1H), 0.93 (s, 9H), 1.46 (s, 9H), 2.27 (s, 3H), 2.33-2.40 (m, 2H), 3.39 (dd, J = 11.2, 1.0 Hz, 1H), 3.49-3.57 (m, 3H), 3.98 (q, J = 2.4 Hz, 2H), 4.17-4.30 (m, 1H), 4.63 (s, 2H), 4.76 (s, 2H), 5.79-5.88 (m, 1H), 6.56 (d, J = 1.7 Hz, 1H), 6.69 (dd, J = 8.3, 1.7 Hz, 1H), 6.98-7.10 (m, 1H), 7.17-7.30 (m, 3H), 7.42 (d, J = 7.6 Hz, 1H). ^{13}C NMR (101 MHz, $CDCl_3$): δ -5.2, 4.0, 4.1, 12.6, 18.3, 22.8, 25.9, 27.4, 28.5, 40.9, 43.6, 51.8, 52.2, 53.2, 63.4, 79.6, 107.7, 112.7, 120.5, 122.7, 125.3, 125.7, 127.1, 127.7, 127.9, 135.0, 135.3, 138.3, 139.1, 139.1, 154.8, 168.8.

$[\alpha_D]^{22} = +110$ (c = 0.1, MeOH). ν_{max} (neat): 2929, 2856, 1692, 1651, 1516, 1365, 1336, 1291, 1240, 1168, 1113, 1063, 956, 835, 775, 732, 666 cm^{-1} .

HRMS: ($C_{37}H_{53}N_3O_4Si$) $[M+H]^+$ requires 632.3878, found $[M+H]^+$ 632.3884.

1-(2-Cyclopropyl-4-(2-(hydroxymethyl)benzyl)-6-(1,2,3,6-tetrahydropyridin-4-yl)-3,4-dihydroquinoxalin-1(2*H*)-yl)ethanone



To a solution of (S)-*tert*-butyl 4-(1-acetyl-4-(2-(((*tert*-butyldimethylsilyl)oxy)methyl)benzyl)-2-cyclopropyl-1,2,3,4-tetrahydroquinoxalin-6-yl)-5,6-dihydropyridine-1(2*H*)-carboxylate (S)-**2.134** (26 mg, 0.041 mmol) in MeOH (0.4 mL) was added HCl (0.8 mL, 1 M in Et_2O , 0.823 mmol), and the reaction was stirred at rt for 6 h. The reaction was purified by ion exchange

chromatography (sulphonic acid (SCX) 1 g, sequential solvents MeOH, 2 M $NH_3/MeOH$), fractions were evaporated *in vacuo* and further purified by silica chromatography (0-100% (3:1 EtOAc:EtOH)/cyclohexane). Appropriate fractions were evaporated *in vacuo* and further

purified using Formic MDAP, after evaporation the product was freebased using ion exchange chromatography (sulphonic acid (SCX) 500 mg, sequential solvents MeOH, 2 M NH₃/MeOH), fractions were evaporated to afford (S)-1-(2-cyclopropyl-4-(2-(hydroxymethyl)benzyl)-6-(1,2,3,6-tetrahydropyridin-4-yl)-3,4-dihydroquinoxalin-1(2H)yl)ethanone (8 mg, 0.019 mmol, 47%).

$[\alpha_D]^{22\text{ }^\circ\text{C}} = +119$ (c = 0.1, MeOH). Analysis matched racemate (pp 217).

4.3 Compound Synthesis and Characterisation - Design and Synthesis of BRPF1 Bromodomain Inhibitors

General Procedure A – Warhead Amide Formation

To a solution of the respective heterocyclic carboxylic acid (1 eq), HATU (1.2 eq) and DIPEA (3 eq) in DMF (0.3 M) was added the respective amine (2 eq), and the reaction was stirred at rt for 2 h. The reaction mixture was filtered and purified by High pH MDAP. The appropriate fractions were evaporated to dryness to afford the product.

General Procedure B – Pyrazolopyrimidine Suzuki

5-chloro-*N*-methylpyrazolo[1,5-*a*]pyrimidine-3-carboxamide **3.030** (1 eq.), Pd(PPh₃)₄ (5 mol%), sodium carbonate (2 eq.) and the respective boronic acid or pinacol ester (1.5 eq) were placed in a microwave vial, which was sealed and placed under an atmosphere of nitrogen. Toluene, EtOH and water (2:1:1, 0.15 M) were added and the reaction was heated in a Biotage Initiator microwave to 120 °C for 20 min. The reaction mixture was filtered through Celite and evaporated to dryness. The residue was purified by silica chromatography or MDAP and the fractions evaporated to dryness to afford the product.

General Procedure C - S_NAr

To a solution of 5-chloro-*N*-methylpyrazolo[1,5-*a*]pyrimidine-3-carboxamide **3** (1 eq) in DMSO (0.3 M) was added DIPEA (3 eq) and the respective amine (2 eq). The reaction was stirred at rt or heated in a Biotage Initiator microwave reaction to 90-120 °C until complete.

After cooling the reaction mixture was diluted with MeOH (0.4 mL) and purified directly by High pH MDAP. The solvent was evaporated to afford the product.

General Procedure D - Boc Deprotection

To a solution of the Boc-amine in DCM (0.5 mL) was added TFA (0.1 mL), and the reaction was stirred at rt for 90 min. The reaction mixture was purified directly by ion exchange chromatography (sulphonic acid (SCX), sequential solvents MeOH, 2 M NH₃/MeOH). The appropriate fractions were combined and evaporated *in vacuo* to give the product.

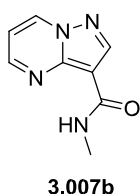
General Procedure E – Amine Acylation

To a solution of a primary or secondary amine (1 eq) and pyridine (2 eq) in DCM (0.14 M) was added the respective acylating agent (1.5 eq). The reaction mixture was stirred at rt for 2 h, then diluted with DCM (5 mL) and washed with sat. aq. NaHCO₃ (5 mL). The aqueous layer was extracted with DCM (5 mL), dried through a hydrophobic frit and evaporated to dryness. The residue was purified by silica chromatography (0-100% (3:1 EtOAc:EtOH)/cyclohexane), and the appropriate fractions were evaporated to dryness to afford the product.

General Procedure F – Reductive Amination

A suspension of the desired amine (1 eq), aldehyde (1.5 eq) and magnesium sulphate in DCM (0.1 M) was stirred at rt for 24 h. The reaction mixture was filtered and evaporated to dryness. The residue was dissolved in MeOH (0.1 M) and sodium borohydride (5 eq) was added portionwise. The reaction was stirred at rt for 1 h, then quenched with water and evaporated. The residue was partitioned between water (10 mL) and EtOAc (10 mL) and the aqueous layer was extracted with EtOAc (2 x 10 mL). The combined organics were washed with brine, dried through a hydrophobic frit and evaporated to dryness. The crude product was purified by silica chromatography or MDAP to afford the product.

***N*-Methylpyrazolo[1,5-*a*]pyrimidine-3-carboxamide**



Synthesised according to General Procedure A using pyrazolo[1,5-*a*]pyrimidine-3-carboxylic acid **3.006** (100 mg, 0.61 mmol) and MeNH₂ (919 μ L, 2 M in THF 1.839 mmol). The crude product was purified by silica chromatography (10-50% (3:1 EtOAc:EtOH)/cyclohexane), fractions were evaporated *in vacuo* and further purified by High pH MDAP to afford *N*-

methylpyrazolo[1,5-*a*]pyrimidine-3-carboxamide (87 mg, 0.494 mmol, 81%) as a white solid.

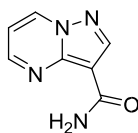
LCMS (High pH, ES⁺): t_R =0.50 min, [M+H]⁺ 177.2, (100% purity). ¹H NMR (400 MHz, MeOD-*d*₄): δ 3.01 (s, 3H), 7.19 (dd, J = 7.0, 4.2 Hz, 1H), 8.53 (s, 1H),

8.74 (dd, J = 4.2, 1.6 Hz, 1H), 9.04 (dd, J = 7.0, 1.6 Hz, 1H). Amide proton not observed. ¹³

C NMR (101 MHz, MeOD-*d*₄): δ 24.7, 104.7, 109.6, 136.8, 145.5, 145.9, 152.0, 163.7. M.pt.: 159-161 °C. ν_{max} (neat): 3372, 3103, 2509, 1644, 1612, 1560, 1527, 1496, 1445, 1399, 1385, 1325, 1295, 1265, 1230, 1212, 1170, 1109, 1021, 906, 776 cm⁻¹.

HRMS: (C₈H₈N₄O) [M+H]⁺ requires 177.0776, found [M+H]⁺ 177.0779.

Pyrazolo[1,5-a]pyrimidine-3-carboxamide

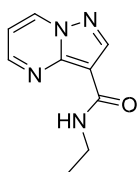


3.007b

Synthesised according to General Procedure A using pyrazolo[1,5-a]pyrimidine-3-carboxylic acid **3.006** (25 mg, 0.15 mmol) and ammonium chloride (16 mg, 0.31 mmol), to afford pyrazolo[1,5-a]pyrimidine-3-carboxamide (15 mg, 0.09 mmol, 60%).

LCMS (High pH, ES⁺): t_R =0.42 min, [M+H]⁺ 163.2, (100% purity). ¹H NMR (400 MHz, MeOD-d₄): δ 7.20 (dd, J = 7.0, 4.2 Hz, 1H), 8.57 (s, 1H), 8.77 (dd, J = 4.2, 1.6 Hz, 1H), 9.07 (dd, J = 7.0, 1.6 Hz, 1H). Exchangeable protons were not observed.

N-Ethylpyrazolo[1,5-a]pyrimidine-3-carboxamide



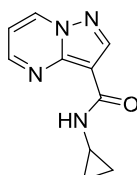
3.007c

Synthesised according to General Procedure A using pyrazolo[1,5-a]pyrimidine-3-carboxylic acid **3.006** (25 mg, 0.15 mmol) and EtNH₂ (0.15 mL, 2 M in THF, 0.31 mmol), to afford *N*-ethylpyrazolo[1,5-a]pyrimidine-3-carboxamide (23 mg, 0.121 mmol, 79%).

LCMS (High pH, ES⁺): t_R =0.60 min, [M+H]⁺ 191.2, (100% purity). ¹

H NMR (400 MHz, MeOD-d₄): δ 1.31-1.41 (m, 3H), 3.55-3.65 (m, 2H), 7.24-7.34 (m, 1H), 8.66 (s, 1H), 8.82-8.89 (m, 1H), 9.11-9.19 (m, 1H). Amide proton not observed.

N-Cyclopropylpyrazolo[1,5-a]pyrimidine-3-carboxamide

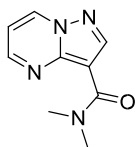


3.007d

Synthesised according to General Procedure A using pyrazolo[1,5-a]pyrimidine-3-carboxylic acid **3.006** (25 mg, 0.15 mmol) and cyclopropylamine (18 mg, 0.31 mmol), to afford *N*-cyclopropylpyrazolo[1,5-a]pyrimidine-3-carboxamide (15 mg, 0.07 mmol, 48%).

LCMS (High pH, ES⁺): t_R =0.62 min, [M+H]⁺ 203.3, (100% purity). ¹H NMR (400 MHz, MeOD-d₄): δ 0.61-0.70 (m, 2H), 0.81-0.92 (m, 2H), 2.84-2.94 (m, 1H), 7.15-7.24 (m, 1H), 8.56 (s, 1H), 8.70-8.79 (m, 1H), 9.01-9.09 (m, 1H). Exchangeable protons were not observed.

N,N-Dimethylpyrazolo[1,5-a]pyrimidine-3-carboxamide

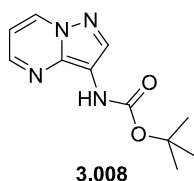


3.007e

Synthesised according to General Procedure A using pyrazolo[1,5-a]pyrimidine-3-carboxylic acid **3.006** (25 mg, 0.15 mmol) and dimethylamine, (0.039 mL, 40% wt. in H₂O, 0.31 mmol), to afford *N,N*-dimethylpyrazolo[1,5-a]pyrimidine-3-carboxamide (8 mg, 0.042 mmol, 27%).

LCMS (High pH, ES⁺): t_R =0.48 min, [M+H]⁺ 191.2, (100% purity). ¹H NMR (400 MHz, MeOD-d₄): δ 3.10-3.22 (m, 6H), 7.13 (dd, J = 7.0, 4.2 Hz, 1H), 8.36 (s, 1H), 8.68 (dd, J = 4.2, 1.6 Hz, 1H), 8.99 (dd, J = 7.0, 1.6 Hz, 1H).

***tert*-Butyl pyrazolo[1,5-*a*]pyrimidin-3-ylcarbamate**



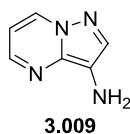
To a suspension of pyrazolo[1,5-*a*]pyrimidine-3-carboxylic acid **3.006** (100 mg, 0.613 mmol) and triethylamine (171 μ L, 1.226 mmol) in toluene (4 mL) stirred under N₂ at rt was added diphenyl phosphorazidate (198 μ L, 0.919 mmol). The reaction mixture was stirred at rt for 15 min, then heated to 100 °C for 2.5 h. *tert*-Butanol (0.6 mL, 6.13 mmol) was added

and the reaction was heated to 100 °C for 2.5 h. The reaction mixture was then cooled to rt and partitioned between EtOAc (10 mL) and water (25 mL). The aqueous was extracted with EtOAc (3 x 10 mL) and the combined organics were dried using a hydrophobic frit and evaporated *in vacuo*. The crude product was purified by silica chromatography (10-50% (3:1 EtOAc:EtOH)), appropriate fractions were evaporated *in vacuo* to afford *tert*-butyl pyrazolo[1,5-*a*]pyrimidin-3-ylcarbamate (85 mg, 0.363 mmol, 59%) as a yellow solid.

LCMS (High pH, ES⁺): t_R = 0.79 min, [M-H]⁺ 233.2, (75% purity).

¹H NMR (400 MHz, DMSO-*d*₆): δ 1.46 (s, 9H), 6.98 (dd, *J* = 7.1, 4.0 Hz, 1H), 8.23 (br. s., 1H), 8.48 (dd, *J* = 4.0, 1.6 Hz, 1H), 8.89 (br. s, 1H), 8.99 (dd, *J* = 7.1, 1.6 Hz, 1H).

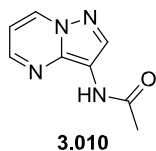
Pyrazolo[1,5-*a*]pyrimidin-3-amine



To a solution of *tert*-butyl pyrazolo[1,5-*a*]pyrimidin-3-ylcarbamate **3.008** (85 mg, 0.363 mmol) in DCM (3.6 mL) was added TFA (559 μ L, 7.26 mmol) and the mixture was stirred at rt for 4 h. The reaction mixture was purified by ion exchange chromatography (SCX 5 g, sequential solvents: MeOH/2 M NH₃ in MeOH). The appropriate fractions were combined and concentrated under reduced pressure to give pyrazolo[1,5-*a*]pyrimidin-3-amine (43 mg, 0.321 mmol, 88%) as an orange solid.

LCMS (High pH, ES⁺): t_R = 0.36 min, no mass ion observed, (100% purity). ¹H NMR (400 MHz, DMSO-*d*₆): δ 4.24 (br. s., 2H), 6.73 (dd, *J* = 7.1, 3.9 Hz, 1H), 7.71 (s, 1H), 8.20 (dd, *J* = 3.9, 1.6 Hz, 1H), 8.75 (dd, *J* = 7.1, 1.6 Hz, 1H).

***N*-(Pyrazolo[1,5-*a*]pyrimidin-3-yl)acetamide**



To a solution of pyrazolo[1,5-*a*]pyrimidin-3-amine **3.009** (15 mg, 0.112 mmol) and pyridine (18 μ L, 0.224 mmol) in DCM (0.5 mL) was added acetyl chloride (12 μ L, 0.168 mmol). The reaction mixture was stirred at rt for 2 h, and then diluted with DCM (5 mL) and washed with sat. aq. NaHCO₃ (5 mL). The aqueous was extracted with DCM (5 mL), dried through a hydrophobic frit and evaporated to dryness. The residue was purified by silica chromatography (0-90% 3:1 EtOAc:EtOH/cyclohexane), appropriate fractions were evaporated to dryness to afford *N*-(pyrazolo[1,5-*a*]pyrimidin-3-yl)acetamide (15 mg, 0.085 mmol, 76%) as a yellow solid.

LCMS (High pH, ES⁺): t_R = 0.38 min, [M+H]⁺ 177.2, (100% purity). ¹H NMR (400 MHz, DMSO-d₆): δ 2.09 (s, 3H), 7.00 (dd, J = 7.1, 3.9 Hz, 1H), 8.48 (dd, J =

4.0, 1.6 Hz, 1H), 8.52 (s, 1H), 9.01 (dd, J = 7.1, 1.7 Hz, 1H), 10.09 (s, 1H).

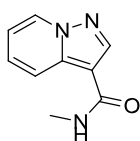
¹³

C NMR (126 MHz, DMSO-d₆): δ 23.3, 108.9, 111.2, 136.1, 138.2, 138.9, 148.7, 168.6. M.pt.: 220-223 °C.

v_{max} (neat): 3232, 3119, 3072, 3030, 1676, 1628, 1591, 1541, 1480, 1408, 1379, 1359, 1336, 1306, 1266, 1168, 1136, 1110, 1003, 907, 797, 770, 751, 733, 658 cm⁻¹.

HRMS: (C₈H₈N₄O) [M+H]⁺ requires 177.0771, found [M+H]⁺ 177.0776.

N-Methylpyrazolo[1,5-a]pyridine-3-carboxamide



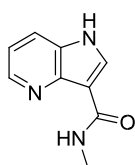
3.012

To a suspension of pyrazolo[1,5-a]pyridine-3-carboxylic acid **3.011** (72 mg, 0.44 mmol) and oxalyl chloride (78 μL, 0.89 mmol) in DCM (2.5 mL) stirred under N₂ at rt was added DMF (3 μL, 0.04 mmol). The reaction mixture was stirred at rt for 3 h, until the suspension became a clear brown solution. The reaction mixture was evaporated *in vacuo*, redissolved in THF (2.5 mL) and cooled to 0 °C. MeNH₂ (666 μL, 2 M in THF, 1.33 mmol) was added and the reaction was stirred at 0 °C for 1 h. The reaction mixture was diluted with EtOAc (10 mL) and sat. aq. NaHCO₃ (5 mL) and the aqueous layer was extracted with EtOAc (3 x 10 mL). The combined organic layers were dried through a hydrophobic frit and evaporated to dryness. The crude product was purified by silica chromatography (0-25% EtOH/EtOAc), fractions were evaporated *in vacuo* to afford *N*-methylpyrazolo[1,5-a]pyridine-3-carboxamide (64 mg, 0.365 mmol, 82%) as a white solid

LCMS (High pH, ES⁺): t_R = 0.55 min, [M+] 175.2, (95% pure). ¹H NMR (400 MHz, CDCl₃): δ 3.03 (d, J = 4.9 Hz, 3H), 5.79-5.97 (m, 1H), 6.92 (ddd, J = 7.1,

6.8, 1.2 Hz, 1H), 7.35 (ddd, J = 9.1, 6.8, 1.0 Hz, 1H), 8.12 (s, 1H), 8.29-8.34 (m, 1H), 8.46-8.50 (m, 1H).

N-Methyl-1H-pyrrolo[3,2-b]pyridine-3-carboxamide



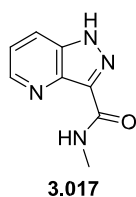
3.016

Synthesised according to General Procedure A using pyrrolo[3,2-b]pyridine-3-carboxylic acid **3.013** (200 mg, 1.23 mmol) and MeNH₂ (1.9 mL, 2 M in THF, 3.70 mmol), affording *N*-methyl-1H-pyrrolo[3,2-b]pyridine-3-carboxamide (130 mg, 0.74 mmol, 60%).

LCMS (High pH, ES⁺): t_R=0.62 min, [M+H]⁺ 176.2, (91% purity). ¹H NMR (400 MHz, CDCl₃): δ 3.15 (d, J = 4.9 Hz, 3H), 7.22 (dd, J = 8.3, 4.6 Hz, 1H), 7.82 (dd, J = 8.3, 1.0 Hz, 1H), 8.15 (d, J = 3.2 Hz, 1H), 8.52 (dd, J = 4.6, 1.0 Hz, 1H), 8.97 (br. s., 1H), 9.85 (br. s., 1H). ¹³C NMR (101 MHz, CDCl₃): δ 25.9, 110.6, 117.5, 120.1, 129.7, 131.9, 143.0, 143.5, 166.1. M.pt.: 143-148 °C. v_{max} (neat): 3136, 3098, 3055, 2933, 2888, 1620, 1575, 1498, 1454, 1413, 1336, 1283, 1205, 1160, 1130, 1083, 998, 888, 764 cm⁻¹.

HRMS: (C₉H₉N₃O) [M+H]⁺ requires 176.0818, found [M+H]⁺ 176.0816.

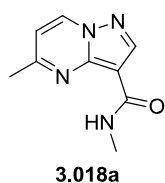
***N*-Methyl-1*H*-pyrazolo[4,3-*b*]pyridine-3-carboxamide**



Synthesised according to General Procedure A using pyrazolo[4,3-*b*]pyridine-3-carboxylic acid **3.014** (50 mg, 0.306 mmol) and MeNH₂ (0.49 mL, 2 M in THF, 0.99 mmol), affording *N*-methyl-1*H*-pyrazolo[4,3-*b*]pyridine-3-carboxamide (2.4 mg, 0.014 mmol, 4%).

LCMS (High pH, ES⁺): t_R=0.51 min, [M+H]⁺ 177.0, (70% purity). ¹H NMR (400 MHz, CDCl₃): δ 3.27 (d, *J* = 4.9 Hz, 3H), 7.46 (dd, *J* = 8.4, 4.5 Hz, 1H), 8.63-8.70 (m, 2H), 8.89 (q, *J* = 4.9 Hz, 1H), 13.85-14.30 (m, 1H).

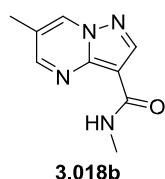
***N*,5-Dimethylpyrazolo[1,5-*a*]pyrimidine-3-carboxamide**



Synthesised according to General Procedure A using 5-methylpyrazolo[1,5-*a*]pyrimidine-3-carboxylic acid **3.015a** (50 mg, 0.282 mmol) and MeNH₂ (0.49 mL, 2 M in THF, 0.99 mmol), affording *N*,5-dimethylpyrazolo[1,5-*a*]pyrimidine-3-carboxamide (27 mg, 0.142 mmol, 50%).

LCMS (High pH, ES⁺): t_R=0.57 min, [M+H]⁺ 191.2, (100% purity). ¹H NMR (400 MHz, CDCl₃): δ 2.71 (s, 3H), 3.08 (d, *J* = 4.9 Hz, 3H), 6.83 (d, *J* = 7.1 Hz, 1H), 7.87 (br. s., 1H), 8.57-8.64 (m, 2H)

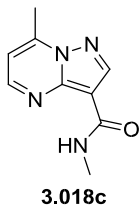
***N*,6-Dimethylpyrazolo[1,5-*a*]pyrimidine-3-carboxamide**



Synthesised according to General Procedure A using 6-methylpyrazolo[1,5-*a*]pyrimidine-3-carboxylic acid **3.015b** (50 mg, 0.282 mmol) and MeNH₂ (0.49 mL, 2 M in THF, 0.99 mmol), affording *N*,6-dimethylpyrazolo[1,5-*a*]pyrimidine-3-carboxamide (32 mg, 0.168 mmol, 60%).

LCMS (High pH, ES⁺): t_R=0.57 min, [M+H]⁺ 191.2, (100% purity). ¹H NMR (400 MHz, CDCl₃): δ 2.46 (d, *J* = 0.7 Hz, 3H), 3.08 (d, *J* = 4.9 Hz, 3H), 7.79 (br. s., 1H), 8.50 (d, *J* = 2.0 Hz, 1H), 8.58 (dd, *J* = 2.0, 0.7 Hz, 1H), 8.63 (s, 1H).

***N*,7-Dimethylpyrazolo[1,5-*a*]pyrimidine-3-carboxamide**



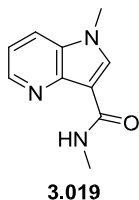
Synthesised according to General Procedure A using 7-methylpyrazolo[1,5-*a*]pyrimidine-3-carboxylic acid **3.018c** (50 mg, 0.282 mmol) and MeNH₂ (0.49 mL, 2 M in THF, 0.99 mmol), affording *N*,7-dimethylpyrazolo[1,5-*a*]pyrimidine-3-carboxamide (42 mg, 0.221 mmol, 75%).

LCMS (High pH, ES⁺): t_R=0.56 min, [M+H]⁺ 191.2, (100% purity). ¹H NMR (400 MHz, CDCl₃): δ 2.88 (d, *J* = 0.7 Hz, 3H), 3.09 (d, *J* = 4.9 Hz, 3H), 6.87 (dd, *J* = 4.4, 0.7 Hz, 1H), 7.95 (br. s., 1H), 8.52 (d, *J* = 4.4 Hz, 1H), 8.72 (s, 1H). M.pt.: 171-173 °C. ¹³C NMR (101 MHz, CDCl₃): δ 17.2, 25.8, 106.2, 108.5, 146.0, 146.2, 147.9, 150.0, 162.9. ν_{max}

(neat): 3350, 3062, 1645, 1552, 1414, 1389, 1335, 1267, 1244, 1169, 1037, 940, 857, 802, 779, 716 cm⁻¹.

HRMS: (C₉H₁₀ON₄) [M+H]⁺ requires 191.0933, found [M+H]⁺ 191.0936.

***N*,1-Dimethyl-1*H*-pyrrolo[3,2-*b*]pyridine-3-carboxamide**



A solution of *N*-methyl-1*H*-pyrrolo[3,2-*b*]pyridine-3-carboxamide **3.016** (10 mg, 0.057 mmol), tetrabutylammonium hydrogen sulfate (2 mg, 5.71 μmol) and 50% aq. potassium hydroxide (11 μL, 0.057 mmol) in DCM (0.5 mL) was stirred vigorously at rt for 5 min. Methyl iodide (4 μL, 0.068 mmol) was added and the reaction mixture was stirred vigorously at rt for 18 h. The reaction

mixture was partitioned between DCM (5 mL) and sat. aq. NaHCO₃ (5 mL). The aqueous was extracted with DCM (2 x 5 mL) and the combined organics were evaporated to dryness. The crude product was purified by silica chromatography (0-100% (3:1

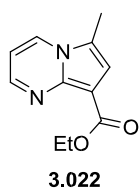
EtOAc/EtOH)/cyclohexane), appropriate fractions were evaporated to dryness and further purified by SPE (sulphonic acid (SCX) 1g, sequential solvents MeOH, 2 M NH₃/MeOH). Appropriate fractions were evaporated *in vacuo* to give *N*,1-dimethyl-1*H*-pyrrolo[3,2*b*]pyridine-3-carboxamide (8.5 mg, 0.045 mmol, 79%) as a white solid.

LCMS (High pH, ES⁺): t_R=0.69 min, [M+H]⁺ 190.2, (97% purity). ¹H NMR (400 MHz, CDCl₃): δ 3.08 (d, *J* = 4.9 Hz, 3H), 3.85 (s, 3H), 7.20 (dd, *J* = 8.3, 4.6 Hz, 1H), 7.67 (dd, *J* = 8.3, 1.2 Hz, 1H), 7.99 (s, 1H), 8.49 (dd, *J* = 4.8, 1.3 Hz, 1H), 8.70 (br. s., 1H). ¹³C NMR (101 MHz, CDCl₃): δ 25.7, 33.4, 110.8, 117.0, 117.5, 130.1, 135.6, 143.3, 143.4, 164.6.

M.pt.: 170-171 °C. ν_{max} (neat): 3332, 3060, 1644, 1610, 1558, 1451, 1415, 1387, 1334, 1312, 1266, 1229, 1144, 1072, 981, 923, 780 cm⁻¹.

HRMS: (C₁₀H₁₁N₃O) [M+H]⁺ requires 190.0975 found [M+H]⁺ 190.0976.

Ethyl 6-methylpyrrolo[1,2-*a*]pyrimidine-8-carboxylate



A suspension of ethyl 2-amino-5-methyl-1*H*-pyrrole-3-carboxylate **3.021** (100 mg, 0.595 mmol) and 1,1,3,3-tetramethoxypropane (0.157 mL, 0.951 mmol) in acetic acid (0.6 mL) was heated to 100 °C in a sealed tube (oil bath) for 1 h. The reaction mixture was cooled to rt, neutralised with sat. aq. NaHCO₃ (15 mL) and extracted with EtOAc (3 x 15 mL). The organics were dried through a

hydrophobic frit and evaporated to dryness. Purified by silica chromatography (50-100% EtOAc/cyclohexane), appropriate fractions were evaporated to afford ethyl 6-methylpyrrolo[1,2-*a*]pyrimidine-8-carboxylate (21 mg, 0.103 mmol, 17%) as a yellow gum.

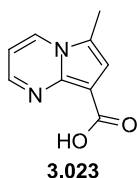
LCMS (Formic, ES⁺): t_R=0.76 min, [M+H]⁺ 205.0, (90% pure). ¹H NMR (400 MHz, CDCl₃): δ 1.41 (t, *J* = 7.2 Hz, 3H), 2.47 (s, 3H), 4.41 (q, *J* = 7.2 Hz, 2H), 6.79 (dd, *J* = 7.1, 4.0 Hz, 1H), 7.22 (s, 1H), 8.08 (dd, *J* = 7.1, 1.8 Hz, 1H), 8.43 (dd, *J* = 4.0,

1.8 Hz, 1H). ¹³C NMR (101 MHz, CDCl₃): δ 11.0, 14.7, 59.9, 102.4, 107.8, 117.1, 117.9, 129.5, 140.9, 146.0, 164.1.

ν_{\max} (neat): 2981, 1682, 1620, 1557, 1524, 1503, 1436, 1328, 1277, 1239, 1208, 1127, 1073, 1041, 779 cm⁻¹.

HRMS: (C₁₁H₁₂N₂O₂) [M+H]⁺ requires 205.0972, found [M+H]⁺ 205.0970.

6-Methylpyrrolo[1,2-a]pyrimidine-8-carboxylic acid

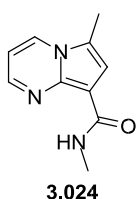


To a solution of ethyl 6-methylpyrrolo[1,2-a]pyrimidine-8-carboxylate **3.022** (32 mg, 0.157 mmol) in MeOH (1.5 mL) was added 4M aq. KOH (118 μL, 0.470 mmol), and the reaction was heated to 80 °C for 1 h. The reaction mixture was cooled and purified by SPE (aminopropyl (NH₂), 2 g, sequential solvents MeOH/1.25 M HCl in MeOH). The product did not absorb to the column and the appropriate fractions were evaporated *in vacuo* to afford 6-methylpyrrolo[1,2-a]pyrimidine-8-carboxylic acid, potassium salt (46 mg, 0.150 mmol, 95%) as a yellow solid. Used for further chemistry without purification.

LCMS (Formic, ES⁺): t_R =0.56 min, [M+H]⁺ 177.0, (100% purity). ¹H NMR (400 MHz, DMSO-d₆): δ 2.38 (s, 3H), 6.66 (dd, J = 7.0, 3.8 Hz, 1H), 6.93 (s, 1H),

8.06-8.09 (m, 1H), 8.33 (dd, J = 7.0, 1.6 Hz, 1H). Acid proton not observed.

N,6-Dimethylpyrrolo[1,2-a]pyrimidine-8-carboxamide



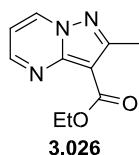
Synthesised according to General Procedure A using potassium 6-methylpyrrolo[1,2-a]pyrimidine-8-carboxylate **3.023** (43 mg, 0.140 mmol) and MeNH₂, (0.140 mL, 2 M in THF, 0.281 mmol). After 90 min, further HATU (59 mg, 0.155 mmol), MeNH₂, (0.140 mL, 2 M in THF, 0.281 mmol) and DIPEA (0.074 mL, 0.421 mmol) were added and the reaction was stood for 18 hr. After High pH MDAP, the product contained residual DIPEA and silicone grease so was dried under vacuum, loaded onto a plug of silica, washed with cyclohexane and eluted with EtOAc. The solvent was evaporated *in vacuo* to afford N,6-dimethylpyrrolo[1,2-a]pyrimidine-8-carboxamide (9 mg, 0.048 mmol, 34%) as a yellow solid.

LCMS (High pH, ES⁺): t_R =0.65 min, [M+H]⁺ 190.2, (96% purity). ¹H NMR (400 MHz, MeOD-d₄): δ 2.49 (d, J = 0.7 Hz, 3H), 3.02 (s, 3H), 6.89 (dd, J = 7.1, 4.2 Hz, 1H), 7.17 (q, J = 0.7 Hz, 1H), 8.32 (dd, J = 4.0, 1.6 Hz, 1H), 8.47 (dd, J = 7.1, 1.5 Hz, 1H). NH was not observed. ¹³C NMR (101 MHz, MeOD-d₄): δ 9.3, 24.6, 103.8, 107.3, 114.6, 118.7, 130.7, 138.8, 144.7, 166.1. M.pt.: 70-73 °C.

ν_{\max} (neat): 3460, 3317, 2919, 1618, 1600, 1563, 1508, 1440, 1379, 1331, 1284, 1260, 1092, 843, 774, 622, 556 cm⁻¹.

HRMS: (C₁₀H₁₁N₃O) [M+H]⁺ requires 190.0975, found [M+H]⁺ 190.0974.

6-Methylpyrrolo[1,2-a]pyrimidine-8-carboxylic acid



A suspension of ethyl 5-amino-3-methyl-1H-pyrazolo[1,5-a]pyrimidine-3-carboxylate **3.025** (230 mg, 1.359 mmol) and 1,1,3,3-tetramethoxypropane (0.302 mL, 1.835 mmol) in 5 M HCl (1 mL) was heated to 95 °C in a sealed tube for 5 min. The reaction mixture was cooled to rt, neutralised with sat. aq. NaHCO₃ (15 mL)

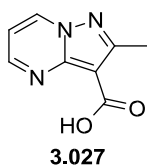
and extracted with EtOAc (3 x 15 mL). The organics were dried through a hydrophobic frit and evaporated to dryness. Purified by silica chromatography (50-100%

EtOAc/cyclohexane), appropriate fractions were evaporated *in vacuo* to afford ethyl 2-methylpyrazolo[1,5-a]pyrimidine-3-carboxylate (155 mg, 0.755 mmol, 56%) as a yellow solid.

LCMS (High pH, ES⁺): t_R=0.72 min, [M+EtO⁻] 160.1, (96% pure).

¹H NMR (400 MHz, CDCl₃): δ 1.45 (t, *J* = 7.1 Hz, 3H), 2.74 (s, 3H), 4.48 (q, *J* = 7.1 Hz, 2H), 6.97 (dd, *J* = 7.0, 4.3 Hz, 1H), 8.66 (dd, *J* = 7.0, 2.0 Hz, 1H), 8.75 (dd, *J* = 4.3, 2.0 Hz, 1H).

2-Methylpyrazolo[1,5-a]pyrimidine-3-carboxylic acid



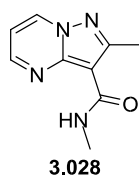
A solution of ethyl 2-methylpyrazolo[1,5-a]pyrimidine-3-carboxylate **3.026** (155 mg, 0.76 mmol) and NaOH (2.3 mL, 1 M aq., 2.3 mmol) in MeOH (2.5 mL) and THF (2.5 mL) was stirred at rt for 18 h. The reaction mixture was acidified to pH 1 with 5 M HCl and evaporated to dryness. The residue was

dissolved in DMSO, filtered and purified TFA MDAP to afford 2-methylpyrazolo[1,5a]pyrimidine-3-carboxylic acid (54 mg, 0.305 mmol, 40%) as an off-white solid.

LCMS (TFA, ES⁺): t_R=0.41 min, [M+H]⁺ 178.1, (100% pure). ¹H NMR (400 MHz, DMSO-d₆): δ 2.60 (s, 3H), 7.19 (dd, *J* = 7.1, 4.2 Hz, 1H), 8.73 (dd, *J* =

4.2, 1.7 Hz, 1H), 9.13 (dd, *J* = 6.8, 1.7 Hz, 1H), 12.26 (br. s, 1H).

N,2-Dimethylpyrazolo[1,5-a]pyrimidine-3-carboxamide



Synthesised according to General Procedure A using 2-methylpyrazolo[1,5a]pyrimidine-3-carboxylic acid **3.027** (25 mg, 0.14 mmol) and MeNH₂, 2 M in THF (0.14 mL, 0.28 mmol). The reaction mixture was filtered and purified by TFA MDAP. The solvent was evaporated and the residue was

purified by ion exchange chromatography (sulphonic acid (SCX) 500 mg, MeOH). The solvent was evaporated *in vacuo* to afford N,2-dimethylpyrazolo[1,5-a]pyrimidine-3-carboxamide (24 mg, 0.13 mmol, 89%) as a white solid. LCMS (TFA, ES⁺): t_R=0.49 min, [M+H]⁺ 191.0, (100% purity). ¹H NMR (400 MHz, DMSO-d₆): δ 2.64 (s, 3H), 2.88 (d, *J* = 4.6 Hz, 3H), 7.19 (dd, *J* = 7.0, 4.3 Hz, 1H), 7.93-8.05 (m, 1H), 8.73 (dd, *J* = 4.3, 1.7 Hz, 1H), 9.18 (dd, *J* = 7.0, 1.7 Hz, 1H).

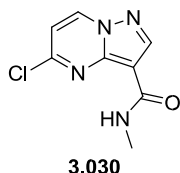
¹³C

NMR (101 MHz, DMSO-d₆): δ 14.8, 25.9, 101.8, 109.7, 137.1, 146.6, 152.0, 156.8, 163.1. M.pt.: 160-164 °C.

ν_{\max} (neat): 3363, 3070, 1615, 1532, 1424, 1399, 1353, 1275, 1226, 1146, 1023, 840, 785, 683 cm^{-1} .

HRMS: ($\text{C}_9\text{H}_{10}\text{N}_4\text{O}$) $[\text{M}+\text{H}]^+$ requires 191.0927, found $[\text{M}+\text{H}]^+$ 191.0928.

5-Chloro-*N*-methylpyrazolo[1,5-*a*]pyrimidine-3-carboxamide



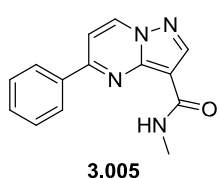
To a suspension of 5-chloropyrazolo[1,5-*a*]pyrimidine-3-carboxylic acid **3.029** (2.5 g, 12.7 mmol) and oxalyl chloride (2.22 mL, 25.3 mmol) in DCM (75 mL) stirred under N_2 at rt was added DMF (0.08 mL, 1.0 mmol). The reaction mixture was stirred at rt for 4 h, until the suspension became a clear brown solution. The reaction mixture was evaporated *in vacuo* and the residue was redissolved in DCM and evaporated to dryness to afford the acid chloride (2.96 g, 97%).

The residue was redissolved in THF (30 mL) and MeNH_2 (19 mL, 2 M in THF, 37.8 mmol) was added under N_2 at 0 °C. The reaction mixture was stirred at 0 °C for 1 h. The reaction mixture was then diluted with EtOAc (100 mL) and sat. aq. NaHCO_3 (50 mL) and the aqueous layer was extracted with EtOAc (4 x 50 mL). The combined organic layers were washed with brine (20 mL), dried through a hydrophobic frit and evaporated to dryness. The crude product was purified by silica chromatography (75-100% EtOAc/cyclohexane), appropriate fractions were evaporated *in vacuo* to afford 5-chloro-*N*-methylpyrazolo[1,5-*a*]pyrimidine-3-carboxamide (1.70 g, 8.07 mmol, 82%) as a cream solid.

LCMS (High pH, ES^+): t_{R} = 0.63 min, $[\text{M}+\text{H}]^+$ 211.2, (93% purity). ^1H NMR (400 MHz, CDCl_3): δ 3.08 (d, J = 4.9 Hz, 3H), 6.96 (d, J = 7.3 Hz, 1H), 7.43 (br. s., 1H), 8.67 (d, J = 7.3 Hz, 1H), 8.68 (s, 1H). ^{13}C NMR (101 MHz, CDCl_3): δ 26.0, 106.4, 110.0, 137.3, 144.6, 148.0, 152.7, 161.9. M.pt.: 212-213 °C. ν_{\max} (neat): 3376, 3110, 3066, 1648, 1609, 1563, 1515, 1400, 1306, 1237, 1220, 1151, 1132, 1113, 1067, 959, 932, 921, 805, 775, 743, 720 cm^{-1} .

HRMS: ($\text{C}_8\text{H}_7\text{ClN}_4\text{O}$) $[\text{M}+\text{H}]^+$ requires 211.0381, found $[\text{M}+\text{H}]^+$ 211.0381.

N-Methyl-5-phenylpyrazolo[1,5-*a*]pyrimidine-3-carboxamide

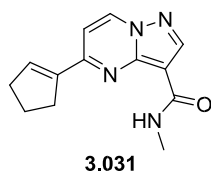


Prepared according to General Procedure B, with 5-chloro-*N*-methylpyrazolo[1,5-*a*]pyrimidine-3-carboxamide **3.030** (25 mg, 0.12 mmol) and phenylboronic acid (17 mg, 0.14 mmol). Purified by High pH MDAP to afford *N*-methyl-5-phenylpyrazolo[1,5-*a*]pyrimidine-3-carboxamide (20 mg, 0.08 mmol, 67%).

LCMS (High pH, ES^+): t_{R} = 0.87 min, $[\text{M}+\text{H}]^+$ 253.2, (100% purity). ^1H NMR (400 MHz, CDCl_3): δ 3.11 (d, J = 4.9 Hz, 3H), 7.41 (d, J = 7.3 Hz, 1H), 7.56-7.62 (m, 3H), 7.87-7.99 (m, 1H), 8.05-8.12 (m, 2H), 8.67 (s, 1H), 8.77 (d, J = 7.3 Hz, 1H). ^{13}C NMR (101 MHz, CDCl_3): δ 26.0, 106.2, 106.5, 127.5, 129.3, 131.4, 136.1, 136.3, 145.7, 147.4, 158.2, 162.9. M.pt.: 145-147 °C. ν_{\max} (neat): 1652, 1615, 1560, 1490, 1472, 1415, 1288, 1227, 785, 770, 748, 691 cm^{-1} .

HRMS: (C₁₄H₁₂N₄O) [M+H]⁺ requires 253.1084, found [M+H]⁺ 253.1083.

5-(Cyclopent-1-en-1-yl)-*N*-methylpyrazolo[1,5-*a*]pyrimidine-3-carboxamide

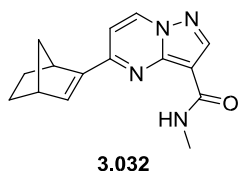


Prepared according to General Procedure B, with 5-chloro-*N*-methylpyrazolo[1,5-*a*]pyrimidine-3-carboxamide **3.030** (25 mg, 0.12 mmol) and 2-(cyclopent-1-en-1-yl)-4,4,5,5-tetramethyl-1,3,2dioxaborolane. Purification by High pH MDAP, affording 5-

(cyclopent-1-en-1-yl)-*N*-methylpyrazolo[1,5-*a*]pyrimidine-3-carboxamide (6 mg, 0.025 mmol, 21%) as a yellow solid.

LCMS (High pH, ES⁺): t_R = 0.92 min, [M+H]⁺ 243.3, (90% purity). ¹H NMR (400 MHz, CDCl₃): δ 2.07-2.16 (m, 2H), 2.70 (tq, *J* = 7.5, 2.5 Hz, 2H), 2.88-2.96 (m, 2H), 3.06 (d, *J* = 4.9 Hz, 3H), 6.79-6.85 (m, 1H), 7.14 (d, *J* = 7.3 Hz, 1H), 7.92 (br. s., 1H), 8.57 (d, *J* = 7.3 Hz, 1H), 8.59 (s, 1H).

5-(Bicyclo[2.2.1]hept-2-en-2-yl)-*N*-methylpyrazolo[1,5-*a*]pyrimidine-3-carboxamide

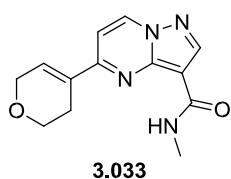


Prepared according to General Procedure B, with 5-chloro-*N*-methylpyrazolo[1,5-*a*]pyrimidine-3-carboxamide **3.030** (25 mg, 0.12 mmol) and 3,6-dihydro-2*H*-pyran-4-ylboronic acid pinacol ester (30 mg, 0.14 mmol). Purified by HPLC (Zorbax SB C8 21.2 x 150mm, 7 μm, 35-99% (0.1% Trifluoroacetic Acid in water)/MeCN),³⁸⁵ fractions

were evaporated to dryness and further purified by High pH MDAP to afford 5-(bicyclo[2.2.1]hept-2-en-2-yl)-*N*-methylpyrazolo[1,5-*a*]pyrimidine-3-carboxamide (8 mg, 0.03 mmol, 25%).

LCMS (High pH, ES⁺): t_R = 1.01 min, [M+H]⁺ 269.2, (97% purity). ¹H NMR (400 MHz, CDCl₃): δ 1.13-1.27 (m, 2H), 1.35-1.41 (m, 1H), 1.59-1.67 (m, 1H), 1.84-1.97 (m, 2H), 3.08 (d, *J* = 4.9 Hz, 3H), 3.15-3.20 (m, 1H), 3.65-3.70 (m, 1H), 6.96 (d, *J* = 3.2 Hz, 1H), 7.03 (d, *J* = 7.6 Hz, 1H), 7.96 (br. s., 1H), 8.54 (d, *J* = 7.5 Hz, 1H), 8.58 (s, 1H).

5-(3,6-Dihydro-2*H*-pyran-4-yl)-*N*-methylpyrazolo[1,5-*a*]pyrimidine-3-carboxamide

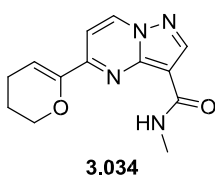


Prepared according to General Procedure B, with 5-chloro-*N*-methylpyrazolo[1,5-*a*]pyrimidine-3-carboxamide **3.030** (25 mg, 0.12 mmol) and 3,6-dihydro-2*H*-pyran-4-ylboronic acid pinacol ester (30 mg, 0.14 mmol). Purified by High pH MDAP to afford 5-(3,6-dihydro-2*H*-pyran-4-yl)-*N*-methylpyrazolo[1,5-*a*]pyrimidine-3-carboxamide (19

mg, 0.074 mmol, 62%)

LCMS (High pH, ES⁺): t_R = 0.69 min, [M+H]⁺ 259.2, (98% purity). ¹H NMR (400 MHz, CDCl₃): δ 2.71-2.77 (m, 2H), 3.07 (d, *J* = 4.89 Hz, 3H), 3.99 (t, *J* = 5.50 Hz, 2H), 4.43-4.48 (m, 2H), 6.83-6.89 (m, 1H), 7.14 (d, *J* = 7.34 Hz, 1H), 7.72-7.85 (m, 1H), 8.60 (s, 1H), 8.64 (d, *J* = 7.34 Hz, 1H).

5-(3,4-Dihydro-2H-pyran-6-yl)-N-methylpyrazolo[1,5-a]pyrimidine-3-carboxamide



Prepared according to General Procedure B, with 5-chloro-N-methylpyrazolo[1,5-a]pyrimidine-3-carboxamide **3.030** (25 mg, 0.12 mmol) and 2-(3,4-dihydro-2H-pyran-6-yl)-4,4,5,5-tetramethyl-1,3,2-dioxaborolane (30 mg, 0.142 mmol) and purified by High pH MDAP.

The solvent was evaporated to afford 5-(3,4-dihydro-2H-pyran-6-yl)-N-methylpyrazolo[1,5-a]pyrimidine-3-carboxamide (22 mg, 0.085 mmol, 72%) as a yellow solid.

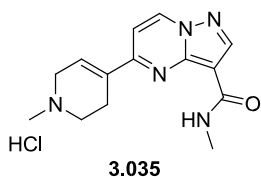
LCMS (High pH, ES⁺): t_R = 0.82 min, [M+H⁺] 259.2, (98% purity).

¹H NMR (400 MHz, CDCl₃): δ 1.95-2.03 (m, 2H), 2.36 (td, J = 6.2, 4.4 Hz, 2H), 3.08 (d, J = 4.9 Hz, 3H), 4.22-4.28 (m, 2H), 6.28 (t, J = 4.5 Hz, 1H), 7.28 (d, J = 7.3 Hz, 1H), 7.80 (br. s., 1H), 8.63 (s, 1H), 8.67 (d, J = 7.3 Hz, 1H).¹³

C NMR (101 MHz, CDCl₃): δ 21.0, 21.9, 26.0, 66.9, 104.9, 105.5, 105.6, 136.0, 145.2, 147.2, 149.1, 154.4, 162.9. M. pt.: 179-181 °C. ν_{max} (neat): 3364, 3052, 3002, 2929, 1648, 1610, 1560, 1509, 1421, 1348, 1279, 1232, 1174, 1087, 1065, 913, 838, 771 cm⁻¹.

HRMS: (C₁₃H₁₄N₄O₂) [M+H]⁺ requires 259.1190, found [M+H]⁺ 259.1190.

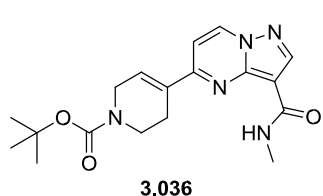
N-Methyl-5-(1-methyl-1,2,3,6-tetrahydropyridin-4-yl)pyrazolo[1,5-a]pyrimidine-3-carboxamide hydrochloride



Prepared according to General Procedure B, with 5-chloro-N-methylpyrazolo[1,5-a]pyrimidine-3-carboxamide **3.030** (25 mg, 0.12 mmol) and 1-methyl-4-(4,4,5,5-tetramethyl-1,3,2-dioxaborolan-2-yl)1,2,3,6-tetrahydropyridine (31.8 mg, 0.142 mmol) and purified by

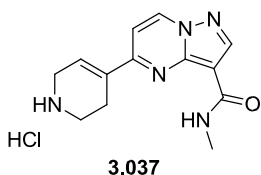
High pH MDAP. The solvent was evaporated *in vacuo*, dissolved in DCM (3 mL) and HCl (119 μL, 2 M in Et₂O, 0.237 mmol) was added dropwise with stirring. The resulting precipitate was collected by filtration and dried under vacuum to afford N-methyl-5-(1-methyl-1,2,3,6-tetrahydropyridin-4-yl)pyrazolo[1,5-a]pyrimidine-3-carboxamide hydrochloride (4 mg, 0.013 mmol, 11%) as a brown solid. LCMS (High pH, ES⁺): t_R = 0.68 min, [M+H⁺] 272.2, (92% purity). ¹H NMR (400 MHz, DMSO-d₆): δ 2.91 (d, J = 4.6 Hz, 3H), 3.17 (s, 3H), 3.61-3.71 (m, 2H), 3.86-3.98 (m, 2H), 4.09-4.14 (m, 1H), 4.15-4.20 (m, 1H), 7.09-7.15 (m, 1H), 7.59 (d, J = 7.3 Hz, 1H), 7.78 (q, J = 4.2 Hz, 1H), 8.54 (s, 1H), 9.26 (d, J = 7.3 Hz, 1H), 10.39-10.53 (m, 1H).

tert-Butyl 4-(3-(methylcarbamoyl)pyrazolo[1,5-a]pyrimidin-5-yl)-5,6-dihydropyridine-1(2H)-carboxylate



Prepared according to General Procedure B, with 5-chloro-*N*-methylpyrazolo[1,5-*a*]pyrimidine-3-carboxamide **3.030** (100 mg, 0.475 mmol) and *tert*-butyl 4-(4,4,5,5-tetramethyl-1,3,2-dioxaborolan-2-yl)-5,6-dihydropyridine-1(2*H*)-carboxylate (176 mg, 0.570 mmol). Purified by silica chromatography (0-100% EtOAc/cyclohexane), affording *tert*-butyl 4-(3-(methylcarbamoyl)pyrazolo[1,5-*a*]pyrimidin-5-yl)-5,6-dihydropyridine-1(2*H*)-carboxylate (135 mg, 0.302 mmol, 64%) as a green gum, which was 80% pure by NMR and used for further chemistry without further purification. LCMS (High pH, ES⁺): $t_R = 0.98$ min, $[M+H]^+$ 358.4, (84% purity).

***N*-Methyl-5-(1,2,3,6-tetrahydropyridin-4-yl)pyrazolo[1,5-*a*]pyrimidine-3-carboxamide hydrochloride**



A solution of *tert*-butyl 4-(3-(methylcarbamoyl)pyrazolo[1,5-*a*]pyrimidin-5-yl)-5,6-dihydropyridine-1(2*H*)-carboxylate **3.036** (130 mg, 0.291 mmol) in DCM (2 mL) and TFA (1 mL) was stirred at rt for 1 h. The reaction mixture was evaporated, azeotroped with

MeCN and purified by High pH MDAP. The fractions were evaporated to dryness and the residue was dissolved in DCM (3 mL). HCl (0.145 mL, 4 M in 1,4-dioxane, 0.582 mmol) was added dropwise with stirring. The resulting suspension was filtered and the solid dried under vacuum to afford *N*-methyl-5-(1,2,3,6-tetrahydropyridin-4-yl)pyrazolo[1,5-*a*]pyrimidine-3-carboxamide hydrochloride (42 mg, 0.143 mmol, 49%) as a yellow solid.

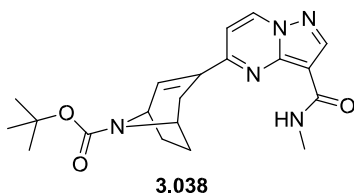
LCMS (High pH, ES⁺): $t_R = 0.58$ min, $[M+H]^+$ 258.2, (100% pure). ¹H NMR (400 MHz, DMSO-*d*₆): δ 2.91 (d, $J = 4.6$ Hz, 3H), 2.92-2.97 (m, 2H), 3.29-3.41 (m, 2H), 3.86-3.96 (m, 2H), 7.13 (br. s., 1H), 7.58 (d, $J = 7.6$ Hz, 1H), 7.78 (q, $J = 4.6$ Hz, 1H), 8.53 (s, 1H), 9.25 (d, $J = 7.6$ Hz, 1H), 9.35 (br. s., 2H).

¹³C NMR (101 MHz, DMSO-*d*₆): δ 21.6, 26.3, 40.5, 42.1, 100.0, 106.0, 127.6, 133.5, 137.5, 145.0, 146.5, 157.1, 162.1. M.pt.: 260 °C (decomp).

ν_{max} (neat): 3366, 2936, 2789, 1641, 1611, 1562, 1509, 1420, 1319, 1272, 1232, 1182, 1095, 1088, 834, 806, 775 cm⁻¹.

HRMS: (C₁₃H₁₅N₅O) $[M+H]^+$ requires 258.1349, found $[M+H]^+$ 258.1348

***tert*-Butyl 3-(3-(methylcarbamoyl)pyrazolo[1,5-*a*]pyrimidin-5-yl)-8-azabicyclo[3.2.1]oct-2-ene-8-carboxylate**



Prepared according to General Procedure B, with 5-chloro-*N*-methylpyrazolo[1,5-*a*]pyrimidine-3-carboxamide

3.030

(50 mg, 0.237 mmol), *tert*-butyl 3-(4,4,5,5-tetramethyl-1,3,2-dioxaborolan-2-yl)-8-azabicyclo[3.2.1]oct-2-ene-

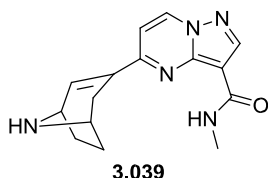
8-carboxylate (96 mg, 0.285 mmol) and purified by silica

chromatography (0-90% 3:1 EtOAc/EtOH:cyclohexane), appropriate fractions were evaporated *in vacuo* and further purified by High pH MDAP, affording *tert*-butyl 3-(3(methylcarbamoyl)pyrazolo[1,5-*a*]pyrimidin-5-yl)-8-azabicyclo[3.2.1]oct-2-ene-8-carboxylate (36 mg, 0.094 mmol, 40%) as a yellow solid.

LCMS (High pH, ES⁺): t_R = 1.03 min, [M+H⁺] 384.5, (100% purity). ¹

¹H NMR (400 MHz, DMSO-*d*₆): δ 1.39 (s, 9H), 1.62-1.75 (m, 1H), 1.89-2.04 (m, 2H), 2.092.26 (m, 1H), 2.57-2.71 (m, 1H), 2.92 (d, *J* = 4.6 Hz, 3H), 2.97-3.13 (m, 1H), 4.39-4.49 (m, 1H), 4.50-4.57 (m, 1H), 7.46-7.48 (m, 1H), 7.50 (d, *J* = 7.6 Hz, 1H), 7.79 (q, *J* = 4.6 Hz, 1H),

8.48 (s, 1H), 9.15 (d, *J* = 7.3 Hz, 1H) **5-(8-Azabicyclo[3.2.1]oct-2-en-3-yl)-*N*-**



methylpyrazolo[1,5-*a*]pyrimidine-3-carboxamide To a solution of

tert-butyl 3-(3-(methylcarbamoyl)pyrazolo[1,5-*a*]pyrimidin-5-yl)-8-azabicyclo[3.2.1]oct-2-ene-8-carboxylate **3.038** (36 mg, 0.094 mmol) in DCM (1 mL) was added TFA (72 μL, 0.939 mmol) and the reaction

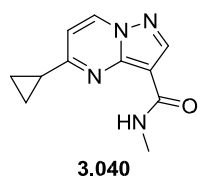
was stirred at rt for 1 h. The reaction mixture was purified by ion exchange chromatography (sulphonic

acid (SCX) 2 g, sequential solvents MeOH, 2 M NH₃/MeOH). The appropriate fractions were combined, evaporated *in vacuo* and purified by High pH MDAP. The solvent was evaporated *in vacuo* to afford 5-(8-azabicyclo[3.2.1]oct-2-en-3-yl)-*N*-methylpyrazolo[1,5-*a*]pyrimidine-3-carboxamide (3 mg, 10.59 μmol, 11%) as a yellow gum. LCMS (High pH, ES⁺): t_R = 0.63 min, [M+H⁺] 284.3, (93% purity). ¹

¹H NMR (400 MHz, MeOD-*d*₄): δ 1.82-1.93 (m, 1H), 2.06-2.18 (m, 1H), 2.20-2.33 (m, 2H), 2.78 (d, *J* = 18.1 Hz, 1H), 3.05 (s, 3H), 3.11-3.21 (m, 1H), 4.10-4.16 (m, 1H), 4.17-4.23 (m, 1H), 7.28-7.35 (m, 1H), 7.47 (d, *J* = 7.3 Hz, 1H), 8.50 (s, 1H), 8.92 (d, *J* = 7.6 Hz, 1H).

Exchangeable protons were not observed.

5-Cyclopropyl-*N*-methylpyrazolo[1,5-*a*]pyrimidine-3-carboxamide



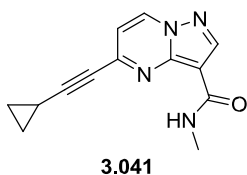
5-Chloro-*N*-methylpyrazolo[1,5-*a*]pyrimidine-3-carboxamide **3.030** (25 mg, 0.12 mmol), palladium (II) acetate (1.1 mg, 4.75 μmol), potassium cyclopropyltrifluoroborate (26 mg, 0.18 mmol), di(adamantan-1yl)(butyl)phosphine (cataCXium® A, 2.6 mg, 7.12 μmol) and cesium

carbonate (116 mg, 0.36 mmol) were sealed in a microwave vial and

placed under N₂. Toluene (0.4 mL) and water (0.4 mL) were added by syringe and the reaction was heated to 100 °C in a Biotage Initiator microwave reactor for 2 h. The reaction mixture was filtered through Celite and evaporated to dryness. The residue was purified by silica chromatography (0-12% EtOH/EtOAc), appropriate fractions were evaporated *in vacuo* to afford 5-cyclopropyl-*N*-methylpyrazolo[1,5-*a*]pyrimidine-3-carboxamide (24 mg, 0.11 mmol, 94%) as a white solid.

LCMS (High pH, ES⁺): t_R = 0.73 min, [M+H⁺] 217.2, (97% purity). ¹H NMR (400 MHz, CDCl₃): δ 1.19-1.32 (m, 4H), 2.13-2.24 (m, 1H), 3.06 (d, *J* = 4.9 Hz, 3H), 6.80 (d, *J* = 7.3 Hz, 1H), 7.73 (br. s., 1H), 8.55 (d, *J* = 7.3 Hz, 1H), 8.57 (s, 1H).

5-(Cyclopropylethynyl)-*N*-methylpyrazolo[1,5-*a*]pyrimidine-3-carboxamide 5-Chloro-*N*-methylpyrazolo[1,5-*a*]pyrimidine-3-carboxamide **3.030** (25 mg, 0.119 mmol), Pd(PPh₃)₂Cl₂ (4.2 mg, 5.93 μmol) and CuI (1.1 mg, 5.93 μmol) were sealed in a microwave vial and placed under N₂. Triethylamine (66 μL, 0.475 mmol), ethynylcyclopropane (28 μL, 70% wt in toluene, 0.237 mmol) and anhydrous DMF (0.6 mL) were added



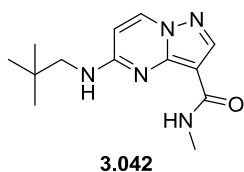
by syringe and microwave reactor to 120 °C for 20 min. The reaction mixture was filtered through Celite and evaporated to dryness. The residue was purified by High pH MDAP. The solvent was evaporated *in vacuo* to afford 5-(cyclopropylethynyl)-*N*-methylpyrazolo[1,5-*a*]pyrimidine-3-carboxamide (14 mg, 0.058 mmol, 49%) as a brown solid.

LCMS (High pH, ES⁺): t_R = 0.83 min, [M+H⁺] 241.3, (95% pure). ¹H NMR (400 MHz, CDCl₃): δ 0.97-1.11 (m, 4H), 1.53-1.64 (m, 1H), 3.07 (d, *J* = 4.9 Hz, 3H),

6.91 (d, *J* = 7.1 Hz, 1H), 7.71 (br. s., 1H), 8.62 (d, *J* = 7.1 Hz, 1H), 8.65 (s, 1H). ¹³C NMR (101 MHz, CDCl₃): δ 0.4, 9.5, 26.0, 74.8, 101.5, 106.1, 111.8, 135.3, 144.6, 145.3, 147.4, 162.5.

M.pt.: 178-180 °C. ν_{max} (neat): 3385, 3053, 3004, 2223, 1650, 1608, 1551, 1506, 1460, 1420, 1300, 1228, 1169, 980, 917, 831, 776 cm⁻¹.

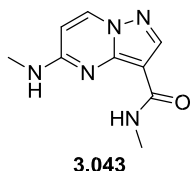
***N*-Methyl-5-(neopentylamino)pyrazolo[1,5-*a*]pyrimidine-3-carboxamide**



Prepared according to General Procedure C, with 5-chloro-*N*-methylpyrazolo[1,5-*a*]pyrimidine-3-carboxamide **3.030** (30 mg, 0.14 mmol), DIPEA (37 μL, 0.21 mmol) and neopentylamine (33 μL, 0.29 mmol) at 120 °C, affording *N*-methyl-5-(neopentylamino)pyrazolo[1,5-*a*]pyrimidine-3-carboxamide (33 mg, 0.126 mmol, 89%) as a white solid.

LCMS (High pH, ES⁺): t_R = 0.89 min, [M+H⁺] 262.3, (90% purity). ¹H NMR (400 MHz, CDCl₃): δ 1.05 (s, 9H), 3.04 (d, *J* = 4.9 Hz, 3H), 3.26-3.40 (m, 2H), 5.47 (t, *J* = 5.1 Hz, 1H), 6.19 (d, *J* = 7.6 Hz, 1H), 7.69-7.87 (m, 1H), 8.15-8.28 (m, 1H), 8.35 (s, 1H).

***N*-Methyl-5-(methylamino)pyrazolo[1,5-*a*]pyrimidine-3-carboxamide** Prepared



according to General Procedure C, with 5-chloro-*N*-methylpyrazolo[1,5-*a*]pyrimidine-3-carboxamide **3.030** (20 mg, 0.095 mmol), DIPEA (25 μ L, 0.14 mmol) and 2 M methylamine in THF (95 μ L,

0.19 mmol) at rt for 1 h, affording *N*-methyl-5-(methylamino)pyrazolo[1,5-*a*]pyrimidine-3-carboxamide (14 mg, 0.068 mmol, 72%) as a white solid.

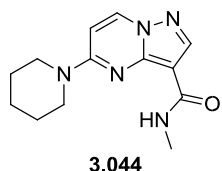
LCMS (High pH, ES⁺): t_R = 0.55 min, [M+H]⁺ 206.2, (100% purity) ¹H NMR (400 MHz, DMSO-*d*₆): δ 2.85 (d, J = 4.6 Hz, 3H), 2.93 (d, J = 4.9 Hz, 3H), 6.34 (d, J = 7.6 Hz, 1H), 7.80 (q, J = 4.6 Hz, 1H), 8.02 (q, J = 3.7 Hz, 1H), 8.08 (s, 1H), 8.52 (d, J = 7.6 Hz, 1H). ¹³

C NMR (101 MHz, DMSO-*d*₆): δ 25.9, 27.7, 101.2, 101.7, 136.0, 144.4, 146.7, 157.5, 163.1. M.pt.: 296-298 °C.

ν_{max} (neat): 3273, 3132, 1631, 1570, 1511, 1448, 1407, 1245, 1171, 954, 881, 822, 770, 704, 627, 580 cm⁻¹.

HRMS: (C₉H₁₁N₅O) [M+H]⁺ requires 206.1037, found [M+H]⁺ 206.1036.

***N*-Methyl-5-(piperidin-1-yl)pyrazolo[1,5-*a*]pyrimidine-3-carboxamide** Prepared



according to General Procedure C, with 5-chloro-*N*-methylpyrazolo[1,5-*a*]pyrimidine-3-carboxamide **3.030** (30 mg, 0.14 mmol), DIPEA (37 μ L, 0.21 mmol) and piperidine (28 μ L, 0.29 mmol) at

120 °C, affording *N*-methyl-5-(piperidin-1-yl)pyrazolo[1,5-*a*]pyrimidine-3-carboxamide (29 mg, 0.11 mmol, 79%) as a white solid.

LCMS (High pH, ES⁺): t_R = 0.84 min, [M+H]⁺ 260.1, (90% purity) ¹H NMR (400 MHz, CDCl₃): δ 1.63-1.82 (m, 6H), 3.03 (d, J = 4.9 Hz, 3H), 3.60-3.77 (m, 4H),

6.40 (d, J = 7.8 Hz, 1H), 7.65 (br. s., 1H), 8.25 (d, J = 7.8 Hz, 1H), 8.36 (s, 1H). ¹³

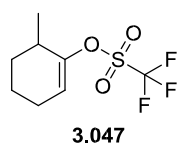
C NMR (101 MHz, CDCl₃): δ 24.4, 25.6, 25.8, 46.2, 96.7, 102.0, 136.0, 146.2, 146.4, 155.9, 163.9.

M.pt.: 193-195 °C.

ν_{max} (neat): 3357, 2939, 1648, 1568, 1634, 1488, 1460, 1446, 1255, 1224, 895, 777 cm⁻¹.

HRMS: (C₁₃H₁₇N₅O) [M+H]⁺ requires 260.1506, found [M+H]⁺ 260.1507.

6-Methylcyclohex-1-en-1-yl trifluoromethanesulfonate



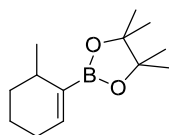
To a solution of 2-methylcyclohexanone **3.046** (486 μ L, 4 mmol) in DME (13 mL) stirred under N₂ at -78 °C was added LDA (2.4 mL, 2.0 M in THF/heptane/ethylbenzene 4.80 mmol) dropwise. The reaction mixture was stirred at -78 °C for 2 h, then a solution of 1,1,1-trifluoro-*N*-phenyl-

N((trifluoromethyl)sulfonyl)methanesulfonamide (1572 mg, 4.40 mmol) in DME (13 mL) was added dropwise and the reaction was allowed to warm to 0 °C and stirred for 5 h. The reaction mixture was evaporated to dryness and purified by silica chromatography (cyclohexane) to afford 6-methylcyclohex-1-en-1-yl trifluoromethanesulfonate (455 mg, 1.86

mmol, 47%) as a colourless oil. ^1H NMR (400 MHz, CDCl_3): δ 1.14 (d, $J = 7.1$ Hz, 3H), 1.41-1.51 (m, 1H), 1.51-1.61 (m, 1H), 1.61-1.71 (m, 1H), 1.88-1.98 (m, 1H), 2.17 (s, 2H), 2.48-2.60 (m, 1H), 5.73 (td, $J = 4.1, 1.3$ Hz, 1H).¹⁹ 386,387

F NMR (376 MHz, CDCl_3): δ -74.30. Analysis consistent with literature.

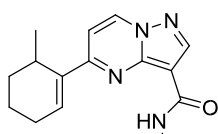
4,4,5,5-Tetramethyl-2-(6-methylcyclohex-1-en-1-yl)-1,3,2-dioxaborolane



3.048

A solution of 6-methylcyclohex-1-en-1-yl trifluoromethanesulfonate **3.047** (440 mg, 1.802 mmol), *bis*(pinacolato)diboron (686 mg, 2.70 mmol), $\text{PdCl}_2(\text{dppf})$ (65.9 mg, 0.090 mmol) and potassium acetate (530 mg, 5.40 mmol) in DMF (9 mL) was placed under N_2 and stirred at 85 °C for 20 h. The reaction mixture was filtered through Celite and evaporated to dryness. The crude product was dry-loaded onto silica and purified by silica chromatography (0-12% EtOAc/cyclohexane), appropriate fractions were evaporated *in vacuo* to afford 4,4,5,5-tetramethyl-2-(6-methylcyclohex-1-en-1-yl)-1,3,2-dioxaborolane (220 mg, 0.495 mmol, 28%) as a colourless oil. Analysis was consistent with the literature,³⁸⁸ ~50% pure, taken forward to further chemistry without purification.

N-Methyl-5-(6-methylcyclohex-1-en-1-yl)pyrazolo[1,5-*a*]pyrimidine-3-carboxamide



3.049

Prepared according to General Procedure B, with 5-chloro-*N*-methylpyrazolo[1,5-*a*]pyrimidine-3-carboxamide **3.030** (50 mg, 0.237 mmol) and 4,4,5,5-tetramethyl-2-(6-methylcyclohex-1-en-1-yl)-1,3,2-dioxaborolane (50% pure, 127 mg, 0.285 mmol). Purified by silica chromatography (70-100% EtOAc/cyclohexane), appropriate fractions were evaporated *in vacuo* and further purified by High pH MDAP to afford *N*-methyl-5-(6-methylcyclohex-1-en-1-yl)pyrazolo[1,5-*a*]pyrimidine-3-carboxamide (7 mg, 0.026 mmol, 11%) as a yellow solid.

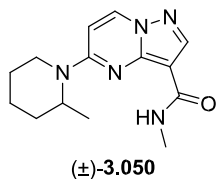
LCMS (High pH, ES⁺): $t_{\text{R}}=1.06$ min, $[\text{M}+\text{H}]^+$ 271.1, (100% purity). ^1H NMR (400 MHz, CDCl_3): δ 1.18 (d, $J = 6.8$ Hz, 3H), 1.72-1.92 (m, 4H), 2.31-2.40 (m, 2H),

3.08 (d, $J = 4.9$ Hz, 3H), 3.18-3.29 (m, 1H), 6.78 (t, $J = 4.0$ Hz, 1H), 7.12 (d, $J = 7.3$ Hz, 1H), 7.92-8.00 (m, 1H), 8.59-8.62 (m, 2H), ^{13}C NMR (101 MHz, CDCl_3): δ 17.5, 19.9, 25.9, 26.7, 28.1, 29.9, 105.7, 106.1, 135.1, 135.2,

135.4, 140.7, 146.7, 159.5, 163.2 M.pt.: 64-66 °C v_{max} (neat): 3358, 2932, 1641, 1615, 1559, 1509, 1465, 1415, 1267, 1216, 1180, 1118, 1085, 989, 900, 803, 777, 722, 695, 636, 559, 536 cm^{-1} .

HRMS: ($\text{C}_{15}\text{H}_{18}\text{N}_4\text{O}$) $[\text{M}+\text{H}]^+$ requires 271.1553, found $[\text{M}+\text{H}]^+$ 271.1551.

***N*-Methyl-5-(2-methylpiperidin-1-yl)pyrazolo[1,5-*a*]pyrimidine-3-carboxamide**



Prepared according to General Procedure C, with 5-chloro-*N*-methylpyrazolo[1,5-*a*]pyrimidine-3-carboxamide **3.030** (40 mg, 0.190 mmol), 2-methylpiperidine (45 μ L, 0.380 mmol) and DIPEA (50 μ L, 0.285 mmol) at 120 °C. The reaction mixture was diluted with water (20 mL) and extracted with EtOAc (3 x 10 mL). The combined organics

were washed with brine, dried through a hydrophobic frit and evaporated to dryness. The residue was purified by silica chromatography (0-25% EtOH/EtOAc), appropriate fractions were evaporated *in vacuo* to afford (±)-*N*-methyl-5-(2-methylpiperidin-1-yl)pyrazolo[1,5-*a*]pyrimidine-3-carboxamide (48 mg, 0.176 mmol, 92%) as an off-white solid.

LCMS (High pH, ES⁺): t_R = 0.89 min, [M+H⁺] 274.5, (93% purity). ¹H NMR (400 MHz, CDCl₃): δ 1.31 (d, J = 6.8 Hz, 3H), 1.70-1.93 (m, 6H), 3.04 (d, J = 4.9 Hz, 3H), 3.13 (td, J = 13.3, 3.3 Hz, 1H), 4.23-4.31 (m, 1H), 4.63-4.72 (m, 1H), 6.41 (d, J = 8.1 Hz, 1H), 7.63-7.74 (m, 1H), 8.28 (d, J = 8.1 Hz, 1H), 8.38 (s, 1H). ¹³C NMR (101 MHz, CDCl₃): δ 15.2, 18.5, 25.4, 25.8, 30.3, 39.9, 47.9, 96.9, 101.9, 136.0, 146.1, 146.4, 155.9, 163.9.

M.pt.: 158-160 °C.

ν_{max} (neat): 3338, 2950, 2852, 1635, 1567, 1428, 1452, 1358, 1263, 1223, 1181, 1150 1051, 882, 796, 774 cm⁻¹.

HRMS: (C₁₄H₁₉N₅O) [M+H]⁺ requires 274.1662, found [M+H]⁺ 274.1662.

The enantiomers were separated by chiral HPLC³³⁶ (30%EtOH/Heptane, f = 30 mL/min, Column 30 mm x 25 cm Chiralpak AS-H):

(*R*)-*N*-methyl-5-(2-methylpiperidin-1-yl)pyrazolo[1,5-*a*]pyrimidine-3-carboxamide (18 mg, 0.066 mmol, 35%). Second eluting isomer, >99%*ee* by Chiral HPLC.

White solid

$[\alpha_D]^{25\text{ }^\circ\text{C}}$ = -128 (c = 0.13, MeOH).

LCMS (High pH, ES⁺): t_R = 0.91 min, [M+H⁺] 274.3, (100% purity).

(*S*)-*N*-methyl-5-(2-methylpiperidin-1-yl)pyrazolo[1,5-*a*]pyrimidine-3-carboxamide (15 mg, 0.055 mmol, 30%). First eluting isomer, >99%*ee* by Chiral HPLC.

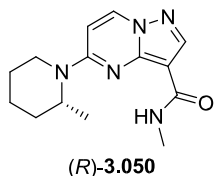
White solid.

$[\alpha_D]^{25\text{ }^\circ\text{C}}$ = +118 (c = 0.13, MeOH).

LCMS (High pH, ES⁺): t_R = 0.91 min, [M+H⁺] 274.3, (100% purity).

All other characterisation data was in accordance with the racemate.

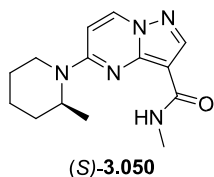
(R)-N-Methyl-5-(2-methylpiperidin-1-yl)pyrazolo[1,5-a]pyrimidine-3-carboxamide



Prepared according to General Procedure C, with 5-chloro-N-methylpyrazolo[1,5-a]pyrimidine-3-carboxamide **3.030** (25 mg, 0.119 mmol), (*R*)-2-methylpiperidine (0.025 mL, 0.208 mmol) and DIPEA (0.041 mL, 0.237 mmol) at rt, affording (*R*)-*N*-Methyl-5-(2-methylpiperidin-1-yl)pyrazolo[1,5-a]pyrimidine-3-carboxamide (26 mg,

0.095 mmol, 80%) as an off-white solid. Analysis matched racemate (pp 241).

(S)-N-Methyl-5-(2-methylpiperidin-1-yl)pyrazolo[1,5-a]pyrimidine-3-carboxamide



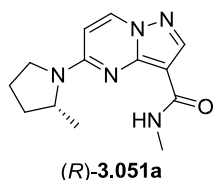
Prepared according to General Procedure C, with 5-chloro-N-methylpyrazolo[1,5-a]pyrimidine-3-carboxamide **3.030** (30 mg, 0.142 mmol), (*S*)-2-methylpiperidine (34 μ L, 0.285 mmol) and DIPEA (37 μ L, 0.214 mmol) at rt, affording (*S*)-*N*-Methyl-5-(2-methylpiperidin-1-yl)pyrazolo[1,5-a]pyrimidine-3-carboxamide (32 mg, 0.117 mmol, 82%)

as an and (*S*)-2-methylpyrrolidine (31 mg, 0.36 mmol) at rt., affording (*R*)-*N*-methyl-5-(2-methylpyrrolidin-1-yl)pyrazolo[1,5-a]pyrimidine-3-carboxamide (35 mg, 0.135 mmol, 72%).

LCMS (High pH, ES⁺): t_R = 0.84 min, [M+H]⁺ 260.0, (100% purity). ¹

¹H NMR (400 MHz, DMSO-*d*₆, 393K): δ 1.30 (d, J = 6.1 Hz, 3H), 1.75-1.83 (m, 1H), 1.962.23 (m, 3H), 2.89 (d, J = 4.4 Hz, 3H), 3.53-3.62 (m, 1H), 3.69 (ddd, J = 11.1, 7.5, 3.7 Hz, 1H), 4.30-4.39 (m, 1H), 6.47 (d, J = 7.8 Hz, 1H), 7.68 (br. s., 1H), 8.10 (s, 1H), 8.56 (d, J = 7.8 Hz, 1H).

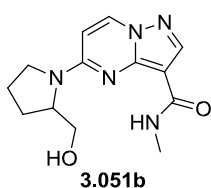
(R)-N-Methyl-5-(2-methylpyrrolidin-1-yl)pyrazolo[1,5-a]pyrimidine-3-carboxamide



Prepared according to General Procedure C with **3.030** (38 mg, 0.18 mmol), DIPEA (0.095 mL, 0.541 mmol) and (*R*)-2-methylpyrrolidine (31 mg, 0.36 mmol) at rt, affording (*R*)-*N*-methyl-5-(2-methylpyrrolidin-1-yl)pyrazolo[1,5-a]pyrimidine-3-carboxamide (35 mg, 0.135 mmol, 70%).

LCMS (High pH, ES⁺): t_R = 0.84 min, [M+H]⁺ 260.0, (100% purity). NMR matched (*S*)-**4a**.

5-(2-(Hydroxymethyl)pyrrolidin-1-yl)-*N*-methylpyrazolo[1,5-a]pyrimidine-3carboxamide



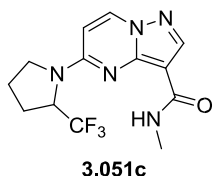
Prepared according to General Procedure C with **3.030** (38 mg, 0.18 mmol), DIPEA (0.095 mL, 0.541 mmol) and pyrrolidin-2-ylmethanol (*S*)-2-methylpyrrolidine (37 mg, 0.36 mmol) at rt, affording 5-(2-

(Hydroxymethyl)pyrrolidin-1-yl)-*N*-methylpyrazolo[1,5-a]pyrimidine-3carboxamide (34 mg, 0.125 mmol, 66%).

LCMS (High pH, ES⁺): t_R = 0.63 min, [M+H]⁺ 276.0, (100% purity). ¹

¹H NMR (400 MHz, DMSO-*d*₆, 393K): δ 1.95-2.15 (m, 4H), 2.88 (d, *J* = 4.6 Hz, 3H), 3.523.71 (m, 4H), 4.20-4.29 (m, 1H), 4.49 (t, *J* = 5.0 Hz, 1H), 6.55 (d, *J* = 7.7 Hz, 1H), 7.67 (br. s., 1H), 8.10 (s, 1H), 8.56 (d, *J* = 7.7 Hz, 1H).

***N*-Methyl-5-(2-(trifluoromethyl)pyrrolidin-1-yl)pyrazolo[1,5-*a*]pyrimidine-3-carboxamide**



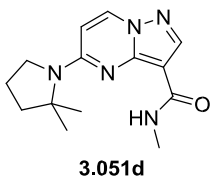
3.051c

Prepared according to General Procedure C, with **3.030** (38 mg, 0.18 mmol), DIPEA (0.095 mL, 0.541 mmol), 2-trifluoromethylpyrrolidine (50 mg, 0.36 mmol) and heating to 120 °C, affording *N*-methyl-5-(2(trifluoromethyl)pyrrolidin-1-yl)pyrazolo[1,5-*a*]pyrimidine-3-carboxamide (40 mg, 0.129 mmol, 68%).

LCMS (High pH, ES⁺): t_R = 0.83 min, [M+H]⁺ 314.0, (100% purity). ¹H NMR (400 MHz, CDCl₃): δ 2.15-2.40 (m, 4H), 2.99 (d, *J* = 4.9 Hz, 3H), 3.57-3.68 (m, 1H), 3.75-3.83 (m, 1H), 4.82 (br. s., 1H), 6.33 (d, *J* = 7.6 Hz, 1H), 7.62 (d, *J* = 3.9 Hz, 1H), 8.35 (d, *J* = 7.8 Hz, 1H), 8.36 (s, 1H). ¹³C NMR (101 MHz, CDCl₃): δ 23.2, 25.6, 26.5, 48.6, 58.8 (q, *J* = 32.3 Hz), 97.8, 102.7, 125.9 (q, *J* = 283.9 Hz), 136.3, 145.6, 146.2, 155.2, 163.4. M.pt.: 220-221 °C.

v_{max} (neat): 3353, 3101, 3051, 2974, 1636, 1571, 1439, 1451, 1385, 1282, 1238, 1159, 1145, 1127, 1072, 994, 914, 803, 777, 712, 670 cm⁻¹.

HRMS: (C₁₃H₁₄F₃N₅O) [M+H]⁺ requires 314.1223, found [M+H]⁺ 314.1225. **5-(2,2-**



3.051d

Dimethylpyrrolidin-1-yl)-*N*-methylpyrazolo[1,5-*a*]pyrimidine-3-

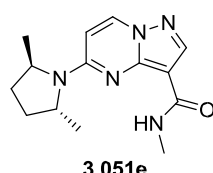
carboxamide Prepared according to General Procedure C, with **3.030** (38 mg, 0.18 mmol), DIPEA (0.095 mL, 0.541 mmol), 2,2-dimethylpyrrolidine (36 mg, 0.36 mmol) and heating to 120 °C, affording 5-(2,2-

dimethylpyrrolidin-1-yl)-*N*-methylpyrazolo[1,5-*a*]pyrimidine-3-carboxamide (29 mg, 0.105 mmol, 55%)

LCMS (High pH, ES⁺): t_R = 0.89 min, [M+H]⁺ 274.0, (100% purity). ¹H NMR (600 MHz, DMSO-*d*₆): δ 1.57 (br. s., 6H), 1.94 (br. s., 4H), 2.86 (d, *J* = 4.5 Hz, 3H),

3.52-3.66 (m, 2H), 6.38-6.51 (m, 1H), 7.74-7.82 (m, 1H), 8.12 (s, 1H), 8.60-8.70 (m, 1H).

5-((2*R*,5*R*)-2,5-Dimethylpyrrolidin-1-yl)-*N*-methylpyrazolo[1,5-*a*]pyrimidine-3carboxamide



3.051e

Prepared according to General Procedure C, with 5-chloro-*N*-methylpyrazolo[1,5-*a*]pyrimidine-3-carboxamide **3.030** (40 mg, 0.190 mmol), (2*R*,5*R*)-2,5-dimethylpyrrolidine (44 μL, 0.380 mmol) and DIPEA (50 μL, 0.285 mmol) at 120 °C. The reaction mixture was diluted with water (20 mL) and extracted with EtOAc (3 x 10 mL). The combined organics were washed with brine, dried through a hydrophobic frit and evaporated to dryness. The crude product was purified by silica chromatography (0-25% EtOH/EtOAc), appropriate fractions were evaporated *in vacuo* and further purified by High pH MDAP and

HPLC,³⁸⁵ to afford 5-((2*R*,5*R*)-2,5-dimethylpyrrolidin-1-yl)-*N*-methylpyrazolo[1,5-*a*]pyrimidine-3-carboxamide (27 mg, 0.099 mmol, 52%) as a white solid.

LCMS (High pH, ES⁺): t_R=0.91 min, [M+H]⁺ 274.3, (100% purity). ¹H NMR (400 MHz, CDCl₃): δ 1.18-1.39 (m, 6H), 1.71-1.84 (m, 2H), 2.24-2.43 (m, 2H), 3.02 (d, *J* = 4.9 Hz, 3H), 4.08-4.19 (m, 1H), 4.46-4.58 (m, 1H), 6.21 (d, *J* = 7.8 Hz, 1H), 7.84-7.94 (m, 1H), 8.26 (d, *J* = 7.8 Hz, 1H), 8.36 (s, 1H). ¹³C NMR (101 MHz, CDCl₃): δ 18.0, 19.3, 25.7, 29.5, 30.7, 54.0, 54.1, 98.8, 101.7, 135.5, 145.7, 146.8, 153.3, 164.1.

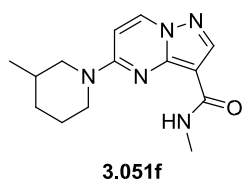
M.pt. 136-138 °C

[α]_D²⁵ °C = -127 (c=0.3, MeOH).

v_{max} (neat): 3427, 3337, 2971, 1629, 1571, 1488, 1459, 1381, 1345, 1235, 1155, 1039, 1019, 893, 799, 774 cm⁻¹.

HRMS: (C₁₄H₁₉N₅O) [M+H]⁺ requires 274.1662, found [M+H]⁺ 274.1662.

***N*-Methyl-5-(3-methylpiperidin-1-yl)pyrazolo[1,5-*a*]pyrimidine-3-carboxamide**

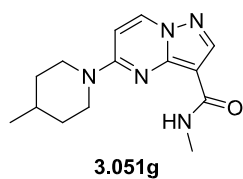


Prepared according to General Procedure C with **3.030** (38 mg, 0.18 mmol), DIPEA (0.095 mL, 0.541 mmol) and 3-methylpiperidine (36 mg, 0.36 mmol) at rt, affording *N*-methyl-5-(3-methylpiperidin-1-yl)pyrazolo[1,5-*a*]pyrimidine-3-carboxamide (43 mg, 0.156 mmol,

82%).

LCMS (High pH, ES⁺): t_R = 0.92 min, [M+H]⁺ 274.0, (100% purity). ¹H NMR (600 MHz, DMSO-*d*₆): δ 0.94 (d, *J* = 6.8 Hz, 3H), 1.18-1.28 (m, 1H), 1.42-1.52 (m, 1H), 1.58-1.68 (m, 1H), 1.71-1.77 (m, 1H), 1.78-1.85 (m, 1H), 2.73-2.82 (m, 1H), 2.86 (d, *J* = 4.5 Hz, 3H), 3.02-3.10 (m, 1H), 4.18-4.47 (m, 2H), 6.86 (d, *J* = 7.9 Hz, 1H), 7.58-7.65 (m, 1H), 8.12 (s, 1H), 8.67 (d, *J* = 7.9 Hz, 1H).

***N*-Methyl-5-(4-methylpiperidin-1-yl)pyrazolo[1,5-*a*]pyrimidine-3-carboxamide**

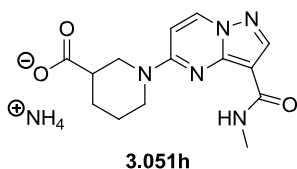


Prepared according to General Procedure C with **3.030** (38 mg, 0.18 mmol), DIPEA (0.095 mL, 0.541 mmol) and 4-methylpiperidine (36 mg, 0.36 mmol) at rt, affording *N*-methyl-5-(4-methylpiperidin-1-yl)pyrazolo[1,5-*a*]pyrimidine-3-carboxamide (45 mg, 0.165 mmol,

87%).

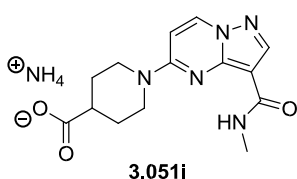
LCMS (High pH, ES⁺): t_R = 0.92 min, [M+H]⁺ 274.0, (100% purity). ¹H NMR (600 MHz, DMSO-*d*₆): δ 0.93 (d, *J* = 6.0 Hz, 3H), 1.07-1.17 (m, 2H), 1.66-1.78 (m, 3H), 2.85 (d, *J* = 4.2 Hz, 3H), 3.02 (t, *J* = 12.5 Hz, 2H), 4.35-4.52 (m, 2H), 6.84 (d, *J* = 7.9 Hz, 1H), 7.59 (q, *J* = 4.2 Hz, 1H), 8.12 (s, 1H), 8.63-8.69 (m, 1H).

1-(3-(Methylcarbamoyl)pyrazolo[1,5-*a*]pyrimidin-5-yl)piperidine-3-carboxylic acid, ammonium salt



Prepared according to General Procedure C with **3.030** (38 mg, 0.18 mmol), DIPEA (0.095 mL, 0.541 mmol) and piperidine-3carboxylic acid (47 mg, 0.36 mmol) at rt, affording 1-(3-(methylcarbamoyl)pyrazolo[1,5-a]pyrimidin-5-yl)piperidine-3-carboxylic acid, ammonium salt (19 mg, 0.060 mmol, 30%). LCMS (High pH, ES⁺): t_R = 0.44 min, [M+H]⁺ 304.0, (100% purity). ¹H NMR (600 MHz, DMSO-d₆): δ 1.44-1.55 (m, 1H), 1.70-1.79 (m, 2H), 1.94 (br. s., 1H), 2.84 (d, J = 4.5 Hz, 3H), 3.26-3.79 (m, 7H), 4.06 (br. s., 2H), 6.85 (d, J = 7.9 Hz, 1H), 7.67 (br. s., 1H), 8.13 (s, 1H), 8.68 (d, J = 7.9 Hz, 1H).

1-(3-(Methylcarbamoyl)pyrazolo[1,5-a]pyrimidin-5-yl)piperidine-4-carboxylic acid, ammonium salt

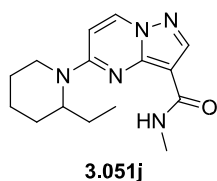


Prepared according to General Procedure C with **3.030** (38 mg, 0.18 mmol), DIPEA (0.095 mL, 0.541 mmol) and piperidine-4carboxylic acid (47 mg, 0.36 mmol) at rt, affording 1-(3-(methylcarbamoyl)pyrazolo[1,5-a]pyrimidin-5-yl)piperidine-4carboxylic acid, ammonium salt (30 mg, 0.092 mmol, 46%). LCMS (High pH, ES⁺): t_R = 0.44 min, [M+H]⁺ 304.0, (100% purity).

1

¹H NMR (600 MHz, DMSO-*d*₆): δ 1.54-1.64 (m, 2H), 1.94 (d, *J* = 11.0 Hz, 2H), 2.58 (m, 1H), 2.86 (d, *J* = 4.9 Hz, 3H), 3.21 (t, *J* = 11.9 Hz, 2H), 3.42 (br. s., 4H), 4.34 (br. s., 2H), 6.85 (d, *J* = 7.9 Hz, 1H), 7.58 (q, *J* = 4.5 Hz, 1H), 8.13 (s, 1H), 8.69 (d, *J* = 7.9 Hz, 1H).

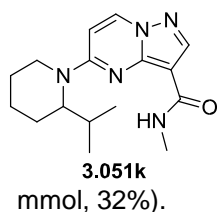
5-(2-Ethylpiperidin-1-yl)-*N*-methylpyrazolo[1,5-*a*]pyrimidine-3-carboxamide



Prepared according to General Procedure C, with **3.030** (38 mg, 0.18 mmol), DIPEA (0.095 mL, 0.541 mmol) and 2-ethylpiperidine (41 mg, 0.36 mmol) at rt, affording 5-(2-ethylpiperidin-1-yl)-*N*-methylpyrazolo[1,5-*a*]pyrimidine-3-carboxamide (36 mg, 0.126 mmol, 67%).

LCMS (High pH, ES⁺): *t*_R = 0.97 min, [M+H]⁺ 288.0, (100% purity). ¹H NMR (600 MHz, DMSO-*d*₆): δ 0.85 (t, *J* = 7.4 Hz, 3H), 1.39-1.49 (m, 1H), 1.53-1.79 (m, 7H), 2.85 (d, *J* = 4.5 Hz, 3H), 2.97-3.07 (m, 1H), 4.24-4.64 (m, 2H), 6.84 (d, *J* = 8.3 Hz, 1H), 7.59-7.67 (m, 1H), 8.12 (s, 1H), 8.65 (d, *J* = 7.9 Hz, 1H).

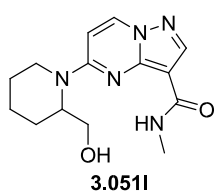
5-(2-Isopropylpiperidin-1-yl)-*N*-methylpyrazolo[1,5-*a*]pyrimidine-3-carboxamide



Prepared according to General Procedure C, with **3.030** (38 mg, 0.18 mmol), 2-isopropylpiperidine (46 mg, 0.36 mmol), DIPEA (0.095 mL, 0.541 mmol) and heating to 120 °C, affording 5-(2-isopropylpiperidin-1-yl)-*N*-methylpyrazolo[1,5-*a*]pyrimidine-3-carboxamide (18.2 mg, 0.060

LCMS (High pH, ES⁺): *t*_R = 1.03 min, [M+H]⁺ 302.1, (100% purity). ¹H NMR (600 MHz, DMSO-*d*₆): δ 0.77 (d, *J* = 6.4 Hz, 3H), 1.00 (d, *J* = 6.4 Hz, 3H), 1.38-1.60 (m, 3H), 1.64-1.77 (m, 2H), 1.90 (d, *J* = 13.6 Hz, 1H), 2.25-2.35 (m, 1H), 2.85 (d, *J* = 4.5 Hz, 3H), 2.90-3.08 (m, 1H), 3.82-4.85 (m, 2H), 6.87 (d, *J* = 7.6 Hz, 1H), 7.60-7.67 (m, 1H), 8.11 (s, 1H), 8.63 (d, *J* = 7.9 Hz, 1H).

5-(2-(Hydroxymethyl)piperidin-1-yl)-*N*-methylpyrazolo[1,5-*a*]pyrimidine-3-carboxamide



Prepared according to General Procedure C, with **3.030** (50 mg, 0.237 mmol), piperidin-2-ylmethanol (41.0 mg, 0.356 mmol) and DIPEA (83 μL, 0.475 mmol), with stirring at rt for 18 h then heating to 90 °C in a Biotage Initiator microwave reactor for 20 min. The reaction mixture was diluted

with sat. aq. NaHCO₃ (15 mL) and EtOAc (15 mL) and the aqueous layer was extracted with EtOAc (5 x 10 mL) and DCM (5 x 10 mL). The combined organics were dried through a hydrophobic frit, evaporated to dryness and purified by silica chromatography (10-100% (3:1 EtOAc:EtOH)/cyclohexane). The solvent was evaporated *in*

1
vacuo to give 5-(2-(hydroxymethyl)piperidin-1-yl)-*N*-methylpyrazolo[1,5-*a*]pyrimidine-3-carboxamide (49 mg, 0.169 mmol, 71%) as a yellow solid.

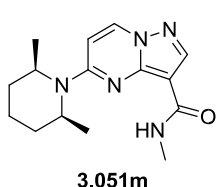
LCMS (High pH, ES⁺): t_R = 0.68 min, [M+H]⁺ 290.2, (100% purity).

¹H NMR (400 MHz, CDCl₃): δ 1.64-1.83 (m, 3H), 1.87 (d, J = 12.7 Hz, 2H), 2.97 (d, J = 4.9 Hz, 3H), 3.21 (td, J = 13.2, 2.9 Hz, 1H), 3.74 (d, J = 10.8 Hz, 1H), 4.25 (t, J = 10.8 Hz, 1H), 4.51 (br. s., 3H), 6.56 (d, J = 8.1 Hz, 1H), 7.66 (q, J = 4.9 Hz, 1H), 8.05 (s, 1H), 8.07 (d, J = 8.1 Hz, 1H). OH not observed. ¹³C NMR (101 MHz, CDCl₃): δ 19.5, 25.3, 25.8, 26.0, 39.4, 54.9, 61.4, 97.9, 100.0, 100.9, 135.3, 145.2, 157.0, 164.2. M.pt.: 213-214 °C.

ν_{max} (neat): 3224, 2862, 1648, 1577, 1472, 1459, 1263, 1233, 1178, 1128, 1067, 874, 769, 713 cm⁻¹.

HRMS: (C₁₄H₁₉N₅O₂) [M+H]⁺ requires 290.1612, found [M+H]⁺ 290.1604.

5-(*cis*-2,6-Dimethylpiperidin-1-yl)-*N*-methylpyrazolo[1,5-*a*]pyrimidine-3-carboxamide



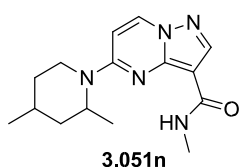
Prepared according to General Procedure C, with **3.030** (30 mg, 0.142 mmol), *cis*-2,6-dimethylpiperidine (38 μ L, 0.285 mmol) and DIPEA (37 μ L, 0.214 mmol). The reaction was heated to 120 °C in a Biotage Initiator microwave for 3 h, to afford 5-(*cis*-2,6-Dimethylpiperidin-1-yl)-

N-methylpyrazolo[1,5-*a*]pyrimidine-3-carboxamide (6 mg, 0.021 mmol, 15%) as a brown solid.

LCMS (High pH, ES⁺): t_R = 0.97 min, [M+H]⁺ 288.3, (98% purity). ¹H NMR (400 MHz, CDCl₃): δ 1.34 (d, J = 7.1 Hz, 6H), 1.61-1.68 (m, 2H), 1.76-2.01 (m, 4H),

3.03 (d, J = 4.9 Hz, 3H), 4.61 (br. s., 2H), 6.41 (d, J = 8.1 Hz, 1H), 7.80 (br. s., 1H), 8.30 (d, J = 8.1 Hz, 1H), 8.38 (s, 1H).

5-(2,4-Dimethylpiperidin-1-yl)-*N*-methylpyrazolo[1,5-*a*]pyrimidine-3-carboxamide

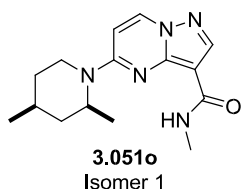


Prepared according to General Procedure C, with 5-chloro-*N*-methylpyrazolo[1,5-*a*]pyrimidine-3-carboxamide **3.030** (35 mg, 0.166 mmol), 2,4-dimethylpiperidine (37.6 mg, 0.332 mmol) and DIPEA (0.058 mL, 0.332 mmol). The reaction was stirred at rt for 18 h. The

reaction mixture was then purified directly by High pH MDAP. The solvent was evaporated *in vacuo* to give 5-(2,4-dimethylpiperidin-1-yl)-*N*-methylpyrazolo[1,5-*a*]pyrimidine-3-carboxamide (43 mg, 90%), 3:1 mixture of diastereomers. The mixture was purified by chiral HPLC³³⁶ (30% EtOH/Heptane, f =30 mL/min, Column 30 mm x 25 cm Chirapak AS-H) to afford the following products:

5-((2*S**,4*S**)-2,4-Dimethylpiperidin-1-yl)-*N*-methylpyrazolo[1,5-*a*]pyrimidine-3-carboxamide

1



First eluting isomer, (16 mg, 0.056 mmol, 34%). White solid.

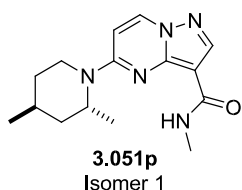
LCMS (High pH, ES⁺): $t_R = 0.99$ min, $[M+H]^+$ 288.2, (98% purity).

¹H NMR (400 MHz, CDCl₃): δ 1.08 (d, $J = 6.8$ Hz, 3H), 1.34 (d, $J = 6.4$ Hz, 3H), 1.36-1.47 (m, 2H), 1.67-1.79 (m, 1H), 1.96 (ddd, $J = 13.5, 6.4, 4.0$ Hz, 1H), 2.05-2.17 (m, 1H), 3.04 (d, $J =$

4.9 Hz, 3H), 3.32 (ddd, $J = 14.1, 11.0, 6.2$ Hz, 1H), 4.10 (ddd, $J = 14.1, 7.5, 2.1$ Hz, 1H), 4.22-4.33 (m, 1H), 6.33 (d, $J = 7.8$ Hz, 1H), 7.72-7.79 (m, 1H), 8.26 (d, $J = 7.8$ Hz, 1H), 8.37 (s, 1H).

The opposite enantiomer of **3.051o** was not obtained. A 5:1 mixture of diastereoisomers, eluting second, was also obtained, which was further purified by chiral HPLC³³⁶ (60% EtOH(+0.2%isopropylamine)/Heptane(+0.2%isopropylamine), $f=25$ mL/min, Column 30 mm x 25 cm Chirapak IC) to afford the single enantiomer products.

5-((2S*,4R*)-2,4-Dimethylpiperidin-1-yl)-N-methylpyrazolo[1,5-a]pyrimidine-3carboxamide

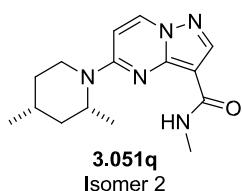


First eluting isomer, (1 mg, 3.48 μ mol, 2.1%), white solid.

LCMS (High pH, ES⁺): $t_R = 0.99$ min, $[M+H]^+$ 288.2, (95% purity). ¹H NMR (600 MHz, CDCl₃): δ 1.02 (d, $J = 6.6$ Hz, 3H), 1.23 (qd, $J = 12.8, 4.6$ Hz, 1H), 1.31 (d, $J = 7.0$ Hz, 3H), 1.47 (td, $J = 12.8, 5.5$ Hz,

1H), 1.74 (dquin, $J = 13.4, 1.6, 1.6, 1.6, 1.6$ Hz, 1H), 1.84-1.90 (m, 1H), 1.91-2.00 (m, 1H), 3.05 (d, $J = 4.8$ Hz, 3H), 3.11-3.19 (m, 1H), 4.15-4.44 (m, 1H), 4.574.85 (m, 1H), 6.42 (d, $J = 7.8$ Hz, 1H), 7.64-7.73 (m, 1H), 8.28 (d, $J = 7.8$ Hz, 1H), 8.39 (s, 1H).

5-((2R*,4R*)-2,4-Dimethylpiperidin-1-yl)-N-methylpyrazolo[1,5-a]pyrimidine-3carboxamide



First eluting isomer, (8 mg, 0.028 mmol, 17%), white solid.

LCMS (High pH, ES⁺): $t_R = 0.99$ min, $[M+H]^+$ 288.3, (99% purity).

NMR matches **3.051o**.

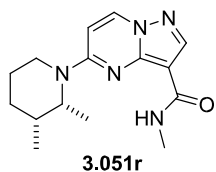
5-(cis-2,3-Dimethylpiperidin-1-yl)-N-methylpyrazolo[1,5-a]pyrimidine-3-carboxamide
and **5-(trans-2,3-Dimethylpiperidin-1-yl)-N-methylpyrazolo[1,5-a]pyrimidine-3carboxamide**

Prepared according to General Procedure C, with 5-chloro-N-methylpyrazolo[1,5a]pyrimidine-3-carboxamide **3.030** (75 mg, 0.356 mmol), 2,3-dimethylpiperidine (mixture of isomers, 81 mg, 0.712 mmol) and DIPEA (124 μ L, 0.712 mmol) at rt. The reaction mixture was diluted with

¹
EtOAc (10 mL) and sat. aq NaHCO₃ (10 mL) and the aqueous layer was extracted with EtOAc (3 x 10 mL). The combined organics were washed with brine and

evaporated to dryness. The product was purified by HPLC³⁸⁵ (CSH C18 150x30 mm, 5 μ m, 10 mM aq. $\text{NH}_4\text{HCO}_3/\text{MeCN}$, $f=40$ mL/min) to afford the products:

5-(*Cis*-2,3-dimethylpiperidin-1-yl)-*N*-methylpyrazolo[1,5-*a*]pyrimidine-3-carboxamide



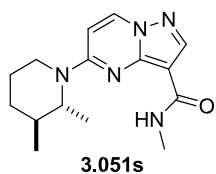
3.051r

First eluting isomer, 6 mg, 0.021 mmol, 6% yield, off-white glass.

LCMS (High pH, ES⁺): $t_R = 0.96$ min, $[\text{M}+\text{H}]^+ 288.2$, (100% purity). ¹H NMR (400 MHz, CDCl_3): δ 1.11 (d, $J = 7.1$ Hz, 3H), 1.35 (d, $J = 6.8$

Hz, 3H), 1.44-1.53 (m, 1H), 1.65-1.70 (m, 1H), 1.80-2.02 (m, 3H), 3.05 (d, $J = 4.9$ Hz, 3H), 3.13 (td, $J = 13.1, 3.9$ Hz, 1H), 4.23 (qd, $J = 6.8, 1.0$ Hz, 1H), 4.28-4.36 (m, 1H), 6.40 (d, $J = 8.0$ Hz, 1H), 7.72 (br. s., 1H), 8.27 (d, $J = 8.0$ Hz, 1H), 8.38 (s, 1H).

5-(*Trans*-2,3-dimethylpiperidin-1-yl)-*N*-methylpyrazolo[1,5-*a*]pyrimidine-3-carboxamide



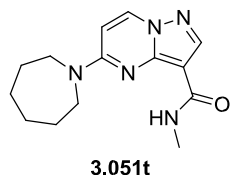
3.051s

Second eluting isomer, 81 mg, 0.282 mmol, 79 % yield, white solid.

LCMS (High pH, ES⁺): $t_R = 0.98$ min, $[\text{M}+\text{H}]^+ 288.3$, (100% purity). ¹H NMR (400 MHz, 393 K, $\text{DMSO}-d_6$): δ 0.97 (d, $J = 7.1$ Hz, 3H), 1.14

(d, $J = 6.8$ Hz, 3H), 1.45-1.64 (m, 3H), 1.77-1.94 (m, 2H), 2.89 (d, $J = 4.9$ Hz, 3H), 3.04-3.14 (m, 1H), 4.25-4.34 (m, 1H), 4.60 (qd, $J = 6.8, 6.0$ Hz, 1H), 6.76 (d, $J = 8.0$ Hz, 1H), 7.53 (br. s., 1H), 8.11 (s, 1H), 8.55 (d, $J = 8.0$ Hz, 1H).

5-(Azepan-1-yl)-*N*-methylpyrazolo[1,5-*a*]pyrimidine-3-carboxamide Prepared



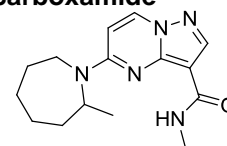
3.051t

according to General Procedure C with **3.030** (38 mg, 0.18 mmol), DIPEA (95 μ L, 0.541 mmol) and azepane (36 mg, 0.36 mmol) at rt, affording 5-(azepan-1-yl)-*N*-methylpyrazolo[1,5-*a*]pyrimidine-3carboxamide (43 mg, 0.158 mmol, 83%).

LCMS (High pH, ES⁺): $t_R = 0.89$ min, $[\text{M}+\text{H}]^+ 274.0$, (100% purity). ¹H NMR (400 MHz, CDCl_3): δ 1.52-1.64 (m, 4H), 1.84 (br. s., 4H), 2.99 (d, $J = 4.9$ Hz, 3H), 3.49-3.86 (m, 4H), 6.28 (d, $J = 7.8$ Hz, 1H), 7.74 (q, $J = 3.4$ Hz, 1H), 8.21 (d, $J = 7.8$ Hz, 1H), 8.31 (s, 1H). ¹³C NMR (101 MHz, CDCl_3): δ 25.7, 26.4 – 27.2 (br), 26.7, 47.6 – 49.4 (br), 96.5, 101.7, 135.8, 145.8, 146.6, 155.6, 163.9. M.pt.: 191-192 °C. ν_{max} (neat): 3335, 2922, 1631, 1570, 1504, 1462, 1438, 1370, 1276, 1233, 1203, 1177, 1079, 999, 883, 806, 777 cm^{-1} .

HRMS: ($\text{C}_{14}\text{H}_{19}\text{N}_5\text{O}$) $[\text{M}+\text{H}]^+$ requires 274.1662, found $[\text{M}+\text{H}]^+ 274.1661$.

***N*-Methyl-5-(2-methylazepan-1-yl)pyrazolo[1,5-*a*]pyrimidine-3-carboxamide**

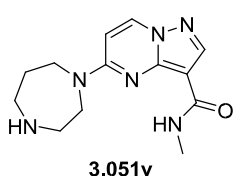


3.051u

Prepared according to General Procedure C with **3.030** (15 mg, 0.071 mmol), 2-methylazepane (16 mg, 0.142 mmol) and DIPEA (37 μ L, 0.214 mmol) at rt, affording *N*-methyl-5-(2-methylazepan-1-yl)pyrazolo[1,5-*a*]pyrimidine-3carboxamide (14 mg, 0.047 mmol, 66%) as a yellow solid. LCMS (High pH, ES⁺): $t_R = 0.97$

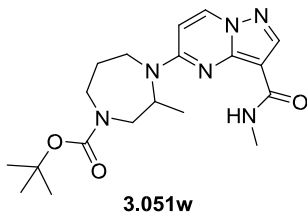
min, $[M+H]^+$ 288.3, (100% purity). 1H NMR (400 MHz, DMSO- d_6): δ 1.20-1.31 (m, 1H), 1.25 (d, $J = 6.3$ Hz, 3H), 1.36-1.51 (m, 1H), 1.57-1.69 (m, 2H), 1.72-1.91 (m, 3H), 2.07-2.20 (m, 1H), 2.89 (d, $J = 4.8$ Hz, 3H), 3.263.38 (m, 1H), 3.97 (s, 1H), 4.36-4.49 (m, 1H), 6.61 (d, $J = 8.1$ Hz, 1H), 7.59 (br. s., 1H), 8.10 (s, 1H), 8.52 (d, $J = 7.8$ Hz, 1H).

5-(1,4-Diazepan-1-yl)-*N*-methylpyrazolo[1,5-*a*]pyrimidine-3-carboxamide



Prepared according to General Procedure C with **3.030** (20 mg, 0.095 mmol), 1,4-diazepane (67 mg, 0.665 mmol) and DIPEA (33 μ L, 0.190 mmol) at rt, affording 5-(1,4-diazepan-1-yl)-*N*-methylpyrazolo[1,5-*a*]pyrimidine-3-carboxamide (16 mg, 0.058 mmol, 61%). LCMS (High pH, ES⁺): $t_R = 0.56$ min, $[M+H]^+$ 275.3, (100% purity). 1H NMR (400 MHz, DMSO- d_6): δ 1.68-1.90 (m, 2H), 2.37 (br. s., 1H), 2.68 (br. s., 2H), 2.812.98 (m, 1H), 2.85 (d, $J = 4.2$ Hz, 3H), 3.62-3.94 (m, 4H), 6.72 (d, $J = 7.8$ Hz, 1H), 7.64-7.79 (m, 1H), 8.12 (s, 1H), 8.69 (d, $J = 7.8$ Hz, 1H). Diazepane NH not observed.

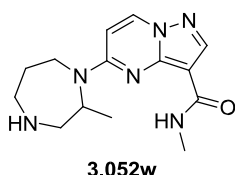
***tert*-Butyl 5-methyl-4-(3-(methylcarbamoyl)pyrazolo[1,5-*a*]pyrimidin-5-yl)-1,4-diazepane-1-carboxylate**



Prepared according to General Procedure C with **3.030** (38 mg, 0.18 mmol), DIPEA (95 μ L, 0.541 mmol) and *tert*-butyl 5-methyl-1,4-diazepane-1-carboxylate (77 mg, 0.36 mmol) at rt, affording *tert*-butyl 5-methyl-4-(3-(methylcarbamoyl)pyrazolo[1,5-*a*]pyrimidin-5-yl)-1,4-diazepane-1-carboxylate (51 mg, 0.131 mmol, 69%).

LCMS (High pH, ES⁺): $t_R = 0.94$ min, $[M]^+$ 388.0, (100% purity). 1H NMR (400 MHz, DMSO- d_6): δ 1.31 (d, $J = 6.8$ Hz, 3H), 1.34 (s, 9H), 1.73 (dtd, $J = 15.0, 8.3, 2.3$ Hz, 1H), 2.14-2.24 (m, 1H), 2.89 (d, $J = 4.9$ Hz, 3H), 3.11 (ddd, $J = 14.5, 8.4, 2.4$ Hz, 1H), 3.42-3.54 (m, 2H), 3.68 (ddd, $J = 14.5, 7.9, 1.6$ Hz, 1H), 3.74-3.83 (m, 1H), 4.11-4.22 (m, 1H), 4.51-4.64 (m, 1H), 6.72 (d, $J = 8.1$ Hz, 1H), 7.49-7.59 (m, 1H), 8.12 (s, 1H), 8.59 (d, $J = 7.8$ Hz, 1H).

***N*-Methyl-5-(2-methyl-1,4-diazepan-1-yl)pyrazolo[1,5-*a*]pyrimidine-3-carboxamide**



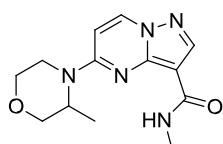
Prepared according to General Procedure D with **3.051w** (30 mg, 0.077 mmol) affording *N*-methyl-5-(2-methyl-1,4-diazepan-1-yl)pyrazolo[1,5-*a*]pyrimidine-3-carboxamide (21 mg, 0.073 mmol, 94%).

LCMS (High pH, ES⁺): $t_R = 0.59$ min, $[M+H]^+$ 289.3, (100% purity). 1H

NMR (400 MHz, DMSO- d_6 , 393K): δ 1.26 (d, $J = 6.4$ Hz, 3H), 1.70-1.81 (m, 1H), 2.162.25 (m, 1H), 2.45 (ddd, $J = 13.7, 9.4, 0.7$ Hz, 1H), 2.77 (ddd, $J = 13.0, 10.5, 1.7$ Hz, 1H), 2.88 (d,

$J = 4.9$ Hz, 3H), 3.02 (dd, $J = 13.7, 7.2$ Hz, 1H), 3.09 (dd, $J = 13.0, 3.5$ Hz, 1H), 3.37 (ddd, $J = 15.0, 10.5, 1.7$ Hz, 1H), 4.08 (d, $J = 15.0$ Hz, 1H), 4.38-4.51 (m, 1H), 6.64 (d, $J = 8.0$ Hz, 1H), 7.60 (br. s., 1H), 8.11 (s, 1H), 8.56 (d, $J = 8.0$ Hz, 1H). NH not observed.

***N*-Methyl-5-(3-methylmorpholino)pyrazolo[1,5-*a*]pyrimidine-3-carboxamide**



3.051x

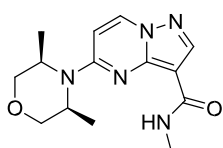
Prepared according to General Procedure C with **3.030** (38 mg, 0.18 mmol), DIPEA (95 μ L, 0.541 mmol) and 3-methylmorpholine (37 mg, 0.36 mmol) at rt, affording *N*-methyl-5-(3-methylmorpholino)pyrazolo[1,5-*a*]pyrimidine-3-carboxamide (33 mg,

0.119 mmol, 63%).

LCMS (High pH, ES⁺): $t_R = 0.67$ min, $[M+H]^+$ 276.0, (100% purity). ¹

¹H NMR (600 MHz, DMSO- d_6): δ 1.24 (d, $J = 6.8$ Hz, 3H), 2.85 (d, $J = 4.9$ Hz, 3H), 3.25 (ddd, $J = 13.0, 11.5, 2.7$ Hz, 1H), 3.50 (ddd, $J = 11.5, 11.5, 2.6$ Hz, 1H), 3.65 (dd, $J = 11.3, 2.3$ Hz, 1H), 3.76 (d, $J = 11.3$ Hz, 1H), 3.98 (dd, $J = 11.5, 2.7$ Hz, 1H), 4.18 (d, $J = 13.0$ Hz, 1H), 4.43-4.53 (m, 1H), 6.80 (d, $J = 7.9$ Hz, 1H), 7.58 (q, $J = 4.2$ Hz, 1H), 8.16 (s, 1H), 8.72-8.79 (m, 1H).

5-(*cis*-3,5-Dimethylmorpholino)-*N*-methylpyrazolo[1,5-*a*]pyrimidine-3-carboxamide

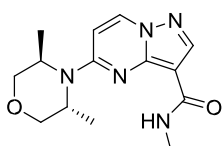


3.051y

Prepared according to General Procedure C, with **3.030** (38 mg, 0.18 mmol), DIPEA (95 μ L, 0.541 mmol), *cis*-3,5-dimethylmorpholine (42 mg, 0.36 mmol) and heating to 120 $^{\circ}$ C, affording 5-(*cis*-3,5-dimethylmorpholino)-*N*-methylpyrazolo[1,5-*a*]pyrimidine-3-carboxamide (6.1 mg, 0.021 mmol, 11%).

LCMS (High pH, ES⁺): $t_R = 0.74$ min, $[M+H]^+$ 290.0, (100% purity). ¹H NMR (600 MHz, DMSO- d_6): δ 1.31 (d, $J = 6.8$ Hz, 6H), 2.85 (d, $J = 4.5$ Hz, 3H), 3.65 (dd, $J = 11.3, 3.4$ Hz, 2H), 3.82 (d, $J = 11.3$ Hz, 2H), 4.33-4.43 (m, 2H), 6.76 (d, $J = 7.9$ Hz, 1H), 7.64-7.72 (m, 1H), 8.16 (s, 1H), 8.77 (d, $J = 7.9$ Hz, 1H).

5-((3*R*,5*R*)-3,5-Dimethylmorpholino)-*N*-methylpyrazolo[1,5-*a*]pyrimidine-3-carboxamide



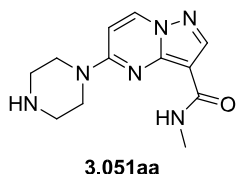
3.051z

Prepared according to General Procedure C, with **3.030** (38 mg, 0.18 mmol), DIPEA (95 μ L, 0.541 mmol), (3*R*,5*R*)-3,5-dimethylmorpholine (42 mg, 0.36 mmol) and heating to 120 $^{\circ}$ C, affording 5-((3*R*,5*R*)-3,5-dimethylmorpholino)-*N*-methylpyrazolo[1,5-*a*]pyrimidine-3-carboxamide (25 mg, 0.085 mmol, 45%).

LCMS (High pH, ES⁺): $t_R = 0.72$ min, $[M+H]^+$ 290.0, (100% purity).

¹H NMR (600 MHz, DMSO- d_6): δ 1.36 (d, $J = 6.8$ Hz, 6H), 2.85 (d, $J = 4.5$ Hz, 3H), 3.72 (dd, $J = 11.3, 1.9$ Hz, 2H), 4.16 (dd, $J = 11.3, 2.3$ Hz, 2H), 4.25-4.31 (m, 2H), 6.72 (d, $J = 7.9$ Hz, 1H), 7.72 (q, $J = 4.5$ Hz, 1H), 8.18 (s, 1H), 8.78 (d, $J = 7.9$ Hz, 1H).

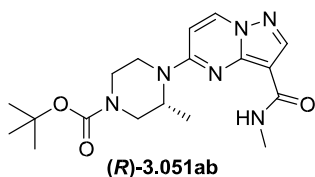
***N*-Methyl-5-(piperazin-1-yl)pyrazolo[1,5-*a*]pyrimidine-3-carboxamide**



Prepared according to General Procedure C with **3.030** (20 mg, 0.095 mmol), piperazine (57 mg, 0.665 mmol) and DIPEA (33 μ L, 0.190 mmol), affording *N*-methyl-5-(piperazin-1-yl)pyrazolo[1,5-*a*]pyrimidine-3-carboxamide (21 mg, 0.081 mmol, 85%).

LCMS (High pH, ES⁺): t_R = 0.51 min, [M+H]⁺ 261.2, (100% purity). ¹H NMR (400 MHz, DMSO-*d*₆): δ 2.78-2.82 (m, 4H), 2.85 (d, J = 4.9 Hz, 3H), 3.66 (br. s., 4H), 6.83 (d, J = 8.1 Hz, 1H), 7.58 (q, J = 4.9 Hz, 1H), 8.14 (s, 1H), 8.71 (d, J = 8.1 Hz, 1H). Piperazine NH was not observed.

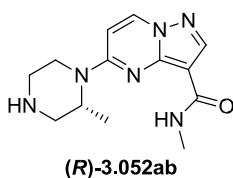
***(R)*-*tert*-Butyl 3-methyl-4-(3-(methylcarbamoyl)pyrazolo[1,5-*a*]pyrimidin-5-yl)piperazine-1-carboxylate**



Prepared according to General Procedure C, with **3.030** (38 mg, 0.18 mmol), DIPEA (95 μ L, 0.541 mmol) and (*R*)-*tert*-butyl 3-methylpiperazine-1-carboxylate (72 mg, 0.36 mmol) at rt, affording (*R*)-*tert*-butyl 3-methyl-4-(3-(methylcarbamoyl)pyrazolo[1,5-*a*]pyrimidin-5-yl)piperazine-1-carboxylate (52 mg, 0.139 mmol, 73%).

LCMS (High pH, ES⁺): t_R = 0.94 min, [M+H]⁺ 375.0, (100% purity). ¹H NMR (400 MHz, DMSO-*d*₆, 393K): δ 1.25 (d, J = 6.6 Hz, 3H), 1.48 (s, 9H), 2.87-2.93 (m, 3H), 3.10-3.43 (m, 3H), 3.86 (s, 1H), 3.93-4.01 (m, 1H), 4.21 (dt, J = 13.7, 3.5 Hz, 1H), 4.604.70 (m, 1H), 6.74 (d, J = 8.1 Hz, 1H), 7.43-7.53 (m, 1H), 8.15 (s, 1H), 8.64 (d, J = 8.1 Hz, 1H).

***(R)*-*N*-Methyl-5-(2-methylpiperazin-1-yl)pyrazolo[1,5-*a*]pyrimidine-3-carboxamide**



Prepared according to General Procedure D with (***R***)-**3.051ab** (30 mg, 0.08 mmol) affording (*R*)-*N*-methyl-5-(2-methylpiperazin-1-yl)pyrazolo[1,5-*a*]pyrimidine-3-carboxamide (19 mg, 0.069 mmol, 86%). LCMS (High pH, ES⁺): t_R = 0.56 min, [M+H]⁺ 275.2, (100% purity).

¹H NMR (400 MHz, MeOD-*d*₄): δ 1.37 (d, J = 6.8 Hz, 3H), 2.83 (td, J = 12.6, 3.7 Hz, 1H), 2.97-3.02 (m, 1H), 3.00 (s, 3H), 3.06 (dd, J = 13.0, 4.2 Hz, 1H), 3.10-3.18 (m, 1H), 3.26 (td, J = 13.0, 3.5 Hz, 1H), 4.26 (dd, J = 13.4, 1.5 Hz, 1H), 4.53-4.65 (m, 1H), 6.75 (d, J = 7.8 Hz, 1H), 8.22 (s, 1H), 8.47 (d, J = 8.1 Hz, 1H). Exchangeable protons were not observed. ¹³

¹³C NMR (101 MHz, MeOD-*d*₄): δ 12.9, 24.6, 39.6, 44.7, 47.7, 49.1, 97.6, 100.6, 136.0, 144.6, 146.6, 156.5, 164.8.

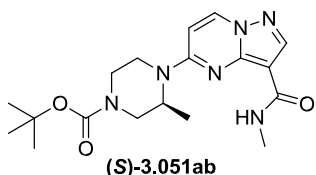
M.pt.: 176-177 °C.

$[\alpha_D]^{22} = -104$ (c = 0.13, MeOH).

ν_{max} (neat): 3301, 2937, 1635, 1571, 1488, 1465, 1443, 1224, 1167, 1065, 994, 892, 865, 803, 773, 692 cm^{-1} .

HRMS: (C₁₃H₁₈N₆O) [M+H]⁺ requires 275.1615, found [M+H]⁺ 275.1617.

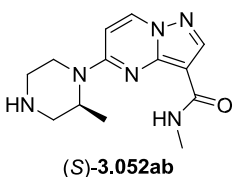
(S)-tert-Butyl 3-methyl-4-(3-(methylcarbamoyl)pyrazolo[1,5-a]pyrimidin-5-yl)piperazine-1-carboxylate



Prepared according to General Procedure C, with **3.030** (30 mg, 0.14 mmol), (S)-tert-butyl 3-methylpiperazine-1-carboxylate (57 mg, 0.29 mmol) and DIPEA (37 μ L, 0.214 mmol) at rt affording (S)-tert-butyl 3-methyl-4-(3-

(methylcarbamoyl)pyrazolo[1,5-a]pyrimidin-5-yl)piperazine-1-carboxylate (34 mg, 0.091 mmol, 64%) as a yellow solid. LCMS (High pH, ES⁺): t_R = 0.94 min, [M+H]⁺ 375.2, (98% purity). ¹H NMR (400 MHz, CDCl₃): δ 1.32 (d, J = 6.6 Hz, 3H), 1.53 (s, 9H), 3.05 (d, J = 4.9 Hz, 3H), 3.07-3.21 (m, 1H), 3.24-3.32 (m, 1H), 3.35-3.45 (m, 1H), 3.97-4.30 (m, 3H), 4.45-4.56 (m, 1H), 6.40 (d, J = 8.1 Hz, 1H), 7.52-7.59 (m, 1H), 8.36 (d, J = 8.1 Hz, 1H), 8.42 (s, 1H).

(S)-N-Methyl-5-(2-methylpiperazin-1-yl)pyrazolo[1,5-a]pyrimidine-3-carboxamide

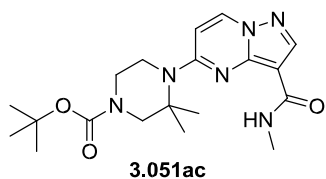


Prepared according to General Procedure D with (S)-**3.051ab** (32 mg, 0.09 mmol) affording (R)-N-methyl-5-(2-methylpiperazin-1-yl)pyrazolo[1,5-a]pyrimidine-3-carboxamide (23 mg, 0.084 mmol, 98%).

LCMS (High pH, ES⁺): t_R = 0.56 min, [M+H]⁺ 275.0, (94% purity).

NMR matches (R)-**3.052ab** (pp 253).

tert-Butyl 3,3-dimethyl-4-(3-(methylcarbamoyl)pyrazolo[1,5-a]pyrimidin-5-yl)piperazine-1-carboxylate

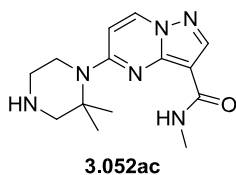


Prepared according to General Procedure C with **3.030** (38 mg, 0.18 mmol), DIPEA (95 μ L, 0.541 mmol), tert-butyl 3,3dimethylpiperazine-1-carboxylate (77 mg, 0.36 mmol) and heating to 120 °C, affording tert-butyl 3,3-dimethyl-4-(3-(methylcarbamoyl)pyrazolo[1,5-a]pyrimidin-5-yl)piperazine-1-

carboxylate (12 mg, 0.030 mmol, 16%).

LCMS (High pH, ES⁺): t_R = 0.97 min, [M+H]⁺ 389.0, (100% purity). ¹H NMR (600 MHz, DMSO-d₆): δ 1.43 (s, 9H), 1.56 (s, 6H), 2.86 (d, J = 4.5 Hz, 3H), 3.433.53 (m, 4H), 3.93 (br. s., 2H), 6.76-6.81 (m, 1H), 7.67 (br. s., 1H), 8.16 (s, 1H), 8.70 (d, J =

7.9 Hz, 1H). **5-(2,2-Dimethylpiperazin-1-yl)-*N*-methylpyrazolo[1,5-*a*]pyrimidine-3-carboxamide**

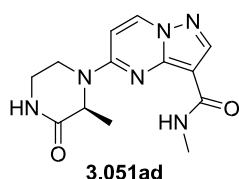


Prepared according to General Procedure D with **3.051ac** (9.5 mg, 0.024 mmol) affording 5-(2,2-dimethylpiperazin-1-yl)-*N*-methylpyrazolo[1,5-*a*]pyrimidine-3-carboxamide (6.8 mg, 0.024 mmol, 98%).

LCMS (High pH, ES⁺): *t*_R = 0.61 min, [M+H]⁺ 289.0, (98% purity).

¹H NMR (400 MHz, MeOD-*d*₄): δ 1.65 (s, 6H), 2.90 (s, 2H), 2.99-3.02 (m, 3H), 3.11-3.17 (m, 2H), 3.70-3.75 (m, 2H), 6.84 (d, *J* = 8.1 Hz, 1H), 8.00-8.08 (m, 1H), 8.26 (s, 1H), 8.51 (d, *J* = 8.1 Hz, 1H). NH was not observed and the amide proton was partially exchanged.

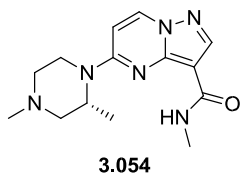
(*S*)-*N*-Methyl-5-(2-methyl-3-oxopiperazin-1-yl)pyrazolo[1,5-*a*]pyrimidine-3-carboxamide



Prepared according to General Procedure C with **3.030** (38 mg, 0.18 mmol), DIPEA (95 μL, 0.541 mmol) and (*S*)-3-methylpiperazin-2-one (41 mg, 0.36 mmol) at rt, affording (*S*)-*N*-methyl-5-(2-methyl-3-oxopiperazin-1-yl)pyrazolo[1,5-*a*]pyrimidine-3-carboxamide (46 mg, 0.158 mmol, 83%).

LCMS (High pH, ES⁺): *t*_R = 0.53 min, [M+H]⁺ 289.0, (100% purity). ¹H NMR (600 MHz, DMSO-*d*₆): δ 1.43 (d, *J* = 7.2 Hz, 3H), 2.86 (d, *J* = 4.5 Hz, 3H), 3.26-3.50 (m, 3H), 4.32-4.51 (m, 1H), 4.75-4.86 (m, 1H), 6.84 (d, *J* = 7.9 Hz, 1H), 7.54-7.60 (m, 1H), 8.17-8.20 (m, 2H), 8.76 (d, *J* = 7.6 Hz, 1H).

(*R*)-*N*-Methyl-5-(2-methylpiperazin-1-yl)pyrazolo[1,5-*a*]pyrimidine-3-carboxamide To

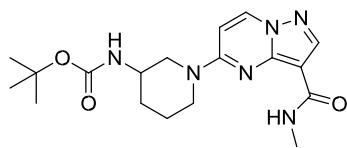


a solution of (*R*)-*N*-methyl-5-(2-methylpiperazin-1-yl)pyrazolo[1,5-*a*]pyrimidine-3-carboxamide (***R***-**3.052ab**) (10 mg, 0.036 mmol) in formic acid (0.5 mL) at rt was added formaldehyde (0.136 mL, 37% wt. in H₂O, 1.823 mmol). The reaction mixture was stirred at

70 °C for 5 h. The reaction was purified by ion exchange chromatography (sulphonic acid (SCX) 500 mg, sequential solvents MeOH, 2 M NH₃/MeOH). The appropriate fractions were combined and evaporated *in vacuo* to give (*R*)-5-(2,4-dimethylpiperazin-1-yl)-*N*-methylpyrazolo[1,5-*a*]pyrimidine-3-carboxamide (6 mg, 0.021 mmol, 57%) as a white solid.

LCMS (High pH, ES⁺): *t*_R = 0.67 min, [M+H]⁺ 289.2, (99% purity). ¹H NMR (400 MHz, MeOD-*d*₄): δ 1.39 (d, *J* = 6.8 Hz, 3H), 2.14 (ddd, *J* = 12.0, 12.0, 3.5 Hz, 1H), 2.29 – 2.38 (m, 4H), 2.90 (d, *J* = 12.0 Hz, 1H), 2.96-3.01 (m, 1H), 3 (d, *J* = 4.9 Hz, 3H), 3.32-3.39 (m, 1H), 4.33 (d, *J* = 13.4 Hz, 1H), 4.62 – 4.72 (m, 1H), 6.76 (d, *J* = 8.0 Hz, 1H), 7.93-8.03 (m, 1H), 8.23 (s, 1H), 8.49 (d, *J* = 8.0 Hz, 1H).

***tert*-Butyl (1-(3-(methylcarbamoyl)pyrazolo[1,5-*a*]pyrimidin-5-yl)piperidin-3-yl)carbamate**



3.051ae

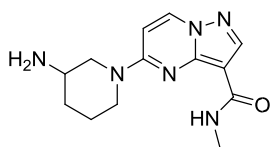
Prepared according to General Procedure C, with **3.030** (38 mg, 0.18 mmol), DIPEA (0.095 mL, 0.541 mmol) and *tert*-butyl piperidine-3-ylcarbamate (72 mg, 0.36 mmol) at rt, affording *tert*-butyl (1-(3-(methylcarbamoyl)pyrazolo[1,5-*a*]pyrimidin-5-yl)piperidin-3-yl)carbamate (62 mg, 0.165

mmol, 87%).

LCMS (High pH, ES⁺): *t*_R = 0.89 min, [M+H]⁺ 375.0, (100% purity). ¹H NMR (600 MHz, DMSO-*d*₆): δ 1.40 (s, 9H), 1.43-1.59 (m, 2H), 1.74-1.90 (m, 2H), 2.89 (d, *J* = 3.8 Hz, 3H), 2.93-3.10 (m, 1H), 3.36-3.43 (m, 1H), 4.00-4.13 (m, 1H), 4.62 (br.s, 1H),

6.76-6.84 (m, 1H), 6.98 (d, *J* = 5.3 Hz, 1H), 7.63-7.63 (m, 1H), 7.63-7.71 (m, 1H), 8.13 (s, 1H), 8.69 (d, *J* = 7.9 Hz, 1H).

5-(3-Aminopiperidin-1-yl)-*N*-methylpyrazolo[1,5-*a*]pyrimidine-3-carboxamide



3.052ae

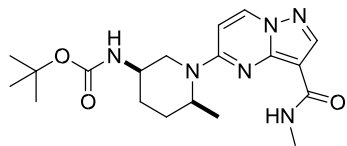
Prepared according to General Procedure D with **3.051ae** (30 mg, 0.08 mmol) affording 5-(3-aminopiperidin-1-yl)-*N*-methylpyrazolo[1,5-*a*]pyrimidine-3-carboxamide (18 mg, 0.066 mmol, 82%).

LCMS (High pH, ES⁺): *t*_R = 0.57 min, [M+H]⁺ 275.3, (99% purity).

¹

H NMR (400 MHz, DMSO-*d*₆): δ 1.28-1.40 (m, 1H), 1.41-1.54 (m, 1H), 1.73-1.84 (m, 1H), 1.85-1.95 (m, 1H), 2.01 (br. s., 2H), 2.70-2.80 (m, 1H), 2.87 (d, *J* = 4.9 Hz, 3H), 2.85-2.93 (m, 1H), 3.15 (ddd, *J* = 13.4, 10.8, 2.9 Hz, 1H), 4.22 (br. s., 2H), 6.82 (d, *J* = 8.0 Hz, 1H), 7.59 (q, *J* = 4.6 Hz, 1H), 8.12 (s, 1H), 8.68 (d, *J* = 8.0 Hz, 1H)

***tert*-Butyl (*cis*-6-Methyl-1-(3-(methylcarbamoyl)pyrazolo[1,5-*a*]pyrimidin-5-yl)piperidin-3-yl)carbamate**



3.051af

Prepared according to General Procedure C, with **3.030** (50 mg, 0.237 mmol) *tert*-butyl ((3*R*,6*S*)-6-methylpiperidin-3-yl)carbamate (102 mg, 0.475 mmol), DIPEA (62 μL, 0.356 mmol) and heating to 90 °C in a Biotage Initiator microwave reactor for 1 h. The reaction mixture was diluted with EtOAc (20 mL) and washed with 0.5 M aq. HCl (2 x 10 mL) and sat. aq. NaHCO₃ (2 x 10 mL). The aqueous layers were extracted with EtOAc (10 mL) and the combined organics were washed with brine, dried through a hydrophobic frit and evaporated to dryness. The residue was purified by silica chromatography 10-80% (3:1 EtOAc:EtOH)/cyclohexane to afford *tert*-butyl

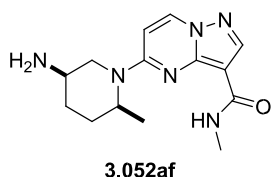
(*cis*-6-methyl-1-(3-(methylcarbamoyl)pyrazolo[1,5-*a*]pyrimidin-5-yl)piperidin-3-yl)carbamate (77 mg, 0.198 mmol, 83%).

LCMS (High pH, ES⁺): *t*_R = 0.98 min, [M+H]⁺ 389.4 (92% purity).

¹H NMR (400 MHz, CDCl₃): δ 1.33 (d, *J* = 7.1 Hz, 3H), 1.50 (s, 9H), 1.61-1.69 (m, 1H), 1.741.84 (m, 1H), 1.85-2.00 (m, 2H), 2.77 (t, *J* = 12.1 Hz, 1H), 3.07 (d, *J* = 4.9 Hz, 3H), 3.50-3.63 (m, 1H), 4.50-4.59 (m, 1H), 4.60-4.69 (m, 1H), 4.74-4.88 (m, 1H), 6.46 (d, *J* = 8.1 Hz, 1H),

7.65-7.73 (m, 1H), 8.31 (d, *J* = 8.1 Hz, 1H), 8.40 (s, 1H).

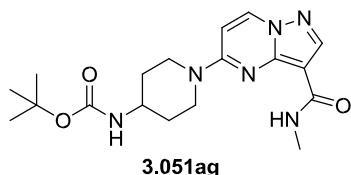
5-(*cis*-5-Amino-2-methylpiperidin-1-yl)-*N*-methylpyrazolo[1,5-*a*]pyrimidine-3-carboxamide



Prepared according to General Procedure D with **3.051af** (26 mg, 0.067 mmol) affording 5-(*cis*-5-amino-2-methylpiperidin-1-yl)-*N*-methylpyrazolo[1,5-*a*]pyrimidine-3-carboxamide (19 mg, 0.066 mmol, 98%) as a white solid.

LCMS (High pH, ES⁺): *t*_R = 0.62 min, [M+H]⁺ 289.3, (100% purity). ¹H NMR (400 MHz, DMSO-*d*₆): δ 1.20 (d, *J* = 6.8 Hz, 3H), 1.39-1.54 (m, 1H), 1.62-1.79 (m, 3H), 2.58-2.73 (m, 2H), 2.87 (d, *J* = 4.9 Hz, 3H), 3.29 (br. s., 2H), 4.34 (br. s., 1H), 4.73 (br. s., 1H), 6.81 (d, *J* = 8.1 Hz, 1H), 7.61 (q, *J* = 4.6 Hz, 1H), 8.13 (s, 1H), 8.69 (d, *J* = 8.1 Hz, 1H).

tert-Butyl (1-(3-(methylcarbamoyl)pyrazolo[1,5-*a*]pyrimidin-5-yl)piperidin-4-yl)carbamate

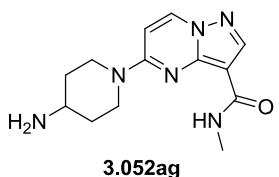


Prepared according to General Procedure C with **3.030** (20 mg, 0.095 mmol), DIPEA (33 μL, 0.190 mmol) and *tert*-butyl piperidine-4-ylcarbamate (29 mg, 0.142 mmol) at rt, affording *tert*-butyl (1-(3-(methylcarbamoyl)pyrazolo[1,5-*a*]pyrimidin-5-yl)piperidin-4-yl)carbamate (35 mg, 0.093 mmol, 98%).

LCMS (High pH, ES⁺): *t*_R = 0.88 min, [M+H]⁺ 375.3, (100% purity). ¹

¹H NMR (400 MHz, CDCl₃): δ 1.43-1.55 (m, 11H), 2.08-2.19 (m, 2H), 3.02 (d, *J* = 4.6 Hz, 3H), 3.20 (ddd, *J* = 13.8, 11.3, 2.5 Hz, 2H), 3.72-3.86 (m, 1H), 4.32 (d, *J* = 13.8 Hz, 2H), 4.44-4.59 (m, 1H), 6.40 (d, *J* = 8.0 Hz, 1H), 7.54 (q, *J* = 4.6 Hz, 1H), 8.29 (d, *J* = 8.0 Hz, 1H), 8.38 (s, 1H).

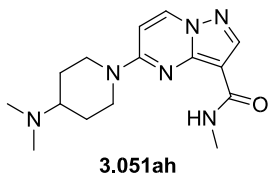
5-(4-Aminopiperidin-1-yl)-*N*-methylpyrazolo[1,5-*a*]pyrimidine-3-carboxamide



Prepared according to General Procedure D with **3.051ag** (22 mg, 0.06 mmol) affording 5-(4-aminopiperidin-1-yl)-*N*-methylpyrazolo[1,5-*a*]pyrimidine-3-carboxamide (12 mg, 0.044 mmol, 73%).

LCMS (High pH, ES⁺): *t*_R = 0.56 min, [M+H]⁺ 275.2, (100% purity).

¹H NMR (400 MHz, CDCl₃): δ 1.40 (br. s, 2H), 1.38-1.50 (m, 2H), 1.95-2.06 (m, 2H), 3.04 (d, *J* = 4.9 Hz, 3H), 3.05-3.12 (m, 1H), 3.20 (ddd, *J* = 13.6, 11.3, 2.8 Hz, 2H), 4.33 (d, *J* = 13.6 Hz, 2H), 6.42 (d, *J* = 8.0 Hz, 1H), 7.54-7.67 (m, 1H), 8.29 (d, *J* = 8.0 Hz, 1H), 8.38 (s, 1H). **5-(4-(Dimethylamino)piperidin-1-yl)-*N*-methylpyrazolo[1,5-*a*]pyrimidine-3-carboxamide**



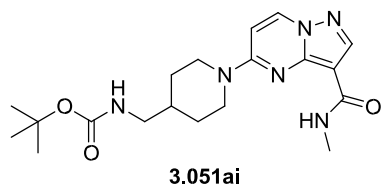
3.051ah

Prepared according to General Procedure C with **3.030** (20 mg, 0.095 mmol), DIPEA (33 μL, 0.190 mmol) and *N,N*-dimethylpiperidine-4-amine (18 mg, 0.142 mmol) at rt, affording 5-

(4-(dimethylamino)piperidin-1-yl)-*N*-methylpyrazolo[1,5-*a*]pyrimidine-3-carboxamide (27 mg, 0.089 mmol, 94%) LCMS (High pH, ES⁺): *t*_R

= 0.66 min, [M+H]⁺ 303.4, (100% purity). ¹H NMR (400 MHz, CDCl₃): δ 1.51-1.63 (m, 2H), 1.96-2.05 (m, 2H), 2.32 (s, 6H), 2.42-2.53 (m, 1H), 3.03 (d, *J* = 4.9 Hz, 3H), 3.06-3.15 (m, 2H), 4.40 (d, *J* = 13.0 Hz, 2H), 6.41 (d, *J* = 8.0 Hz, 1H), 7.55-7.63 (m, 1H), 8.28 (d, *J* = 8.0 Hz, 1H), 8.38 (s, 1H).

***tert*-Butyl ((1-(3-(methylcarbamoyl)pyrazolo[1,5-*a*]pyrimidin-5-yl)piperidin-4-yl)methyl)carbamate**



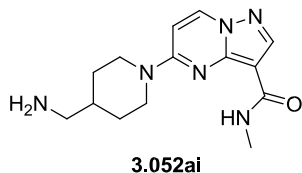
3.051ai

Prepared according to General Procedure C with **3.030** (20 mg, 0.095 mmol), DIPEA (33 μL, 0.190 mmol) and *tert*-butyl (piperidine-4-ylmethyl)carbamate (31 mg, 0.142 mmol) at rt, affording *tert*-butyl ((1-(3-(methylcarbamoyl)pyrazolo[1,5-*a*]pyrimidin-5-yl)piperidin-

4-yl)methyl)carbamate (30 mg, 0.077 mmol, 81%)

LCMS (High pH, ES⁺): *t*_R = 0.90 min, [M+H]⁺ 389.4, (100% purity). ¹H NMR (400 MHz, CDCl₃): δ 1.29 (dd, *J* = 12.3, 3.1 Hz, 2H), 1.45 (s, 9H), 1.79-1.94 (m, 3H), 3.02 (d, *J* = 4.6 Hz, 3H), 3.04-3.11 (m, 4H), 4.41 (d, *J* = 13.0 Hz, 2H), 4.60-4.71 (m, 1H), 6.39 (d, *J* = 8.0 Hz, 1H), 7.59 (q, *J* = 4.6 Hz, 1H), 8.27 (d, *J* = 8.0 Hz, 1H), 8.37 (s, 1H).

5-(4-(Aminomethyl)piperidin-1-yl)-*N*-methylpyrazolo[1,5-*a*]pyrimidine-3-carboxamide

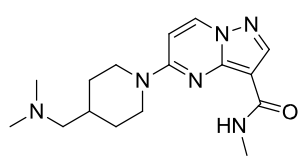


3.052ai

Prepared according to General Procedure D with **3.051ai** (23 mg, 0.06 mmol) affording 5-(4-(aminomethyl)piperidin-1-yl)-*N*-methylpyrazolo[1,5-*a*]pyrimidine-3-carboxamide (12 mg, 0.042 mmol, 69%).

LCMS (High pH, ES⁺): *t*_R = 0.61 min, [M+H]⁺ 289.0, (98% purity). ¹H NMR (400 MHz, CDCl₃): δ 1.22-1.35 (m, 2H), 1.41 (br. s., 2H), 1.63-1.75 (m, 1H), 1.901.98 (m, 2H), 2.67 (d, *J* = 6.4 Hz, 2H), 3.02 (d, *J* = 4.6 Hz, 3H), 3.07 (td, *J* = 13.0, 2.4 Hz, 2H), 4.43 (d, *J* = 13.0 Hz, 2H), 6.41 (d, *J* = 8.0 Hz, 1H), 7.62 (q, *J* = 4.6 Hz, 1H), 8.26 (d, *J* =

8.0 Hz, 1H), 8.36 (s, 1H). **5-(4-((Dimethylamino)methyl)piperidin-1-yl)-*N*-methylpyrazolo[1,5-*a*]pyrimidine-3-carboxamide**

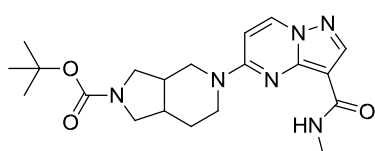


3.051aj

Prepared according to General Procedure C with **3.030** (20 mg, 0.095 mmol), DIPEA (33 μ L, 0.190 mmol) and *N,N*-dimethylpiperidine-4-amine (18 mg, 0.142 mmol) at rt, affording

5-(4-((dimethylamino)methyl)piperidin-1-yl)-*N*-methylpyrazolo[1,5-*a*]pyrimidine-3-carboxamide (23 mg, 0.073 mmol, 77%) LCMS (High pH, ES⁺): t_R = 0.75 min, [M+H]⁺ 317.3, (100% purity). ¹H NMR (400 MHz, CDCl₃): δ 1.20-1.32 (m, 2H), 1.77-1.89 (m, 1H), 1.95 (dq, J = 13.2, 2.5 Hz, 2H), 2.17 (d, J = 7.5 Hz, 2H), 2.23 (s, 6H), 3.02 (d, J = 4.6 Hz, 3H), 3.07 (td, J = 12.5, 2.5 Hz, 2H), 4.38 (d, J = 12.5 Hz, 2H), 6.40 (d, J = 8.0 Hz, 1H), 7.58-7.67 (m, 1H), 8.26 (d, J = 8.0 Hz, 1H), 8.36 (s, 1H).

***tert*-Butyl 5-(3-(methylcarbamoyl)pyrazolo[1,5-*a*]pyrimidin-5-yl)hexahydro-1*H*pyrrolo[3,4-*c*]pyridine-2(3*H*)-carboxylate**



3.051ak

Prepared according to General Procedure C with **3.030** (20 mg, 0.095 mmol), DIPEA (33 μ L, 0.190 mmol) and *tert*-butyl hexahydro-1*H*-pyrrolo[3,4-*c*]pyridine-2(3*H*)-carboxylate hydrochloride (37.4 mg, 0.142 mmol) at rt. The

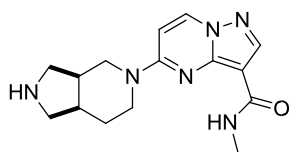
reaction mixture was filtered and purified by High pH

MDAP. The solvent was evaporated *in vacuo* to give *tert*-butyl 5-(3-(methylcarbamoyl)pyrazolo[1,5-*a*]pyrimidin-5-yl)hexahydro-1*H*-pyrrolo[3,4-*c*]pyridine-2(3*H*)carboxylate (45 mg) as a colourless glass.

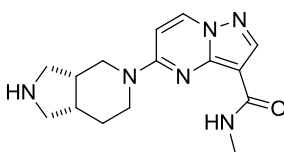
LCMS (High pH, ES⁺): t_R = 0.92 min, [M+H]⁺ 401.2, (100% purity).

Impure by NMR, carried forward to further chemistry without further purification.

5-((3,7-*cis*)Hexahydro-1*H*-pyrrolo[3,4-*c*]pyridin-5(6*H*)-yl)-*N*-methylpyrazolo[1,5-*a*]pyrimidine-3-carboxamide



Isomer 1
3.052ak



Isomer 2
3.052al

Prepared according to General Procedure D with *tert*-butyl 5-(3-

(methylcarbamoyl)pyrazolo[1,5-*a*]pyrimidin-5-yl)hexahydro-1*H*-pyrrolo[3,4-*c*]pyridine-2(3*H*)-carboxylate **3.051ak** (45 mg, 0.112 mmol) and TFA (0.173 mL, 2.247 mmol). The reaction mixture was purified by ion exchange chromatography (sulphonic acid (SCX) 1g, sequential solvents MeOH, 2 M NH₃/MeOH). The appropriate fractions were combined and evaporated *in vacuo*. The mixture of isomers was separated by Chiral HPLC³³⁶ (75% EtOH (+0.2% isopropylamine) / Heptane (+0.2% isopropylamine), f = 30 mL/min, wavelength, 215 nm, 30

mm x 25 cm x 5 μ m Chiralpak IC Column) to afford the products. **5-((3,7-*cis*)Hexahydro-1*H*-pyrrolo[3,4-*c*]pyridin-5(6*H*)-yl)-*N*-methylpyrazolo[1,5-*a*]pyrimidine-3-carboxamide, Isomer 1** (10 mg, 0.033 mmol, 30%).

LCMS (High pH, ES⁺): t_R = 0.57 min, [M+H]⁺ 301.3, (97% purity).

¹H NMR (CDCl₃, 600MHz): δ 1.78 (dtd, J = 14.1, 9.9, 4.4 Hz, 1H), 2.03 (dtd, J = 14.1, 5.7, 4.0 Hz, 1H), 2.39 (tq, J = 9.0, 6.0 Hz, 1H), 2.50 (qt, J = 8.3, 6.2 Hz, 1H), 2.72 (dd, J = 10.8, 6.2 Hz, 1H), 2.79 (dd, J = 10.8, 5.5 Hz, 1H), 3.03 (d, J = 5.0 Hz, 3H), 3.18 (dd, J = 10.8, 7.7 Hz, 1H), 3.22 (dd, J = 10.8, 7.3 Hz, 1H), 3.45-3.53 (m, 1H), 3.56 (br dd, J = 13.4, 8.3 Hz, 1H), 3.78-3.85 (m, 1H), 3.88-3.98 (m, 1H), 6.34 (d, J = 7.9 Hz, 1H), 7.65 (br q, J = 5.0 Hz, 1H), 8.29 (d, J = 7.9 Hz, 1H), 8.38 (s, 1H). NH not observed.

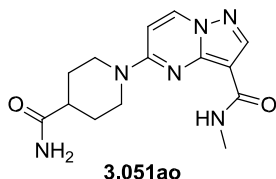
¹³

C NMR (CDCl₃, 151MHz): δ 25.2, 25.8, 36.0, 38.1, 43.4, 43.4, 50.3, 52.3, 96.5, 102.0, 136.0, 146.2, 146.3, 156.1, 163.9.

5-((3,7-*cis*)hexahydro-1*H*-pyrrolo[3,4-*c*]pyridin-5(6*H*)-yl)-*N*-methylpyrazolo[1,5-*a*]pyrimidine-3-carboxamide, Isomer 2 (9 mg, 0.030 mmol, 27%)

LCMS (High pH, ES⁺): t_R = 0.57 min, [M+H]⁺ 301.3, (98% purity). NMR matched **3.052ak**.

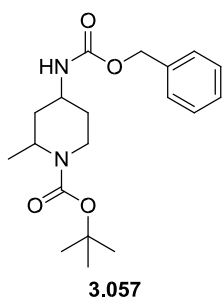
5-(4-carbamoylpiperidin-1-yl)-*N*-methylpyrazolo[1,5-*a*]pyrimidine-3-carboxamide



Prepared according to General Procedure C with **3.030** (20 mg, 0.095 mmol), DIPEA (33 μ L, 0.190 mmol) and piperidine-4carboxamide (18.26 mg, 0.142 mmol) at rt. The product precipitated from the reaction mixture and was collected by filtration, washed with EtOAc and dried under vacuum to afford 5(4-carbamoylpiperidin-1-yl)-*N*-methylpyrazolo[1,5-*a*]pyrimidine-3-carboxamide (16 mg, 0.052 mmol, 55%) as a white solid. LCMS (High pH, ES⁺): t_R = 0.52 min, [M+H]⁺ 303.2, (94% purity). ¹

¹H NMR (400 MHz, DMSO-*d*₆): δ 1.58 (qd, J = 12.0, 3.9 Hz, 2H), 1.79-1.92 (m, 2H), 2.412.50 (m, 1H), 2.86 (d, J = 4.9 Hz, 3H), 3.05-3.17 (m, 2H), 4.39-4.54 (m, 2H), 6.80 (br. s., 1H), 6.86 (d, J = 8.1 Hz, 1H), 7.30 (br. s., 1H), 7.59 (q, J = 4.9 Hz, 1H), 8.14 (s, 1H), 8.70 (d, J = 7.8 Hz, 1H).

***tert*-Butyl 4-(((benzyloxy)carbonyl)amino)-2-methylpiperidine-1-carboxylate**

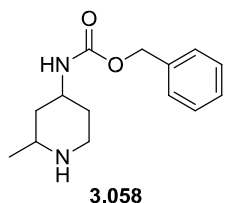


A suspension of *tert*-butyl 4-amino-2-methylpiperidine-1-carboxylate **3.056** (250 mg, 1.167 mmol), benzyl chloroformate (0.20 mL, 1.400 mmol) and potassium carbonate (322 mg, 2.333 mmol) was stirred at rt for 18 h. The reaction mixture was diluted with water (20 mL) and extracted with EtOAc (4 x 15 mL). The combined organics were washed with brine, dried through a hydrophobic frit and evaporated to dryness. The crude product was purified by silica chromatography (550% EtOAc/cyclohexane), appropriate fractions were evaporated *in vacuo* to afford *tert*-butyl 4-

((benzyloxy)carbonyl)amino)-2-methylpiperidine-1-carboxylate (275 mg, 0.789 mmol, 68%). ~10:1 *dr*, major isomer unknown.

LCMS (High pH, ES⁺): t_R = 1.24 min, [M+H]⁺ 349.2 (66% purity). ¹H NMR (400 MHz, CDCl₃): δ 1.24 (d, J = 6.8 Hz, 3H), 1.48 (s, 9H), 1.66 (s, 1H), 1.87-2.01 (m, 2H), 3.10 (ddd, J = 14.1, 11.6, 3.9 Hz, 1H), 3.76-3.92 (m, 2H), 4.12-4.23 (m, 1H), 4.73 (d, J = 5.9 Hz, 1H), 4.76-4.83 (m, 1H), 5.12 (s, 2H), 7.30-7.40 (m, 5H).

Benzyl (2-methylpiperidin-4-yl)carbamate

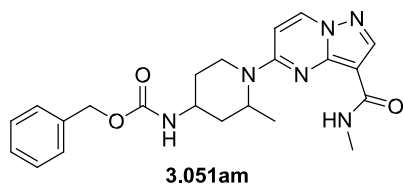


Prepared according to General Procedure D with *tert*-butyl 4(((benzyloxy)carbonyl)amino)-2-methylpiperidine-1-carboxylate **3.057** (275 mg, 0.789 mmol) and TFA (1.2 mL, 15.8 mmol), affording benzyl (2-methylpiperidin-4-yl)carbamate (170 mg, 0.685 mmol, 87%) as a colourless oil. ~10:1 *dr*, major isomer unknown.

LCMS (High pH, ES⁺): t_R = 0.80 min, [M+H]⁺ 249.3, (89% purity). ¹H NMR (400 MHz, CDCl₃): δ 0.92 (q, J = 11.7 Hz, 1H), 1.10 (d, J = 6.4 Hz, 3H), 1.23 (qd, J = 12.5, 4.3 Hz, 1H), 1.93-2.05 (m, 2H), 2.63-2.79 (m, 2H), 3.11 (dq, J = 12.5, 2.4 Hz, 1H),

3.61 (d, J = 7.3 Hz, 1H), 4.63 (br. s., 1H), 5.11 (s, 2H), 7.30-7.41 (m, 5H). NH not observed.

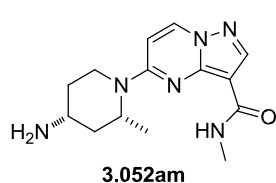
Benzyl (2-methyl-1-(3-(methylcarbamoyl)pyrazolo[1,5-a]pyrimidin-5-yl)piperidin-4-yl)carbamate



Prepared according to General Procedure C with **3.030** (60 mg, 0.285 mmol), DIPEA (75 μ L, 0.427 mmol) and benzyl (2-methylpiperidin-4-yl)carbamate (106 mg, 0.427 mmol). The reaction was stirred at rt for 18 h, then heated to 90 °C in a Biotage Initiator

microwave

reactor for 2 h. The reaction mixture was diluted with EtOAc (20 mL) and washed with 0.5 M HCl (2 x 10 mL) and sat. aq. NaHCO₃ (2 x 10 mL). The aqueous layers were back-extracted with EtOAc (10 mL) and the combined organics were washed with brine, dried through a hydrophobic frit and evaporated to dryness. The crude product was purified by silica chromatography (10-80% (3:1 EtOAc:EtOH)/cyclohexane) to afford benzyl (2-methyl-1-(3(methylcarbamoyl)pyrazolo[1,5-a]pyrimidin-5-yl)piperidin-4-yl)carbamate (76 mg, 0.180 mmol, 63%). ~5:1 *dr* by NMR, major isomer unknown. LCMS (High pH, ES⁺): t_R = 0.95 min, [M+H]⁺ 423.3 (97% purity). ¹H NMR (400 MHz, CDCl₃): δ 1.39 (d, J = 6.6 Hz, 3H), 1.85 (s, 2H), 2.15-2.25 (m, 2H), 3.04 (d, J = 4.9 Hz, 3H), 3.39 (ddd, J = 14.1, 11.9, 4.6 Hz, 1H), 3.87-3.97 (m, 1H), 4.20 (ddd, J = 13.7, 5.9, 2.7 Hz, 1H), 4.43-4.54 (m, 1H), 4.79-4.90 (m, 1H), 5.14 (s, 2H), 6.36 (d, J = 7.8 Hz, 1H), 7.32-7.43 (m, 5H), 7.62 (q, J = 4.9 Hz, 1H), 8.29-8.34 (m, 1H), 8.38-8.41 (m, 1H). **5-(*cis*-4-Amino-2-methylpiperidin-1-yl)-*N*-methylpyrazolo[1,5-a]pyrimidine-3carboxamide**

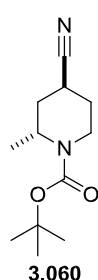


A solution of benzyl (2-methyl-1-(3-(methylcarbamoyl)pyrazolo[1,5-a]pyrimidin-5-yl)piperidin-4-yl)carbamate **3.051am** (75 mg, 0.178 mmol) in HBr (33% wt. in AcOH, 1.56 mL) was stirred at rt for 15 min. The reaction mixture was purified directly by ion exchange chromatography (sulphonic acid (SCX) 2 g, sequential solvents MeOH, 2 M NH₃/MeOH). Fractions were combined and evaporated *in vacuo* to give 5-(4-amino-2-methylpiperidin-1-yl)-*N*-methylpyrazolo[1,5-a]pyrimidine-3-carboxamide (38 mg, 0.132 mmol, 74%) as an off-white solid. The diastereoisomers were separated by HPLC³⁸⁵

(CSH C18 150 x 30mm, 5 μm I.D., 0-100% MeCN/ 0.1% aq. TFA), affording 5-(*cis*-4-amino-2-methylpiperidin-1-yl)-*N*-methylpyrazolo[1,5-a]pyrimidine-3-carboxamide (5.4 mg, 0.019 mmol, 12%). The corresponding *trans* isomer was not obtained in significant quantity.

LCMS (High pH, ES⁺): t_R = 0.59 min, [M+H⁺] 289.3 (100% purity). ¹H NMR (400 MHz, MeOD-d₄): δ 1.42 (d, *J* = 6.6 Hz, 3H), 1.77 (dddd, *J* = 13.7, 7.8, 6.3, 1.8 Hz, 1H), 1.91 (ddd, *J* = 13.1, 12.0, 9.8 Hz, 1H), 2.30 (ddd, *J* = 13.1, 6.3, 4.0 Hz, 1H), 2.392.51 (m, 1H), 3.00 (d, *J* = 4.9 Hz, 3H), 3.35-3.44 (m, 1H), 3.53 (ddd, *J* = 14.5, 11.2, 6.1 Hz, 1H), 4.38 (ddd, *J* = 14.5, 7.1, 1.2 Hz, 1H), 4.51 (m, *J* = 12.0, 6.6 Hz, 1H), 6.74 (d, *J* = 8.1 Hz, 1H), 8.01 (q, *J* = 4.9 Hz, 1H), 8.23 (s, 1H), 8.50 (d, *J* = 8.1 Hz, 1H). NH₂ was not observed.

***tert*-Butyl 4-cyano-2-methylpiperidine-1-carboxylate**

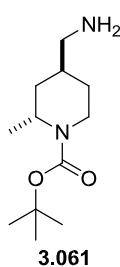


To a solution of *tert*-butyl 2-methyl-4-oxopiperidine-1-carboxylate **3.059** (295 mg, 1.383 mmol) and TosMIC (405 mg, 2.075 mmol) in DME (18 mL) at rt was added potassium *tert*-butoxide (466 mg, 4.15 mmol) portionwise. The reaction was stirred under N₂ at rt for 18 h. Water (20 mL) was added and the reaction was stirred at rt for 30 min. The mixture was extracted with EtOAc (3 x 20 mL) and the combined organics were dried through a hydrophobic frit and evaporated to dryness. The crude product was purified by silica chromatography (0-35% EtOAc/cyclohexane). The appropriate fractions were evaporated to dryness to afford (*trans*)*tert*-butyl 4-cyano-2-methylpiperidine-1-carboxylate (100 mg, 0.446 mmol, 32%) as an offwhite oil.

R_f = 0.5 (30% EtOAc/cyclohexane), stains with KMnO₄. ¹H NMR (400 MHz, DMSO-d₆): δ 1.07 (d, *J* = 7.1 Hz, 3H), 1.40 (s, 9H), 1.43-1.55 (m, 1H), 1.68-1.78 (m, 1H), 1.82-1.89 (m, 1H), 1.91-1.99 (m, 1H), 2.81 (td, *J* = 13.5, 2.7 Hz, 1H), 3.08 (tt, *J* = 12.5, 3.7 Hz, 1H), 3.82 (ddd, *J* = 13.5, 4.4, 2.2 Hz, 1H), 4.26-4.36 (m, 1H).

¹³C NMR (101 MHz, DMSO-d₆): δ 15.7, 21.7, 28.5, 28.9, 33.1, 37.3, 45.4, 79.4, 123.1, 154.1
 ν_{max} (neat): 2975, 2241 (weak, CN stretch), 1685, 1408, 1365, 1345, 1279, 1164, 1122, 1073, 1014, 875, 770 cm⁻¹

(*trans*)-*tert*-Butyl 4-(aminomethyl)-2-methylpiperidine-1-carboxylate

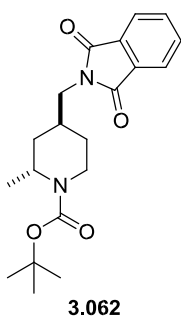


To a solution of (*trans*)-*tert*-butyl 4-cyano-2-methylpiperidine-1-carboxylate **3.060** (305 mg, 1.360 mmol) in THF (5 mL) at 0 °C was added boranetetrahydrofuran complex (4.08 mL, 1 M in THF, 4.08 mmol). The reaction was stirred under N₂ at 75 °C for 5 h. The reaction mixture was cooled to rt and quenched with a mixture of ammonium chloride and sat. NaHCO₃ solution. The mixture was extracted with EtOAc (4 x 20 mL) and the combined organic layers

were washed with brine, dried through a hydrophobic frit and evaporated. The crude product was purified by ion exchange chromatography (sulphonic acid (SCX) 10 g, sequential solvents MeOH, 2 M NH₃/MeOH). The appropriate fractions were combined and evaporated *in vacuo* to give (*trans*)-*tert*-butyl 4-(aminomethyl)-2-methylpiperidine-1-carboxylate (195 mg, 0.854 mmol, 63%) as a colourless gum. ¹H NMR (400 MHz, CDCl₃): δ 1.04 (qd, *J* = 12.5, 4.5 Hz, 1H), 1.15 (d, *J* = 7.1 Hz, 3H), 1.231.43 (m, 2H), 1.48 (s, 9H), 1.54-1.78 (m, 4H), 2.57 (d, *J* = 6.1 Hz, 2H), 2.79-2.94 (m, 1H), 3.93-4.09 (m, 1H), 4.35-4.56 (m, 1H).

ν_{\max} (neat): 2973, 2923, 1683, 1455, 1409, 1364, 1339, 1250, 1159, 1064, 897, 770 cm⁻¹.

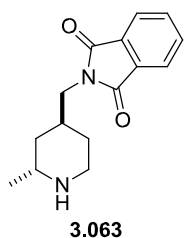
(*trans*)-*tert*-Butyl 4-((1,3-dioxisoindolin-2-yl)methyl)-2-methylpiperidine-1-carboxylate



A solution of (*trans*)-*tert*-butyl 4-(aminomethyl)-2-methylpiperidine-1-carboxylate **3.061** (175 mg, 0.766 mmol) and phthalic anhydride (114 mg, 0.766 mmol) in toluene (5 mL) was stirred at 120 °C for 3 h. The reaction was concentrated and the residue was purified by silica chromatography (0-30% EtOAc/cyclohexane). Fractions were evaporated *in vacuo* to afford (*trans*)-*tert*-butyl 4-((1,3-dioxisoindolin-2-yl)methyl)-2-methylpiperidine-1-carboxylate (260 mg, 0.725 mmol, 95%) as a colourless oil. LCMS (High pH, ES⁺): *t*_R = 1.28 min, [M+H]⁺ 359.3, (97% purity).

¹H NMR (400 MHz, CDCl₃): δ 1.11 (d, *J* = 7.1 Hz, 3H), 1.46 (s, 9H), 1.51-1.69 (m, 4H), 2.112.25 (m, 1H), 2.74-2.87 (m, 1H), 3.57 (d, *J* = 7.1 Hz, 2H), 3.93-4.07 (m, 1H), 4.36-4.59 (m, 1H), 7.71-7.77 (m, 2H), 7.83-7.91 (m, 2H).

2-(*trans*-2-Methylpiperidin-4-yl)methyl)isoindoline-1,3-dione



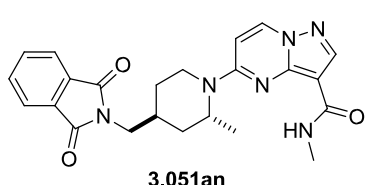
Prepared according to General Procedure D with (*trans*)-*tert*-butyl 4-((1,3-dioxisoindolin-2-yl)methyl)-2-methylpiperidine-1-carboxylate **3.062** (250 mg, 0.697 mmol) and TFA (2 mL, 26.0 mmol) in DCM (6 mL), affording 2-(*trans*-2-Methylpiperidin-4-yl)methyl)isoindoline-1,3-dione (165 mg, 0.639 mmol, 92%) as a white solid.

LCMS (High pH, ES⁺): *t*_R = 0.81 min, [M+H]⁺ 259.3, (90% purity).

¹H NMR (400 MHz, CDCl₃): δ 1.09 (d, *J* = 6.4 Hz, 3H), 1.34-1.45 (m, 2H), 1.50 (dt, *J* = 13.5, 3.8 Hz, 1H), 1.67 (ddt, *J* = 13.9, 9.4, 4.6, 4.6 Hz, 1H), 2.26-2.39 (m, 1H), 2.88 (dt, *J* = 12.5,

4.7 Hz, 1H), 2.95-3.04 (m, 1H), 3.11 ((quint, $J = 6.2, 3.1$ Hz, 1H), 3.66-3.84 (m, 2H), 7.69-7.80 (m, 2H), 7.82-7.93 (m, 2H). NH not observed. ^{13}C NMR (CDCl_3 , 151MHz): δ 21.7, 28.7, 30.9, 36.2, 41.0, 41.1, 46.6, 123.2, 132.1, 133.9, 168.6. ν_{max} (neat): 3229, 2311, 1774, 1702, 1439, 1394, 1372, 1358, 1341, 1068, 1029, 959, 921, 856, 772, 724, 712 cm^{-1} . HRMS: ($\text{C}_{15}\text{H}_{18}\text{O}_2\text{N}_2$) $[\text{M}+\text{H}]^+$ requires 259.1447, found $[\text{M}+\text{H}]^+$ 259.1441.

5-(*trans*-4-((1,3-Dioxoisindolin-2-yl)methyl)-2-methylpiperidin-1-yl)-*N*-methylpyrazolo[1,5-*a*]pyrimidine-3-carboxamide

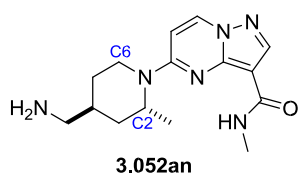


Prepared according to General Procedure C with **3.030** (40 mg, 0.190 mmol), DIPEA (66 μL , 0.380 mmol) and 2((*trans*-2-methylpiperidin-4-yl)methyl)isindoline-1,3-dione **3.063** (74 mg, 0.285 mmol) at rt. The reaction mixture was

diluted with sat. aq. NaHCO_3 (20 mL) and extracted with EtOAc (3 x 20 mL). The combined organics were washed with brine, dried through a hydrophobic frit and evaporated to dryness. The crude product was purified by silica chromatography (10-50% (3:1 EtOAc:EtOH)/cyclohexane), the fractions were evaporated to dryness, evaporated again from diethyl ether and dried under vacuum to afford 5-(*trans*-4-((1,3-dioxoisindolin-2-yl)methyl)-2-methylpiperidin-1-yl)-*N*-methylpyrazolo[1,5-*a*]pyrimidine-3-carboxamide (80 mg, 0.185 mmol, 97%) as a white solid.

LCMS (High pH, ES⁺): $t_{\text{R}} = 0.99$ min, $[\text{M}+\text{H}]^+$ 433.4, (99% purity). ^1H NMR (400 MHz, CDCl_3): δ 1.28 (d, $J = 6.8$ Hz, 3H), 1.33-1.46 (m, 1H), 1.59-1.70 (m, 1H), 1.76-1.84 (m, 1H), 1.87-1.96 (m, 1H), 2.29-2.43 (m, 1H), 3.03 (d, $J = 4.9$ Hz, 3H), 3.06-3.17 (m, 1H), 3.67 (d, $J = 7.1$ Hz, 2H), 4.22-4.47 (m, 1H), 4.64-4.88 (m, 1H), 6.40 (d, $J = 8.1$ Hz, 1H), 7.57-7.63 (m, 1H), 7.74-7.81 (m, 2H), 7.86-7.93 (m, 2H), 8.29 (d, $J = 8.1$ Hz, 1H), 8.39 (s, 1H).

5-(*trans*-4-Amino-2-methylpiperidin-1-yl)-*N*-methylpyrazolo[1,5-*a*]pyrimidine-3-carboxamide



A solution of 5-(*trans*-4-((1,3-dioxoisindolin-2-yl)methyl)-2-methylpiperidin-1-yl)-*N*-methylpyrazolo[1,5-*a*]pyrimidine-3-carboxamide **3.051an** (75 mg, 0.173 mmol) in MeNH_2 (33% in EtOH, 250 μL , 2.008 mmol) was heated to 120 $^\circ\text{C}$ in a Biotage

Initiator microwave reactor for 1 h. The reaction stalled, so the reaction was concentrated under a stream of nitrogen, redissolved in MeNH_2 (33% in EtOH, 250 μL , 2.008 mmol) and heated to 120 $^\circ\text{C}$ in a Biotage Initiator microwave reactor for 90 min. The reaction was evaporated to dryness and purified by High pH MDAP. Collection failed and the product was sent to the waste. The waste was evaporated and purified by ion exchange chromatography (sulphonic acid (SCX) 2g, sequential solvents MeOH, 2 M

NH₃/MeOH). The appropriate fractions were combined and evaporated *in vacuo* to give 5(*trans*-4-(aminomethyl)-2-methylpiperidin-1-yl)-*N*-methylpyrazolo[1,5-*a*]pyrimidine-3carboxamide (27 mg, 0.089 mmol, 52%) as a hygroscopic brown gum.

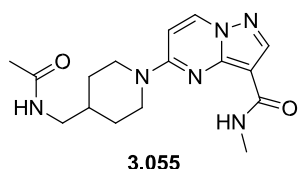
LCMS (High pH, ES⁺): t_R = 0.60 min, [M+H]⁺ 303.3, (98% purity). ¹H NMR (500 MHz, DMSO-d₆): δ 1.01-1.13 (m, 1H), 1.21 (d, *J* = 6.9 Hz, 3H), 1.28-1.38 (m, 1H), 1.71-1.82 (m, 2H), 1.90 (d, *J* = 12.9 Hz, 1H), 2.46 (d, *J* = 5.8 Hz, 2H), 2.87 (d, *J* = 4.9 Hz, 3H), 2.97-3.21 (m, 3H), 3.93-5.43 (m, 2H), 6.86 (d, *J* = 8.1 Hz, 1H), 7.63 (q, *J* = 4.9 Hz, 1H), 8.12-8.17 (m, 1H), 8.70 (d, *J* = 8.1 Hz, 1H).

¹³C NMR (126 MHz, DMSO-d₆): δ 15.9, 26.0, 29.9, 33.2, 34.9, 48.1, 98.4, 101.4, 137.1, 145.2, 146.2, 156.3, 163.0. Piperidine C2 and C6 not observed due to peak broadening.

ν_{max} (neat): 3342, 2932, 1631, 1568, 1484, 1440, 1229, 1140, 1085, 1006, 899, 864, 774 cm⁻¹.

HRMS: (C₁₅H₂₂N₆O) [M+H]⁺ requires 303.1928, found [M+H]⁺ 303.1936.

5-(*cis*-4-Amino-2-methylpiperidin-1-yl)-*N*-methylpyrazolo[1,5-*a*]pyrimidine-3carboxamide



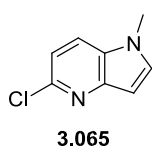
To a suspension of 5-(4-(aminomethyl)piperidin-1-yl)-*N*-methylpyrazolo[1,5-*a*]pyrimidine-3-carboxamide **3.052ai** (10 mg, 0.035 mmol) and pyridine (5.6 μL, 0.069 mmol) in DCM (0.5 mL) was added acetyl chloride (3.7 μL, 0.052 mmol). The reaction mixture was stirred at rt for 18 h. Further pyridine (5.6 μL, 0.069

mmol) and acetyl chloride (3.7 μL, 0.052 mmol) were added and the reaction was stirred at rt for 18 h. The reaction mixture was diluted with DCM (10 mL) and sat. aq. NaHCO₃ (10 mL). The aqueous layer was extracted with DCM (3 x 10 mL), dried through a hydrophobic frit and evaporated to dryness. The residue was purified by silica chromatography (0-15% MeOH/DCM) and the appropriate fractions were evaporated to dryness to afford 5-(4(acetamidomethyl)piperidin-1-yl)-*N*-methylpyrazolo[1,5-*a*]pyrimidine-3-carboxamide (6.5 mg,

0.020 mmol, 57%) as a white solid.

LCMS (Formic, ES⁺): t_R = 0.60 min, [M+H]⁺ 331.3, (100% purity). ¹H NMR (400 MHz, CDCl₃): δ 1.26-1.40 (m, 2H), 1.86-1.99 (m, 3H), 2.03 (s, 3H), 3.03 (d, *J* = 4.9 Hz, 3H), 3.03-3.11 (m, 2H), 3.23 (t, *J* = 6.2 Hz, 2H), 4.41 (d, *J* = 12.7 Hz, 2H), 5.83 (t, *J* = 5.1 Hz, 1H), 6.40 (d, *J* = 7.8 Hz, 1H), 7.60 (q, *J* = 4.4 Hz, 1H), 8.27 (d, *J* = 7.8 Hz, 1H), 8.36 (s, 1H).

5-Chloro-1-methyl-1*H*-pyrrolo[3,2-*b*]pyridine

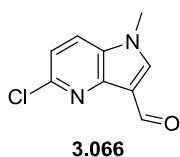


To a solution of 5-chloro-1*H*-pyrrolo[3,2-*b*]pyridine **3.064** (600 mg, 3.93 mmol) in DMF (10 mL) at 0 °C was added sodium hydride (60% in mineral oil, 629 mg, 15.73 mmol), and the reaction was stirred for 15 min. Methyl iodide (0.49 mL, 7.86 mmol) was added and the reaction was allowed to warm to rt and stirred for 1 h. The reaction was cooled to 0 °C and cautiously quenched with water. When bubbling ceased the reaction was diluted with water (600 mL) and the aqueous layer was extracted with diethyl ether (3 x 20 mL). The combined organics were washed with brine, dried through a hydrophobic frit and evaporated to dryness. Purified by silica chromatography (0-50% EtOAc/cyclohexane), appropriate fractions were evaporated *in vacuo* to afford 5-chloro-1-methyl-1*H*-pyrrolo[3,2-*b*]pyridine (540 mg, 3.24 mmol, 82%) as a white solid.

LCMS (High pH, ES⁺): *t_R* = 0.82 min, [M+H]⁺ 167.0, (96% purity). ¹H NMR (400 MHz, CDCl₃): δ 3.84 (s, 3H), 6.64 (dd, *J* = 3.3, 0.7 Hz, 1H), 7.15 (d, *J* = 8.6 Hz, 1H), 7.31 (d, *J* = 3.3 Hz, 1H), 7.59 (dd, *J* = 8.6, 0.7 Hz, 1H). ¹³C NMR (101 MHz, CDCl₃): δ 33.3, 102.0, 116.3, 119.0, 128.4, 133.0, 144.0, 146.2. M.pt.: 71-72 °C. *v*_{max} (neat): 1604, 1548, 1502, 1434, 1412, 1344, 1811, 1261, 1217, 1143, 1111, 1089, 1077, 1007, 910, 809, 769, 750, 711 cm⁻¹.

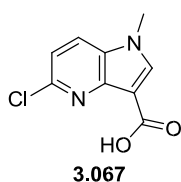
HRMS: (C₈H₇ClN₂) [M+H]⁺ requires 167.0371, found [M+H]⁺ 167.0371.

5-Chloro-1-methyl-1*H*-pyrrolo[3,2-*b*]pyridine-3-carbaldehyde



To DMF (5 mL) at 0 °C under N₂ was added POCl₃ (0.554 mL, 5.94 mmol), and the reaction was stirred at 0 °C for 15 min. To this solution was added a solution of 5-chloro-1-methyl-1*H*-pyrrolo[3,2-*b*]pyridine **3.065** (495 mg, 2.97 mmol) in DMF (2 mL) dropwise. The reaction mixture was stirred at rt for 2 h. The reaction mixture was poured into an ice/water mixture and the pH was adjusted to 7 by adding 1 N NaOH (~18 mL). A white precipitate formed and was collected by filtration, washed with water and dried under vacuum to afford 5-chloro-1-methyl-1*H*-pyrrolo[3,2-*b*]pyridine-3-carbaldehyde (245 mg, 1.259 mmol, 42%) as a white solid. The aqueous filtrate was extracted with EtOAc (5 x 20 mL) and DCM (3 x 20 mL). The combined organic layers were dried through a hydrophobic frit and evaporated *in vacuo* to afford further 5-chloro-1-methyl-1*H*-pyrrolo[3,2-*b*]pyridine-3-carbaldehyde (265 mg, 1.362 mmol, 46%) as a white solid. LCMS (High pH, ES⁺): *t_R* = 0.67 min, [M+H]⁺ 195.1, (98% purity). ¹H NMR (400 MHz, CDCl₃): δ 3.91 (s, 3H), 7.27 (d, *J* = 8.6 Hz, 1H), 7.66 (d, *J* = 8.6 Hz, 1H), 7.97 (s, 1H), 10.36 (s, 1H). ¹³C NMR (101 MHz, CDCl₃): δ 34.3, 116.6, 118.6, 120.3, 129.0, 136.7, 144.3, 147.1, 184.3. M.pt.: 208-210 °C *v*_{max} (neat): 3101, 3072, 2836, 1669, 1602, 1556, 1528, 1448, 1421, 1405, 1376, 1356, 1310, 1272, 1222, 1155, 1117, 1067, 1016, 882, 827, 772, 781, 722 cm⁻¹.

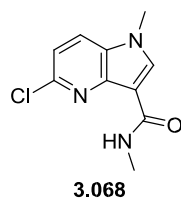
HRMS: (C₉H₇ClN₂O) [M+H]⁺ requires 195.0320, found [M+H]⁺ 195.0320. **5-Chloro-1-methyl-1*H*-pyrrolo[3,2-*b*]pyridine-3-carboxylic acid**



To a suspension of 5-chloro-1-methyl-1*H*-pyrrolo[3,2-*b*]pyridine-3-carbaldehyde **3.066** (360 mg, 1.850 mmol) in THF (30 mL) and water (6 mL) at 0 °C was added sulfamic acid (1.08 g, 11.10 mmol), followed by a solution of sodium chlorite (314 mg, 2.77 mmol) and sodium dihydrogen phosphate (2.67 g, 22.20 mmol) in water (18 mL) dropwise. The reaction was stirred at rt for 18 h. A white precipitate formed and was filtered off, washed with water and dried under vacuum to afford 5-chloro-1-methyl-1*H*-pyrrolo[3,2-*b*]pyridine-3-carboxylic acid (300 mg, 1.282 mmol, 69%) as a white solid, which contained ~10% aldehyde SM by LCMS and NMR and was used without further purification.

LCMS (High pH, ES⁺): t_R = 0.40 min, [M+H]⁺ 211.2, (80% purity). ¹H NMR (400 MHz, CDCl₃): δ 3.89 (s, 3H), 7.31 (d, J = 8.6 Hz, 1H), 8.06 (d, J = 8.6 Hz, 1H), 8.33 (s, 1H), 11.48-12.39 (m, 1H).

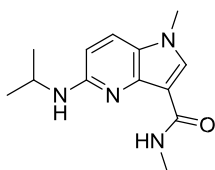
5-Chloro-*N*,1-dimethyl-1*H*-pyrrolo[3,2-*b*]pyridine-3-carboxamide



To a suspension of 5-chloro-1-methyl-1*H*-pyrrolo[3,2-*b*]pyridine-3-carboxylic acid **3.067** (300 mg, 1.282 mmol) and oxalyl chloride (224 μL, 2.56 mmol) in DCM (6.5 mL) stirred under N₂ at rt was added DMF (5 μL, 0.064 mmol). The reaction mixture was stirred at rt for 5 h. The reaction mixture was evaporated *in vacuo* and the residue was redissolved in anhydrous DCM and evaporated again. The acyl chloride was dissolved in THF (6.5 mL) and stirred under N₂ at 0 °C. MeNH₂ (2M in THF, 961 μL, 1.923 mmol) was added and the resulting thick slurry was stirred at rt for 18 h. The reaction mixture was concentrated *in vacuo* and dissolved in EtOAc (30 mL) and sat. aq. NaHCO₃ (30 mL). The aqueous layer was extracted with EtOAc (5 x 30 mL) and the combined organics were dried through a hydrophobic frit and evaporated to dryness. The crude product was purified by silica chromatography (10-60% (3:1/EtOAc:EtOH)/cyclohexane), and fractions were evaporated *in vacuo* to afford 5-chloro-*N*,1-dimethyl-1*H*-pyrrolo[3,2-*b*]pyridine-3-carboxamide (150 mg, 0.671 mmol, 52%) as a white solid.

LCMS (High pH, ES⁺): t_R = 0.83 min, [M+H]⁺ 224.1, (92% purity). ¹H NMR (400 MHz, CDCl₃): δ 3.10 (d, J = 4.9 Hz, 3H), 3.88 (s, 3H), 7.23 (d, J = 8.6 Hz, 1H), 7.65 (d, J = 8.6 Hz, 1H), 8.02 (s, 1H), 8.21 (br. s., 1H). ¹³C NMR (101 MHz, CDCl₃): δ 25.8, 33.8, 110.7, 117.3, 120.1, 128.8, 136.6, 142.6, 145.0, 163.7. ν_{max} (neat): 3351, 3093, 1656, 1606, 1561, 1452, 1415, 1376, 1354, 1291, 1255, 1194, 1150, 1112, 1070, 986, 920, 848, 808, 780, 763 cm⁻¹. M.pt.: 184-187 °C.

HRMS: (C₁₀H₁₀ClN₃O) [M+H]⁺ requires 224.0585, found [M+H]⁺ 224.0599. **5-(Isopropylamino)-*N*,1-dimethyl-1*H*-pyrrolo[3,2-*b*]pyridine-3-carboxamide**



3.069

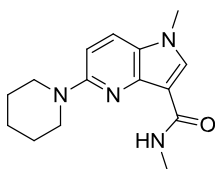
5-Chloro-*N*,1-dimethyl-1*H*-pyrrolo[3,2-*b*]pyridine-3-carboxamide **3.068** (25 mg, 0.112 mmol), NaO^tBu (32 mg, 0.335 mmol), Pd(OAc)₂ (2.5 mg, 0.011 mmol) and BINAP (14 mg, 0.022 mmol) were dissolved in 1,4-dioxane (750 μL) and stirred at rt for 10 min under N₂.

Isopropylamine

(19 μL, 0.224 mmol) was added and the reaction was heated to 100 °C

in an oil bath for 5 h. The reaction mixture was filtered through Celite, evaporated to dryness and purified by silica chromatography (30-90% (3:1 EtOAc:EtOH)/cyclohexane). The appropriate fractions were evaporated to dryness to afford 5-(isopropylamino)-*N*,1-dimethyl-1*H*-pyrrolo[3,2-*b*]pyridine-3-carboxamide (17 mg, 0.069 mmol, 62%) as a white solid. LCMS (High pH, ES⁺): t_R = 0.90 min, [M+H]⁺ 247.2, (100% purity). ¹H NMR (400 MHz, CDCl₃): δ 1.30 (d, *J* = 6.4 Hz, 6H), 3.04 (d, *J* = 4.9 Hz, 3H), 3.75 (s, 3H), 4.02 (br. s., 1H), 4.26 (br. s., 1H), 6.32 (d, *J* = 9.0 Hz, 1H), 7.42 (d, *J* = 9.0 Hz, 1H), 7.72 (s, 1H), 8.69 (br. s., 1H).

***N*,1-Dimethyl-5-(piperidin-1-yl)-1*H*-pyrrolo[3,2-*b*]pyridine-3-carboxamide**



3.070

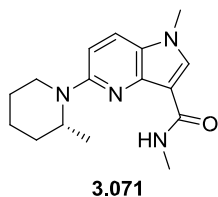
5-Chloro-*N*,1-dimethyl-1*H*-pyrrolo[3,2-*b*]pyridine-3-carboxamide **3.068** (30 mg, 0.134 mmol), NaO^tBu (39 mg, 0.402 mmol), Pd(OAc)₂ (3 mg, 0.013 mmol) and BINAP (17 mg, 0.027 mmol) were dissolved in 1,4-dioxane (900 μL) and stirred at rt for 10 min under N₂. Piperidine (27 μL, 0.268 mmol) was added and the reaction was heated to 100 °C

in an oil bath for 18 h. The reaction mixture was filtered through Celite, evaporated to dryness and purified by silica chromatography (10-60% (3:1 EtOAc:EtOH)/cyclohexane). The appropriate fractions were evaporated to dryness to afford *N*,1-dimethyl-5-(piperidin-1-yl)-1*H*-pyrrolo[3,2-*b*]pyridine-3-carboxamide (12 mg, 0.044 mmol, 33%).

LCMS (High pH, ES⁺): t_R = 1.05 min, [M+H]⁺ 273.3, (92% purity). ¹H NMR (400 MHz, CDCl₃): δ 1.63-1.81 (m, 6H), 3.03-3.11 (m, 3H), 3.51-3.61 (m, 4H), 3.78 (s, 3H), 6.72 (d, *J* = 9.0 Hz, 1H), 7.50 (d, *J* = 9.0 Hz, 1H), 7.78 (s, 1H), 8.71 (br. s., 1H). ¹³

C NMR (101 MHz, CDCl₃): δ 24.7, 25.6, 25.6, 33.5, 47.8, 104.3, 109.4, 119.9, 124.3, 133.5, 141.3, 156.8, 165.3. M.pt.: 188-191 °C. ν_{max} (neat): 3314, 3105, 2930, 2852, 2808, 1642, 1610, 1578, 1556, 1474, 1450, 1419, 1382, 1296, 1276, 1259, 1235, 1164, 1127, 1073, 1029, 943, 855, 798, 783, 757, 670 cm⁻¹.

HRMS: (C₁₅H₂₀N₄O) [M+H]⁺ requires 273.1710, found [M+H]⁺ 273.1723.

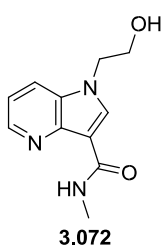
(R)-N,1-Dimethyl-5-(2-methylpiperidin-1-yl)-1H-pyrrolo[3,2-b]pyridine-3-carboxamide5-Chloro-*N*,1-dimethyl-1*H*-pyrrolo[3,2-*b*]pyridine-3-carboxamide

3.068 (30 mg, 0.134 mmol), NaO^tBu (39 mg, 0.402 mmol), Pd(OAc)₂ (3 mg,

0.013 mmol) and BINAP (17 mg, 0.027 mmol) were dissolved in 1,4-dioxane (900 μL) and stirred at rt for 10 min under N₂. (*R*)-2-Methylpiperidine (32 μL, 0.268 mmol) was added and the reaction was heated to 100 °C in an oil bath for 24 h. The reaction mixture was filtered through Celite, evaporated to dryness and purified by silica chromatography (0-80% (3:1 EtOAc:EtOH)/cyclohexane). The appropriate fractions were evaporated to dryness and further purified by High pH MDAP to afford (*R*)-*N*,1-dimethyl-5-(2-methylpiperidin-1-yl)-1*H*-pyrrolo[3,2-*b*]pyridine-3-carboxamide (6 mg, 0.021 mmol, 16%) as a white solid.

LCMS (High pH, ES⁺): t_R = 1.12 min, [M+H]⁺ 287.2, (88% purity). ¹H NMR (400 MHz, DMSO-*d*₆): δ 1.10 (d, *J* = 6.6 Hz, 3H), 1.43-1.82 (m, 5H), 2.89 (d, *J* = 4.6 Hz, 3H), 2.94 (td, *J* = 12.7, 2.9 Hz, 2H), 3.78 (s, 3H), 4.00-4.09 (m, 1H), 4.54-4.63 (m, 1H),

6.83 (d, *J* = 9.0 Hz, 1H), 7.77 (d, *J* = 9.0 Hz, 1H), 7.85 (s, 1H), 8.52-8.61 (m, 1H).

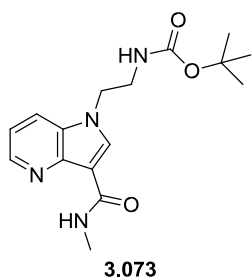
1-(2-Hydroxyethyl)-*N*-methyl-1H-pyrrolo[3,2-*b*]pyridine-3-carboxamide

A solution of *N*-methyl-1*H*-pyrrolo[3,2-*b*]pyridine-3-carboxamide **3.016** (27 mg, 0.154 mmol), potassium carbonate (64 mg, 0.462 mmol) and 1,3-dioxolan-2-one (41 mg, 0.462 mmol), in DMF (750 μL) was stirred at 110 °C for 1 h. The reaction mixture was diluted with water (10 mL) and extracted with EtOAc (4 x 15 mL) and DCM (3 x 10 mL). The combined organics were dried through a hydrophobic frit and evaporated to dryness. The crude

product was purified by silica chromatography (0-100% (3:1/EtOAc:EtOH)/cyclohexane), appropriate fractions were evaporated *in vacuo* to afford 1-(2-hydroxyethyl)-*N*-methyl-1*H*-pyrrolo[3,2-*b*]pyridine-3-carboxamide (30 mg, 0.137 mmol, 89%) as a white solid.

LCMS (High pH, ES⁺): t_R = 0.61 min, [M+H]⁺ 220.2, (100% purity). ¹H NMR (400 MHz, CDCl₃): δ 2.70 (d, *J* = 4.6 Hz, 3H), 4.02 (t, *J* = 5.1 Hz, 2H), 4.28 (t, *J* = 5.1 Hz, 2H), 4.55 (br. s, 1H), 7.17 (dd, *J* = 8.3, 4.7 Hz, 1H), 7.75 (dd, *J* = 8.3, 1.2 Hz, 1H),

8.04 (s, 1H), 8.45 (dd, *J* = 4.7, 1.2 Hz, 1H), 8.66 (q, *J* = 4.6 Hz, 1H).

***tert*-Butyl (2-(3-(methylcarbamoyl)-1H-pyrrolo[3,2-*b*]pyridin-1-yl)ethyl)carbamate**

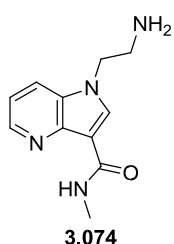
A solution of *N*-methyl-1*H*-pyrrolo[3,2-*b*]pyridine-3-carboxamide **3.016** (25 mg, 0.143 mmol), potassium carbonate (59 mg, 0.462 mmol) and *tert*-butyl (2-chloroethyl)carbamate (51 mg, 0.285 mmol), in DMF (714 μL) was stirred at 110 °C for 2 h. The reaction mixture was diluted with water (10 mL) and extracted with EtOAc (4 x 15 mL)

and DCM (3 x 10 mL). The combined organics were dried through a hydrophobic frit and evaporated to dryness. The crude product was purified by silica chromatography (0-45% (3:1/EtOAc:EtOH)/cyclohexane), appropriate fractions were evaporated *in vacuo* to afford *tert*-butyl (2-(3-(methylcarbamoyl)1*H*-pyrrolo[3,2-*b*]pyridin-1-yl)ethyl)carbamate (43 mg, 0.135 mmol, 95%) as a white solid.

LCMS (High pH, ES⁺): *t*_R = 0.88 min, [M+H]⁺ 319.2, (100% purity).

¹H NMR (400 MHz, DMSO-*d*₆): δ 1.26 (s, 9H), 2.91 (d, *J* = 4.6 Hz, 3H), 3.29-3.35 (m, 2H), 4.31 (t, *J* = 5.1 Hz, 2H), 6.90 (t, *J* = 5.3 Hz, 1H), 7.29 (dd, *J* = 8.3, 4.6 Hz, 1H), 8.02 (d, *J* = 8.3 Hz, 1H), 8.15 (s, 1H), 8.47 (dd, *J* = 4.6, 1.2 Hz, 1H), 8.58 (q, *J* = 4.6 Hz, 1H).

1-(2-Aminoethyl)-*N*-methyl-1*H*-pyrrolo[3,2-*b*]pyridine-3-carboxamide



To a solution of *tert*-butyl (2-(3-(methylcarbamoyl)1*H*-pyrrolo[3,2-*b*]pyridin-1-yl)ethyl)carbamate **3.073** (38 mg, 0.119 mmol) in DCM (600 μL) was added TFA (184 μL, 2.387 mmol) and the reaction was stirred at rt for 4 h. The reaction was purified by ion exchange chromatography (sulphonic acid (SCX) 1 g, sequential solvents MeOH, 2 M NH₃/MeOH). The appropriate fractions were combined and evaporated *in vacuo* to give 1-(2-aminoethyl)-*N*-methyl-1*H*-pyrrolo[3,2-*b*]pyridine-3-carboxamide (26 mg, 0.119 mmol, 100%) as an offwhite oil which solidified on standing.

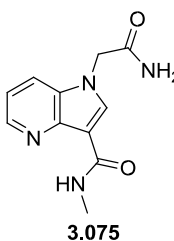
LCMS (High pH, ES⁺): *t*_R = 0.57 min, [M+H]⁺ 219.2, (100% pure). ¹H NMR (400 MHz, CDCl₃): δ 1.22 (br. s., 2H), 3.10 (d, *J* = 4.9 Hz, 3H), 3.17 (t, *J* = 5.9 Hz, 2H), 4.22 (t, *J* = 5.9 Hz, 2H), 7.21 (dd, *J* = 8.3, 4.6 Hz, 1H), 7.75 (d, *J* = 7.8 Hz, 1H), 8.11 (s, 1H), 8.51 (d, *J* = 3.9 Hz, 1H), 8.75 (br. s., 1H). ¹³C NMR (101 MHz, CDCl₃): δ 25.7, 41.9, 50.2, 110.9, 117.1, 117.8, 129.7, 134.9, 143.4, 143.6, 164.7.

M.pt.: 77-79 °C.

*v*_{max} (neat): 3451, 3347, 3309, 1627, 1563, 1432, 1406, 1338, 1270, 1171, 1025, 940, 893, 859, 782 cm⁻¹.

HRMS: (C₁₁H₁₄N₄O) [M+H]⁺ requires 219.1240, found [M+H]⁺ 219.1244.

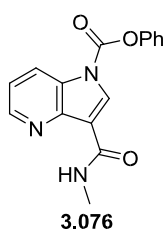
1-(2-Amino-2-oxoethyl)-*N*-methyl-1*H*-pyrrolo[3,2-*b*]pyridine-3-carboxamide A



solution of *N*-methyl-1*H*-pyrrolo[3,2-*b*]pyridine-3-carboxamide **3.016** (22 mg, 0.126 mmol), potassium carbonate (52 mg, 0.377 mmol) and 2-iodoacetamide (47 mg, 0.251 mmol), in DMF (630 μL) was stirred at 80 °C for 2 h. The reaction mixture was filtered and purified by High pH MDAP to afford 1-(2-amino-2-oxoethyl)-*N*-methyl-1*H*-pyrrolo[3,2-*b*]pyridine-3-carboxamide (11 mg, 0.047 mmol, 38%) as a white solid.

LCMS (High pH, ES⁺): *t*_R = 0.54 min, [M+H]⁺ 233.2, (100% purity). ¹H NMR (400 MHz, DMSO-*d*₆): δ 2.93 (d, *J* = 4.7 Hz, 3H), 4.94 (s, 2H), 7.25-7.33 (m, 2H), 7.67 (br. s., 1H), 7.92 (dd, *J* = 8.3, 1.2 Hz, 1H), 8.17 (s, 1H), 8.49 (dd, *J* = 4.6, 1.2 Hz, 1H), 8.60 (q, *J* = 4.7 Hz, 1H).

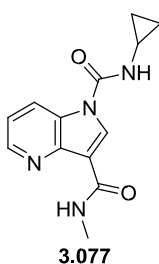
3-(Methylcarbamoyl)-1*H*-pyrrolo[3,2-*b*]pyridine-1-carboxylate



To a solution of *N*-methyl-1*H*-pyrrolo[3,2-*b*]pyridine-3-carboxamide **3.016** (45 mg, 0.257 mmol) and triethylamine (72 μ L, 0.514 mmol) in THF (1.25 mL) at 0 °C was added phenyl chloroformate (40 μ L, 0.321 mmol), and the reaction was allowed to warm to rt and stirred for 2 h. The reaction mixture was diluted with water (10 mL) and extracted with EtOAc (3 x 15 mL). The combined organics were dried through a hydrophobic frit and evaporated to dryness to afford phenyl 3-(methylcarbamoyl)-1*H*-pyrrolo[3,2-*b*]pyridine-1-carboxylate (82 mg, 0.250 mmol, 97%) as a white solid. The product was 90% pure by NMR and was used for further chemistry without additional purification.

LCMS (High pH, ES⁺): t_R = 1.05 min, [M+H]⁺ 296.1, (100% purity). ¹H NMR (400 MHz, CDCl₃): δ 3.14 (d, J = 4.9 Hz, 3H), 7.29-7.56 (m, 6H), 8.56 (d, J = 8.3 Hz, 1H), 8.62 (dd, J = 4.9, 1.5 Hz, 1H), 8.74 (s, 1H), 8.90-9.00 (m, 1H).

*N*1-Cyclopropyl-*N*3-methyl-1*H*-pyrrolo[3,2-*b*]pyridine-1,3-dicarboxamide

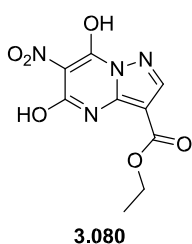


To a solution of phenyl 3-(methylcarbamoyl)-1*H*-pyrrolo[3,2-*b*]pyridine-1-carboxylate **3.076** (25 mg, 0.076 mmol) and triethylamine (32 μ L, 0.229 mmol) in DMSO (380 μ L) at rt was added cyclopropylamine (11 μ L, 0.152 mmol). The reaction was stirred at rt for 18 h, then purified by silica chromatography (0-50% (3:1 EtOAc:EtOH)/cyclohexane). Appropriate fractions were evaporated *in vacuo* and further purified by High pH MDAP.

The solvent was evaporated *in vacuo* to give *N*1-cyclopropyl-*N*3-methyl-1*H*-pyrrolo[3,2-*b*]pyridine-1,3-dicarboxamide (3 mg, 0.012 mmol, 15%) as a white solid.

LCMS (High pH, ES⁺): t_R = 0.80 min, [M+H]⁺ 259.1, (100% purity). ¹H NMR (400 MHz, DMSO-*d*₆): δ 0.64-0.78 (m, 4H), 2.78-2.86 (m, 1H), 2.94 (d, J = 4.8 Hz, 3H), 7.43 (dd, J = 8.4, 4.8 Hz, 1H), 8.57-8.63 (m, 2H), 8.64 (q, J = 2.7 Hz, 1H), 8.74 (s, 1H), 8.76 (q, J = 4.7 Hz, 1H).

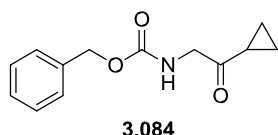
Ethyl 5,7-dihydroxy-6-nitropyrzolo[1,5-*a*]pyrimidine-3-carboxylate



Sodium (0.296 g, 12.89 mmol) was added to anhydrous ethanol (18.96 ml) with stirring at 0 °C until all the metal had reacted. To the resulting solution was added ethyl 5-amino-1*H*-pyrazole-4-carboxylate **3.079** (1 g, 6.45 mmol) followed by diethyl 2-nitromalonate **3.078** (1.24 mL, 7.09 mmol). The reaction mixture was then heated to 90 °C for 7 days. The reaction mixture was filtered and the residue was washed with EtOH and

dissolved in water. Addition of conc. HCl failed to precipitate product, and the product could not be extracted from the aqueous with EtOAc or 10% DCM/MeOH at pH 1-5. The aqueous was evaporated to dryness and the residue suspended in MeOH, filtered and the filtrate evaporated *in vacuo* to afford ethyl 5,7-dihydroxy-6-nitropyrazolo[1,5-*a*]pyrimidine-3-carboxylate (1.67 g, 6.23 mmol, 97%) as a yellow solid. This contained an indeterminate amount of residual salts and was taken forward to further chemistry without purification. LCMS (Formic, ES⁺): $t_R = 0.78$ min, [M⁺] 268.9, (100% pure)

Benzyl (2-cyclopropyl-2-oxoethyl)carbamate



To a solution of benzyl (2-(methoxy(methyl)amino)-2-oxoethyl)carbamate **3.083** (1 g, 3.96 mmol) in THF (13 ml) stirred under N₂ at -5 °C was added cyclopropylmagnesium bromide (0.5 M in THF, 20 mL, 9.91 mmol) dropwise. The reaction mixture was stirred at 0 °C for 1.5 h. The reaction was warmed to rt and stirred for 2 h. Incomplete conversion, so further cyclopropylmagnesium bromide (0.5 M in THF, 20 mL, 9.91 mmol) was added and the reaction was stirred at rt for 18 h. The reaction mixture was quenched with saturated ammonium chloride (3 mL), and concentrated *in vacuo*. The resulting suspension was filtered and washed with DCM, and the filtrate was diluted with water (10 mL). The aqueous layer was extracted with DCM (3 x 20 mL) and the combined organics were dried through a hydrophobic frit and evaporated to dryness. The residue was purified by silica chromatography (0-50% EtOAc/cyclohexane) appropriate fractions were evaporated *in vacuo* to afford benzyl (2-cyclopropyl-2-oxoethyl)carbamate (650 mg, 2.79 mmol, 70%) as a white solid.

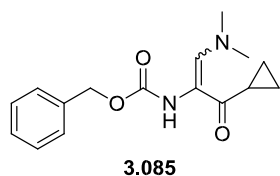
LCMS (Formic, ES⁺): $t_R = 0.93$ min, [M+H⁺] 234.1, (100% purity). ¹H NMR (400 MHz, CDCl₃): δ 0.94-1.03 (m, 2H), 1.11-1.16 (m, 2H), 1.87-1.97 (m, 1H), 4.27 (d, $J = 4.6$ Hz, 2H), 5.12 (s, 2H), 5.52 (br. s., 1H), 7.28-7.39 (m, 5H).

¹³

C NMR (101 MHz, CDCl₃) \square 11.4, 18.6, 51.0, 66.9, 128.1, 128.1, 128.5, 136.4, 156.1, 205.0.
M.pt.: 54 °C ν_{max} (neat): 3336, 1712, 1685, 1533, 1416, 1393, 1284, 1257, 1157, 1077, 1039, 975, 750, 722, 670 cm⁻¹

HRMS: (C₁₃H₁₅NO₃) [M+Na]⁺ requires 256.0950, found [M+Na]⁺ 256.09.

Benzyl (3-cyclopropyl-1-(dimethylamino)-3-oxoprop-1-en-2-yl)carbamate



A solution of benzyl (2-cyclopropyl-2-oxoethyl)carbamate **3.084** (540 mg, 2.315 mmol) in DMF-DMA (4.6 mL, 34.7 mmol) was stirred at 85 °C for 18 h. The reaction mixture was evaporated to dryness and purified by silica chromatography (0-100% (3:1 EtOAc/EtOH)/cyclohexane), appropriate fractions were evaporated *in vacuo* to afford benzyl

(3-cyclopropyl-1-(dimethylamino)-3-oxoprop-1-en-2-yl)carbamate (516 mg, 1.790 mmol, 77%) as a white solid.

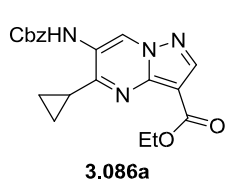
LCMS (Formic, ES⁺): t_R = 0.91 min, [M+H]⁺ 289.1, (87% purity).

¹H NMR (400 MHz, CDCl₃): δ 0.62-0.82 (m, 2H), 0.90-1.09 (m, 2H), 2.00-2.16 (m, 1H), 3.07 (s, 6H), 5.17 (s, 2H), 5.62-6.04 (m, 1H), 7.29-7.50 (m, 5H). ~3.5:1 mixture of alkene isomers, major isomer not determined, NH not observed.

Ethyl 6-(((benzyloxy)carbonyl)amino)-5-cyclopropylpyrazolo[1,5-a]pyrimidine-3-carboxylate and ethyl 6-(((benzyloxy)carbonyl)amino)-7-cyclopropylpyrazolo[1,5-a]pyrimidine-3-carboxylate

A solution of benzyl (3-cyclopropyl-1-(dimethylamino)-3-oxoprop-1-en-2-yl)carbamate **3.085** (399 mg, 1.382 mmol) and ethyl 5-amino-1*H*-pyrazole-4-carboxylate **3.079** (165 mg, 1.063 mmol) in AcOH (10.6 mL) was sealed in a microwave vial and heated to 140 °C in a Biotage Initiator microwave reactor for 30 min. The reaction mixture was evaporated to dryness and purified by silica chromatography (20-70% EtOAc/cyclohexane). The appropriate fractions were evaporated to afford the products. Structures were assigned by ¹⁵N HMBC.³⁸⁵

Ethyl 6-(((benzyloxy)carbonyl)amino)-5-cyclopropylpyrazolo[1,5-a]pyrimidine-3-carboxylate



23 mg, 0.060 mmol, 5.7%, yellow solid.

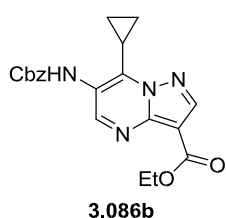
LCMS (Formic, ES⁺): t_R=1.07 min, [M+H]⁺ 381.1, (98% purity). ¹

¹H NMR (400 MHz, CDCl₃): δ 1.13-1.19 (m, 2H), 1.36-1.40 (m, 2H), 1.42 (t, *J* = 7.2 Hz, 3H), 2.04-2.12 (m, 1H), 4.38 (q, *J* = 7.2 Hz, 2H),

5.27 (s, 2H), 7.02 (br. s., 1H), 7.33-7.46 (m, 5H), 8.47 (s, 1H), 9.30 (br. s., 1H). ¹³C NMR (151 MHz, CDCl₃): δ 10.1, 13.4, 14.4, 60.0, 68.1, 101.9, 122.3, 126.8, 127.9-129.0 (m, 5C), 135.3, 144.6, 147.6, 153.5, 159.1, 162.7. M.pt.: 143-145 °C *v*_{max} (neat): 3285, 3038, 2982, 1693, 1543, 1498, 1429, 1382, 1288, 1251, 1202, 1178, 1065, 888, 866, 778, 745, 698, 671 cm⁻¹.

HRMS: (C₂₀H₂₀N₄O₄) [M+H]⁺ requires 381.1557, found [M+H]⁺ 381.1556.

Ethyl 6-(((benzyloxy)carbonyl)amino)-7-cyclopropylpyrazolo[1,5-a]pyrimidine-3-carboxylate



365 mg, 0.960 mmol, 90%, yellow solid

LCMS (Formic, ES⁺): t_R=1.14 min, [M+H]⁺ 381.1, (95% purity). ¹

¹H NMR (400 MHz, CDCl₃): δ 1.08-1.17 (m, 2H), 1.31 (t, *J* = 7.2 Hz, 3H), 1.47-1.61 (m, 2H), 2.22-2.29 (m, 1H), 4.31 (q, *J* = 7.2 Hz, 2H),

5.16 (s, 2H), 7.23-7.37 (m, 5H), 7.61 (s, 1H), 8.42 (s, 1H), 8.66 (br. s., 1H).

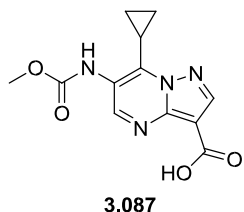
¹³C NMR (151 MHz, CDCl₃): δ 7.5, 9.8, 14.5, 60.2, 67.7, 102.4, 121.3, 128.3, 128.4, 128.5, 135.7, 145.7, 146.6, 147.0, 151.5, 154.9, 162.5.

M.pt.: 119-122 °C

ν_{\max} (neat): 3286, 2981, 1720, 1698, 1682, 1560, 1536, 1501, 1369, 1271, 1213, 1196, 1163, 1132, 1061, 936, 783, 758, 734, 696 cm^{-1} .

HRMS: ($\text{C}_{20}\text{H}_{20}\text{N}_4\text{O}_4$) $[\text{M}+\text{H}]^+$ requires 381.1557, found $[\text{M}+\text{H}]^+$ 381.1556.

6-(((Methoxy)carbonyl)amino)-7-cyclopropylpyrazolo[1,5-a]pyrimidine-3-carboxylic acid

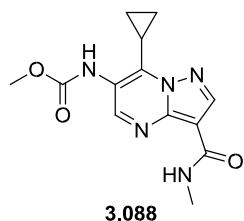


To a solution of ethyl 6-(((benzyloxy)carbonyl)amino)-7-cyclopropylpyrazolo[1,5-a]pyrimidine-3-carboxylate **3.086b** (325 mg, 0.854 mmol) in MeOH (8.5 mL) was added 4M KOH (640 μL , 2.56 mmol), and the reaction was stirred at rt for 1 h. The reaction mixture was heated to 80 °C for 1 h. The reaction was cooled to rt, further 4M KOH (641 μL , 2.56 mmol) was added and the reaction was stirred for 7 days at rt. The reaction mixture was concentrated *in vacuo* and partitioned between EtOAc and water. The aqueous layer was extracted with EtOAc (2 x 20 mL), the organics were discarded. The aqueous layer was adjusted to pH 1 and extracted with EtOAc (5 x 20 mL). The combined organics were washed with brine, dried through a hydrophobic frit and evaporated to dryness to afford 7-cyclopropyl-6-(((methoxycarbonyl)amino)pyrazolo[1,5-a]pyrimidine-3-carboxylic acid (196 mg, 0.710 mmol, 83%) as a light yellow solid. Used for without purification.

LCMS (Formic, ES^+): $t_{\text{R}}=0.58$ min, $[\text{M}+\text{H}]^+$ 277.2, (96% purity). ¹

$^1\text{H NMR}$ (400 MHz, DMSO-d_6): δ 1.14-1.24 (m, 2H), 1.60-1.68 (m, 2H), 2.36-2.47 (m, 1H), 3.70 (s, 3H), 8.56 (s, 1H), 8.60 (s, 1H), 9.47 (br. s, 1H), 12.32 (br. s, 1H).

Methyl (7-cyclopropyl-3-(methylcarbamoyl)pyrazolo[1,5-a]pyrimidin-6-yl)carbamate



To a suspension of 7-cyclopropyl-6-(((methoxycarbonyl)amino)pyrazolo[1,5-a]pyrimidine-3-carboxylic acid **3.087** (195 mg, 0.706 mmol) and oxalyl chloride (74 μL , 0.847 mmol) in DCM (4 mL) at rt was added DMF (4 μL , 0.056 mmol). The reaction mixture was stirred at rt for 3 h, until the suspension became a clear yellow solution. The reaction mixture was evaporated *in vacuo* and the residue was redissolved in 2-MeTHF (4 mL). MeNH_2 (2M in THF, 529 μL , 1.059 mmol) was added and the reaction was stirred at rt for 1 h. The reaction mixture was diluted with EtOAc (10 mL) and sat. aq. NaHCO_3 (5 mL), separated and the aqueous layer was extracted with EtOAc (3 x 10 mL). The combined organic layers were dried through a hydrophobic frit and evaporated. The crude product was purified by silica chromatography (0-25% EtOH/EtOAc), appropriate fractions were evaporated and further purified by High pH MDAP. The solvent was evaporated *in vacuo* to give methyl (7-cyclopropyl-3-

(methylcarbamoyl)pyrazolo[1,5-*a*]pyrimidin-6-yl)carbamate (68 mg, 0.235 mmol, 33%) as an off-white solid.

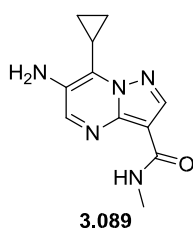
LCMS (High pH, ES⁺): t_R=0.64 min, [M+H]⁺ 290.0, (100% pure).

¹H NMR (400 MHz, CDCl₃): δ 1.24-1.33 (m, 2H), 1.63-1.79 (m, 2H), 2.26-2.38 (m, 1H), 3.04 (d, *J* = 4.8 Hz, 3H), 3.84 (s, 3H), 7.24 (br. s., 1H), 7.88 (q, *J* = 4.8 Hz, 1H), 8.55 (s, 1H), 8.65 (br. s., 1H). ¹³C NMR (101 MHz, CDCl₃): δ 7.6, 9.6, 25.9, 53.2, 105.4, 120.6, 144.6, 145.4, 146.0, 149.7, 155.4, 162.9.

M.pt.: 199-201 °C. ν_{max} (neat): 3363, 3287, 2950, 1702, 1662, 1635, 1540, 1396, 1243, 1162, 1075, 939, 884, 806, 777, 697, 664 cm⁻¹.

HRMS: (C₁₃H₁₅N₅O₃) [M+H]⁺ requires 290.1248, found [M+H]⁺ 290.1248.

6-Amino-7-cyclopropyl-*N*-methylpyrazolo[1,5-*a*]pyrimidine-3-carboxamide



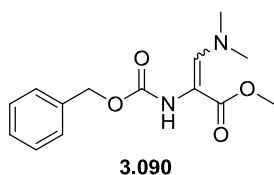
To a solution of methyl (7-cyclopropyl-3-(methylcarbamoyl)pyrazolo[1,5*a*]pyrimidin-6-yl)carbamate **3.088** (58 mg, 0.200 mmol) in MeOH (4 mL) in a sealed tube was added 1 M NaOH (1.2 mL, 1.203 mmol), and the reaction was stirred at 80 °C for 18 h. The reaction mixture was concentrated *in vacuo*, redissolved in MeOH and water, acidified with

1.25 M HCl in MeOH, and purified by ion exchange chromatography (sulphonic acid (SCX) 2 g, sequential solvents MeOH, 2 M NH₃/MeOH) and High pH MDAP. The solvent was evaporated *in vacuo* to give 6-amino-7-cyclopropyl-*N*-methylpyrazolo[1,5*a*]pyrimidine-3-carboxamide (2 mg, 8.65 μmol, 4.3%) as an off-white gum.

LCMS (High pH, ES⁺): t_R=0.57 min, [M+H]⁺ 232.4 (100% purity). ¹

¹H NMR (400 MHz, MeOD-*d*₄): δ 1.15-1.24 (m, 2H), 1.25-1.34 (m, 2H), 2.03-2.12 (m, 1H), 3.00 (s, 3H), 8.36 (s, 1H), 8.45 (s, 1H), 8.57 (s, 1H). NH₂ not observed, amide partially exchanged.

Methyl 2-(((benzyloxy)carbonyl)amino)-3-(dimethylamino)acrylate

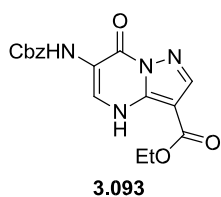


A solution of methyl 2-(((benzyloxy)carbonyl)amino)acetate **3.090** (545 mg, 2.441 mmol) and 1-*tert*-butoxy-*N,N,N',N'*-tetramethylmethanediamine **3.091** (529 μL, 2.56 mmol) in toluene (2 mL) was stirred at 110 °C for 4 h. Further 1-*tert*-

tert-butoxy-*N,N,N',N'*-tetramethylmethanediamine (150 μL) was added and the reaction was stirred at 110 °C for 2 h. The reaction mixture was evaporated to dryness and purified by silica chromatography (0-60% (3:1 EtOAc/EtOH)/cyclohexane) appropriate fractions were evaporated *in vacuo* to afford methyl 2-(((benzyloxy)carbonyl)amino)-3-(dimethylamino)acrylate (620 mg, 2.228 mmol, 91%) as a thick yellow oil. Data consistent with literature.³⁶³

LCMS (Formic, ES⁺): t_R=0.85 min, [M+H]⁺ 279.0, (52% purity). ¹H NMR (400 MHz, CDCl₃): δ 2.95-3.08 (m, 6H), 3.60-3.72 (m, 3H), 5.18 (s, 2H), 5.54 (br. s., 1H), 7.30-7.44 (m, 6H). ~4:1 mixture of alkene isomers, major isomer not determined.

Ethyl 6-(((benzyloxy)carbonyl)amino)-7-oxo-4,7-dihydropyrazolo[1,5-a]pyrimidine-3-carboxylate



A solution of methyl 2-(((benzyloxy)carbonyl)amino)-3-(dimethylamino)acrylate **3.092** (233 mg, 0.838 mmol) and ethyl 5-amino-1*H*-pyrazole-4-carboxylate (100 mg, 0.645 mmol) in acetic acid (4 mL) was sealed in a microwave vial and heated to 140 °C in a Biotage Initiator microwave reactor for 30 min. The reaction mixture

was evaporated to dryness and purified by silica chromatography (0-100% (3:1 EtOAc:EtOH)/cyclohexane). The appropriate fractions were evaporated to afford ethyl 6-(((benzyloxy)carbonyl)amino)-7-oxo-4,7-dihydropyrazolo[1,5-a]pyrimidine-3-carboxylate (156 mg, 0.438 mmol, 68%).

LCMS (Formic, ES⁺): t_R=0.91 min, [M+H]⁺ 357.0, (97% purity). ¹H NMR (400 MHz, CDCl₃): δ 1.41 (t, *J* = 7.1 Hz, 3H), 4.40 (q, *J* = 7.3 Hz, 2H), 5.25 (s, 2H),

7.34-7.44 (m, 5H), 7.47 (s, 1H), 8.23 (s, 1H), 8.76 (s, 1H), 9.95 (br. s., 1H) ¹³

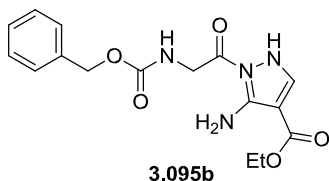
C NMR (151 MHz, CDCl₃): δ 14.4, 60.9, 67.6, 96.5, 114.6, 123.7, 128.1, 128.5, 128.6, 135.5, 142.4, 144.2, 152.8, 153.5, 163.3. M.pt.: 221-222 °C. ν_{max} (neat): 3294, 3063, 1694, 1661, 1612, 1535, 1510, 1446, 1361, 1291, 1220, 1174, 1116, 1080, 1028, 997, 953, 852, 771, 746, 699, 617, 579, 553 cm⁻¹.

HRMS: (C₁₇H₁₆N₄O₅) [M+H]⁺ requires 357.1194, found [M+H]⁺ 357.1193.

Ethyl 5-amino-1-(2-(((benzyloxy)carbonyl)amino)acetyl)-1*H*-pyrazole-4-carboxylate and ethyl 3-amino-1-(2-(((benzyloxy)carbonyl)amino)acetyl)-1*H*-pyrazole-4-carboxylate To a solution of Cbz-Glycine (148 mg, 0.709 mmol) in DMF (4 mL) was added HATU (270 mg, 0.709 mmol), and the reaction was stirred at rt for 5 min. Ethyl 5-amino-1*H*-pyrazole-4-carboxylate **3.079** (100 mg, 0.645 mmol) and DIPEA (0.281 mL, 1.611 mmol) were added and the reaction was stirred at rt for 6 h. The reaction mixture was partitioned between water (50 mL) and EtOAc (25 mL) and the aqueous layer was extracted with EtOAc (2 x 25 mL). The combined organics were dried through a hydrophobic frit and evaporated to dryness. The crude product was purified by silica chromatography (0-100% (3:1 EtOAc/EtOH)/cyclohexane) and fractions evaporated *in vacuo* to afford the products:

Ethyl 5-amino-1-(2-(((benzyloxy)carbonyl)amino)acetyl)-1*H*-pyrazole-4-carboxylate

30 mg, 0.087 mmol, 13%



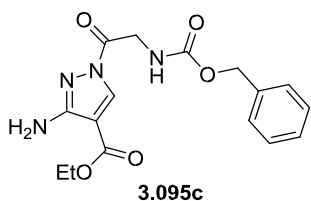
LCMS (High pH, ES⁺): t_R=1.06 min, [M]⁺ 347.3 (89% purity). ¹H NMR (600MHz, CDCl₃): δ 1.35 (t, *J* = 7.2 Hz, 3H), 4.29 (q, *J* = 7.2 Hz, 2H), 4.69 (br d, *J* = 5.5 Hz, 2H), 5.17 (s, 2H), 5.44

(br s, 1H), 6.98 (br s, 2H), 7.31-7.40 (m, 2H), 7.32-7.38 (m, 2H), 7.34-7.38 (m, 1H), 7.70 (s, 1H).

¹³

C NMR (CDCl₃, 151MHz): δ 14.4, 44.5, 60.0, 67.3, 94.8, 128.1, 128.2, 128.5, 136.1, 144.1, 153.3, 156.4, 163.7, 171.9.

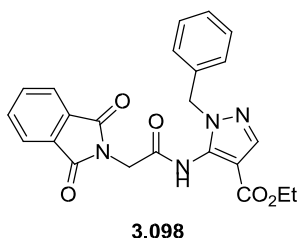
Ethyl 3-amino-1-(2-(((benzyloxy)carbonyl)amino)acetyl)-1H-pyrazole-4-carboxylate



100 mg, 0.289 mmol, 45%.

LCMS (High pH, ES⁺): t_R=1.01 min, [M⁺] 347.2 (56% purity). ¹H NMR (600 MHz, CDCl₃) δ 1.36 (t, J = 7.1 Hz, 3H), 4.30 (q, J = 7.1 Hz, 2H), 4.70 (d, J = 5.5 Hz, 2H), 5.15-5.19 (m, 2H), 5.51 (br. s., 1H), 6.99 (br. s., 2H), 7.31-7.41 (m, 5H), 7.71 (s, 1H).

Ethyl 1-benzyl-5-(2-(1,3-dioxisoindolin-2-yl)acetamido)-1H-pyrazole-4-carboxylate



To a solution of ethyl 5-amino-1-benzyl-1H-pyrazole-4-carboxylate **3.096** (100 mg, 0.408 mmol) and pyridine (49 μL, 0.612 mmol) in CHCl₃ (4 mL) was added 2-(1,3-dioxisoindolin-2-yl)acetyl chloride **3.097** (365 mg, 1.631 mmol), and the reaction was stirred at rt for 1 h. The reaction mixture was diluted with DCM (10 mL) and washed with sat. aq. NaHCO₃. (10 mL). The aqueous layer

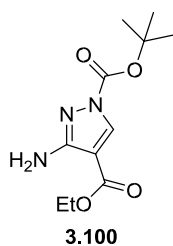
was extracted with DCM (10 mL) and the combined organics were dried through a hydrophobic frit and evaporated to dryness. The crude product was purified by silica chromatography (0-100% EtOAc/cyclohexane), fractions were evaporated to afford ethyl 1-benzyl-5-(2-(1,3-dioxisoindolin-2-yl)acetamido)-1H-pyrazole-4-carboxylate (92 mg, 0.213 mmol, 52%) as a white solid.

LCMS (High pH, ES⁺): t_R = 1.03 min, [M+H]⁺ 433.3, (97% purity). ¹H NMR (400 MHz, DMSO-d₆): δ 1.29 (t, J = 7.1 Hz, 3H), 4.20 (q, J = 7.1 Hz, 2H), 4.48 (s, 2H), 5.17 (s, 2H), 7.21-7.38 (m, 5H), 7.84-8.00 (m, 5H), 10.59 (s, 1H). ¹³C NMR (101 MHz, DMSO-d₆): δ 14.6, 40.8, 52.3, 60.1, 108.5, 123.8, 128.3, 128.5, 129.0, 132.2, 135.2, 136.5, 137.7, 140.8, 162.0, 167.0, 167.8. M.pt.: 243-245 °C.

ν_{max} (neat): 3203, 3567, 1776, 1708, 1726, 1687, 1554, 1481, 1417, 1395, 1320, 1281, 1262, 1194, 1173, 1415, 1100, 1078, 1027, 949, 772, 755, 713, 696, 607, 560, 530 cm⁻¹.

HRMS: (C₂₃H₂₀N₄O₅) [M+H]⁺ requires 433.1507, found [M+H]⁺ 433.1507.

1-tert-Butyl 4-ethyl 3-amino-1H-pyrazole-1,4-dicarboxylate



To a solution of ethyl 5-amino-1*H*-pyrazole-4-carboxylate **3.079** (1.0 g, 6.45 mmol) and pyridine (0.782 mL, 9.67 mmol) in DCM (43 mL) was added Boc₂O (1.477 g, 6.77 mmol), and the reaction was stirred at rt for 18 h. The reaction mixture was partitioned between sat. aq. NaHCO₃ (20 mL) and DCM (20 mL) and the aqueous layer was extracted with DCM (2 x 20 mL).

The combined organics were dried through a hydrophobic frit and evaporated to dryness. The crude product was purified by silica chromatography (0-60% 3:1 EtOAc/EtOH in cyclohexane) to afford 1-*tert*-butyl 4-ethyl 3-amino-1*H*-pyrazole-1,4-dicarboxylate (1.25 g, 4.90 mmol, 76%).

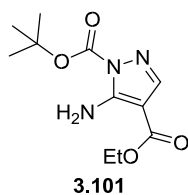
LCMS (High pH, ES⁺): t_R = 0.98 min, [M+H]⁺ 256.2, (51% purity) ¹H NMR (400 MHz, CDCl₃): δ 1.38 (t, *J* = 7.1 Hz, 3H), 1.65 (s, 9H), 4.33 (q, *J* = 7.1 Hz, 2H),

4.96 (br. s., 2H), 8.31 (s, 1H). 94% pure by NMR. ¹³

C NMR (101 MHz, CDCl₃): δ 14.3, 27.9, 60.5, 85.7, 104.5, 134.5, 142.8, 156.9, 163.5. M.pt.: 136-137 °C. ν_{max} (neat): 3480, 3275, 2982, 1732, 1699, 1625, 1578, 1518, 1438, 1411, 1393, 1369, 1293, 1245, 1145, 1092, 1021, 965, 850, 778, 763 cm⁻¹.

HRMS: (C₁₁H₁₇N₃O₄) [M+H]⁺ requires 256.1292, found [M+H]⁺ 256.1291.

1-*tert*-Butyl 4-ethyl 5-amino-1*H*-pyrazole-1,4-dicarboxylate



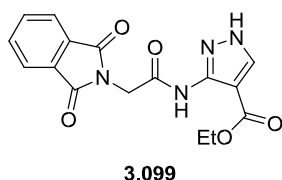
To a solution of ethyl 5-amino-1*H*-pyrazole-4-carboxylate (100 mg, 0.645 mmol) and pyridine (0.078 mL, 0.967 mmol) in DCM (5 mL) was added Boc₂O (148 mg, 0.677 mmol), and the reaction was stirred at rt for 7 h. The reaction mixture was partitioned between sat. aq. NaHCO₃ (20 mL) and DCM (20 mL) and the aqueous layer was extracted with DCM (2 x 20

mL). The combined organics were dried through a hydrophobic frit and evaporated to dryness. The crude product was purified by silica chromatography (0-60% (3:1 EtOAc:EtOH)/cyclohexane), fractions were evaporated *in vacuo* to afford 1-*tert*-butyl 4-ethyl 5-amino-1*H*-pyrazole-1,4-dicarboxylate (32 mg, 0.125 mmol, 19%).

LCMS (Formic, ES⁺): t_R = 1.00 min, [(M-^tBu)+H]⁺ 200.0, (100% purity) ¹H NMR (400 MHz, CDCl₃): δ 1.37 (t, *J* = 7.1 Hz, 3H), 1.68 (s, 9H), 4.30 (q, *J* = 7.1 Hz, 2H),

6.86 (br. s, 2H), 7.72 (s, 1H).

Ethyl 3-(2-(1,3-dioxisoindolin-2-yl)acetamido)-1*H*-pyrazole-4-carboxylate



One-pot amidation/deprotection from 3.100

To a solution of 1-*tert*-butyl 4-ethyl 3-amino-1*H*-pyrazole-1,4-dicarboxylate **3.100** (725 mg, 2.84 mmol) and pyridine (229 μL, 2.84 mmol) in DCM (28 mL) was added 2-(1,3-dioxisoindolin-2-yl)acetyl chloride **3.097** (1.27 g, 5.68 mmol), and the reaction was stirred at rt for 18 h. TFA (3.28 mL, 42.6 mmol) was added and the reaction was stirred at rt for 4 h. The reaction mixture was neutralised with sat. aq. NaHCO₃ solution (28 mL) and the

aqueous layer was extracted with DCM (2 x 40 mL). The combined organics were dried through a hydrophobic frit and evaporated to dryness. Purification by silica chromatography (0-4% DCM/MeOH) and evaporation of the appropriate fractions afforded ethyl 3-(2-(1,3-dioxoisindolin-2-yl)acetamido)-1*H*-pyrazole-4-carboxylate (655 mg, 1.913 mmol, 67%) as a white solid.

One-pot protection/amidation/deprotection from 3.079

To a solution of ethyl 3-amino-1*H*-pyrazole-4-carboxylate **3.079** (4.00 g, 25.8 mmol) and pyridine (2.08 mL, 25.8 mmol) in DCM (129 mL) was added di-*tert*-butyl dicarbonate (6.19 g, 28.4 mmol), and the reaction was stirred at rt for 18 h. 2-(1,3-Dioxoisindolin-2-yl)acetyl chloride **3.097** (6.92 g, 30.9 mmol) was added and the reaction was stirred at rt for 4 h. TFA (20 mL, 258 mmol) was added and the reaction was stirred at rt for 2 h. The reaction mixture was neutralised by dropwise addition of sat. aq. NaHCO₃ solution (170 mL) and stirred for 15 min once the addition was complete. The mixture was filtered and the collected solid was washed with DCM (30 mL) and sat. aq. NaHCO₃ (30 mL), and dried under vacuum to afford ethyl 3-(2-(1,3-dioxoisindolin-2-yl)acetamido)-1*H*-pyrazole-4-carboxylate (4.33 g, 12.65 mmol, 49%) as a white solid.

The filtrate was separated and the aqueous layer was extracted with DCM (3 x 50 mL). The combined organics were dried through a hydrophobic frit and evaporated to dryness. The residue was triturated with DCM (50 mL), filtered and the solid was washed with DCM (20 mL) and dried under vacuum to afford further ethyl 3-(2-(1,3-dioxoisindolin-2-yl)acetamido)-1*H*-pyrazole-4-carboxylate (1.7 g, 4.97 mmol, 19%) as a white solid.

LCMS (High pH, ES⁺): t_R = 0.83 min, [M+H]⁺ 343.2, (97% purity). ¹H NMR (400 MHz, CDCl₃): δ 1.35 (t, *J* = 7.1 Hz, 3H), 4.32 (q, *J* = 7.1 Hz, 2H), 4.62 (s, 2H),

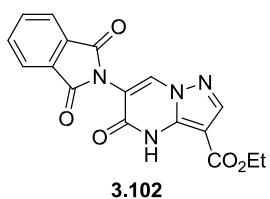
7.72-7.84 (m, 3H), 7.88-7.98 (m, 2H), 9.93 (br. s., 1H), 11.11-12.01 (m, 1H). ¹³C

NMR (101 MHz, CDCl₃): δ 14.3, 40.7, 60.6, 98.7, 123.9, 131.9, 134.5, 139.1, 142.2, 164.4, 165.4, 167.4. M.pt.: 227-230 °C.

v_{max} (neat): 3313, 1777, 1719, 1678, 1590, 1529, 1490, 1416, 1395, 1376, 1266, 1173, 1108, 1071, 1019, 956, 936, 889, 781, 752, 712, 681 cm⁻¹.

HRMS: (C₁₆H₁₄N₄O₅) [M+H]⁺ requires 343.1037 found [M+H]⁺ 343.1041.

Ethyl 6-(1,3-dioxoisindolin-2-yl)-5-oxo-4,5-dihydropyrazolo[1,5-*a*]pyrimidine-3carboxylate



To a suspension of ethyl 3-(2-(1,3-dioxoisindolin-2-yl)acetamido)-1*H*-pyrazole-4-carboxylate **3.099** (1.66 g, 4.85 mmol) in toluene

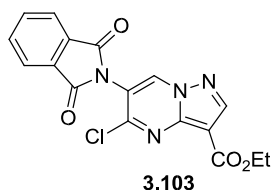
(13 mL) was added 1-*tert*-butoxy-*N,N,N,N*-tetramethylmethanedi-amine **3.091** (2.0 mL, 9.70 mmol), and the

reaction was stirred at 110 °C for 3 h. A deep red solution

developed. The reaction mixture was evaporated to dryness, suspended in acetic acid (6.5 ml) and heated to 110 °C for 30 min. The reaction mixture was evaporated *in vacuo*. The resulting gum was triturated with ether and filtered to afford ethyl 6-(1,3-dioxoisindolin-2-yl)5-oxo-4,5-dihydropyrazolo[1,5-a]pyrimidine-3-carboxylate (1.85 g, 4.46 mmol, 92%) as an off-white solid. This was taken forward to further chemistry without purification.

LCMS (High pH, ES⁺): t_R = 0.61 min, [M+H]⁺ 353.0, (85% purity). ¹H NMR (400 MHz, DMSO-d₆): δ 1.28 (t, *J* = 7.1 Hz, 3H), 4.22 (q, *J* = 7.1 Hz, 2H), 7.92-8.02 (m, 5H), 8.08 (s, 1H), 8.72 (s, 1H).

Ethyl 5-chloro-6-(1,3-dioxoisindolin-2-yl)pyrazolo[1,5-a]pyrimidine-3-carboxylate



To a solution of ethyl 6-(1,3-dioxoisindolin-2-yl)-5-oxo-4,5-dihydropyrazolo[1,5-a]pyrimidine-3-carboxylate **3.102** (1.85 g, 5.25 mmol) in POCl₃ (20 mL, 210 mmol) was added DMF (1.2 mL, 15.75 mmol) and the reaction was heated to 100 °C for 36 h. The mixture was cooled to rt and concentrated *in vacuo*. The residue was

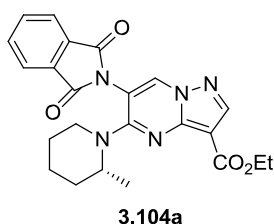
treated with saturated aq. NaHCO₃ (30 mL) and stood for 2 h until the quench had ceased. The aqueous phase was extracted with EtOAc (3 x 20 mL). The combined organic layers were washed with brine, dried through a hydrophobic frit and concentrated *in vacuo*. The residue was purified by silica chromatography (0-50% EtOAc/cyclohexane), appropriate fractions were evaporated *in vacuo* to afford ethyl 5-chloro-6-(1,3-dioxoisindolin-2-yl)pyrazolo[1,5-a]pyrimidine-3-carboxylate (1.06 g, 2.86 mmol, 54%) as a white solid. 60% yield overall for two steps.

LCMS (High pH, ES⁺): t_R = 1.06 min, [M+H]⁺ 371.1, (89% purity). ¹H NMR (400 MHz, CDCl₃): δ 1.45 (t, *J* = 7.1 Hz, 3H), 4.46 (q, *J* = 7.1 Hz, 2H), 7.86-7.94 (m, 2H), 8.00-8.07 (m, 2H), 8.66 (s, 1H), 8.82 (s, 1H). ¹³C NMR (101 MHz, CDCl₃): δ 14.4, 60.8, 104.2, 114.8, 124.5, 131.5, 135.2, 137.7, 146.0, 149.6, 153.0, 161.5, 165.9. M.pt.: 150-152 °C.

ν_{max} (neat): 3076, 2978, 1729, 1633, 1562, 1499, 1468, 1419, 1373, 1347, 1302, 1209, 1134, 1067, 1021, 879, 780, 718 cm⁻¹.

HRMS: (C₁₇H₁₁ClN₄O₄) [M+H]⁺ requires 371.0542, found [M+H]⁺ 371.054, [M+Na]⁺ requires 393.0361, found [M+Na]⁺ 393.0363.

(R)-Ethyl 6-(1,3-dioxoisindolin-2-yl)-5-(2-methylpiperidin-1-yl)pyrazolo[1,5-a]pyrimidine-3-carboxylate

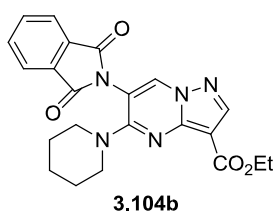


To a solution of ethyl 5-chloro-6-(1,3-dioxoisindolin-2-yl)pyrazolo[1,5-a]pyrimidine-3-carboxylate **3.103** (1 g, 2.70 mmol) in DMSO (7 ml) was added (*R*)-2-methylpiperidine (0.650 mL, 5.39 mmol) and DIPEA (0.707 mL, 4.05 mmol). The reaction was stirred at rt for 24 h, then diluted with EtOAc (20 mL)

and the organic layer was washed with 1 M HCl (2 x 15 mL) and sat. aq. NaHCO₃ (15 mL). The separate aqueous layers were each extracted with EtOAc (20 mL) and the combined organics were dried through a hydrophobic frit and evaporated to dryness to afford (*R*)-ethyl 6-(1,3-dioxoisindolin-2-yl)-5-(2-methylpiperidin-1-yl)pyrazolo[1,5-*a*]pyrimidine-3-carboxylate (1.17 g, 2.70 mmol, 100%) as an orange solid.

LCMS (High pH, ES⁺): t_R = 1.24 min, [M+H]⁺ 434.3, (87% purity). ¹H NMR (400 MHz, CDCl₃): δ 1.25 (d, *J* = 6.8 Hz, 3H), 1.43 (t, *J* = 7.1 Hz, 3H), 1.46-1.56 (m, 4H), 1.60-1.71 (m, 1H), 1.71-1.83 (m, 1H), 3.10-3.20 (m, 1H), 3.73 (dt, *J* = 13.4, 3.4 Hz, 1H), 4.33-4.43 (m, 2H), 4.49-4.59 (m, 1H), 7.86-7.90 (m, 2H), 7.98-8.05 (m, 2H), 8.29 (s, 1H), 8.40 (s, 1H).

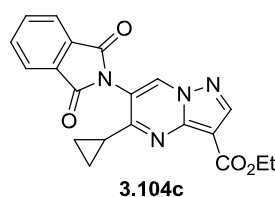
Ethyl 6-(1,3-dioxoisindolin-2-yl)-5-(piperidin-1-yl)pyrazolo[1,5-*a*]pyrimidine-3-carboxylate



To a solution of ethyl 5-chloro-6-(1,3-dioxoisindolin-2-yl)pyrazolo[1,5-*a*]pyrimidine-3-carboxylate **3.103** (150 mg, 0.405 mmol) in DMSO (1 mL) was added piperidine (0.060 mL, 0.607 mmol) and DIPEA (0.106 mL, 0.607 mmol). The reaction was stirred at rt for 90 min. The reaction mixture was diluted with EtOAc (20 mL) and washed with 1 M HCl (2 x 15 mL) and sat. aq. NaHCO₃ (15 mL). The separate aqueous layers were each extracted with EtOAc (20 mL) and the combined organics were dried through a hydrophobic frit and evaporated to dryness to afford ethyl 6-(1,3-dioxoisindolin-2-yl)-5-(piperidin-1-yl)pyrazolo[1,5-*a*]pyrimidine-3-carboxylate (168 mg, 0.401 mmol, 99%) as a white solid.

LCMS (High pH, ES⁺): t_R = 1.17 min, [M+H]⁺ 420.3, (93% purity). ¹H NMR (400 MHz, DMSO-*d*₆): δ 1.32 (t, *J* = 7.1 Hz, 3H), 1.42-1.50 (m, 4H), 1.51-1.59 (m, 2H), 3.49-3.56 (m, 4H), 4.24 (q, *J* = 7.1 Hz, 2H), 7.96-8.02 (m, 2H), 8.05-8.10 (m, 2H), 8.39 (s, 1H), 9.14 (s, 1H).

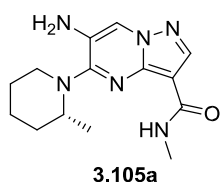
Ethyl 5-cyclopropyl-6-(1,3-dioxoisindolin-2-yl)pyrazolo[1,5-*a*]pyrimidine-3-carboxylate



A solution of ethyl 5-chloro-6-(1,3-dioxoisindolin-2-yl)pyrazolo[1,5-*a*]pyrimidine-3-carboxylate **3.103** (800 mg, 2.158 mmol), K₂CO₃ (596 mg, 4.32 mmol), Pd(PPh₃)₄ (249 mg, 0.216 mmol) and cyclopropylboronic acid (278 mg, 3.24 mmol) in 1,4-dioxane (8.5 mL) was degassed with N₂, then heated to 100 °C for 18 h. The reaction mixture was filtered through Celite and evaporated to dryness. The residue was purified by silica chromatography (0-30% (3:1 EtOAc:EtOH)/cyclohexane) and the relevant fractions were evaporated to dryness to afford ethyl 5-cyclopropyl-6-(1,3-dioxoisindolin-2-yl)pyrazolo[1,5-*a*]pyrimidine-3-carboxylate (21

mg, 0.046 mmol, 34%) as an off-white solid. This contained ~16% residual triphenylphosphine oxide and was used for further chemistry without further purification. LCMS (High pH, ES⁺): t_R = 1.10 min, [M+H]⁺ 377.2, (96% purity). ¹H NMR (400 MHz, CDCl₃): δ 1.10 (s, 2H), 1.42 (t, *J* = 7.1 Hz, 3H), 1.44-1.48 (m, 2H), 1.841.93 (m, 1H), 4.39 (q, *J* = 7.1 Hz, 2H), 7.88 (dd, *J* = 5.5, 3.1 Hz, 2H), 8.03 (dd, *J* = 5.5, 3.1 Hz, 2H), 8.56 (s, 1H), 8.59 (s, 1H).

(*R*)-6-Amino-*N*-methyl-5-(2-methylpiperidin-1-yl)pyrazolo[1,5-*a*]pyrimidine-3carboxamide



To a solution of DABAL-Me₃ (473 mg, 1.846 mmol) in anhydrous THF (1.5 mL) in a sealed tube was added MeNH₂, 2 M in THF (1.38 mL, 2.77 mmol). The reaction mixture was stirred at 40 °C in an oil bath for 30 min. A solution of (*R*)-ethyl 6-(1,3-dioxoisindolin-2-yl)-5-(2methylpiperidin-1-yl)pyrazolo[1,5-*a*]pyrimidine-3-carboxylate **3.104a** (400 mg, 0.923 mmol) in THF (3 mL) was added and the reaction was heated to 70 °C for 12 h. The reaction mixture was cooled to rt and quenched with aqueous 2 M HCl. The aqueous phase was neutralised with sat. aq. NaHCO₃ and extracted with EtOAc (5 x 20 mL). The combined organics were dried using a hydrophobic frit and evaporated *in vacuo*. The crude product was purified by silica chromatography (10-60% (3:1 EtOAc:EtOH)/cyclohexane), appropriate fractions were evaporated *in vacuo* and further purified by High pH MDAP to give

(*R*)-6-amino-*N*-methyl-5-(2-methylpiperidin-1-yl)pyrazolo[1,5-*a*]pyrimidine-3carboxamide (130 mg, 0.451 mmol, 49%) as an orange solid. LCMS (High pH, ES⁺): t_R = 0.89 min, [M+H]⁺ 289.2, (99% purity). ¹H NMR (400 MHz, CDCl₃): δ 1.24 (d, *J* = 6.6 Hz, 3H), 1.55-1.94 (m, 6H), 3.02 (d, *J* = 4.9 Hz, 3H), 3.29-3.37 (m, 1H), 3.44 (dt, *J* = 13.0, 4.2 Hz, 1H), 3.55 (s, 2H), 4.15-4.25 (m, 1H), 7.71 (d, *J* = 3.2 Hz, 1H), 8.00 (s, 1H), 8.33 (s, 1H). ¹³C NMR (101 MHz, CDCl₃): δ 16.2, 19.9, 25.7, 25.8, 31.3, 44.3, 50.3, 102.9, 119.3, 126.2, 141.1, 143.6, 155.3, 163.8.

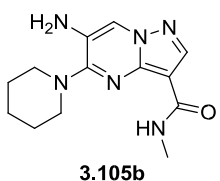
M.pt.: 75-80 °C

[α_D]²⁵ °C = -10 (c = 0.1, MeOH).

ν_{max} (neat): 3350, 3204, 2936, 2863, 1640, 1558, 1444, 1374, 1335, 1277, 1227, 1194, 1178, 1129, 1066, 1036, 1006, 863, 772, 734 cm⁻¹.

HRMS: (C₁₄H₂₀N₆O) [M+H]⁺ requires 289.1771, found [M+H]⁺ 289.1779.

6-Amino-*N*-methyl-5-(piperidin-1-yl)pyrazolo[1,5-*a*]pyrimidine-3-carboxamide

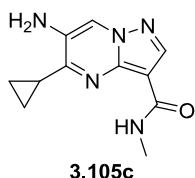


To a solution of DABAL-Me₃ (400 mg, 1.559 mmol) in anhydrous THF (1.3 mL) stirred under N₂ at rt in a sealed tube was added MeNH₂ (1169 μL, 2 M in THF, 2.339 mmol). The reaction mixture was stirred at 40 °C in an sand bath for 1 h. A solution of ethyl 6-(1,3-dioxoisindolin-2-yl)-5-(piperidin-1-yl)pyrazolo[1,5-*a*]pyrimidine-3-carboxylate **3.104b** (327 mg,

0.780 mmol) in THF (2.6 mL) was added and the reaction was heated to 70 °C for 18 h. The reaction mixture was cooled to rt and quenched with aqueous 2 M HCl. The aqueous layer was neutralised with sat. aq. NaHCO₃ and extracted with EtOAc (4 x 30 mL). The combined organics were dried using a hydrophobic frit and evaporated *in vacuo*. The crude product was purified by silica chromatography (10-70% (3:1 EtOAc:EtOH)/cyclohexane), appropriate fractions were evaporated *in vacuo* and further purified by High pH MDAP to afford 6-amino-*N*-methyl-5-(piperidin-1-yl)pyrazolo[1,5-*a*]pyrimidine-3-carboxamide (110 mg, 0.401 mmol, 51%) as an off-white solid.

LCMS (High pH, ES⁺): t_R = 0.83 min, [M+H]⁺ 275.2, (90% purity). ¹H NMR (400 MHz, CDCl₃): δ 1.71-1.84 (m, 6H), 3.05 (d, *J* = 4.9 Hz, 3H), 3.40-3.45 (m, 4H), 3.49 (s, 2H), 7.66-7.73 (m, 1H), 8.01 (s, 1H), 8.36 (s, 1H).

6-Amino-5-cyclopropyl-*N*-methylpyrazolo[1,5-*a*]pyrimidine-3-carboxamide To a solution of DABAL-Me₃ (324 mg, 1.265 mmol) in anhydrous THF (1 mL) stirred under N₂ at rt in a sealed tube was added MeNH₂ (1265 μL, 2 M in THF, 2.53 mmol). The reaction mixture was stirred at 40 °C in an oil bath for 30 min. A solution of ethyl 5-cyclopropyl-6-(1,3-dioxoisindolin-2-yl)pyrazolo[1,5-*a*]pyrimidine-3-carboxylate **3.104c** (280 mg, 0.632 mmol)



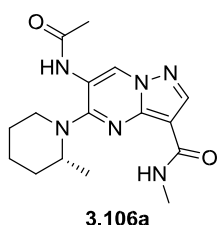
in THF (2 mL) was added and the reaction was heated to 70 °C for 3 h. The reaction mixture was cooled to rt and quenched with aqueous 2 M HCl. The aqueous layer was neutralised with sat. aq. NaHCO₃ and extracted with EtOAc (5 x 10 mL). The combined organics were dried using a hydrophobic frit and evaporated *in vacuo*. The crude product was purified by silica chromatography (10-90% (3:1 EtOAc:EtOH)/cyclohexane), appropriate fractions were evaporated *in vacuo* to afford 6-amino-5-cyclopropyl-*N*-methylpyrazolo[1,5-*a*]pyrimidine-3-carboxamide (114 mg, 0.493 mmol, 78%) as a yellow solid. LCMS (High pH, ES⁺): t_R = 0.62 min, [M+H]⁺ 232.2, (98% purity). ¹H NMR (400 MHz, MeOD-*d*₄): δ 1.17-1.28 (m, 4H), 2.28-2.37 (m, 1H), 3.00 (s, 3H), 8.21 (s, 1H), 8.22 (s, 1H). Exchangeable protons were not observed. ¹³C NMR (101 MHz, MeOD-*d*₄): δ 10.0, 12.0, 24.6, 102.5, 116.7, 133.1, 140.7, 142.8, 159.4, 164.3.

M.pt.: 215-220 °C (decomp)

ν_{max} (neat): 3224, 1641, 1556, 1435, 1316, 1283, 1216, 1195, 1159, 1128, 1058, 870, 826, 768 cm⁻¹.

HRMS: (C₁₁H₁₃N₅O) [M+H]⁺ requires 232.1193, found [M+H]⁺ 232.1193.

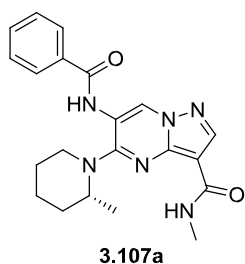
(*R*)-6-Acetamido-*N*-methyl-5-(2-methylpiperidin-1-yl)pyrazolo[1,5-*a*]pyrimidine-3-carboxamide



Prepared according to General Procedure E, with **3.105a** (20 mg, 0.069 mmol) and acetyl chloride (7 μ L, 0.104 mmol), affording (*R*)-6-acetamido-*N*-methyl-5-(2-methylpiperidin-1-yl)pyrazolo[1,5-*a*]pyrimidine-3-carboxamide (19 mg, 0.058 mmol, 83%) as an off-white solid.

LCMS (High pH, ES⁺): t_R = 0.77 min, [M+H]⁺ 331.2, (100% purity). ¹H NMR (400 MHz, CDCl₃): δ 1.21 (d, J = 6.5 Hz, 3H), 1.57-1.96 (m, 6H), 2.28 (s, 3H), 3.03 (d, J = 4.6 Hz, 3H), 3.16-3.30 (m, 2H), 3.78-3.88 (m, 1H), 7.56 (q, J = 4.6 Hz, 1H), 7.67 (s, 1H), 8.44 (s, 1H), 9.47 (s, 1H)

(*R*)-6-Benzamido-*N*-methyl-5-(2-methylpiperidin-1-yl)pyrazolo[1,5-*a*]pyrimidine-3-carboxamide

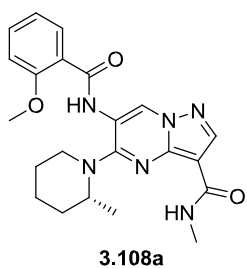


Prepared according to General Procedure E, with **3.105a** (20 mg, 0.069 mmol) and benzoyl chloride (0.012 mL, 0.104 mmol), affording (*R*)-6-benzamido-*N*-methyl-5-(2-methylpiperidin-1-yl)pyrazolo[1,5-*a*]pyrimidine-3-carboxamide (23 mg, 0.059 mmol, 84%) as an offwhite solid.

LCMS (High pH, ES⁺): t_R = 1.01 min, [M+H]⁺ 393.3, (95% purity).

¹H NMR (400 MHz, CDCl₃): δ 1.19 (d, J = 6.5 Hz, 3H), 1.61-1.74 (m, 2H), 1.75-2.04 (m, 4H), 3.08 (d, J = 4.6 Hz, 3H), 3.10-3.16 (m, 1H), 3.30-3.38 (m, 1H), 3.76-3.82 (m, 1H), 7.54-7.62 (m, 3H), 7.63-7.68 (m, 1H), 7.91-7.96 (m, 2H), 8.52 (s, 1H), 8.56 (s, 1H), 9.94 (s, 1H).

(*R*)-6-(2-Methoxybenzamido)-*N*-methyl-5-(2-methylpiperidin-1-yl)pyrazolo[1,5-*a*]pyrimidine-3-carboxamide

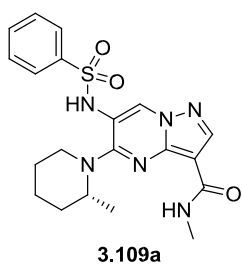


Prepared according to General Procedure E, with **3.105a** (20 mg, 0.069 mmol) and 2-methoxybenzoyl chloride (0.014 mL, 0.104 mmol). The product was further purified by high pH MDAP, affording as an off-white solid.

LCMS (High pH, ES⁺): t_R = 1.12 min, [M+H]⁺ 423.3, (100% purity).

¹H NMR (400 MHz, CDCl₃): δ 1.20 (d, J = 6.6 Hz, 3H), 1.59-1.79 (m, 3H), 1.81-1.91 (m, 2H), 1.96-2.05 (m, 1H), 3.05 (d, J = 4.6 Hz, 3H), 3.09-3.18 (m, 1H), 3.30-3.39 (m, 1H), 3.86-3.94 (m, 1H), 4.12 (s, 3H), 7.09 (d, J = 8.2 Hz, 1H), 7.19 (ddd, J = 7.8, 7.3, 1.0 Hz, 1H), 7.56 (ddd, J = 8.2, 7.3, 1.8 Hz, 1H), 7.61 (q, J = 4.6 Hz, 1H), 8.32 (dd, J = 7.8, 1.8 Hz, 1H), 8.50 (s, 1H), 9.91 (s, 1H), 10.13 (s, 1H).

(*R*)-*N*-methyl-5-(2-methylpiperidin-1-yl)-6-(phenylsulfonamido)pyrazolo[1,5-*a*]pyrimidine-3-carboxamide



Prepared according to General Procedure E, with **3.105a** (20 mg, 0.069 mmol) and benzenesulfonyl chloride (0.013 mL, 0.104 mmol), stirring for 36 h. Further purified by high pH MDAP, affording (*R*)-*N*-methyl-5-(2-methylpiperidin-1-yl)-6-(phenylsulfonamido)pyrazolo[1,5-a]pyrimidine-3-carboxamide (12 mg, 0.028 mmol, 40%) as a brown solid.

LCMS (High pH, ES⁺): $t_R = 0.79$ min, $[M+H]^+$ 429.2, (94% purity). ¹

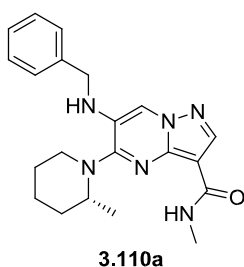
¹H NMR (400 MHz, CDCl₃): δ 1.05 (d, $J = 6.6$ Hz, 3H), 1.43-1.86 (m, 6H), 2.92 (ddd, $J = 12.8, 8.1, 4.5$ Hz, 1H), 2.99 (d, $J = 4.9$ Hz, 3H), 3.28 (dt, $J = 13.0, 4.5$ Hz, 1H), 3.82-3.92 (m, 1H), 6.91-7.20 (m, 1H), 7.47-7.55 (m, 3H), 7.59-7.65 (m, 1H), 7.81-7.87 (m, 2H), 8.42 (s, 1H), 8.50 (s, 1H). ¹³C NMR (101 MHz, CDCl₃): δ 16.7, 20.3, 25.5, 25.9, 31.5, 46.7, 52.2, 103.8, 115.3, 127.2, 129.5, 131.0, 133.8, 138.8, 143.1, 146.7, 156.7, 163.1. M.pt.: 96-99 °C.

$[\alpha_D]^{22} = -35$ ($c = 0.2$, MeOH).

ν_{max} (neat): 3349, 3066, 2939, 1635, 1568, 1477, 1447, 1344, 1268, 1242, 1165, 1093, 921, 557, 730, 689 cm⁻¹.

HRMS: (C₂₀H₂₄N₆O₃S) $[M+H]^+$ requires 429.1703, found $[M+H]^+$ 429.1707.

(*R*)-6-(Benzamido)-*N*-methyl-5-(2-methylpiperidin-1-yl)pyrazolo[1,5-*a*]pyrimidine-3-carboxamide

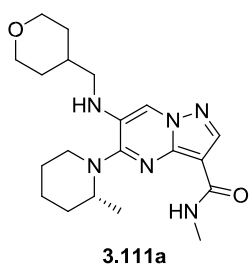


Prepared according to General Procedure F, with **3.105a** (25 mg, 0.087 mmol) and benzaldehyde (13.22 μ L, 0.130 mmol). The crude product was purified by silica chromatography (10-40% (3:1 EtOAc:EtOH)/cyclohexane), appropriate fractions were evaporated *in vacuo* and further purified by High pH MDAP to give (*R*)-6-

(benzylamino)-*N*-methyl-5-(2-methylpiperidin-1-yl)pyrazolo[1,5-a]pyrimidine-3-carboxamide (10 mg, 0.026 mmol, 31%).

LCMS (High pH, ES⁺): $t_R = 1.24$ min, $[M]^+$ 379.3, (100% pure). ¹H NMR (400 MHz, CDCl₃): δ 1.23 (d, $J = 6.4$ Hz, 3H), 1.56-1.95 (m, 6H), 3.05 (d, $J = 4.6$ Hz, 3H), 3.26-3.35 (m, 1H), 3.36-3.45 (m, 1H), 4.07-4.15 (m, 1H), 4.18-4.27 (m, 1H), 4.27-4.34 (m, 2H), 7.31-7.46 (m, 5H), 7.69 (q, $J = 4.6$ Hz, 1H), 7.79 (s, 1H), 8.34 (s, 1H).

(*R*)-*N*-Methyl-5-(2-methylpiperidin-1-yl)-6-(((tetrahydro-2*H*-pyran-4-yl)methyl)amino)pyrazolo[1,5-*a*]pyrimidine-3-carboxamide



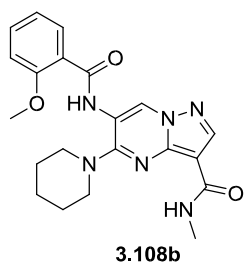
Prepared according to General Procedure F, with **3.105a** (23 mg, 0.080 mmol) and tetrahydro-2H-pyran-4-carbaldehyde (14 mg, 0.120 mmol). The product was purified by silica chromatography (0-45% (3:1 EtOAc:EtOH)/cyclohexane), appropriate fractions were evaporated *in vacuo* and further purified by Formic MDAP to give (*R*)-

N-methyl-5-(2-methylpiperidin-1-yl)-6-(((tetrahydro-2H-pyran-4-yl)methyl)amino)pyrazolo[1,5-a]pyrimidine-3-carboxamide (14 mg, 0.036 mmol, 45%) as a white solid.

LCMS (High pH, ES⁺): $t_R = 1.07$ min, $[M+H]^+$ 387.3, (100% pure).

¹H NMR (400 MHz, CDCl₃): δ 1.20 (d, $J = 6.6$ Hz, 3H), 1.46 (qd, $J = 12.0, 4.2$ Hz, 2H), 1.572.01 (m, 9H), 2.95 (t, $J = 6.0$ Hz, 2H), 3.02 (d, $J = 4.9$ Hz, 3H), 3.18-3.27 (m, 1H), 3.33 (s, 1H), 3.44 (td, $J = 11.8, 2.1$ Hz, 2H), 3.79 (t, $J = 5.6$ Hz, 1H), 3.98-4.08 (m, 2H), 7.65 (q, $J = 4.9$ Hz, 1H), 7.79 (s, 1H), 8.34 (s, 1H). NH not observed.

6-(2-Methoxybenzamido)-*N*-methyl-5-(piperidin-1-yl)pyrazolo[1,5-a]pyrimidine-3carboxamide



Prepared according to General Procedure E, with **3.105b** (8 mg, 0.029 mmol) and 2-methoxybenzoyl chloride (6 μ L, 0.044 mmol). The product was purified by silica chromatography (0-50% (3:1 EtOAc:EtOH)/cyclohexane), appropriate fractions were evaporated *in vacuo* to afford 6-(2-methoxybenzamido)-*N*-methyl-5-(piperidin-1-yl)pyrazolo[1,5-a]pyrimidine-3-carboxamide (9 mg, 0.022 mmol, 76%)

as a white solid.

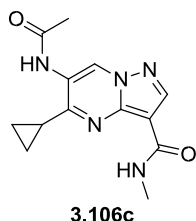
LCMS (High pH, ES⁺): $t_R = 1.06$ min, $[M+H]^+$ 409.3, (97% purity). ¹H NMR (400 MHz, CDCl₃): δ 1.69-1.84 (m, 6H), 3.05 (d, $J = 4.9$ Hz, 3H), 3.31-3.35 (m, 4H), 4.12 (s, 3H), 7.09 (d, $J = 8.1$ Hz, 1H), 7.15-7.21 (m, 1H), 7.56 (ddd, $J = 8.4, 7.4, 1.8$ Hz, 1H),

7.60-7.66 (m, 1H), 8.31 (dd, $J = 7.8, 1.7$ Hz, 1H), 8.47 (s, 1H), 9.81 (s, 1H), 9.98 (s, 1H). ¹³C

NMR (101 MHz, CDCl₃): δ 24.1, 25.5, 25.9, 50.6, 56.4, 104.0, 111.7, 117.1, 120.6, 122.0, 128.7, 132.8, 134.0, 142.1, 146.0, 156.7, 157.3, 163.2, 163.3. M.pt.: 209-210 °C. ν_{max} (neat): 3386, 3273, 2945, 1649, 1660, 1540, 1483, 1429, 1373, 1303, 1287, 1244, 1212, 1168, 1097, 1014, 944, 861, 754, 690 cm⁻¹.

HRMS: (C₂₁H₂₄N₆O₃) $[M+H]^+$ requires 409.1983, found $[M+H]^+$ 409.1994.

6-Acetamido-5-cyclopropyl-*N*-methylpyrazolo[1,5-*a*]pyrimidine-3-carboxamide



Prepared according to General Procedure E, with **3.105c** (17 mg, 0.074 mmol) and acetyl chloride (8 μ L, 0.110 mmol) in THF (0.05 M) affording 6-acetamido-5-cyclopropyl-*N*-methylpyrazolo[1,5-*a*]pyrimidine-3-carboxamide (11 mg, 0.040 mmol, 55%) as a white solid. LCMS (High pH, ES⁺): t_R = 0.60 min, [M+H]⁺ 274.2, (100% purity). ¹

¹H NMR (400 MHz, DMSO-*d*₆): δ 1.16-1.29 (m, 4H), 2.16 (s, 3H), 2.41-2.48 (m, 1H), 2.88 (d, J = 4.9 Hz, 3H), 7.57 (q, J = 4.6 Hz, 1H), 8.42 (s, 1H), 9.20 (s, 1H), 9.96 (s, 1H).

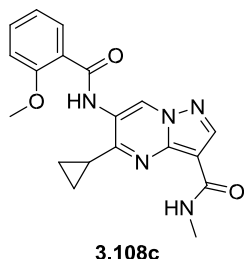
¹³C NMR (101 MHz, DMSO-*d*₆): δ 12.9, 13.3, 23.5, 26.1, 104.3, 121.7, 132.4, 143.4, 146.3, 162.2, 163.8, 170.2.

M.pt.: 230-236 °C (decomp).

ν_{max} (neat): 3372, 3268, 3037, 1657, 1559, 1536, 1491, 1426, 1377, 1291, 1221, 1184, 1148, 1124, 1059, 992, 934, 907, 869, 771, 749, 720 cm⁻¹.

HRMS: (C₁₃H₁₅N₅O₂) [M+H]⁺ requires 274.1299, found [M+H]⁺ 274.1304.

5-Cyclopropyl-6-(2-methoxybenzamido)-*N*-methylpyrazolo[1,5-*a*]pyrimidine-3-carboxamide

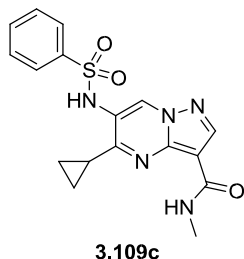


Prepared according to General Procedure E, with **3.105c** (17 mg, 0.074 mmol) and 2-methoxybenzoyl chloride (0.015 mL, 0.110 mmol) in THF (1.5 mL) affording 5-cyclopropyl-6-(2-methoxybenzamido)-*N*-methylpyrazolo[1,5-*a*]pyrimidine-3-carboxamide (1.5 mg, 4.11 μ mol, 6%) as an off-white solid.

LCMS (High pH, ES⁺): t_R = 0.95 min, [M-H]⁻ 364.4, (100% purity). ¹

¹H NMR (400 MHz, DMSO-*d*₆): δ 1.19-1.34 (m, 4H), 2.43-2.49 (m, 1H), 2.90 (d, J = 4.9 Hz, 3H), 4.01 (s, 3H), 7.15 (t, J = 7.7 Hz, 1H), 7.28 (d, J = 8.3 Hz, 1H), 7.58-7.66 (m, 2H), 7.93 (dd, J = 7.7, 1.8 Hz, 1H), 8.46 (s, 1H), 9.48 (s, 1H), 10.30 (s, 1H).

5-Cyclopropyl-6-(phenylsulfonamido)-*N*-methylpyrazolo[1,5-*a*]pyrimidine-3-carboxamide



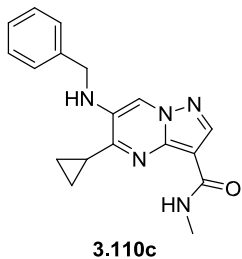
Prepared according to General Procedure E, with **3.105c** (17 mg, 0.074 mmol) and benzenesulfonyl chloride (0.014 mL, 0.110 mmol) in THF (1.5 mL) affording 5-cyclopropyl-*N*-methyl-6-(phenylsulfonamido)pyrazolo[1,5-*a*]pyrimidine-3-carboxamide (15 mg, 0.040 mmol, 55%) as a white solid.

LCMS (High pH, ES⁺): t_R = 0.66 min, [M+H]⁺ 372.3, (100% purity). ¹

1

¹H NMR (400 MHz, DMSO-*d*₆): δ 0.74-0.81 (m, 2H), 0.92-0.98 (m, 2H), 2.09-2.18 (m, 1H), 2.84 (d, *J* = 4.9 Hz, 3H), 7.48 (q, *J* = 4.9 Hz, 1H), 7.55-7.61 (m, 2H), 7.66-7.73 (m, 3H), 8.45 (s, 1H), 8.81 (s, 1H), 10.44 (s, 1H).

6-(Benzylamino)-5-cyclopropyl-*N*-methylpyrazolo[1,5-*a*]pyrimidine-3-carboxamide

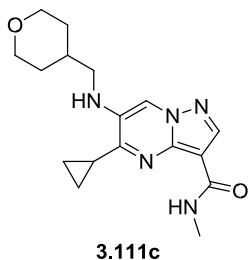


Prepared according to General Procedure F, with **3.105c** (16 mg, 0.069 mmol) and benzaldehyde (11 μL, 0.104 mmol). Slow conversion was observed so further magnesium sulphate and TsOH (7 mg, 0.035 mmol) were added and the reaction was stirred at rt for 6 h. 10 eq NaBH₄ were required, with stirring for 24 h. The crude product was purified by High pH MDAP to give 6-(benzylamino)-5-cyclopropyl-*N*-

methylpyrazolo[1,5-*a*]pyrimidine-3-carboxamide (3 mg, 9.33 μmol, 13%) as an off-white solid.

LCMS (High pH, ES⁺): t_R = 1.00 min, [M+H]⁺ 321.2, (100% pure). ¹H NMR (400 MHz, MeOD-*d*₄): δ 1.27-1.30 (m, 4H), 2.39-2.48 (m, 1H), 3.00 (s, 3H), 4.47 (s, 2H), 7.28 (m, *J* = 7.3 Hz, 1H), 7.38 (s, 2H), 7.47 (d, *J* = 7.3 Hz, 2H), 7.81 (s, 1H), 8.19 (s, 1H). Exchangeable protons were not observed.

5-Cyclopropyl-*N*-methyl-6-(((tetrahydro-2*H*-pyran-4-yl)methyl)amino)pyrazolo[1,5-*a*]pyrimidine-3-carboxamide

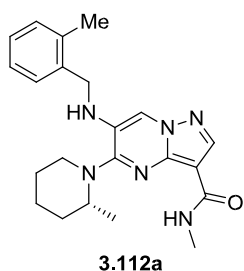


Prepared according to General Procedure F, with **3.105c** (16 mg, 0.069 mmol) and tetrahydro-2*H*-pyran-4-carbaldehyde (12 mg, 0.104 mmol). Slow conversion was observed so further magnesium sulphate and TsOH (7 mg, 0.035 mmol) were added and the reaction was stirred at rt for 6 h. In total, 10 eq NaBH₄ were required, with stirring for 24 h. The crude product was purified by High pH MDAP to give 5-cyclopropyl-*N*-methyl-6-(((tetrahydro-2*H*-pyran-4-yl)methyl)amino)pyrazolo[1,5-*a*]pyrimidine-3-carboxamide (4 mg, 0.012 mmol, 18%) as an off-white solid.

LCMS (High pH, ES⁺): t_R = 0.83 min, [M+H]⁺ 330.3, (90% pure). ¹

¹H NMR (400 MHz, MeOD-*d*₄): δ 1.22-1.27 (m, 4H), 1.42 (qd, *J* = 12.0, 4.4 Hz, 2H), 1.84 (dq, *J* = 13.0, 2.0 Hz, 2H), 2.00-2.13 (m, 1H), 2.32-2.40 (m, 1H), 3.01 (s, 3H), 3.09 (d, *J* = 6.8 Hz, 2H), 3.47 (td, *J* = 12.0, 2.0 Hz, 2H), 4.00 (dd, *J* = 11.2, 3.2 Hz, 2H), 8.04 (s, 1H), 8.24 (s, 1H). Exchangeable protons were not observed.

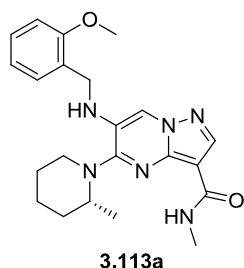
(*R*)-*N*-Methyl-6-((2-methylbenzyl)amino)-5-(2-methylpiperidin-1-yl)pyrazolo[1,5-*a*]pyrimidine-3-carboxamide



Prepared according to General Procedure F, with **3.105a** (25 mg, 0.087 mmol), 2-methylbenzaldehyde (15 μ L, 0.130 mmol) and acetic acid (5 μ L, 0.087 mmol). The crude product was purified by High pH MDAP to give (*R*)-*N*-methyl-6-((2-methylbenzyl)amino)-5-(2-methylpiperidin-1-yl)pyrazolo[1,5-*a*]pyrimidine-3-carboxamide (27 mg, 0.069 mmol, 79%).

LCMS (High pH, ES⁺): t_R = 1.31 min, [M+H]⁺ 393.4, (96% pure). ¹H NMR (400 MHz, CDCl₃): δ 1.20 (d, J = 6.6 Hz, 3H), 1.52-1.65 (m, 2H), 1.66-1.75 (m, 2H), 1.76-1.91 (m, 2H), 2.38 (s, 3H), 3.03 (d, J = 4.6 Hz, 3H), 3.26 (dt, J = 12.8, 4.8 Hz, 1H), 3.32-3.41 (m, 1H), 4.00-4.11 (m, 2H), 4.22 (d, J = 5.4 Hz, 2H), 7.18-7.32 (m, 4H), 7.67 (q, J = 4.6 Hz, 1H), 7.79 (s, 1H), 8.33 (s, 1H).

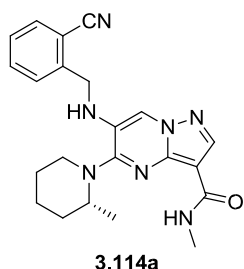
(*R*)-*N*-Methyl-6-((2-methoxybenzyl)amino)-5-(2-methylpiperidin-1-yl)pyrazolo[1,5-*a*]pyrimidine-3-carboxamide



Prepared according to General Procedure F, with **3.105a** (25 mg, 0.087 mmol), 2-methoxybenzaldehyde (16 μ L, 0.130 mmol) and acetic acid (5 μ L, 0.087 mmol). The crude product was purified by High pH MDAP to give (*R*)-6-((2-methoxybenzyl)amino)-*N*-methyl-5-(2-methylpiperidin-1-yl)pyrazolo[1,5-*a*]pyrimidine-3-carboxamide (26 mg, 0.064 mmol, 73%).

LCMS (High pH, ES⁺): t_R = 1.27 min, [M+H]⁺ 409.4, (96% pure). ¹H NMR (400 MHz, CDCl₃): δ 1.20 (d, J = 6.6 Hz, 3H), 1.53-1.68 (m, 2H), 1.69-1.77 (m, 2H), 1.78-1.92 (m, 2H), 3.02 (d, J = 4.6 Hz, 3H), 3.22-3.38 (m, 2H), 3.89 (s, 3H), 4.06 (s, 1H), 4.27 (d, J = 5.7 Hz, 2H), 4.39 (t, J = 5.7 Hz, 1H), 6.89-6.97 (m, 2H), 7.26-7.32 (m, 2H), 7.68 (q, J = 4.6 Hz, 1H), 7.82 (s, 1H), 8.31 (s, 1H).

(*R*)-6-((2-Cyanobenzyl)amino)-*N*-methyl-5-(2-methylpiperidin-1-yl)pyrazolo[1,5-*a*]pyrimidine-3-carboxamide



Prepared according to General Procedure F, with **3.105a** (25 mg, 0.087 mmol), 2-formylbenzonitrile (17 mg, 0.130 mmol) and acetic acid (5 μ L, 0.087 mmol). The crude product was purified by High pH MDAP to give (*R*)-6-((2-cyanobenzyl)amino)-*N*-methyl-5-(2-methylpiperidin-1-yl)pyrazolo[1,5-*a*]pyrimidine-3-carboxamide (31 mg, 0.077 mmol, 89%).

1

LCMS (High pH, ES⁺): t_R = 1.15 min, [M+H]⁺ 404.3, (93% pure).

¹H NMR (400 MHz, CDCl₃): δ 1.21 (d, J = 6.4 Hz, 3H), 1.56-1.65 (m, 2H), 1.71-1.96 (m, 4H), 3.02 (d, J = 4.9 Hz, 3H), 3.25 (dt, J = 12.8, 4.8 Hz, 1H), 3.35-3.44 (m, 1H), 4.01-4.10 (m, 1H), 4.41-4.60 (m, 3H), 7.44 (td, J = 7.6, 1.2 Hz, 1H), 7.51-7.54 (m, 1H), 7.58-7.66 (m, 2H),

7.73 (s, 1H), 7.72-7.75 (m, 1H), 8.32 (s, 1H). ^{13}C NMR (101 MHz, CDCl_3): δ 17.0, 20.8, 25.8, 25.8, 31.9, 46.5, 47.3, 51.7, 103.8, 111.9, 115.3, 117.2, 127.8, 128.4, 128.5, 133.3, 133.8, 140.2, 141.1, 143.9, 155.5, 163.5. M.pt.: 118-122 °C.

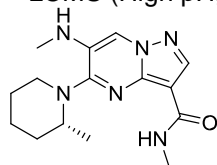
$[\alpha_D]^{23} = +27$ (c = 0.24, MeOH). ν_{max} (neat): 3334, 2935, 2224, 1645, 1564, 1456, 1276, 1265, 1245, 1198, 1174, 1130, 1092, 1064, 972, 920, 882, 815, 771, 740, 728 cm^{-1} .

HRMS: ($\text{C}_{22}\text{H}_{25}\text{N}_7\text{O}$) $[\text{M}+\text{H}]^+$ requires 404.2193, found $[\text{M}+\text{H}]^+$ 404.2199.

(R)-N-Methyl-6-(methylamino)-5-(2-methylpiperidin-1-yl)pyrazolo[1,5-a]pyrimidine-3-carboxamide and (R)-6-(dimethylamino)-N-methyl-5-(2-methylpiperidin-1-yl)pyrazolo[1,5-a]pyrimidine-3-carboxamide

To a solution of **3.105a** (42 mg, 0.146 mmol) and potassium carbonate (80 mg, 0.582 mmol) in DMF (1.5 mL) was added methyl iodide (12 μL , 0.350 mmol). The reaction mixture was stirred at 90 °C for 16 h. The reaction mixture was cooled, neutralised with sat. aq. NaHCO_3 (25 mL) and the aqueous phase was extracted with EtOAc (3 x 15 mL). The combined organics were dried through a hydrophobic frit and evaporated to dryness. The crude product was purified by High pH MDAP afford the products: **(R)-N-methyl-6-(methylamino)-5-(2-methylpiperidin-1-yl)pyrazolo[1,5-a]pyrimidine-3-carboxamide** 7 mg, 0.023 mmol, 16 %.

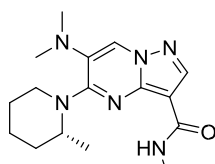
LCMS (High pH, ES⁺): t_R = 1.00 min, $[\text{M}+\text{H}]^+$ 303.2, (100% pure). ¹



3.115a

^1H NMR (400 MHz, CDCl_3): δ 1.19 (d, J = 6.6 Hz, 3H), 1.61-1.94 (m, 6H), 2.84 (d, J = 5.4 Hz, 3H), 3.02 (d, J = 4.9 Hz, 3H), 3.20-3.27 (m, 1H), 3.30-3.37 (m, 1H), 3.72-3.83 (m, 1H), 4.01-4.09 (m, 1H), 7.65-7.72 (m, 1H), 7.78 (s, 1H), 8.34 (s, 1H).

(R)-6-(dimethylamino)-N-methyl-5-(2-methylpiperidin-1-yl)pyrazolo[1,5-a]pyrimidine-3-carboxamide



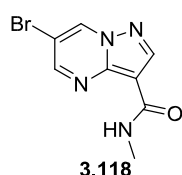
3.116a

2 mg, 6.32 μmol , 4%.

LCMS (High pH, ES⁺): t_R = 1.13 min, $[\text{M}+\text{H}]^+$ 317.1, (100% pure). ¹

^1H NMR (400 MHz, CDCl_3): δ 1.25 (d, J = 6.8 Hz, 3H), 1.62-1.96 (m, 6H), 2.72 (s, 6H), 3.01 (d, J = 4.9 Hz, 3H), 3.18 (s, 1H), 4.28-4.36 (m, 1H), 4.95-5.04 (m, 1H), 7.71-7.77 (m, 1H), 8.01 (s, 1H), 8.33 (s, 1H).

6-Bromo-N-methylpyrazolo[1,5-a]pyrimidine-3-carboxamide



3.118

To a suspension of 6-bromopyrazolo[1,5-a]pyrimidine-3-carboxylic acid **3.117** (900 mg, 3.72 mmol) and oxalyl chloride (0.651 mL, 7.44 mmol) in DCM (22 mL) stirred under N_2 at rt was added DMF (14 μL , 0.186 mmol).

The reaction mixture was stirred at rt for 5 h, until the suspension became a clear solution. The reaction mixture was evaporated *in vacuo*, redissolved in anhydrous DCM and evaporated again. The residue was dissolved in THF (9 mL) and stirred under N_2 at 0 °C.

MeNH₂ (7.44 mL, 2 M in THF, 14.87 mmol) was added and the resulting thick slurry was stirred at rt for 2 h. Further MeNH₂ (7.44 mL, 2 M in THF, 14.87 mmol) was added and the reaction stirred for 2 h. The reaction mixture was concentrated *in vacuo* and suspended in EtOAc (100 mL) and sat. aq. NaHCO₃ (50 mL). The mixture was filtered, washed with ether, and the solid dried under vacuum to afford 6-bromo-*N*-methylpyrazolo[1,5-*a*]pyrimidine-3-carboxamide (685 mg, 2.69 mmol, 72%) as an off-white solid.

The filtrate was separated and the aqueous layer was extracted with EtOAc (3 x 50 mL). The combined organics were washed with brine (10 mL), dried through a hydrophobic frit and evaporated to dryness. The crude product was purified by silica chromatography (0-60% (3:1 EtOAc:EtOH)/cyclohexane), appropriate fractions were evaporated *in vacuo* to afford additional 6-bromo-*N*-methylpyrazolo[1,5-*a*]pyrimidine-3-carboxamide (127 mg, 0.498 mmol, 13%) as a cream solid.

LCMS (High pH, ES⁺): t_R = 0.64 min, [M+H]⁺ 255.0, 257.0, (100% purity). ¹H NMR (400 MHz, DMSO-*d*₆): δ 2.87 (d, *J* = 4.5 Hz, 3H), 7.79 (q, *J* = 4.5 Hz, 1H), 8.56 (s, 1H), 8.87 (d, *J* = 2.1 Hz, 1H), 9.79 (d, *J* = 2.1 Hz, 1H).

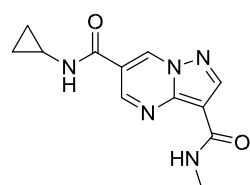
¹³C NMR (101 MHz, DMSO-*d*₆): δ 26.2, 105.3, 106.4, 137.9, 144.0, 146.7, 152.9, 161.7/ M.pt.: 194-195 °C. ν_{max} (neat): 3416, 3045, 1673, 1660, 1561, 1527, 1502, 1456, 1421, 1368, 1259, 1222, 1194, 1081, 914, 825, 770, 690, 632, 576, 529 cm⁻¹.

HRMS: (C₈H₇ON₄Br) [M+H]⁺ requires 254.9881, found [M+H]⁺ 254.9879.

N6-Cyclopropyl-N3-methylpyrazolo[1,5-*a*]pyrimidine-3,6-dicarboxamide, 6-(cyclopropylamino)-*N*-methylpyrazolo[1,5-*a*]pyrimidine-3-carboxamide and 7-(cyclopropylamino)-*N*-methylpyrazolo[1,5-*a*]pyrimidine-3-carboxamide

A solution of 6-bromo-*N*-methylpyrazolo[1,5-*a*]pyrimidine-3-carboxamide **3.118** (30 mg, 0.118 mmol), cyclopropanamine (34 mg, 0.588 mmol), Pd(OAc)₂ (13 mg, 0.059 mmol), Xantphos (41 mg, 0.071 mmol) and triethylamine (33 μL, 0.235 mmol) in DMF (235 μL) was evacuated and backfilled with carbon monoxide (CO) twice. The reaction was placed under a balloon of CO and heated to 60 °C for 4 h. The reaction was filtered through Celite and evaporated to dryness. The crude product was purified by High pH MDAP. The solvent was blown down to give the three products:

N6-Cyclopropyl-N3-methylpyrazolo[1,5-*a*]pyrimidine-3,6-dicarboxamide



3 mg, 0.012 mmol, 10%.

LCMS (High pH, ES⁺): t_R = 0.57 min, [M+H]⁺ 260.3, (95% purity).

¹H NMR (400 MHz, DMSO-*d*₆): δ 0.59-0.65 (m, 2H), 0.73-0.80 (m, 2H), 2.86-2.93 (m, 1H), 2.89 (d, *J* = 4.6 Hz, 3H), 7.82-7.89 (m, 1H), 8.67 (s, 1H), 8.76 (d, *J* = 3.7 Hz, 1H), 9.08 (d, *J* = 2.0 Hz, 1H), 9.63 (d, *J* = 2.2 Hz, 1H).

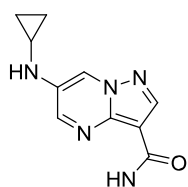
¹³C NMR (101 MHz, DMSO-d₆): δ 6.2, 23.5, 26.2, 106.4, 117.1, 137.4, 145.7, 148.1, 151.4, 161.7, 163.6.

M.pt.: 160-200 °C (decomp.).

ν_{max} (neat): 3363, 3279, 1665, 1624, 1567, 1541, 1508, 1409, 1392, 1321, 1260, 1081, 1022, 940, 911, 841, 782 cm⁻¹.

HRMS: (C₁₂H₁₄O₂N₅) [M+H]⁺ requires 260.1142, found [M+H]⁺ 260.1146.

6-(Cyclopropylamino)-N-methylpyrazolo[1,5-a]pyrimidine-3-carboxamide 5



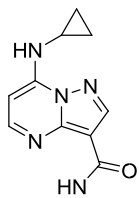
3.120

mg, 0.022 mmol, 18%.

LCMS (High pH, ES⁺): t_R = 0.67 min, [M+H]⁺ 232.2, (95% purity). ¹H NMR (400 MHz, CDCl₃): δ 0.60-0.66 (m, 2H), 0.84-0.91 (m, 2H), 2.47 (tt, J = 6.6, 3.4 Hz, 1H), 3.06 (d, J = 4.9 Hz, 3H), 4.34 (br. s., 1H), 7.68 (br. s., 1H), 8.25 (d, J = 2.4 Hz, 1H), 8.33 (d, J = 2.4 Hz, 1H), 8.50 (s, 1H). 7-

(Cyclopropylamino)-N-methylpyrazolo[1,5-a]pyrimidine-3-

carboxamide 3 mg, 0.013 mmol, 11%.



3.121

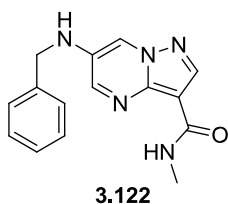
LCMS (High pH, ES⁺): t_R = 0.75 min, [M+H]⁺ 232.3, (84% purity). ¹H NMR (400 MHz, DMSO-d₆): δ 0.71-0.79 (m, 2H), 0.83 – 0.92 (m, 2H), 2.702.78 (m, 1H), 2.87 (d, J = 4.6 Hz, 3H), 6.52 (d, J = 5.4 Hz, 1H), 7.96-8.05 (m, 1H), 8.37 (d, J = 5.4 Hz, 1H), 8.40 (s, 1H). Amine NH not observed.

N6-Cyclopropyl-N3-methylpyrazolo[1,5-a]pyrimidine-3,6-dicarboxamide In the

reaction chamber of the COware³⁷² two-chamber glassware, 6bromo-N-methylpyrazolo[1,5-a]pyrimidine-3-carboxamide **3.118** (60 mg, 0.235 mmol), cyclopropanamine (0.049 mL, 0.706 mmol), triethylamine (0.066 mL, 0.470 mmol) and Xantphos Pd G3 (11 mg, 0.012 mmol) were dissolved in 1,4-dioxane (0.5 mL). In the CO-generating chamber was placed 9-methyl-9H-fluorene-9-carbonyl chloride (114 mg, 0.470 mmol), Pd₂(dba)₃ (4.3 mg, 4.70 μmol) and tri-*tert*-butylphosphonium tetrafluoroborate (1.4 mg, 4.70 μmol). The vessel was purged with nitrogen, then triethylamine (0.098 mL, 0.706 mmol) and 1,4-dioxane (0.5 mL) were added to the CO-generating chamber and the vessel was sealed. The reaction was heated to 50 °C in a sand bath for 18 h. The reaction mixture was cooled and the contents of the reaction chamber were evaporated to dryness. The residue was dry-loaded onto silica and purified by silica chromatography (10-60% (3:1 EtOAc:EtOH)/cyclohexane). The appropriate fractions were evaporated to afford N6-cyclopropyl-N3-methylpyrazolo[1,5-a]pyrimidine-3,6-dicarboxamide (34 mg, 0.131 mmol, 56% yield) as a yellow solid.

Analysis was consistent with material obtained *via* the previous method (pp 289).

6-(Benzylamino)-*N*-methylpyrazolo[1,5-*a*]pyrimidine-3-carboxamide A



solution of 6-bromo-*N*-methylpyrazolo[1,5-*a*]pyrimidine-3-carboxamide **3.118** (20 mg, 0.078 mmol), Pd(OAc)₂ (0.88 mg, 3.92 μmol), Xantphos (2.7 mg, 4.70 μmol), benzylamine (43 μL, 0.392 mmol) and triethylamine (22 μL, 0.157 mmol) in DMF (157 μL) was heated to 60 °C under N₂ in a sand bath for 3 h. The reaction was

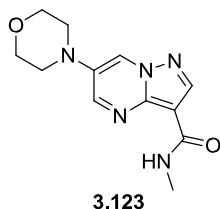
filtered through Celite, evaporated to dryness and purified by silica chromatography (0-50% (3:1 EtOAc:EtOH)/cyclohexane). The appropriate fractions were evaporated to dryness to afford 6-(benzylamino)-*N*-methylpyrazolo[1,5-*a*]pyrimidine-3-carboxamide (12 mg, 0.043 mmol, 54%) as an off-white solid.

LCMS (High pH, ES⁺): t_R = 0.84 min, [M+H]⁺ 282.2, (94% purity).

¹H NMR (400 MHz, CDCl₃): δ 3.05 (d, *J* = 4.9 Hz, 3H), 4.32-4.37 (m, 2H), 4.42 (t, *J* = 4.6 Hz, 1H), 7.31-7.43 (m, 5H), 7.67 (br. s., 1H), 7.93 (d, *J* = 2.7 Hz, 1H), 8.34 (d, *J* = 2.7 Hz, 1H), 8.44 (s, 1H). ¹³C NMR (101 MHz, CDCl₃): δ 25.9, 48.5, 105.8, 115.2, 127.4, 128.1, 129.1, 133.8, 136.7, 141.0, 144.5, 144.7, 163.0. M.pt.: 190-192 °C. ν_{max} (neat): 3367, 3293, 3081, 2885, 1630, 1564, 1501, 1458, 1402, 1320, 1261, 1221, 1188, 1132, 1075, 998, 878, 808, 772, 740, 698 cm⁻¹.

HRMS: (C₁₅H₁₅N₅O) [M+H]⁺ requires 282.1349, found [M+H]⁺ 282.1348.

N-Methyl-6-morpholinopyrazolo[1,5-*a*]pyrimidine-3-carboxamide A



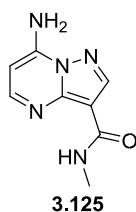
solution of 6-bromo-*N*-methylpyrazolo[1,5-*a*]pyrimidine-3-carboxamide **3.118** (20 mg, 0.078 mmol), Pd(OAc)₂ (0.88 mg, 3.92 μmol), Xantphos (2.7 mg, 4.70 μmol), morpholine (34 μL, 0.392 mmol) and triethylamine (22 μL, 0.157 mmol) in DMF (157 μL) was heated to 80 °C under N₂ in a sand bath for 18 h. The reaction was filtered

through Celite, evaporated to dryness and purified by silica chromatography (0-50% 3:1 EtOH:EtOAc/cyclohexane). The appropriate fractions were evaporated to dryness to afford *N*-methyl-6-morpholinopyrazolo[1,5-*a*]pyrimidine-3-carboxamide (8 mg, 0.031 mmol, 39%) as an off-white solid.

LCMS (High pH, ES⁺): t_R = 0.60 min, [M+H]⁺ 262.2, (88% purity).

¹H NMR (400 MHz, CDCl₃): δ 3.05 (d, *J* = 4.9 Hz, 3H), 3.15 (dd, *J* = 5.6, 3.9 Hz, 4H), 3.90-3.95 (m, 4H), 7.60-7.71 (m, 1H), 8.18 (d, *J* = 2.7 Hz, 1H), 8.53-8.56 (m, 2H).

7-Amino-*N*-methylpyrazolo[1,5-*a*]pyrimidine-3-carboxamide

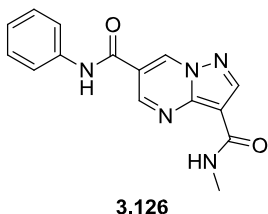


A solution of 6-bromo-*N*-methylpyrazolo[1,5-*a*]pyrimidine-3-carboxamide **3.118** (20 mg, 0.078 mmol), Pd(OAc)₂ (0.88 mg, 3.92 μmol), Xantphos (2.7 mg, 4.70 μmol), ammonium chloride (21 mg, 0.392 mmol) and triethylamine (77 μL, 0.55 mmol) in DMF (157 μL) was heated to 80 °C under N₂ in a sand bath for 18 h.

3.125 The reaction mixture was filtered through Celite, evaporated to dryness and purified by High pH MDAP. The solvent was blown down to afford 7-amino-*N*-methylpyrazolo[1,5-*a*]pyrimidine-3-carboxamide (3 mg, 0.016 mmol, 20%) as an off-white solid.

LCMS (High pH, ES⁺): t_R = 0.52 min, [M+H]⁺ 192.2, (100% purity). ¹H NMR (400 MHz, DMSO-d₆): δ 2.86 (d, *J* = 4.6 Hz, 3H), 6.26 (d, *J* = 5.4 Hz, 1H), 8.01 (q, *J* = 4.6 Hz, 1H), 8.13-8.21 (m, 2H), 8.23 (d, *J* = 5.4 Hz, 1H), 8.40 (s, 1H).

***N*3-Methyl-*N*6-phenylpyrazolo[1,5-*a*]pyrimidine-3,6-dicarboxamide**



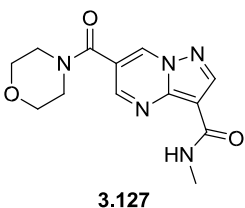
6-Bromo-*N*-methylpyrazolo[1,5-*a*]pyrimidine-3-carboxamide **3.118** (25 mg, 0.098 mmol), aniline (18 μL, 0.196 mmol), Co₂(CO)₈ (8 mg, 0.025 mmol), Pd(OAc)₂ (1.1 mg, 4.90 μmol), Xantphos (2.8 mg, 4.90 μmol) and DMAP (24 mg, 0.196 mmol) were sealed in a vial and placed under N₂. 1,4-Dioxane (980 μL) was added and the reaction

was degassed. The reaction was heated to 60 °C for 6 h

in a sand bath, then to 75 °C for 18 h. The reaction mixture was cooled, filtered through Celite and evaporated to dryness. The residue was purified by High pH MDAP. The solvent was blown down to give *N*3-methyl-*N*6-phenylpyrazolo[1,5-*a*]pyrimidine-3,6-dicarboxamide (5 mg, 0.017 mmol, 17%) as an off-white solid.

LCMS (High pH, ES⁺): t_R = 0.79 min, no mass ion, (90% purity). ¹H NMR (400 MHz, CDCl₃): δ 3.11 (d, *J* = 4.9 Hz, 3H), 7.22-7.28 (m, 1H), 7.46 (t, *J* = 7.9 Hz, 2H), 7.69-7.75 (m, 1H), 7.78 (d, *J* = 7.8 Hz, 2H), 8.53 (s, 1H), 8.82 (br. s., 1H), 9.00 (d, *J* = 2.2 Hz, 1H), 9.18 (d, *J* = 2.2 Hz, 1H).

***N*3-Methyl-*N*6-phenylpyrazolo[1,5-*a*]pyrimidine-3,6-dicarboxamide**

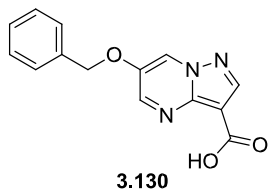


6-Bromo-*N*-methylpyrazolo[1,5-*a*]pyrimidine-3-carboxamide **3.118** (25 mg, 0.098 mmol), morpholine (17 μL, 0.196 mmol), Co₂(CO)₈ (8 mg, 0.025 mmol), Pd(OAc)₂ (1.1 mg, 4.90 μmol), Xantphos (2.8 mg, 4.90 μmol) and DMAP (24 mg, 0.196 mmol) were sealed in a vial and placed under N₂. 1,4-Dioxane (980 μL) was added and the

reaction was degassed. The reaction was heated to 60 °C for 6 h in a sand bath, then to 75 °C for 18 h. The reaction mixture was cooled, filtered through Celite and evaporated to dryness. The residue was purified by High pH MDAP. The solvent was blown down to give *N*-methyl-6-(morpholine-4-carbonyl)pyrazolo[1,5-*a*]pyrimidine-3-carboxamide (8 mg, 0.028 mmol, 28%) as an off-white solid.

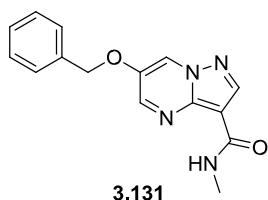
LCMS (High pH, ES⁺): t_R = 0.51 min, [M+H]⁺ 290.2, (90% purity). ¹H NMR (400 MHz, MeOD-d₄): δ 3.03 (s, 3H), 3.75 (br. s., 8H), 8.64 (s, 1H), 8.83 (d, *J* = 2.0 Hz, 1H), 9.30 (d, *J* = 2.0 Hz, 1H). Exchangeable protons were not observed.

6-(Benzyloxy)pyrazolo[1,5-*a*]pyrimidine-3-carboxylic acid



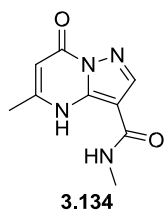
To a solution of oxalyl chloride (0.600 mL, 6.86 mmol) in DCM (15 mL) at -78 °C was added a solution of DMSO (1.2 mL, 16.91 mmol) in DCM (2 mL) dropwise and the reaction was stirred for 10 min. A solution of 2-(benzyloxy)propane-1,3-diol **3.128** (500 mg, 2.74 mmol) in DCM (2 mL) was added dropwise and the reaction was stirred for 15 min. Triethylamine (4.6 mL, 33.0 mmol) was added dropwise and the reaction was stirred at -78 °C for 1 h. The cold bath was removed and 6 M aq. HCl (6 mL, 36.0 mmol) was added, followed by 3-amino-1*H*-pyrazole-4-carboxylic acid **3.129** (349 mg, 2.74 mmol). The reaction was heated to 70 °C for 90 min. The aqueous layer was extracted with DCM (3 x 20 mL) and the combined organics were dried through a hydrophobic frit and evaporated to dryness. The residue was purified by silica chromatography (0-40% (3:1 EtOAc/EtOH + 2% AcOH)/cyclohexane) and the appropriate fractions were evaporated to dryness to afford 6-(benzyloxy)pyrazolo[1,5-*a*]pyrimidine-3-carboxylic acid (135 mg, 0.501 mmol, 18%). The product contained a significant amount of an unknown impurity, possibly benzoylpropanediol related, and was used for further chemistry without further purification. LCMS (High pH, ES⁺): t_R = 0.81 min, [M+H]⁺ 270.1, (100% purity).

6-(Benzyloxy)-*N*-methylpyrazolo[1,5-*a*]pyrimidine-3-carboxamide



A solution of 6-(benzyloxy)pyrazolo[1,5-*a*]pyrimidine-3-carboxylic acid **3.130** (135 mg, 0.50 mmol), HATU (286 mg, 0.75 mmol) and DIPEA (175 μL, 1.00 mmol) in DMF (1.25 mL) was stirred at rt for 15 min. MeNH₂ (1.0 mL, 2 M in THF, 2.00 mmol) was added and the reaction was stirred at rt for 18 h. The reaction mixture was poured into water (20 mL) and extracted with EtOAc (3 x 15 mL). The combined organics were dried through a hydrophobic frit and evaporated to dryness. The crude product was purified by silica chromatography (10-40% (3:1/EtOAc:EtOH)/cyclohexane), appropriate fractions were evaporated to afford 6-(benzyloxy)-*N*-methylpyrazolo[1,5-*a*]pyrimidine-3carboxamide (11 mg, 0.039 mmol, 8%) as a yellow solid. LCMS (High pH, ES⁺): t_R = 0.93 min, [M+H]⁺ 283.2, (81% purity). ¹H NMR (400 MHz, CDCl₃): δ 3.05 (d, *J* = 4.9 Hz, 3H), 5.13 (s, 2H), 7.36-7.48 (m, 5H), 7.60-7.71 (m, 1H), 8.33 (d, *J* = 2.7 Hz, 1H), 8.53 (d, *J* = 2.7 Hz, 1H), 8.55 (s, 1H).

***N*,5-Dimethyl-7-oxo-4,7-dihydropyrazolo[1,5-*a*]pyrimidine-3-carboxamide**

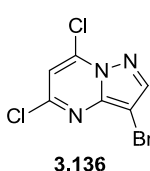


To a solution of 5-methyl-7-oxo-4,7-dihydropyrazolo[1,5-*a*]pyrimidine-3-carboxylic acid **3.133** (43 mg, 0.223 mmol) and HATU (93 mg, 0.245 mmol) in DMSO (2 mL) stirred under N₂ at rt was added MeNH₂ (0.223 mL, 2 M in THF, 0.445 mmol) and DIPEA (0.078 mL, 0.445 mmol). The reaction mixture was stirred at rt for 24 h. The reaction mixture was purified directly

by High pH MDAP. The solvent was evaporated *in vacuo* to give *N*,5-dimethyl-7-oxo-4,7-dihydropyrazolo[1,5-*a*]pyrimidine-3-carboxamide (7 mg, 0.034 mmol, 15%) as a white solid. LCMS (High pH, ES⁺): t_R = 0.46 min, [M+H]⁺ 207.3, (99% purity). ¹H NMR (400 MHz, DMSO-*d*₆): δ 2.31 (br. s., 3H), 2.80 (d, *J* = 4.6 Hz, 3H), 5.47-5.69 (m, 1H), 6.74-7.50 (m, 1H), 7.99-8.20 (m, 1H), 8.27-8.37 (m, 1H).

v_{max} (neat): 3336, 3174, 3006, 1683, 1610, 1582, 1544, 1490, 1459, 1439, 1422, 1364, 1275, 1189, 1135, 1018, 998, 918, 805, 785, 772, 671, 660 cm⁻¹. **3-Bromo-5,7-**

dichloropyrazolo[1,5-*a*]pyrimidine

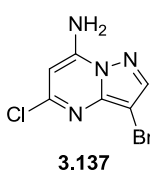


To a solution of 5,7-dichloropyrazolo[1,5-*a*]pyrimidine **3.135** (830 mg, 4.41 mmol) in CHCl₃ (22 mL) stirred under N₂ at rt was added NBS (864 mg, 4.86 mmol) and the reaction mixture was stirred at rt for 1 h. The reaction mixture was quenched with water and the aqueous was extracted with

dichloromethane (3 x 10 mL). The combined organics were dried using a hydrophobic frit and evaporated *in vacuo*. The crude product was purified by silica chromatography (0-10% EtOAc/cyclohexane), the solvent was evaporated *in vacuo* to afford to afford 3-bromo-5,7-dichloropyrazolo[1,5-*a*]pyrimidine (1.11 g, 4.16 mmol, 94%) as a yellow solid.

LCMS (High pH, ES⁺): t_R = 1.05 min, [M+H]⁺ 265.6, (95% purity). ¹H NMR (400 MHz, CDCl₃): δ 7.04 (s, 1H), 8.22 (s, 1H). ¹³C NMR (101 MHz, CDCl₃): δ 86.2, 109.5, 140.5, 145.0, 146.3, 150.6. Analysis consistent with literature.³⁶⁷

3-bromo-5-chloropyrazolo[1,5-*a*]pyrimidin-7-amine



A suspension of 3-bromo-5,7-dichloropyrazolo[1,5-*a*]pyrimidine **3.136** (865 mg, 3.24 mmol) in 33% ammonium hydroxide solution (15 mL, 385 mmol) in a sealed tube was heated to 85 °C in an oil bath for 18 h. The reaction mixture was cooled and evaporated to dryness. The residue was suspended

in water and filtered, the solid was washed with water (20 mL) and Et₂O (20 mL) and dried under vacuum to afford 3-bromo-5-chloropyrazolo[1,5-*a*]pyrimidin-7-amine (640 mg, 2.59 mmol, 80%) as a yellow solid.

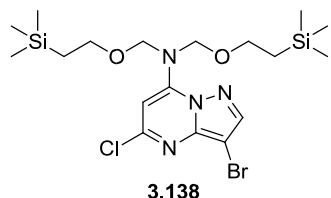
LCMS (High pH, ES⁺): t_R = 0.82 min, [M+H]⁺ 247.2, 249.0, 250.9, (99% purity). ¹H NMR (400 MHz, DMSO-*d*₆): δ 6.11 (s, 1H), 8.28 (br. s, 2H), 8.27 (s, 1H).

¹³C NMR (101 MHz, DMSO-*d*₆): δ 81.2, 87.5, 144.7, 145.0, 149.7, 151.6.

ν_{\max} (neat): 3447, 3089, 7645, 1592, 1558, 1463, 1350, 1332, 1305, 1154, 1142, 1185, 1050, 980, 911, 787 cm^{-1} .

HRMS: ($\text{C}_6\text{H}_4\text{N}_4\text{ClBr}$) $[\text{M}+\text{H}]^+$ requires 246.9381, found $[\text{M}+\text{H}]^+$ 246.9385.

3-Bromo-5-chloro-*N,N*-bis((2-(trimethylsilyl)ethoxy)methyl)pyrazolo[1,5-*a*]pyrimidin-7-amine

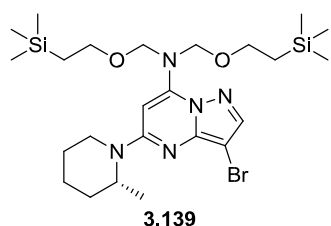


To a suspension of 3-bromo-5-chloropyrazolo[1,5-*a*]pyrimidin-7-amine **3.137** (640 mg, 2.59 mmol) and DIPEA (2.71 mL, 15.52 mmol) in DCM (7 mL) was added SEM-Cl (1.84 mL, 10.34 mmol), and the reaction was heated to 45 °C for 8 h. The reaction mixture was cooled and diluted with DCM (10 mL) and water (15 mL) and extracted. The organic layer was washed with water (15 mL) and the combined aqueous layers were extracted with DCM (10 mL). The combined organics were dried through a hydrophobic frit and evaporated. The crude product was purified by silica chromatography (0-10% EtOAc/cyclohexane), fractions were evaporated *in vacuo* to afford 3-bromo-5-chloro-*N,N*-bis((2-(trimethylsilyl)ethoxy)methyl)pyrazolo[1,5-*a*]pyrimidin-7-amine (1.16 g, 2.055 mmol, 79%) as a colourless oil.

LCMS (High pH, ES⁺): t_{R} = 1.79 min, $[\text{M}+\text{H}]^+$ 507.2, 509.2, 511.2, (95% purity). ¹H NMR (400 MHz, CDCl_3): δ 0.00-0.03 (m, 18H), 0.93-0.98 (m, 4H), 3.65-3.71 (m, 4H), 5.24 (s, 4H), 6.57 (s, 1H), 8.03 (s, 1H). ¹³C NMR (101 MHz, CDCl_3): δ -1.4, 18.1, 66.2, 79.7, 94.3, 95.1, 144.1, 146.3, 149.3, 152.6. ν_{\max} (neat): 2953, 1603, 1543, 1248, 1156, 1072, 976, 913, 856, 831, 758, 692 cm^{-1} .

HRMS: ($\text{C}_{18}\text{H}_{32}\text{N}_4\text{O}_2\text{Si}_2\text{BrCl}$) $[\text{M}+\text{H}]^+$ requires 507.1009, found $[\text{M}+\text{H}]^+$ 507.1011.

(*R*)-3-Bromo-5-(2-methylpiperidin-1-yl)-*N,N*-bis((2-(trimethylsilyl)ethoxy)methyl)pyrazolo[1,5-*a*]pyrimidin-7-amine



To a solution of 3-bromo-5-chloro-*N,N*-bis((2-(trimethylsilyl)ethoxy)methyl)pyrazolo[1,5-*a*]pyrimidin-7-amine **3.138** (400 mg, 0.709 mmol) and sodium carbonate (751 mg, 7.09 mmol) in NMP (1.5 mL) in a sealed tube was added (*R*)-2-methylpiperidine (0.384 mL, 3.19 mmol). The reaction was heated to 110 °C for 20 h. The reaction was diluted with water (20 mL) and the aqueous layer was extracted with diethyl ether (4 x 30 mL). The combined organics were washed with brine, dried through a hydrophobic frit evaporated to dryness. The crude product was purified by silica chromatography (0-8% EtOAc/cyclohexane), fractions were evaporated *in vacuo* to afford (*R*)-3-bromo-5-(2-methylpiperidin-1-yl)-*N,N*-bis((2-(trimethylsilyl)ethoxy)methyl)pyrazolo[1,5-*a*]pyrimidin-7-amine (374 mg, 0.655 mmol, 92%) as a colourless gum.

LCMS (High pH, ES⁺): t_R = 1.93 min, [M+H]⁺ 570.4, 572.3, (100% purity) ¹H NMR (400 MHz, CDCl₃): δ -0.02 (s, 18H), 0.85-0.96 (m, 4H), 1.21 (d, J = 6.8 Hz, 3H), 1.48-1.84 (m, 6H), 2.99 (td, J = 13.1, 3.1 Hz, 1H), 3.56-3.65 (m, 4H), 4.35-4.44 (m, 1H),

4.62-4.72 (m, 1H), 5.09 (s, 4H), 6.14 (s, 1H), 7.76 (s, 1H). ¹³C NMR (101 MHz CDCl₃): δ -1.4, 14.9, 18.1, 18.8, 25.7, 30.4, 39.3, 47.2, 65.8, 78.3, 80.2,

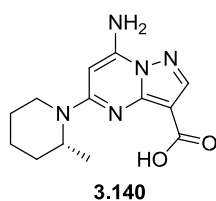
83.9, 143.0, 147.2, 148.9, 157.3.

[α_D]^{22 °C} = -37 (c = 0.21, MeOH). ν_{max} (neat): 2950, 1624, 1558, 1515, 1454,

1249, 1067, 855, 836 cm⁻¹. HRMS: (C₂₄H₄₄N₅O₂Si₂Br) [M+H]⁺ requires

570.2290, found [M+H]⁺ 570.2295.

(R)-7-Amino-5-(2-methylpiperidin-1-yl)pyrazolo[1,5-a]pyrimidine-3-carboxylic acid



To a solution of ⁿBuLi (1.6 M in hexanes, 2.19 mL, 3.50 mmol) in THF (3.5 mL) stirred under N₂ at -78 °C was added a solution of (R)-3-bromo-5-(2-methylpiperidin-1-yl)-N,N-

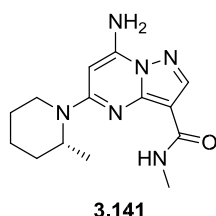
bis((2(trimethylsilyl)ethoxy)methyl)pyrazolo[1,5-a]pyrimidin-7-amine

3.139 (200 mg, 0.350 mmol) in THF (3.5 mL). The reaction mixture was

stirred at -78 °C for 20 min. Dry ice was sublimed in a separate flask at rt and the resulting CO₂ was bubbled through the reaction at -78 °C, with gradual warming to rt, for 4 h. The reaction mixture was quenched with 2 M HCl and stirred at rt for 2 days. The aqueous layer was adjusted to pH 6 and extracted with EtOAc (4 x 10 mL) and the combined organics were washed with brine, dried using a hydrophobic frit and evaporated *in vacuo*. The crude product was purified by Formic MDAP and the solvent was evaporated *in vacuo* to give (R)-7-amino-5-(2-methylpiperidin-1-yl)pyrazolo[1,5-a]pyrimidine-3-carboxylic acid (17 mg, 0.056 mmol, 16%) as an off-white solid.

LCMS (Formic, ES⁺): t_R = 0.78 min, [M+H]⁺ 276.1, (89% purity). ¹H NMR (400 MHz, DMSO-d₆) δ 1.16 (d, J=6.8 Hz, 3 H), 1.32-1.48 (m, 1 H), 1.52-1.79 (m, 5 H), 2.93 (td, J=13.1, 2.6 Hz, 1 H), 4.19-4.30 (m, 1 H), 4.53-4.64 (m, 1 H), 5.64 (s, 1 H), 7.32 (s, 2 H), 8.13 (s, 1 H), 8.34 (s, 1 H). 90% pure, used for further chemistry without further purification.

(R)-7-Amino-N-methyl-5-(2-methylpiperidin-1-yl)pyrazolo[1,5-a]pyrimidine-3carboxamide



(R)-7-amino-5-(2-methylpiperidin-1-yl)pyrazolo[1,5-a]pyrimidine-3carboxylic acid 3.140 (22 mg, 0.080 mmol) and HATU (37 mg, 0.096 mmol) in DMF (1 mL) was added DIPEA (0.028 mL, 0.160 mmol) and MeNH₂ (0.120 mL, 2 M in THF, 0.240 mmol). The reaction mixture was stirred at rt for 3 h. Further HATU (36.5 mg, 0.096 mmol) and MeNH₂

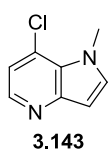
(0.120 mL, 2 M in THF, 0.240 mmol) were added and the reaction was stirred at rt for 3 days. The reaction mixture was diluted with water (20 mL) and extracted with EtOAc (3 x 10 mL). The combined organics were washed with brine, dried through a

hydrophobic frit and evaporated to dryness. The crude product was purified by silica chromatography (10-70% (3:1 EtOAc:EtOH)/cyclohexane), fractions were evaporated *in vacuo* and further purified by High pH MDAP to afford (*R*)-7-amino-*N*-methyl-5-(2methylpiperidin-1-yl)pyrazolo[1,5-*a*]pyrimidine-3-carboxamide (2 mg, 6.94 μ mol, 9%) as a white solid.

LCMS (High pH, ES⁺): t_R = 0.91 min, [M+H]⁺ 289.3, (100% purity). ¹H NMR (400 MHz, DMSO-*d*₆): δ 1.17 (d, J = 6.8 Hz, 3H), 1.35-1.53 (m, 1H), 1.54-1.81 (m, 5H), 2.84 (d, J = 4.8 Hz, 3H), 2.97 (td, J = 13.1, 2.9 Hz, 1H), 4.08-4.18 (m, 1H), 4.49-4.59 (m, 1H), 5.63 (s, 1H), 7.33 (s, 2H), 7.81 (q, J = 4.8 Hz, 1H), 8.09 (s, 1H). ¹³C NMR (126 MHz, DMSO-*d*₆): δ 14.9, 18.7, 25.6, 25.8, 30.4, 39.1, 47.3, 73.4, 100.9, 144.1, 147.1, 149.1, 158.3, 163.4.

ν_{max} (neat): 3329, 3194, 2939, 1664, 1623, 1564, 1488, 1379, 1239, 1179, 1130, 871, 778, 765, 674 cm^{-1} .

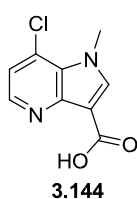
HRMS: (C₁₄H₂₀N₆O) [M+H]⁺ requires 289.1771, found [M+H]⁺ 289.1774. **7-Chloro-1-methyl-1*H*-pyrrolo[3,2-*b*]pyridine**



To a solution of 7-chloro-1*H*-pyrrolo[3,2-*b*]pyridine **3.142** (445 mg, 2.92 mmol) in DMF (10 mL) at 0 °C was added sodium hydride (60% in mineral oil, 350 mg, 8.75 mmol), and the reaction was stirred for 15 min. Methyl iodide (0.365 mL, 5.83 mmol) was added and the reaction was stirred at 0 °C for 1 h. The reaction was quenched with water (100 mL) and the aqueous layer was extracted with diethyl ether (3 x 20 mL). The combined organics were washed with brine, dried through a hydrophobic frit and evaporated to dryness. Purified by silica chromatography (10-90% EtOAc/cyclohexane) the appropriate fractions were evaporated to dryness to afford 7-chloro-1-methyl-1*H*-pyrrolo[3,2-*b*]pyridine (350 mg, 2.101 mmol, 72%) as a white solid.

LCMS (High pH, ES⁺): t_R = 0.85 min, [M+H]⁺ 167.1, (100% purity) ¹H NMR (400 MHz, CDCl₃): δ 4.15 (s, 3H), 6.70 (d, J = 3.2 Hz, 1H), 7.10 (d, J = 5.1 Hz, 1H), 7.26 (d, J = 3.2 Hz, 1H), 8.30 (d, J = 5.1 Hz, 1H).

7-Chloro-1-methyl-1*H*-pyrrolo[3,2-*b*]pyridine-3-carboxylic acid



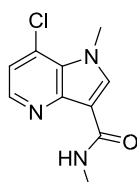
To DMF (1.7 mL) at 0 °C under N₂ was added POCl₃ (380 μ L, 4.08 mmol), and the reaction was stirred at 0°C for 15 min. To this solution was added a solution of 7-chloro-1-methyl-1*H*-pyrrolo[3,2-*b*]pyridine **3.143** (340 mg, 2.041 mmol) in DMF (3.4 mL) dropwise. The reaction mixture was stirred at rt for 18 h. Further POCl₃ (380 μ L, 4.08 mmol) was added and the reaction was heated

to 60 °C for 18 h. Further POCl₃ (200 μ L, 2.15 mmol) was added and the reaction was heated to 60 °C for 18 h. The reaction mixture was poured into an ice/water mixture and the pH was adjusted to 7 by adding 2 N NaOH. The aqueous was extracted with EtOAc (5 x 20 mL) and the combined organic layers were dried through a hydrophobic frit and evaporated *in vacuo*. and water (2.5 mL) and cooled to 0°C. Sulfamic acid (691 mg, 7.12 mmol) was added, followed by a solution of sodium chlorite (201 mg, 1.780 mmol) and sodium dihydrogen phosphate (1.71 g, 14.24 mmol) in water (8 mL) dropwise. The reaction was stirred at rt for 18 h. A precipitate

had formed and was filtered off, washed with diethyl ether and dried under vacuum to afford 7-chloro-1-methyl-1*H*-pyrrolo[3,2-*b*]pyridine-3-carboxylic acid (135 mg, 0.641 mmol, 31% over two steps) as a white solid.

LCMS (Formic, ES⁺): $t_R = 0.37$ min, [M+H]⁺ 211.0, (100% purity). ¹H NMR (400 MHz, DMSO-*d*₆): δ 4.16 (s, 3H), 7.39 (d, $J = 5.1$ Hz, 1H), 8.40 (d, $J = 5.1$ Hz, 1H), 8.40 (s, 1H), 9.06-11.73 (m, 1H).

7-Chloro-*N*,1-dimethyl-1*H*-pyrrolo[3,2-*b*]pyridine-3-carboxamide



3.145

To a solution of 7-chloro-1-methyl-1*H*-pyrrolo[3,2-*b*]pyridine-3-carboxylic acid **3.144** (135 mg, 0.641 mmol) and HATU (292 mg, 0.769 mmol) in DMF (2.5 mL) was added DIPEA (168 μ L, 0.961 mmol) and MeNH₂ (961 μ L, 2 M in THF, 1.923 mmol). The reaction mixture was stirred at rt for 2 h. The reaction mixture was diluted with EtOAc (10 mL) and sat. aq. NaHCO₃ (20 mL). The aqueous phase was extracted with EtOAc (3 x 10 mL), dried through a hydrophobic frit and evaporated to dryness. The residue was purified by silica chromatography (10-50% (3:1 EtOAc:EtOH)/cyclohexane) and the appropriate fractions evaporated to dryness to afford 7-chloro-*N*,1-dimethyl-1*H*-pyrrolo[3,2-*b*]pyridine-3-carboxamide (85 mg, 0.380 mmol, 59%) as a white solid. LCMS (High pH, ES⁺): $t_R = 0.86$ min, [M+H]⁺ 224.23, (100% purity). ¹H NMR (400 MHz, DMSO-*d*₆): δ 2.90 (d, $J = 4.6$ Hz, 3H), 4.15 (s, 3H), 7.39 (d, $J = 5.1$ Hz, 1H), 8.28 (s, 1H), 8.39 (d, $J = 5.1$ Hz, 1H), 8.55 (q, $J = 4.6$ Hz, 1H).

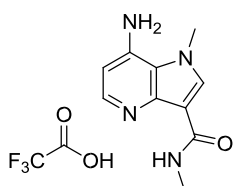
¹³

C NMR (101 MHz, DMSO-*d*₆): δ 25.8, 37.2, 110.2, 118.8, 126.1, 127.2, 139.5, 144.3, 145.0, 163.1.

M.pt.: 184-188 °C. ν_{max} (neat): 3305, 3095, 1645, 1601, 1563, 1444, 1403, 1336, 1316, 1296, 1267, 1211, 1139, 1088, 850, 828, 808, 783 cm⁻¹.

HRMS: (C₁₀H₁₀N₃OCl) [M+H]⁺ requires 224.0585, found [M+H]⁺ 224.0575.

7-Amino-*N*,1-dimethyl-1*H*-pyrrolo[3,2-*b*]pyridine-3-carboxamide, TFA salt



3.146

7-Chloro-*N*,1-dimethyl-1*H*-pyrrolo[3,2-*b*]pyridine-3-carboxamide **3.145** (40 mg, 0.179 mmol), sodium *tert*-butoxide (51.6 mg, 0.537 mmol), PdOAc₂ (4.02 mg, 0.018 mmol) and BINAP (22.27 mg, 0.036 mmol) were dissolved in 1,4-dioxane (1.2 mL) and stirred at rt for 10 min under N₂. 4-Methoxybenzylamine (0.047 mL, 0.358 mmol) was added and the reaction was heated to 100 °C in an oil bath for 6 h. The reaction mixture was filtered through Celite and evaporated to dryness. The residue was dissolved in TFA (1 mL) and stirred at rt for 3 h. The reaction mixture was purified by ion exchange chromatography (2 g SCX, MeOH/2 M NH₃ in MeOH), solvent was evaporated *in vacuo* and the product was further purified by silica chromatography (0-10% 2 M NH₃ in MeOH/DCM). The fractions were evaporated *in vacuo* and the product was further purified by HPLC³⁸⁵ (CSH C18 150 x 30 mm,

5 μm column using MeCN/water with a TFA modifier), affording 7-amino-*N*,1-dimethyl-1*H*-pyrrolo[3,2-*b*]pyridine-3-carboxamide, trifluoroacetic acid salt (41 mg, 0.129 mmol, 72%).

LCMS (High pH, ES⁺): t_{R} = 0.56 min, [M+H]⁺ 205.2, (69% purity). ¹H NMR (400 MHz, DMSO-*d*₆): δ 2.81 (d, J = 4.5 Hz, 3H), 4.13 (s, 3H), 6.63 (d, J = 6.6 Hz, 1H), 7.11 (t, J = 50.4 Hz, 1H), 7.81-7.98 (m, 1H), 7.94 (t, J = 6.6 Hz, 1H), 8.15 (s, 1H), 8.38 (q, J = 4.5 Hz, 1H), 12.87 (br. s., 1H).¹⁹

¹⁹F NMR (376 MHz, DMSO-*d*₆): δ -73.99.

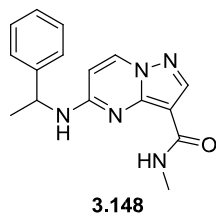
¹³C NMR (101 MHz, DMSO-*d*₆): δ 25.8, 37.9, 103.4, 104.8, 117.8, 135.5, 135.8, 136.8, 148.6, 163.2. TFA salt carbon not observed.

M.pt.: 145-147 °C.

ν_{max} (neat): 3233, 1642, 1616, 1572, 1489, 1415, 1363, 1304, 1191, 1151, 1129, 785, 725, 705 cm^{-1} .

HRMS: (C₁₀H₁₂N₄O) [M+H]⁺ requires 205.1084, found [M+H]⁺ 205.1082.

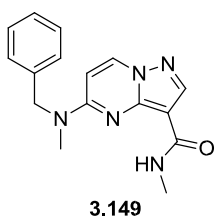
***N*-Methyl-5-((1-phenylethyl)amino)pyrazolo[1,5-*a*]pyrimidine-3-carboxamide**



Prepared according to General Procedure C, with **3.030** (25 mg, 0.119 mmol), α -methylbenzylamine (22 mg, 0.178 mmol) and DIPEA (42 μL , 0.237 mmol) at rt, affording *N*-methyl-5-((1-phenylethyl)amino)pyrazolo[1,5-*a*]pyrimidine-3-carboxamide (32 mg, 0.108 mmol, 91%).

LCMS (High pH, ES⁺): t_{R} = 0.85 min, [M+H]⁺ 296.2, (100% purity). ¹H NMR (400 MHz, CDCl₃): δ 1.66 (d, J = 6.8 Hz, 3H), 2.95 (d, J = 4.9 Hz, 3H), 5.00-5.11 (m, 1H), 5.38-5.48 (m, 1H), 6.13 (d, J = 7.8 Hz, 1H), 7.29-7.43 (m, 6H), 8.24 (d, J = 7.8 Hz, 1H), 8.33 (s, 1H).

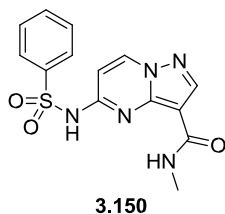
5-(Benzyl(methyl)amino)-*N*-methylpyrazolo[1,5-*a*]pyrimidine-3-carboxamide



Prepared according to General Procedure C, with **3.030** (25 mg, 0.119 mmol), *N*-methylbenzylamine (22 mg, 0.178 mmol) and DIPEA (42 μL , 0.237 mmol) at rt, affording 5-(benzyl(methyl)amino)-*N*-methylpyrazolo[1,5-*a*]pyrimidine-3-carboxamide (15 mg, 0.051 mmol, 43%).

LCMS (High pH, ES⁺): t_{R} = 0.88 min, [M+H]⁺ 296.2, (100% purity). ¹H NMR (400 MHz, CDCl₃): δ 2.97 (d, J = 4.4 Hz, 3H), 3.31 (s, 3H), 4.86 (s, 2H), 6.37 (d, J = 7.8 Hz, 1H), 7.22-7.43 (m, 5H), 7.51-7.72 (m, 1H), 8.31 (d, J = 7.8 Hz, 1H), 8.40 (s, 1H).

***N*-Methyl-5-(phenylsulfonamido)pyrazolo[1,5-*a*]pyrimidine-3-carboxamide**



To a suspension of **3.030** (40 mg, 0.190 mmol) and cesium carbonate (186 mg, 0.570 mmol) in DME (3 mL) was added benzenesulfonamide (45 mg, 0.285 mmol) and the reaction mixture was stirred at 90 °C for 18 h. The reaction was diluted with EtOAc (10 mL) and 1 M HCl (20 mL) and the aqueous phase was extracted with EtOAc (4 x 10 mL). The combined organics were washed with brine, dried through a hydrophobic frit and evaporated to dryness. The residue was purified by silica chromatography (0-15% MeOH/DCM), appropriate fractions were evaporated *in vacuo* to afford *N*-methyl-5-(phenylsulfonamido)pyrazolo[1,5-*a*]pyrimidine-3-carboxamide (40 mg, 0.121 mmol, 64%) as a white solid.

LCMS (Formic, ES⁺): t_R = 0.68 min, [M+H]⁺ 332.0, (100% purity).

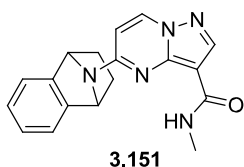
¹H NMR (400 MHz, DMSO-*d*₆): δ 2.85 (d, *J* = 4.6 Hz, 3H), 6.57 (d, *J* = 7.6 Hz, 1H), 7.43-7.50 (m, 1H), 7.56-7.67 (m, 3H), 7.94 (dd, *J* = 7.7, 1.8 Hz, 2H), 8.19 (s, 1H), 8.82 (d, *J* = 7.3 Hz, 1H), 12.10-12.52 (m, 1H).

¹³C NMR (101 MHz, DMSO-*d*₆): δ 25.7, 102.8, 103.2, 126.9, 129.6, 132.9, 138.1, 142.2, 145.1, 145.2, 154.8, 162.4. M.pt.: 235-238 °C.

ν_{max} (neat): 2928, 1625, 1572, 1466, 1420, 1344, 1236, 1162, 1124, 1082, 896, 809, 775, 750, 718, 687 cm⁻¹.

HRMS: (C₁₄H₁₃N₅O₃S) [M+H]⁺ requires 332.0812, found [M+H]⁺ 332.0808.

***N*-Methyl-5-(1,2,3,4-tetrahydro-1,4-epiminonaphthalen-9-yl)pyrazolo[1,5-*a*]pyrimidine-3-carboxamide**



Prepared according to General Procedure C, with **3.030** (25 mg, 0.119 mmol), 1,2,3,4-tetrahydro-1,4-epiminonaphthalene (25.9 mg, 0.178 mmol) and DIPEA (42 μL, 0.237 mmol) at 90 °C, affording *N*-methyl-5-(1,2,3,4-tetrahydro-1,4-epiminonaphthalen-9-yl)pyrazolo[1,5-*a*]pyrimidine-3-carboxamide (32 mg, 0.100 mmol, 84%) as an off-white solid.

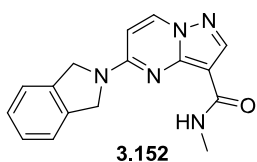
LCMS (High pH, ES⁺): t_R = 0.95 min, [M+H]⁺ 320.2, (100% purity). ¹H NMR (400 MHz, DMSO-*d*₆): δ 1.32-1.38 (m, 2H), 2.09-2.17 (m, 2H), 2.94 (d, *J* = 4.6 Hz, 3H), 5.84 (br. s., 2H), 6.88 (d, *J* = 7.8 Hz, 1H), 7.18 (dd, *J* = 5.4, 3.0 Hz, 2H), 7.39 (dd, *J* =

5.4, 3.0 Hz, 2H), 7.68 (q, *J* = 4.6 Hz, 1H), 8.19 (s, 1H), 8.80 (d, *J* = 7.8 Hz, 1H).

¹³C NMR (101 MHz, DMSO-*d*₆): δ 26.2, 26.5, 61.4, 100.3, 102.4, 120.2, 127.0, 137.8, 145.0, 145.4, 145.8, 156.3, 162.7. M.pt.: 128-131 °C ν_{max} (neat): 3355, 2950, 1628, 1567, 1480, 1434, 1351, 1225, 1174, 1113, 1080, 911, 886, 842, 800, 774, 759, 691 cm⁻¹.

HRMS: (C₁₈H₁₇N₅O) [M+H]⁺ requires 320.1506, found [M+H]⁺ 320.1520.

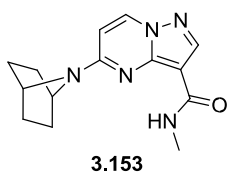
5-(Isoindolin-2-yl)-*N*-methylpyrazolo[1,5-*a*]pyrimidine-3-carboxamide



Prepared according to General Procedure C, with **3.030** (20 mg, 0.095 mmol), isoindoline (16 μ L, 0.142 mmol) and DIPEA (33 μ L, 0.190 mmol) at rt. The product precipitated from the reaction mixture and was collected by filtration, then washed with EtOAc and dried under vacuum to afford 5-(isoindolin-2-yl)-*N*-methylpyrazolo[1,5-*a*]pyrimidine-3-carboxamide (18 mg, 0.061 mmol, 64%) as a white solid.

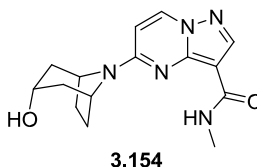
LCMS (High pH, ES⁺): t_R = 0.91 min, [M+H]⁺ 294.2, (99% purity). ¹H NMR (400 MHz, CDCl₃): δ 3.12 (d, J = 4.9 Hz, 3H), 4.93 (br. s., 2H), 5.05 (br. s., 2H), 6.35 (d, J = 7.6 Hz, 1H), 7.35-7.50 (m, 4H), 7.74-7.85 (m, 1H), 8.41 (d, J = 7.6 Hz, 1H), 8.44

(s, 1H) **5-(7-Azabicyclo[2.2.1]heptan-7-yl)-*N*-methylpyrazolo[1,5-*a*]pyrimidine-3-**



carboxamide Prepared according to General Procedure C, with **3.030** (20 mg, 0.095 mmol), 7-azabicyclo[2.2.1]heptane hydrochloride (19 mg, 0.142 mmol) and DIPEA (33 μ L, 0.190 mmol) at 90 °C, affording 5-(7-azabicyclo[2.2.1]heptan-7-yl)-*N*-methylpyrazolo[1,5-*a*]pyrimidine-3-carboxamide (4 mg, 0.015 mmol, 16%) as a yellow solid. LCMS (High pH, ES⁺): t_R = 0.84 min, [M+H]⁺ 272.2, (97% purity). ¹H NMR (400 MHz, CDCl₃): δ 1.59-1.67 (m, 4H), 1.91 (s, 4H), 3.06 (d, J = 4.6 Hz, 3H), 4.59 (br. s., 2H), 6.34 (d, J = 7.8 Hz, 1H), 7.70 (br. s., 1H), 8.29 (d, J = 7.6 Hz, 1H), 8.40 (s, 1H).

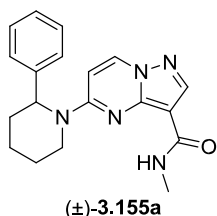
5-(3-Hydroxy-8-azabicyclo[3.2.1]octan-8-yl)-*N*-methylpyrazolo[1,5-*a*]pyrimidine-3-carboxamide



Prepared according to General Procedure C, with **3.030** (20 mg, 0.095 mmol), nortropine (18 mg, 0.142 mmol) and DIPEA (33 μ L, 0.190 mmol) at rt, affording 5-(3-hydroxy-8-azabicyclo[3.2.1]octan-8-yl)-*N*-methylpyrazolo[1,5-*a*]pyrimidine-3-carboxamide (20 mg, 0.066 mmol, 70%) as a white solid.

LCMS (High pH, ES⁺): t_R = 0.65 min, [M+H]⁺ 302.1, (100% purity). ¹H NMR (400 MHz, DMSO-*d*₆): δ 1.77 (d, J = 13.9 Hz, 2H), 1.83-2.21 (m, 4H), 2.35 (d, J = 7.3 Hz, 2H), 2.86 (d, J = 4.6 Hz, 3H), 3.89 (br. s., 1H), 4.45-4.60 (m, 1H), 4.69 (d, J = 2.4 Hz, 1H), 4.76-4.91 (m, 1H), 6.69 (d, J = 7.8 Hz, 1H), 7.66 (q, J = 4.6 Hz, 1H), 8.11 (s, 1H), 8.68 (d, J = 7.8 Hz, 1H).

(±)-*N*-Methyl-5-(2-phenylpiperidin-1-yl)pyrazolo[1,5-*a*]pyrimidine-3-carboxamide



Prepared according to General Procedure C, with **3.030** (40 mg, 0.190 mmol), 2-phenylpiperidine (46 mg, 0.285 mmol) and DIPEA (66 μ L, 0.380 mmol) at 90 °C. The reaction mixture was diluted with EtOAc (10 mL) and sat. aq NaHCO₃ (10 mL) and the aqueous was extracted with EtOAc (3 x 10 mL). The combined organics were washed with brine, evaporated to dryness and purified by silica chromatography (10-70% (3:1 EtOAc:EtOH)/cyclohexane), appropriate fractions were evaporated *in vacuo* and further

purified by ion-exchange chromatography (sulphonic acid (SCX) 2 g, eluting with methanol). The solvent was evaporated *in vacuo* to give *N*-methyl-5-(2-phenylpiperidin-1-yl)pyrazolo[1,5-*a*]pyrimidine-3-carboxamide (50 mg, 0.149 mmol, 78%) as a white solid.

LCMS (High pH, ES⁺): $t_R = 1.03$ min, $[M+H]^+$ 336.3, (89% purity). ¹H NMR (400 MHz, CDCl₃): δ 1.64-1.94 (m, 4H), 2.07-2.19 (m, 1H), 2.40 (dq, $J = 13.8, 3.4$ Hz, 1H), 2.95 (d, $J = 4.6$ Hz, 3H), 3.37 (ddd, $J = 13.8, 11.5, 4.0$ Hz, 1H), 4.31-4.42 (m, 1H),

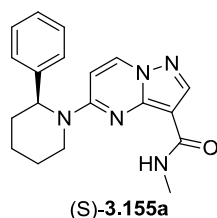
5.60 (br. s., 1H), 6.40 (d, $J = 8.0$ Hz, 1H), 7.22-7.33 (m, 3H), 7.34-7.43 (m, 2H), 7.51 (br. s., 1H), 8.28 (d, $J = 8.0$ Hz, 1H), 8.38 (s, 1H).

¹³C NMR (101 MHz, CDCl₃): δ 18.6, 24.5, 25.7, 29.5, 41.7, 56.0, 96.9, 102.1, 126.2, 127.1, 128.9, 136.1, 139.8, 146.2, 146.2, 156.6, 163.8. M.pt.: 206-208 °C.

ν_{max} (neat): 1631, 1655, 1441, 1267, 1225, 1180, 1128, 1023, 894, 776, 697 cm⁻¹.

HRMS: (C₁₉H₂₁N₅O) $[M+H]^+$ requires 336.1819, found $[M+H]^+$ 336.1817.

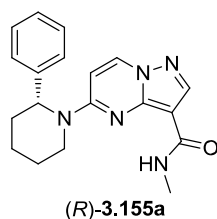
(*S*)-*N*-Methyl-5-(2-phenylpiperidin-1-yl)pyrazolo[1,5-*a*]pyrimidine-3-carboxamide



Prepared according to General Procedure C, with **3.030** (23 mg, 0.109 mmol), (*S*)-2-phenylpiperidine (26 mg, 0.164 mmol) and DIPEA (38 μ L, 0.218 mmol) at 90 °C, affording (*S*)-*N*-methyl-5-(2-phenylpiperidin-1-yl)pyrazolo[1,5-*a*]pyrimidine-3-carboxamide (13 mg, 0.038 mmol, 35%).
LCMS (High pH, ES⁺): $t_R = 1.03$ min, $[M+H]^+$ 336.3, (100% purity).

$[\alpha_D]^{22} = -231$ ($c = 0.2$, MeOH). >99% ee by chiral HPLC. NMR consistent with racemate.

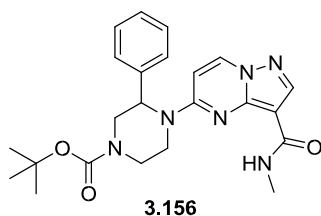
(*R*)-*N*-Methyl-5-(2-phenylpiperidin-1-yl)pyrazolo[1,5-*a*]pyrimidine-3-carboxamide



Prepared according to General Procedure C, with **3.030** (23 mg, 0.109 mmol), (*R*)-2-phenylpiperidine (26 mg, 0.164 mmol) and DIPEA (38 μ L, 0.218 mmol) at 90 °C, affording (*S*)-*N*-methyl-5-(2-phenylpiperidin-1-yl)pyrazolo[1,5-*a*]pyrimidine-3-carboxamide (22 mg, 0.064 mmol, 59%).
LCMS (High pH, ES⁺): $t_R = 1.03$ min, $[M+H]^+$ 336.3, (100% purity).

$[\alpha_D]^{22} = +110$ ($c = 0.2$, MeOH). >99% ee by chiral HPLC. NMR consistent with racemate.

tert-Butyl 4-(3-(methylcarbamoyl)pyrazolo[1,5-*a*]pyrimidin-5-yl)-3-phenylpiperazine-1-carboxylate

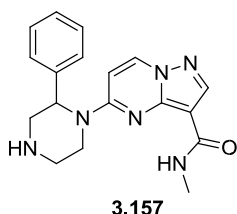


Prepared according to General Procedure C, with **3.030** (20 mg, 0.095 mmol), *tert*-butyl 3-phenylpiperazine-1-carboxylate (37 mg, 0.142 mmol) and DIPEA (33 μ L, 0.190 mmol) at 90 °C for 2 hr. Further *tert*-butyl 3-phenylpiperazine-1-carboxylate (37 mg, 0.142 mmol) was added and the reaction was heated to 90

°C for a further 1 hr. The product was purified by High pH MDAP and ion exchange chromatography (sulphonic acid (SCX) 1 g, eluting with MeOH), fractions were evaporated to give *tert*-butyl 4-(3-(methylcarbamoyl)pyrazolo[1,5-*a*]pyrimidin-5-yl)-3-phenylpiperazine-

1carboxylate (17 mg, 0.039 mmol, 41%) as an off-white solid. LCMS (High pH, ES⁺): t_R = 1.04 min, [M+H]⁺ 437.2, (100% purity). ¹H NMR (400 MHz, CDCl₃): δ 1.32-1.48 (m, 9H), 2.96 (d, J = 3.9 Hz, 3H), 3.38-3.65 (m, 1H), 3.71-3.90 (m, 2H), 3.91-4.09 (m, 1H), 4.11-4.48 (m, 2H), 5.39 (br. s., 1H), 6.26-6.37 (m, 1H), 7.29-7.43 (m, 6H), 8.31 (d, J = 7.6 Hz, 1H), 8.40 (s, 1H).

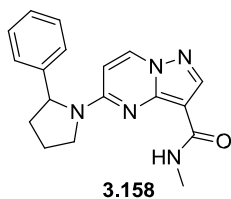
***N*-Methyl-5-(2-phenylpiperazin-1-yl)pyrazolo[1,5-*a*]pyrimidine-3-carboxamide**



Prepared according to General Procedure D with *tert*-butyl 4-(3-(methylcarbamoyl)pyrazolo[1,5-*a*]pyrimidin-5-yl)-3-phenylpiperazine-1-carboxylate **3.156** (17 mg, 0.039 mmol) and TFA (120 μL, 1.558 mmol) in DCM (0.4 mL), at rt for 18 h, affording *N*-methyl-5-(2-phenylpiperazin-1-yl)pyrazolo[1,5-*a*]pyrimidine-3-carboxamide (12 mg, 0.036 mmol, 92%) as a yellow solid.

LCMS (High pH, ES⁺): t_R = 0.70 min, [M+H]⁺ 337.3, (100% purity). ¹H NMR (400 MHz, DMSO-*d*₆): δ 2.79 (d, J = 4.6 Hz, 3H), 2.83 (td, J = 11.7, 3.9 Hz, 1H), 3.06-3.13 (m, 1H), 3.16 (dd, J = 12.7, 5.1 Hz, 1H), 3.31-3.42 (m, 3H), 4.30-4.41 (m, 1H), 5.50-5.57 (m, 1H), 6.81 (d, J = 7.8 Hz, 1H), 7.19-7.26 (m, 1H), 7.29-7.38 (m, 4H), 7.42-7.50 (m, 1H), 8.13 (s, 1H), 8.72 (d, J = 7.8 Hz, 1H).

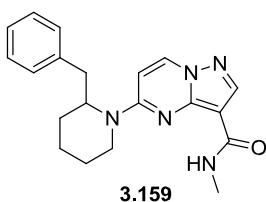
***N*-Methyl-5-(2-phenylpyrrolidin-1-yl)pyrazolo[1,5-*a*]pyrimidine-3-carboxamide**



Prepared according to General Procedure C, with **3.030** (20 mg, 0.095 mmol), 2-phenylpyrrolidine (21 mg, 0.142 mmol) and DIPEA (33 μL, 0.190 mmol) at 90 °C for 90 min, affording *N*-Methyl-5-(2-phenylpyrrolidin-1-yl)pyrazolo[1,5-*a*]pyrimidine-3-carboxamide (23 mg, 0.072 mmol, 75%).

LCMS (High pH, ES⁺): t_R = 0.96 min, [M+H]⁺ 322.3, (100% purity). ¹H NMR (400 MHz, 393 K, DMSO-*d*₆): δ 1.88-1.97 (m, 1H), 2.02-2.16 (m, 2H), 2.48-2.58 (m, 1H), 2.76 (d, J = 4.9 Hz, 3H), 3.83 (dt, J = 10.7, 7.6 Hz, 1H), 3.95-4.03 (m, 1H), 5.26 (dd, J = 8.1, 3.7 Hz, 1H), 6.41 (q, J = 4.9 Hz, 1H), 7.20-7.39 (m, 6H), 8.05 (s, 1H), 8.55 (d, J = 7.6 Hz, 1H).

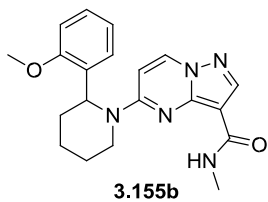
***N*-Methyl-5-(2-benzylpiperidin-1-yl)pyrazolo[1,5-*a*]pyrimidine-3-carboxamide**



Prepared according to General Procedure C, with **3.030** (20 mg, 0.095 mmol), 2-benzylpiperidine (25 mg, 0.142 mmol) and DIPEA (33 μL, 0.190 mmol) at 90 °C for 30 min. The reaction mixture was diluted with sat. aq. NaHCO₃ (15 mL) and EtOAc (15 mL) and the aqueous phase was extracted with EtOAc (3 x 10 mL). The

combined organics were dried through a hydrophobic frit, evaporated and purified by High pH MDAP. The solvent was evaporated *in vacuo* to give 5-(2-benzylpiperidin-1-yl)-*N*-methylpyrazolo[1,5-*a*]pyrimidine-3-carboxamide (24 mg, 0.069 mmol, 72%) as a yellow solid. LCMS (High pH, ES⁺): *t*_R = 1.08 min, [M+H]⁺ 350.3, (100% purity). ¹H NMR (400 MHz, CDCl₃): δ 1.61-1.99 (m, 6H), 2.97-3.02 (m, 2H), 3.06 (d, *J* = 4.9 Hz, 3H), 3.30 (td, *J* = 13.2, 2.7 Hz, 1H), 4.28 (br. s., 1H), 4.86 (br. s., 1H), 6.27 (d, *J* = 7.8 Hz, 1H), 7.18-7.25 (m, 3H), 7.26-7.33 (m, 2H), 7.63 (q, *J* = 4.9 Hz, 1H), 8.19 (d, *J* = 7.8 Hz, 1H), 8.38 (s, 1H).

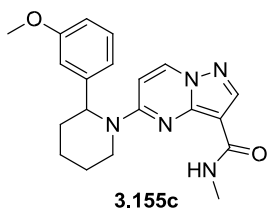
5-(2-(2-Methoxyphenyl)piperidin-1-yl)-*N*-methylpyrazolo[1,5-*a*]pyrimidine-3carboxamide



Prepared according to General Procedure C, with **3.030** (20 mg, 0.095 mmol), 2-(2-methoxyphenyl)piperidine (27 mg, 0.142 mmol) and DIPEA (33 μL, 0.190 mmol) at 90 °C for 1 h, affording 5-(2-(2-methoxyphenyl)piperidin-1-yl)-*N*-methylpyrazolo[1,5-*a*]pyrimidine-3carboxamide (26 mg, 0.071 mmol, 75%) as a yellow solid.

LCMS (High pH, ES⁺): *t*_R = 1.08 min, [M+H]⁺ 366.3, (94% purity). ¹H NMR (400 MHz, CDCl₃): δ 1.60-1.73 (m, 2H), 1.79-1.93 (m, 1H), 1.96-2.07 (m, 1H), 2.102.19 (m, 2H), 2.99 (d, *J* = 4.9 Hz, 3H), 3.64 (ddd, *J* = 13.4, 11.7, 4.9 Hz, 1H), 3.94 (s, 3H), 4.45-4.56 (m, 1H), 5.59 (t, *J* = 5.3 Hz, 1H), 6.25 (d, *J* = 7.8 Hz, 1H), 6.88 (ddd, *J* = 7.5, 7.5, 1.0 Hz, 1H), 6.96 (d, *J* = 8.1 Hz, 1H), 7.05 (dd, *J* = 7.5, 1.0 Hz, 1H), 7.23-7.28 (m, 1H), 7.60 (q, *J* = 4.9 Hz, 1H), 8.19 (d, *J* = 7.8 Hz, 1H), 8.35 (s, 1H).

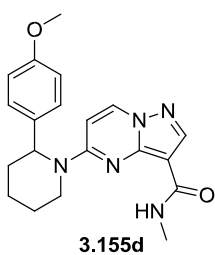
5-(2-(3-Methoxyphenyl)piperidin-1-yl)-*N*-methylpyrazolo[1,5-*a*]pyrimidine-3carboxamide



Prepared according to General Procedure C, with **3.030** (20 mg, 0.095 mmol), 2-(3-methoxyphenyl)piperidine (27 mg, 0.142 mmol) and DIPEA (33 μL, 0.190 mmol) at 90 °C for 90 min, affording 5-(2-(3-methoxyphenyl)piperidin-1-yl)-*N*-methylpyrazolo[1,5-*a*]pyrimidine-3-carboxamide (21 mg, 0.057 mmol, 61%) as a white solid.

LCMS (Formic, ES⁺): *t*_R = 1.01 min, [M+H]⁺ 366.2, (100% purity). ¹H NMR (400 MHz, CDCl₃): δ 1.57-1.93 (m, 4H), 2.12 (s, 1H), 2.35 (s, 1H), 2.95 (d, *J* = 4.9 Hz, 3H), 3.38 (ddd, *J* = 13.6, 11.5, 4.0 Hz, 1H), 3.80 (s, 3H), 4.30-4.39 (m, 1H), 5.55 (br. s., 1H), 6.39 (d, *J* = 7.8 Hz, 1H), 6.75-6.86 (m, 3H), 7.28-7.33 (m, 1H), 7.50 (q, *J* = 4.9 Hz, 1H), 8.27 (d, *J* = 7.8 Hz, 1H), 8.37 (s, 1H).

5-(2-(4-Methoxyphenyl)piperidin-1-yl)-*N*-methylpyrazolo[1,5-*a*]pyrimidine-3carboxamide



3.155d

1

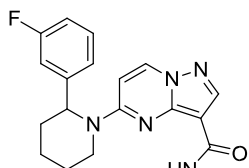
Prepared according to General Procedure C, with **3.030** (20 mg, 0.095 mmol), 2-(4-methoxyphenyl)piperidine (27 mg, 0.142 mmol) and DIPEA (33 μ L, 0.190 mmol) at 90 °C for 1 h, affording 5-(2-(4-methoxyphenyl)piperidin-1-yl)-*N*-methylpyrazolo[1,5-*a*]pyrimidine-3-carboxamide (28 mg, 0.077 mmol, 81%) as a yellow solid. LCMS (High pH, ES⁺): t_R = 1.03 min, [M+H]⁺ 366.3, (88% purity).

¹H NMR (400 MHz, CDCl₃): δ 1.58-1.80 (m, 3H), 1.87 (d, J = 3.9 Hz, 1H), 2.03-2.14 (m, 1H), 2.30-2.41 (m, 1H), 2.96 (d, J = 4.9 Hz, 3H), 3.25-3.37 (m, 1H), 3.81 (s, 3H), 4.30-4.42 (m, 1H), 5.55 (br. s., 1H), 6.39 (d, J = 7.8 Hz, 1H), 6.86-6.94 (m, 2H), 7.10-7.19 (m, 2H), 7.55 (q, J = 4.2 Hz, 1H), 8.26 (d, J = 7.8 Hz, 1H), 8.37 (s, 1H). ¹³C NMR (101 MHz, CDCl₃): δ 18.7, 24.6, 25.7, 29.5, 41.4, 55.3, 55.4, 96.8, 102.1, 114.3, 127.4, 131.4, 136.1, 146.2, 146.3, 156.6, 158.6, 163.8. M.pt.: 146-148 °C.

ν_{max} (neat): 3362, 2939, 1630, 1564, 1509, 1439, 1245, 1225, 1176, 1025, 895, 839, 821, 793, 776 cm⁻¹.

HRMS: (C₂₀H₂₃N₅O₂) [M+H]⁺ requires 366.1925, found [M+H]⁺ 366.1934.

5-(2-(3-Fluorophenyl)piperidin-1-yl)-*N*-methylpyrazolo[1,5-*a*]pyrimidine-3-carboxamide

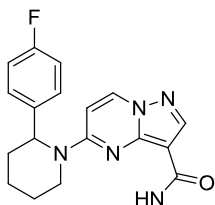


3.155e

Prepared according to General Procedure C, with **3.030** (20 mg, 0.095 mmol), 2-(3-fluorophenyl)piperidine (26 mg, 0.142 mmol) and DIPEA (33 μ L, 0.190 mmol) at 90 °C for 1 h, affording 5-(2-(3-fluorophenyl)piperidin-1-yl)-*N*-methylpyrazolo[1,5-*a*]pyrimidine-3-carboxamide (25 mg, 0.071 mmol, 75%) as a light brown solid.

LCMS (High pH, ES⁺): t_R = 1.04 min, [M+H]⁺ 354.3, (100% purity). ¹H NMR (400 MHz, CDCl₃): δ 1.59-1.71 (m, 1H), 1.71-1.85 (m, 2H), 1.85-1.94 (m, 1H), 2.072.20 (m, 1H), 2.30-2.40 (m, 1H), 2.94 (d, J = 4.9 Hz, 3H), 3.37 (ddd, J = 13.6, 11.4, 3.9 Hz, 1H), 4.27-4.37 (m, 1H), 5.59-5.65 (m, 1H), 6.41 (d, J = 7.8 Hz, 1H), 6.92-7.07 (m, 3H), 7.32-7.39 (m, 1H), 7.40-7.47 (m, 1H), 8.31 (d, J = 7.8 Hz, 1H), 8.39 (s, 1H).

5-(2-(4-Fluorophenyl)piperidin-1-yl)-*N*-methylpyrazolo[1,5-*a*]pyrimidine-3-carboxamide



3.155f

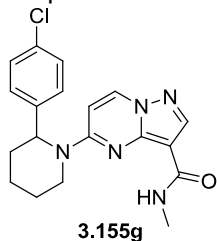
Prepared according to General Procedure C, with **3.030** (20 mg, 0.095 mmol), 2-(4-fluorophenyl)piperidine (26 mg, 0.142 mmol) and DIPEA (33 μ L, 0.190 mmol) at 90 °C for 90 min. The product precipitated from the reaction mixture and was collected by filtration, washed with Et₂O and dried under vacuum to afford 5-(2-(4-fluorophenyl)piperidin-1-yl)-*N*-methylpyrazolo[1,5-*a*]pyrimidine-3-carboxamide (20 mg, 0.057 mmol,

60%) as an off-white solid.

LCMS (High pH, ES⁺): t_R = 1.04 min, [M+H]⁺ 354.3, (100% purity). ¹H NMR (400 MHz, CDCl₃): δ 1.60-1.93 (m, 4H), 2.06-2.19 (m, 1H), 2.32-2.42 (m, 1H), 2.95 (d, J = 4.9 Hz, 3H), 3.32 (ddd, J = 13.7, 11.5, 3.9 Hz, 1H), 4.28-4.39 (m, 1H), 5.61 (br. s., 1H), 6.40 (d, J = 8.1 Hz, 1H), 7.04-7.11 (m, 2H), 7.17-7.28 (m, 2H), 7.43-7.52 (m, 1H), 8.30 (d, J = 8.1 Hz, 1H), 8.39 (s, 1H).

5-(2-(4-Chlorophenyl)piperidin-1-yl)-N-methylpyrazolo[1,5-a]pyrimidine-3-carboxamide

Prepared according to General Procedure C, with **3.030** (20 mg, 0.095 mmol), 2-(4-chlorophenyl)piperidine (28 mg, 0.142 mmol) and DIPEA

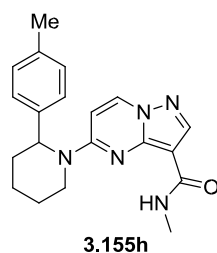


(33 μL, 0.190 mmol) at 90 °C for 90 min, affording 5-(2-(4chlorophenyl)piperidin-1-yl)-N-methylpyrazolo[1,5-a]pyrimidine-3-carboxamide (23 mg, 0.062 mmol, 66%).

LCMS (High pH, ES⁺): t_R = 1.12 min, [M+H]⁺ 370.4 (94% purity).

¹H NMR (400 MHz, CDCl₃): δ 1.59-1.93 (m, 4H), 2.06-2.18 (m, 1H), 2.31-2.40 (m, 1H), 2.95 (d, J = 4.9 Hz, 3H), 3.32 (ddd, J = 13.6, 11.4, 4.0 Hz, 1H), 4.27-4.39 (m, 1H), 5.56-5.65 (m, 1H), 6.39 (d, J = 7.9 Hz, 1H), 7.19 (d, J = 8.3 Hz, 2H), 7.36 (d, J = 8.3 Hz, 2H), 7.42-7.48 (m, 1H), 8.31 (d, J = 7.9 Hz, 1H), 8.40 (s, 1H).

5-(2-(p-Tolyl)piperidin-1-yl)-N-methylpyrazolo[1,5-a]pyrimidine-3-carboxamide

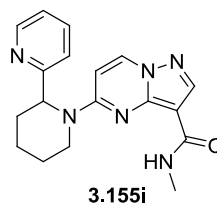


Prepared according to General Procedure C, with **3.030** (20 mg, 0.095 mmol), 2-(p-tolyl)piperidine (25 mg, 0.142 mmol) and DIPEA (33 μL, 0.190 mmol) at 90 °C for 90 min, affording 5-(2-(p-Tolyl)piperidin-1-yl)-N-methylpyrazolo[1,5-a]pyrimidine-3-carboxamide (24 mg, 0.069 mmol, 72%).

LCMS (High pH, ES⁺): t_R = 1.11 min, [M+H]⁺ 350.3, (100% purity).

¹H NMR (400 MHz, CDCl₃): δ 1.61-1.92 (m, 4H), 2.04-2.16 (m, 1H), 2.36 (s, 3H), 2.37-2.42 (m, 1H), 2.96 (d, J = 4.9 Hz, 3H), 3.35 (ddd, J = 13.6, 11.4, 4.0 Hz, 1H), 4.34-4.43 (m, 1H), 5.52-5.59 (m, 1H), 6.38 (d, J = 8.1 Hz, 1H), 7.13 (d, J = 8.3 Hz, 2H), 7.19 (d, J = 8.3 Hz, 2H), 7.48-7.58 (m, 1H), 8.27 (d, J = 8.1 Hz, 1H), 8.38 (s, 1H).

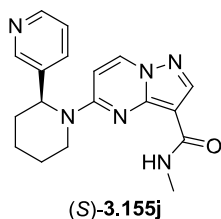
5-(2-(Pyridin-2-yl)piperidin-1-yl)-N-methylpyrazolo[1,5-a]pyrimidine-3-carboxamide



Prepared according to General Procedure C, with **3.030** (20 mg, 0.095 mmol), 2-(piperidin-2-yl)pyridine (23 mg, 0.142 mmol) and DIPEA (33 μL, 0.190 mmol) at 90 °C for 90 min, affording 5-(2-(pyridin-2yl)piperidin-1-yl)-N-methylpyrazolo[1,5-a]pyrimidine-3-carboxamide (24 mg, 0.071 mmol, 75%).

LCMS (High pH, ES⁺): t_R = 0.84 min, [M+H]⁺ 337.3, (100% purity). ¹H NMR (400 MHz, CDCl₃): δ 1.50-1.86 (m, 3H), 1.89-1.99 (m, 1H), 2.05-2.18 (m, 1H), 2.52-2.62 (m, 1H), 2.96 (d, J = 4.9 Hz, 3H), 3.49-3.60 (m, 1H), 4.28-4.37 (m, 1H), 5.65 (br. s., 1H), 6.46 (d, J = 8.1 Hz, 1H), 7.13-7.22 (m, 2H), 7.42-7.51 (m, 1H), 7.66 (td, J = 7.8, 1.8 Hz, 1H),

8.29 (d, $J = 8.1$ Hz, 1H), 8.37 (s, 1H), 8.60-8.63 (m, 1H). **(S)-5-(2-(Pyridin-3-yl)piperidin-1-yl)-*N*-methylpyrazolo[1,5-*a*]pyrimidine-3-carboxamide** Prepared



(S)-3.155j

according to General Procedure C, with **3.030** (20 mg, 0.095 mmol), (-)-anabasine (23 mg, 0.142 mmol) and DIPEA (33 μ L, 0.190 mmol) at 90 $^{\circ}$ C for 1 h, affording (S)-5-(2-(pyridin-3-yl)piperidin-1-yl)-

N-methylpyrazolo[1,5-*a*]pyrimidine-3-carboxamide (17 mg, 0.051 mmol,

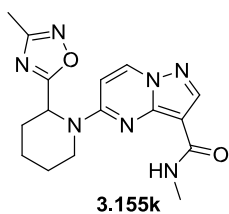
53%) as a brown solid.

LCMS (High pH, ES⁺): $t_R = 0.77$ min, $[M+H]^+$ 337.3, (100% purity). 1 H NMR (400 MHz, CDCl₃):

δ 1.57-1.71 (m, 1H), 1.72-1.85 (m, 2H), 1.86-1.95 (m, 1H), 2.18 (dddd, $J = 14.1, 12.1, 5.7, 4.0$ Hz, 1H), 2.35-2.44 (m, 1H), 2.93 (d, $J = 4.9$ Hz, 3H), 3.35 (ddd, $J = 13.6, 11.4, 4.0$ Hz, 1H), 4.29 (d, $J = 14.1$ Hz, 1H), 5.75 (t, $J = 4.0$ Hz, 1H), 6.44 (d, $J = 7.8$ Hz, 1H), 7.31 (dd, $J = 7.9, 4.8$ Hz, 1H), 7.36 (q, $J = 4.9$ Hz, 1H), 7.53-7.58 (m, 1H),

8.33 (d, $J = 7.8$ Hz, 1H), 8.39 (s, 1H), 8.56 (dd, $J = 4.8, 1.1$ Hz, 1H), 8.60 (d, $J = 2.2$ Hz, 1H).

***N*-Methyl-5-(2-(3-methyl-1,2,4-oxadiazol-5-yl)piperidin-1-yl)pyrazolo[1,5-*a*]pyrimidine-3-carboxamide**



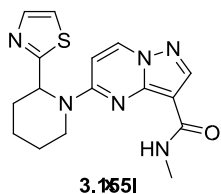
3.155k

Prepared according to General Procedure C, with **3.030** (20 mg, 0.095 mmol), 3-methyl-5-(piperidin-2-yl)-1,2,4-oxadiazole hydrochloride (29 mg, 0.142 mmol) and DIPEA (66 μ L, 0.380 mmol) at 90 $^{\circ}$ C for 1 h, affording *N*-methyl-5-(2-(3-methyl-1,2,4-oxadiazol-5-yl)piperidin-1-yl)pyrazolo[1,5-*a*]pyrimidine-3-carboxamide (22 mg, 0.064 mmol, 68%)

as a light yellow solid.

LCMS (High pH, ES⁺): $t_R = 0.81$ min, $[M+H]^+$ 342.2, (100% purity). 1 H NMR (400 MHz, CDCl₃): δ 1.66-1.92 (m, 3H), 1.99-2.07 (m, 1H), 2.08-2.20 (m, 1H), 2.262.34 (m, 1H), 2.39 (s, 3H), 3.06 (d, $J = 4.9$ Hz, 3H), 3.67 (td, $J = 12.4, 3.3$ Hz, 1H), 4.05-4.15 (m, 1H), 5.98 (dd, $J = 5.7, 1.6$ Hz, 1H), 6.55 (d, $J = 8.1$ Hz, 1H), 7.35-7.45 (m, 1H), 8.39 (d, $J = 8.1$ Hz, 1H), 8.42 (s, 1H).

***N*-Methyl-5-(2-(thiazol-2-yl)piperidin-1-yl)pyrazolo[1,5-*a*]pyrimidine-3-carboxamide**

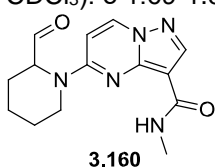


3.165l

Prepared according to General Procedure C, with **3.030** (20 mg, 0.095 mmol), 2-(piperidin-2-yl)thiazole (24 mg, 0.142 mmol) and DIPEA (33 μ L, 0.190 mmol) at 90 $^{\circ}$ C for 1 h, affording *N*-methyl-5-(2-(thiazol-2-yl)piperidin-1-yl)pyrazolo[1,5-*a*]pyrimidine-3-carboxamide (21 mg, 0.061 mmol, 65%) as a yellow solid.

LCMS (High pH, ES⁺): $t_R = 0.84$ min, $[M+H]^+$ 343.2, (94% purity). 1 H NMR (400 MHz,

CDCl₃): δ 1.69-1.88 (m, 3H), 1.90-1.99 (m, 1H), 2.09-2.19 (m, 1H), 2.512.59 (m, 1H), 3.00 (d, $J = 4.9$ Hz, 3H), 3.43-3.54 (m, 1H), 4.14-4.29 (m, 1H), 6.07 (d, $J = 3.4$ Hz, 1H), 6.51 (d, $J = 7.8$ Hz, 1H), 7.31 (d, $J = 3.3$ Hz, 1H), 7.43-7.55 (m, 1H), 7.76 (d, $J = 3.3$ Hz, 1H), 8.35 (d, $J = 7.8$ Hz, 1H), 8.41 (s, 1H). **5-(2-**



3.160

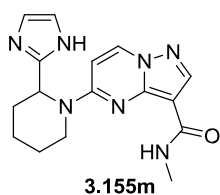
Formylpiperidin-1-yl)-N-methylpyrazolo[1,5-a]pyrimidine-3-carboxamide To a suspension of 5-(2-(hydroxymethyl)piperidin-1-yl)-N-methylpyrazolo[1,5-a]pyrimidine-3-carboxamide **3.0511** (41 mg, 0.142 mmol) in DCM (3 mL) was added Dess-Martin periodinane (78 mg,

0.184 mmol). The solid dissolved and the reaction was stirred at rt for 3 h. The reaction mixture was diluted with sat. aq. NaHCO₃ (20 mL) and sodium thiosulfate pentahydrate (352 mg, 1.417 mmol) was added. The mixture was vigorously stirred for 30 min, then extracted with DCM (5 x 10 mL). The combined organics were dried through a hydrophobic frit and evaporated to dryness to give 5-(2-formylpiperidin-1-yl)-N-methylpyrazolo[1,5-a]pyrimidine-3-carboxamide (40 mg, 0.139 mmol, 98%) as a yellow gum.

The product was used crude without purification.

LCMS (High pH, ES⁺): t_R = 0.74 min, [M+H]⁺ 288.2, (82% purity). ¹H NMR (400 MHz, CDCl₃): δ 1.65-1.86 (m, 4H), 1.93-2.04 (m, 1H), 2.08-2.18 (m, 1H), 3.04 (d, J = 4.9 Hz, 3H), 3.58-3.67 (m, 1H), 3.73 (s, 1H), 4.59-4.68 (m, 1H), 6.53 (d, J = 7.8 Hz, 1H), 7.06 (br. s., 1H), 8.40 (d, J = 7.8 Hz, 1H), 8.43 (s, 1H), 9.64 (d, J = 1.2 Hz, 1H). 90% pure by NMR.

5-(2-(1H-imidazol-2-yl)piperidin-1-yl)-N-methyl-pyrazolo[1,5-a]pyrimidine-3-carboxamide



To a suspension of 5-(2-formylpiperidin-1-yl)-N-methylpyrazolo[1,5-a]pyrimidine-3-carboxamide **3.160** (40 mg, 0.139 mmol) and 30% ammonium hydroxide solution (108 μL, 0.835 mmol) in MeOH (300 μL) was added glyoxal (64 μL, 40% in water, 0.557 mmol) dropwise. The reaction was stirred at rt for 18 h. The reaction was evaporated *in vacuo*

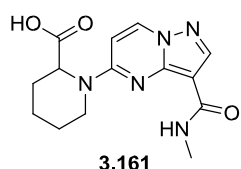
and the residue was purified by High pH MDAP. The solvent was evaporated *in vacuo* to give 5-(2-(1H-imidazol-2-yl)piperidin-1-yl)-N-methylpyrazolo[1,5-a]pyrimidine-3-carboxamide (12 mg, 0.037 mmol, 27%) as a powdery white solid.

LCMS (High pH, ES⁺): t_R = 0.63 min, [M+H]⁺ 326.2, (95% purity). ¹

¹H NMR (500 MHz, DMSO-d₆): δ 1.58 (br. s., 3H), 1.72-1.83 (m, 1H), 1.85-1.96 (m, 1H), 2.30-2.39 (m, 1H), 2.83 (d, J = 4.7 Hz, 3H), 3.22-3.31 (m, 1H), 4.38 (br. s., 1H), 5.82 (br. s., 1H), 6.81 (s, 1H), 6.91 (d, J = 8.0 Hz, 1H), 7.06 (s, 1H), 7.48-7.57 (m, 1H), 8.15 (s, 1H), 8.72 (d, J = 7.7 Hz, 1H), 11.81 (br. s., 1H).

¹³C NMR (126 MHz, DMSO-d₆): δ 19.7, 25.0, 25.9, 28.7, 42.4, 50.9, 98.7, 101.6, 116.9, 127.7, 137.0, 145.2, 145.9, 146.7, 157.3, 162.9. M.pt.: 160-200 °C (decomp). ν_{max} (neat): 2938, 1632, 1565, 1482, 1444, 1269, 1224, 1167, 1085, 1030, 964, 894, 795, 776, 745 cm⁻¹.

HRMS: (C₁₆H₁₉N₇O) [M+H]⁺ requires 326.1724, found [M+H]⁺ 326.1722. **1-(3-**



(Methylcarbamoyl)pyrazolo[1,5-a]pyrimidin-5-yl)piperidine-2-

carboxylic acid Prepared according to General Procedure C, with

3.030 (50 mg, 0.237 mmol), piperidine-2-carboxylic acid (46 mg, 0.356 mmol) and DIPEA (166 μL, 0.950 mmol) at 90 °C for 90 min. The

reaction mixture was poured into 2 M HCl (15 mL) and exhaustively extracted with EtOAc.

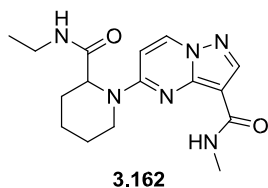
The combined organics were dried through a hydrophobic frit and evaporated to dryness.

The crude product was purified by Formic MDAP and the solvent was evaporated to give 1-(3-(methylcarbamoyl)pyrazolo[1,5-a]pyrimidin-5-yl)piperidine-2-carboxylic acid (20 mg, 0.066 mmol, 28%) as a white solid.

LCMS (Formic, ES⁺): t_R = 0.68 min, [M+H]⁺ 304.1, (100% purity). ¹

¹H NMR (400 MHz, DMSO-d₆): δ 1.33-1.48 (m, 1H), 1.50-1.64 (m, 1H), 1.65-1.77 (m, 1H), 1.78-1.90 (m, 2H), 2.13-2.25 (m, 1H), 2.84 (d, *J* = 4.9 Hz, 3H), 4.19 (br. s., 1H), 5.05-5.12 (m, 1H), 6.93 (d, *J* = 8.1 Hz, 1H), 7.58 (q, *J* = 4.9 Hz, 1H), 8.17 (s, 1H), 8.78 (d, *J* = 8.1 Hz, 1H), 12.92 (br. s., 1H). Piperidine C2-H not observed due to peak broadening by the acid.

5-(2-(Ethylcarbamoyl)piperidin-1-yl)-*N*-methylpyrazolo[1,5-a]pyrimidine-3-carboxamide



To a solution of 1-(3-(methylcarbamoyl)pyrazolo[1,5-a]pyrimidin-5-yl)piperidine-2-carboxylic acid **3.161** (10 mg, 0.033 mmol) and HATU (15.04 mg, 0.040 mmol) in DMF (0.5 mL) was added DIPEA (0.017 mL, 0.099 mmol) and ethanamine (0.033 mL, 2 M in THF,

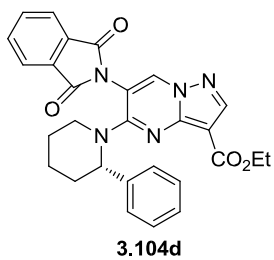
0.066 mmol). The reaction mixture was stirred at rt for 3 h, then

purified directly by Formic MDAP. The solvent was evaporated *in vacuo* and the residue was purified by ion exchange chromatography (sulphonic acid (SCX) 500 mg, eluting with MeOH).

The appropriate fractions were combined and evaporated *in vacuo* to give 5-(2(ethylcarbamoyl)piperidin-1-yl)-*N*-methylpyrazolo[1,5-a]pyrimidine-3-carboxamide (8 mg, 0.024 mmol, 73%) as a white solid.

LCMS (High pH, ES⁺): t_R = 0.67 min, [M+H]⁺ 331.3, (100% purity). ¹H NMR (400 MHz, DMSO-d₆): δ 1.00 (t, *J* = 7.2 Hz, 3H), 1.36-1.69 (m, 3H), 1.75-1.88 (m, 2H), 2.08-2.18 (m, 1H), 2.86 (d, *J* = 4.9 Hz, 3H), 3.02-3.17 (m, 2H), 4.04-4.24 (m, 1H), 4.98 (br. s., 1H), 6.88 (d, *J* = 8.0 Hz, 1H), 7.51 (q, *J* = 4.9 Hz, 1H), 8.03 (t, *J* = 5.1 Hz, 1H), 8.15 (s, 1H), 8.74 (d, *J* = 8.0 Hz, 1H). Piperidine C2-H was not observed due to peak broadening by the amide.

(S)-Ethyl 6-(1,3-dioxoisindolin-2-yl)-5-(2-phenylpiperidin-1-yl)pyrazolo[1,5a]pyrimidine-3-carboxylate



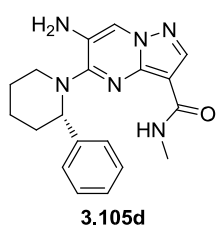
Prepared according to General Procedure C, with **3.103** (200 mg, 0.539 mmol), (*S*)-2-phenylpiperidine (130 mg, 0.809 mmol) and DIPEA (188 μ L, 1.079 mmol) at 90 °C for 2 h. Further (*S*)-2-phenylpiperidine (50 mg, 0.310 mmol) was added and the reaction was heated to 90 °C for 1 h. The reaction was diluted with sat. aq. NaHCO₃ (20 mL) and Et₂O (20 mL) and extracted. The aqueous layer was extracted with Et₂O (2 x 15 mL) and EtOAc (10 mL) and the combined organics were washed with brine, dried through a hydrophobic frit and evaporated to dryness. The crude product was purified by silica chromatography (0-25% (3:1 EtOAc:EtOH)/cyclohexane), and the appropriate fractions were evaporated *in vacuo* to afford (*S*)-ethyl 6-(1,3-dioxoisindolin-2-yl)-5-(2-phenylpiperidin-1-yl)pyrazolo[1,5-*a*]pyrimidine-3-carboxylate (230 mg, 0.418 mmol, 77%). The product was 90% pure by NMR and was used for further chemistry without further purification.

LCMS (High pH, ES⁺): *t*_R = 1.35 min, [M+H]⁺ 496.1, (87% purity). ¹H NMR (400 MHz, DMSO-*d*₆): δ 1.27 (t, *J* = 7.1 Hz, 3H), 1.32-1.39 (m, 1H), 1.45-1.58 (m, 2H), 1.65-1.78 (m, 1H), 1.86-2.00 (m, 1H), 2.07-2.20 (m, 1H), 3.07-3.17 (m, 1H), 4.10-4.18 (m, 1H), 4.19-4.27 (m, 2H), 5.25 (t, *J* = 4.4 Hz, 1H), 6.96-7.03 (m, 1H), 7.08-7.14 (m, 2H), 7.15-7.20 (m, 2H), 7.73-7.94 (m, 4H), 8.42 (s, 1H), 9.23 (s, 1H).

(*S*)-6-Amino-*N*-methyl-5-(2-phenylpiperidin-1-yl)pyrazolo[1,5-*a*]pyrimidine-3-carboxamide and (*S*)-ethyl 6-amino-5-(2-phenylpiperidin-1-yl)pyrazolo[1,5-*a*]pyrimidine-3-carboxylate

To a solution of DABAL-Me₃ (214 mg, 0.835 mmol) in anhydrous THF (0.7 mL) stirred under N₂ at rt in a sealed tube was added MeNH₂ (627 μ L, 2 M in THF, 1.253 mmol). The reaction mixture was stirred at 40 °C in an oil bath for 30 min. A solution of (*S*)-ethyl 6-(1,3-dioxoisindolin-2-yl)-5-(2-phenylpiperidin-1-yl)pyrazolo[1,5-*a*]pyrimidine-3-carboxylate **3.104d** (230 mg, 0.418 mmol) in THF (1.4 mL) was added and the reaction was heated to 70 °C for 12 h. Further MeNH₂ (627 μ L, 2 M in THF, 1.253 mmol) and DABAL-Me₃ (214 mg, 0.835 mmol) were added and the reaction was heated to 90 °C for 8 h. The reaction mixture was cooled to rt and quenched with aqueous 2 M HCl. The aqueous was neutralised with sat. aq. NaHCO₃ and extracted with EtOAc (5 x 20 mL). The combined organics were dried using a hydrophobic frit and evaporated *in vacuo*. The crude was purified by silica chromatography (5-60% (3:1 EtOAc:EtOH)/cyclohexane) to afford the products:

(*S*)-6-Amino-*N*-methyl-5-(2-phenylpiperidin-1-yl)pyrazolo[1,5-*a*]pyrimidine-3-carboxamide



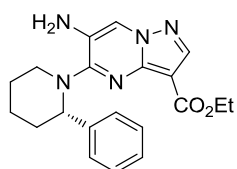
3.105d

16 mg, 0.046 mmol, 11 % yield, yellow solid.

LCMS (High pH, ES⁺): t_R = 0.99 min, [M+H]⁺ 351.2, (91% purity). ¹H

NMR (400 MHz, CDCl₃): δ 1.63-1.89 (m, 3H), 1.90-1.98 (m, 2H), 2.02-2.12 (m, 1H), 2.86-2.96 (m, 1H), 3.02 (d, J = 4.9 Hz, 3H), 3.75-3.85 (m, 3H), 4.65 (dd, J = 9.7, 3.3 Hz, 1H), 7.08-7.16 (m, 1H), 7.18-7.27 (m, 5H), 8.02 (s, 1H), 8.26 (s, 1H). 95% pure.

(S)-Ethyl 6-amino-5-(2-phenylpiperidin-1-yl)pyrazolo[1,5-a]pyrimidine-3-carboxylate



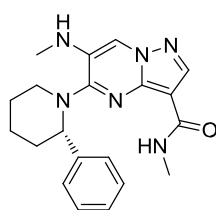
3.163

116 mg, 0.270 mmol, 65 % yield, yellow solid.

LCMS (High pH, ES⁺): t_R = 1.19 min, [M+H]⁺ 366.2, (87% purity). ¹H

NMR (400 MHz, CDCl₃): δ 1.45 (t, J = 6.8 Hz, 3H), 1.62-1.70 (m, 1H), 1.71-1.82 (m, 1H), 1.82-1.91 (m, 1H), 1.92-2.11 (m, 3H), 3.15-3.26 (m, 1H), 3.48-3.57 (m, 1H), 3.73 (s, 2H), 4.28-4.48 (m, 2H), 4.97 (dd, J = 8.7, 4.0 Hz, 1H), 7.09-7.15 (m, 1H), 7.18 – 7.24 (m, 2H), 7.38 – 7.44 (m, 2H), 7.94 (s, 1H), 8.23 (s, 1H). 85% pure by NMR.

(S)-N-Methyl-(6-methylamino)-5-(2-phenylpiperidin-1-yl)pyrazolo[1,5-a]pyrimidine-3-carboxamide



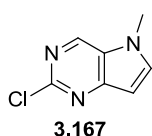
3.115d

To a solution of (S)-6-amino-N-methyl-5-(2-phenylpiperidin-1-yl)pyrazolo[1,5-a]pyrimidine-3-carboxamide **3.105d** (16 mg, 0.046 mmol) and potassium carbonate (25 mg, 0.183 mmol) in anhydrous DMF (913 μL) was added methyl iodide (5.7 μL, 0.091 mmol). The reaction mixture was heated to 90 °C for 18 h. Further methyl iodide

(5.7 μL, 0.091 mmol) and potassium carbonate (25 mg, 0.183 mmol) were added and the reaction was heated to 90 °C for 24 h. The reaction mixture was cooled to rt, poured into sat. aq. NaHCO₃ (10 mL) and extracted with EtOAc (4 x 10 mL). The combined organics were dried using a hydrophobic frit and evaporated *in vacuo*. The crude product as purified by High pH MDAP, the solvent was blown down to afford (S)-N-methyl-6(methylamino)-5-(2-phenylpiperidin-1-yl)pyrazolo[1,5-a]pyrimidine-3-carboxamide (1.5 mg, 4.12 μmol, 9%) as a yellow solid.

LCMS (High pH, ES⁺): t_R = 1.08 min, [M+H]⁺ 365.3, (97% purity). ¹H NMR (400 MHz, CDCl₃): δ 1.64-1.74 (m, 1H), 1.81 (br. s., 2H), 1.89-2.01 (m, 2H), 2.02-2.11 (m, 1H), 2.76-2.84 (m, 1H), 2.92 (d, J = 5.4 Hz, 3H), 3.03 (d, J = 4.9 Hz, 3H), 3.71-3.79 (m, 1H), 4.16 (q, J = 5.4 Hz, 1H), 4.57 (dd, J = 10.4, 3.3 Hz, 1H), 7.07-7.14 (m, 1H), 7.16-7.27 (m, 5H), 7.77 (s, 1H), 8.25 (s, 1H).

2-Chloro-5-methyl-5H-pyrrolo[3,2-d]pyrimidine



To a solution of 2-chloro-5*H*-pyrrolo[3,2-*d*]pyrimidine **3.166** (500 mg, 3.26 mmol) and potassium carbonate (900 mg, 6.51 mmol) in DMF (5 mL) was added methyl iodide (0.30 mL, 4.88 mmol), and the reaction was stirred at rt for 3 h. The reaction was diluted with water (30 mL) and the aqueous was extracted with EtOAc (6 x 10 mL). The combined organics were washed with brine, dried through a hydrophobic frit and evaporated to dryness. The crude product was purified by silica chromatography (20-90% EtOAc/cyclohexane), the appropriate fractions were evaporated to dryness to afford 2-chloro-5-methyl-5*H*-pyrrolo[3,2-*d*]pyrimidine (453 mg, 2.70 mmol, 83%) as a white solid.

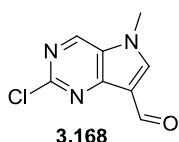
LCMS (High pH, ES⁺): t_R = 0.60 min, [M⁺] 167.9, 170.1, (100% purity) ¹H NMR (400 MHz, CDCl₃): δ 3.93 (s, 3H), 6.62 (d, J = 3.2 Hz, 1H), 7.48 (d, J = 3.2 Hz, 1H),

8.69 (s, 1H). ¹³C NMR (101 MHz, CDCl₃): δ 33.7, 101.7, 127.1, 137.7, 139.8, 152.6, 153.0.

M.pt.: 151-153 °C. ν_{max} (neat): 3071, 1605, 1581, 1497, 1450, 1430, 1401, 1375, 1319, 1261, 1156, 1092, 1005, 927, 787, 752, 670 cm⁻¹.

HRMS: (C₇H₆N₃Cl) [M+H]⁺ requires 168.0323, found [M+H]⁺ 168.0329.

2-Chloro-5-methyl-5*H*-pyrrolo[3,2-*d*]pyrimidine-7-carbaldehyde



To DMF (4 mL) at 0 °C under N₂ was added POCl₃ (0.445 mL, 4.77 mmol), and the reaction was stirred at 0 °C for 15 min. To this solution was added a solution of 2-chloro-5-methyl-5*H*-pyrrolo[3,2-*d*]pyrimidine **3.167** (400 mg, 2.387 mmol) in DMF (2 mL) dropwise. The reaction mixture was stirred at rt for 40 h, then poured into an ice/water mixture. The pH was adjusted to 7 with sat. aq. NaHCO₃ and the aqueous was extracted with EtOAc (5 x 20 mL) and DCM (5 x 15 mL), the combined organic layers were dried through a hydrophobic frit and evaporated *in vacuo* to afford 2-chloro-5-methyl-5*H*-pyrrolo[3,2-*d*]pyrimidine-7-carbaldehyde (422 mg, 2.157 mmol, 90%) as an offwhite solid.

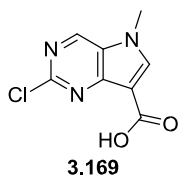
LCMS (High pH, ES⁺): t_R = 0.54 min, [M+H]⁺ 196.0, (99% purity). ¹H NMR (400 MHz, DMSO-*d*₆): δ 4.01 (s, 3H), 8.72 (s, 1H), 9.15 (s, 1H), 10.08 (s, 1H).

¹³C NMR (101 MHz, DMSO-*d*₆): δ 34.9, 115.2, 128.6, 144.0, 144.8, 150.3, 154.1, 183.4. M.pt.: 194-198 °C.

ν_{max} (neat): 3094, 1658, 1596, 1513, 1465, 1374, 1329, 1252, 1219, 1135, 1070, 1009, 919, 891, 786, 714 cm⁻¹.

HRMS: (C₈H₆N₃OCl) [M+H]⁺ requires 196.0272, found [M+H]⁺ 196.0277.

2-Chloro-5-methyl-5*H*-pyrrolo[3,2-*d*]pyrimidine-7-carboxylic acid



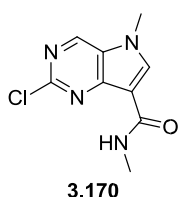
To a suspension of 2-chloro-5-methyl-5*H*-pyrrolo[3,2-*d*]pyrimidine-7-carbaldehyde **3.168** (400 mg, 2.045 mmol) in THF (25 mL) and water (5 mL) at 0 °C was added sulfamic acid (1.19 g, 12.27 mmol), followed by a

solution of sodium chlorite (347 mg, 3.07 mmol) and sodium dihydrogen phosphate (2.95 g, 24.54 mmol) in water (15 mL) dropwise. The reaction was stirred at rt for 24 h, then concentrated to remove the organic solvent. A precipitate formed and was filtered off, washed with diethyl ether and dried under vacuum to afford 2-chloro-5-methyl-5*H*-pyrrolo[3,2-*d*]pyrimidine-7-carboxylic acid (402 mg, 1.900 mmol, 93%) as an off-white solid.

LCMS (Formic, ES⁺): $t_R = 0.47$ min, [M+H]⁺ 212.1, (96% purity).

¹H NMR (400 MHz, DMSO-*d*₆): δ 3.97 (s, 3H), 8.54 (s, 1H), 9.07 (s, 1H). Acid proton was not observed.

2-Chloro-*N*,5-methyl-5*H*-pyrrolo[3,2-*d*]pyrimidine-7-carboxamide



A solution of 2-chloro-5-methyl-5*H*-pyrrolo[3,2-*d*]pyrimidine-7-carboxylic acid **3.169** (400 mg, 1.890 mmol), HATU (863 mg, 2.268 mmol) and DIPEA (0.495 mL, 2.84 mmol) in DMF (6 mL) was stirred under N₂ at rt for 10 min until all the solid dissolved. MeNH₂ (1.13 mL, 2 M in THF, 2.268 mmol) was added and a precipitate immediately formed. The reaction mixture was

stirred at rt for 2 h. The reaction mixture was filtered, the solid was washed with diethyl ether and dried to afford 2-chloro-*N*,5-dimethyl-5*H*-pyrrolo[3,2-*d*]pyrimidine-7-carboxamide (232 mg, 1.033 mmol, 55%) as a white solid.

The filtrate contained residual product, and was diluted with EtOAc (10 mL) and sat. aq. NaHCO₃ (20 mL). The aqueous layer was separated, extracted with EtOAc (6 x 10 mL), and the combined organics were dried through a hydrophobic frit and evaporated to dryness. The residue was purified by silica chromatography (20-90% (3:1 EtOAc:EtOH)/cyclohexane), appropriate fractions were evaporated *in vacuo* and further purified by ion exchange chromatography (sulphonic acid (SCX) 5 g, eluting with MeOH). The appropriate fractions were evaporated *in vacuo* to give further 2-chloro-*N*,5-dimethyl-5*H*-pyrrolo[3,2-*d*]pyrimidine-7-carboxamide (130 mg, 0.579 mmol, 31%) as a white solid.

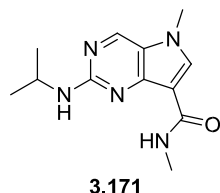
LCMS (Formic, ES⁺): $t_R = 0.62$ min, [M+H]⁺ 225.1, (99% purity). ¹H NMR (400 MHz, DMSO-*d*₆): δ 2.91 (d, $J = 4.6$ Hz, 3H), 3.97 (s, 3H), 7.71 (q, $J = 4.6$ Hz, 1H), 8.49 (s, 1H), 9.11 (s, 1H).

¹³C NMR (101 MHz, DMSO-*d*₆): δ 26.1, 34.4, 109.5, 128.0, 142.5, 143.5, 148.4, 152.5, 162.3.

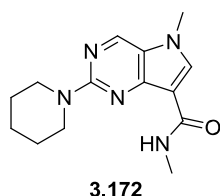
M.pt.: 186-200 °C (decomp).

ν_{max} (neat): 3360, 3049, 1644, 1606, 1651, 1462, 1398, 1360, 1270, 1250, 1198, 1160, 1133, 1073, 989, 856, 788 cm⁻¹.

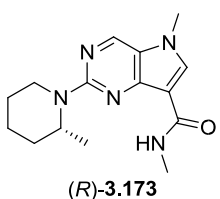
HRMS: (C₉H₉N₄OCl) [M+H]⁺ requires 225.0538, found [M+H]⁺ 225.0539.

2-(Isopropylamino)-*N*,5-dimethyl-5*H*-pyrrolo[3,2-*d*]pyrimidine-7-carboxamide

To a solution of 2-chloro-*N*,5-dimethyl-5*H*-pyrrolo[3,2-*d*]pyrimidine-7-carboxamide **3.170** (30 mg, 0.134 mmol) in DMSO (0.5 mL) was added propan-2-amine (23 μ L, 0.267 mmol) and DIPEA (47 μ L, 0.267 mmol). The reaction was heated to 90 $^{\circ}$ C in a Biotage Initiator microwave reactor for 5 h. Further propan-2-amine (23 μ L, 0.267 mmol) and DIPEA (47 μ L, 0.267 mmol) were added and the reaction was heated to 160 $^{\circ}$ C in a Biotage Initiator microwave reactor for 5 h, followed by direct purification by High pH MDAP. The solvent was blown down to give 2-(isopropylamino)-*N*,5-dimethyl-5*H*-pyrrolo[3,2-*d*]pyrimidine-7-carboxamide (9 mg, 0.036 mmol, 27%) as an off-white solid. LCMS (Formic, ES⁺): t_R = 0.53 min, [M+H]⁺ 248.4, (97% purity). ¹H NMR (400 MHz, CDCl₃): δ 1.32 (d, J = 6.4 Hz, 6H), 3.06 (d, J = 4.9 Hz, 3H), 3.83 (s, 3H), 4.11-4.23 (m, 1H), 4.94-5.09 (m, 1H), 7.85 (s, 1H), 8.24-8.35 (m, 1H), 8.44 (s, 1H).

***N*,5-Dimethyl-2-(piperidin-1-yl)-5*H*-pyrrolo[3,2-*d*]pyrimidine-7-carboxamide**

To a solution of 2-chloro-*N*,5-dimethyl-5*H*-pyrrolo[3,2-*d*]pyrimidine-7-carboxamide **3.170** (30 mg, 0.134 mmol) in DMSO (0.5 mL) was added piperidine (20 μ L, 0.20 mmol) and DIPEA (47 μ L, 0.267 mmol). The reaction was heated to 90 $^{\circ}$ C in a Biotage Initiator microwave reactor for 5 h. Further piperidine (10 μ L, 0.10 mmol) was added and the reaction was heated to 160 $^{\circ}$ C in a Biotage Initiator microwave reactor for 5 h, followed by direct purification by High pH MDAP. The solvent was blown down to give *N*,5-dimethyl-2-(piperidin-1-yl)-5*H*-pyrrolo[3,2-*d*]pyrimidine-7-carboxamide (23 mg, 0.084 mmol, 63%) as a white solid. LCMS (Formic, ES⁺): t_R = 0.82 min, [M+H]⁺ 274.2, (100% purity). ¹H NMR (400 MHz, CDCl₃): δ 1.63-1.76 (m, 6H), 3.07 (d, J = 4.9 Hz, 3H), 3.80-3.86 (m, 7H), 7.83 (s, 1H), 8.26 (br. s., 1H), 8.49 (s, 1H).

(*R*)-*N*,5-Dimethyl-2-(2-methylpiperidin-1-yl)-5*H*-pyrrolo[3,2-*d*]pyrimidine-7-carboxamide

To a solution of 2-chloro-*N*,5-dimethyl-5*H*-pyrrolo[3,2-*d*]pyrimidine-7-carboxamide **3.170** (30 mg, 0.134 mmol) in DMSO (0.5 mL) was added (*R*)-2-methylpiperidine (27 mg, 0.267 mmol) and DIPEA (47 μ L, 0.267 mmol). The reaction was heated to 90 $^{\circ}$ C in a Biotage Initiator microwave reactor for 5 h, then heated to 160 $^{\circ}$ C in a sand bath for 72 h. The reaction mixture was diluted with EtOAc (20 mL) and sat. aq. NaHCO₃ (15 mL). The aqueous layer was extracted with EtOAc (3 x 20 mL) and the combined organics were dried through a hydrophobic frit and evaporated. The crude product was purified by High pH MDAP. The solvent was blown down to give (*R*)-*N*,5-dimethyl-2-(2-methylpiperidin-1-yl)-5*H*-pyrrolo[3,2-*d*]pyrimidine-7-carboxamide (28 mg, 0.097 mmol, 73%) as a brown solid.

LCMS (Formic, ES⁺): t_R = 0.90 min, [M+H]⁺ 288.3, (100% purity). ¹H NMR (400 MHz, CDCl₃): δ 1.23 (d, J = 6.8 Hz, 3H), 1.50-1.58 (m, 1H), 1.64-1.87 (m, 5H), 3.04 (td, J = 13.0, 2.9 Hz,

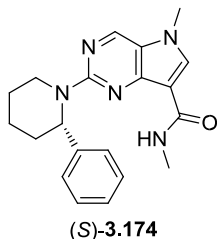
1H), 3.07 (d, $J = 4.9$ Hz, 3H), 3.82 (s, 3H), 4.60 (dd, $J = 13.3, 2.6$ Hz, 1H), 5.08 (s, 1H), 7.82 (s, 1H), 8.30 (br. s., 1H), 8.49 (s, 1H). ^{13}C NMR (101 MHz, CDCl_3): δ 14.3, 19.1, 25.7, 25.9, 30.5, 33.8, 39.3, 46.5, 108.6, 123.2, 137.6, 140.3, 149.1, 158.4, 164.4. M.pt.: 131-133 °C. 22 °C

$[\alpha_D] = -111$ ($c = 0.25$, MeOH).

ν_{max} (neat): 3327, 2930, 1647, 1604, 1565, 1475, 1448, 1415, 1387, 1250, 1178, 1146, 1078, 1036, 966, 938, 910, 870, 793 cm^{-1} .

HRMS: ($\text{C}_{15}\text{H}_{21}\text{N}_5\text{O}$) $[\text{M}+\text{H}]^+$ requires 288.1819, found $[\text{M}+\text{H}]^+$ 288.1828.

(S)-N,5-Dimethyl-2-(2-phenylpiperidin-1-yl)-5H-pyrrolo[3,2-d]pyrimidine-7-carboxamide



To a solution of 2-chloro-*N*,5-dimethyl-5*H*-pyrrolo[3,2-*d*]pyrimidine-7-carboxamide **3.170** (30 mg, 0.134 mmol) in DMSO (0.5 mL) was added (*S*)-2-phenylpiperidine (43 mg, 0.267 mmol) and DIPEA (47 μL , 0.267 mmol). The reaction was heated to 90 °C in a Biotage Initiator microwave reactor for 5 h, then heated to 160 °C in a sand bath for 72 h. The reaction mixture was diluted with EtOAc (20 mL) and sat. aq. NaHCO_3 (15 mL). The aqueous layer was extracted with EtOAc (3 x 20 mL) and the combined organics were dried through a hydrophobic frit and evaporated to dryness. The crude product was purified by High pH MDAP. The solvent was blown down to give (*S*)-*N*,5dimethyl-2-(2-phenylpiperidin-1-yl)-5*H*-pyrrolo[3,2-*d*]pyrimidine-7-carboxamide (18 mg, 0.052 mmol, 39%) as a brown solid.

LCMS (Formic, ES^+): $t_R = 1.15$ min, $[\text{M}+\text{H}]^+ 350.3$, (100% purity). ^1H NMR (400 MHz, CDCl_3): δ 1.60-1.82 (m, 4H), 2.00-2.11 (m, 1H), 2.35-2.43 (m, 1H), 2.98 (d, $J = 4.9$ Hz, 3H), 3.22 (ddd, $J = 13.4, 11.4, 3.8$ Hz, 1H), 3.81 (s, 3H), 4.72-4.81 (m, 1H), 6.08 (dd, $J = 4.9, 2.9$ Hz, 1H), 7.22 (d, $J = 7.1$ Hz, 1H), 7.26-7.35 (m, 4H), 7.81 (s, 1H), 8.06-8.15 (m, 1H), 8.49 (s, 1H).

4.4 Supplementary Protocols

CLND Solubility

Solubility was determined by precipitation of 10 mM DMSO stock concentration to 5% DMSO pH7.4 phosphate buffered saline, with quantification by ChemiLuminescent Nitrogen Detection.

FaSSIF solubility

Compounds were dissolved in DMSO at 2.5 mg/mL and then diluted in Fast State Simulated Intestinal Fluid (FaSSIF pH 6.5) at 125 $\mu\text{g}/\text{mL}$ (final DMSO concentration is 5%). After 16h of incubation at 25°C, the suspension was filtered. The concentration of the compound was determined by a fast HPLC gradient. The ratio of the peak areas obtained from the standards and the sample filtrate was used to calculate the solubility of the compound.

ChromLogD_{7.4}

Carried out according to literature protocols,³¹⁷ using a Waters Aquity UPLC System, Phenomenex Gemini NX 50x2 mm, 3 μm HPLC column, 0-100% pH 7.40 ammonium acetate buffer/acetonitrile gradient. Retention time was compared to standards of known pH to derive Chromatographic Hydrophobicity Index (CHI). ChromLogD = 0.0857CHI – 2.

Artificial membrane permeability measurement.

Permeability across a lipid membrane was measured using the published protocol.³⁸⁹

FRET Assays

BET proteins were produced using protocols given in the literature.¹³¹ Compounds were screened against either 6H-Thr BRD4 (1-477) (Y390A) (BRD4 BD2 mutation to monitor compound binding to BD1) or 6H-Thr BRD4 (1-477) (Y97A) (BRD4 BD1 mutation to monitor compound binding to BD2) in a dose-response format in a TR-FRET assay measuring competition between test compound and an Alexa Fluor 647 derivative of I-BET762.1 Compounds were titrated from 10 mM in 100% DMSO and 50 nL transferred to a low volume black 384 well micro titre plate using a Labcyte Echo 555. A Thermo Scientific Multidrop Combi was used to dispense 5 μL of 20 nM protein in an assay buffer of 50 mM HEPES, 150 mM NaCl, 5% glycerol, 1 mM DTT and 1 mM CHAPS, pH 7.4, and in the presence of 100 nM fluorescent ligand (~*K_d* concentration for the interaction between BRD4 BD1 and ligand). After equilibrating for 30 min in the dark at rt, the bromodomain protein:fluorescent ligand interaction was detected using TR-FRET following a 5 μL addition of 3 nM europium chelate labelled anti-6His antibody (Perkin Elmer, W1024, AD0111) in assay buffer. Time resolved fluorescence (TRF) was then detected on a TRF laser equipped Perkin Elmer Envision multimode plate reader (excitation = 337 nm; emission 1 = 615 nm; emission 2 = 665 nm; dual wavelength bias dichroic = 400 nm, 630 nm). TR-FRET ratio was calculated using the following equation: Ratio = ((Acceptor fluorescence at 665 nm) / (Donor fluorescence at 615 nm)) * 1000. TR-FRET ratio data was normalised to high (DMSO) and low (compound control derivative of I-BET762) controls and IC50 values determined for each of the compounds tested by fitting the fluorescence ratio data to a four parameter model: $y = a + ((b - a) / (1 + (10^x / 10^c)^d))$ where 'a' is the minimum, 'b' is the Hill slope, 'c' is the IC50 and 'd' is the maximum.

BRPF proteins were produced using protocols given in the literature.¹⁹⁴ Compounds were screened against 6H-Flag-Tev-BRPF1 (622-738), 6HisFlag-Tev-BRPF2 (also known as BRD1) (551-673) or 6His-Flag-Tev-BRPF3 (579-706) protein in dose-response format in a TR-FRET assay measuring competition between test compound and a synthetic fluorescent ligand. Compounds were titrated from 10 mM in 100% DMSO and 100 nL transferred to a low volume black 384 well micro titre plate using a Labcyte Echo 555. A Thermo Scientific Multidrop Combi was used to dispense 5 μL of 4 nM BRPF1, 20 nM BRPF2 or 40 nM BRPF3

protein respectively in an assay buffer of 50 mM HEPES, 150 mM NaCl, 5% glycerol, 1mM DTT and 1 mM CHAPS, pH 7.4, and in the presence of the appropriate fluorescent ligand concentration (~*K_d* concentration for the interaction between protein and ligand). After equilibrating for 30 min in the dark at rt, the bromodomain protein:fluorescent ligand interaction was detected using TR-FRET following a 5 μ L addition of either 3 nM Lanthascreen Elite Tb-anti His antibody (Invitrogen PV5863) for the Alexa 488 ligands, or 3 nM europium chelate labelled anti-6His antibody (Perkin Elmer, W1024, AD0111) for the Alexa 647 ligand, in assay buffer. Time resolved fluorescence energy transfer (TR-FRET) was then detected on a time-resolved fluorescence laser equipped Perkin Elmer Envision multimode plate reader using the appropriate protocol (excitation = 337 nm; emission 1 Alexa 488 = 495 nm; emission 2 Alexa 488 = 520 nm, emission 1 Alexa 647 = 615 nm; emission 2 Alexa 647= 665 nm). TR-FRET ratio was calculated using the following equation: Ratio = ((Acceptor fluorescence at 520 or 665 nm) / (Donor fluorescence at 495 or 615 nm)) * 1000. Data were analysed as for the BRD4 assay.

FRET assays for Brd9 were carried out using literature protocols.²¹¹ FRET assays against BAZ2A, BTPF, Brd7, CECR2, PCAF and TIF1a were carried out using similar methodology. Brd4, BAZ2A, BTPF, Brd7, CECR2, PCAF, TIF1a, BRPF2 and BRPF3 assays (and some BRPF1 runs) were carried out by Laurie Gordon, Cassie Messenger and Melanie Leverage.

BROMOscan® Bromodomain Profiling

BROMOscan® bromodomain profiling was provided by DiscoverX Corp. (Fremont, CA, USA, <http://www.discoverx.com>). Determination of the *K_d* between test compounds and DNA tagged bromodomains was achieved through binding competition against a proprietary reference immobilized ligand.

5. References

- (1) Hughes, J. P.; Rees, S.; Kalindjian, S. B.; Philpott, K. L. *Br. J. Pharmacol.* **2011**, *162* (6), 1239.
- (2) Anighoro, A.; Bajorath, J.; Rastelli, G. *J. Med. Chem.* **2014**, *57* (19), 7874.
- (3) Weiss, W. A.; Taylor, S. S.; Shokat, K. M. *Nat. Chem. Biol.* **2007**, *3* (12), 739.
- (4) Bunnage, M. E.; Chekler, E. L. P.; Jones, L. H. *Nat. Chem. Biol.* **2013**, *9* (4), 195.
- (5) Sweis, R. F. *ACS Med. Chem. Lett.* **2015**, *6* (6), 618.
- (6) Arrowsmith, C. H.; Audia, J. E.; Austin, C.; Baell, J.; Bennett, J.; Blagg, J.; Bountra, C.; Brennan, P. E.; Brown, P. J.; Bunnage, M. E.; Buser-Doepner, C.; Campbell, R. M.; Carter, A. J.; Cohen, P.; Copeland, R. a; Cravatt, B.; Dahlin, J. L.; Dhanak, D.; Edwards, A. M.; Frye, S. V.; Gray, N.; Grimshaw, C. E.; Hepworth, D.; Howe, T.; Huber, K. V. M.; Jin, J.; Knapp, S.; Kotz, J. D.; Kruger, R. G.; Lowe, D.; Mader, M. M.; Marsden, B.; Mueller-Farnow, A.; Müller, S.; O'Hagan, R. C.; Overington, J. P.; Owen, D. R.; Rosenberg, S. H.; Roth, B.; Ross, R.; Schapira, M.; Schreiber, S. L.; Shoichet, B.; Sundström, M.; Superti-Furga, G.; Taunton, J.; Toledo-Sherman, L.; Walpole, C.; Walters, M. a; Willson, T. M.; Workman, P.; Young, R. N.; Zuercher, W. J. *Nat. Chem. Biol.* **2015**, *11* (8), 536.
- (7) Workman, P.; Collins, I. *Chem. Biol.* **2010**, *17* (6), 561.
- (8) Frye, S. V. *Nat. Chem. Biol.* **2010**, *6* (3), 159.
- (9) Kola, I.; Landis, J. *Nat. Rev. Drug Discov.* **2004**, *3* (8), 711.
- (10) Hann, M. M. *Medchemcomm* **2011**, *2* (5), 349.
- (11) Gleeson, M. P.; Hersey, A.; Montanari, D.; Overington, J. *Nat. Rev. Drug Discov.* **2011**, *10* (3), 197.
- (12) Wenlock, M. C.; Austin, R. P.; Barton, P.; Davis, A. M.; Leeson, P. D. *J. Med. Chem.* **2003**, *46*

- (7), 1250.
- (13) Lipinski, C. A.; Lombardo, F.; Dominy, B. W.; Feeney, P. J. *Adv. Drug Deliv. Rev.* **2001**, *46* (1-3), 3.
- (14) Shultz, M. D. *Bioorg. Med. Chem. Lett.* **2013**, *23* (21), 5980.
- (15) Leeson, P. D.; Springthorpe, B. *Nat. Rev. Drug Discov.* **2007**, *6* (11), 881.
- (16) Young, R. J.; Green, D. V. S.; Luscombe, C. N.; Hill, A. P. *Drug Discov. Today* **2011**, *16* (1718), 822.
- (17) Ertl, P.; Rohde, B.; Selzer, P. *J. Med. Chem.* **2000**, *43* (20), 3714.
- (18) Hughes, J. D.; Blagg, J.; Price, D. A.; Bailey, S.; Decrescenzo, G. A.; Devraj, R. V; Ellsworth, E.; Fobian, Y. M.; Gibbs, M. E.; Gilles, R. W.; Greene, N.; Huang, E.; Krieger-Burke, T.; Loesel, J.; Wager, T.; Whiteley, L.; Zhang, Y. *Bioorg. Med. Chem. Lett.* **2008**, *18* (17), 4872.
- (19) Ritchie, T. J.; Macdonald, S. J. F. *Drug Discov. Today* **2009**, *14* (21-22), 1011.
- (20) Ritchie, T. J.; Macdonald, S. J. F.; Young, R. J.; Pickett, S. D. *Drug Discov. Today* **2011**, *16* (34), 164.
- (21) Lovering, F.; Bikker, J.; Humblet, C. *J. Med. Chem.* **2009**, *52* (21), 6752.
- (22) Muthas, D.; Boyer, S.; Hasselgren, C. *Med. Chem. Commun.* **2013**, *4* (7), 1058.
- (23) Kenny, P. W.; Montanari, C. A. *J. Comput. Aided Mol. Des.* **2013**, *27* (1), 1.
- (24) Waring, M. J.; Arrowsmith, J.; Leach, A. R.; Leeson, P. D.; Mandrell, S.; Owen, R. M.; Pairaudeau, G.; Pennie, W. D.; Pickett, S. D.; Wang, J.; Wallace, O.; Weir, A. *Nat. Rev. Drug Discov.* **2015**, *14* (7), 475.
- (25) Bhattachar, S. N.; Wesley, J. A.; Seadeek, C. *J. Pharm. Biomed. Anal.* **2006**, *41* (1), 152.
- (26) Di, L.; Artursson, P.; Avdeef, A.; Ecker, G. F.; Faller, B.; Fischer, H.; Houston, J. B.; Kansy, M.; Kerns, E. H.; Krämer, S. D.; Lennernäs, H.; Sugano, K. *Drug Discov. Today* **2012**, *17* (15-16), 905.
- (27) Dobson, P. D.; Kell, D. B. *Nat. Rev. Drug Discov.* **2008**, *7* (3), 205.
- (28) Artursson, P. *J. Pharm. Sci.* **1990**, *79* (6), 476.
- (29) Faller, B. *Curr. Drug Metab.* **2008**, *9* (9), 886.
- (30) Kuntz, I. D.; Chen, K.; Sharp, K. a; Kollman, P. a. *Proc. Natl. Acad. Sci. USA* **1999**, *96* (18), 9997.
- (31) Hopkins, A. L.; Groom, C. R.; Alex, A. *Drug Discov. Today* **2004**, *9* (10), 430.
- (32) Shultz, M. D. *ACS Med. Chem. Lett.* **2014**, *5* (1), 2.
- (33) Murray, C. W.; Erlanson, D. A.; Hopkins, A. L.; Keserü, G. M.; Leeson, P. D.; Rees, D. C.; Reynolds, C. H.; Richmond, N. J. *ACS Med. Chem. Lett.* **2014**, *5* (6), 616.
- (34) Mortenson, P. N.; Murray, C. W. *J. Comput. Aided Mol. Des.* **2011**, *25* (7), 663.
- (35) Hopkins, A. L.; Keserü, G. M.; Leeson, P. D.; Rees, D. C.; Reynolds, C. H. *Nat. Rev. Drug Discov.* **2014**, *13* (2), 105.
- (36) Hann, M. M.; Keserü, G. M. *Nat. Rev. Drug Discov.* **2012**, *11*, 355.
- (37) Arrowsmith, C. H.; Bountra, C.; Fish, P. V; Lee, K.; Schapira, M. *Nat. Rev. Drug Discov.* **2012**, *11* (5), 384.
- (38) International Human Genome Sequencing Consortium. *Nature* **2004**, *431* (7011), 931.
- (39) Luger, K.; Mäder, A. W.; Richmond, R. K.; Sargent, D. F.; Richmond, T. J. *Nature* **1997**, *389* (6648), 251.
- (40) Thoma, F.; Koller, T.; Klug, A. *J. Cell. Biol.* **1979**, *83* (2), 403.
- (41) Tough, D. F.; Lewis, H. D.; Rioja, I.; Lindon, M. J.; Prinjha, R. K. *Br. J. Pharmacol.* **2014**, *171*, 4981.
- (42) Furdas, S. D.; Carlino, L.; Sippl, W.; Jung, M. *Med. Chem. Commun.* **2012**, *3*, 123.
- (43) Strahl, B. D.; Allis, C. D. *Nature* **2000**, *403*, 41.
- (44) Jenuwein, T.; Allis, C. D. *Science (80-)*. **2001**, *293*, 1074.
- (45) Katan-Khaykovich, Y.; Struhl, K. *Genes Dev.* **2002**, *16* (6), 743.
- (46) Radman-Livaja, M.; Liu, C. L.; Friedman, N.; Schreiber, S. L.; Rando, O. J. *PLoS Genet.* **2010**, *6* (2), 223.
- (47) Tsukada, Y.; Fang, J.; Erdjument-Bromage, H.; Warren, M. E.; Borchers, C. H.; Tempst, P.; Zhang, Y. *Nature* **2006**, *439*, 811.
- (48) Shi, Y.; Lan, F.; Matson, C.; Mulligan, P.; Whetstone, J. R.; Cole, P. A.; Casero, R. A.; Shi, Y. *Cell* **2004**, *119*, 941.
- (49) Copeland, R. A. *Clin. Cancer Res.* **2013**, *19* (23), 6344.
- (50) Huang, Y.; Fang, J.; Bedford, M. T.; Zhang, Y.; Xu, R.-M. *Science (80-)*. **2006**, *312* (5774), 748.
- (51) Jones, D. O.; Cowell, I. G.; Singh, P. B. *Bioessays* **2000**, *22* (2), 124.
- (52) Shahbazian, M. D.; Grunstein, M. *Annu. Rev. Biochem.* **2007**, *76*, 75.
- (53) Winogradoff, D.; Echeverria, I.; Potoyan, D. A.; Papoian, G. A. *J. Am. Chem. Soc.* **2015**, *137* (19), 6245.
- (54) Morinière, J.; Rousseaux, S.; Steuerwald, U.; Soler-López, M.; Curtet, S.; Vitte, A.-L.; Govin, J.; Gaucher, J.; Sadoul, K.; Hart, D. J.; Krijgsveld, J.; Khochbin, S.; Müller, C. W.; Petosa, C. *Nature* **2009**, *461*, 664.

- (55) Filippakopoulos, P.; Picaud, S.; Mangos, M.; Keates, T.; Lambert, J.-P.; Barsyte-Lovejoy, D.; Felletar, I.; Volkmer, R.; Müller, S.; Pawson, T.; Gingras, A.-C.; Arrowsmith, C. H.; Knapp, S. *Cell* **2012**, *149* (1), 214.
- (56) Dion, M. F.; Altschuler, S. J.; Wu, L. F.; Rando, O. J. *Proc. Natl. Acad. Sci. U. S. A.* **2005**, *102* (15), 5501.
- (57) Richon, V. M. *Br. J. Cancer* **2006**, *95*, S2.
- (58) Richardson, P. G.; Mitsiades, C. S.; Laubach, J. P.; Hajek, R.; Spicka, I.; Dimopoulos, M. A.; Moreau, P.; Siegel, D. S.; Jagannath, S.; Anderson, K. C. *Leuk. Res.* **2013**, *37* (7), 829.
- (59) Vigushin, D. M.; Coombes, R. C. *Curr. Cancer Drug Targets* **2004**, *4* (2), 205.
- (60) Ueda, H.; Manda, T.; Matsumoto, S.; Mukumoto, S.; Nishigaki, F.; Kawamura, I.; Shimomura, K. *J. Antibiot.* **1994**, *47* (3), 315.
- (61) Ueda, H.; Nakajima, H.; Hori, Y.; Fujita, T.; Nishimura, M.; Goto, T.; Okuhara, M. *J. Antibiot.* **1994**, *47* (3), 301.
- (62) Shigematsu, N.; Ueda, H.; Takase, S.; Tanaka, H.; Yamamoto, K.; Tada, T. *J. Antibiot.* **1994**, *47* (3), 311.
- (63) Marks, P. a; Breslow, R. *Nat. Biotechnol.* **2007**, *25* (1), 84.
- (64) Tamkun, J. W.; Deuring, R.; Scott, M. P.; Kissinger, M.; Pattatucci, M.; Kaufman, T. C.; Kennison, J. *Cell* **1992**, *68*, 561.
- (65) Belkina, A. C.; Denis, G. V. *Nat. Rev. Cancer* **2012**, *12*, 465.
- (66) Flynn, E. M.; Huang, O. W.; Poy, F.; Oppikofer, M.; Bellon, S. F.; Tang, Y.; Cochran, A. G. *Structure* **2015**, *23* (10), 1801.
- (67) Tan, M.; Luo, H.; Lee, S.; Jin, F.; Yang, J. S.; Montellier, E.; Buchou, T.; Cheng, Z.; Rousseaux, S.; Rajagopal, N.; Lu, Z.; Ye, Z.; Zhu, Q.; Wysocka, J.; Ye, Y.; Khochbin, S.; Ren, B.; Zhao, Y. *Cell* **2011**, *146* (6), 1016.
- (68) Liu, L.; Zhen, X. T.; Denton, E.; Marsden, B. D.; Schapira, M. *Bioinformatics* **2012**, *28* (16), 2205.
- (69) Fukazawa, H.; Masumi, A. *Biol. Pharm. Bull.* **2012**, *35* (11), 2064.
- (70) Berkovits, B. D.; Wolgemuth, D. J. In *Current Topics in Developmental Biology*; Elsevier Inc., 2013; Vol. 102, pp 293–326.
- (71) Rahman, S.; Sowa, M. E.; Ottinger, M.; Smith, J. A.; Shi, Y.; Harper, J. W.; Howley, P. M. *Mol. Cell. Biol.* **2011**, *31* (13), 2641.
- (72) Dey, A.; Ellenberg, J.; Farina, A.; Coleman, A. E.; Maruyama, T.; Sciortino, S.; Ellenberg, J. A. N.; Lippincott-schwartz, J.; Ozato, K. *Mol. Cell. Biol.* **2000**, *20* (17), 6537.
- (73) Korb, E.; Herre, M.; Zucker-Scharff, I.; Darnell, R. B.; Allis, C. D. *Nat. Neurosci.* **2015**.
- (74) French, C.; Ramirez, C. L.; Kolmakova, J.; Hickman, T. T.; Cameron, M. J.; Thyne, M. E.; Kutok, J. L.; Toretsky, J.; Tadavarthy, K.; Kees, U. R.; Fletcher, J.; Aster, J. C. *Oncogene* **2008**, *27*, 2237.
- (75) Filippakopoulos, P.; Qi, J.; Picaud, S.; Shen, Y.; Smith, W. B.; Fedorov, O.; Morse, E. M.; Keates, T.; Hickman, T. T.; Felletar, I.; Philpott, M.; Munro, S.; McKeown, M. R.; Wang, Y.; Christie, A. L.; West, N.; Cameron, M. J.; Schwartz, B.; Heightman, T. D.; La Thangue, N.; French, C. a; Wiest, O.; Kung, A. L.; Knapp, S.; Bradner, J. E. *Nature* **2010**, *468* (7327), 1067.
- (76) Mertz, J. A.; Conery, A. R.; Bryant, B. M.; Sandy, P.; Balasubramanian, S.; Mele, D. A.; Bergeron, L.; Sims, R. J. *Proc. Natl. Acad. Sci. USA* **2011**, *108* (40), 16669.
- (77) Zuber, J.; Shi, J.; Wang, E.; Rappaport, A. R.; Herrmann, H.; Sison, E. a; Magoon, D.; Qi, J.; Blatt, K.; Wunderlich, M.; Taylor, M. J.; Johns, C.; Chicas, A.; Mulloy, J. C.; Kogan, S. C.; Brown, P.; Valent, P.; Bradner, J. E.; Lowe, S. W.; Vakoc, C. R. *Nature* **2011**, *478* (7370), 524.
- (78) Chen, C.; Liu, Y.; Lu, C.; Cross, J. R.; Morris, J. P.; Shroff, A. S.; Ward, P. S.; Bradner, J. E.; Thompson, C.; Lowe, S. W. *Genes Dev* **2013**, *27* (18), 1974.
- (79) Dawson, M. A.; Prinjha, R. K.; Dittmann, A.; Giotopoulos, G.; Bantscheff, M.; Chan, W.-I.; Robson, S. C.; Chung, C.; Hopf, C.; Savitski, M. M.; Huthmacher, C.; Gudgin, E.; Lugo, D.; Beinke, S.; Chapman, T. D.; Roberts, E. J.; Soden, P. E.; Auger, K. R.; Mirquet, O.; Doehner, K.; Delwel, R.; Burnett, A. K.; Jeffrey, P.; Drewes, G.; Lee, K.; Huntly, B. J. P.; Kouzarides, T. *Nature* **2011**, *478* (7370), 529.
- (80) Baratta, M. G.; Schinzel, A. C.; Zwang, Y.; Bandopadhyay, P.; Bowman-Colin, C.; Kutt, J.; Curtis, J.; Piao, H.; Wong, L. C.; Kung, A. L.; Beroukhim, R.; Bradner, J. E.; Drapkin, R.; Hahn, W. C.; Liu, J. F.; Livingston, D. M. *Proc. Natl. Acad. Sci.* **2015**, *112* (1), 232.
- (81) Asangani, I. A.; Dommeti, V. L.; Wang, X.; Malik, R.; Cieslik, M.; Yang, R.; Escara-Wilke, J.; Wilder-Romans, K.; Dhanireddy, S.; Engelke, C.; Iyer, M. K.; Jing, X.; Wu, Y.-M.; Cao, X.; Qin, Z. S.; Wang, S.; Feng, F. Y.; Chinnaiyan, A. M. *Nature* **2014**, *510* (7504), 278.
- (82) Henssen, A.; Thor, T.; Odersky, A.; Heukamp, L.; El-Hindy, N.; Beckers, A.; Speleman, F.; Althoff, K.; Schäfers, S.; Schramm, A.; Sure, U.; Fleischhack, G.; Eggert, A.; Schulte, J. H. *Oncotarget* **2013**, *4* (11), 2080.
- (83) Cheng, Z.; Gong, Y.; Ma, Y.; Lu, K.; Lu, X.; Pierce, L. A.; Thompson, R. C.; Muller, S.; Knapp, S.; Wang, J. *Clin. Cancer Res.* **2013**, *19* (7), 1748.

- (84) Puissant, A.; Frumm, S. M.; Alexe, G.; Bassil, C. F.; Qi, J.; Chanthery, Y. H.; Nekritz, E. A.; Zeid, R.; Gustafson, W. C.; Greninger, P.; Garnett, M. J.; McDermott, U.; Benes, C. H.; Kung, A. L.; Weiss, W. A.; Bradner, J. E.; Stegmaier, K. *Cancer Discov.* **2013**, *3* (3), 308.
- (85) ClinicalTrials.gov. NCT01943851: A Dose Escalation Study to Investigate the Safety, Pharmacokinetics (PK), Pharmacodynamics (PD) and Clinical Activity of GSK525762 in Subjects With Relapsed, Refractory Hematologic Malignancies <https://clinicaltrials.gov/ct2/show/NCT01943851> (accessed Jul 2, 2015).
- (86) ClinicalTrials.gov. NCT02296476: A Trial With Dose Optimization of OTX015 in Recurrent Glioblastoma Multiforme (GBM) Patients <https://clinicaltrials.gov/ct2/show/NCT02296476> (accessed Jul 2, 2015).
- (87) ClinicalTrials.gov. NCT01713582: A Phase I, Dose-finding Study of the Bromodomain (Brd) Inhibitor OTX015 in Haematological Malignancies <https://clinicaltrials.gov/ct2/show/NCT01713582> (accessed Jul 2, 2015).
- (88) ClinicalTrials.gov. NCT02259114: A Phase IB Trial With OTX015, a Small Molecule Inhibitor of the Bromodomain and Extra-Terminal (BET) Proteins, in Patients With Selected Advanced Solid Tumors <https://clinicaltrials.gov/ct2/show/NCT02259114> (accessed Jul 2, 2015).
- (89) ClinicalTrials.gov. NCT01949883: A Phase 1 Study Evaluating CPI-0610 in Patients With Progressive Lymphoma <https://clinicaltrials.gov/ct2/show/NCT01949883> (accessed Jul 2, 2015).
- (90) ClinicalTrials.gov. NCT01587703: A Study to Investigate the Safety, Pharmacokinetics, Pharmacodynamics, and Clinical Activity of GSK525762 in Subjects With NUT Midline Carcinoma (NMC) and Other Cancers <https://clinicaltrials.gov/ct2/show/NCT01587703> (accessed Jul 2, 2015).
- (91) Delmore, J. E.; Issa, G. C.; Lemieux, M. E.; Rahl, P. B.; Shi, J.; Jacobs, H. M.; Kastiris, E.; Gilpatrick, T.; Paranal, R. M.; Qi, J.; Chesi, M.; Schinzel, A. C.; McKeown, M. R.; Heffernan, T. P.; Vakoc, C. R.; Bergsagel, P. L.; Ghobrial, I. M.; Richardson, P. G.; Young, R. A.; Hahn, W. C.; Anderson, K. C.; Kung, A. L.; Bradner, J. E.; Mitsiades, C. S. *Cell* **2011**, *146* (6), 904.
- (92) Lovén, J.; Hoke, H.; Lin, C. Y.; Lau, A.; Orlando, D.; Vakoc, C. R.; Bradner, J. E.; Lee, T. I.; Young, R. *Cell* **2013**, *153* (2), 320.
- (93) Chapuy, B.; McKeown, M. R.; Lin, C. Y.; Monti, S.; Roemer, M. G. M.; Qi, J.; Rahl, P. B.; Sun, H. H.; Yeda, K. T.; Doench, J. G.; Reichert, E.; Kung, A. L.; Rodig, S. J.; Young, R. A.; Shipp, M. A.; Bradner, J. E. *Cancer Cell* **2013**, *24* (6), 777.
- (94) Tolani, B.; Gopalakrishnan, R.; Punj, V.; Matta, H.; Chaudhary, P. M. *Oncogene* **2014**, *33* (22), 2928.
- (95) Floyd, S. R.; Pacold, M. E.; Huang, Q.; Clarke, S. M.; Lam, F. C.; Cannell, I. G.; Bryson, B. D.; Rameseder, J.; Lee, M. J.; Blake, E. J.; Fydrych, A.; Ho, R.; Greenberger, B. A.; Chen, G. C.; Maffa, A.; Del Rosario, A. M.; Root, D. E.; Carpenter, A. E.; Hahn, W. C.; Sabatini, D. M.; Chen, C. C.; White, F. M.; Bradner, J. E.; Yaffe, M. B. *Nature* **2013**, *498* (7453), 246.
- (96) Shimamura, T.; Chen, Z.; Soucheray, M.; Carretero, J.; Kikuchi, E.; Tchaicha, J. H.; Gao, Y.; Cheng, K. A.; Cohoon, T. J.; Qi, J.; Akbay, E.; Kimmelman, A. C.; Kung, A. L.; Bradner, J. E.; Wong, K.-K. *Clin. Cancer Res.* **2013**, *19* (22), 6183.
- (97) Lu, J.; Qian, Y.; Altieri, M.; Dong, H.; Wang, J.; Raina, K.; Hines, J.; Winkler, J. D.; Crew, A. P.; Coleman, K.; Crews, C. M. *Chem. Biol.* **2015**, *22* (6), 755.
- (98) Fong, C. Y.; Gilan, O.; Lam, E. Y. N.; Rubin, A. F.; Ftouni, S.; Tyler, D.; Stanley, K.; Sinha, D.; Yeh, P.; Morison, J.; Giotopoulos, G.; Lugo, D.; Jeffrey, P.; Lee, S. C.-W.; Carpenter, C.; Gregory, R.; Ramsay, R. G.; Lane, S. W.; Abdel-Wahab, O.; Kouzarides, T.; Johnstone, R. W.; Dawson, S.-J.; Huntly, B. J. P.; Prinjha, R. K.; Papenfuss, A. T.; Dawson, M. A. *Nature* **2015**, *525* (7570), 538.
- (99) Rathert, P.; Roth, M.; Neumann, T.; Muerdter, F.; Roe, J.-S.; Muhar, M.; Deswal, S.; CernyReiterer, S.; Peter, B.; Jude, J.; Hoffmann, T.; Boryń, Ł. M.; Axelsson, E.; Schweifer, N.; Tontsch-Grunt, U.; Dow, L. E.; Gianni, D.; Pearson, M.; Valent, P.; Stark, A.; Kraut, N.; Vakoc, C. R.; Zuber, J. *Nature* **2015**, *525* (7570), 543.
- (100) Nicodeme, E.; Jeffrey, K. L.; Schaefer, U.; Beinke, S.; Dewell, S.; Chung, C.-W.; Chandwani, R.; Marazzi, I.; Wilson, P.; Coste, H.; White, J.; Kirilovsky, J.; Rice, C. M.; Lora, J. M.; Prinjha, R. K.; Lee, K.; Tarakhovsky, A. *Nature* **2010**, *468*, 1119.
- (101) Belkina, A. C.; Nikolajczyk, B. S.; Denis, G. V. *J. Immunol.* **2013**, *190* (7), 3670.
- (102) Bandukwala, H. S.; Gagnon, J.; Togher, S.; Greenbaum, J. a; Lamperti, E. D.; Parr, N. J.; Molesworth, A. M. H.; Smithers, N.; Lee, K.; Witherington, J.; Tough, D. F.; Prinjha, R. K.; Peters, B.; Rao, A. *Proc. Natl. Acad. Sci. USA* **2012**, *109* (36), 14532.
- (103) Park-Min, K.-H.; Lim, E.; Lee, M. J.; Park, S. H.; Giannopoulou, E.; Yamilina, A.; van der Meulen, M.; Zhao, B.; Smithers, N.; Witherington, J.; Lee, K.; Tak, P. P.; Prinjha, R. K.; Ivashkiv, L. B. *Nat. Commun.* **2014**, *5*, 5418.
- (104) Klein, K.; Kabala, P. A.; Grabiec, A. M.; Gay, R. E.; Kolling, C.; Lin, L.-L.; Gay, S.; Tak, P. P.; Prinjha, R. K.; Ospelt, C.; Reedquist, K. A. *Ann. Rheum. Dis.* **2014**, *1*.

- (105) Chan, C. H.; Fang, C.; Qiao, Y.; Yarinina, A.; Prinjha, R. K.; Ivashkiv, L. B. *Eur. J. Immunol.* **2015**, *45* (1), 287.
- (106) Bisgrove, D. A.; Mahmoudi, T.; Henklein, P.; Verdin, E. *Proc. Natl. Acad. Sci. USA* **2007**, *104* (34), 13690.
- (107) Banerjee, C.; Archin, N.; Michaels, D.; Belkina, A. C.; Denis, G. V.; Bradner, J.; Sebastiani, P.; Margolis, D. M.; Montano, M. *J. Leukoc. Biol.* **2012**, *92* (6), 1147.
- (108) Li, Z.; Guo, J.; Wu, Y.; Zhou, Q. *Nucleic Acids Res.* **2013**, *41* (1), 277.
- (109) Boehm, D.; Calvanese, V.; Dar, R. D.; Xing, S.; Schroeder, S.; Martins, L.; Aull, K.; Li, P.-C.; Planelles, V.; Bradner, J. E.; Zhou, M.-M.; Siliciano, R. F.; Weinberger, L.; Verdin, E.; Ott, M. *Cell Cycle* **2013**, *12* (3), 452.
- (110) Jones, M. H.; Numata, M.; Shimane, M. *Genomics* **1997**, *45* (3), 529.
- (111) Plaseski, T.; Noveski, P.; Popeska, Z.; Efremov, G. D.; Plaseska-Karanfilska, D. *J. Androl.* **2012**, *33* (4), 675.
- (112) Theofel, I.; Bartkuhn, M.; Hundertmark, T.; Boettger, T.; Gärtner, S. M. K.; Leser, K.; Awe, S.; Schipper, M.; Renkawitz-Pohl, R.; Rathke, C. *PLoS One* **2014**, *9* (9), e108267.
- (113) Matzuk, M. M.; McKeown, M. R.; Filippakopoulos, P.; Li, Q.; Ma, L.; Agno, J. E.; Lemieux, M. E.; Picaud, S.; Yu, R. N.; Qi, J.; Knapp, S.; Bradner, J. E. *Cell* **2012**, *150* (4), 673.
- (114) Gosmini, R.; Nguyen, V. L.; Toum, J.; Simon, C.; Brusq, J. G.; Krysa, G.; Mirguet, O.; RiouEymard, A. M.; Boursier, E. V.; Trottet, L.; Bamborough, P.; Clark, H.; Chung, C.; Cutler, L.; Demont, E. H.; Kaur, R.; Lewis, A. J.; Schilling, M. B.; Soden, P. E.; Taylor, S.; Walker, A. L.; Walker, M. D.; Prinjha, R. K.; Nicodème, E. *J. Med. Chem.* **2014**, *57* (19), 8111.
- (115) Mirguet, O.; Lamotte, Y.; Donche, F.; Toum, J.; Gellibert, F.; Bouillot, A.; Gosmini, R.; Nguyen, V.-L.; Delannée, D.; Seal, J.; Blandel, F.; Boullay, A.-B.; Boursier, E.; Martin, S.; Brusq, J.-M.; Krysa, G.; Riou, A.; Tellier, R.; Costaz, A.; Huet, P.; Dudit, Y.; Trottet, L.; Kirilovsky, J.; Nicodeme, E. *Bioorg. Med. Chem. Lett.* **2012**, *22* (8), 2963.
- (116) McNeill, E. *Curr. Opin. Investig. Drugs* **2010**, *11* (3), 357.
- (117) McLure, K. G.; Gesner, E. M.; Tsujikawa, L.; Kharenko, O. a.; Atwell, S.; Campeau, E.; Wasiak, S.; Stein, A.; White, A.; Fontano, E.; Suto, R. K.; Wong, N. C. W.; Wagner, G. S.; Hansen, H. C.; Young, P. R. *PLoS One* **2013**, *8* (12), e83190.
- (118) Wong, N. C. *Curr. Opin. Investig. Drugs* **2007**, *8* (9), 718.
- (119) ClinicalTrials.gov. NCT01067820: ApoA-I Synthesis Stimulation and Intravascular Ultrasound for Coronary Atheroma Regression Evaluation (ASSURE I) <https://clinicaltrials.gov/ct2/show/NCT01067820> (accessed Sep 1, 2015).
- (120) ClinicalTrials.gov. NCT01423188: The Study of Quantitative Serial Trends in Lipids With ApolipoproteinA-I Stimulation (SUSTAIN) <https://clinicaltrials.gov/ct2/show/NCT01423188> (accessed Sep 1, 2015).
- (121) ClinicalTrials.gov. NCT01058018: Clinical Trial for Dose Finding and Safety of RVX000222 in Subjects With Stable Coronary Artery Disease (ASSERT) <https://clinicaltrials.gov/ct2/show/NCT01058018> (accessed Sep 1, 2015).
- (122) ClinicalTrials.gov. NCT01863225: Characterization of Multi-dose RVX000222 in Combination With Statin Treatment in Dyslipidemia <https://clinicaltrials.gov/ct2/show/NCT01863225> (accessed Sep 1, 2015).
- (123) Bailey, D.; Jahagirdar, R.; Gordon, A.; Hafiane, A.; Campbell, S.; Chatur, S.; Wagner, G. S.; Hansen, H. C.; Chiacchia, F. S.; Johansson, J.; Krimbou, L.; Wong, N. C. W.; Genest, J. *J. Am. Coll. Cardiol.* **2010**, *55* (23), 2580.
- (124) Nicholls, S. J.; Gordon, A.; Johansson, J.; Wolski, K.; Ballantyne, C. M.; Kastelein, J. J. P.; Taylor, A.; Borgman, M.; Nissen, S. E. *J. Am. Coll. Cardiol.* **2011**, *57* (9), 1111.
- (125) Puri, R.; Kataoka, Y.; Wolski, K.; Gordon, A.; Johansson, J.; Wong, N.; Nissen, S.; Nicholls, S. *J. Am. Coll. Cardiol.* **2014**, *63* (12), A1451.
- (126) Nicholls, S. J.; Puri, R.; Wolski, K.; Ballantyne, C. M.; Barter, P. J.; Brewer, H. B.; Kastelein, J. J. P.; Hu, B.; Uno, K.; Kataoka, Y.; Herrman, J.-P. R.; Merkely, B.; Borgman, M.; Nissen, S. E. *Am. J. Cardiovasc. Drugs* **2015**.
- (127) Picaud, S.; Wells, C.; Felletar, I.; Brotherton, D.; Martin, S.; Savitsky, P.; Diez-Dacal, B.; Philpott, M.; Bountra, C.; Lingard, H.; Fedorov, O.; Müller, S.; Brennan, P. E.; Knapp, S.; Filippakopoulos, P. *Proc. Natl. Acad. Sci. USA* **2013**, *110* (49), 19754.
- (128) Zhao, Y.; Yang, C.; Wang, S. *J. Med. Chem.* **2013**, *56* (19), 7498.
- (129) Mirguet, O.; Gosmini, R.; Toum, J.; Clément, C. a; Barnathan, M.; Brusq, J.-M.; Mordaunt, J. E.; Grimes, R. M.; Crowe, M.; Pineau, O.; Ajakane, M.; Daugan, A.; Jeffrey, P.; Cutler, L.; Haynes, A. C.; Smithers, N. N.; Chung, C.-W.; Bamborough, P.; Uings, I. J.; Lewis, A.; Witherington, J.; Parr, N.; Prinjha, R. K.; Nicodème, E. *J. Med. Chem.* **2013**, *56* (19), 7501.
- (130) Boi, M.; Gaudio, E.; Bonetti, P.; Kwee, I.; Bernasconi, E.; Tarantelli, C.; Rinaldi, a.; Testoni, M.; Cascione, L.; Ponzoni, M.; Mensah, a. a.; Stathis, a.; Stussi, G.; Riveiro, M. E.; Herait, P.; Inghirami, G.; Cvitkovic, E.; Zucca, E.; Bertoni, F. *Clin. Cancer Res.* **2015**, *21* (3), 1628.

- (131) Chung, C.; Coste, H.; White, J. H.; Mirguet, O.; Wilde, J.; Gosmini, R. L.; Delves, C.; Magny, S. M.; Woodward, R.; Hughes, S. A.; Boursier, E. V.; Flynn, H.; Bouillot, A. M.; Bamborough, P.; Brusq, J.-M. G.; Gellibert, F. J.; Jones, E. J.; Riou, A. M.; Homes, P.; Martin, S. L.; Uings, I. J.; Toum, .; Cl ment, C. A.; Boullay, A.-B.; Grimley, R. L.; Blandel, F. M.; Prinjha, R. K.; Lee, K.; Kirilovsky, J.; Nicodeme, E. *J. Med. Chem.* **2011**, *54* (11), 3827.
- (132) Philpott, M.; Yang, J.; Tumber, T.; Fedorov, O.; Uttarkar, S.; Filippakopoulos, P.; Picaud, S.; Keates, T.; Felletar, I.; Ciulli, A.; Knapp, S.; Heightman, T. D. *Mol. BioSyst* **2011**, *7* (10), 2899.
- (133) Hewings, D. S.; Wang, M.; Philpott, M.; Fedorov, O.; Uttarkar, S.; Filippakopoulos, P.; Picaud, S.; Vuppusetty, C.; Marsden, B.; Knapp, S.; Conway, S. J.; Heightman, T. D. *J. Med. Chem.* **2011**, *54* (19), 6761.
- (134) Hewings, D. S.; Fedorov, O.; Filippakopoulos, P.; Martin, S.; Picaud, S.; Tumber, A.; Wells, C.; Olcina, M. M.; Freeman, K.; Gill, A.; Ritchie, A. J.; Sheppard, D. W.; Russell, A. J.; Hammond, E. M.; Knapp, S.; Brennan, P. E.; Conway, S. J. *J. Med. Chem.* **2013**, *56* (8), 3217.
- (135) Hay, D.; Fedorov, O.; Filippakopoulos, P.; Martin, S.; Philpott, M.; Picaud, S.; Hewings, D. S.; Uttakar, S.; Heightman, T. D.; Conway, S. J.; Knapp, S.; Brennan, P. E. *Med. Chem. Commun.* **2013**, *4* (1), 140.
- (136) Bamborough, P.; Diallo, H.; Goodacre, J. D.; Gordon, L.; Lewis, A.; Seal, J. T.; Wilson, D. M.; Woodrow, M. D.; Chung, C.-W. *J. Med. Chem.* **2012**, *55* (2), 587.
- (137) Seal, J.; Lamotte, Y.; Donche, F.; Bouillot, A.; Mirguet, O.; Gellibert, F.; Nicodeme, E.; Krysa, G.; Kirilovsky, J.; Beinke, S.; McCleary, S.; Rioja, I.; Bamborough, P.; Chung, C.-W.; Gordon, L.; Lewis, T.; Walker, A. L.; Cutler, L.; Lugo, D.; Wilson, D. M.; Witherington, J.; Lee, K.; Prinjha, R. K. *Bioorg. Med. Chem. Lett.* **2012**, *22* (8), 2968.
- (138) Ran, X.; Zhao, Y.; Liu, L.; Bai, L.; Yang, C.-Y.; Zhou, B.; Meagher, J. L.; Chinnaswamy, K.; Stuckey, J. a.; Wang, S. *J. Med. Chem.* **2015**, *58* (12), 4927.
- (139) Chung, C.-W.; Dean, A. W.; Woolven, J. M.; Bamborough, P. *J. Med. Chem.* **2012**, *55* (2), 576.
- (140) Zhao, L.; Cao, D.; Chen, T.; Wang, Y.; Miao, Z.; Xu, Y.; Chen, W.; Wang, X.; Li, Y.; Du, Z.; Xiong, B.; Li, J.; Xu, C.; Zhang, N.; He, J.; Shen, J. *J. Med. Chem.* **2013**, *56* (10), 3833.
- (141) Zhao, L.; Wang, Y.; Cao, D.; Chen, T.; Wang, Q.; Li, Y.; Xu, Y.; Zhang, N.; Wang, X.; Chen, D.; Chen, L.; Chen, Y.; Xia, G.; Shi, Z.; Liu, Y.; Lin, Y.; Miao, Z.; Shen, J.; Xiong, B. *J. Med. Chem.* **2015**, *58* (3), 1281.
- (142) Fish, P. V.; Filippakopoulos, P.; Bish, G.; Brennan, P. E.; Bunnage, M. E.; Cook, A. S.; Federov, O.; Gerstenberger, B. S.; Jones, H.; Knapp, S.; Marsden, B.; Nocka, K.; Owen, D. R.; Philpott, M.; Picaud, S.; Primiano, M. J.; Ralph, M. J.; Sciammetta, N.; Trzuppek, J. D. *J. Med. Chem.* **2012**, *55* (22), 9831.
- (143) Picaud, S.; Da Costa, D.; Thanasopoulou, A.; Filippakopoulos, P.; Fish, P. V.; Philpott, M.; Fedorov, O.; Brennan, P.; Bunnage, M. E.; Owen, D. R.; Bradner, J. E.; Taniere, P.; O'Sullivan, B.; Müller, S.; Schwaller, J.; Stankovic, T.; Knapp, S. *Cancer Res.* **2013**, *73* (11), 3336.
- (144) Wu, J.; Shin, J.; Williams, C. M. M.; Geoghegan, K. F.; Wright, S. W.; Limburg, D. C.; Sahasrabudhe, P.; Bonin, P. D.; Lefker, B. a.; Ramsey, S. J. *Med. Chem. Commun.* **2014**, *5*, 1871.
- (145) Zhang, G.; Plotnikov, A. N.; Rusinova, E.; Shen, T.; Morohashi, K.; Joshua, J.; Zeng, L.; Mujtaba, S.; Ohlmeyer, M.; Zhou, M.-M. *J. Med. Chem.* **2013**, *56* (22), 9251.
- (146) Gacias, M.; Gerona-Navarro, G.; Plotnikov, A. N.; Zhang, G.; Zeng, L.; Kaur, J.; Moy, G.; Rusinova, E.; Rodriguez, Y.; Matikainen, B.; Vincek, A.; Joshua, J.; Casaccia, P.; Zhou, M.-M. *Chem. Biol.* **2014**, *21* (7), 841.
- (147) Baud, M. G. J.; Lin-Shiao, E.; Cardote, T.; Tallant, C.; Pschibul, A.; Chan, K.-H.; Zengerle, M.; Garcia, J. R.; Kwan, T. T.-L.; Ferguson, F. M.; Ciulli, A. *Science (80-)*. **2014**, *346*, 638.
- (148) Baud, M. G. J.; Lin-Shiao, E.; Zengerle, M.; Tallant, C.; Ciulli, A. *J. Med. Chem.* **2016**, *59* (4), 1492.
- (149) Devaiah, B. N.; Lewis, B. a.; Cherman, N.; Hewitt, M. C.; Albrecht, B. K.; Robey, P. G.; Ozato, K.; Sims, R. J.; Singer, D. S. *Proc. Natl. Acad. Sci.* **2012**, *109* (18), 6927.
- (150) Ciceri, P.; Müller, S.; O'Mahony, A.; Fedorov, O.; Filippakopoulos, P.; Hunt, J. P.; Lasater, E. A.; Pallares, G.; Picaud, S.; Wells, C.; Martin, S.; Wodicka, L. M.; Shah, N. P.; Treiber, D. K.; Knapp, S. *Nat. Chem. Biol.* **2014**, *10* (4), 305.
- (151) Martin, M. P.; Olesen, S. H.; Georg, G. I.; Schönbrunn, E. *ACS Chem. Biol.* **2013**, *8* (11), 2360.
- (152) Ember, S. W. J.; Zhu, J. Y.; Olesen, S. H.; Martin, M. P.; Becker, A.; Berndt, N.; Georg, G. I.; Schonbrunn, E. *ACS Chem. Biol.* **2014**, *9* (5), 1160.
- (153) Chen, L.; Yap, J. L.; Yoshioka, M.; Lanning, M. E.; Fountain, R. N.; Rajee, M.; Scheenstra, J. a.; Strovel, J. W.; Fletcher, S. *ACS Med. Chem. Lett.* **2015**, *6* (7), 764.
- (154) Winter, G. E.; Buckley, D. L.; Paulk, J.; Roberts, J. M.; Souza, A.; Dhe-paganon, S.; Bradner, J. E. *Science (80-)*. **2015**, *348* (6241), 1376.
- (155) Zengerle, M.; Chan, K.-H.; Ciulli, A. *ACS Chem. Biol.* **2015**, *10* (8), 1770.
- (156) Brand, M.; Measures, A. M.; Wilson, B. G.; Cortopassi, W. a.; Alexander, R.; Höss, M.; Hewings, D. S.; Rooney, T. P. C.; Paton, R. S.; Conway, S. J. *ACS Chem. Biol.* **2015**, *10* (1), 22.

- (157) Vidler, L. R.; Brown, N.; Knapp, S.; Hoelder, S. *J. Med. Chem.* **2012**, *55*, 7346.
- (158) Boussoeur, F.; Jamshidikia, M.; Morozumi, Y.; Rousseaux, S.; Khochbin, S. *Biochim. Biophys. Acta - Gene Regul. Mech.* **2013**, *1829* (10), 1010.
- (159) Ciro, M.; Prosperini, E.; Quarto, M.; Grazini, U.; Walfridsson, J.; McBlane, F.; Nucifero, P.; Pacchiana, G.; Capra, M.; Christensen, J.; Helin, K. *Cancer Res.* **2009**, *69* (21), 8491.
- (160) Caron, C.; Lestrat, C.; Marsal, S.; Escoffier, E.; Curtet, S.; Virolle, V.; Barbry, P.; Debernardi, A.; Brambilla, C.; Brambilla, E.; Rousseaux, S.; Khochbin, S. *Oncogene* **2010**, *29* (37), 5171.
- (161) Wu, G.; Lu, X.; Wang, Y.; He, H.; Meng, X.; Xia, S.; Zhen, K.; Liu, Y. *Int. J. Oncol.* **2014**, *45*, 351.
- (162) Zou, J. X.; Guo, L.; Revenko, A. S.; Tepper, C. G.; Gemo, A. T.; Kung, H.-J.; Chen, H.-W. *Cancer Res.* **2009**, *69* (8), 3339.
- (163) Chaikuad, A.; Petros, A. M.; Fedorov, O.; Xu, J.; Knapp, S. *Med. Chem. Commun.* **2014**, *00*, 1.
- (164) Mary J. Harner, Brian A. Chauder, Jason Phan, and S. W. F. *J. Med. Chem.* **2014**, *57*, 9687.
- (165) Devine, S. M.; Mulcair, M. D.; Debono, C. O.; Leung, E. W. W.; Nissink, J. W. M.; Lim, S. S.; Chandrashekar, I. R.; Vazirani, M.; Mohanty, B.; Simpson, J. S.; Baell, J. B.; Scammells, P. J.; Norton, R. S.; Scanlon, M. J. *J. Med. Chem.* **2015**, *58* (3), 1205.
- (166) Demont, E. H.; Chung, C.; Furze, R. C.; Grandi, P.; Michon, A.-M.; Wellaway, C.; Barrett, N.; Bridges, A. M.; Craggs, P. D.; Diallo, H.; Dixon, D. P.; Douault, C.; Emmons, A. J.; Jones, E. J.; Karamshi, B. V.; Locke, K.; Mitchell, D. J.; Mouzon, B. H.; Prinjha, R. K.; Roberts, A. D.; Sheppard, R. J.; Watson, R. J.; Bamborough, P. *J. Med. Chem.* **2015**, *58* (14), 5649.
- (167) Bamborough, P.; Chung, C.; Furze, R. C.; Grandi, P.; Michon, A.-M.; Sheppard, R. J.; Barnett, H.; Diallo, H.; Dixon, D. P.; Douault, C.; Jones, E. J.; Karamshi, B.; Mitchell, D. J.; Prinjha, R. K.; Rau, C.; Watson, R. J.; Werner, T.; Demont, E. H. *J. Med. Chem.* **2015**, *58* (15), 6151. (168) Jones, M. H.; Hamana, N.; Nezu, J. i; Shimane, M. *Genomics* **2000**, *63*, 40.
- (169) Guetg, C.; Lienemann, P.; Sirri, V.; Grummt, I.; Hernandez-Verdun, D.; Hottiger, M. O.; Fussenegger, M.; Santoro, R. *EMBO J.* **2010**, *29*, 2135.
- (170) Ferguson, F. M.; Fedorov, O.; Chaikuad, A.; Philpott, M.; Muniz, J. R. C.; Felletar, I.; Von Delft, F.; Heightman, T.; Knapp, S.; Abell, C.; Ciulli, A. *J. Med. Chem.* **2013**, *56*, 10183.
- (171) Drouin, L.; McGrath, S.; Vidler, L. R.; Chaikuad, A.; Monteiro, O.; Tallant, C.; Philpott, M.; Rogers, C.; Fedorov, O.; Liu, M.; Akhtar, W.; Hayes, A.; Raynaud, F.; Müller, S.; Knapp, S.; Hoelder, S. *J. Med. Chem.* **2015**, *58*, 2553.
- (172) Chen, P.; Chaikuad, A.; Bamborough, P.; Bantscheff, M.; Bountra, C.; Chung, C.-W.; Fedorov, O.; Grandi, P.; Jung, D.; Lesniak, R.; Lindon, M.; Müller, S.; Philpott, M.; Prinjha, R.; Rogers, C.; Selenski, C.; Tallant, C.; Werner, T.; Willson, T. M.; Knapp, S.; Drewry, D. H. *J. Med. Chem.* **2016**, *59* (4), 1410.
- (173) Jones, M. H.; Hamana, N.; Shimane, M. *Genomics* **2000**, *63* (1), 35.
- (174) Xiao, H.; Sandaltzopoulos, R.; Wang, H.-M.; Hamiche, A.; Ranallo, R.; Lee, K.-M.; Fu, D.; Wu, C. *Mol. Cell* **2001**, *8* (3), 531.
- (175) Landry, J.; Sharov, A. A.; Piao, Y.; Sharova, L. V.; Xiao, H.; Southon, E.; Matta, J.; Tessarollo, L.; Zhang, Y. E.; Ko, M. S. H.; Kuehn, M. R.; Yamaguchi, T. P.; Wu, C. *PLoS Genet.* **2008**, *4* (10), e1000241.
- (176) Ruthenburg, A. J.; Li, H.; Milne, T. A.; Dewell, S.; McGinty, R. K.; Yuen, M.; Ueberheide, B.; Dou, Y.; Muir, T. W.; Patel, D. J.; Allis, C. D. *Cell* **2011**, *145* (5), 692.
- (177) Kim, K.; Punj, V.; Choi, J.; Heo, K.; Kim, J.-M.; Laird, P. W.; An, W. *Epigeneti. Chromatin* **2013**, *6* (1), 34.
- (178) Xiao, S.; Liu, L.; Lu, X.; Long, J.; Zhou, X.; Fang, M. *J. Cancer Res. Clin. Oncol.* **2015**, *141* (8), 1465.
- (179) Dar, A. A.; Nosrati, M.; Bezrookove, V.; de Semir, D.; Majid, S.; Thummala, S.; Sun, V.; Tong, S.; Leong, S. P. L.; Minor, D.; Billings, P. R.; Soroceanu, L.; Debs, R.; Miller, J. R.; Sagebiel, R. W.; Kashani-Sabet, M. *JNCI J. Natl. Cancer Inst.* **2015**, *107* (5), djv034.
- (180) Urick, A. K.; Hawk, L. M. L.; Cassel, M. K.; Mishra, N. K.; Liu, S.; Adhikari, N.; Zhang, W.; dos Santos, C. O.; Hall, J. L.; Pomerantz, W. C. K. *ACS Chem. Biol.* **2015**, *10* (10), 2246.
- (181) Carlson, S.; Glass, K. C. *J. Cell. Physiol.* **2014**, *229* (11), 1571.
- (182) Camós, M.; Esteve, J.; Jares, P.; Colomer, D.; Rozman, M.; Villamor, N.; Costa, D.; Carrió, A.; Nomdedéu, J.; Montserrat, E.; Campo, E. *Cancer Res.* **2006**, *66* (14), 6947.
- (183) Laue, K.; Daujat, S.; Crump, J. G.; Plaster, N.; Roehl, H. H.; Kimmel, C. B.; Schneider, R.; Hammerschmidt, M. *Development* **2008**, *135* (11), 1935.
- (184) Perez-campo, F. M.; Borrow, J.; Kouskoff, V.; Lacaud, G. *Blood* **2009**, *113* (20), 4866.
- (185) Hibiya, K.; Katsumoto, T.; Kondo, T.; Kitabayashi, I.; Kudo, A. *Dev. Biol.* **2009**, *329* (2), 176.
- (186) You, L.; Yan, K.; Zhou, J.; Zhao, H.; Bertos, N. R.; Park, M.; Wang, E.; Yang, X.-J. *PLOS Genet.* **2015**, *11* (3), e1005034.

- (187) Mishima, Y.; Miyagi, S.; Saraya, A.; Negishi, M.; Endoh, M.; Endo, T. A.; Toyoda, T.; Shinga, J.; Katsumoto, T.; Chiba, T.; Yamaguchi, N.; Kitabayashi, I.; Koseki, H.; Iwama, A. *Blood* **2011**, *118* (9), 2443.
- (188) Severinsen, J. E.; Bjarkam, C. R.; Kiaer-Larsen, S.; Olsen, I. M.; Nielsen, M. M.; Blechingberg, J.; Nielsen, A. L.; Holm, I. E.; Foldager, L.; Young, B. D.; Muir, W. J.; Blackwood, D. H. R.; Corydon, T. J.; Mors, O.; Børglum, A. D. *Mol. Psychiatry* **2006**, *11* (12), 1126.
- (189) van der Zwaag, B.; Franke, L.; Poot, M.; Hochstenbach, R.; Spierenburg, H. A.; Vorstman, J. A. S.; van Daalen, E.; de Jonge, M. V.; Verbeek, N. E.; Brilstra, E. H.; van 't Slot, R.; Ophoff, R. A.; van Es, M. A.; Blauw, H. M.; Veldink, J. H.; Buizer-Voskamp, J. E.; Beemer, F. A.; van den Berg, L. H.; Wijmenga, C.; van Amstel, H. K. P.; van Engeland, H.; Burbach, J. P. H.; Staal, W. G. *PLoS One* **2009**, *4* (5), e5324.
- (190) Nyegaard, M.; Severinsen, J. E.; Als, T. D.; Hedemand, A.; Straarup, S.; Nordentoft, M.; McQuillin, A.; Bass, N.; Lawrence, J.; Thirumalai, S.; Pereira, A. C. P.; Kandaswamy, R.; Lydall, G. J.; Sklar, P.; Scolnick, E.; Purcell, S.; Curtis, D.; Gurling, H. M. D.; Mortensen, P. B.; Mors, O.; Børglum, A. D. *Am. J. Med. Genet. B. Neuropsychiatr. Genet.* **2010**, *153B* (2), 582.
- (191) Bjarkam, C. R.; Corydon, T. J.; Olsen, I. M. L.; Pallesen, J.; Nyegaard, M.; Fryland, T.; Mors, O.; Børglum, A. D. *Brain Struct. Funct.* **2009**, *214* (1), 37.
- (192) Kushima, I.; Aleksic, B.; Ikeda, M.; Yamanouchi, Y.; Kinoshita, Y.; Ito, Y.; Nakamura, Y.; Inada, T.; Iwata, N.; Ozaki, N. *Am. J. Med. Genet. B. Neuropsychiatr. Genet.* **2010**, *153B* (3), 786.
- (193) Poplawski, A.; Hu, K.; Lee, W.; Natesan, S.; Peng, D.; Carlson, S.; Shi, X.; Balaz, S.; Markley, J. L.; Glass, K. C. *J. Mol. Biol.* **2014**, *426* (8), 1661.
- (194) Demont, E. H.; Bamborough, P.; Chung, C.; Craggs, P. D.; Fallon, D.; Gordon, L. J.; Grandi, P.; Hobbs, C. I.; Hussain, J.; Jones, E. J.; Le Gall, A.; Michon, A.-M.; Mitchell, D. J.; Prinjha, R. K.; Roberts, A. D.; Sheppard, R. J.; Watson, R. J. *ACS Med. Chem. Lett.* **2014**, *5* (11), 1190.
- (195) The Structural Genomics Consortium. PFI-4 - a chemical probe for BRPF1B <http://www.thesgc.org/chemical-probes/PFI-4> (accessed Jul 27, 2015).
- (196) The Structural Genomics Consortium. OF-1 - a chemical probe for BRPF bromodomains <http://www.thesgc.org/chemical-probes/OF-1> (accessed Jul 27, 2015).
- (197) The Structural Genomics Consortium. NI-57 - a chemical probe for BRPF bromodomains <http://www.thesgc.org/chemical-probes/NI-57> (accessed Jul 27, 2015).
- (198) Palmer, W. S.; Poncet-Montange, G.; Liu, G.; Petrocchi, A.; Reyna, N.; Subramanian, G.; Theroff, J.; Yau, A.; Kost-Alimova, M.; Bardenhagen, J. P.; Leo, E.; Shepard, H. E.; Tieu, T. N.; Shi, X.; Zhan, Y.; Zhao, S.; Barton, M. C.; Draetta, G.; Toniatti, C.; Jones, P.; Geck Do, M.; Andersen, J. N. *J. Med. Chem.* **2016**, *59* (4), 1440.
- (199) Bennett, J.; Fedorov, O.; Tallant, C.; Monteiro, O.; Meier, J.; Gamble, V.; Savitsky, P.; NunezAlonso, G. a; Haendler, B.; Rogers, C.; Brennan, P. E.; Müller, S.; Knapp, S. *J. Med. Chem.* **2016**, *59* (4), 1642.
- (200) Middeljans, E.; Wan, X.; Jansen, P. W.; Sharma, V.; Stunnenberg, H. G.; Logie, C. *PLoS One* **2012**, *7* (3), e33834.
- (201) Kadoch, C.; Hargreaves, D. C.; Hodges, C.; Elias, L.; Ho, L.; Ranish, J.; Crabtree, G. R. *Nat. Genet.* **2013**, *45* (6), 592.
- (202) Hohmann, A. F.; Vakoc, C. R. *Trends Genet.* **2014**, *30* (8), 356.
- (203) Sun, H.; Liu, J.; Zhang, J.; Shen, W.; Huang, H.; Xu, C.; Dai, H.; Wu, J.; Shi, Y. *Biochem. Biophys. Res. Commun.* **2007**, *358* (2), 435.
- (204) Zhu, B.; Tian, J.; Zhong, R.; Tian, Y.; Chen, W.; Qian, J.; Zou, L.; Xiao, M.; Shen, N.; Yang, H.; Lou, J.; Qiu, Q.; Ke, J.; Lu, X.; Song, W.; Li, H.; Liu, L.; Wang, L.; Miao, X. *Mol. Carcinog.* **2015**, *54* (9), 761.
- (205) Drost, J.; Mantovani, F.; Tocco, F.; Elkon, R.; Comel, A.; Holstege, H.; Kerkhoven, R.; Jonkers, J.; Voorhoeve, P. M.; Agami, R.; Del Sal, G. *Nat. Cell Biol.* **2010**, *12* (4), 380.
- (206) Chiu, Y.-H.; Lee, J. Y.; Cantley, L. C. *Mol. Cell* **2014**, *54* (1), 193.
- (207) Scotto, L.; Narayan, G.; Nandula, S. V.; Subramaniam, S.; Kaufmann, A. M.; Wright, J. D.; Pothuri, B.; Mansukhani, M.; Schneider, A.; Arias-Pulido, H.; Murty, V. V. *Mol. Cancer* **2008**, *7* (1), 58.
- (208) Clark, P. G. K.; Vieira, L. C. C.; Tallant, C.; Fedorov, O.; Singleton, D. C.; Rogers, C. M.; Monteiro, O. P.; Bennett, J. M.; Baronio, R.; Müller, S.; Daniels, D. L.; Méndez, J.; Knapp, S.; Brennan, P. E.; Dixon, D. J. *Angew. Chem. Int. Ed. Engl.* **2015**, *54* (21), 6217.
- (209) Hay, D.; Brennan, P.; Fedorov, O.; Tallant, C.; Monteiro, O.; Muller-Knapp, S.; Knapp, S.; Schofield, C. J.; Martin, S.; Rogers, C. *Med. Chem. Commun.* **2015**, *6*, 1381.
- (210) The Structural Genomics Consortium. BI-9564 - A chemical probe for BRD9 and BRD7 <http://www.thesgc.org/chemical-probes/BI-9564> (accessed Aug 3, 2015).
- (211) Theodoulou, N. H.; Bamborough, P.; Bannister, A. J.; Becher, I.; Bit, R. a; Che, K. H.; Chung, C.-W.; Dittmann, A.; Drewes, G.; Drewry, D. H.; Gordon, L.; Grandi, P.; Leveridge, M.; Lindon, M.; Michon, A.-M.; Molnar, J.; Robson, S. C.; Tomkinson, N. C. O.; Kouzarides, T.; Prinjha, R.

- K.; Humphreys, P. G. *J. Med. Chem.* **2016**, *59* (4), 1425.
- (212) Monden, T.; Wondisford, F. E.; Hollenberg, A. N. *J. Biol. Chem.* **1997**, *272* (47), 29834.
- (213) Doyon, Y.; Côté, J. *Curr. Opin. Genet. Dev.* **2004**, *14* (2), 147.
- (214) Yamada, H. Y.; Rao, C. V. *Int. J. Oncol.* **2009**, *35* (5), 1101.
- (215) Couture, J.-P.; Nolet, G.; Beaulieu, E.; Blouin, R.; Gévry, N. *Endocrinology* **2012**, *153* (12), 5796.
- (216) Smith, T. F.; Gaitatzes, C.; Saxena, K.; Neer, E. J. *Trends Biochem. Sci.* **1999**, *24* (5), 181.
- (217) Philipps, D. L.; Wigglesworth, K.; Hartford, S. A.; Sun, F.; Pattabiraman, S.; Schimenti, K.; Handel, M.; Eppig, J. J.; Schimenti, J. C. *Dev. Biol.* **2008**, *317* (1), 72.
- (218) Farhang-Fallah, J.; Randhawa, V. K.; Nimmual, A.; Klip, A.; Bar-Sagi, D.; Rozakis-Adcock, M. *Mol. Cell. Biol.* **2002**, *22* (20), 7325.
- (219) Podcheko, A.; Northcott, P.; Bikopoulos, G.; Lee, A.; Bommarreddi, S. R.; Kushner, J. A.; Farhang-Fallah, J.; Rozakis-Adcock, M. *Mol. Cell. Biol.* **2007**, *27* (18), 6484.
- (220) Jin, J.; Arias, E. E.; Chen, J.; Harper, J. W.; Walter, J. C. *Mol. Cell* **2006**, *23* (5), 709.
- (221) Grotto, S.; Drouin-Garraud, V.; Ounap, K.; Puusepp-Benazzouz, H.; Schuurs-Hoeijmakers, J.; Le Meur, N.; Chambon, P.; Fehrenbach, S.; van Bokhoven, H.; Frébourg, T.; de Brouwer, A. P. M.; Saugier-veber, P. *Eur. J. Med. Genet.* **2014**, *57* (5), 200.
- (222) Field, M.; Tarpey, P. S.; Smith, R.; Edkins, S.; O'Meara, S.; Stevens, C.; Tofts, C.; Teague, J.; Butler, A.; Dicks, E.; Barthorpe, S.; Buck, G.; Cole, J.; Gray, K.; Halliday, K.; Hills, K.; Jenkinson, A.; Jones, D.; Menzies, A.; Mironenko, T.; Perry, J.; Raine, K.; Richardson, D.; Shepherd, R.; Small, A.; Varian, J.; West, S.; Widaa, S.; Mallya, U.; Wooster, R.; Moon, J.; Luo, Y.; Hughes, H.; Shaw, M.; Friend, K. L.; Corbett, M.; Turner, G.; Partington, M.; Mulley, J.; Bobrow, M.; Schwartz, C.; Stevenson, R.; Gecz, J.; Stratton, M. R.; Futreal, P. A.; Raymond, F. L. *Am. J. Hum. Genet.* **2007**, *81* (2), 367.
- (223) Hino-Fukuyo, N.; Kikuchi, A.; Arai-Ichinoi, N.; Niihori, T.; Sato, R.; Suzuki, T.; Kudo, H.; Sato, Y.; Nakayama, T.; Kakisaka, Y.; Kubota, Y.; Kobayashi, T.; Funayama, R.; Nakayama, K.; Uematsu, M.; Aoki, Y.; Haginoya, K.; Kure, S. *Hum. Genet.* **2015**, *134* (6), 649.
- (224) Banting, G. S.; Barak, O.; Ames, T. M.; Burnham, A. C.; Kardel, M. D.; Cooch, N. S.; Davidson, C. E.; Godbout, R.; McDermid, H. E.; Shiekhhattar, R. *Hum. Mol. Genet.* **2005**, *14* (4), 513.
- (225) Thompson, P. J.; Norton, K. A.; Niri, F. H.; Dawe, C. E.; McDermid, H. E. *J. Mol. Biol.* **2012**, *415* (5), 793.
- (226) Lee, S.-K.; Park, E.-J.; Lee, H.-S.; Lee, Y. S.; Kwon, J. *Mol. Cells* **2012**, *34* (1), 85.
- (227) The Structural Genomics Consortium. NVS-1 - A chemical probe for CECR2 <http://www.thesgc.org/chemical-probes/NVS-1> (accessed Aug 2, 2015).
- (228) Levine, A. J. *Cell* **1997**, *88* (3), 323.
- (229) Mujtaba, S.; He, Y.; Zeng, L.; Yan, S.; Plotnikova, O.; Sachchidanand; Sanchez, R.; ZeleznikLe, N. J.; Ronai, Z.; Zhou, M. M. *Mol. Cell* **2004**, *13* (2), 251.
- (230) Hay, D. A.; Fedorov, O.; Martin, S.; Singleton, D. C.; Tallant, C.; Wells, C.; Picaud, S.; Philpott, M.; Monteiro, O. P.; Rogers, C. M.; Conway, S. J.; Rooney, T. P. C.; Tumber, A.; Yapp, C.; Filippakopoulos, P.; Bunnage, M. E.; Müller, S.; Knapp, S.; Schofield, C. J.; Brennan, P. E. *J. Am. Chem. Soc.* **2014**, *136* (26), 9308.
- (231) Rooney, T. P. C.; Filippakopoulos, P.; Fedorov, O.; Picaud, S.; Cortopassi, W. A.; Hay, D. A.; Martin, S.; Tumber, A.; Rogers, C. M.; Philpott, M.; Wang, M.; Thompson, A. L.; Heightman, T. D.; Pryde, D. C.; Cook, A.; Paton, R. S.; Müller, S.; Knapp, S.; Brennan, P. E.; Conway, S. J. *Angew. Chem. Int. Ed.* **2014**, *53* (24), 6126.
- (232) The Structural Genomics Consortium. I-CBP112 - a CREBBP/EP300-selective chemical probe <http://www.thesgc.org/chemical-probes/ICBP112> (accessed Jul 26, 2015).
- (233) Picaud, S.; Fedorov, O.; Thanasopoulou, A.; Leonards, K.; Jones, K.; Meier, J.; Olzscha, H.; Monteiro, O.; Martin, S.; Philpott, M.; Tumber, A.; Filippakopoulos, P.; Yapp, C.; Wells, C.; Che, K. H.; Bannister, A.; Robson, S.; Kumar, U.; Parr, N.; Lee, K.; Lugo, D.; Jeffrey, P.; Taylor, S.; Vecellio, M. L.; Bountra, C.; Brennan, P. E.; O'Mahony, A.; Velichko, S.; Muller, S.; Hay, D.; Daniels, D. L.; Urh, M.; La Thangue, N. B.; Kouzarides, T.; Prinjha, R.; Schwaller, J.; Knapp, S. *Cancer Res.* **2015**, *75* (23), 5106.
- (234) Xu, M.; Unzue, A.; Dong, J.; Spiliotopoulos, D.; Nevado, C.; Caffisch, A. *J. Med. Chem.* **2016**, *59* (4), 1340.
- (235) Unzue, A.; Xu, M.; Dong, J.; Wiedmer, L.; Spiliotopoulos, D.; Caffisch, A.; Nevado, C. *J. Med. Chem.* **2016**, *59* (4), 1350.
- (236) Thompson, M. *Biochimie* **2009**, *91* (3), 309.
- (237) Chandrasekaran, R.; Thompson, M. *Biochem. Biophys. Res. Commun.* **2007**, *355* (3), 661.
- (238) Xue, Y.; Canman, J. C.; Lee, C. S.; Nie, Z.; Yang, D.; Moreno, G. T.; Young, M. K.; Salmon, E. D.; Wang, W. *Proc. Natl. Acad. Sci. U. S. A.* **2000**, *97* (24), 13015.
- (239) Huang, X.; Gao, X.; Diaz-Trelles, R.; Ruiz-Lozano, P.; Wang, Z. *Dev. Biol.* **2008**, *319* (2), 258.
- (240) Xia, W.; Nagase, S.; Montia, A. G.; Kalachikov, S. M.; Keniry, M.; Su, T.; Memeo, L.; Hibshoosh, H.; Parsons, R. *Cancer Res.* **2008**, *68* (6), 1667.

- (241) Varela, I.; Tarpey, P.; Raine, K.; Huang, D.; Ong, C. K.; Stephens, P.; Davies, H.; Jones, D.; Lin, M.-L.; Teague, J.; Bignell, G.; Butler, A.; Cho, J.; Dalgliesh, G. L.; Galappaththige, D.; Greenman, C.; Hardy, C.; Jia, M.; Latimer, C.; Lau, K. W.; Marshall, J.; McLaren, S.; Menzies, A.; Mudie, L.; Stebbings, L.; Largaespada, D. A.; Wessels, L. F. A.; Richard, S.; Kahnoski, R. J.; Anema, J.; Tuveson, D. A.; Perez-Mancera, P. A.; Mustonen, V.; Fischer, A.; Adams, D. J.; Rust, A.; Chanon, W.; Subimerb, C.; Dykema, K.; Furge, K.; Campbell, P. J.; Teh, B. T.; Stratton, M. R.; Futreal, P. A. *Nature* **2011**, *469* (7331), 539.
- (242) Wilson, B. G.; Roberts, C. W. M. *Nat. Rev. Cancer* **2011**, *11* (7), 481.
- (243) Oike, T.; Ogiwara, H.; Tominaga, Y.; Ito, K.; Ando, O.; Tsuta, K.; Mizukami, T.; Shimada, Y.; Isomura, H.; Komachi, M.; Furuta, K.; Watanabe, S.-I.; Nakano, T.; Yokota, J.; Kohno, T. *Cancer Res.* **2013**, *73* (17), 5508.
- (244) Hoffman, G. R.; Rahal, R.; Buxton, F.; Xiang, K.; McAllister, G.; Frias, E.; Bagdasarian, L.; Huber, J.; Lindeman, A.; Chen, D.; Romero, R.; Ramadan, N.; Phadke, T.; Haas, K.; Jaskelioff, M.; Wilson, B. G.; Meyer, M. J.; Saenz-Vash, V.; Zhai, H.; Myer, V. E.; Porter, J. A.; Keen, N.; McLaughlin, M. E.; Mickanin, C.; Roberts, C. W. M.; Stegmeier, F.; Jagani, Z. *Proc. Natl. Acad. Sci. U. S. A.* **2014**, *111* (8), 3128.
- (245) Wilson, B. G.; Helming, K. C.; Wang, X.; Kim, Y.; Vazquez, F.; Jagani, Z.; Hahn, W. C.; Roberts, C. W. M. *Mol. Cell. Biol.* **2014**, *34* (6), 1136.
- (246) Vangamudi, B.; Paul, T. A.; Shah, P. K.; Kost-Alimova, M.; Nottebaum, L.; Shi, X.; Zhan, Y.; Leo, E.; Mahadeshwar, H. S.; Protopopov, A.; Futreal, A.; Tieu, T. N.; Peoples, M.; Heffernan, T. P.; Marszalek, J. R.; Toniatti, C.; Petrocchi, A.; Verhelle, D.; Owen, D. R.; Draetta, G.; Jones, P.; Palmer, W. S.; Sharma, S.; Andersen, J. N. *Cancer Res.* **2015**, *75* (18), 3865.
- (247) The Structural Genomics Consortium. PFI-3: Selective chemical probe for SMARCA bromodomains <http://www.thesgc.org/chemical-probes/PFI-3> (accessed Aug 4, 2015).
- (248) Filippakopoulos, P.; Picaud, S.; von Delft, F.; Arrowsmith, C.H., Edwards, A.M., Bountra, C., Knapp, S., S. G. C. (SGC). RSC Protein Data Bank: Crystal Structure of the fifth bromodomain of Human Poly-bromodomain containing protein 1 (PB1) in complex with a hydroxyphenylpropenone ligand (Entry 4QUO) <http://www.rcsb.org/pdb/explore/explore.do?structureId=4q0o> (accessed Aug 4, 2015).
- (249) Bamborough, P.; Chung, C. *Med. Chem. Commun.* **2015**, *6* (9), 1587.
- (250) Dhalluin, C.; Carlson, J. E.; Zeng, L.; He, C.; Aggarwal, A. K.; Zhou, M. M. *Nature* **1999**, *399* (6735), 491.
- (251) Kanno, T.; Kanno, Y.; Siegel, R. M.; Jang, M. K.; Lenardo, M. J.; Ozato, K. *Mol. Cell* **2004**, *13* (1), 33.
- (252) Ott, M.; Schnölzer, M.; Garnica, J.; Fischle, W.; Emiliani, S.; Rackwitz, H. R.; Verdin, E. *Curr. Biol.* **1999**, *9* (24), 1489.
- (253) Mujtaba, S.; He, Y.; Zeng, L.; Farooq, A.; Carlson, J. E.; Ott, M.; Verdin, E.; Zhou, M.-M. *Mol. Cell* **2002**, *9* (3), 575.
- (254) Zeng, L.; Li, J.; Muller, M.; Yan, S.; Mujtaba, S.; Pan, C.; Wang, Z.; Zhou, M. M. *J. Am. Chem. Soc.* **2005**, *127* (8), 2376.
- (255) Pan, C.; Mezei, M.; Mujtaba, S.; Muller, M.; Zeng, L.; Li, J.; Wang, Z.; Zhou, M. M. *J. Med. Chem.* **2007**, *50* (10), 2285.
- (256) Wang, Q.; Wang, R.; Zhang, B.; Zhang, S.; Zheng, Y.; Wang, Z. *Med. Chem. Commun.* **2013**, *4* (4), 737.
- (257) Bloch, D. B.; de la Monte, S. M.; Guigaouri, P.; Filippov, A.; Bloch, K. D. *J. Biol. Chem.* **1996**, *271* (46), 29198.
- (258) Zucchelli, C.; Tamburri, S.; Quilici, G.; Palagano, E.; Berardi, A.; Saare, M.; Peterson, P.; Bachi, A.; Musco, G. *FEBS J.* **2014**, *281* (1), 216.
- (259) Bernardi, R.; Pandolfi, P. P. *Nat. Rev. Mol. Cell Biol.* **2007**, *8* (12), 1006.
- (260) Stepp, W. H.; Meyers, J. M.; McBride, A. A. *MBio* **2013**, *4* (6), e00845.
- (261) Tavalai, N.; Adler, M.; Scherer, M.; Riedl, Y.; Stamminger, T. *J. Virol.* **2011**, *85* (18), 9447.
- (262) Granito, A.; Yang, W.-H.; Muratori, L.; Lim, M. J.; Nakajima, A.; Ferri, S.; Pappas, G.; Quarneri, C.; Bianchi, F. B.; Bloch, D. B.; Muratori, P. *Am. J. Gastroenterol.* **2010**, *105* (1), 125.
- (263) Szosteki, C.; Guldner, H. H.; Netter, H. J.; Will, H. *J. Immunol.* **1990**, *145* (12), 4338.
- (264) Bloch, D. B.; Nakajima, A.; Gulick, T.; Chiche, J. D.; Orth, D.; de La Monte, S. M.; Bloch, K. D. *Mol. Cell. Biol.* **2000**, *20* (16), 6138.
- (265) Roscioli, T.; Cliffe, S. T.; Bloch, D. B.; Bell, C. G.; Mullan, G.; Taylor, P. J.; Sarris, M.; Wang, J.; Donald, J. A.; Kirk, E. P.; Ziegler, J. B.; Salzer, U.; McDonald, G. B.; Wong, M.; Lindeman, R.; Buckley, M. F. *Nat. Genet.* **2006**, *38* (6), 620.
- (266) Madani, N.; Millette, R.; Platt, E. J.; Marin, M.; Kozak, S. L.; Bloch, D. B.; Kabat, D. *J. Virol.* **2002**, *76* (21), 11133.

- (267) Franke, A.; McGovern, D. P. B.; Barrett, J. C.; Wang, K.; Radford-Smith, G. L.; Ahmad, T.; Lees, C. W.; Balschun, T.; Lee, J.; Roberts, R.; Anderson, C. A.; Bis, J. C.; Bumpstead, S.; Ellinghaus, D.; Festen, E. M.; Georges, M.; Green, T.; Haritunians, T.; Jostins, L.; Latiano, A.; Mathew, C. G.; Montgomery, G. W.; Prescott, N. J.; Raychaudhuri, S.; Rotter, J. I.; Schumm, P.; Sharma, Y.; Simms, L. A.; Taylor, K. D.; Whiteman, D.; Wijmenga, C.; Baldassano, R. N.; Barclay, M.; Bayless, T. M.; Brand, S.; Büning, C.; Cohen, A.; Colombel, J.-F.; Cottone, M.; Stronati, L.; Denson, T.; De Vos, M.; D'Inca, R.; Dubinsky, M.; Edwards, C.; Florin, T.; Franchimont, D.; Gearry, R.; Glas, J.; Van Gossum, A.; Guthery, S. L.; Halfvarson, J.; Verspaget, H. W.; Hugot, J.-P.; Karban, A.; Laukens, D.; Lawrance, I.; Lemann, M.; Levine, A.; Libioulle, C.; Louis, E.; Mowat, C.; Newman, W.; Panés, J.; Phillips, A.; Proctor, D. D.; Regueiro, M.; Russell, R.; Rutgeerts, P.; Sanderson, J.; Sans, M.; Seibold, F.; Steinhart, A. H.; Stokkers, P. C. F.; Torkvist, L.; Kullak-Ublick, G.; Wilson, D.; Walters, T.; Targan, S. R.; Brant, S. R.; Rioux, J. D.; D'Amato, M.; Weersma, R. K.; Kugathasan, S.; Griffiths, A. M.; Mansfield, J. C.; Vermeire, S.; Duerr, R. H.; Silverberg, M. S.; Satsangi, J.; Schreiber, S.; Cho, J. H.; Annese, V.; Hakonarson, H.; Daly, M. J.; Parkes, M. *Nat. Genet.* **2010**, *42* (12), 1118.
- (268) Di Bernardo, M. C.; Crowther-Swanepoel, D.; Broderick, P.; Webb, E.; Sellick, G.; Wild, R.; Sullivan, K.; Vijayakrishnan, J.; Wang, Y.; Pittman, A. M.; Sunter, N. J.; Hall, A. G.; Dyer, M. J. S.; Matutes, E.; Dearden, C.; Mainou-Fowler, T.; Jackson, G. H.; Summerfield, G.; Harris, R. J.; Pettitt, A. R.; Hillmen, P.; Allsup, D. J.; Bailey, J. R.; Pratt, G.; Pepper, C.; Fegan, C.; Allan, J. M.; Catovsky, D.; Houlston, R. S. *Nat. Genet.* **2008**, *40* (10), 1204.
- (269) Tallant, C., Nunez-Alonso, G., Savitsky, P., Newman, J., Krojer, T., Szykowska, A., BurgessBrown, N., Filippakopoulos, P., von Delft, F., Arrowsmith, C.H., Edwards, A.M., Bountra, C., Knapp, S. RSC Protein Data Bank: Crystal structure of human SP100 PHD-Bromodomain in the free state (Entry 4PTB) <http://www.rcsb.org/pdb/explore.do?structureId=4PTB> (accessed Aug 4, 2015).
- (270) Prinjha, R. K.; Witherington, J.; Lee, K. *Trends Pharmacol. Sci.* **2012**, *33* (3), 146.
- (271) Jacobson, R. H.; Ladurner, A. G.; King, D. S.; Tjian, R. *Science* (80-.). **2000**, *288* (5470), 1422.
- (272) Wassarman, D. A.; Sauer, F. *J. Cell Sci.* **2001**, *114* (Pt 16), 2895.
- (273) Wang, P. J.; Page, D. C. *Hum. Mol. Genet.* **2002**, *11* (19), 2341.
- (274) Tavassoli, P.; Wafa, L. A.; Cheng, H.; Zoubeidi, A.; Fazli, L.; Gleave, M.; Snoek, R.; Rennie, P. S. *Mol. Endocrinol.* **2010**, *24* (4), 696.
- (275) O'Rawe, J.; Wu, Y.; Rope, A.; Jimenez Barrón, L. T.; Swensen, J.; Fang, H.; Mittelman, D.; Highnam, G.; Robison, R.; Yang, E.; Wang, K.; Lyon, G. *bioRxiv* **2015**, 014050.
- (276) Hu, H.; Haas, S. A.; Chelly, J.; Van Esch, H.; Raynaud, M.; de Brouwer, A. P. M.; Weinert, S.; Froyen, G.; Frints, S. G. M.; Laumonier, F.; Zemojtel, T.; Love, M. I.; Richard, H.; Emde, A.-K.; Bienek, M.; Jensen, C.; Hambrock, M.; Fischer, U.; Langnick, C.; Feldkamp, M.; WissinkLindhout, W.; Lebrun, N.; Castelnau, L.; Rucci, J.; Montjean, R.; Dorseuil, O.; Billuart, P.; Stuhlmann, T.; Shaw, M.; Corbett, M. A.; Gardner, A.; Willis-Owen, S.; Tan, C.; Friend, K. L.; Belet, S.; van Roozendaal, K. E. P.; Jimenez-Pocquet, M.; Moizard, M.-P.; Ronce, N.; Sun, R.; O'Keeffe, S.; Chenna, R.; van Bömmel, A.; Göke, J.; Hackett, A.; Field, M.; Christie, L.; Boyle, J.; Haan, E.; Nelson, J.; Turner, G.; Baynam, G.; Gillissen-Kaesbach, G.; Müller, U.; Steinberger, D.; Budny, B.; Badura-Stronka, M.; Latos-Bieleńska, A.; Ousager, L. B.; Wieacker, P.; Rodríguez Criado, G.; Bondeson, M.-L.; Annerén, G.; Dufke, A.; Cohen, M.; Van Maldergem, L.; Vincent-Delorme, C.; Echenne, B.; Simon-Bouy, B.; Kleefstra, T.; Willemsen, M.; Fryns, J.-P.; Devriendt, K.; Ullmann, R.; Vingron, M.; Wrogemann, K.; Wienker, T. F.; Tzschach, A.; van Bokhoven, H.; Gecz, J.; Jentsch, T. J.; Chen, W.; Ropers, H.-H.; Kalscheuer, V. M. *Mol. Psychiatry* **2016**, *21* (1), 133.
- (277) Makino, S.; Kaji, R.; Ando, S.; Tomizawa, M.; Yasuno, K.; Goto, S.; Matsumoto, S.; Tabuena, M. D.; Maranon, E.; Dantes, M.; Lee, L. V.; Ogasawara, K.; Tooyama, I.; Akatsu, H.; Nishimura, M.; Tamiya, G. *Am. J. Hum. Genet.* **2007**, *80* (3), 393.
- (278) Allende-Vega, N.; Saville, M. K.; Meek, D. W. *Oncogene* **2007**, *26* (29), 4234.
- (279) Zhao, S.; Choi, M.; Overton, J. D.; Bellone, S.; Roque, D. M.; Cocco, E.; Guzzo, F.; English, D. P.; Varughese, J.; Gasparrini, S.; Bortolomai, I.; Buza, N.; Hui, P.; Abu-Khalaf, M.; Ravaggi, A.; Bignotti, E.; Bandiera, E.; Romani, C.; Todeschini, P.; Tassi, R.; Zanotti, L.; Carrara, L.; Pecorelli, S.; Silasi, D.-A.; Ratner, E.; Azodi, M.; Schwartz, P. E.; Rutherford, T. J.; Stiegler, A. L.; Mane, S.; Boggon, T. J.; Schlessinger, J.; Lifton, R. P.; Santin, A. D. *Proc. Natl. Acad. Sci. U. S. A.* **2013**, *110* (8), 2916.
- (280) Tsai, W.-W.; Wang, Z.; Yiu, T. T.; Akdemir, K. C.; Xia, W.; Winter, S.; Tsai, C.-Y.; Shi, X.; Schwarzer, D.; Plunkett, W.; Aronow, B.; Gozani, O.; Fischle, W.; Hung, M.-C.; Patel, D. J.; Barton, M. C. *Nature* **2010**, *468* (7326), 927.
- (281) Le Douarin, B.; Nielsen, A. L.; Garnier, J. M.; Ichinose, H.; Jeanmougin, F.; Losson, R.; Chambon, P. *EMBO J.* **1996**, *15* (23), 6701.

- (282) Allton, K.; Jain, A. K.; Herz, H.-M.; Tsai, W.-W.; Jung, S. Y.; Qin, J.; Bergmann, A.; Johnson, R. L.; Barton, M. C. *Proc. Natl. Acad. Sci. USA* **2009**, *106* (28), 11612.
- (283) Cui, Z.; Cao, W.; Li, J.; Song, X.; Mao, L.; Chen, W. *PLoS One* **2013**, *8* (5), e63887.
- (284) Zhang, L.-H.; Yin, A.-A.; Cheng, J.-X.; Huang, H.-Y.; Li, X.-M.; Zhang, Y.-Q.; Han, N.; Zhang, X. *Oncogene* **2015**, *34* (5), 600.
- (285) Miao, Z.-F.; Wang, Z.-N.; Zhao, T.-T.; Xu, Y.-Y.; Wu, J.-H.; Liu, X.-Y.; Xu, H.; You, Y.; Xu, H.M. *Virchows Arch.* **2015**, *466* (5), 525.
- (286) Li, H.; Sun, L.; Tang, Z.; Fu, L.; Xu, Y.; Li, Z.; Luo, W.; Qiu, X.; Wang, E. *PLoS One* **2012**, *7* (5), e37657.
- (287) Katritzky, A.; Rachwal, S.; Rachwal, B. *Tetrahedron* **1996**, *52* (48), 15031.
- (288) Shamovsky, I.; Ripa, L.; Blomberg, N.; Eriksson, L. A.; Hansen, P.; Mee, C.; Tyrchan, C.; O'Donovan, M.; Sjö, P. *Chem. Res. Toxicol.* **2012**, *25*, 2236.
- (289) *The MAK Collection for Occupational Health and Safety*. 2012, pp 46–61.
- (290) Hirst, D.; Wellaway, C.; Harrison, L.; Bamborough, P. *GSK Unpublished Work*.
- (291) Zou, Z.; Huang, B.; Wu, X.; Zhang, H.; Qi, J.; Bradner, J.; Nair, S.; Chen, L.-F. *Oncogene* **2013**, *33*, 2395.
- (292) Chung, C.-W. GSK X-Ray Crystallography.
- (293) Hewings, D. S.; Rooney, T. P. C.; Jennings, L. E.; Hay, D. a; Schofield, C. J.; Brennan, P. E.; Knapp, S.; Conway, S. J. *J. Med. Chem.* **2012**.
- (294) Suzuki, R.; Mikami, A.; Tanaka, H.; Fukushima, H. Compounds having 11 β -HSD1 inhibitory activity. WO 2009001817 A1, 2008.
- (295) Venier, O.; Pascal, C.; Braun, A.; Namane, C.; Mougnot, P.; Crespin, O.; Pacquet, F.; Mougnot, C.; Monseau, C.; Onofri, B.; Dadjji-Faihun, R.; Leger, C.; Ben-Hassine, M.; VanPham, T.; Ragot, J.-L.; Philippo, C.; Güssregen, S.; Engel, C.; Farjot, G.; Noah, L.; Maniani, K.; Nicolaï, E. *Bioorg. Med. Chem. Lett.* **2011**, *21* (8), 2244.
- (296) Tanimori, S.; Kashiwagi, H.; Nishimura, T.; Kirihata, M. *Adv. Synth. Cat.* **2010**, *352* (14-15), 2531.
- (297) Mann, A. In *The Practice of Medicinal Chemistry, 3rd Edition*; 2008; pp 363–379.
- (298) Ley, K.; Seng, F. *Synthesis (Stuttg)*. **1975**, 415.
- (299) Haddadin, M. J.; Issidores, C. H. *Tetrahedron Lett.* **1965**, No. 36, 3253.
- (300) Issidorides, C. H.; Haddadin, M. J. *J. Org. Chem.* **1966**, *31* (12), 4067.
- (301) Shoker, T. a; Ghattass, K. I.; Fettinger, J. C.; Kurth, M. J.; Haddadin, M. J. *Org. Lett.* **2012**, *14* (14), 3704.
- (302) Haddadin, M.; Alkaysi, H.; Saheb, S. *Tetrahedron* **1970**, *26*, 1115.
- (303) Takeda, K.; Akagi, Y.; Saiki, A.; Tsukahara, T.; Ogura, H. *Tetrahedron Lett.* **1983**, *24*, 4569.
- (304) Demont, E. H.; Garton, N. S.; Gosmini, R. L. M.; Hayhow, T. G. C.; Seal, J.; Wilson, D. M.; Woodrow, M. D. WO 2011054841 A1 - Tetrahydroquinoline derivatives as bromodomain inhibitors and their preparation and use in the treatment of cancer, chronic autoimmune and inflammatory diseases. WO 2011054841 A1, 2011.
- (305) Katritzky, A.; Pilarski, B.; Urogdi, L. *Synthesis (Stuttg)*. **1989**, 1989 (12), 949.
- (306) Topliss, J. G. *J. Med. Chem.* **1972**, *15* (10), 1006.
- (307) Smith, D. A.; Allerton, C.; Kubinyi, H.; Waterbeemd, H.; Walker, D. K.; Mannhold, R.; Kubinyi, H.; Folkers, G. *Pharmacokinetics and Metabolism in Drug Design, Volume 51, 3rd Edition*, 3rd ed.; 2012.
- (308) Yadav, J. S.; Reddy, a. R.; Narsaiah, a. V.; Reddy, B. V. S. *J. Mol. Cat. A Chem.* **2007**, *261* (2), 207.
- (309) Ahmed, N.; Kumar, H.; Babu, B. V. *Synth. Commun.* **2013**, *43* (4), 567.
- (310) Swamy, N. R.; Goud, T. V.; Reddy, S. M.; Krishnaiah, P.; Venkateswarlu, Y. *Synth. Commun.* **2004**, *34* (4), 727.
- (311) Pasto, M.; Moyano, A.; Perica, M. A.; Riera, A. *J. Org. Chem.* **1996**, *3263* (61), 6033.
- (312) Khaksar, S.; Heydari, A.; Tajbakhsh, M.; Bijanzadeh, H. R. *J. Fluor. Chem.* **2010**, *131* (1), 106.
- (313) Das, U.; Crousse, B.; Kesavan, V.; Bonnet-Delpon, D.; Begue, J. *J. Org. Chem.* **2000**, *65* (20), 6749.
- (314) Wang, Z.; Cui, Y.-T.; Xu, Z.-B.; Qu, J. *J. Org. Chem.* **2008**, *73* (6), 2270.
- (315) Molander, G. A.; Canturk, B.; Kennedy, L. E. *J. Org. Chem.* **2009**, *74* (3), 973.
- (316) GSK. *Unpublished Work*; 2011.
- (317) Valko, K.; Nunhock, S.; Bevan, C.; Abraham, M.; Reynolds, D. *J. Pharm. Sci.* **2003**, *92* (11), 2236.
- (318) Hepworth, J. D.; Tittensor, E. *J. Chem. Soc.* **1965**, 1558.
- (319) *Compounds purchased from commercial vendors*.
- (320) TenBrink, R. E.; Im, W. B.; Sethy, V. H.; Tang, A. H.; Carter, D. B. *J. Med. Chem.* **1994**, *37* (6), 758.
- (321) Apodaca, R.; Xiao, W. *Org. Lett.* **2001**, *3* (11), 1745.

- (322) Smil, D.; Manku, S.; Chantigny, Y. A.; Leit, S.; Wahhab, A.; Yan, T. P.; Fournel, M.; Maroun, C.; Li, Z.; Lemieux, A.-M.; Nicolescu, A.; Rahil, J.; Lefebvre, S.; Panetta, A.; Besterman, J. M.; Déziel, R. *Bioorg. Med. Chem. Lett.* **2009**, *19* (3), 688.
- (323) Leit, S.; Wahhab, A.; Allan, M.; Smil, D.; Tessier, P.; Deziel, R.; Chantigny, Y. A. Benzodiazepine and benzopiperazine analog inhibitors of histone deacetylase. WO2007022638 A1, 2007.
- (324) Lucia, L. A.; Burton, R. D.; Schanze, K. S. *J. Phys. Chem.* **1993**, *97*, 9078.
- (325) Mannam, S.; Sekar, G. *Tetrahedron Lett.* **2008**, *49* (6), 1083.
- (326) Talukdar, D.; Sharma, K.; Bharadwaj, S.; Thakur, A. *Synlett* **2013**, *24* (08), 963.
- (327) Hunsen, M. *Synthesis (Stuttg.)* **2005**, No. 15, 2487.
- (328) Falorni, M.; Giacomelli, G.; Satta, M.; Cossu, S. *Synthesis (Stuttg.)* **1994**, *4*, 391.
- (329) Zhao, M. M.; Li, J.; Mano, E.; Song, Z. J.; Tschaen, D. M. *Org. Synth.* **2005**, *81*, 195.
- (330) Chavan, S. P.; Dumare, N. B.; Harale, K. R.; Kalkote, U. R. *Tetrahedron Lett.* **2011**, *52* (3), 404.
- (331) Arkin, M. R.; McDowell, R. S.; Oslob, J. D.; Raimundo, B. C.; Waal, N. D.; Yu, C. H. Smallmolecule inhibitors of interleukin-2. WO 2003051797, 2003.
- (332) Yamamoto, N.; Obora, Y.; Ishii, Y. *J. Org. Chem.* **2011**, *76* (8), 2937.
- (333) Owston, N.; Parker, A. J.; Williams, J. M. J. *Chem. Commun.* **2008**, No. 5, 624.
- (334) Owston, N.; Nixon, T.; Parker, A.; Whittlesey, M.; Williams, J. *Synthesis (Stuttg.)* **2009**, *2009* (09), 1578.
- (335) Shultz, M. D. *Bioorg. Med. Chem. Lett.* **2013**, *23* (21), 5992.
- (336) Hortense, E.; Jackson, S. *GSK Chiral Analysis and Purification*.
- (337) Cartigny, D.; Berhal, F.; Nagano, T.; Phansavath, P.; Ayad, T.; Genêt, J.-P.; Ohshima, T.; Mashima, K.; Ratovelomanana-Vidal, V. *J. Org. Chem.* **2012**, *77* (10), 4544.
- (338) Mrcic, N.; Jerphagnon, T.; Minnaard, A.; Feringa, B.; de Vries, J. *Adv. Synth. Cat.* **2009**, *351* (16), 2549.
- (339) Qin, J.; Chen, F.; Ding, Z.; He, Y.-M.; Xu, L.; Fan, Q.-H. *Org. Lett.* **2011**, *13* (24), 6568.
- (340) Tang, W.; Xu, L.; Fan, Q.-H.; Wang, J.; Fan, B.; Zhou, Z.; Lam, K.-H.; Chan, A. S. C. *Angew. Chem. Int. Ed.* **2009**, *48* (48), 9135.
- (341) Wang, D.-W.; Wang, D.; Chen, Q.; Zhou, Y. *Chem. Eur. J.* **2010**, *16* (4), 1133.
- (342) Parker, W. L.; Hanson, R. L.; Goldberg, S. L.; Tully, T. P.; Goswami, A. *Org. Proc. Res. Dev.* **2012**, *16* (3), 464.
- (343) Fabian, M. A.; Biggs, W. H.; Treiber, D. K.; Atteridge, C. E.; Azimioara, M. D.; Benedetti, M. G.; Carter, T. A.; Ciceri, P.; Edeen, P. T.; Floyd, M.; Ford, J. M.; Galvin, M.; Gerlach, J. L.; Grotzfeld, R. M.; Herrgard, S.; Insko, D. E.; Insko, M. A.; Lai, A. G.; Lélías, J.-M.; Mehta, S. A.; Milanov, Z. V.; Velasco, A. M.; Wodicka, L. M.; Patel, H. K.; Zarrinkar, P. P.; Lockhart, D. J. *Nat. Biotechnol.* **2005**, *23*, 329.
- (344) Bair, K. W.; Herberitz, T.; Kauffman, G. S.; Kayser-Bricker, K. J.; Luke, G. P.; Martin, M. W.; Millan, D. S.; Schiller, S. E. R.; Talbot, A. C.; Tebbe, M. J. Benzopiperazine compositions as bet bromodomain inhibitors. WO 2015074081 A1, 2015.
- (345) Le Gall, A.; Watson, R. J.; Mitchell, D. J. *GSK Unpublished Work*; 2014.
- (346) Zhu, S.; MacMillan, D. W. C. *J. Am. Chem. Soc.* **2012**, *134* (26), 10815.
- (347) Molander, G. A.; Gormisky, P. E. *J. Org. Chem.* **2008**, *73* (19), 7481.
- (348) Winstead, R. C.; Simpsont, T. H.; Lock, G. A.; Schiavellit, M. D.; Thompson, D. W. *J. Org. Chem.* **1986**, No. 51, 277.
- (349) Hatley, R. *GSK Unpublished Work*; 2015.
- (350) Mycka, R. J.; Duez, S.; Bernhardt, S.; Heppekausen, J.; Knochel, P.; Fleming, F. F. *J. Org. Chem.* **2012**, *77* (17), 7671.
- (351) Bordwell, F. G.; Van der Puy, M.; Vanier, N. R. *J. Org. Chem.* **1976**, *41* (10), 1885.
- (352) Oldenziel, O. H.; Van Leusen, D.; Van Leusen, A. M. *J. Org. Chem.* **1977**, *42* (19), 3114.
- (353) March, J. *Advanced Organic Chemistry*, 4th ed.; Wiley-Interscience, 1992.
- (354) Xing, Q.; Shi, L.; Lang, R.; Xia, C.; Li, F. *Chem. Commun.* **2012**, *48* (89), 11023.
- (355) Paruch, K.; Dwyer, M. P.; Alvarez, C.; Brown, C.; Chan, T.-Y.; Doll, R. J.; Keertikar, K.; Knutson, C.; McKittrick, B.; Rivera, J.; Rossmann, R.; Tucker, G.; Fischmann, T.; Hruza, A.; Madison, V.; Nomeir, A. A.; Wang, Y.; Kirschmeier, P.; Lees, E.; Parry, D.; Sgambellone, N.; Seghezzi, W.; Schultz, L.; Shanahan, F.; Wiswell, D.; Xu, X.; Zhou, Q.; James, R. A.; Paradkar, V. M.; Park, H.; Rokosz, L. R.; Stauffer, T. M.; Guzi, T. J. *ACS Med. Chem. Lett.* **2010**, *1* (5), 204.
- (356) Saito, T.; Obitsu, T.; Minamoto, C.; Sugiura, T.; Matsumura, N.; Ueno, S.; Kishi, A.; Katsumata, S.; Nakai, H.; Toda, M. *Bioorg. Med. Chem.* **2011**, *19* (20), 5955.
- (357) Kenda, B.; Quesnel, Y.; Ates, A.; Michel, P.; Turet, L.; Mercier, J. No Title. WO 2006128693, 2006.
- (358) Jimenez, J.-M.; Knegtel, R.; Charrier, J.-D.; Stamos, D.; Li, P.; Come, J.; Arnov, A. Pyrazolo[1,5-a]pyrimidines useful as inhibitors of protein kinases. WO 2006/052913 A1, February 1, 2006.

- (359) Tashiro, S.; Matsuoka, K.; Minoda, A.; Shionoya, M. *Angew. Chem. Int. Ed. Engl.* **2012**, *51* (52), 13123.
- (360) Hussein, A. M.; Ishak, E. A.; Atalla, A. A.; Hafiz, S. A.; Elnagdi, M. H. *Phosphorus. Sulfur. Silicon Relat. Elem.* **2007**, *182* (12), 2897.
- (361) Kim, I.; Song, J. H.; Park, C. M.; Jeong, J. W.; Kim, H. R.; Ha, J. R.; No, Z.; Hyun, Y.-L.; Cho, Y. S.; Sook Kang, N.; Jeon, D. J. *Bioorg. Med. Chem. Lett.* **2010**, *20* (3), 922.
- (362) Powell, D.; Gopalsamy, A.; Wang, Y. D.; Zhang, N.; Miranda, M.; McGinnis, J. P.; Rabindran, S. K. *Bioorg. Med. Chem. Lett.* **2007**, *17* (6), 1641.
- (363) Urich, R.; Wishart, G.; Kiczun, M.; Richters, A.; Tidten-Luksch, N.; Rauh, D.; Sherborne, B.; Wyatt, P. G.; Brenk, R. *ACS Chem. Biol.* **2013**, *8* (5), 1044.
- (364) Cebasek, P.; Waggener, J.; Bevk, D.; Jakse, R.; Svete, J.; Stanovnik, B. *J. Comb. Chem.* **2010**, *6* (3), 356.
- (365) Gavrin, L. K.; Lee, A.; Provencher, B. a; Massefski, W. W.; Huhn, S. D.; Ciszewski, G. M.; Cole, D. C.; McKew, J. C. *J. Org. Chem.* **2007**, *72* (3), 1043.
- (366) Novak, A.; Humphreys, L. D.; Walker, M. D.; Woodward, S. *Tetrahedron Lett.* **2006**, *47* (32), 5767.
- (367) Kosugi, T.; Mitchell, D. R.; Fujino, A.; Imai, M.; Kambe, M.; Kobayashi, S.; Makino, H.; Matsueda, Y.; Oue, Y.; Komatsu, K.; Imaizumi, K.; Sakai, Y.; Sugiura, S.; Takenouchi, O.; Unoki, G.; Yamakoshi, Y.; Cunliffe, V.; Frearson, J.; Gordon, R.; John Harris, C.; KallooHosein, H.; Le, J.; Patel, G.; Simpson, D. J.; Sherborne, B.; Thomas, P. S.; Suzuki, N.; Takimoto-Kamimura, M.; Kataoka, K. I. *J. Med. Chem.* **2012**, *55* (15), 6700.
- (368) Dowling, J. E.; Chuaqui, C.; Pontz, T. W.; Lyne, P. D.; Larsen, N. A.; Block, M. H.; Chen, H.; Su, N.; Wu, A.; Russell, D.; Pollard, H.; Lee, J. W.; Peng, B.; Thakur, K.; Ye, Q.; Zhang, T.; Brassil, P.; Raciocot, V.; Bao, L.; Denz, C. R.; Cooke, E. *ACS Med. Chem. Lett.* **2012**, *3* (4), 278.
- (369) Bedford, R. B.; Durrant, S. J.; Montgomery, M. *Angew. Chem. Int. Ed. Engl.* **2015**, *54* (30), 8787.
- (370) Baburajan, P.; Elango, K. P. *Tetrahedron Lett.* **2014**, *55* (5), 1006.
- (371) Friis, S. D.; Skrydstrup, T.; Buchwald, S. L. **2015**, 8.
- (372) Hermange, P.; Lindhardt, A. T.; Taaning, R. H.; Bjerglund, K.; Lupp, D.; Skrydstrup, T. *J. Am. Chem. Soc.* **2011**, *133* (15), 6061.
- (373) Arora, N.; Chen, S.; Hermann, J. C.; Kuglstatter, A.; Labadie, S. S.; Lin, C. J. J.; Lucas, M. C.; Moore, A. G.; Papp, E.; Talamas, F. X.; Wanner, J.; Zhai, Y. Pyrazolo[1,5-a]pyrimidine and thieno[3,2-b]pyrimidine derivatives as IRAK4 modulators. WO2012007375, 2012.
- (374) Fraser, R. R.; Bruce Grindley, T. *Tetrahedron Lett.* **1974**, *15* (47), 4169.
- (375) Guzi, T.; Paruch, K.; Dwyer, M.; Parry, D. US 20070082900 A1 Methods for inhibiting protein kinases. US 20070082900 A1, 2006.
- (376) Blaney, J.; Gibbons, P. A.; Hanan, E.; Lyssikatos, J. P.; Magnuson, S. R.; Pastor, R.; Rawson, T. E.; Zhou, A.; Zhu, B.-Y. Pyrazolopyrimidine Jak inhibitor compounds and methods. WO 2010051549 A1, 2010.
- (377) Almansa, C.; de Arriba, A. F.; Cavalcanti, F. L.; Gómez, L. A.; Miralles, A.; Merlos, M.; GarcíaRafanell, J.; Forn, J. *J. Med. Chem.* **2001**, *44* (3), 350.
- (378) Popowycz, F.; Schneider, C.; DeBonis, S.; Skoufias, D. A.; Kozielski, F.; Galmarini, C. M.; Joseph, B. *Bioorg. Med. Chem.* **2009**, *17* (9), 3471.
- (379) He, L.; Gilligan, P. J.; Zaczek, R.; Fitzgerald, L. W.; McElroy, J.; Shen, H.-S. L.; Saye, J. A.; Kalin, N. H.; Shelton, S.; Christ, D.; Trainor, G.; Hartig, P. *J. Med. Chem.* **2000**, *43* (3), 449.
- (380) Senga, K.; O'Brien, D. E.; Scholten, M. B.; Novinson, T.; Miller, J. P.; Robins, R. K. *J. Med. Chem.* **1982**, *25* (3), 243.
- (381) Harris, C. M.; Ericsson, A. M.; Argiriadi, M. A.; Barberis, C.; Borhani, D. W.; Burchat, A.; Calderwood, D. J.; Cunha, G. A.; Dixon, R. W.; Frank, K. E.; Johnson, E. F.; Kamens, J.; Kwak, S.; Li, B.; Mullen, K. D.; Perron, D. C.; Wang, L.; Wishart, N.; Wu, X.; Zhang, X.; Zmetra, T. R.; Talanian, R. V. *Bioorg. Med. Chem. Lett.* **2010**, *20* (1), 334.
- (382) Würtz, S.; Lohre, C.; Fröhlich, R.; Bergander, K.; Glorius, F. *J. Am. Chem. Soc.* **2009**, *131*, 8344.
- (383) Song, X.-G.; Zhu, S.-F.; Xie, X.-L.; Zhou, Q.-L. *Angew. Chem. Int. Ed. Engl.* **2013**, *52* (9), 2555.
- (384) Blaszykowski, C.; Aktoudianakis, E.; Alberico, D.; Bressy, C.; Hulcoop, D. G.; Jafarpour, F.; Joushaghani, A.; Laleu, B.; Lautens, M. *J. Org. Chem.* **2008**, *73* (5), 1888.
- (385) Hobbs, A.; Briers, R.; Lynn, S. *GSK Purification and Analysis Services*.
- (386) Mc Murry, J. E.; Scott, W. J. *Tetrahedron Lett.* **1983**, *24* (10), 979.
- (387) Graczyk, P. P.; Dimopoulos, P.; Khan, A.; Bhatia, G. S.; Farthing, C. N. 7-azaindole derivatives and their use in the inhibition of c-jun n-terminal kinase. WO2008095944A, 2008.
- (388) Takagi, J.; Takahashi, K.; Ishiyama, T.; Miyaura, N. *J. Am. Chem. Soc.* **2002**, *124* (27), 8001.
- (389) Balléll, L.; Bates, R. H.; Young, R. J.; Alvarez-Gomez, D.; Alvarez-Ruiz, E.; Barroso, V.; Blanco, D.; Crespo, B.; Escribano, J.; González, R.; Lozano, S.; Huss, S.; Santos-Villarejo, A.; Martín-Plaza, J. J.; Mendoza, A.; Rebollo-Lopez, M. J.; Remuiñán-Blanco, M.; Lavandera, J. L.; Pérez-

Herran, E.; Gamo-Benito, F. J.; García-Bustos, J. F.; Barros, D.; Castro, J. P.; Cammack, N.
ChemMedChem **2013**, *8* (2), 313.